

Site descriptive modelling Forsmark, stage 2.2

A fracture domain concept as a basis for the statistical modelling of fractures and minor deformation zones, and interdisciplinary coordination

Isabelle Olofsson, Assen Simeonov
Svensk Kärnbränslehantering AB

Michael Stephens, Geological Survey of Sweden (SGU)

Sven Follin, SF GeoLogic AB

Ann-Chatrin Nilsson, Geosigma AB

Kennert Röshoff, Ulrika Lindberg, Flavio Lanaro
Bergbyggkonsult AB

Anders Fredriksson, Lars Persson
Golder Associates AB

April 2007

Svensk Kärnbränslehantering AB

Swedish Nuclear Fuel
and Waste Management Co
Box 5864
SE-102 40 Stockholm Sweden
Tel 08-459 84 00
+46 8 459 84 00
Fax 08-661 57 19
+46 8 661 57 19



Site descriptive modelling Forsmark, stage 2.2

A fracture domain concept as a basis for the statistical modelling of fractures and minor deformation zones, and interdisciplinary coordination

Isabelle Olofsson, Assen Simeonov
Svensk Kärnbränslehantering AB

Michael Stephens, Geological Survey of Sweden (SGU)

Sven Follin, SF GeoLogic AB

Ann-Chatrin Nilsson, Geosigma AB

Kennert Röshoff, Ulrika Lindberg, Flavio Lanaro
Bergbyggkonsult AB

Anders Fredriksson, Lars Persson
Golder Associates AB

April 2007

This report concerns a study which was conducted for SKB. The conclusions and viewpoints presented in the report are those of the authors and do not necessarily coincide with those of the client.

A pdf version of this document can be downloaded from www.skb.se

Abstract

The Swedish Nuclear Fuel and Waste Management Company (SKB) is undertaking site characterization at two different locations, Forsmark and Simpevarp/Laxemar, with the objective of siting a final waste repository at depth for spent nuclear fuel. The programme is built upon the development of site descriptive models after each data freeze. This report describes the first attempt to define fracture domains for the Forsmark site modelling in stage 2.2.

Already during model version 1.2 at Forsmark, significant spatial variability in the fracture pattern was observed. The variability appeared to be so significant that it provoked the need for a subdivision of the model volume for the treatment of geological and hydrogeological data into sub-volumes. Subsequent analyses of data collected up to data freeze 2.1 led to a better understanding of the site and a concept for the definition of fracture domains based on geological characteristics matured.

The main objectives of this report are to identify and describe fracture domains at the site on the basis of geological data and to compile hydrogeological, hydrogeochemical and rock mechanics data within each fracture domain and address the implications of this integration activity.

On the basis of borehole data, six fracture domains (FFM01–FFM06) have been recognized inside and immediately around the candidate volume. Three of these domains (FFM01, FFM02 and FFM06) lie inside the target volume for a potential repository in the northwestern part of the candidate area, and need to be addressed in the geological DFN modelling work.

The hydrogeological data support the subdivision of the bedrock into fracture domains FFM01, FFM02 and FFM03. Few or no data are available for the other three domains. The hydrogeochemical data also support the subdivision into fracture domains FFM01 and FFM02. Since few data are available from the bedrock between deformation zones inside FFM03, there is little information on the hydrogeochemical character of the groundwater in this domain. No significant differences in mechanical properties of the intact rock have been observed between the different fracture domains, except for those that more likely depend on different mineralogical composition.

The results of the work are compiled in tables and several figures for each borehole that document the occurrence of rock domains, deformation zones and fracture domains in each borehole as well as hydrogeological, hydrogeochemical and rock mechanics data in relation to rock domains, deformation zones and fracture domains. A 3D geometric model for fracture domains inside the target volume, based on the data in the boreholes, is also presented.

Sammanfattning

Svensk Kärnbränslehantering AB (SKB) bedriver platsundersökningar på två platser, Forsmark och Simpevarp/Laxemar, för en eventuell lokalisering av ett djupförvar för använt kärnbränsle på någon av dessa platser. Programmet för platskaraktärisering tar avstamp från platsbeskrivande modeller som tas fram efter varje datafrys. Denna rapport beskriver det första försöket att definiera sprickdomäner i Forsmark för platsmodelleringen i modellsteg 2.2.

Redan under arbetet med att ta fram modellversion 1.2 för Forsmark observerades betydande skillnader i bergets sprickighet mellan olika delar inom kandidatområdet. Dessa skillnader visade på ett behov av att dela upp modellvolymen i olika delvolymmer för bearbetning av geologiska och hydrogeologiska data. Den större förståelse av berget i Forsmarks som uppnått i och med de efterföljande analyserna av data ingående i datafrys 2.1 gav ytterligare stöd för konceptet att berget kan delas in i olika enheter, sprickdomäner, och hur denna indelning kan göras baserat på bergets geologiska egenskaper.

Det huvudsakliga syftet med denna rapport är att identifiera och beskriva sprickdomäner utifrån geologiska data och att sammanställa hydrogeologiska, hydrogeokemiska och bergmekaniska primärdata för varje sprickdomän samt att belysa betydelsen av denna samordnade aktivitet.

Baserat på borrhålsdata har sex sprickdomäner identifierats inom och direkt utanför kandidatområdet. Tre av dessa domäner (FFM01, FFM02 och FFM03) ligger inom det tilltänkta förvarsområdet i den nordvästra delen av kandidatområdet. Dessa domäner behöver därför adresseras i den geologiska DFN modelleringen.

Indelningen av berget i sprickdomänerna FFM01, FFM02 och FFM03 stöds av de sammanställda hydrogeologiska primärdata. Få eller inga data finns för de övriga domänerna. Även hydrogeokemiska data stöder indelningen i sprickdomänerna FFM01 och FFM02. Eftersom endast få data finns från berget mellan deformationszonerna i sprickdomän FFM03 är informationen om grundvattnets karaktär i denna domän liten. Inga signifikanta skillnader i det intakta bergets mekaniska egenskaper mellan de olika sprickdomänerna har noterats, förutom de som snarare beror på skillnader i bergets mineralogiska sammansättning.

Resultatet av arbetet är sammanställt i tabeller och flera figurer för varje borrhål. Dessa dokumenterar var bergdomäner, deformationszoner och sprickdomäner finns i varje borrhål samt visar hydrogeologiska, hydrogeokemiska och bergmekaniska data i relation till bergdomäner, deformationszoner och sprickdomäner. En geometrisk modell i 3D för sprickdomänerna i det tilltänkta förvarsberget, som baseras på data från borrhålen, redovisas också.

Contents

1	Introduction	7
1.1	Background	7
1.2	Objective and scope	7
1.3	Presentation of the Forsmark site	8
1.4	Structure of the report	8
2	Terminology	11
3	Available primary data	13
3.1	Overview of investigations	13
3.2	Late data	13
3.3	Nonconformities	14
4	Fracture data in boreholes	15
4.1	Data selection	15
4.2	Borehole logs and the results of the single-hole interpretation	18
4.3	Modifications of single-hole interpretation in connection with geological modelling and extended single-hole interpretation work	21
4.3.1	Modifications of possible deformation zones during modelling work	22
4.3.2	Additional possible deformation zones identified by the extended single-hole interpretation	26
4.4	Identification of vuggy rock in connection with quartz dissolution	27
4.5	Fracture frequency distribution in each borehole	30
5	Fracture domain concept	33
5.1	Presentation of the fracture domain concept	33
5.2	Presentation of fracture domains in each borehole	37
5.3	Geometric model for fracture domains inside the target volume	40
5.4	Uncertainties	43
6	Hydrogeological data in the context of fracture domains and deformation zones	47
6.1	Available hydrogeological data and data selection	47
6.2	Flow anomalies by depth, deformation zone and fracture domain	48
6.2.1	Drill site 1	49
6.2.2	Drill site 2	51
6.2.3	Drill site 3	52
6.2.4	Drill site 4	53
6.2.5	Drill site 5	54
6.2.6	Drill site 6	55
6.2.7	Drill site 7	57
6.2.8	Drill site 8	59
6.2.9	Drill site 10	61
6.3	Summary	62
6.3.1	Summary of PFL-f fracture transmissivities in different fracture domains	62
6.3.2	Orientation and statistics of flowing features associated with the PFL-f fracture transmissivities	63
7	Hydrogeochemical data in the context of fracture domains and deformation zones	67
7.1	Data selection	67
7.1.1	Investigations	67
7.1.2	Components and parameters	68

7.2	Drill site overview	71
7.2.1	Drill site 1	71
7.2.2	Drill site 2	74
7.2.3	Drill site 3	75
7.2.4	Drill site 4	76
7.2.5	Drill site 5	77
7.2.6	Drill site 6	78
7.2.7	Drill site 7	80
7.2.8	Drill site 8	81
7.2.9	Drill site 9	83
7.3	Summary and discussion	84
8	Rock mechanics data in the context of fracture domains and deformation zones	91
8.1	Available rock mechanics data and data selection	91
8.2	Drill site overview	93
8.2.1	Intact rock properties	93
8.2.2	Fracture properties	99
8.3	Overview of test results	103
8.3.1	Tests on intact rock	103
8.3.2	Tests on fractures	111
8.3.3	Rock mass characterization	117
8.3.4	Rock stress measurements	118
8.4	Summary and discussion	120
9	Discussion and summary	131
9.1	Visualization of borehole data	131
9.2	Implications of the fracture domain model for geological DFN modelling	132
9.3	Feedback from other disciplines to geology	132
10	Conclusions	135
	Acknowledgements	136
	References	137
Appendix 1	Specification of available data	139
Appendix 2	WellCad diagrams for geological data	161
Appendix 3	Fracture frequency distribution diagrams for all boreholes	183
Appendix 4	Presentation of fracture domains in each cored borehole	195
Appendix 5	WellCad diagrams for hydrogeochemical data	217
Appendix 6	WellCad diagrams for rock mechanics data	221
Appendix 7	P-wave velocity plots	237
Appendix 8	Integrated WellCad diagrams	239
Appendix 9	Documentation of data files on the CD-Rom	261

1 Introduction

1.1 Background

The Swedish Nuclear Fuel and Waste Management Company (SKB) is undertaking site characterization at two different locations, Forsmark and Simpevarp/Laxemar, with the objective of siting a repository for spent nuclear fuel. The programme is built upon the development of site descriptive models after each data freeze.

Already during model version 1.2 at Forsmark, significant spatial variability in the fracture pattern was observed. The gently dipping deformation zone ZFMA2 was identified as a major structural feature steering both the hydrogeological and fracture properties at the site /SKB 2005a/. Moreover, the conditions close to the surface in the north-western part of the model volume appeared to be different from the conditions observed at depth. The variability appeared to be so significant that it provoked the need for a subdivision of the model volume for the treatment of geological and hydrogeological data into sub-volumes.

This report describes the first attempt to define fracture domains for the Forsmark site modelling in stage 2.2.

1.2 Objective and scope

No geological DFN modelling work was performed during stage 2.1. However, data collected up to the data freeze 2.1 were interpreted in the framework of the development of the deformation zone and rock domain models. These analyses led to a better understanding of the site and a concept for the definition of fracture domains based on geological characteristics matured /SKB 2006/.

The geological model is composed of three main components: the rock domain model, the deformation zone model, and the geological DFN model. The deformation zone model aims to define the larger structural features in the model volume, while the aim of the geological DFN model is to provide a statistical description of the features below the resolution threshold for the definition of deterministic deformation zones and fractures (see also Chapter 2). This involves an important interaction between the models, as primary data need to be addressed in the appropriate manner. Moreover, other disciplines are dependent on the assumptions made in the overall geological modelling work.

The main objectives of this report is to:

- identify and describe fracture domains at the site on the basis of geological data, so as to specify the set of data to be used in deformation zone modelling work and the set of data to be used in geological DFN modelling work,
- compile hydrogeological, hydrogeochemical and rock mechanical data within each fracture domain and address the implications of this integration activity,
- present an overview of the primary data available at stage 2.2.

The report is written as a support for the modelling in stage 2.2 and as such contains a limited amount of data analyses. It is intended to constitute a basis for the geological DFN and other modelling work by defining the different sub-domains in which the geological DFN should be represented. Hence, the geological DFN modelling team will use the fracture domain concept presented herein as a working hypothesis. Based on the outcome of statistical analyses of the fractures and the potential correlation between these statistics and other geological parameters, the definitions of the fracture domains may be modified, or complementary sub-domains may be recognised.

1.3 Presentation of the Forsmark site

The Forsmark site is located in northern Uppland within the municipality of Östhammar about 170 km north of Stockholm. Figure 1-1 illustrates the candidate area with the ten drill sites where borehole data have been acquired up to data freeze 2.2. Figure 1-2 presents detailed maps of the actual drill sites for the report. Data from boreholes at drill sites 11 and 12 are not included in the data set for data freeze 2.2.

1.4 Structure of the report

Chapter 2 presents the terminology used in this report in order to facilitate an understanding of the different expressions used to describe the geological model.

The primary data from investigations that were available at data freeze 2.2 are compiled and defined in Chapter 3 of this report. Chapter 4 describes the process of defining the fracture domains and involves an analysis of relevant geological data. The fracture domains are identified and described in Chapter 5. Hydrogeological, hydrogeochemical and rock mechanics data

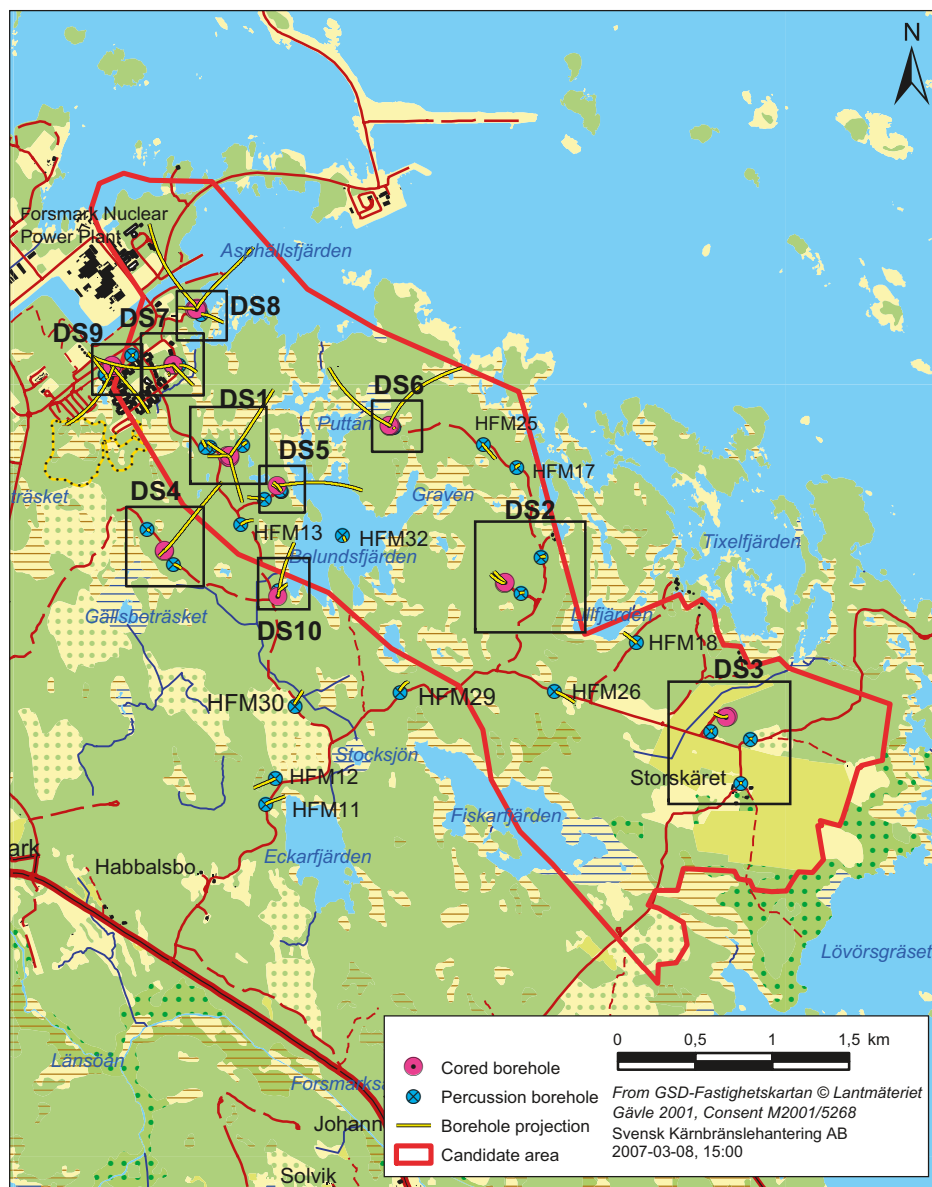


Figure 1-1. Drill sites in and close to the candidate area.

are presented and interpreted in the framework of the fracture domain concept in Chapters 6, 7 and 8. The purpose is to seek support from other disciplines for the fracture domain concept, which has been developed solely on the basis of geological information. The lessons learned from the integration exercise are discussed and conclusions are drawn in Chapters 9 and 10.

In order to facilitate the reading of the report, most of the illustrations are presented in appendices and a few examples of each illustration type are included in the main body of the report. All illustrations and 3D models are provided on a CD. The 3D models will also be made available in the SKB model database. An additional outcome of the work presented in this report is three tables not included in this report. One of these tables documents borehole intersections of rock domains, deformation zones and fracture domains in the geological model based on data freeze 2.2. Table 5-1 is an extract of this table and the full table will be made available in Sicada¹. The other two tables contain compilations of hydrogeochemical and rock mechanics data, respectively, within the framework of the geometries of the geological model. These two tables will be made available in the SKB model database.

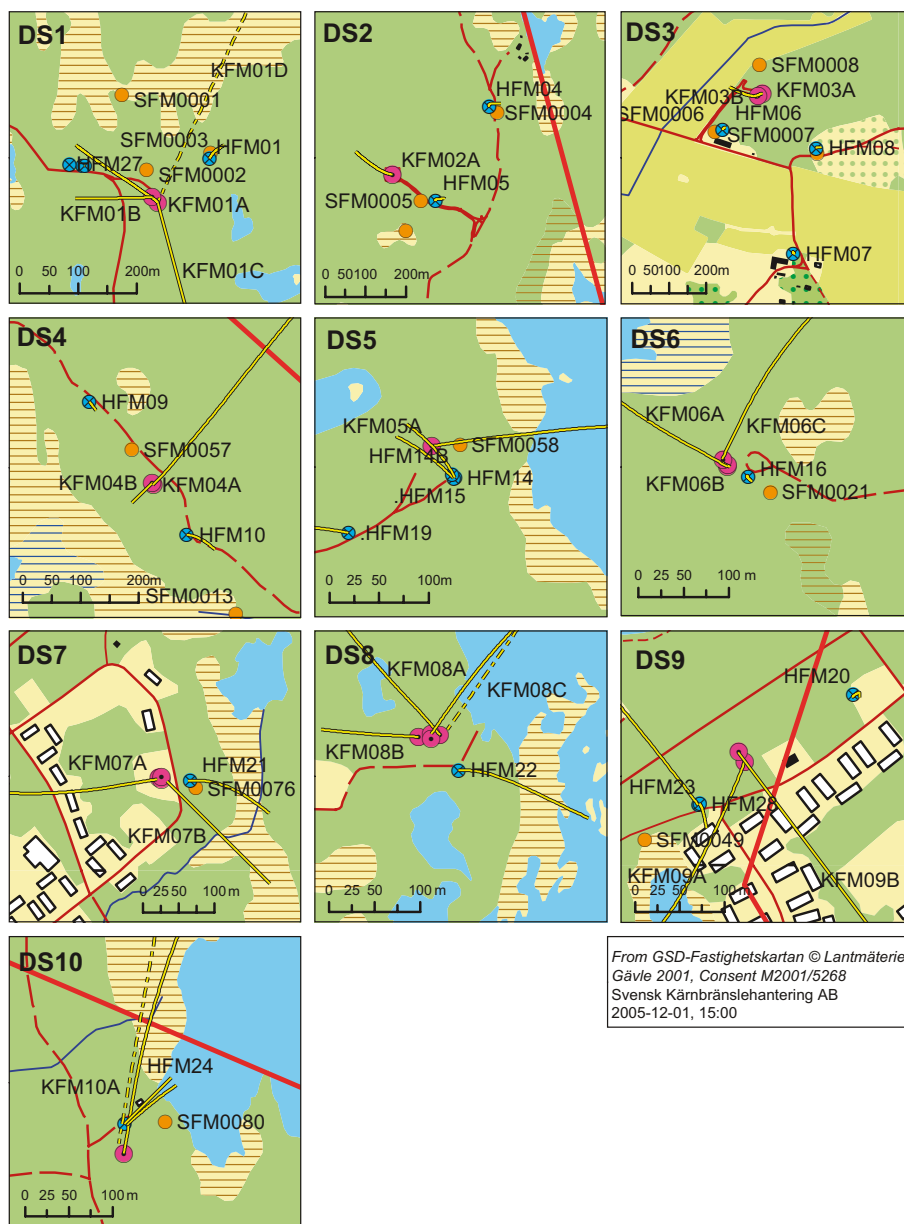


Figure 1-2. Detailed documentation of the drill sites. See Figure 1-1 for legend.

¹ The work with adding these data to Sicada is ongoing at the time of preparing this report.

2 Terminology

The terminology used in the site characterisation work is considered to be a possible pitfall as different disciplines apply the same term with different meanings. For this reason, definitions are provided here for terms that are crucial in the geological modelling work. The definitions below are based on the general guidelines provided in /Munier and Hermansson 2001/ and /Munier et al. 2003/. The recognition of both rock domains for one purpose and fracture domains for another (see below) follows the guidelines presented in /Munier et al. 2003, p 63/. In the following text, the general terms used in these reports have been more strictly defined in relation to the geological situation and the needs of other disciplines at Forsmark.

- **Rock unit (RU).** A rock unit is defined on the basis of one or several combined properties including rock composition, grain size, degree of bedrock homogeneity, degree and style of ductile deformation, early-stage alteration (albitization) and fracture frequency. Both dominant rock type and subordinate rock types are defined for the rock units that are defined solely or partly on the basis of rock composition. The term rock unit is used in the bedrock mapping work at the surface (2D structure) and in connection with the single hole interpretation work (essentially a 1D structure). Rock units are referred to as RUxx, where the ID is coupled to the boreholes. Thus, there is no unique ID for the rock units at the site.
- **Rock domain (RD).** A rock domain refers to a rock volume in which rock units that show similar composition, grain size, degree of bedrock homogeneity, and degree and style of ductile deformation have been combined and distinguished from each other. Rock volumes that show early-stage alteration (albitization) are also distinguished as separate rock domains. The term rock domain is used in the 3D geometric modelling work and different rock domains at Forsmark are referred to as RFMxxx. The recognition of rock domains as defined here aims primarily to meet the needs of colleagues working with the discipline thermal modelling.
- **Deformation zone (DZ).** A deformation zone is a general term referring to an essentially 2D structure along which there is a concentration of brittle, ductile or combined brittle and ductile deformation. The term fracture zone is used to denote a brittle deformation zone without any specification whether there has or has not been a shear sense of movement along the zone. A fracture zone that shows a shear sense of movement is referred to as a fault zone. In the single-hole interpretation, deformation zones are referred to as DZxx, where the ID is coupled to the boreholes.

Table 2-1 presents the terminology for brittle structures based on trace length and thickness as presented in /Andersson et al. 2000/. The borderlines between the different structures are approximate. For purposes of linguistic simplicity, these structures are referred to in the text that follows as regional, major and minor deformation zones.

Based on the scale of the structure and bearing in mind the resolution scale of the current deterministic modelling work, a distinction is made between:

- 1) Deformation zones, which are longer than 1,000 m and modelled deterministically. These are referred to as ZFMxxx and are included in the DZ block model.
- 2) Minor deformation zones, which are shorter than 1,000 m and modelled deterministically. These are referred to as ZFMxxx, but are not included in the DZ block models.

Table 2-1. Terminology and general description (length and width are approximate) of the brittle structures in the bedrock based on /Andersson et al. 2000/.

Terminology	Length	Width	Geometrical description
Regional deformation zone	> 10 km	> 100 m	Deterministic
Local major deformation zone	1 km – 10 km	5 m – 100 m	Deterministic (with scale-dependent description of uncertainty)
Local minor deformation zone	10 m – 1 km	0.1 m – 5 m	Statistical (if possible, deterministic)
Fracture	< 10 m	< 0.1 m	Statistical

3) Possible deformation zones, which have been recognised in the single hole interpretation, but have not been linked to other features (e.g. a low magnetic lineament, a seismic reflector) that provide a basis for modelling in 3D space. For this reason, these structures are not modelled deterministically and are probably minor zones. The term deformation zone is used at all stages in the geological work, bedrock surface mapping, single-hole interpretation and 3D modelling.

- Fracture domain (FD). A fracture domain refers to a rock volume outside deformation zones in which rock units show similar fracture frequency characteristics. Fracture domains at Forsmark are defined on the basis of the single-hole interpretation work and its modifications and extensions, and the results of the initial statistical treatment of fractures. Both deformation zones that have been modelled geometrically, and possible deformation zones that have been identified in the single hole interpretation but have not been modelled geometrically, are excluded from fracture domains. The term is used in the first hand as a basis for the discrete fracture network modelling work (geological DFN) and different fracture domains at Forsmark are referred to as FFMxxx. The recognition of fracture domains as defined here aims primarily to meet the needs of colleagues working with the disciplines hydrogeology, hydrogeochemistry and rock mechanics.
- Discrete fracture network (geological DFN). The fracturing in the bedrock is described on the basis of a standardized statistical procedure, which provides geometries, directions and spatial distributions for the fractures within defined fracture domains.
- Candidate area/volume. The area at the ground surface, and its extension at depth, in a municipality that was recognised as suitable for a site investigation, following the feasibility study work /SKB 2000/.
- Target volume. The target volume includes the rock volume that has been identified as suitable for the excavation of the waste repository /SKB 2005b/. In connection with the stage 2.2 modelling work, this volume is defined as the parts of rock domain RFM029, as well as rock domain RFM045, that are situated north-west of the steeply dipping zone ZFMNE0065 and beneath the gently dipping zones ZFMA2, ZFMA3 and ZFMF1. The target volume defines the boundaries of the volume in which geological DFN modelling work will be carried out during stage 2.2.

3 Available primary data

3.1 Overview of investigations

Analyses and modelling work are performed on quality controlled data from Forsmark stored in the SKB database Sicada and the SKB Geographic Information System (GIS) at data freeze 2.2. No data posterior to the data freeze 2.2 or otherwise reported will be used for geological DFN modelling.

Tables A1-1 to A1-4 in Appendix 1 summarise the investigations that have been carried out on the site up to data freeze 2.2 for geology, hydrogeology, hydrochemistry and rock mechanics. These tables also include data collected for versions 1.1, 1.2, 2.1, as well as any supplementary data that may have been available before the start of the site investigation programme. The reports mentioned in these tables are listed in Table A1-5 in Appendix 1. Note that the reference to the P-reports does not refer to the reference to the data in Sicada. Both references are presented in the tables in Appendix 1.

All data that are included in these tables have not been used and analyzed in the framework of this report. Nevertheless, they are meant to support the modelling teams in the preparation of their work. The data analyzed in this report are specified under each relevant section (e.g. section 4.1 for geology).

3.2 Late data

Some data needed in the dataset for data freeze 2.2 were not available at the time of the data freeze and are therefore referred to as late data. This delay has implications for the modelling work. First of all, these data cannot be integrated in this report, and they need to be added to the dataset afterwards. The late data reported are:

- Geological data from single-hole interpretation of cored borehole KFM07C and percussion borehole HFM26.
- Rock stress measurements: overcoring measurements in cored boreholes KFM02B and KFM07C and hydraulic measurements (HF/HTPF) in KFM07A, KFM07C, KFM08A, KFM09A and KFM09B.
- Uniaxial compressive tests in KFM01C – these data were available in Sicada before completion of the report and are presented in the WellCad plots (Appendix 6 and 8), but not included in the compilation of rock mechanics data presented in Chapter 8.
- Triaxial compressive tests in KFM02B.
- Observations of indirect rock stress indicators by means of borehole breakout study in several boreholes.
- Empirical characterization of rock mass quality by means of Q and RMR for KFM07C – these data were available in Sicada before completion of the report and are presented in the WellCad plots (Appendix 6 and 8), but not included in the compilation of the rock mechanics data presented in Chapter 8.
- Results from direct tensile tests.

3.3 Nonconformities

Due to updates in the mapping procedure or discrepancies in the application of the instructions for bedrock mapping, some parameters do not conform in all boreholes. An overview of the identified and reported nonconformities is available in /SKB document ID 1073601/.

The most important parameters for the analysis and understanding of data in Forsmark that are affected by nonconformities are listed below:

- Aperture measurements along fractures in KFM01A, KFM02A, KFM03A and KFM03B: aperture was defined as 0 mm, 1 mm or a value greater than 1 mm. For all other boreholes, an aperture size of 0.5 mm was introduced to include fractures that had an aperture too small to be measured in BIPS (resolution limit 1 mm). It should be noted that fracture data from KFM01A have been post-processed based on the new methodology, and an aperture of 0.5 mm is now estimated.
- Documentation of sealed fracture networks was introduced for the first time in January 2004, and was, therefore, first included in KFM01B and KFM04A. Sealed fracture networks have not been mapped in KFM01A, KFM02A, KFM03A and KFM03B.

Even if the data stored in Sicada has been checked and approved for use, some errors may be found during the modelling work. The people involved in the modelling work shall report any detected errors, according to the steering document SDP-517 (version 3.0) “Hantering av fel i primärdata”, to the e-mail address *data.error@skb.se*. The error must be documented in a special error report. More serious errors should be reported as discrepancies according to procedure SD-006. The modellers should also regularly check the data error report list in Sicada.

One “error”, which was discovered after data freeze 2.2 and which could affect the modelling work under stage 2.2, is the error in the orientation data. This error concerns the geometry and position of each borehole as well as the orientation of geological structures including fractures. The uncertainty related to this error was still under analysis at the time of preparation of this report. For this reason, some figures presented in this report may be affected by the result of this uncertainty study, as for example the elevation (metres below sea level) calculated according to the coordinate system RT90-RHB70. However, the fracture positions and the intercept of the modelled structures along the borehole will not be affected. The impact of the uncertainty revealed by this error study should be evaluated by each discipline during the modelling stage 2.2.

4 Fracture data in boreholes

4.1 Data selection

The following data have been selected from Sicada as a basis for defining fracture domains at the Forsmark site:

- The rock units and possible deformation zones defined in the single-hole interpretation of the cored boreholes KFM01A, KFM01B, KFM01C, KFM01D, KFM02A, KFM03A, KFM03B, KFM04A, KFM05A, KFM06A, KFM06B, KFM06C, KFM07A, KFM07B, KFM07C, KFM08A, KFM08B, KFM08C, KFM09A, KFM09B and KFM10A (Figure 1-1 and Figure 1-2). Sicada file reference: p_one_hole_interpret, coordinates calculated, data delivery Sicada_06_193 (2006-09-18) and Sicada_06_283 (2006-11-09).
- The rock units and possible deformation zones defined in the single-hole interpretation of the percussion boreholes HFM01 to HFM32 and HFM38. Sicada file reference: p_one_hole_interpret, coordinates calculated, data delivery Sicada_06_193 (2006-09-18) and Sicada_06_283 (2006-11-09).
- Rock alteration in the cored boreholes listed above except KFM07C, with focus on quartz dissolution. This type of alteration occurs together with porous, vuggy rock in the boreholes. It has not been recognized in any of the percussion boreholes at the site or in KFM07C. Sicada file reference: p_rock_alter, coordinates calculated, data delivery Sicada_06_193 (2006-09-18).
- One metre fracture frequency and elevation data from the cored boreholes listed above. Sicada file reference: p_freq_1m, coordinates calculated and p_freq_1m_shi_rock, coordinates calculated, Sicada_06_193 (2006-09-18) and Sicada_06_283 (2006-11-09).

The division of rock domain RFM029 into sub-volumes, based on the uneven distribution of hydraulic flow anomalies /SKB 2005a, section 8.4.3, p 368–369/ as well as the conceptual understanding of the structural geology of the site prior to model stage 2.2 /SKB 2006, section 3.2.2, p 121–126/, have both provided an inspiration for the establishment of fracture domains. The definition of fracture domains inside the target volume, in both 3D space and extracted from this model in 2D space at the surface and at 400 m depth, has also made use of the stage 2.2 geometric models for rock domains (Figure 4-1) and deterministic deformation zones (Figure 4-2).

Due to the poorer quality of geological data in the percussion boreholes, the lower confidence level in the single hole interpretation work and the limited length of these boreholes, data from the percussion boreholes have not been used to define fracture domains at the site. Nevertheless, fracture domains have been assigned along these boreholes, based on the fracture domains identified in the nearest cored boreholes.

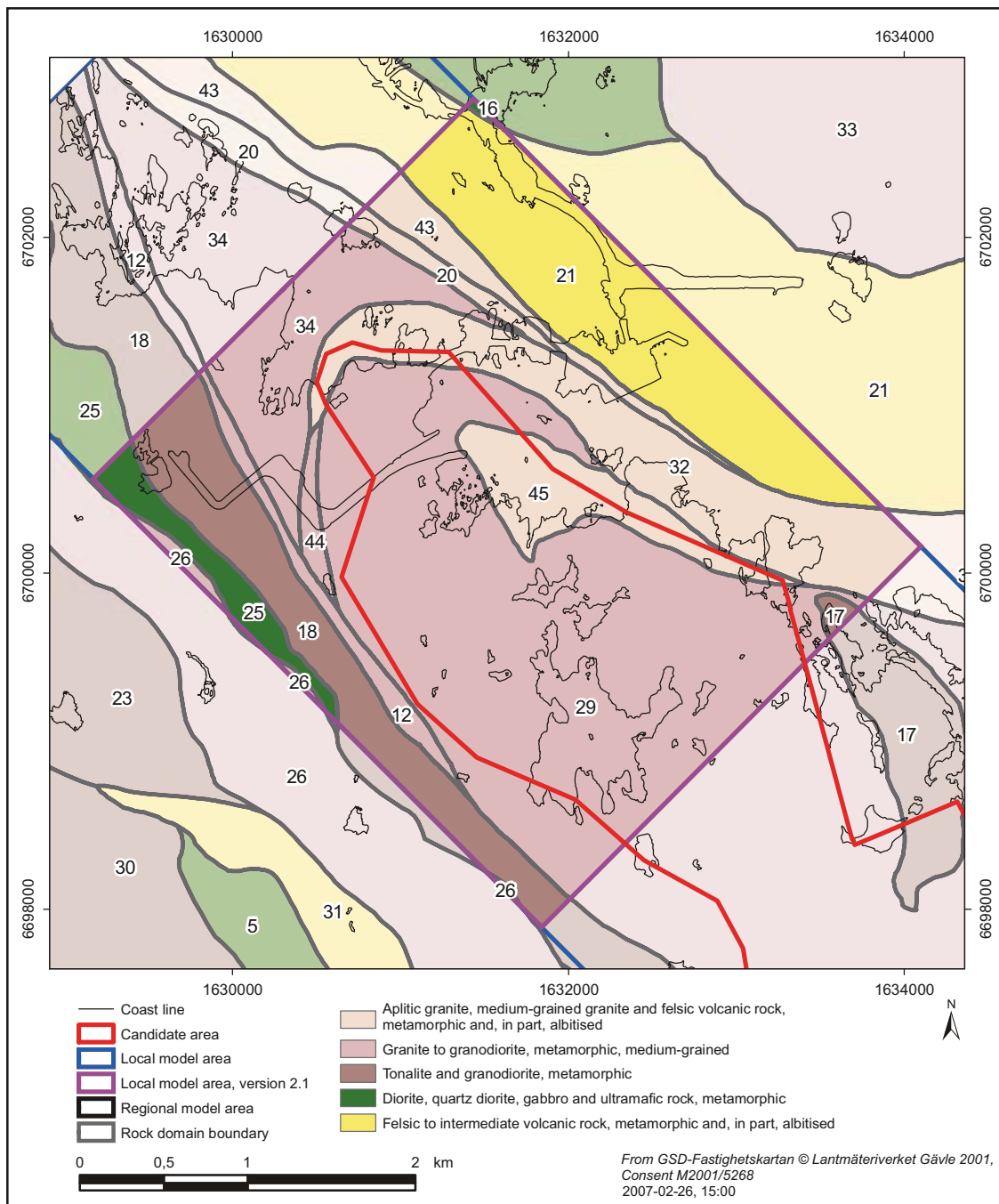


Figure 4-1. Two-dimensional model at the surface for rock domains inside and immediately around the local model area, stage 2.2. Rock domains further away from this area are identical to SDM version 1.2. The colours represent the composition of the dominant rock type in each domain, if necessary in combination with the grain size of the rock. As in previous models, the degree of homogeneity and the style and degree of ductile deformation (not shown here) have also been used to distinguish domains. Coordinates are provided using the RT90 (RAK) system.

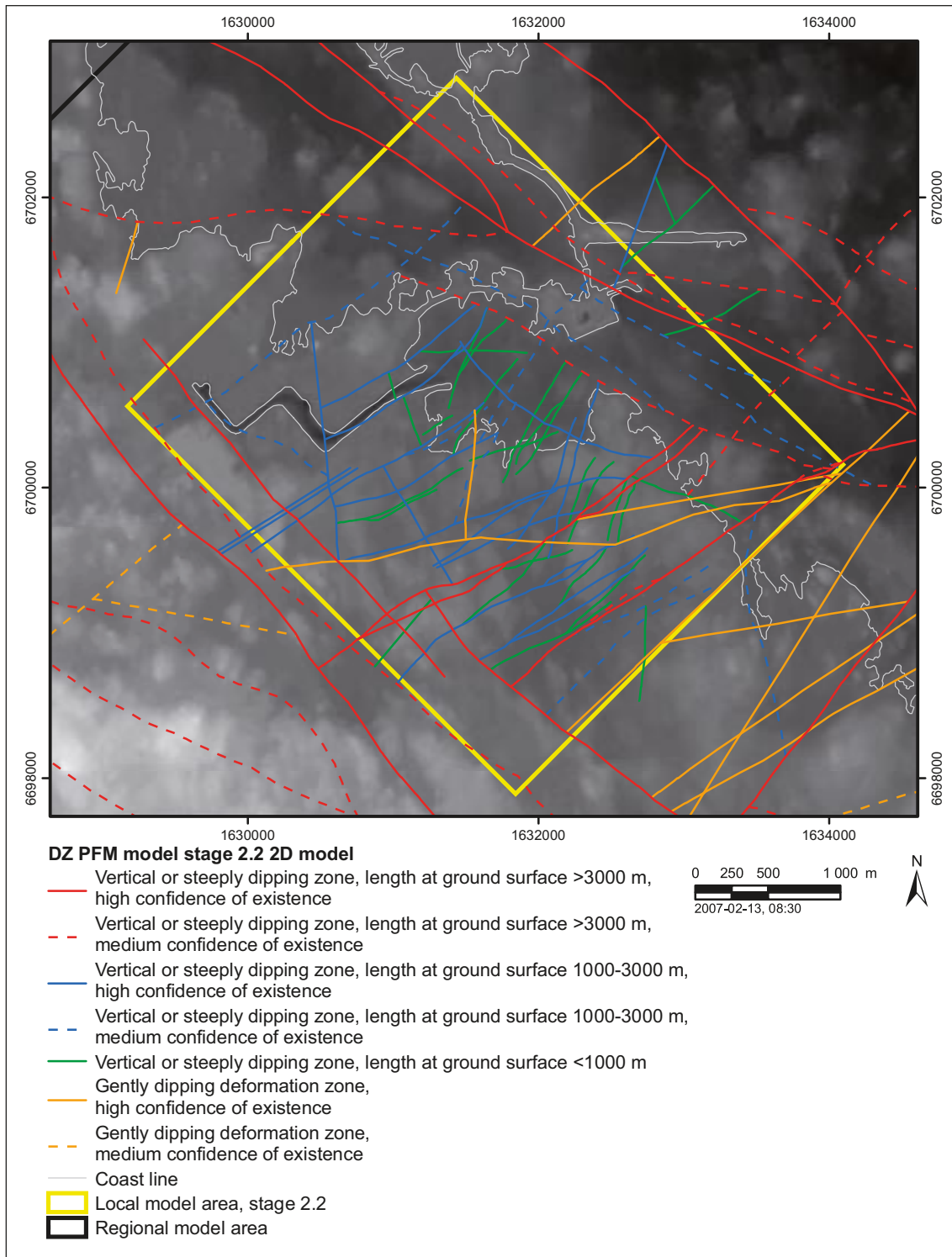


Figure 4-2. Surface intersection of deterministic deformation zones in the local model area, stage 2.2. The background corresponds to the digital elevation model for the site. Coordinates are provided using the RT90 (RAK) system.

4.2 Borehole logs and the results of the single-hole interpretation

Since the identification and description of rock units and especially possible deformation zones in the single-hole interpretations is a key component in the establishment of the fracture domain concept, a selection of the base geological and geophysical data that are used to define these geological entities is shown here. All references to the single-hole interpretation reports are listed in section 3.1. Minor modifications of the single-hole interpretations during the modelling and extended single-hole interpretation work are addressed in section 4.3.

The selected base data have been displayed in a series of WellCad diagrams, one for each cored borehole (Appendix 2). The scale of each borehole figure is identical. One example of a WellCad diagram for the cored borehole KFM07A (Figure 4-3), which is situated in the north-western part of the candidate area (Figure 1-1), is provided here.

The comments below are added to facilitate the reading and understanding of these diagrams:

- As mentioned in section 3.3, sealed fracture networks were not mapped during the first stage of the site investigation programme and are therefore not available for KFM01A, KFM02A, KFM03A and KFM03B.
- As a result of a review of the methodology for mapping aperture, the minimum aperture for open and partly open fractures in KFM02A, KFM03A and KFM03B is 1 mm and not 0.5 mm as for the other cored boreholes, see also section 3.3.
- The fracture frequency for sealed fractures, sealed fracture networks, open crushed and open and partly open fractures is plotted for 1 m of core length. Moving average plots are discussed in section 4.5.

In accordance with the general recommendations in the method description for single-hole interpretation (SKB MD 810.003, version 3.0), rock units (RU) are distinguished in the single-hole interpretation of cored boreholes primarily with the aid of the data sets rock type and rock occurrence, i.e. rock composition. The silicate density, natural gamma radiation and, in some instances, even magnetic susceptibility logs are also used, mainly to check that rock classification has been carried out correctly. One or more rock units extend over the whole length of each borehole and even include the borehole intervals where possible deformation zones have been recognized (Appendix 2).

Outside possible deformation zones, rock units with similar composition are also distinguished on the basis of variations in the frequency of fractures, particularly open and partly open fractures (e.g. rock unit RU1 with a higher frequency of open and partly open fractures and RU2a with a lower frequency in KFM01A, Appendix 2). In a few cases, rock units with similar composition but with a higher degree of ductile deformation (e.g. rock units RU2, RU3a, RU4, RU5 and RU3b in KFM04A) or different grain size (e.g. rock units RU2 and RU3a in KFM05A, Appendix 2) are also distinguished, and, in one minor case, even with a higher degree of static recrystallization (rock units RU2 and RU3 in KFM01D, Appendix 2).

Bedrock geological mapping at the surface recognized the occurrence of Na-K alteration in the granitic rocks close to the margins of and immediately outside the candidate area, in its north-western part /Stephens et al. 2003, 2005/. This alteration affected the granitic rocks prior to and/or during the ductile deformation in the bedrock and is similar to the alteration that has been observed, on a more detailed scale, along the contacts between amphibolite dykes and granitic rocks /Stephens et al. 2005/. Drilling activity, particularly in boreholes KFM06A, KFM06C, KFM08A, KFM08C and KFM09B has confirmed the occurrence of this early-stage alteration at depth, and it is mapped and referred to in Sicada as albitization. It produces a pale grey to whitish, fine-grained rock, in places with isolated knots of biotite and a slightly increased quartz content /Pettersson et al. 2005/. Borehole intersections are of sufficient length that rock units dominated by albitized granitic rock have been identified in all these five boreholes (Appendix 2).

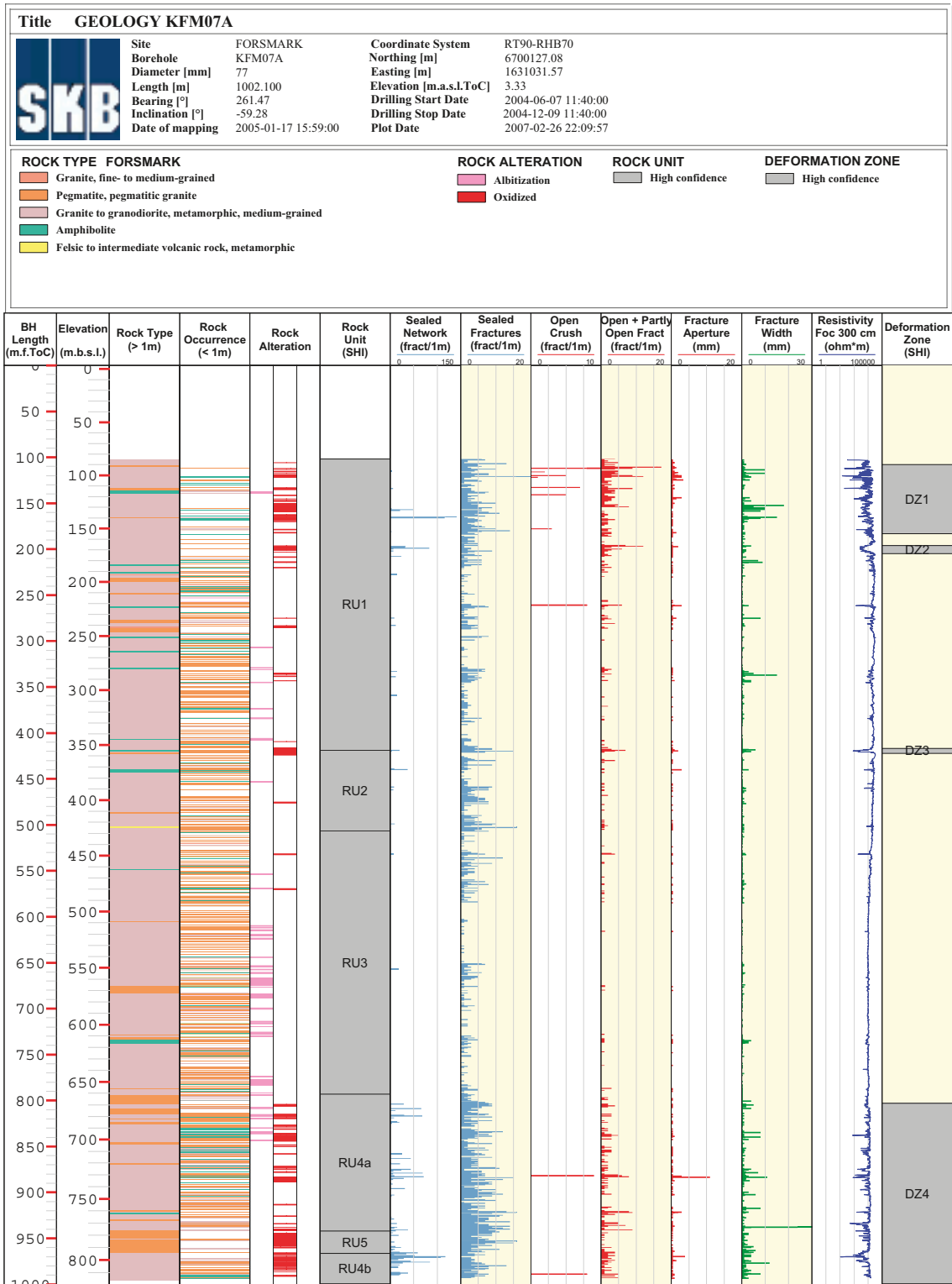


Figure 4-3. Example of a WellCad diagram for the cored borehole KFM07A, showing a selected suite of base geological and geophysical data that have been used to identify rock units and possible deformation zones in the single hole interpretation of this borehole. The identification of rock units follows that recommended in the revised method description for single hole interpretation (SKB MD 810.003, version 3.0).

In accordance with the general recommendations in the method description for single hole interpretation (SKB MD 810.003, version 3.0), possible deformation zones (DZ) are distinguished in the single-hole interpretation of cored boreholes primarily with the aid of the data sets rock alteration, fracture frequency (sealed networks, individual sealed fractures, open crushed zones, and individual open and partly open fractures) and focused resistivity. The type of alteration that is most prominent along the zones is that mapped and referred to in Sicada as oxidation. Other features that also assist in the identification of possible deformation zones include low magnetic susceptibility, which is commonly coincident with the type of alteration referred to as oxidation, and low radar amplitude anomalies in the borehole radar data. The aperture of open and partly open fractures and caliper anomalies are also noted in the description of the possible zones.

With these considerations in mind, the base data that illustrate rock type (> 1 m core length), rock occurrence (< 1 m core length) and the frequency of each type of fracture in consecutive 1 m borehole intervals are selected in each WellCad diagram, in order to illustrate the recognition of rock units in each borehole. Furthermore, the base data that show rock alteration, fracture frequency for each type of fracture, fracture aperture, fracture width, and focused resistivity (300 cm) are selected in each diagram, in order to illustrate the recognition of possible deformation zones in each borehole.

Following an inspection of the diagrams in Appendix 2, and bearing in mind the context of this report, the following features deserve emphasis:

- Rock units that are immediately outside the target volume and are generally affected by strong ductile deformation show an increased frequency of fractures or possible deformation zones. These borehole segments are identified in Table 4-1.
- Rock units outside possible deformation zones but altered by albitization show an increased frequency of fractures, particularly sealed fractures (e.g. borehole KFM06C beneath 337 m below sea level, Appendix 2).
- The two previous points provide further support for the conclusion drawn in the version 1.2 statistical modelling work that fracture intensity is conditioned in part by rock domains /La Pointe et al. 2005/.
- There are rock units outside possible deformation zones in the upper part of several boreholes that show a markedly increased frequency of fractures, particularly open and partly open fractures as well as fractures with larger apertures (e.g. RU1 along KFM01A, Appendix 2). This point is further clarified in section 4.5.
- Rock unit RU2 in KFM07A, which shows an increased frequency of sealed fractures relative to the rock units outside possible deformation zones, both above and below (Figure 4-3), is located directly beneath the possible deformation zone DZ3. It is possible that the increased frequency of fractures within this rock unit is related to this deformation zone. The same phenomenon may be present in, for example, borehole KFM09A, adjacent to the possible deformation zones DZ1 and DZ2 (RU1a, RU2 and RU1b, see Appendix 2), and in borehole KFM09B between the possible deformation zones DZ1 and DZ2 (RU2, RU1b and RU3a, see Appendix 2).
- There is a significant occurrence of sealed fractures, sealed fracture networks and rock alteration (oxidation) along many of the possible deformation zones (e.g. DZ4 along KFM07A, Figure 4-3).
- Relative to the bedrock outside possible deformation zones, there is an increased frequency of open and partly open fractures along many of the zones that are dominated by sealed fractures and sealed fracture networks (e.g. DZ4 along KFM07A, Figure 4-3).
- Some of the possible deformation zones occur along and immediately adjacent to the contacts between rock units. These include, for example, DZ2, DZ3 and DZ5 in KFM03A, which occur in the vicinity of the contact between amphibolite and metagranite (see Appendix 3), and DZ8 in KFM02A which occurs along the contact between metagranite and finer-grained metatonalite (see Appendix 2).

Table 4-1. Borehole segments immediately outside the target volume that, in the single-hole interpretation work, are inferred to contain an increased frequency of fractures or possible deformation zones.

Borehole	Elevation (m.b.s.l.)	Rock unit	Rock domain
KFM04A	2–147	RU2	RFM018
KFM04A	147–420	RU3a, RU4, RU5, RU3b	RFM012
KFM06C	703–776	RU5, RU6	RFM032
KFM07A	657–815	RU4a, RU5, RU4b	RFM044
KFM08A	612–706	RU2, RU3	RFM032
KFM08A	706–753	RU4	RFM034
KFM09A	200–424	RU4, RU5, RU6	RFM044
KFM09A	512–594	RU8	RFM012
KFM09A	594–621	RU9	RFM018

4.3 Modifications of single-hole interpretation in connection with geological modelling and extended single-hole interpretation work

Modifications of the original single-hole interpretation of possible deformation zones have emerged during the modelling work as a result of two approaches:

- A critical reappraisal of the boundaries of all possible deformation zones identified in the original single-hole interpretation.
- An application of the updated instructions for single-hole interpretation with a higher degree of resolution (SKB MB 810.003, version 3.0). Since most of the single-hole interpretations had already been completed when this version of the method description was released during 2006, it was necessary to reassess data and cores in order to identify possible additional deformation zones below the resolution threshold applied during the first stage of the site investigation programme. This is referred to as “extended single-hole interpretation” (ESHI).

In view of the resolution that was applied, the sections identified by extended single-hole interpretation probably correspond to minor deformation zones, since they do not present large intersections in the core. However, since the only information available on these zones comes from boreholes, their extent is difficult to assess.

Based on an assessment of the frequency data for open and partly open fractures as well as the focused resistivity data, changes in the boundaries of two rock units have also been made. These changes concern the base of rock unit RU1 in both KFM01A and KFM01B. On the basis of the same criteria, one new rock unit boundary has been introduced in the upper part of KFM08B.

The revised single-hole interpretations, which include the results of all the changes summarized above, are recorded in the Sicada database under the activity name “extended single hole interpretation” (GE302), and the following files are directly linked to the results of the ESHI process: p_fract_core_ESHI and p_freq_1m_eshi.

A more detailed description of the modifications of the possible deformation zones are presented in the following two sections.

4.3.1 Modifications of possible deformation zones during modelling work

During the geological modelling work, version 1.2 and stage 2.1, a critical reappraisal of the boundaries of all the possible deformation zones intersected in cored boreholes and identified during the single-hole interpretation has been carried out (see, for example, Table 3-3 in /SKB 2006/ for the model stage 2.1). The focus in each reappraisal was on the fracture frequency data for sealed networks, individual sealed fractures, open crushed zones, individual open and partly open fractures and all fractures. Furthermore, the occurrence of the alteration type referred to as oxidation in Sicada was assessed. WellCad diagrams showing data from the geological mapping of the boreholes were also inspected. The same type of analysis has been done for model stage 2.2.

The minor modifications made during the stage 2.2 modelling work, in relation to the original single-hole interpretation, are shown in Table 4-2. This table also provides a comparison of all the possible deformation zones in the single-hole interpretations of cored boreholes with the deformation zones actually modelled geometrically. In summary, the following modifications have been made:

- Modification of one or both of the boundaries of some of the zones defined in the single-hole interpretation, with the result that some zones occupy a slightly longer borehole interval in the modelling work (8 cases).
- Reduction in the extension of some of the zones in the single-hole interpretation, so that only a part (or parts) of the zone in the single-hole interpretation has (have) been modelled geometrically (7 cases).
- Recognition of some new zones for geological modelling that were not identified in the single-hole interpretation (5 cases).
- Recognition of borehole sections that lie adjacent to or are sandwiched between modelled deformation zones and are judged to be affected by a deformation zone (10 cases).

The borehole sections that are affected by, but judged to lie outside deformation zones need to be handled with special attention in geological DFN modelling work (see also section 5.2).

Table 4-2. Comparison of deformation zones (DZ) as inferred from the single-hole interpretation (SHI) of cored boreholes with deformation zones as modelled during stage 2.2.

Borehole	DZ (SHI)	Adjusted SECUP (m)	Adjusted SECLow (m)	Extension or reduction in SHI during modelling work (stage 2.2)	DZ (model stage 2.2)
KFM01A				267–285 m inferred to be a DZ. Not recognized in SHI	ZFMENE1192
KFM01A	DZ2	386	412		ZFMENE1192
KFM01A	DZ3	639	684		ZFMENE2254
KFM01B	DZ1	16	53	53–64 m added	ZFMA2
KFM01B	DZ2	107	135		Possible DZ. Not modelled deterministically
KFM01B	DZ3	415	454		ZFMNNW0404
KFM01C	DZ1	23	48	Fractured rock between 48 and 62 m inferred to be affected by DZ	ZFMA2, ZFMENE2254
KFM01C	DZ2	62	99		ZFMA2
KFM01C	DZ3	235	450	Only borehole intervals 235–252 m and 305–330 m included in the DZ deterministic modelling work. Fractured rock between 252 and 305 m, and 330 and 450 m inferred to be affected by DZ	ZFMENE0060A (235–252 m) / ZFMENE0060C (306–330 m)

Borehole	DZ (SHI)	Adjusted SECUP (m)	Adjusted SECLow (m)	Extension or reduction in SHI during modelling work (stage 2.2)	DZ (model stage 2.2)
KFM01D	DZ1	176	184		Possible DZ. Not modelled deterministically
KFM01D	DZ2	411	421		Possible DZ. Not modelled deterministically
KFM01D	DZ3	488	496		Possible DZ. Not modelled deterministically
KFM01D	DZ4	670	700		ZFMENE0061
KFM01D	DZ5	771	774		Possible DZ. Not modelled deterministically
KFM02A	DZ2	110	122		ZFM866
KFM02A	DZ3	160	184		ZFMA3
KFM02A	DZ4	266	267		ZFM1189
KFM02A	DZ5	303	310		ZFM1189
KFM02A	DZ6	415	520	Divided into two separate zones at 417–442 m and 476–520 m. Fractured rock between 442 and 476 m inferred to be affected by DZ	ZFMA2 (417–442 m) / ZFMF1 (476–520 m)
KFM02A	DZ7	520	600		Possible DZ. Not modelled deterministically
KFM02A	DZ8	893	905		ZFMB4
KFM02A	DZ9	922	925		Possible DZ. Not modelled deterministically
KFM02A	DZ10	976	982		Possible DZ. Not modelled deterministically
KFM03A	DZ1	356	399		ZFMA4
KFM03A	DZ2	448	455		ZFMA7
KFM03A	DZ3	638	646		ZFMB1
KFM03A	DZ4	803	816		ZFMA3
KFM03A	DZ5	942	949		Possible DZ. Not modelled deterministically
KFM03B	DZ1	24	42		ZFMA5
KFM03B	DZ2	62	67		Possible DZ. Not modelled deterministically
KFM04A	DZ1	169	176	110–169 m added	ZFMNW1200
KFM04A	DZ2	202	213	213–232 m added. DZ2 and DZ3 merged	ZFMA2
KFM04A	DZ3	232	242		ZFMA2
KFM04A				290–370 m inferred to be a DZ. Not recognized in SHI	ZFMNE1188
KFM04A	DZ4	412	462		ZFMNE1188
KFM04A	DZ5	654	661		ZFMWNW0123
KFM05A	DZ1	102	114		ZFMA2
KFM05A	DZ2	416	436	395–416 m added	ZFMENE2282
KFM05A	DZ3	590	796	Only borehole intervals 590–616 m and 685–720 m included in the DZ deterministic modelling work. Fractured rock between 616 and 685 m, and 720 and 796 m inferred to be affected by DZ	ZFMENE0401A (685–720 m) / ZFMENE0401B (590–616 m)
KFM05A	DZ4	892	916		ZFMENE0103
KFM05A	DZ5	936	950	950–992 m added	ZFMENE2383
KFM06A	DZ1	126	148	Only borehole interval 128–146 m included in the DZ deterministic modelling work	Possible DZ. Not modelled deterministically

Borehole	DZ (SHI)	Adjusted SECUP (m)	Adjusted SECLow (m)	Extension or reduction in SHI during modelling work (stage 2.2)	DZ (model stage 2.2)
KFM06A	DZ2	195	245	245–260 m added. DZ2 and DZ3 merged	ZFMENE060B
KFM06A	DZ3	260	278		ZFMENE060B
KFM06A	DZ4	318	358		ZFMENE0060A, ZFMB7
KFM06A				518–545 m inferred to be a DZ. Not recognized in SHI	ZFMNNE2273
KFM06A	DZ5	619	624		ZFMNNE2255
KFM06A	DZ6	652	656		Possible DZ. Not modelled deterministically
KFM06A	DZ7	740	775		ZFMNNE0725
KFM06A	DZ8	788	810		ZFMENE0061
KFM06A	DZ9	882	905		Possible DZ. Not modelled deterministically. Lies close to and fracture data resemble ZFMENE0061
KFM06A	DZ10	925	933		Possible DZ. Not modelled deterministically. Lies close to and fracture data resemble ZFMNNE2280
KFM06A	DZ11	950	990		ZFMNNE2280
KFM06B	DZ1	55	93		ZFMA8
KFM06C	DZ1	102	169		Possible DZ. Not modelled deterministically
KFM06C				283–306 m inferred to be a DZ. Not recognized in SHI	ZFMNNE2008
KFM06C	DZ2	359	400		ZFMB7
KFM06C	DZ3	415	489		ZFMNNE2263
KFM06C	DZ4	502	555		ZFMWNW0044
KFM06C	DZ5	623	677		Possible DZ. Not modelled deterministically
KFM07A	DZ1	108	183	183–185 m added	ZFM1203. ZFMNNW0404
KFM07A	DZ2	196	205		Possible DZ. Not modelled deterministically
KFM07A	DZ3	417	422	Fractured rock beneath DZ3, between 422 and 507 m, inferred to be affected by DZ	ZFMENE0159A
KFM07A	DZ4	803	999	Divided into three separate zones at 803–840 m, 857–897 m and 920–999 m. Fractured rock between these modelled zones inferred to be affected by DZ	ZFMENE1208A (857–897 m) / ZFMENE1208B (803–840 m) / ZFMNS0100 (920–999 m). Interference also with ZFMB8 along 920–999 m
KFM07B	DZ1	51	58		Possible DZ. Not modelled deterministically
KFM07B	DZ2	93	102		ZFM1203
KFM07B	DZ3	119	125		Possible DZ. Not modelled deterministically
KFM07B	DZ4	225	245		ZFMENE2320
KFM07C	DZ1	92	103		ZFM1203
KFM07C	DZ2	308	388		ZFMENE2320
KFM07C	DZ3	429	439		ZFMENE2320
KFM08A	DZ1	172	342	Only borehole interval 244–315 m included in the DZ deterministic modelling work. Fractured rock between 172 and 244 m, and 315 and 342 m inferred to be affected by DZ	ZFMENE1061A

Borehole	DZ (SHI)	Adjusted SECUP (m)	Adjusted SECLOW (m)	Extension or reduction in SHI during modelling work (stage 2.2)	DZ (model stage 2.2)
KFM08A	DZ2	479	496		ZFMNNW1204
KFM08A	DZ3	528	557		Possible DZ. Not modelled deterministically. Possibly related to ZFMNNW1204
KFM08A	DZ4	672	693		Possible DZ. Not modelled deterministically
KFM08A	DZ5	775	840	840–843 m added	ZFMENE2248
KFM08A	DZ6	915	946		Possible DZ. Not modelled deterministically. High frequency of fractures along and close to rock domain boundary RFM032–RFM034. Fine-grained rocks in RFM032
KFM08A	DZ7	967	976		Possible DZ. Not modelled deterministically. High frequency of fractures in RFM034
KFM08B	DZ1	133	140		ZFMNNW1205
KFM08B	DZ2	167	185		ZFMNNW1205
KFM08C	DZ1	161	191		Possible DZ. Not modelled deterministically
KFM08C	DZ2	419	542		ZFMNNE2312
KFM08C	DZ3	673	705		ZFMWNW2255
KFM08C	DZ4	829	832		ZFMENE1061A, ZFNENE1061B
KFM08C	DZ5	946	949		ZFMENE1061A
KFM09A	DZ1	15	40		ZFMENE1208A
KFM09A	DZ2	86	116	Fractured rock between 8 and 15 m, 40 and 86 m, and 116 and 124 m inferred to be affected by DZ	ZFMENE1208B
KFM09A	DZ3	217	280		ZFMENE0159A, ZFMNNW0100
KFM09A	DZ4	723	754	Fractured rock between 754 and 770 m inferred to be affected by DZ	ZFMNW1200
KFM09A	DZ5	770	790		ZFMNW1200
KFM09B	DZ1	9	132	Only borehole intervals 9–43 m, 59–78 m and 106–132 m included in the DZ deterministic modelling work. Fractured rock between these modelled zones and between 132 and 308 m inferred to be affected by DZ	ZFMENE1208A (9–43 m) / ZFMENE1208B (59–78 m) / ZFMENE0159A (106–132 m)
KFM09B	DZ2	308	340		Possible DZ. Not modelled deterministically
KFM09B	DZ3	363	413		ZFMENE2320
KFM09B	DZ4	520	550		ZFMENE2325A
KFM09B	DZ5	561	574		ZFMENE2325B
KFM10A	DZ1	62.85	145		ZFMWNW0123
KFM10A				275–284 m inferred to be a DZ. Not recognized in SHI.	ZFMENE2403
KFM10A	DZ2	430	449		ZFMA2
KFM10A	DZ3	478	490		ZFMA2

4.3.2 Additional possible deformation zones identified by the extended single-hole interpretation

The following information was used to delineate additional possible deformation zones in the extended single-hole interpretation (ESHI):

- One metre fracture frequency data, p_freq_1m, Sicada_06_164. The cored borehole KFM07C, for which data was not available by the date of the data freeze 2.2, could not be included in the study.
- WellCad diagrams that show lithology, fracture frequency and geophysical data.
- BIPS images, data logs and photographs of the cores.

This study was conducted in four steps. An initial selection of borehole intervals was done after a study of frequency plots for open and sealed fractures in each borehole. Subsequently, the Wellcad images for the candidate sections were analyzed in detail to see if they could help to confirm or reject the identified sections as additional possible deformation zones. Then the BIPS images of the cores were also analyzed alongside the BOREMAP data file in order to examine the spatial relationship of fractures to other geologic structures in the rock and to each other. Finally, the fourth step involved an inspection of the borehole cores for the remaining candidates. The methodology used in this study, as well as the different candidates with descriptions, are presented in detail in /Fox and Hermanson 2006/.

On the basis of a study of all cored boreholes available at data freeze 2.2 (except KFM07C), seven additional possible deformation zones, which are inferred to be minor zones, were identified. The relevant borehole sections are listed in Table 4-3. A confidence rating from 1 to 3 is assigned, 3 referring to high confidence in existence. None of these zones have been modelled deterministically.

The ESHI study is not a review of the standard, single-hole interpretation work, nor does it cast doubts on the boundaries of potential deformation zones identified in this interpretation. Indeed, the “initial” threshold resolution of the single-hole interpretation did not permit the identification of certain sections of the core as possible deformation zones. Furthermore, some sections identified during the initial part of the ESHI study were also reinterpreted during the modelling process (section 4.3.1), and are currently included as deformation zones in the deterministic geological model. Other sections that were identified in the ESHI study had also been pointed out due to specific characteristics of the bedrock. Since the ESHI study was completed independently of the standard single-hole interpretation work at the site (section 4.2) and the reappraisal during the ongoing modelling work (section 4.3.1), the results of this study provide an increased confidence in the results of the earlier work.

Table 4-3. Additional possible deformation zones identified along cored boreholes at Forsmark by ESHI /Fox and Hermanson 2006/.

Borehole	Adjusted SECUP (m)	Adjusted SECLOW (m)	Level of confidence
KFM01A	216.4	223.9	3
KFM01B	223.65	225.1	3
KFM01C	121.15	123.5	3
KFM04A	953.2	955.8	2
KFM08A	623.6	624.14	2
KFM09A	666.1	667.3	3
KFM09B	283.6	284.1	3

4.4 Identification of vuggy rock in connection with quartz dissolution

One of the anomalies that has been recognised in the bedrock at the Forsmark site concerns the occurrence of vuggy rock, which is associated with a type of alteration mapped and recorded in Sicada as quartz dissolution (Figure 4-4). The occurrences of vuggy rock also show a red staining that is related to the development of a fine-grained hematite dissemination, typical of the alteration mapped and referred to in Sicada as oxidation. Besides alteration, several features in the geophysical logs indicate the occurrence of vuggy rock in the boreholes. These include a decrease in silicate density, resistivity and magnetic susceptibility, an increase in porosity /SKB 2005a, p 190/, and locally, an increase in natural gamma radiation. Vuggy rock was recognized for the first time in KFM02A, where it was the focus of a special study /Möller et al. 2004/.

The intervals of vuggy rock detected in the boreholes are shown in Table 4-4. Several intervals recorded in Sicada occur close to each other and are separated, for example, solely on the basis of the intensity of the alteration. The most spectacular borehole section, in terms of both length and intensity of alteration, is the section between 272.9 m (264.8 m below sea level) and 299.5 m (291.3 m below sea level) in borehole KFM02A. On the basis of these observations, sixteen geologically separate occurrences are inferred to be present (Table 4-4).

Virtually all the occurrences of vuggy rock occur within or immediately adjacent to possible deformation zones in the single-hole interpretations and along the zones modelled deterministically in model stage 2.2 (Table 4-4). Notable exceptions occur along two borehole intervals, 409.9 m (337.9 m below sea level) to 412.0 m (339.7 m below sea level) in KFM08A and 511.8 m (415.7 m below sea level) to 520.0 m (422.0 m below sea level) in KFM09A. On the basis of this strong correlation, it is inferred that the occurrences of vuggy rock represent channels within deformation zones along which, at some time (or times) during geological history, aggressive hydrothermal fluids have moved and affected the quartz content in the bedrock. The occurrences within inferred zones are commonly found close to one side of the zone, implying that the quartz dissolution event is a reactivation of an older geological structure in the bedrock. Bearing in mind the special characteristics of the vuggy rock, not least the high porosity values, the borehole intervals located outside deformation zones should be handled with special attention in geological DFN modelling work (see also section 5.2).

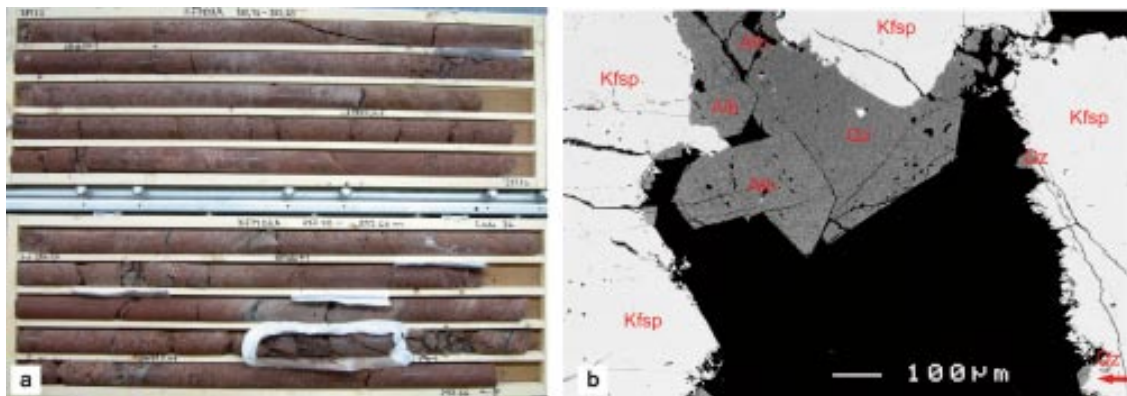


Figure 4-4. a) Strongly altered and vuggy metagranite in borehole KFM02A. The incoherent section (in plastic casing) is a strongly altered amphibolite that has been modified to a rock composed of chlorite, albite, hematite, Ti-oxide and quartz. b) Back-scatter electron (BSE) image that shows euheedral crystals of albite and quartz (medium grey) on a vug wall (black = cavity). The thin rims on K-feldspar grains (light grey) along the vug walls are irregular fringes of K-feldspar (resorbed grains) and small, euheedral crystals of albite and quartz. Scale bar is 0.1 mm. Figure taken from /SKB 2005a/.

Table 4-4. Occurrence of altered vuggy rock in the boreholes, and spatial relationship to possible deformation zones (DZ) in the single-hole interpretation (SHI) and modelled deformation zones, stage 2.2 (ZFMxx).

Occurrence	Borehole	Adjusted SECUP (m)	Adjusted SECLow (m)	Alteration type	Intensity	DZ (SHI) / DZ (model stage 2.2)
1	KFM02A	171.4017	172.0464	Quartz dissolution	Medium	Inside DZ3 / ZFMA3
1	KFM02A	174.3257	174.6049	Quartz dissolution	Medium	Inside DZ3 / ZFMA3
1	KFM02A	174.6069	175.1762	Quartz dissolution	Weak	Inside DZ3 / ZFMA3
1	KFM02A	175.1792	175.2756	Quartz dissolution	Medium	Inside DZ3 / ZFMA3
1	KFM02A	176.9033	177.0077	Quartz dissolution	Faint	Inside DZ3 / ZFMA3
1	KFM02A	179.4226	180.0532	Quartz dissolution	Medium	Inside DZ3 / ZFMA3
2	KFM02A	247.8602	248.2394	Quartz dissolution	Faint	Above DZ4 / ZFM1189
2	KFM02A	248.8501	264.6114	Quartz dissolution	Weak	Above DZ4 / ZFM1189
2	KFM02A	264.6143	266.0617	Quartz dissolution	Medium	Above DZ4 / ZFM1189
2	KFM02A	266.0638	272.9400	Quartz dissolution	Weak	DZ4 and above DZ5 / ZFM1189
2	KFM02A	272.9420	274.9207	Quartz dissolution	Medium	Above DZ5 / ZFM1189
2	KFM02A	274.9238	276.6634	Quartz dissolution	Strong	Above DZ5 / ZFM1189
2	KFM02A	276.6664	279.6094	Quartz dissolution	Medium	Above DZ5 / ZFM1189
2	KFM02A	279.6124	283.1108	Quartz dissolution	Strong	Above DZ5 / ZFM1189
2	KFM02A	283.1138	283.4965	Quartz dissolution	Medium	Above DZ5 / ZFM1189
2	KFM02A	283.4985	284.3242	Quartz dissolution	Strong	Above DZ5 / ZFM1189
2	KFM02A	284.3262	284.8857	Quartz dissolution	Weak	Above DZ5 / ZFM1189
2	KFM02A	284.8867	296.5319	Quartz dissolution	Strong	Above DZ5 / ZFM1189
2	KFM02A	298.8883	299.0470	Quartz dissolution	Strong	Above DZ5 / ZFM1189
2	KFM02A	299.2398	299.5151	Quartz dissolution	Strong	Above DZ5 / ZFM1189
2	KFM02A	301.6063	301.7067	Quartz dissolution	Weak	Above DZ5 / ZFM1189
3	KFM06A	332.4962	332.7465	Quartz dissolution	Medium	Inside DZ4 / ZFME-NE0060A, ZFMB7
4	KFM06A	610.6420	611.0861	Quartz dissolution	Weak	Above DZ5 / ZFMNNE2255
5	KFM06A	770.8406	770.8858	Quartz dissolution	Weak	Inside DZ7 / ZFMNNE0725
6	KFM06B	66.5638	66.9108	Quartz dissolution	Weak	Inside DZ1 / ZFMA8
6	KFM06B	68.6588	69.0540	Quartz dissolution	Medium	Inside DZ1 / ZFMA8
6	KFM06B	69.0570	70.1661	Quartz dissolution	Weak	Inside DZ1 / ZFMA8
7	KFM06C	451.4576	452.2256	Quartz dissolution	Strong	Inside DZ3 / ZFMNNE2263
8	KFM08A	409.8545	412.0399	Quartz dissolution	Strong	No DZ recognized in the SHI
9	KFM08C	454.9640	458.2870	Quartz dissolution	Medium	Inside DZ2 / ZFMNNE2312
9	KFM08C	462.0960	462.2760	Quartz dissolution	Faint	Inside DZ2 / ZFMNNE2312
9	KFM08C	462.2790	462.4950	Quartz dissolution	Medium	Inside DZ2 / ZFMNNE2312
10	KFM08C	497.8410	497.9030	Quartz dissolution	Weak	Inside DZ2 / ZFMNNE2312
10	KFM08C	497.9040	498.9950	Quartz dissolution	Strong	Inside DZ2 / ZFMNNE2312
11	KFM08C	511.6210	511.6410	Quartz dissolution	Faint	Inside DZ2 / ZFMNNE2312

Occurrence	Borehole	Adjusted SECUP (m)	Adjusted SECLOW (m)	Alteration type	Intensity	DZ (SHI) / DZ (model stage 2.2)
11	KFM08C	512.8850	512.9310	Quartz dissolution	Faint	Inside DZ2 / ZFMNNE2312
11	KFM08C	517.2170	517.2880	Quartz dissolution	Faint	Inside DZ2 / ZFMNNE2312
11	KFM08C	519.1460	519.9780	Quartz dissolution	Medium	Inside DZ2 / ZFMNNE2312
11	KFM08C	520.4340	520.7890	Quartz dissolution	Weak	Inside DZ2 / ZFMNNE2312
11	KFM08C	523.1160	523.4460	Quartz dissolution	Weak	Inside DZ2 / ZFMNNE2312
11	KFM08C	523.4510	525.7750	Quartz dissolution	Medium	Inside DZ2 / ZFMNNE2312
11	KFM08C	526.2380	526.4410	Quartz dissolution	Weak	Inside DZ2 / ZFMNNE2312
11	KFM08C	531.5300	531.7940	Quartz dissolution	Medium	Inside DZ2 / ZFMNNE2312
12	KFM09A	511.7505	513.9343	Quartz dissolution	Faint	No DZ recognized in the SHI. Boundary between rock units RU5 and RU7
12	KFM09A	513.9343	515.4333	Quartz dissolution	Weak	No DZ recognized in the SHI. Boundary between rock units RU5 and RU7
12	KFM09A	515.4344	515.7068	Quartz dissolution	Medium	No DZ recognized in the SHI. Boundary between rock units RU5 and RU7
12	KFM09A	515.7068	520.0322	Quartz dissolution	Weak	No DZ recognized in the SHI. Boundary between rock units RU5 and RU7
13	KFM09B	382.3123	382.3254	Quartz dissolution	Weak	Inside DZ3 / ZFMENE2320
14	KFM09B	568.9249	569.3978	Quartz dissolution	Weak	Inside DZ5 / ZFMENE2325B
14	KFM09B	569.3998	572.6340	Quartz dissolution	Medium	Inside DZ5 / ZFMENE2325B
14	KFM09B	572.6360	573.4531	Quartz dissolution	Weak	Inside DZ5 / ZFMENE2325B
15	KFM10A	86.9287	88.7894	Quartz dissolution	Weak	Inside DZ1 / ZFMWNW0123
15	KFM10A	89.3205	89.9060	Quartz dissolution	Weak	Inside DZ1 / ZFMWNW0123
15	KFM10A	92.6009	93.0834	Quartz dissolution	Faint	Inside DZ1 / ZFMWNW0123
15	KFM10A	93.0864	94.2436	Quartz dissolution	Weak	Inside DZ1 / ZFMWNW0123
15	KFM10A	96.6878	97.4517	Quartz dissolution	Weak	Inside DZ1 / ZFMWNW0123
15	KFM10A	98.7714	98.9686	Quartz dissolution	Faint	Inside DZ1 / ZFMWNW0123
15	KFM10A	98.9706	99.8841	Quartz dissolution	Weak	Inside DZ1 / ZFMWNW0123
15	KFM10A	99.8851	100.3489	Quartz dissolution	Medium	Inside DZ1 / ZFMWNW0123
15	KFM10A	100.3509	101.0936	Quartz dissolution	Weak	Inside DZ1 / ZFMWNW0123
15	KFM10A	104.0204	104.7111	Quartz dissolution	Faint	Inside DZ1 / ZFMWNW0123

Occurrence	Borehole	Adjusted SECUP (m)	Adjusted SECLow (m)	Alteration type	Intensity	DZ (SHI) / DZ (model stage 2.2)
15	KFM10A	104.9550	105.4848	Quartz dissolution	Faint	Inside DZ1 / ZFMWNW0123
15	KFM10A	111.4764	111.5854	Quartz dissolution	Faint	Inside DZ1 / ZFMWNW0123
15	KFM10A	111.5874	114.6291	Quartz dissolution	Weak	Inside DZ1 / ZFMWNW0123
15	KFM10A	114.6341	118.5576	Quartz dissolution	Faint	Inside DZ1 / ZFMWNW0123
16	KFM10A	483.5521	487.7752	Quartz dissolution	Faint	Inside DZ3 / ZFMA2

4.5 Fracture frequency distribution in each borehole

The variation in the frequency of different types of fractures at depth is shown for each cored borehole in Appendix 3. These diagrams have been designed to provide an initial assessment of significant variations in fracture frequency in the bedrock outside the influence of geological anomalies such as deformation zones.

The boundaries of the deformation zones modelled during stage 2.2 (section 4.3.1), as well as additional possible deformation zones recognized during the extended single-hole interpretation work, are shown on both the fracture frequency and cumulative frequency plots. These zones can be compared with the boundaries of possible deformation zones that were recognized in the original single-hole interpretation work. The latter are shown in the middle part of each figure. The rapid increase in predominantly sealed fractures over short elevation intervals corresponds to deformation zones.

Since the focus in the statistical modelling work is on the bedrock inside the target volume, the patterns along the borehole intervals inside the marginal rock domains RFM012, RFM018, RFM032 and RFM044 are not addressed further in this section (see also section 5.1). As indicated earlier (point 1 at the end of section 4.2), these domains are generally affected by strong ductile deformation and also show an increased frequency of fractures or possible deformation zones.

Contrasting modes of variation for fracture frequency in the cored boreholes KFM01A and KFM03A were recognized in model version 1.2 /SKB 2005a/. In the context of this report, this observation once again merits special focus.

In borehole KFM01A, there is a marked concentration of open and partly open fractures down to c 200 m below sea level (Figure 4-5). With the exception of the inferred deformation zones, the sealed fractures appear to be more regularly distributed along the borehole. Nevertheless, there is also some tendency towards a concentration of these fractures in the upper part. The patterns in particularly boreholes KFM01D, KFM05A, KFM07B and KFM07C are similar (Appendix 3). Borehole KFM06B, the uppermost part of borehole KFM06A, and down to c 40 m below sea level in borehole KFM08B also contain an abundance of open and partly open fractures, occasional fractures with apertures up to or greater than 5 mm, some minor crush zones and, in KFM08B, generally lower resistivity values (Appendix 2).

Compared to KFM01A, borehole KFM03A shows a distinctly different mode of variation. With the exception of the inferred deformation zones, both the open and partly open fractures as well as the sealed fractures are distributed far more regularly at depth along this borehole (Figure 4-6). The patterns in borehole KFM08C and, after taking account of the occurrence of deformation zones, even in boreholes KFM02A and KFM08A resemble that in KFM03A (Appendix 3).

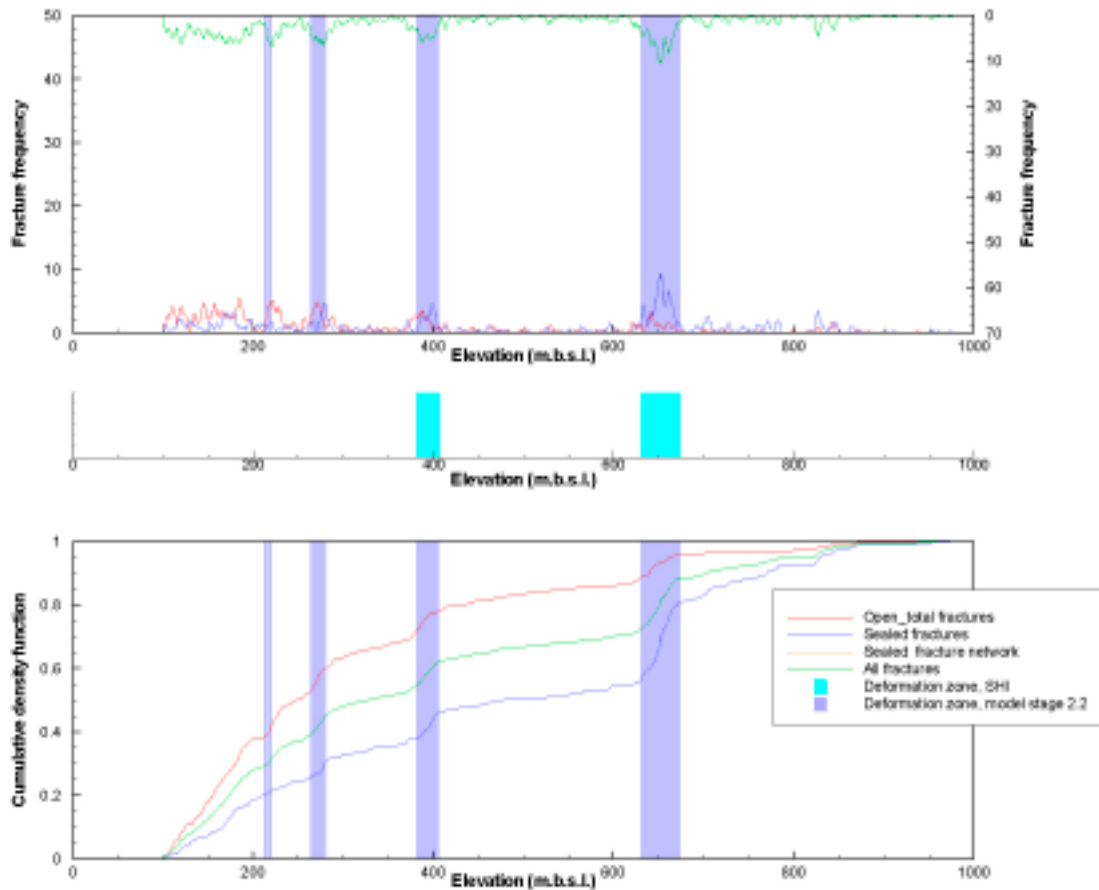


Figure 4-5. Fracture frequency diagrams for the cored borehole KFM01A. The upper diagram is a moving average plot with a 5 m window and 1 m steps, while the lower diagram is a cumulative frequency plot. The scale for all fractures is given to the right in the upper diagram. The deformation zones modelled during stage 2.2, as well as additional possible zones recognized during the extended single-hole interpretation work, are marked on both diagrams. Possible deformation zones, as defined in the single-hole interpretation, are shown for the purpose of comparison in the middle part of the figure.

The above features are illustrated in quantitative terms by again comparing boreholes KFM01A and KFM03A, which both extend downwards to approximately 1,000 m depth. In KFM01A, approximately 40% of all the open and partly open fractures are concentrated in the upper 200 m (Figure 4-5), while in KFM03A less than 10% of all the open and partly open fractures occur above 200 m depth and about 60% above 600 m (Figure 4-6).

On the basis of the observations described above, it is inferred that the north-western and south-eastern parts of the candidate volume differ from each other, particularly in terms of the variation in the frequency of open and partly open fractures down to approximately 1,000 m depth. Furthermore, the boundary between bedrock with an anomalously high frequency of open and partly open fractures (upper part), and bedrock with predominantly sealed fractures (lower part) is not found at the same depth along the boreholes inside the target volume. This depth varies between c 40 m below sea level (KFM08B) and c 200 m below sea level (e.g. KFM01A).

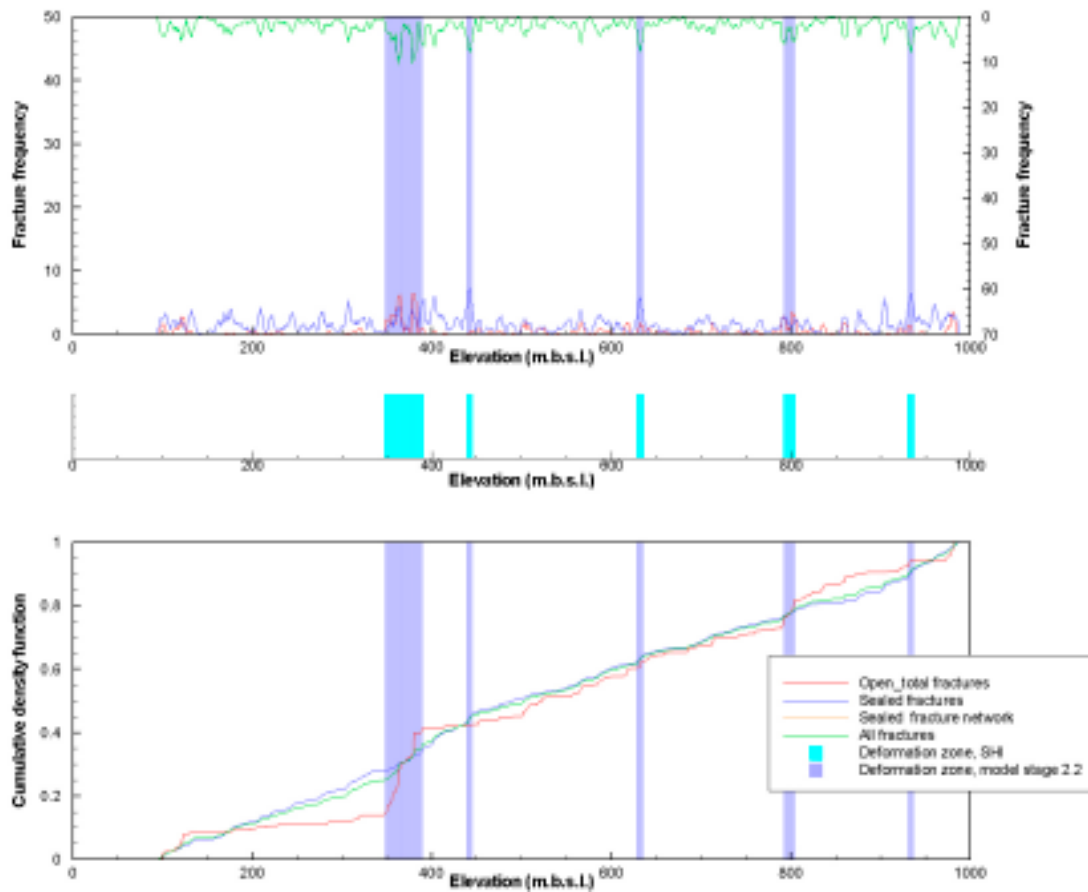


Figure 4-6. Fracture frequency diagrams for the cored borehole KFM03A. The upper diagram is a moving average plot with a 5 m window and 1 m steps, while the lower diagram is a cumulative frequency plot. The scale for all fractures is given to the right in the upper diagram. The deformation zones modelled during stage 2.2 (section 4.3.1) are marked on both diagrams. Possible deformation zones, as defined in the single-hole interpretation, are shown for the purpose of comparison in the middle part of the figure.

5 Fracture domain concept

5.1 Presentation of the fracture domain concept

Deterministic geological modelling at the Forsmark site has so far been concerned with rock domains – which are identified on the basis of variations in rock composition, rock grain size, compositional homogeneity and character of ductile deformation – and deformation zones, along which there is a concentration of strain in the bedrock /SKB 2004, 2005a, 2006/. There is also a need for identification and conceptual understanding of fracture domains at the site, bearing in mind the results of the single-hole interpretation work and the earlier statistical modelling of fractures /La Pointe et al. 2005/.

Prior to any definition of fracture domains, it is necessary to identify deformation zones. For this reason, the following is excluded from fracture domains:

- All deformation zones that have been modelled geometrically during stage 2.2 in RVS. These intervals are referred to as “Modelled DZ” and are provided with a ZFM identification code in Table 5-1 below.
- The possible deformation zones identified in the single-hole interpretation work, which have not been modelled geometrically in RVS. These intervals are referred to as “DZ not modelled” and are identified as “Possible DZ” in Table 5-1 below.
- All the additional, possible minor deformation zones that have been recognized in connection with the renewed appraisal of the cored borehole data (see section 4.3.2). These intervals have not been modelled geometrically in RVS. They are also referred to as “DZ not modelled” and are identified as “Possible DZ” in Table 5-1 below.

The following three considerations control the identification and conceptual understanding of fracture domains at the Forsmark site.

1. Firstly, there is a significant contrast in both the degree and character of the ductile strain and, to a large extent, the compositional homogeneity in the rock domains that form the margins of the target volume on the north-west, north-east and south-west, compared to the rock domains inside the target volume /SKB 2004, 2005a, 2006/. It is suggested that this contrast motivates the inclusion of the former in separate fracture domains. This strategy is also supported by the results of the statistical modelling of fractures during model version 1.2 /La Pointe et al. 2005/.

Tectonic foliation and rock boundaries in the marginal rock domains RFM012 and RFM018, along the south-western margin, show a consistent orientation with steep dips to the south-west. Similar structures in the marginal domains RFM044 and RFM032, which define the north-western and north-eastern margins, are folded. Domain RFM032, in particular, also contains a conspicuous proportion of fine-grained, felsic meta-igneous rocks, and it is anticipated that the size and intensity of fractures in such rock may differ from that in coarser-grained rock. On the basis of these rock domain characteristics, two separate fracture domains are proposed corresponding to the combined rock domains RFM012 and RFM018 and the combined rock domains RFM032 and RFM044.

2. Secondly, there is a marked contrast in the fracture frequency distribution patterns between the boreholes in the north-western and south-eastern parts of the candidate volume. It is suggested that this feature is essentially related to the corresponding contrast in the frequency of gently-dipping deformation zones, with their relatively high frequency of open and partly open fractures, between the two sub-volumes (see below). Since such zones are far less frequent beneath the combined zones ZFMA2 and ZFMF1, which merge together south-east of drill site 2, different fracture domains are anticipated above and beneath these zones.

The fracture frequency distribution patterns also show that the bedrock beneath zone ZFMA2 displays different fracture characteristics close to the surface and at depth. This feature motivates separate fracture domains at different depths beneath this zone.

3. Finally, a subordinate rock domain inside the target volume is dominated by fine-grained, altered (albitized) granitic rock (RFM045). This domain was described for the first time in model stage 2.1 and its presence has been confirmed by the new boreholes analyzed for the first time in the present modelling work. It is judged that both the finer grain size and the somewhat higher quartz content of this rock, as compared to unaltered granitic rock, may be significant for fracture characterization. For this reason, this rock domain is also identified as a separate fracture domain.

The above considerations provide the basis for a conceptual model for fracture domains at the site. Six separate domains are recognized and serve as a basis for the ensuing statistical modelling work. In the short descriptions below, attention is focussed on the fracture domains inside the target volume. Two simplified NW-SE cross-sections along the candidate volume are included here (Figure 5-1), in order to clarify the conceptual understanding of fracture domains FFM01, FFM02, FFM03 and FFM06:

Fracture domain FFM01: This domain is situated within rock domain RFM029 inside the target volume. It lies beneath the gently dipping or sub-horizontal zones ZFMA2, ZFMA3 and ZFMF1 (Figure 5-1) and north-west of the steeply dipping zone ZFMNE0065, at a depth that varies from greater than c 40 m below sea level (large distance from ZFMA2) to greater than c 200 m

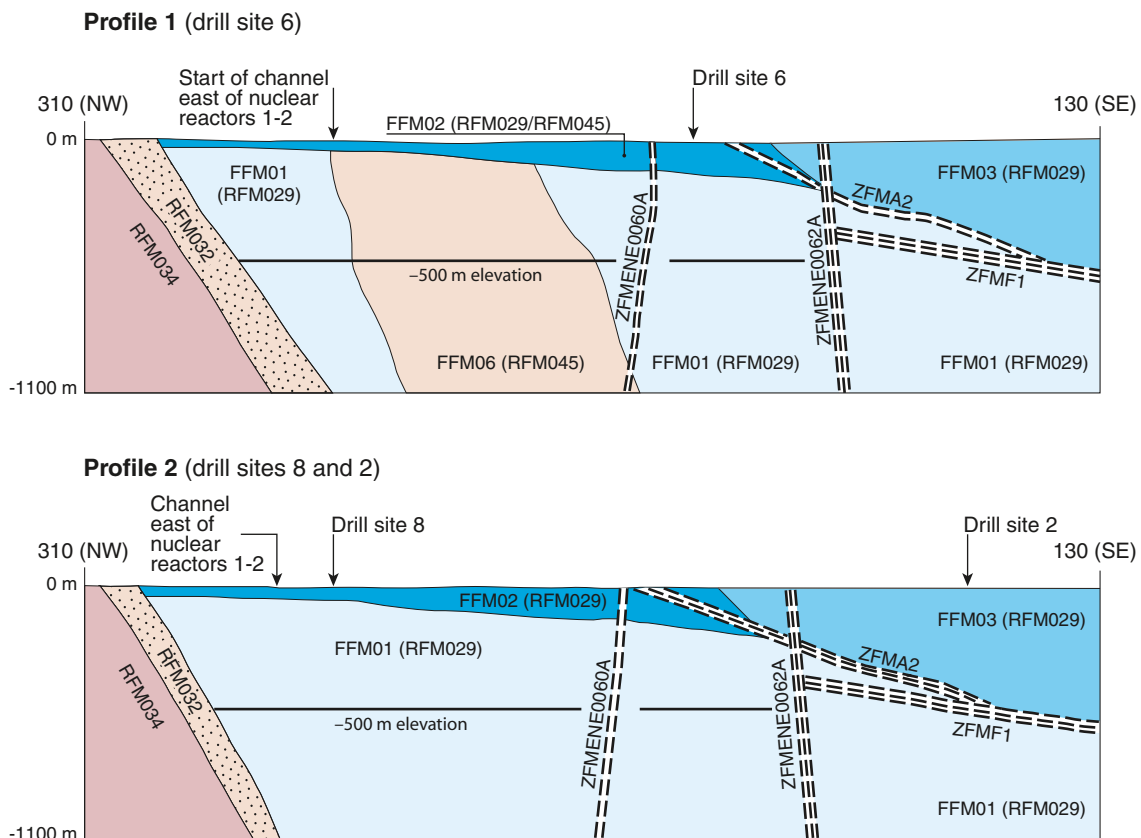


Figure 5-1. Simplified profiles in a NW-SE direction (310°–130°) that pass through drill sites 2 and 8 (lower profile) and drill site 6 (upper profile). The labelled fracture domains (FFM01, FFM02, FFM03 and FFM06) occur inside rock domains RFM029 and RFM045. Only the high confidence deformation zones ZFMA2 (gently dipping), ZFMF1 (sub-horizontal), ZFMENE0060A (steeply dipping, longer than 3,000 m) and ZFMENE0062A (steeply dipping, longer than 3,000 m) are included in the profiles. Note the increased depth of fracture domain FFM02 as zone ZFMA2 is approached in the footwall to the zone, and the occurrence of this domain close to the surface directly above ZFMA2.

below sea level (close to ZFMA2). Relative to the overlying fracture domain FFM02, the bedrock in this domain shows a lower frequency of particularly open and partly open fractures. Gently dipping or sub-horizontal deformation zones are not common inside this domain. In particular, they have not been recognized in the critical depth interval 400–500 m in the north-western part of this domain. It has been suggested that high in situ rock stresses have been able to accumulate inside this volume at one or more times during geological history, in connection with, for example, sedimentary loading processes /SKB 2006, section 3.2.2, p 121–126/.

Fracture domain FFM02: This domain is situated close to the surface inside the target volume, directly above fracture domain FFM01 (Figure 5-1). The domain is characterized by a complex network of gently dipping and sub-horizontal, open and partly open fractures, which are known to merge into at least one deformation zone beneath drill site 7.

It is apparent that geometric modelling must take into account the fact that the transition from more fractured bedrock close to the surface (FFM02) to less fractured bedrock at depth (FFM01) takes place deeper down as the distance from zone ZFMA2 decreases. Thus, the special character of the proposed surface fracture domain FFM02 is not solely determined by elevation. The occurrence of this domain at greater depths beneath ZFMA2 at drill sites 1, 5 and 6, and even above this zone at or close to drill sites 5 and 6, is related to an inferred higher frequency of such older fractures in the vicinity of this zone, to higher rock stresses beneath zone ZFMA2 or to a combination of these two possibilities. The gently dipping and sub-horizontal fractures are oriented at a large angle to the present-day minimum principal stress in the bedrock. This relationship favours their reactivation as extensional joints in the present stress regime, the development of conspicuous apertures along several fractures, and the release of high stress.

Fracture domain FFM03: This domain is situated within rock domains RFM017 and RFM029, outside the target volume. North-west of the steeply dipping zone ZFMNE0065, domain FFM03 lies structurally above zones ZFMA2, ZFMA3 and ZFMF1. It is also found throughout the bedrock volume south-east of zone ZFMNE0065 (Figure 5-1). The domain is characterized by a high frequency of gently dipping deformation zones containing both open and sealed fractures. It is suggested that this structural feature inhibited the build-up of rock stresses in connection with, for example, sedimentary loading processes /SKB 2006, section 3.2.2, p 121–126/. The development of a significant stress-release fracture domain close to the surface with the characteristics of domain FFM02 is also not favoured.

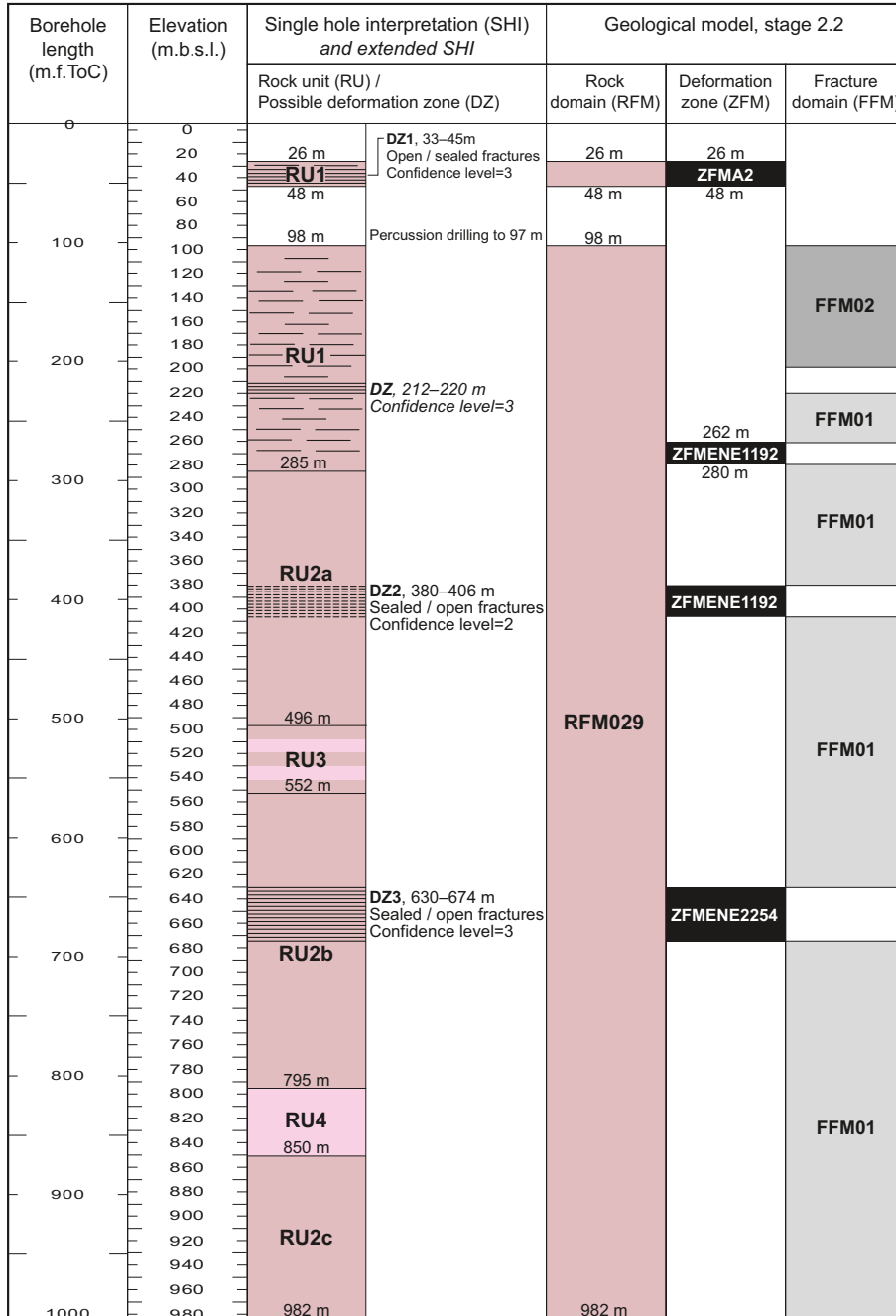
Fracture domain FFM04: This domain is situated within rock domains RFM012 and RFM018 along the south-western margin of and outside the target volume. Strong bedrock anisotropy with high ductile strain and ductile structures that dip steeply to the south-west are prominent in this domain.

Fracture domain FFM05: This domain is situated within rock domains RFM044 and RFM032 along the north-western and north-eastern margins of and outside the target volume. Strong bedrock anisotropy with high ductile strain and folded ductile structures, as well as the occurrence of fine-grained, felsic meta-igneous rocks characterize this domain.

Fracture domain FFM06: This domain is situated within rock domain RFM045, inside the target volume. It resembles fracture domain FFM01 in the sense that it lies beneath both zone ZFMA2 and fracture domain FFM02 (Figure 5-1). It is distinguished from domain FFM01 by the widespread occurrence of fine-grained, altered (albitized) granitic rock, with slightly higher contents of quartz compared to unaltered granitic rock.

Since the target volume lies within rock domains RFM029 and RFM045, north-west of the steeply dipping zone ZFMNE0065 and structurally beneath the gently dipping and sub-horizontal zones ZFMA2, ZFMA3 and ZFMF1, it is apparent that statistical modelling of fractures needs to be implemented in fracture domains FFM01, FFM02 and FFM06 inside rock domains RFM029 and RFM045 (see Figure 5-4 and Figure 5-7 for 3D views of the geometries of these fracture domains).

KFM01A



Legend for single hole interpretation

- Increased frequency of fractures relative to other borehole sections outside deformation zones
- Brittle deformation zone, probable
- Brittle deformation zone, certain

Rock type

- Group C**
 Granodiorite to tonalite, metamorphic, fine- to medium-grained
- Group B**
 Granite (to granodiorite), metamorphic, medium-grained

The elevation of a modelled deformation zone is only provided in the cases where the zone boundaries differ from the single hole interpretation. The base of FFM02 is placed at 199 m beneath sea level

Figure 5-2. Rock units (RU) in the single-hole interpretation (SHI), possible deformation zones (DZ) in the SHI and extended single-hole interpretation (ESHI), and modelled rock domains (RFM), deformation zones (ZFM) and fracture domains (FFM) in borehole KFM01A.

5.2 Presentation of fracture domains in each borehole

With the help of the various criteria used in the development of the fracture domain concept, in particular the three exclusion criteria described in section 5.1, the intervals along which a fracture domain is inferred to be present in each cored borehole are shown in a series of diagrams, one for each cored borehole (Appendix 4). Since rock units and possible deformation zones in the single-hole interpretation of the borehole serve as a basis for the identification of fracture domains, these geological entities are included in each figure. The additional minor zones identified in the extended single-hole interpretation of each borehole (section 4.3.2), as well as the rock domains and deformation zones actually modelled in stage 2.2, are also displayed. An example of these diagrams for cored borehole KFM01A is presented here (Figure 5-2). Furthermore, the contrasting character of fracture domains FFM01 and FFM02 in this borehole is shown in Figure 5-3.

Borehole interval and elevation data for the different geological entities illustrated in the borehole figures (Figure 5-2, Appendix 4) are documented in a table that will be made available in Sicada. Table 5-1 is an extract of this table that presents borehole interval and elevation data for all boreholes, both cored (KFM) and percussion (HFM). The allocation of the borehole intervals in the percussion boreholes to fracture domains has been determined by comparison with the results in the spatially closest cored boreholes. The quality of the data in the percussion boreholes precludes the use of fracture frequency distribution plots (see also section 4.1).

Table 5-1 shows how the base data are treated in modelling stage 2.2. The fields marked as “Modelled DZ” (corresponding to features identified as ZFM in the table) are included in the deterministic modelling work. The fields that include deformation zones that have not been modelled deterministically (features identified as “Possible DZ” in the table) are treated as a single feature with zero thickness in the geological DFN modelling work. All other borehole sections marked with a fracture domain identity should be included in the geological DFN modelling work for the statistical analysis of fractures. The few fracture domain sections identified as “Affected by DZ” or “Vuggy rock outside DZ” should be handled with special attention in the geological DFN modelling work. They can either be integrated in the fracture domain to which they have been allocated in the present study or assigned to a separate fracture domain.

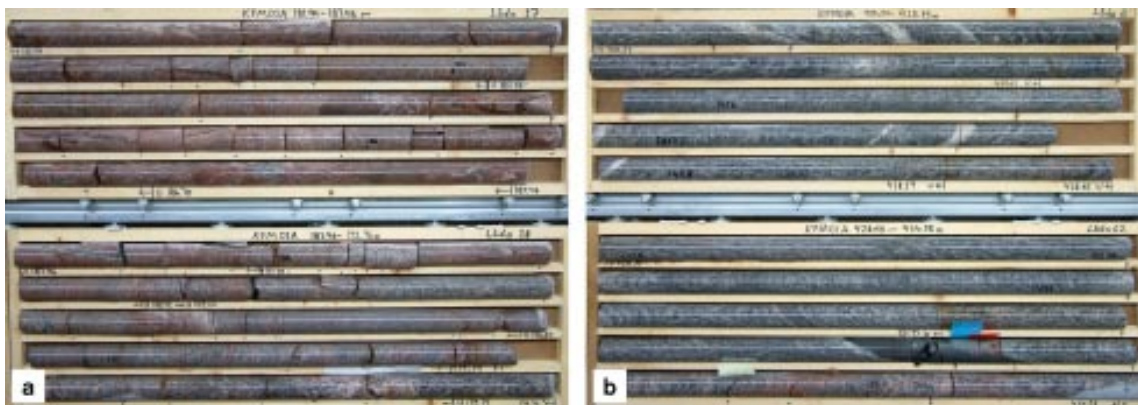


Figure 5-3. a) Character of fracture domain FFM02 in the borehole interval 182–193 m along borehole KFM01A. Note the hematite staining (oxidation) and the high frequency of gently dipping to sub-horizontal fractures that intersect the borehole at a large angle. b) Character of fracture domain FFM01 in the borehole interval 423–435 m along borehole KFM01A. Note the low frequency of open fractures in particular.

Table 5-1. Extract from the table that documents borehole intersections and elevation data for: 1) Rock units and possible deformation zones in the single-hole interpretation. 2) Modified and new rock units and possible deformation zones in the extended and modified single-hole interpretations. 3) Rock domains, deformation zones and fracture domains in the geological model stage 2.2.

Single hole interpretation (SHI) from Sicada/P-reports										Extended SHI (ESHI) and SHI modified during				
Borehole	RU	Confidence	DZ	Confidence	From length (m)	To length (m)	Elevation up (m.b.s.l.)	Elevation low (m.b.s.l.)	Comment	Geological feature	Confidence	From length (m)	To length (m)	Elevation up (m.b.s.l.)
KFM01A	RU1	3			102	290	98	285		Modified RU1	3	102	203	98
										New DZ	3	216	224	212
											New DZ	3	267	285
KFM01A	RU2a	3			290	386	285	380		Modified RU2a	3	203	503	199
KFM01A	RU2a	3	DZ2	2	386	412	380	406						
KFM01A	RU2a	3			412	503	406	496						
KFM01A	RU3	3			503	560	496	552						
KFM01A	RU2b	3			560	639	552	630						
KFM01A	RU2b	3	DZ3	3	639	684	630	674						
KFM01A	RU2b	3			684	808	674	795						
KFM01A	RU4	3			808	865	795	850						
KFM01A	RU2c	3			865	1001	850	982						
KFM01B	RU1	3	DZ1	3	16	53	13	49		Modified DZ1	3	16	64	13
KFM01B	RU1	3			53	107	49	102		Modified RU1	3	16	224	13
KFM01B	RU1	3	DZ2	3	107	135	102	129						
KFM01B	RU1	3			135	141	129	135						
KFM01B	RU2	3			141	415	135	398		New DZ	3	224	225	215
KFM01B	RU2	3	DZ3	3	415	454	398	435						
KFM01B	RU2	3			454	501	435	479						
KFM01C	RU1	3			12	23	6	15						
KFM01C	RU1	3	DZ1	3	23	48	15	34						
KFM01C	RU1	3			48	62	34	44						
KFM01C	RU1	3	DZ2	3	62	99	44	72						
KFM01C	RU1	3			99	235	72	175		New DZ	3	121	124	89
KFM01C	RU1	3	DZ3	3	235	450	175	332		Modified DZ3	3	235	252	175
KFM01C										Modified DZ3	3	252	305	187
KFM01C										Modified DZ3	3	305	330	227
KFM01C										Modified DZ3	3	330	450	245

modelling work			Geological model, version 2.2							
Eleva- tion low (m.b.s.l.)	Comment	Signature	RFM	ZFM (DZ)	FFM	Comment	From length (m)	To length (m)	Eleva- tion up (m.b.s.l.)	Eleva- tion low (m.b.s.l.)
199		MBS/ASi	RFM029		FFM02		102	203	98	199
220		AF/IOL	RFM029		FFM01		203	216	199	212
280		MBS/ASi	RFM029	Possible DZ		DZ not modelled	216	224	212	220
			RFM029		FFM01		224	267	220	262
			RFM029	ZFMENE1192		Modelled DZ	267	285	262	280
			RFM029		FFM01		285	293	280	288
496		MBS/ASi	RFM029		FFM01		293	386	288	380
			RFM029	ZFMENE1192		Modelled DZ	386	412	380	406
			RFM029		FFM01		412	639	406	630
			RFM029							
			RFM029							
			RFM029	ZFMENE2254		Modelled DZ	639	684	630	674
			RFM029		FFM01		684	1001	674	982
			RFM029							
			RFM029							
60		MBS/ASi	RFM029	ZFMA2		Modelled DZ	16	64	13	60
215		MBS/ASi	RFM029		FFM02		64	107	60	102
			RFM029	Possible DZ		DZ not modelled	107	135	102	129
			RFM029		FFM02		135	224	129	215
216		AF/IOL	RFM029	Possible DZ		DZ not modelled	224	225	215	216
			RFM029		FFM01		225	415	216	398
			RFM029	ZFMNNW0404		Modelled DZ	415	454	398	435
			RFM029		FFM01		454	501	435	479
			RFM029		FFM02		12	23	6	15
			RFM029	ZFMA2, ZFMENE1192		Modelled DZ	23	48	15	34
			RFM029		FFM02	Affected by DZ	48	62	34	44
			RFM029	ZFMA2		Modelled DZ	62	99	44	72
			RFM029		FFM02		99	121	72	89
91		AF/IOL	RFM029	Possible DZ		DZ not modelled	121	124	89	91
			RFM029		FFM02		124	235	91	175
187	Modelled DZ	MBS/ASi	RFM029	ZFMENE0060A		Modelled DZ	235	252	175	187
227	Affected by DZ	MBS/ASi	RFM029		FFM01	Affected by DZ	252	305	187	227
245	Modelled DZ	MBS/ASi	RFM029	ZFMENE0060C		Modelled DZ	305	330	227	245
332	Affected by DZ	MBS/ASi	RFM029		FFM01	Affected by DZ	330	450	245	332

5.3 Geometric model for fracture domains inside the target volume

On the basis of borehole data, six separate fracture domains have been recognized within the target volume and its immediate surroundings. Attention is focused in this section on the four domains that have enough data for three-dimensional geometrical modelling, namely FFM01, FFM02, FFM03 and FFM06. The conceptual basis underlying the geometric modelling work, as well as the character of each fracture domain, are presented in section 5.1. In order to facilitate an understanding of the conceptual thinking, two vertical profiles through the fracture domain model were already shown in section 5.1.

In order to define the target volume in the modelling work, the boundaries of the modelled fracture domains coincide with the following planar features:

- The boundary between rock domain RFM029 and the adjacent domain RFM012 in the volume situated north-west of the steeply dipping deformation zone ZFMENE0060A. This zone is longer than 3,000 m.
- The steeply dipping deformation zone ZFMWNW0123 in the volume that is situated south-east of zone ZFMENE0060A. Zone ZFMWNE0123 is also longer than 3,000 m.
- The boundaries between rock domain RFM029 and the adjacent domains RFM044 and RFM032.
- The boundary between rock domains RFM045 and RFM032.
- The south-eastern and basal (1,100 m below sea level) boundaries of the local model volume as defined in model stage 2.2. This is identical to that in model stage 2.1 (see section 2.3.2 in /SKB 2006/).

Three other deformation zones are included in the fracture domain model. Since the deformation zones ZFMA2 and ZFMF1 for the most part define the lower boundary of fracture domain FFM03, these gently dipping zones need to be included in the model. Furthermore, since the steeply dipping deformation zone ZFMENE0062A is also longer than 3,000 m, it is included in the model. The boundaries of rock domains and the geometry of the five deformation zones included in the fracture domain model are taken from model stage 2.2.

Fracture domain FFM02, which is situated in the upper part of the bedrock, is divided into two sub-domains. The north-western part of this domain is located beneath the gently dipping deformation zone ZFMA2 and occupies the uppermost part of the volume within rock domains RFM29 and RFM045. Borehole intersections that constrain the fracture domain boundaries between FFM02 and FFM01 in this volume are summarized in Table 5-2. The south-eastern part of domain FFM02 is located immediately above zone ZFMA2, within the uppermost part of the volume in rock domain RFM029. Fracture domain FFM02 has been modelled to wedge out at depth against zone ZFMA2 (Figure 5-4).

Fracture domain FFM03 is situated above the gently dipping and sub-horizontal zones ZFMA2 and ZFMF1. At depth, this domain lies directly above these zones and FFM01 (Figure 5-1). Closer to the surface, where the FFM02 wedge is present, the lower boundary of fracture domain FFM03 moves away from the gently-dipping deformation zone ZFMA2, so that, at the surface, it is situated to the south-east of this zone (Figure 5-5).

Fracture domains FFM01 and FFM06 are situated beneath the gently dipping and sub-horizontal zones ZFMA2 and ZFMF1, and beneath the near-surface fracture domain FFM02 (Figure 5-1). They are distinguished solely on their alliance to separate rock domains, RFM029 and RFM045. For this reason, the boundary between these two fracture domains coincides with the boundary between these rock domains. Fracture domain FFM06 occupies a significant area at 500 m depth (Figure 5-6).

Table 5-2. Borehole intersections in the boundaries between fracture domain FFM02 and FFM01 that have been used as fixed points in the geometric fracture domain model.

Borehole	Fracture domain boundary	Borehole intersection (m along borehole)	Elevation (m.b.s.l.)
KFM01A	FFM02 – FFM01	203	199
KFM01B	FFM02 – FFM01	225	216
KFM01C	FFM02 – FFM01	244	187
KFM01D	FFM02 – FFM01	191	153
KFM05A	FFM02 – FFM01	237	199
KFM06A	FFM02 – FFM01	137	122
KFM07A	FFM02 – FFM01	147	156
KFM07B	FFM02 – FFM01	195	151
KFM07C	FFM02 – FFM01	123	119
KFM08B	FFM02 – FFM01	46	37
KFM09A	FFM02 – FFM01	124	101
KFM09B	FFM02 – FFM01	119	103

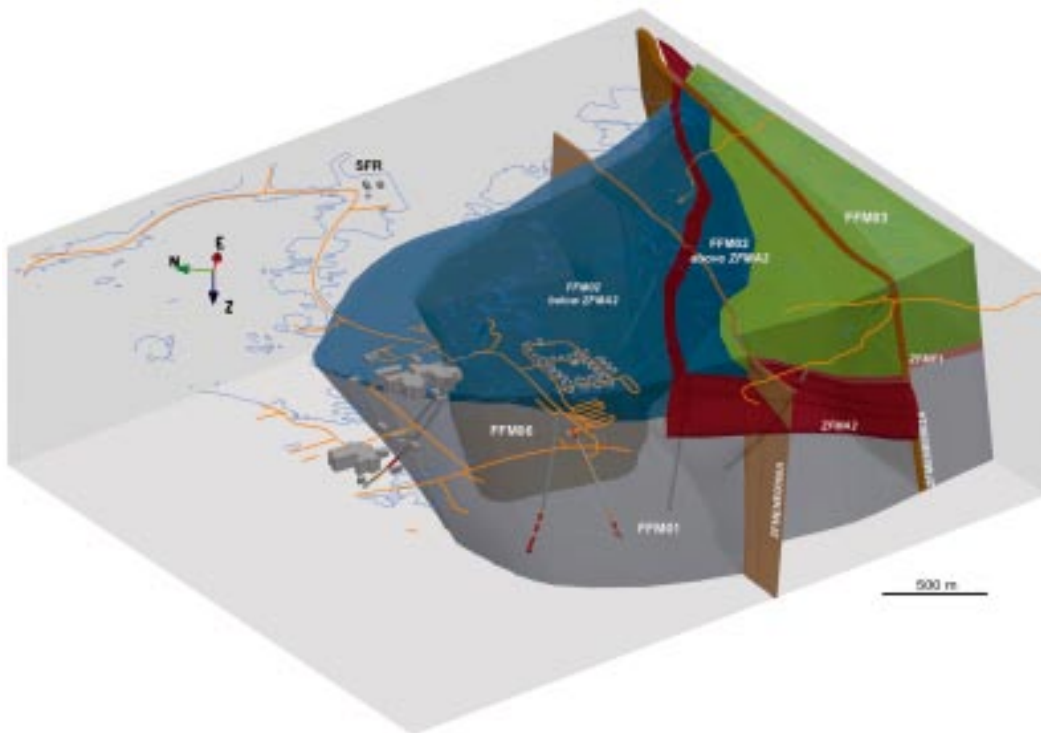


Figure 5-4. View to the east-north-east showing the relationship between zone ZFMA2 (red) and fracture domain FFM02 (blue).

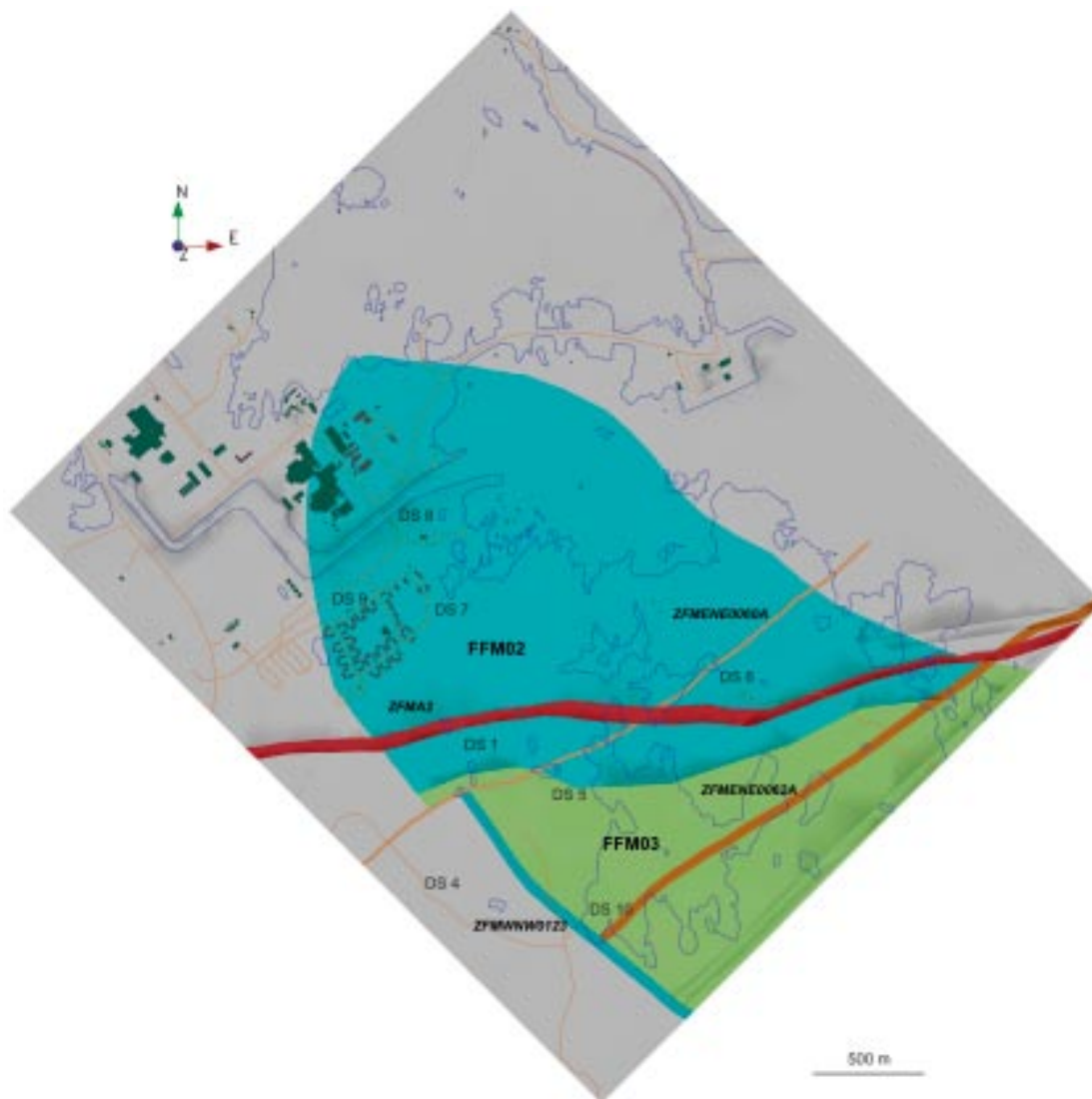


Figure 5-5. Top view of the fracture domain model at the surface. Fracture domain FFM02 is coloured blue while fracture domain FFM03 is coloured green. Four deformation zones – the gently dipping ZFMA2, and the steeply dipping zones ZFMENE0060A, ZFMENE0062A and ZFMWNW0123 – also intersect the surface. The sub-horizontal zone ZFMF1 does not intersect the surface, and is for this reason not present in this figure.

A three-dimensional image of the fracture domain model, which shows the geometrical relationships between domains FFM01, FFM02, FFM03 and FFM06, is shown in Figure 5-7. Fracture domain FFM01 dominates in the lowermost part of the view. The volume coloured dark grey shows the position of FFM06. The uppermost part of the bedrock, in the north-western part of the model, is fracture domain FFM02. This domain dips gently towards the south. Fracture domain FFM03 is situated directly above the gently dipping and sub-horizontal zones ZFMA2 and ZFMF1 at depth, and above domain FFM02 close to the surface.

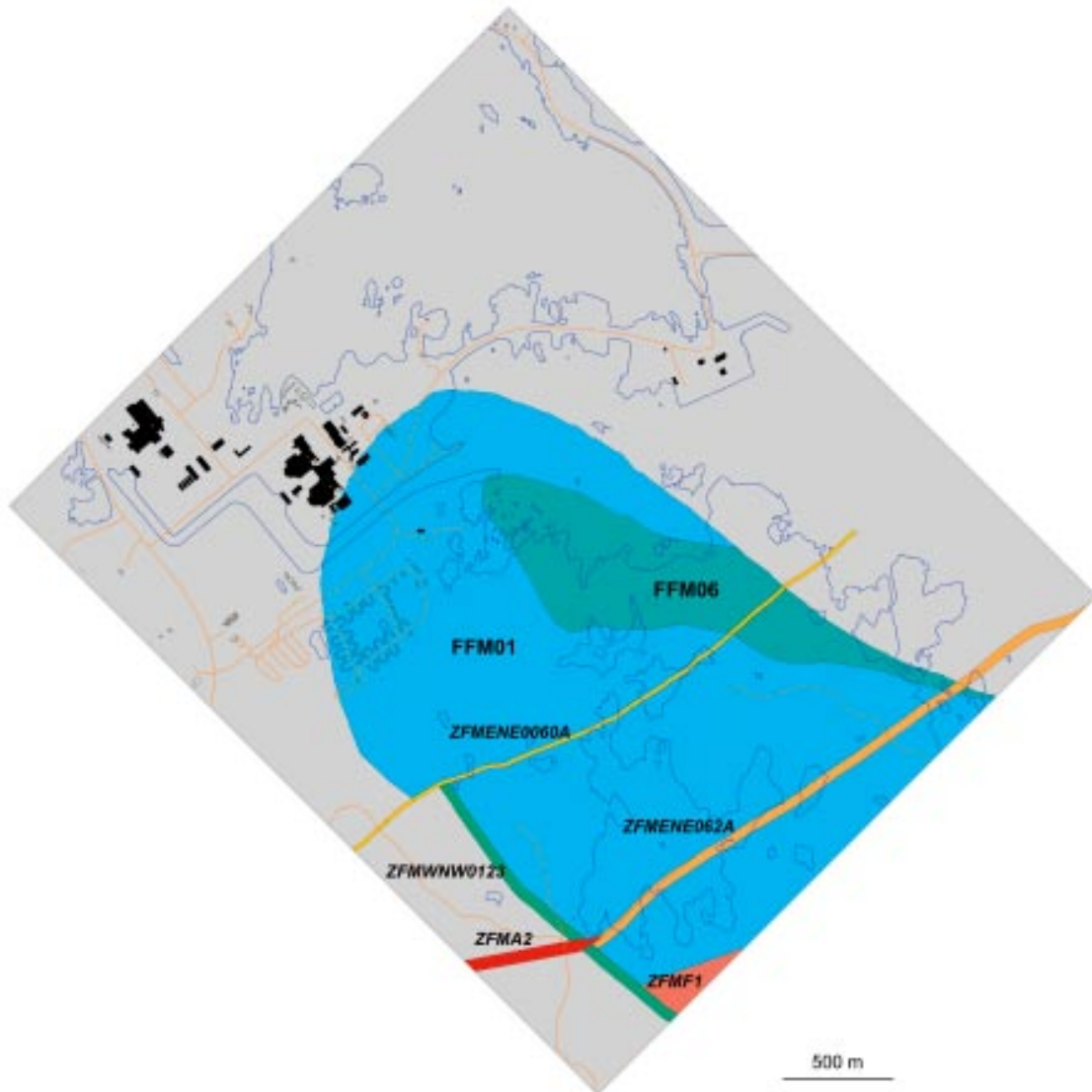


Figure 5-6. Top view of the fracture domain model at 500 metres depth. Fracture domain FFM01 is coloured blue and fracture domain FFM06 is coloured green. Five deformation zones – the gently dipping zone ZFMA2, the sub-horizontal zone ZFMF1, and the three steeply dipping zones ZFMENE0060A, ZFMENE062A and ZFMWNW0123 – longer than 3,000 m, are included in the model.

5.4 Uncertainties

Intrinsic uncertainties in the proposal for fracture domains presented above include all the limitations involved in the rock domain and deformation zone modelling work. Earlier work has addressed many of these uncertainties (see, especially, /SKB 2005a, 2006/) and the remaining uncertainties will be documented again in the modelling report for stage 2.2. These uncertainties are not addressed further here. There are also intrinsic uncertainties in the recognition of fracture domains in the percussion boreholes, due simply to the poorer quality of the geological data in these boreholes. Furthermore, the geometric model for the boundary between fracture domains in the target volume is based on data from a limited number of cored boreholes. For this reason, the geometric model inside the target volume is judged to be highly uncertain.

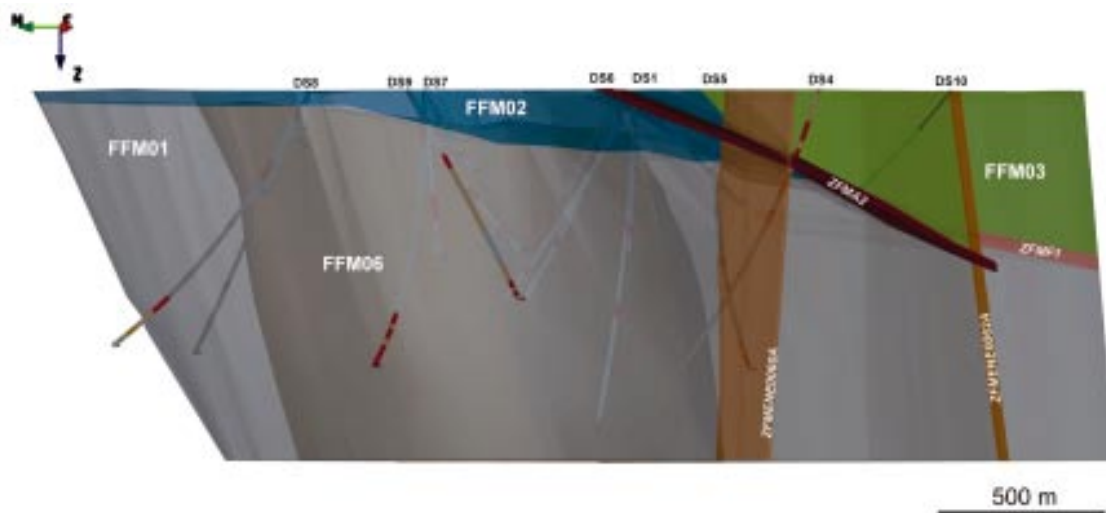


Figure 5-7. Three-dimensional image of the fracture domain model, viewed towards the east-north-east. Fracture domains FFM01, FFM02, FFM03 and FFM06 are coloured grey, dark grey, blue and green, respectively. The gently dipping and sub-horizontal zones ZFMA2 and ZFMF1 as well as the steeply dipping deformation zones ZFMENE0060A and ZFMENE0062A are also shown.

The definition of the boundaries of deformation zones in the single-hole interpretation is probably the most significant uncertainty associated with the definition of fracture domain boundaries in the various boreholes. Care has been taken in the single-hole interpretation work to take into account both the more deformed and the transitional, i.e. less damaged parts of a zone. Nevertheless, the boundary to the bedrock outside the deformation zone is often not sharp. This uncertainty is reflected first and foremost in the modifications of the boundaries of deformation zones that have been made after an evaluation of the relevant data during the modelling work.

Secondly, the uncertainty in the boundaries of deformation zones is reflected in the definition of a few rock units adjacent to zones that are affected more distally by the zone in question. In this context, it is uncertain whether the more fractured bedrock in the borehole sections close to the surface in KFM09A (above 101 m below sea level) and KFM09B (above 242 m below sea level) is a result of this distal deformation (see Table 5-1), stress-release fracturing close to the surface as envisaged in fracture domain FFM02, or a combination of these two possibilities. The geological DFN modelling work should pay special attention to the limited fracture domain sections that have been identified in this work as “Affected by DZ” or “Vuggy rock outside DZ”.

The allocation of the bedrock inside rock domain RFM029 in boreholes KFM08A and KFM08C to fracture domain FFM01 is uncertain, bearing in mind the increased frequency of sealed fractures in particular in this bedrock. An evaluation of new, high-resolution ground magnetic data indicates that there is a swarm of well-defined, low-magnetic lineaments in the hinge and on the north-eastern limb of the major synformal fold structure in the Forsmark target area. These lineaments trend NNE, are discordant with the folded ductile structures in this area, and have not previously been identified as a specific set of structures due to lower resolution airborne geophysical data. Several of these low-magnetic anomalies are related to steeply dipping, brittle deformation zones with NNE strike in the stage 2.2 modelling work. For this reason, it is possible that the bedrock along the boreholes drilled from site 8 and even site 6, which is currently included in fracture domain FFM01, may be particularly influenced by fractures with this orientation. For this reason, it could be argued that these borehole sections should be included in a separate fracture domain. This point poses some uncertainty and underlines the need for a more stringent statistical analysis.

The inclusion of the borehole sections that have been allocated to rock domains RFM034 and RFM044 in fracture domains FFM01 and FFM05, respectively, is uncertain. However, little data are available for these two rock domains and they also lie outside the target volume. For these two reasons, this uncertainty is judged not to be significant.

It is important to keep in mind that the allocation of borehole sections to different fracture domains is a working hypothesis for the statistical modelling of fractures at the Forsmark site. If the statistical analysis indicates that these fracture domains are not adequate to characterize the variability in fracturing within the target volume, alternatives to the existing domains will need to be introduced. The boundaries of the domains may be modified, or sub-domains may be defined.

6 Hydrogeological data in the context of fracture domains and deformation zones

6.1 Available hydrogeological data and data selection

The drilling campaigns and the various single-hole hydraulic investigations carried out in Forsmark are summarized in Table 6-1. The locations of the cored boreholes (KFMxxx) and the percussion-drilled boreholes (HFMxx) are shown in Figure 1-1 and Figure 1-2.

Table 6-2 lists the cored boreholes that have been or will be investigated with the Posiva Flow Log (PLF-f) method (difference flow logging) and the Pipe String System (PSS) method (double-packer injection tests). Percussion-drilled boreholes are investigated with the HTHB method (combined pumping and impeller flow logging). The PFL-f method can be used to detect individual flow anomalies down to a resolution of approximately 0.1 m, has a theoretical detection limit for transmissivity (T) of about $1 \cdot 10^{-9}$ m²/s, and is generally performed after several days of pumping to establish steady state inflow to the entire borehole (line sink). With the PSS method, the shortest packer interval measured is 5 m. It is potentially able to detect smaller flow rates than the PFL-f method, down to T-values of $c 5 \cdot 10^{-10}$ m²/s, and is performed under injection conditions over a short duration of about 20 minutes (point source). The resolution of the HTHB method, finally, is fairly poor. The spatial resolution is a function of the high detection limit, $c 1 \cdot 10^{-6}$ m²/s.

The core-drilled boreholes are typically 5–10 times longer than the percussion-drilled boreholes. Moreover, the geological mapping of the cored boreholes is much better than in the percussion-drilled boreholes. For these two reasons, and because of the high detection limit of the HTHB method, transmissivity data from the percussion-drilled boreholes are not treated in the work presented here.

Table 6-1. List of core- and percussion-drilled boreholes at the time of the different data freezes in Forsmark.

Data freeze	No. of core-drilled boreholes	KFMxxx	No. of percussion-drilled boreholes	HFMxx
1.1 30 Apr 2003	1	KFM01A	8	HFM01–08
1.2 31 Jul 2004		KFM02A–05A KFM01B	11	HFM09–19
2.1 29 Jul 2005		KFM06A–07A KFM03B, -06B	3	HFM020–22
2.2 30 Sep 2006	11	KFM08A–10A KFM06B–09B KFM01C, KFM07C–08C KFM01D	10	HFM23–32
2.3 31 Mar 2007	4	KFM11A–12A KFM02B KFM08D	6	HFM33–38
All	25	KFM01A–12A KFM01B–03B KFM06B–09B KFM01C, KFM07C–08C KFM01D, -08D	38	HFM01–38

Table 6-2. List of PFL and PSS tests in Forsmark.

Data Freeze	No. of PFL tested boreholes	Tested boreholes KFMxxx	No. of PSS tested boreholes	Tested boreholes KFMxxx
1.1 30 Apr 2003	1	KFM01A	0	–
1.2 31 Jul 2004	4	KFM02A–05A	3	KFM01A–03A
2.1 29 Jul 2005	2	KFM06A–07A	6	KFM04A–07A KFM03B, -06B
2.2 30 Sep 2006	5	KFM08A, -10A KFM07C–08C KFM01D	8	KFM08A–09A KFM07B–09B KFM01C, -06C KFM01D
2.3 31 Mar 2007	3	KFM11A KFM07C KFM08D	5	KFM10A–12A KFM07C–08C
All	15	KFM01–08A KFM10A–11A KFM08C KFM01D, -08D	22	KFM01A–12A KFM03B, KFM06B–09B KFM01C, KFM06C–08C KFM01D

Further, a high spatial resolution in the hydraulic measurements is considered necessary for assessing the hydraulic properties of the boreholes with regard to the objectives of the work presented here. The PSS method measures on three scales of resolution: 5 m, 20 m and 100 m. Thus, the highest spatial resolution associated with the PSS method is 5 m. This resolution is considered insufficient with regard to the present objectives, since in several cases the 5 m PSS intervals overlap the boundary between two adjacent fracture domains, or the boundary between a fracture domain and a deformation zone, which makes it difficult to substantiate if there are any significant hydraulic differences present between the different units.

For this reason, fracture transmissivity data acquired by the PFL-f method using a measurement interval of 0.1 m is the only kind of data treated in the work presented here. Among the cored borehole data available at the time of data freeze 2.2, KFM01A, KFM01D, KFM02A, KFM03A, KFM04A, KFM05A, KFM06A, KFM07A, KFM07C, KFM08A, KFM08C and KFM10A are all measured with the PFL-f method using a measurement interval of 0.1 m. The hydraulic information acquired from these twelve boreholes is considered adequate for the objectives of the work presented here. The integrated WellCad plots in Appendix 8 show all single-hole hydraulic test data available for all cored boreholes in Forsmark, i.e. both PFL-f data and PSS data.

6.2 Flow anomalies by depth, deformation zone and fracture domain

Figure 6-1 through Figure 6-12 show the PFL-f fracture transmissivity data observed in the twelve boreholes treated here: KFM01A, KFM01D, KFM02A, KFM03A, KFM04A, KFM05A, KFM06A, KFM07A, KFM07C, KFM08A, KFM08C and KFM10A.

The PFL-f fracture transmissivity data are coloured with regard to their structural association as determined by their position along the boreholes (see Table 6-3): FFM01–FFM06 or a deformation zone. In a few cases, a PFL-f fracture transmissivity value is associated with a “possible deformation zone”.

Table 6-3. Legend to Figure 6-1 through Figure 6-12.

Symbol	Meaning
○	FFM01
●	FFM02
●	FFM03
○	FFM04
●	FFM05
●	FFM06
■	Deformation zone
■	Possible deformation zone

Table 6-4 through Table 6-15 accompany the plots shown in Figure 6-1 through Figure 6-12. The tables provide more detailed geometric information concerning the spatial variability in each borehole, as they also provide information on the units for which there is no associated PFL-f fracture transmissivity data. The figures and tables are presented together for each drill site. All in all, 579 PFL-f fracture transmissivities (flow anomalies) were measured in the twelve cored boreholes treated.

The practical measurement limit of the PFL-f method is shown in the figures. More information about this measurement limit is given in the P-reports for the PFL measurements (see Tables A1-2 and A1-5 in Appendix 1 for identification of these reports).

6.2.1 Drill site 1

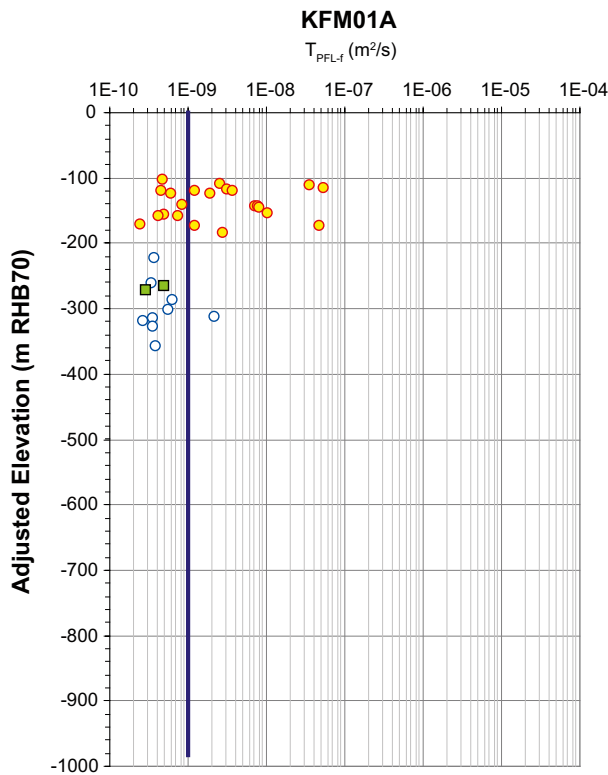


Figure 6-1. Elevation of the 34 PFL-f fracture transmissivity data observed in KFM01A. The fracture transmissivities are coloured with regard to their structural association as determined by their position along the borehole, cf the legend in Table 6-3. The blue line indicates both the practical measurement threshold of the PFL-f method, which is about $1 \cdot 10^{-9} m^2/s$, and the depth of the borehole/PFL-f measurements.

Table 6-4. Compilation of PFL-f transmissivities measured in KFM01A with regard to rock domain (RFM), deformation zone (ZFM), fracture domain (FFM), borehole length (Secup/Seclow) and elevation (Elevup/Elevlow). PFL-f transmissivities are given in [m²/s]. The colours refer to the legend used in the transmissivity plot, cf Table 6-3.

RFM	ZFMxxxx	FFMxx	Secup	Seclow	Elevup	Elevlow	No. PFL-f	Σ T PFL-F
029		02	102	203	98	199	23	1.92E-07
029		01	203	216	199	212	0	0.00E+00
029	Possible		216	224	212	220	0	0.00E+00
029		01	224	267	220	262	2	7.09E-10
029	ENE1192		267	285	262	280	2	7.79E-10
029		01	285	386	280	380	7	4.76E-09
029	ENE1192		386	412	380	406	0	0.00E+00
029		01	412	639	406	630	0	0.00E+00
029	ENE2254		639	684	630	674	0	0.00E+00
029		01	684	1,001	674	982	0	0.00E+00

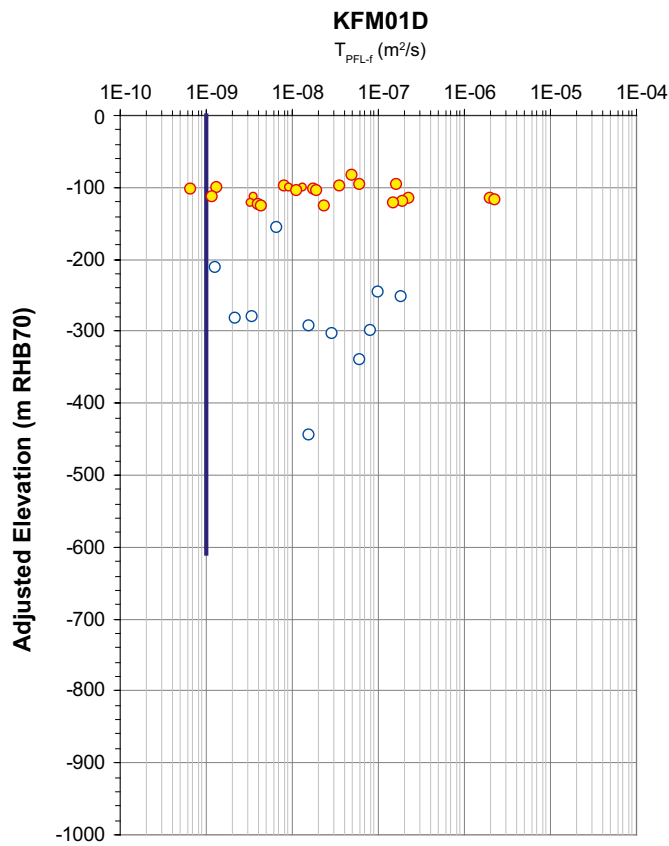


Figure 6-2. Elevation of the 34 PFL-f fracture transmissivity data observed in KFM01D. The fracture transmissivities are coloured with regard to their structural association as determined by their position along the borehole, cf the legend in Table 6-3. The blue line indicates both the practical measurement threshold of the PFL-f method, which is about $1 \cdot 10^{-9} \text{ m}^2/\text{s}$, and the depth of the borehole/PFL-f measurements.

Table 6-5. Compilation of the PFL-f transmissivities measured in KFM01D with regard to rock domain (RFM), deformation zone (ZFM), fracture domain (FFM), borehole length (Secup/Seclow) and elevation (Elevup/Elevlow). The PFL-f transmissivities are given in [m²/s]. The colours refer to the legend used in the transmissivity plot, cf Table 6-3.

RFM	ZFM	FFM	Secup	Seclow	Elevup	Elevlow	No. PFL-f	Σ T PFL-F
029		02	92	176	72	141	23	5.33E-06
029	Possible		176	184	141	147	0	0.00E+00
029		02	184	191	147	153	0	0.00E+00
029		01	191	411	153	325	9	4.22E-07
029	Possible		411	421	325	332	0	0.00E+00
029		01	421	488	332	383	1	6.23E-08
029	Possible		488	496	383	389	0	0.00E+00
029		01	496	670	389	517	1	1.59E-08
029	ENE0061	01	670	700	517	538	0	0.00E+00
029		01	700	771	538	589	0	0.00E+00
029	Possible		771	774	589	591	0	0.00E+00
029		01	774	800	591	609	0	0.00E+00

6.2.2 Drill site 2

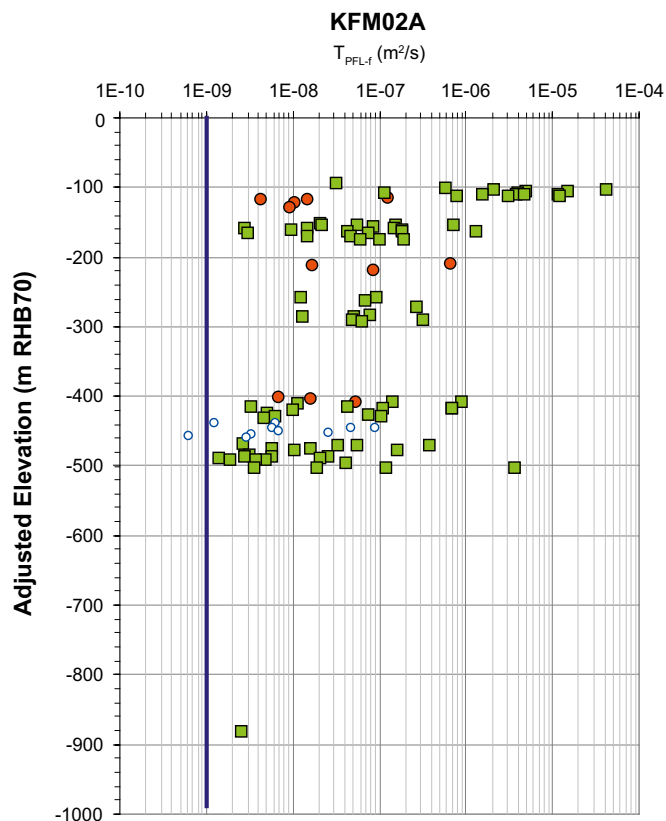


Figure 6-3. Elevation of the 104 PFL-f fracture transmissivity data observed in KFM02A. The fracture transmissivities are coloured with regard to their structural association as determined by their position along the borehole, cf the legend in Table 6-3. The blue line indicates both the practical measurement threshold of the PFL-f method, which is about $1 \cdot 10^{-9} \text{ m}^2/\text{s}$, and the depth of the borehole/PFL-f measurements. In addition to the 104 PFL-f fracture transmissivities in KFM02A there are 21 PFL-f flow anomalies associated with the vuggy granite observed in KFM02A, cf section 4.4. These 21 PFL-f anomalies are of a non-discrete nature meaning that the crystalline rock acts like a porous medium.

Table 6-6. Compilation of the PFL-f transmissivities measured in KFM02A with regard to rock domain (RFM), deformation zone (ZFM), fracture domain (FFM), borehole length (Secup/Seclow) and elevation (Elevup/Elevlow). The PFL-f transmissivities are given in [m²/s]. The colours refer to the legend used in the transmissivity plot, cf Table 6-3.

RFM	ZFM	FFM	Secup	Seclow	Elevup	Elevlow	No. PFL-f	Σ T PFL-F
029		03	100	110	92	102	1	3.28E-08
029	866		110	122	102	114	14	1.07E-04
029		03	122	160	114	152	5	1.66E-07
029	A3		160	184	152	176	21	3.46E-06
029		03	184	240	176	232	3	7.78E-07
029	1189		240	310	232	302	10	1.03E-06
029		03	310	417	302	408	3	7.62E-08
029	A2		417	442	408	433	14	2.85E-06
029		01	442	476	433	467	10	1.90E-07
029	F1		476	520	467	511	22	4.66E-06
029	Possible		520	600	511	590	0	0.00E+00
029		01	600	893	590	881	0	0.00E+00
029	B4		893	905	881	892	1	2.62E-09
029		01	905	922	892	909	0	0.00E+00
029	Possible		922	925	909	912	0	0.00E+00
029		01	925	976	912	963	0	0.00E+00
029	Possible		976	982	963	969	0	0.00E+00
029		01	982	1,001	969	987	0	0.00E+00

6.2.3 Drill site 3

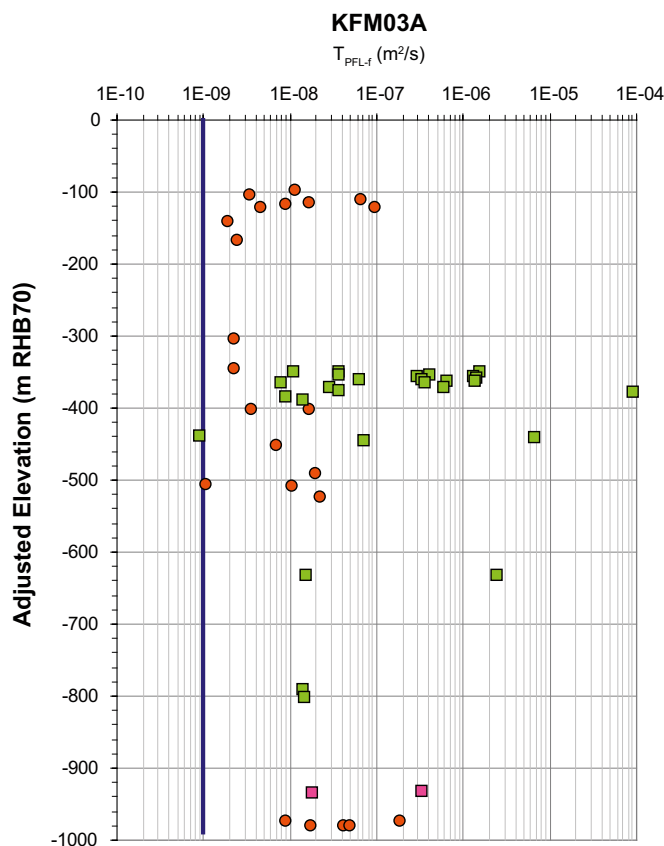


Figure 6-4. Elevation of the 52 PFL-f fracture transmissivity data observed in KFM03A. The fracture transmissivities are coloured with regard to their structural association as determined by their position along the borehole, cf the legend in Table 6-3. The blue line indicates both the practical measurement threshold of the PFL-f method, which is about $1 \cdot 10^{-9}$ m²/s, and the depth of the borehole/PFL-f measurements.

Table 6-7. Compilation of the PFL-f transmissivities measured in KFM03A with regard to rock domain (RFM), deformation zone (ZFM), fracture domain (FFM), borehole length (Secup/Seclow) and elevation (Elevup/Elevlow). The PFL-f transmissivities are given in [m²/s]. The colours refer to the legend used in the transmissivity plot, cf Table 6-3.

RFM	ZFM	FFM	Secup	Seclow	Elevup	Elevlow	No. PFL-f	Σ T PFL-F
029		03	102	220	93	211	9	2.10E-07
017		03	220	293	211	284	0	0.00E+00
029		03	293	356	284	347	2	4.60E-09
029	A4		356	399	347	390	20	1.01E-04
029		03	399	448	390	438	2	2.01E-08
029	A7		448	455	438	445	3	6.72E-06
029		03	455	638	445	627	5	6.06E-08
029	B1		638	646	627	635	2	2.50E-06
029		03	646	803	635	791	0	0.00E+00
029	A3		803	816	791	804	2	2.86E-08
029		03	816	942	804	929	0	0.00E+00
029	Possible		942	949	929	936	2	3.46E-07
029		03	949	1,000	936	987	5	3.06E-07

6.2.4 Drill site 4

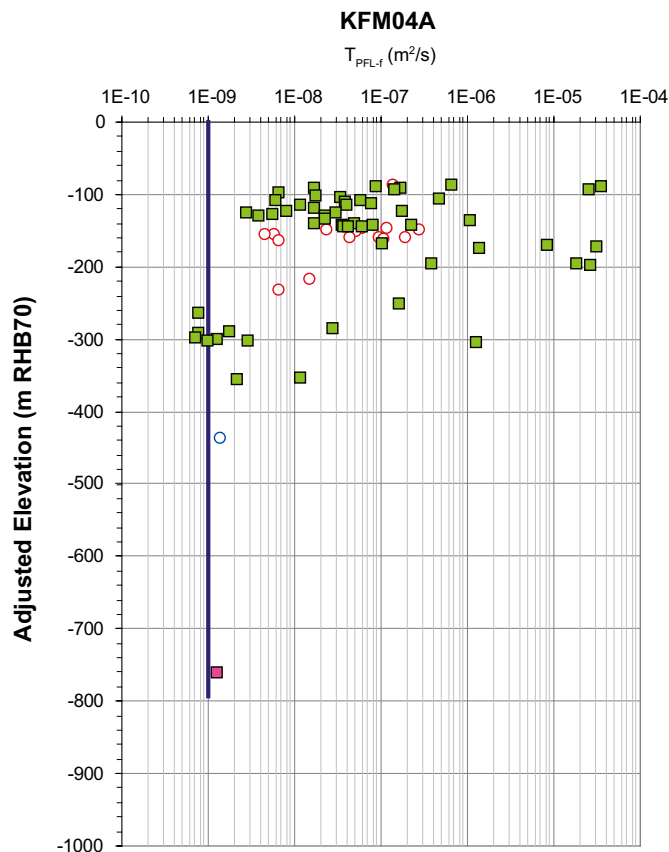


Figure 6-5. Elevation of the 71 PFL-f fracture transmissivity data observed in KFM04A. The fracture transmissivities are coloured with regard to their structural association as determined by their position along the borehole, cf the legend in Table 6-3. The blue line indicates both the practical measurement threshold of the PFL-f method, which is about $1 \cdot 10^{-9}$ m²/s, and the depth of the borehole/PFL-f measurements.

Table 6-8. Compilation of the PFL-f transmissivities measured in KFM04A with regard to rock domain (RFM), deformation zone (ZFM), fracture domain (FFM), borehole length (Secup/Seclow) and elevation (Elevup/Elevlow). The PFL-f transmissivities are given in [m²/s]. The colours refer to the legend used in the transmissivity plot, cf Table 6-3.

RFM	ZFM	FFM	Secup	Seclow	Elevup	Elevlow	No. PFL-f	Σ T PFL-F
018		04	109	110	87	88	1	1.39E-07
018	NW1200		110	176	88	146	35	6.48E-05
018		04	176	177	146	147	0	0.00E+00
012		04	177	202	147	169	12	9.88E-07
012	A2		202	242	169	204	7	8.79E-05
012		04	242	290	204	245	2	2.19E-08
012	NE1188		290	370	245	313	10	1.46E-06
012		04	370	412	313	348	0	0.00E+00
012	NE1188		412	462	348	389	2	1.38E-08
012		04	462	500	389	420	0	0.00E+00
029		01	500	654	420	541	1	1.41E-09
029	NW0123		654	661	541	546	0	0.00E+00
029		01	661	953	546	761	0	0.00E+00
029	Possible		953	956	761	763	1	1.29E-09
029		01	956	1,001	763	794	0	0.00E+00

6.2.5 Drill site 5

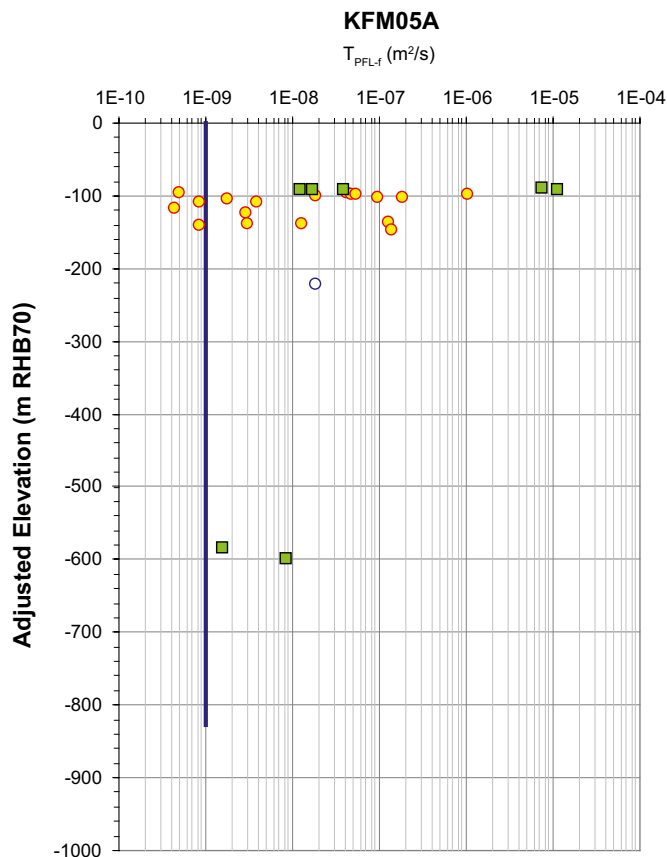


Figure 6-6. Elevation of the 27 PFL-f fracture transmissivity data observed in KFM05A. The fracture transmissivities are coloured with regard to their structural association as determined by their position along the borehole, cf the legend in Table 6-3. The blue line indicates both the practical measurement threshold of the PFL-f method, which is about $1 \cdot 10^{-9}$ m²/s, and the depth of the borehole/PFL-f measurements.

Table 6-9. Compilation of the PFL-f transmissivities measured in KFM05A with regard to rock domain (RFM), deformation zone (ZFM), fracture domain (FFM), borehole length (Secup/Seclow) and elevation (Elevup/Elevlow). The PFL-f transmissivities are given in [m²/s]. The colours refer to the legend used in the transmissivity plot, cf Table 6-3.

RFM	ZFM	FFM	Secup	Seclow	Elevup	Elevlow	No. PFL-f	Σ T PFL-F
029	A2		102	114	83	93	6	1.25E-03
029		02	114	237	93	199	18	1.80E-06
029		01	237	395	199	333	1	1.86E-08
029	ENE2282		395	436	333	366	0	0.00E+00
029		01	436	590	366	492	0	0.00E+00
029	ENE0401B		590	616	492	514	0	0.00E+00
029		01	616	685	514	570	0	0.00E+00
029	ENE0401A		685	720	570	598	2	1.20E-08
029		01	720	892	598	738	0	0.00E+00
029	ENE0103		892	916	738	757	0	0.00E+00
029		01	916	936	757	773	0	0.00E+00
029	ENE2383		936	992	773	818	0	0.00E+00
029		01	992	1,000	818	825	0	0.00E+00

6.2.6 Drill site 6

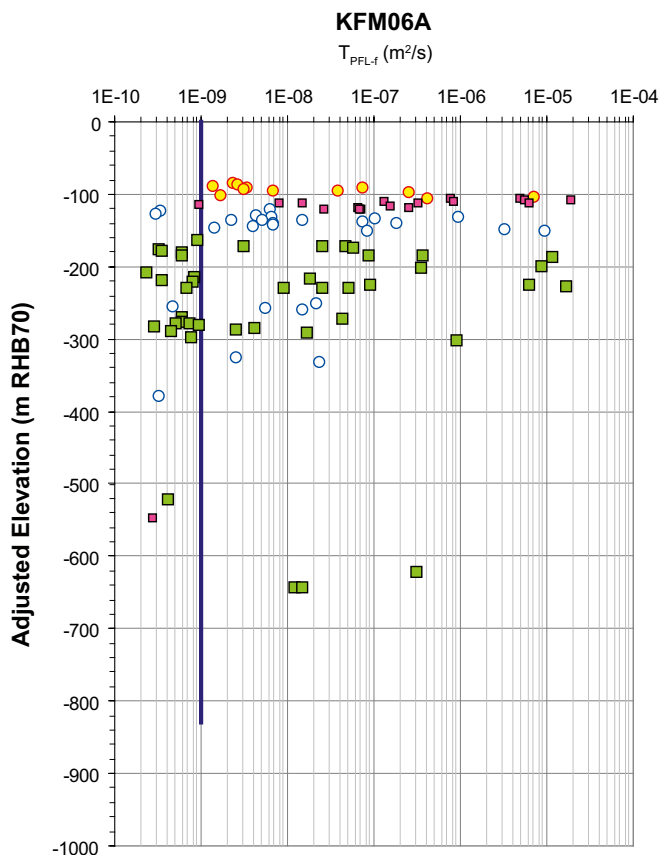


Figure 6-7. Elevation of the 99 PFL-f fracture transmissivity data observed in KFM06A. The fracture transmissivities are coloured with regard to their structural association as determined by their position along the borehole, cf the legend in Table 6-3. The blue line indicates both the practical measurement threshold of the PFL-f method, which is about $1 \cdot 10^{-9}$ m²/s, and the depth of the borehole/PFL-f measurements.

Table 6-10. Compilation of the PFL-f transmissivities measured in KFM06A with regard to rock domain (RFM), deformation zone (ZFM), fracture domain (FFM), borehole length (Secup/Seclow) and elevation (Elevup/Elevlow). The PFL-f transmissivities are given in [m²/s]. The colours refer to the legend used in the transmissivity plot, cf Table 6-3.

RFM	ZFM	FFM	Secup	Seclow	Elevup	Elevlow	No. PFL-f	Σ T PFL-F
029		02	102	128	84	107	12	8.13E-06
029	Possible		128	146	107	122	17	3.90E-05
029		01	146	195	122	164	19	1.42E-05
029	ENE0060B		195	278	164	235	26	4.54E-05
029		01	278	318	235	269	4	4.28E-08
029	ENE0060A, ZFMB7		318	358	269	303	13	9.79E-07
029		01	358	518	303	436	3	2.67E-08
029	NNE2273		518	545	436	459	0	0.00E+00
029		01	545	619	459	520	0	0.00E+00
029	NNE2255		619	624	520	524	1	4.26E-10
029		01	624	652	524	547	0	0.00E+00
029	Possible		652	656	547	551	1	2.74E-10
029		01	656	740	551	620	0	0.00E+00
029	NNE0725		740	775	620	648	1	3.40E-07
045		06	775	788	648	659	0	0.00E+00
045	ENE0061		788	810	659	677	0	0.00E+00
045		06	810	882	677	734	0	0.00E+00
045	Possible		882	905	734	753	0	0.00E+00
045		06	905	925	753	769	0	0.00E+00
045	Possible		925	933	769	775	0	0.00E+00
045		06	933	950	775	789	0	0.00E+00
045	NNE2280		950	990	789	820	0	0.00E+00
045		06	990	998	820	827	0	0.00E+00

6.2.7 Drill site 7

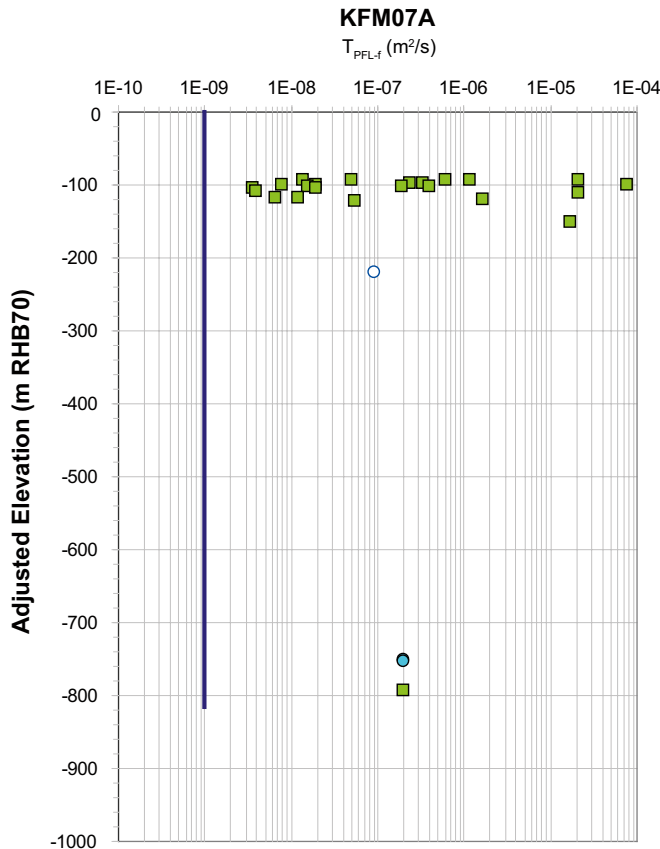


Figure 6-8. Elevation of the 26 PFL-f fracture transmissivity data observed in KFM07A. The fracture transmissivities are coloured with regard to their structural association as determined by their position along the borehole, cf the legend in Table 6-3. The blue line indicates both the practical measurement threshold of the PFL-f method, which is about $1 \cdot 10^{-9} \text{ m}^2/\text{s}$, and the depth of the borehole/PFL-f measurements.

Table 6-11. Compilation of the PFL-f transmissivities measured in KFM07A with regard to rock domain (RFM), deformation zone (ZFM), fracture domain (FFM), borehole length (Secup/Seclow) and elevation (Elevup/Elevlow). The PFL-f transmissivities are given in [m^2/s]. The colours refer to the legend used in the transmissivity plot, cf Table 6-3.

RFM	ZFM	FFM	Secup	Seclow	Elevup	Elevlow	No. PFL-f	$\Sigma T \text{ PFL-F}$
029		02	102	108	85	90	0	0.00E+00
029	1203, NNW0404		108	185	90	156	22	1.41E-04
029		01	185	196	156	165	0	0.00E+00
029	Possible		196	205	165	173	0	0.00E+00
029		01	205	417	173	351	1	9.27E-08
029	ENE0159A		417	422	351	355	0	0.00E+00
029		01	422	793	355	657	0	0.00E+00
044		05	793	803	657	665	0	0.00E+00
044	ENE1208B		803	840	665	694	0	0.00E+00
044		05	840	857	694	708	0	0.00E+00
044	ENE1208A		857	897	708	739	0	0.00E+00
044		05	897	920	739	756	2	4.00E-07
044	NNW0100, B8		920	999	756	815	1	2.00E-07

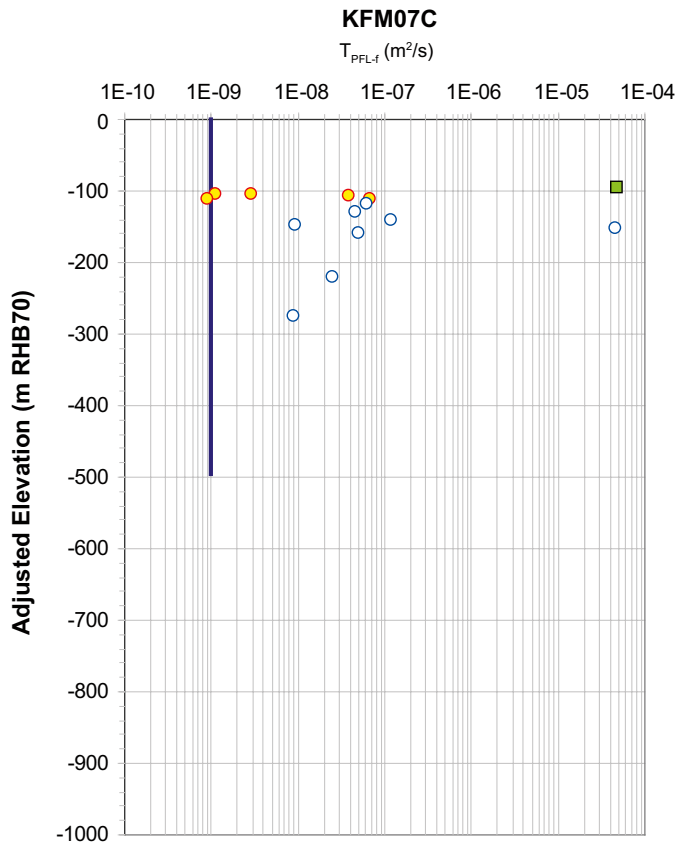


Figure 6-9. Elevation of the 14 PFL-f fracture transmissivity data observed in KFM07C. The fracture transmissivities are coloured with regard to their structural association as determined by their position along the borehole, cf the legend in Table 6-3. The blue line indicates both the practical measurement threshold of the PFL-f method, which is about $1 \cdot 10^{-9} \text{ m}^2/\text{s}$, and the depth of the borehole/PFL-f measurements. It is noted that the PFL-f measurements identified 15 flow anomalies. However, it has been concluded in the post-processing work that anomalies 14 and 15 are located in the same fracture (steeply dipping).

Table 6-12. Compilation of the PFL-f transmissivities measured in KFM07C with regard to rock domain (RFM), deformation zone (ZFM), fracture domain (FFM), borehole length (Secup/Seclow) and elevation (Elevup/Elevlow). The PFL-f transmissivities are given in $[\text{m}^2/\text{s}]$. The colours refer to the legend used in the transmissivity plot, cf Table 6-3.

RFM	ZFM	FFM	Secup	Seclow	Elevup	Elevlow	No. PFL-f	$\Sigma T \text{ PFL-F}$
029		02	85	92	82	88	0	0.00E+00
029	1203		92	103	88	99	1	4.81E-05
029		02	103	123	99	119	5	1.12E-07
029		01	123	308	119	303	8	4.71E-05
029	ENE2320		308	388	303	383	0	0.00E+00
029		01	388	429	383	424	0	0.00E+00
029	ENE2320		429	439	424	434	0	0.00E+00
029		01	439	498	434	493	0	0.00E+00

6.2.8 Drill site 8

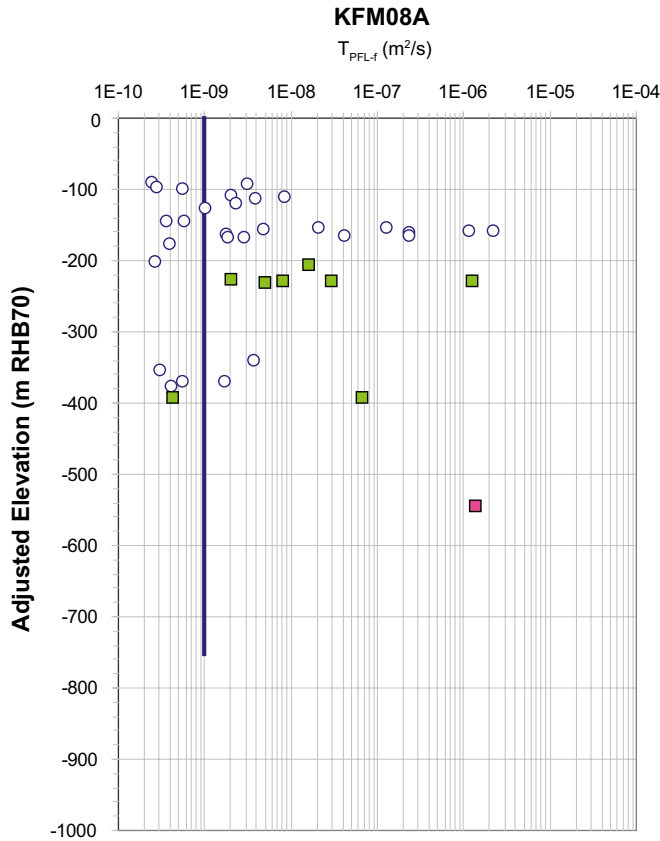


Figure 6-10. Elevation of the 41 PFL-f fracture transmissivity data observed in KFM08A. The fracture transmissivities are coloured with regard to their structural association as determined by their position along the borehole, cf the legend in Table 6-3. The blue line indicates both the practical measurement threshold of the PFL-f method, which is about $1 \cdot 10^{-9}$ m²/s, and the depth of the borehole/PFL-f measurements.

Table 6-13. Compilation of the PFL-f transmissivities measured in KFM08A with regard to rock domain (RFM), deformation zone (ZFM), fracture domain (FFM), borehole length (Secup/Seclow) and elevation (Elevup/Elevlow). The PFL-f transmissivities are given in [m²/s]. The colours refer to the legend used in the transmissivity plot, cf Table 6-3.

RFM	ZFM	FFM	Secup	Seclow	Elevup	Elevlow	No. PFL-f	Σ T PFL-F
029		01	102	172	86	144	9	2.20E-08
029		01	172	244	144	204	15	4.06E-06
029	ENE1061A		244	315	204	262	6	1.31E-06
029		01	315	479	262	392	8	1.47E-08
029	NNW1204		479	496	392	405	2	6.93E-08
029		01	496	528	405	430	0	0.00E+00
029	Possible		528	557	430	451	0	0.00E+00
029		01	557	624	451	500	0	0.00E+00
029	Possible		624	624	500	501	0	0.00E+00
029		01	624	672	501	536	0	0.00E+00
029	Possible		672	693	536	551	1	1.41E-06
029		01	693	775	551	608	0	0.00E+00
029	ENE2248		775	843	608	654	0	0.00E+00
032		05	843	915	654	700	0	0.00E+00
032	Possible		915	946	700	719	0	0.00E+00
034		01	946	967	719	732	0	0.00E+00
034	Possible		967	976	732	738	0	0.00E+00
034		01	976	1,001	738	753	0	0.00E+00

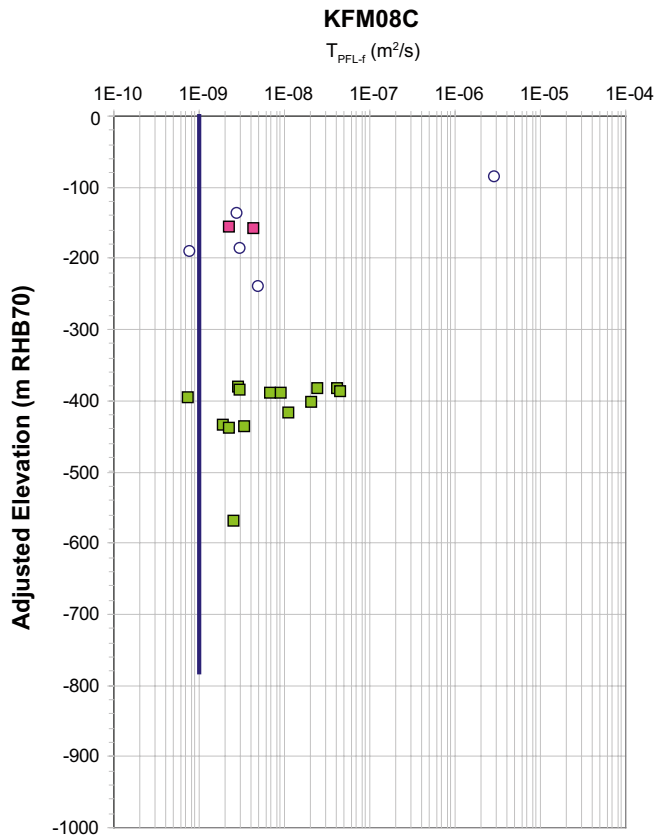


Figure 6-11. Elevation of the 21 PFL-f fracture transmissivity data observed in KFM08C. The fracture transmissivities are coloured with regard to their structural association as determined by their position along the borehole, cf the legend in Table 6-3. The blue line indicates both the practical measurement threshold of the PFL-f method, which is about $1 \cdot 10^{-9} \text{ m}^2/\text{s}$, and the depth of the borehole/PFL-f measurements.

Table 6-14. Compilation of the PFL-f transmissivities measured in KFM08C with regard to rock domain (RFM), deformation zone (ZFM), fracture domain (FFM), borehole length (Secup/Seclow) and elevation (Elevup/Elevlow). The PFL-f transmissivities are given in $[\text{m}^2/\text{s}]$. The colours refer to the legend used in the transmissivity plot, cf Table 6-3.

RFM	ZFM	FFM	Secup	Seclow	Elevup	Elevlow	No. PFL-f	$\Sigma T \text{ PFL-F}$
029		01	102	161	86	137	2	2.95E-06
029	Possible		161	191	137	162	2	6.68E-09
029		01	191	342	162	289	3	8.76E-09
045		06	342	419	289	353	0	0.00E+00
045	NNE2312		419	542	353	454	13	1.76E-07
045		06	542	546	454	457	0	0.00E+00
029		01	546	673	457	561	0	0.00E+00
029	WNW2225		673	705	561	586	1	2.61E-09
029		01	705	829	586	685	0	0.00E+00
029	ENE1061A, ENE1061B		829	832	685	687	0	0.00E+00
029		01	832	946	687	777	0	0.00E+00
029	ENE1061A		946	949	777	779	0	0.00E+00

6.2.9 Drill site 10

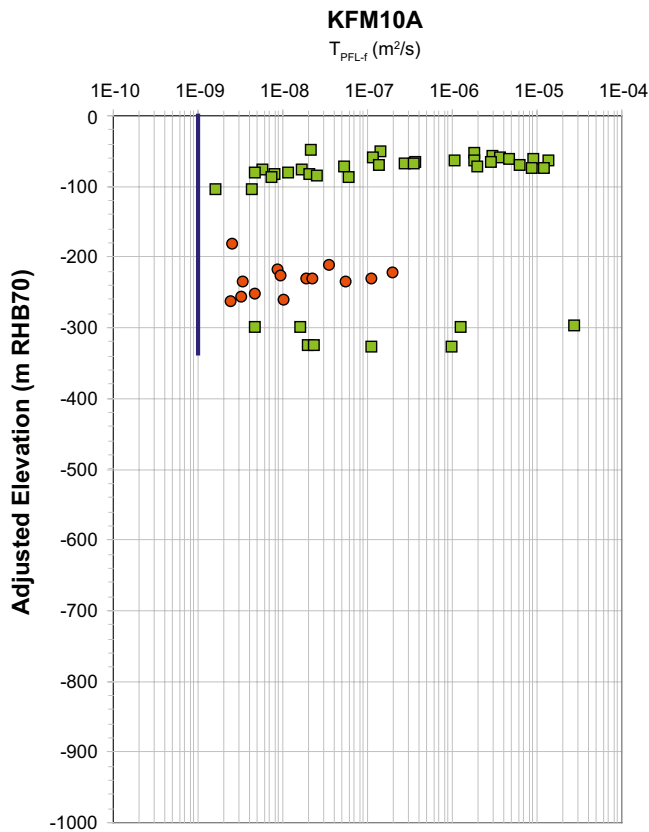


Figure 6-12. Elevation of the 56 PFL-f fracture transmissivity data observed in KFM10A. The fracture transmissivities are coloured with regard to their structural association as determined by their position along the borehole, cf the legend in Table 6-3. The blue line indicates both the practical measurement threshold of the PFL-f method, which is about $1 \cdot 10^{-9}$ m²/s, and the depth of the borehole/PFL-f measurements. It is noted that the two uppermost PFL-f flow anomalies are located in heavily fractured rock, and no core was retrieved during drilling.

Table 6-15. Compilation of the PFL-f transmissivities measured in KFM010A with regard to rock domain (RFM), deformation zone (ZFM), fracture domain (FFM), borehole length (Secup/Seclow) and elevation (Elevup/Elevlow). The PFL-f transmissivities are given in [m²/s]. The colours refer to the legend used in the transmissivity plot, cf Table 6-3.

RFM	ZFM	FFM	Secup	Seclow	Elevup	Elevlow	No. PFL-f	Σ T PFL-F
029	WNW0123		63	145	43	105	34	7.47E-05
029		03	145	275	105	196	1	2.61E-09
029	ENE2403		275	284	196	202	0	0.00E+00
029		03	284	430	202	296	14	4.98E-07
029	A2		430	449	296	307	3	2.92E-05
029		03	449	478	307	324	0	0.00E+00
029	A2		478	490	324	331	4	1.15E-06
029		01	490	500	331	337	0	0.00E+00

6.3 Summary

6.3.1 Summary of PFL-f fracture transmissivities in different fracture domains

It can be concluded from Figure 6-1 through Figure 6-12 that the dominant fracture domains in the site investigation are FFM01, FFM02 and FFM03. There are 103 PFL-f fracture transmissivities for FFM01, 81 for FFM02, 49 for FFM03, 15 for FFM04, 2 for FFM05 and 0 PFL-f fracture transmissivities for FFM06. This means that there are 329 PFL-f fracture transmissivities associated with deformation zones or possible deformation zones and 250 PFL-f fracture transmissivities associated with the fracture domains defined.

A summary of PFL-f fracture transmissivities for each fracture domain FFM01–06 is given in Table 6-16 to Table 6-21. Rough estimates of the bulk hydraulic conductivity over the whole volume of rock for each FFMxx give values of around 10^{-9} to 10^{-8} m/s, but of course this is not evenly distributed, being much higher in the upper rock.

Table 6-16. Summary of PFL-f fracture transmissivity statistics for FFM01. $P_{10,PFL}$ denotes the linear fracture frequency [m^{-1}], T denotes transmissivity [m^2/s].

BH	Σ Length	No. PFL	$P_{10,PFL}$	$P_{10,PFL,corr}$	Σ T PFL	Max T	Min T
KFM01A	693.49	9	0.013	0.019	5.47E-09	2.19E-09	2.67E-10
KFM01D	557.62	11	0.020	0.025	5.01E-07	1.83E-07	1.30E-09
KFM02A	413.36	10	0.024	0.039	1.90E-07	8.89E-08	6.16E-10
KFM03A	0.00	0	0.000	0.000	0.00	0.00	0.00
KFM04A	475.07	1	0.002	0.002	1.41E-09	1.41E-09	1.41E-09
KFM05A	580.12	1	0.002	0.002	1.86E-08	1.86E-08	1.86E-08
KFM06A	435.00	26	0.060	0.094	1.42E-05	9.43E-06	3.02E-10
KFM07A	594.00	1	0.002	0.002	9.27E-08	9.27E-08	9.27E-08
KFM07C	285.67	8	0.028	0.040	4.71E-05	4.68E-05	8.78E-09
KFM08A	536.81	32	0.060	0.092	4.10E-06	2.20E-06	2.48E-10
KFM08C	574.71	4	0.007	0.008	2.96E-06	2.95E-06	7.72E-10
KFM10A	9.98	0	0.000	0.000	0.00	0.00	0.00
All BH	5,155.83	103	0.020	0.030	6.92E-05	4.68E-05	2.48E-10

Table 6-17. Summary of PFL-f fracture transmissivity statistics for FFM02. $P_{10,PFL}$ denotes the linear fracture frequency [m^{-1}], T denotes transmissivity [m^2/s].

BH	Σ Length	No. PFL	$P_{10,PFL}$	$P_{10,PFL,corr}$	Σ T PFL	Max T	Min T
KFM01A	100.33	23	0.229	0.324	1.92E-07	5.31E-08	2.45E-10
KFM01D	91.33	23	0.252	0.334	5.33E-06	2.30E-06	6.59E-10
KFM05A	123.00	18	0.146	0.160	1.80E-06	1.06E-06	4.45E-10
KFM06A	25.79	12	0.465	0.929	8.13E-06	7.31E-06	1.37E-09
KFM07A	5.96	0	0.000	0.000	0.00	0.00	0.00
KFM07C	20.00	5	0.250	0.266	1.12E-07	6.86E-08	8.99E-10
All BH	366.41	81	0.221	0.306	1.56E-05	7.31E-06	2.45E-10

Table 6-18. Summary of PFL-f fracture transmissivity statistics for FFM03. $P_{10,PFL}$ denotes the linear fracture frequency [m^{-1}], T denotes transmissivity [m^2/s].

BH	Σ Length	No. PFL	$P_{10,PFL}$	$P_{10,PFL,corr}$	Σ T-PFL	Max T	Min T
KFM02A	209.46	12	0.057	0.093	1.05E-06	6.77E-07	4.26E-09
KFM03A	819.22	23	0.028	0.071	6.02E-07	1.89E-07	1.09E-09
KFM10A	305.30	14	0.046	0.061	4.98E-07	2.04E-07	2.46E-09
All BH	1,333.98	49	0.037	0.072	2.15E-06	6.77E-07	1.09E-09

Table 6-19. Summary of PFL-f fracture transmissivity statistics for FFM04. $P_{10,PFL}$ denotes the linear fracture frequency [m^{-1}], T denotes transmissivity [m^2/s].

BH	Σ Length	No. PFL	$P_{10,PFL}$	$P_{10,PFL,corr}$	Σ T-PFL	Max T	Min T
KFM04A	154.90	15	0.097	0.160	1.15E-06	2.80E-07	4.59E-09
All BH	154.90	15	0.097	0.160	1.15E-06	2.80E-07	4.59E-09

Table 6-20. Summary of PFL-f fracture transmissivity statistics for FFM05. $P_{10,PFL}$ denotes the linear fracture frequency [m^{-1}], T denotes transmissivity [m^2/s].

BH	Σ Length	No. PFL	$P_{10,PFL}$	$P_{10,PFL,corr}$	Σ T-PFL	Max T	Min T
KFM07A	50.00	2	0.040	0.182	4.00E-07	2.00E-07	2.00E-07
KFM08A	72.00	0	0.000	0.000	0.00	0.00	0.00
All BH	122.00	2	0.016	0.075	4.00E-07	2.00E-07	2.00E-07

Table 6-21. Summary of PFL-f fracture transmissivity statistics for FFM06. $P_{10,PFL}$ denotes the linear fracture frequency [m^{-1}], T denotes transmissivity [m^2/s].

BH	Σ Length	No. PFL	$P_{10,PFL}$	$P_{10,PFL,corr}$	Σ T-PFL	Max T	Min T
KFM06A	129.37	0	0.000	0.000	0.00	0.00	0.00
KFM08C	81.00	0	0.000	0.000	0.00	0.00	0.00
All BH	210.37	0	0.000	0.000	0.00	0.00	0.00

6.3.2 Orientation and statistics of flowing features associated with the PFL-f fracture transmissivities

/Forsman et al. 2004/, /Forsman et al. 2006/ and /Teurneau et al. 2007/ have performed cross-analyses between Boremap data, BIPS data and PFL-f fracture transmissivity data. In effect, each PFL-f fracture transmissivity (flow anomaly) is associated with a fracture mapped in the bore core logs.

Figure 6-13, Figure 6-14 and Figure 6-15 show stereographic pole plots of the orientations of each of the fractures associated with PFL-f fracture transmissivities in fracture domains FFM01, FFM02, and FFM03. For FFM01, the flow is strongly dominated by horizontal and gently-dipping fractures, with a small handful of features that strike NE or NNE. This is also true of FFM02. In both cases, the highest transmissivities are all in horizontal and gently-dipping fractures. The orientation of the gently dipping fractures has a NNE component within the HZ set. Hence, flow is strongly anisotropic in FFM01 and FFM02. In FFM03, flow is more dispersed in terms of orientation, or more isotropic. Although horizontal and gently-dipping fractures still dominate there is less concentration at the centre of the stereonet.

In order to identify any depth dependence, Figure 6-16 and Figure 6-17 show stereonet for FFM01–FFM03 for above and below an elevation of –400 m elevation. The interesting thing here is that even with FFM03 included, fracture transmissivities below –400 m are restricted to horizontal and gently-dipping fractures. Therefore, the distribution of fracture transmissivities is strongly anisotropic for much of the rock influencing the hydrogeology of the site even many kilometres away within the tectonic lens.

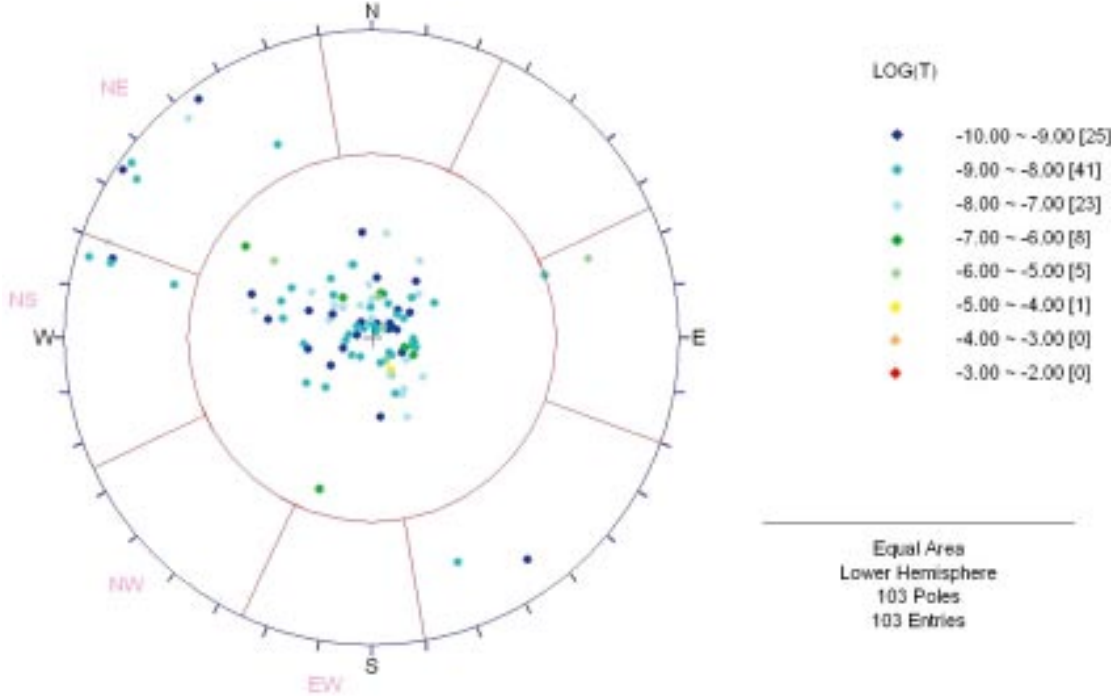


Figure 6-13. Pole plot for PFL-f fracture transmissivities within FFM01 and any borehole. The poles are coloured by LOG10(transmissivity) and use an equal area lower hemisphere projection. A division of the stereonet into sectors is inserted to demonstrate the hard sectors used in the hydrogeological DFN modelling in SDM 1.2 /SKB 2005a/.

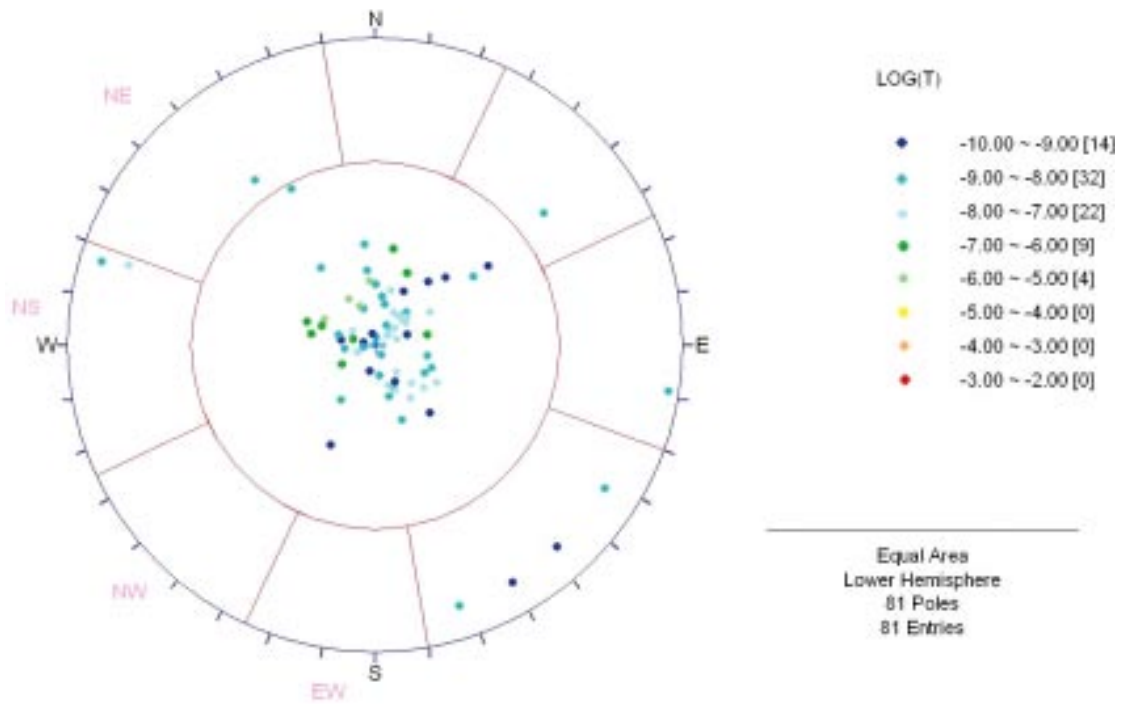


Figure 6-14. Pole plot for PFL-f fracture transmissivities within FFM02 and any borehole. The poles are coloured by LOG10(transmissivity) and use an equal area lower hemisphere projection. A division of the stereonet into sectors is inserted to demonstrate the hard sectors used in the hydrogeological DFN modelling in SDM 1.2 /SKB 2005a/.

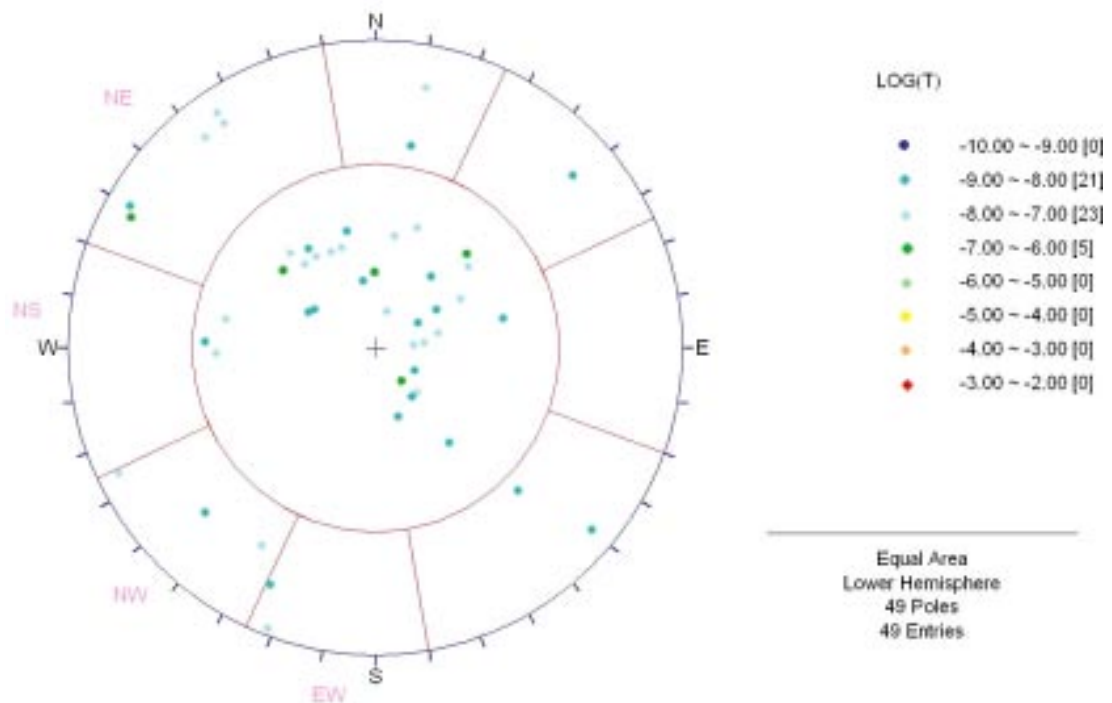


Figure 6-15. Pole plot for PFL-f fracture transmissivities within FFM03 and any borehole. The poles are coloured by LOG10(transmissivity) and use an equal area lower hemisphere projection. A division of the stereonet into sectors is inserted to demonstrate the hard sectors used in the hydrogeological DFN modelling in SDM 1.2 /SKB 2005a/.

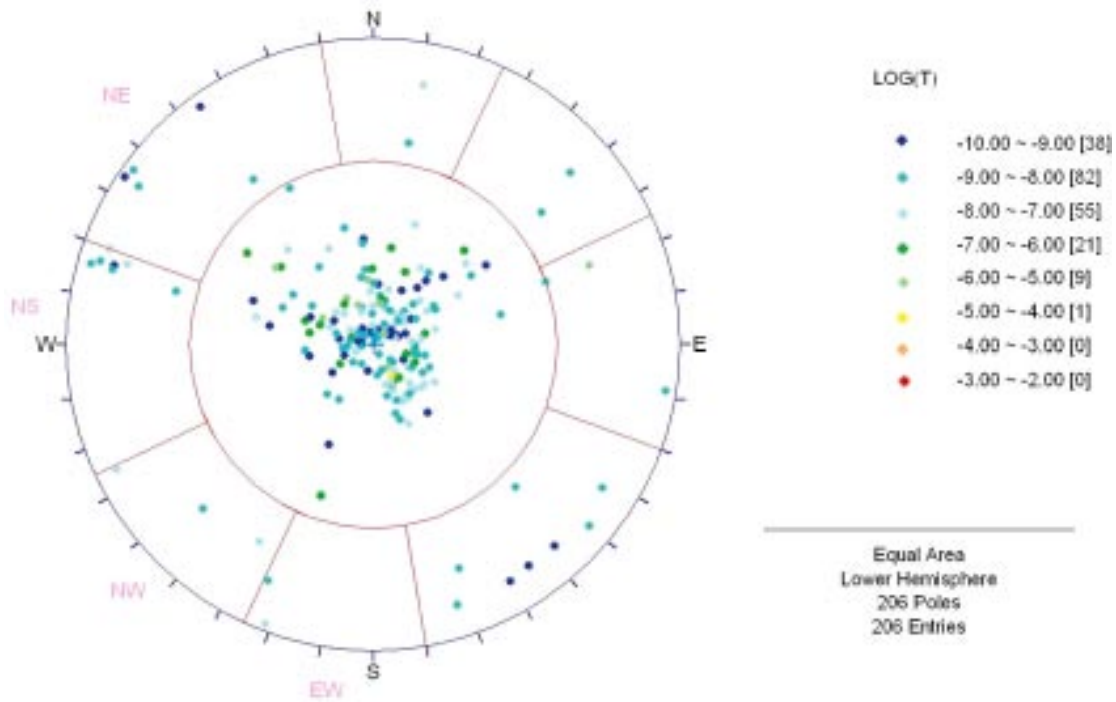


Figure 6-16. Pole plot for PFL flow-anomaly fractures within FFM01–FFM03 above an elevation of 400 m and any borehole. The poles are coloured by LOG10(transmissivity) and use an equal area lower hemisphere projection. A division of the stereonet into sectors is inserted to demonstrate the hard sectors used in the hydrogeological DFN modelling in SDM 1.2 /SKB 2005a/.

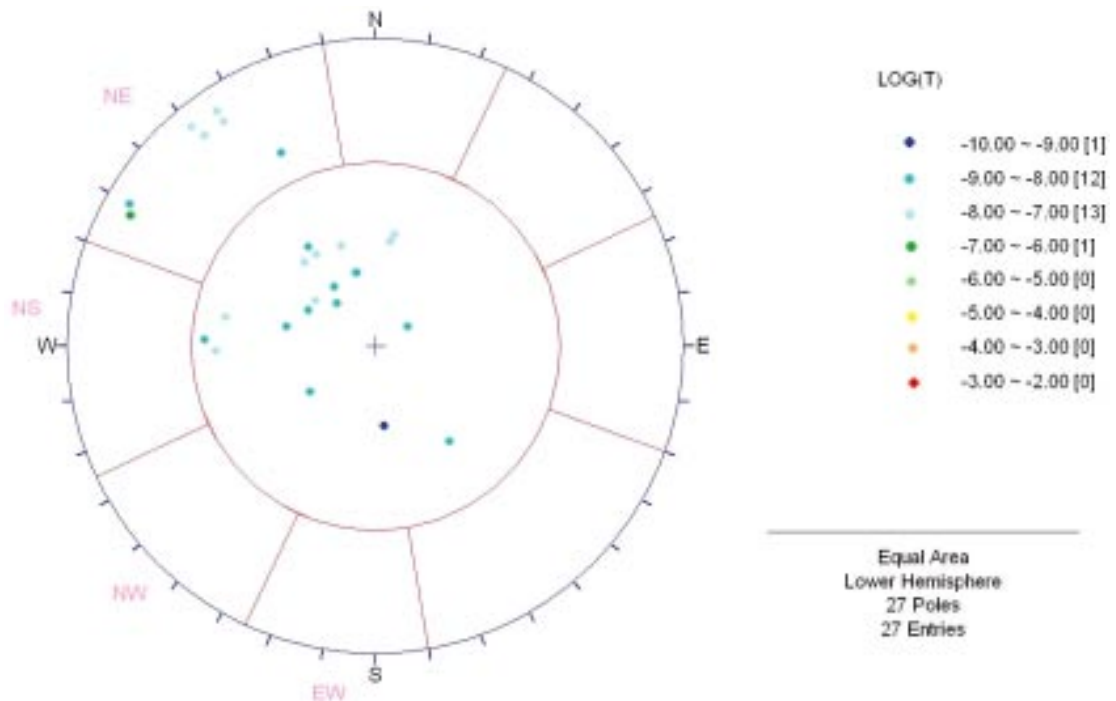


Figure 6-17. Pole plot for PFL flow-anomaly fractures within FFM01–FFM03 below an elevation of 400 m and any borehole. The poles are coloured by LOG10(transmissivity) and use an equal area lower hemisphere projection. A division of the stereonet into sectors is inserted to demonstrate the hard sectors used in the hydrogeological DFN modelling in SDM 1.2 /SKB 2005a/.

7 Hydrogeochemical data in the context of fracture domains and deformation zones

7.1 Data selection

Available hydrogeochemical data are presented in Appendix 1, Table A1-3. Besides groundwater data from boreholes into the bedrock, the table also lists data on precipitation, surface waters and near surface groundwaters in soil pipes. The latter data group is clearly irrelevant from a fracture domain context and is therefore not treated in the present report.

Hydrogeochemical borehole data, selected for the fracture domain discussion, are compiled in a table that will be made available in the SKB model database. The content is explained in more detail in Table 7-1. The compilation is based on the extensive data table produced by the interpretation team Chemnet from the hydrochemical data freeze 2.2 with the following modifications:

- Data on precipitation, surface waters and near surface groundwaters in soil pipes are excluded.
- Hydrogeological and geological information on flow anomalies as well as deformation zones and fracture domains are introduced.
- The intention has been to select one data record for each represented flow anomaly. Therefore, a number of data records from overrepresented fractures or fracture zones are omitted.
- The samples included in data freeze 2.2, and classified as representative (orange coloured data records) or close to representative (green colour) by the interpretation team with the collaboration of responsible site personal, have been preferred. Two additional samples (pink colour) with too large a flushing water content to be included in either of the previous two groups (between 5 and 10%) are also included. These samples provide additional information at supplementary depths.
- Calculated TDS and water density values are included.

Matrix pore water data and associated geological entities are treated briefly in the text and presented in WellCad diagrams in Appendix 5, but are not included in the data compilation table for fracture domains.

7.1.1 Investigations

Groundwater sampling from boreholes for chemical analyses has been performed by several methods and in some boreholes on more than one occasion. The quality and representativity of the water samples with respect to depth, however, differs depending on method used as well as on sampling occasion. High flushing water content and/or sampling at open borehole conditions were two reasons to exclude data from the compilation.

Repeated sampling has been performed in some water-bearing fractures or fracture zones in cored boreholes (KFM01A, KFM02A and KFM03A). These fractures were first chemically characterized during a more than three weeks long investigation campaign, and later on sampling was performed within the long-term hydrochemical monitoring programme. Changes in water composition may be caused either by the existence of the borehole or by the effects of subsequent investigation activities. A sample from the earlier chemical characterization campaign was therefore usually selected to represent the flow anomaly. The percussion boreholes have been investigated either only once by pumping/sampling from the entire borehole in connection with pumping tests or first in connection with pumping tests and later on in shorter packered-off sections within the subsequent hydrochemical monitoring programme. If only one clearly dominant flow anomaly exists, samples from entire boreholes or very long sections were considered representative for that particular flow anomaly. Samples from monitored shorter sections were preferred in cases with stable water composition.

7.1.2 Components and parameters

A large number of chemical constituents and parameters are determined from each groundwater sample. Most of them are compiled in the data compilation for fracture domains together with hydrogeological information on flow anomalies as well as geological information on deformation zones and fracture domains. The content of the data compilation is explained in Table 7-1.

The groundwaters in Forsmark are mixtures of waters of mainly four different origins; 1) water of meteoric origin, 2) Littorina seawater, 3) glacial meltwater and 4) deep saline groundwater (brine) /SKB 2005c/. The constituents and parameters that most clearly reveal or indicate the groundwater character or origin may be of importance for the geological fracture model. These constituents and parameters are discussed below.

Salinity

The spatial distribution of the salinity (or chloride concentration) provides a basic understanding of the hydrogeochemical conditions at the investigation site. The saline component may originate from relict seawater (Littorina) or deep saline groundwater and possibly also from modern Baltic Sea water (brackish water in shallow systems close to the coast).

Chloride concentration, EC (electrical conductivity), TDS (Total Dissolved Solids) and water density are parameters related to the salinity of the sample and show more or less linear relationships, see Figure 7-1 to Figure 7-3. Since chloride is generally conservative in normal groundwater systems, it is often used as one of the variables in X-Y plots in order to study hydrochemical trends. Chloride concentration and EC are measured in the samples. TDS is not determined experimentally (by evaporation to dryness) but the data compilation table available in the SKB model database includes calculated TDS from water composition. A satisfactory estimation of TDS may be obtained from EC by using the expression below, which applies to deep groundwaters in Forsmark.

$$\text{TDS}_{(\text{mg/L})} = 6.2 \times \text{EC}_{(\text{mS/m})}$$

Table 7-1. Groups of parameters and constituents included or excluded from the data compilation table for fracture domains.

Parameter/constituent group	Included	Excluded
Sample identification	X	
Sample location, date and SKB class no.	X	
Coordinate information	(X)	
Inferred flow anomaly (Hydrogeological information)*	X	
SHI from Sicada/P-reports, Geological model version 2.2	X	
Basic physical and chemical parameters including calculated TDS and water density	X	
Major constituents	X	
Nutrients and organic carbon	(X)	
Trace elements	(X)	
Uranium and Thorium (µg/L)	X	
Isotopes Ia (Deuterium, tritium and δ18O)	X	
Isotopes Ib (δ34S, δ37Cl, δ13C, pmC, 10B/11B, 87Sr/86Sr)	(X)	
Isotopes II (238U, 234U, 230Th, 222Rn, 226Ra)	(X)	
Gases (dissolved)		X
Microbes		X
C-organic isotopes		X
Colloids		X

(X) = Hidden columns.

* Transmissivity values are generally selected from PFL flow logging results. The location of the anomaly and fracture transmissivity are given if no more than two flow anomalies are observed within the sampled section. Otherwise, the transmissivities from 5 m sections are presented.

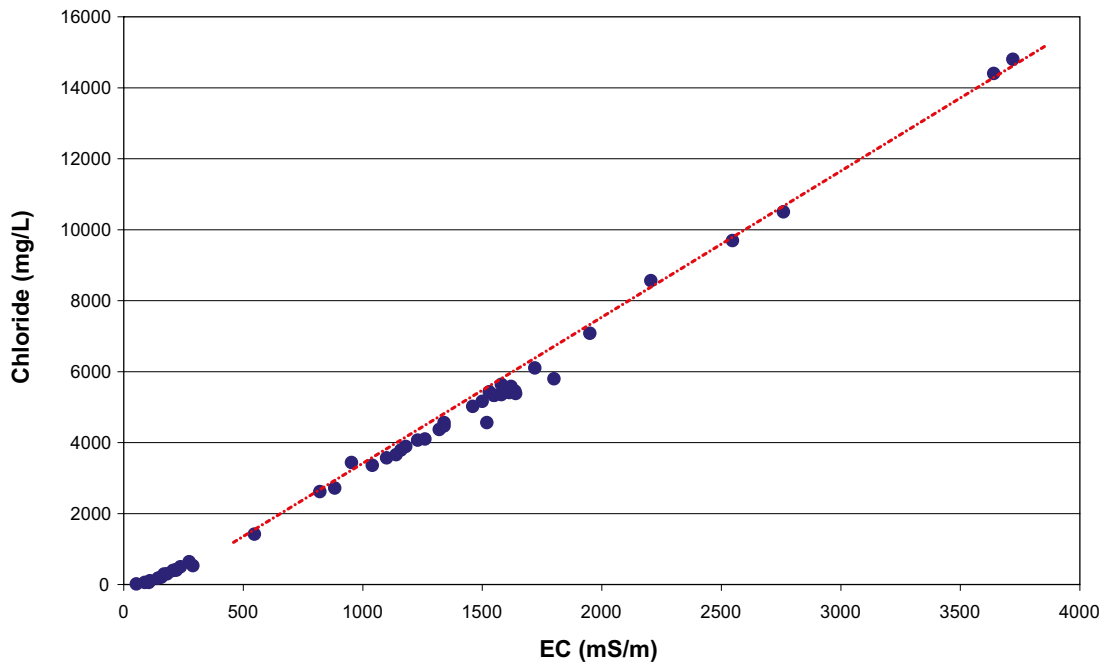


Figure 7-1. Chloride concentration versus electrical conductivity (EC). Groundwater data from Forsmark.

Figure 7-2 shows TDS calculated from water composition versus TDS calculated from EC. The factor to be used to convert EC to TDS varies depending on type of water (generally between 5.5 and 9) and the factor value for surface waters or seawaters, for example, may have other values.

Water density and EC at 25°C have been determined from a number of samples collected from tubes in the borehole installations for pressure monitoring at Forsmark, see Figure 7-3. Linear regression gives the following expression for the line:

$$\text{Density}_{(\text{kg/m}^3)} = 997.075 + 0.004369 \times \text{EC}_{(\text{mS/m})}$$

Calculated water density is included in the data compilation table available in the SKB model database.

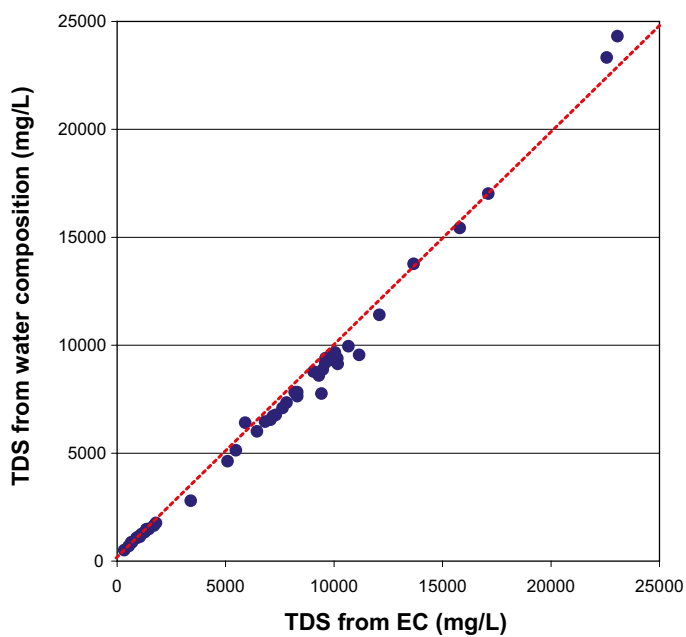


Figure 7-2. TDS from water composition versus TDS calculated from EC. $\text{TDS}_{\text{EC}} = 6.2 \times \text{EC}(\text{mS/m})$.

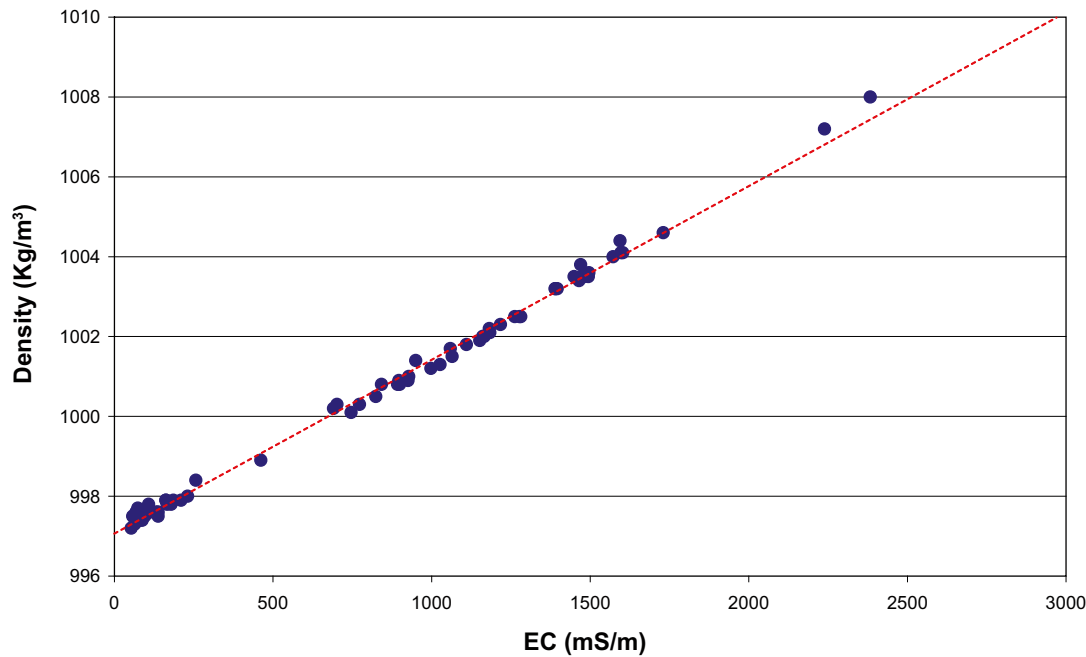


Figure 7-3. Water density (Kg/m³) versus EC(mS/m). Samples collected from tubes in the borehole installations for pressure monitoring at Forsmark. Linear regression gives $density_{25^{\circ}C} = 997.075 + 0.004369 \times EC_{25^{\circ}C}$.

Calcium and sodium

Shallow groundwaters in the overburden often contain high calcium concentrations. This is especially true at the Forsmark site with its calcareous till. Sodium dominates over calcium in the bedrock at shallow and intermediate depths, while calcium is the predominant cation even in the deepest groundwaters. This fact serves as a basis for subdivision into different water types, and the depths at which changes occur are informative.

Magnesium, sulphate and bromide

High magnesium and sulphate concentrations, as well as a low bromide to chloride ratio, indicate a marine origin of the groundwater. Ion exchange processes in the bedrock fracture systems may weaken the marine water signature by causing a decrease in Mg and Na and enrichment of Ca. In Forsmark, however, the observed clear difference in magnesium concentration between intermediate water of Littorina type and deep groundwaters indicates that the effect of ion exchange is less pronounced.

$\delta^{18}O$ signature

A higher $\delta^{18}O$ value generally indicates marine origin and lower $\delta^{18}O$ values for the deeper, more saline groundwaters, indicates a distinct cold climate recharge (glacial) component. However, water-rock interaction also increases the $\delta^{18}O$ values in the groundwater, which complicates the interpretation, especially with regard to matrix pore water. The modelled $\delta^{18}O$ value for Littorina sea water is -4.7% SMOW while the value for fresh glacial meltwater is -25% SMOW. Groundwaters from intermediate depths in Forsmark with chloride concentrations of around 4,000–5,500 mg/L and $\delta^{18}O$ values between -9 and -12% SMOW have been interpreted as Littorina Sea/glacial water mixtures.

Tritium

Tritium contents in excess of the detection limit 0.8 TU reveal the presence of a modern meteoric water component in groundwaters. If groundwater sampled below 200 m depth contains tritium, it is most probably due to flushing water contamination from drilling the borehole. Contact within the fracture network with more shallow modern water is, however, possible.

Redox potential (Eh)

The Eh value does not usually exhibit simple depth dependence and the factors that govern the redox conditions are complex. Nevertheless, the possibility of revealing a pattern in the fracture domain context is worth exploring.

7.2 Drill site overview

7.2.1 Drill site 1

The groundwater composition in the bedrock volume penetrated by the boreholes at drill site 1 (DS1) has been studied thoroughly compared to most other drill sites. Table 7-2 lists the borehole investigations and borehole sections providing the data that are included in the data compilation table available in the SKB model database. Aside from the shallow sections in the percussion boreholes HFM01, HFM02 and HFM27, which represent the deformation zones ZFMA2 and ZFM1203, the groundwater data reflect conditions within the two fracture domains FFM02 (HFM03 and KFM01A) and FFM01 (KFM01D).

The most striking observation at drill site DS1 is the difference in water type between the two investigated shallow sections of borehole KFM01A (at 112 m and 176 m depths) and the two deeper sections of borehole KFM01D (at 341 m and 445 m depths). The groundwaters from the

Table 7-2. Boreholes, investigations and borehole sections providing the selected hydrochemical data at DS1 and assigned geological entities.

IDcode	Investigation	Borehole section (m borehole length)	Secmid elevation (m.b.s.l.)	Fracture domain or deformation zone
HFM01	Sampling in connection with pumping tests (HTHB)	34.5–43.5*	36.5	ZFMA2
HFM02	Long-term hydrochemical monitoring	38.0–48.0	39.9	ZFM1203
HFM03	Sampling in connection with pumping tests (HTHB)	21.0–21.5*	18.1	FFM02
HFM27	Sampling in connection with pumping tests (HTHB)	46.0–58.0	45.6	ZFM1203
KFM01A	Sampling in connection with pumping tests (HTHB)	0.0–100.6	46.9	ZFMA2 (FFM02)
KFM01A	Complete hydrochemical characterization	110.0–120.8 176.8–183.9	111.8 176.3	FFM02 FFM02
KFM01A	Long-term hydrochemical monitoring	109.0–130.0**	110.8	FFM02
KFM01D	Matrix pore water investigation	–	–	See Table 7-3
KFM01D	Complete hydrochemical characterization	428.5–435.6 568.0–575.1	340.9 445.2	FFM01 FFM01
KFM01D	Sampling using hydrotest equipment	314.5–319.5	253.0	FFM01
KFM01D	Sampling of low hydraulic transmissive fractures (LTF)	194.0–196.0 263.8–264.8 354.9–355.9 369.0–370.0	155.7 211.4 282.3 293.1	FFM01 FFM01 FFM01 FFM01

* Flow anomaly position.

** Data record excluded.

two borehole sections in borehole KFM01A display a clearly marine Littorina origin, while the two deeper sections in borehole KFM01D display a mainly non-marine origin. The chemical conditions in the groundwaters at drill site DS1 are summarized in the following points:

- Similar chloride concentrations were observed in the depth ranges 110–180 m in borehole KFM01A and 340–450 m in KFM01D, see Figure 7-4a.
- High magnesium concentrations and low bromide to chloride ratios in the groundwater in the depth range 110–180 m in borehole KFM01A, representing fracture domain FFM02, indicate a marine origin of the water, i.e. Littorina sea water. Low magnesium concentrations and relatively high bromide to chloride ratios in the groundwater in the depth range 340–450 m in borehole KFM01D, representing fracture domain FFM01, indicate a non-marine origin, see Figure 7-4b and Figure 7-4c.
- Relatively low chloride concentrations (3,400–4,000 mg/L) were measured in the groundwaters sampled at the intermediate depths (150–295 m) in the four low transmissive fractures representing fracture domain FFM01, see Figure 7-4a. Furthermore, the magnesium concentrations and the bromide to chloride ratios fall between the two extremes discussed above, see Figure 7-4b and Figure 7-4c. The bedrock properties and the absence of zones seem to prevent saline Littorina sea water from penetrating into the bedrock to the same extent as in fracture domain FFM02. The observations from the highly transmissive fracture at 253 m vertical depth, see next point, indicate that the water composition reflects properties of the groundwater in bedrock between deformation zones at this depth range rather than conditions unique to low transmissive fractures or artefacts due to the use of a special sampling technique /Nilsson et al. 2006/.
- The highly transmissive fracture at 253 m vertical depth in KFM01D also exhibited a rather low chloride concentration (3,890 mg/L). Furthermore the magnesium concentration and the bromide to chloride ratio were similar to corresponding values obtained from the low transmissive fractures.

Fourteen selected short core samples along borehole KFM01D were investigated by out-diffusion experiments to obtain information on the composition of the water in connected pores in the rock material /Waber and Smellie 2007/. Fracture domains or deformation zones associated with each sample are listed in Table 7-3. Figure 7-5 displays chloride concentrations

Table 7-3. Available matrix pore water data along KFM01D and assigned fracture domains or deformation zones.

Matrix pore water	Secup (m borehole length)	Seclow (m borehole length)	Secmid elevation (m.b.s.l.)	Fracture domain or deformation zone
KFM01D	140.47	140.91	112.13	FFM02
KFM01D	191.57	191.89	153.68	FFM01
KFM01D	254.93	255.32	204.57	FFM01
KFM01D	298.94	299.24	239.33	FFM01
KFM01D	351.94	352.20	280.50	FFM01
KFM01D	393.50	393.88	312.47	FFM01
KFM01D	462.59	462.98	365.42	FFM01
KFM01D	499.90	500.20	393.49	FFM01
KFM01D	544.11	544.35	426.54	FFM01
KFM01D	600.10	600.39	468.02	FFM01
KFM01D	642.92	643.31	499.50	FFM01
KFM01D	700.07	700.43	541.00	FFM01 (ZFMENE0061)
KFM01D	747.09	747.49	574.82	FFM01
KFM01D	790.38	790.73	605.62	FFM01

in matrix pore water from borehole KFM01D together with “fracture water” from borehole sections below the deformation zones ZFMA2 and ZFMF1 (the foot wall) i.e. fracture domain FFM01. The WellCad diagram in Appendix 5 permits comparison of matrix pore water data with geological and hydrogeological properties along the borehole on a detailed scale. This is necessary in the case of pore water, since the fracture domain concept is likely to offer too coarse a classification.

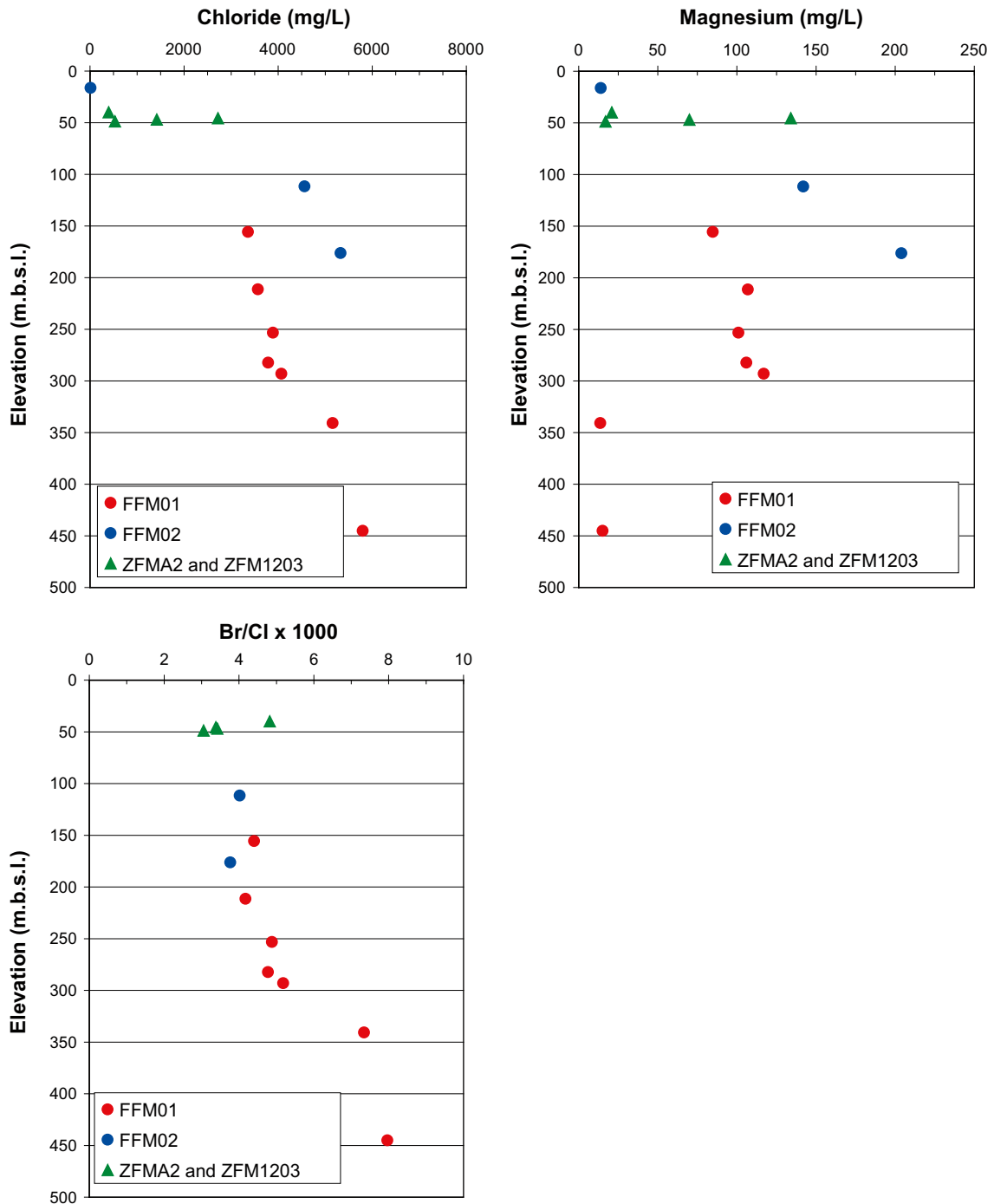


Figure 7-4a–c. Chloride, magnesium and bromide to chloride ratio versus vertical depth in boreholes HFM01, HFM02, HFM03, HFM27, KFM01A and KFM01D at drill site 1. Modelled geological entities are indicated by a colour code.

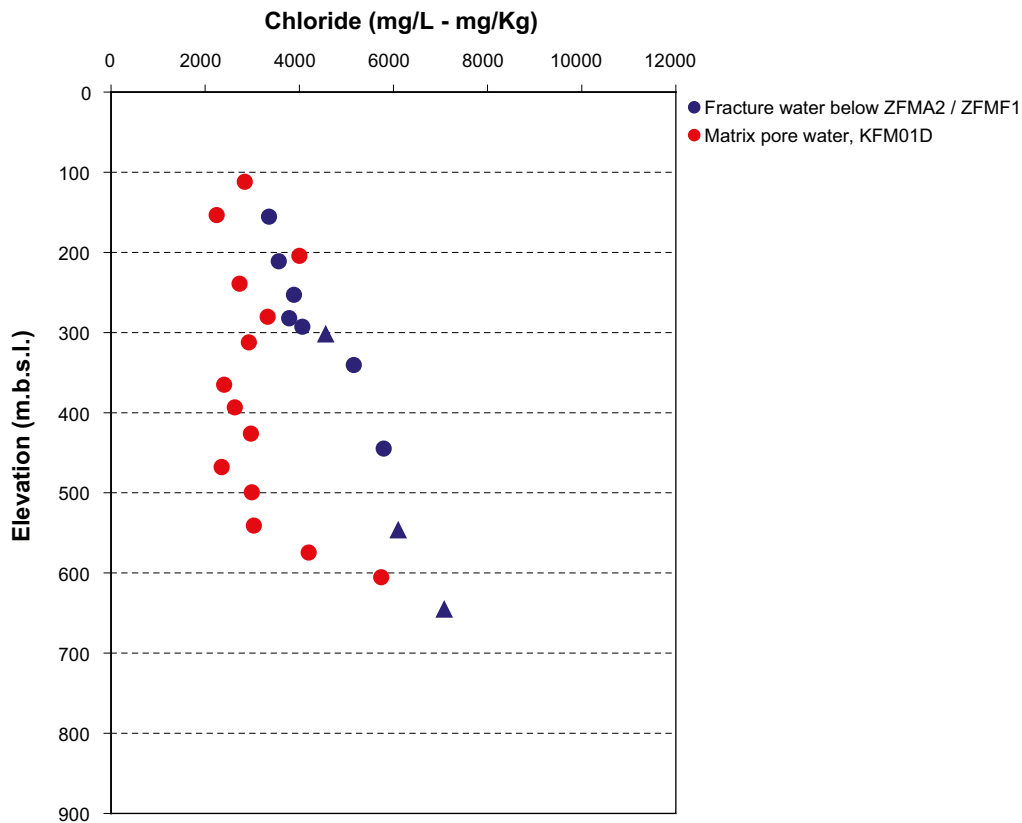


Figure 7-5. Comparison of chloride concentrations between matrix pore water from KFM01D and “fracture water” from borehole sections below deformation zones ZFMA2–ZFMF1 (boreholes HFM22, KFM01D, KFM06A and KFM08A). Samples assigned to fracture domains and deformation zones are shown as filled-in circles and triangles, respectively.

7.2.2 Drill site 2

The groundwater composition in the bedrock volume penetrated by the boreholes at drill site 2 (DS2) has been studied in three boreholes, KFM02A, HFM04, and HFM05. Table 7-4 lists the borehole investigations and borehole sections providing the data that are included in the data compilation table available in the SKB model database. All groundwater data from DS2 reflect conditions within deformation zones, particularly the major zones ZFMA2 and ZFMF1. The shallow sections in HFM04, HFM05 and KFM02A are more extended than the actual zones and also partly include fracture domain FFM03.

Table 7-4. Boreholes, investigations and borehole sections providing the selected hydrochemical data at DS2 and assigned geological entities.

IDcode	Investigation	Borehole section (m borehole length)	Secmid elevation (m.b.s.l.)	Fracture domain or deformation zone
HFM04	Long term hydrochemical monitoring	58.0–66.0	57.9	ZFM866 (FFM03)
HFM05	Sampling in connection with pumping tests (HTHB)	150.0–156.5*	144.6	ZFM866 (FFM03)
KFM02A	Sampling using hydrotest equipment	106.5–126.5	108.9	ZFM866 (FFM03)
		413.5–433.5	414.7	ZFMA2
KFM02A	Complete hydrochemical characterization	509.0–516.1	503.3	ZFMF1
KFM02A	Long-term hydrochemical monitoring	411.0–442.0**	414.7	ZFMA2
		490.0–518.0	494.8	ZFMF1

* Flow anomaly position.

** Data record excluded.

Besides the presence of fresh water or nearly fresh water in the shallow borehole sections between 58 m and 157 m, the deeper groundwaters display a clear Littorina sea water character /SKB 2005c/. The chloride concentration in this limited depth interval is relatively constant and amounts to between 5,380 mg/L and 5,540 mg/L, while the magnesium concentration exceeds 190 mg/L.

7.2.3 Drill site 3

The groundwater composition in the bedrock volume penetrated by the boreholes at drill site 3 (DS3) has mainly been studied in one borehole, KFM03A, although some data exist from percussion boreholes HFM06 and HFM08. Table 7-5 lists the borehole investigations and borehole sections providing the data included in the data compilation table available in the SKB model database. Most of these groundwater data (eight out of ten flow anomalies) reflect the conditions within frequently occurring gently dipping deformation zones. The bedrock between zones from the surface to 1,000 m depth is interpreted as fracture domain FFM03. Borehole KFM03A is the only investigated borehole included in DF 2.2 with samples from flow anomalies that are associated solely with fracture domain FFM03. These two anomalies are found at a very shallow and a very deep location, respectively. A comparison of the hydrogeochemical properties in fracture domain FFM03 with those in fracture domain FFM01 is not possible due to a lack of hydrogeochemical information from bedrock between zones in fracture domain FFM03 in the depth range 100–500 m.

The investigated borehole sections at drill site DS3 reveal a gradual change in the water composition with depth in the gently dipping minor deformation zones penetrating fracture domain FFM03 and within FFM03 itself. This depth dependence is summarized as follows (see Figure 7-6 and WellCad diagram in Appendix 5):

- Sharply increasing chloride concentration and increasing marine character of the groundwater down to approximately 150 m depth. This trend is supported by the increase in magnesium concentration as well as a relatively low bromide to chloride ratio.
- Constant chloride concentration in the depth range between 150 to around 550 m. High magnesium concentrations and low bromide to chloride ratios indicate a marine origin of the water, i.e. Littorina sea water.
- A gradual change of water type from marine origin towards a mixture of glacial meltwater and deep saline groundwater from nearly 600 m depth and increasing chloride concentration from below 600 m.

Table 7-5. Boreholes, investigations and borehole sections providing the selected hydrochemical data at DS3 and assigned geological entities.

IDcode	Investigation	Borehole section (m borehole length)	Secmid elevation (m.b.s.l.)	Fracture domain or deformation zone
HFM06	Sampling in connection with pumping tests (HTHB)	69.0–71.0*	63.0	ZFMA5
HFM08	Sampling in connection with pumping tests (HTHB)	89.5–90.0* 137.5–139.5*	82.4 130.4	FFM03 ZFMA5
KFM03A	Sampling using hydrotest equipment	386.0–391.0 448.0–453.0** 803.2–804.2**	379.1 440.8 792.1	ZFMA4 ZFMA7 ZFMA3
KFM03A	Complete hydrochemical characterization	448.5–455.6 639.0–646.1 939.5–946.6 980.0–1,001.2	442.4 631.9 930.5 977.7	ZFMA7 ZFMB1 DZ*** FFM03
KFM03A	Long-term hydrochemical monitoring	633.5–650.0** 969.5–994.5**	631.1 969.1	ZFMB1 FFM03

* Flow anomaly position.

** Data record excluded.

*** DZ not modelled.

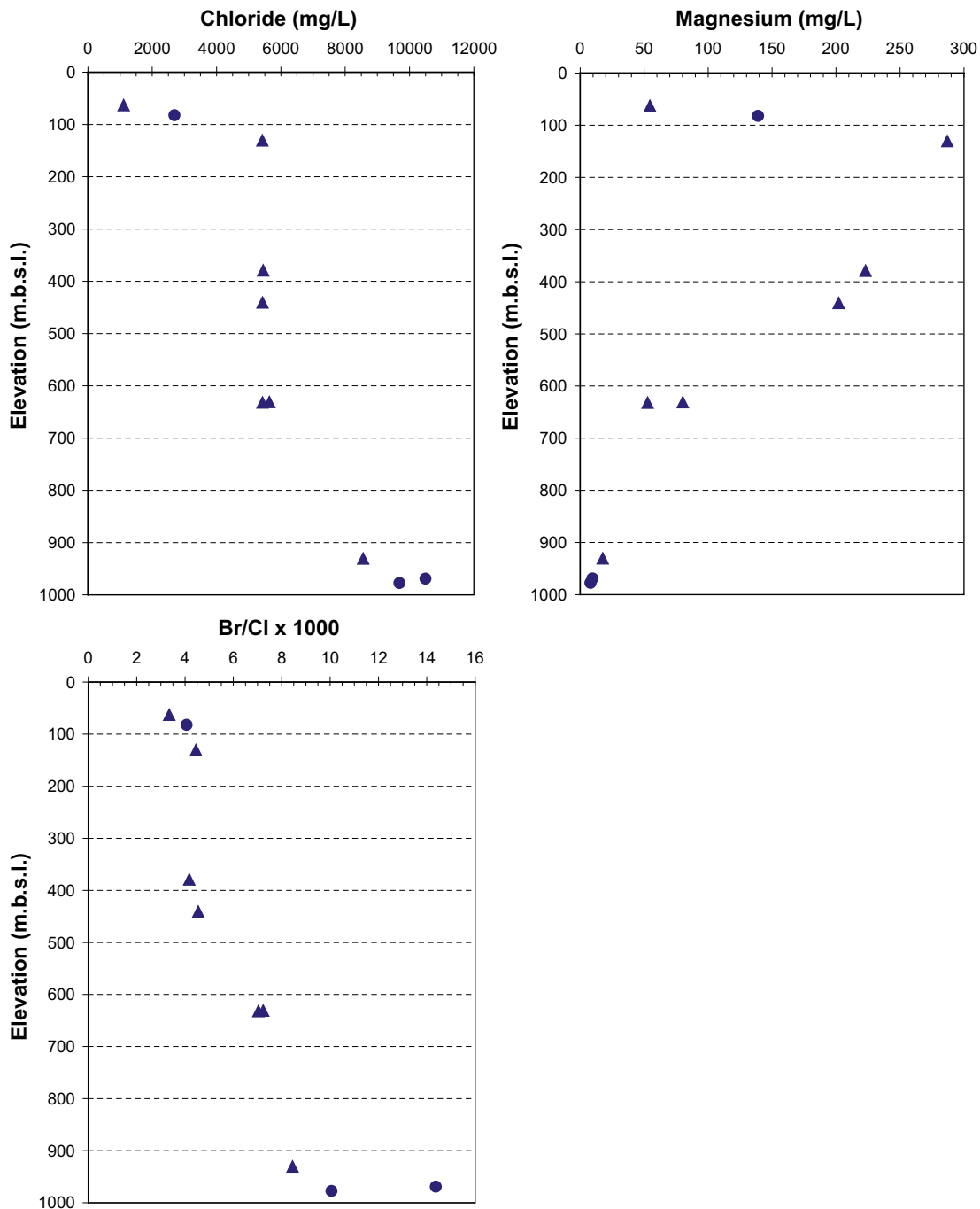


Figure 7-6a-c. Chloride, magnesium and bromide to chloride ratio versus vertical depth. Boreholes HFM06, HFM08 and KFM03A at drill site DS3. The geological entities are fracture domain FFM03 (filled-in circles) and penetrating gently dipping deformation zones (triangles).

7.2.4 Drill site 4

The groundwater composition in the bedrock volume penetrated by the boreholes at drill site 4 (DS4) has been studied in boreholes, KFM04A, HFM09 and HFM10. Table 7-6 lists the borehole investigations and borehole sections providing the data included in the data compilation table available in the SKB model database. The data from borehole KFM04A represent deformation zone ZFMA2 combined with the strongly foliated and banded bedrock with north-west strike along the south-western margin of the candidate area (included in fracture domain FFM04) and also the percussion boreholes represent shallow deformation zones with a large water yield.

Table 7-6. Boreholes, investigations and borehole sections providing the selected hydrochemical data at DS4 and assigned geological entities.

IDcode	Investigation	Borehole section (m borehole length)	Secmid elevation (m.b.s.l.)	Fracture domain or deformation zone
HFM09	Sampling in connection with pumping tests (HTHB)	22.0–29.0*	18.5	ZFMENE0060A
HFM10	Sampling in connection with pumping tests (HTHB)	114.5–121.0*	104.8	DZ*** (FFM04)
KFM04A	Complete hydrochemical characterization	230.5–237.6 354.0–361.1	197.0 302.7	ZFMA2 ZFMNE1188

* Flow anomaly position.

** Data record excluded.

*** DZ not modelled.

Besides fresh water in the shallow borehole section at 22.0–29.0 m, the deeper groundwaters between 104.8 m and 197.0 m depth show clear Littorina sea water character /SKB 2005c/. The section at 302.7 m depth lacks data on most of the basic water constituents, but the EC value indicates a similar water composition as at 197.0 m. In the waters showing Littorina signature, the chloride concentrations amount to 4,470 and 5,580 mg/L and the magnesium concentrations to 173 and 224 mg/L, respectively.

The chemical investigations in this borehole revealed strong electrical earth currents that caused severe corrosion of the chemical downhole equipment during the two week long measurement periods. This condition, which later was verified by self potential measurements, may possibly be related to properties of the strongly foliated and banded bedrock (included in fracture domain FFM04) delimiting the tectonic lens.

7.2.5 Drill site 5

The groundwater composition in the bedrock volume penetrated by the boreholes at drill site 5 (DS5) has been studied in the boreholes, KFM05A, HFM14, HFM15 and HFM19. Table 7-7 lists the borehole investigations and borehole sections providing the data included in the data compilation table in the SKB model database.

Table 7-7. Boreholes, investigations and borehole sections providing the selected hydrochemical data at DS5 and assigned geological entities.

IDcode	Investigation	Borehole section (m borehole length)	Secmid elevation (m.b.s.l.)	Fracture domain or deformation zone
HFM14	Sampling in connection with pumping tests (HTHB)	0.0–150.5*	100	ZFMA2
HFM15	Long-term hydrochemical monitoring	85.0–95.0	59.0	ZFMA2
HFM19	Sampling in connection with pumping tests (HTHB)	170.0–182.5*	150.0	ZFMA2
KFM05A	Sampling during drilling	100.0–121.6	90.4	ZFMA2 (FFM02)
KFM05A	Complete hydrochemical characterization, results rejected	712.6–722.0**	596.3	ZFMENE0401A

* Flow anomaly position.

** Data record excluded.

*** DZ not modelled.

Hydrochemical information from these boreholes is scarce. Data from the only investigated section at depth in borehole KFM05A are considered unsuitable because of short-circuiting around the upper packer, causing less saline borehole water to be drawn from higher up in the bedrock into the sampling section. However, the samples collected at 90.4 and 150.0 m depths in HFM19 and KFM05A show high magnesium concentrations, indicating the presence of a strong Littorina sea water component at relatively shallow depths. The chloride concentrations were 4,370 and 5,330 mg/L, respectively.

7.2.6 Drill site 6

The groundwater composition in the bedrock volume penetrated by the boreholes at drill site 6 (DS6) has been studied in boreholes, KFM06A and HFM16. Table 7-8 lists the borehole investigations and borehole sections providing the data included in the data compilation table stored in the SKB model database.

The sampled borehole sections in borehole KFM06A represent deformation zones and the adjacent modelled fracture domain is FFM01 down to below section 768.0–775.1 m where the domain changes to FFM06. The groundwater from the shallow borehole section at 353.5–360.6 m assigned to ZFMENE0060A revealed a composition less influenced by Littorina sea water compared to groundwaters at corresponding depths in most other boreholes, except KFM01D and KFM08A, see magnesium diagrams in Figure 7-12 and Figure 7-13. The deep section at 768.0–775.1 m borehole length revealed the expected non-marine water character.

Available data from KFM06A also include the composition of the porewater in the rock matrix. A number of selected short core samples along the borehole were investigated by out-diffusion experiments to obtain the composition of the water in connected pores in the rock material, see /Waber and Smellie 2005/. The fracture domain or deformation zone associated with each sample is listed in Table 7-9.

Most of the rock matrix pore water data are associated with fracture domains FFM01 or FFM06. Both domains have similar fracture frequencies and connective properties. Figure 7-7 displays chloride concentrations in matrix pore water from borehole KFM06A together with chloride in “fracture water” from borehole sections below the deformation zones ZFMA2 and ZFMF1 (the foot wall). Both waters reveal similar trends with depth. However, the chloride concentration of the pore water is always lower compared with the fracture water down to around 750 m depth where it increases and approaches concentrations in the same range as in the fracture waters at comparable depths. It has been suggested that the lower concentrations exhibited along two-thirds of the borehole length is due to the fact that the matrix pore water contains a larger proportion of old glacial meltwater compared to the groundwater in the more transmissive fractures. Another possible explanation is that the drilling process and stress release of the core caused an increase of the pore volume in the core samples and that the calculated pore water concentrations will be systematically underestimated due to this. The WellCad diagram in Appendix 5 permits comparison of matrix pore water data with geological and hydrogeological properties along the borehole on a detailed scale.

Table 7-8. Boreholes, investigations and borehole sections providing the selected hydrochemical data at DS6 and assigned geological entities.

IDcode	Investigation	Borehole section (m borehole length)	Secmid elevation (m.b.s.l.)	Fracture domain or deformation zone
HFM16	Long-term hydrochemical monitoring	54.0–67.0	57.2	ZFMA8
KFM06A	Sampling in connection with pumping tests (HTHB)	0.0–100.3	39.4	FFM02 or ZFMA8****
KFM06A	Sampling using hydrotest equipment	266.0–271.0**	227.0	ZFMENE0060B
KFM06A	Complete hydrochemical characterization	353.5–360.6 768.0–775.1	302.0 645.3	ZFMENE0060A ZFMNNE0725
KFM06A	Matrix pore water investigation	–	–	See Table 7-7

* Flow anomaly position.

** Data record excluded.

*** DZ not modelled.

**** Uncertain.

Table 7-9. Available matrix pore water data along KFM06A and assigned fracture domains or deformation zones.

Matrix pore water	Secup (m borehole length)	Seclow (m borehole length)	Secmid elevation (m.b.s.l.)	Fracture domain or deformation zone
KFM06A	146.03	146.39	122.81	FFM01
KFM06A	194.68	194.99	164.83	FFM01 (ZFMENE0060B)
KFM06A	252.53	252.89	214.47	ZFMENE0060B
KFM06A	281.63	282.01	239.33	FFM01
KFM06A	298.45	298.78	253.53	FFM01
KFM06A	355.14	355.44	301.74	ZFMB7
KFM06A	395.24	395.54	335.53	FFM01
KFM06A	440.88	441.24	373.77	FFM01
KFM06A	499.91	500.24	422.98	FFM01
KFM06A	563.3	563.64	475.52	FFM01
KFM06A	575.83	576.16	484.89	FFM01
KFM06A	594.51	594.88	501.35	FFM01
KFM06A	633.44	633.79	533.45	FFM01
KFM06A	660.73	661.14	555.88	FFM01
KFM06A	699.58	699.97	587.61	FFM01
KFM06A	763.27	763.67	639.40	ZFMNNE0725
KFM06A	810.66	810.98	677.57	FFM06
KFM06A	851.5	851.81	710.20	FFM06
KFM06A	900.72	901.12	749.33	Possible DZ, not model.
KFM06A	920.44	920.82	764.91	FFM06
KFM06A	948.48	948.86	786.91	FFM06
KFM06A	977.14	977.47	809.29	ZFMNNE2280
KFM06A	998.22	998.47	825.69	ZFMNNE2280

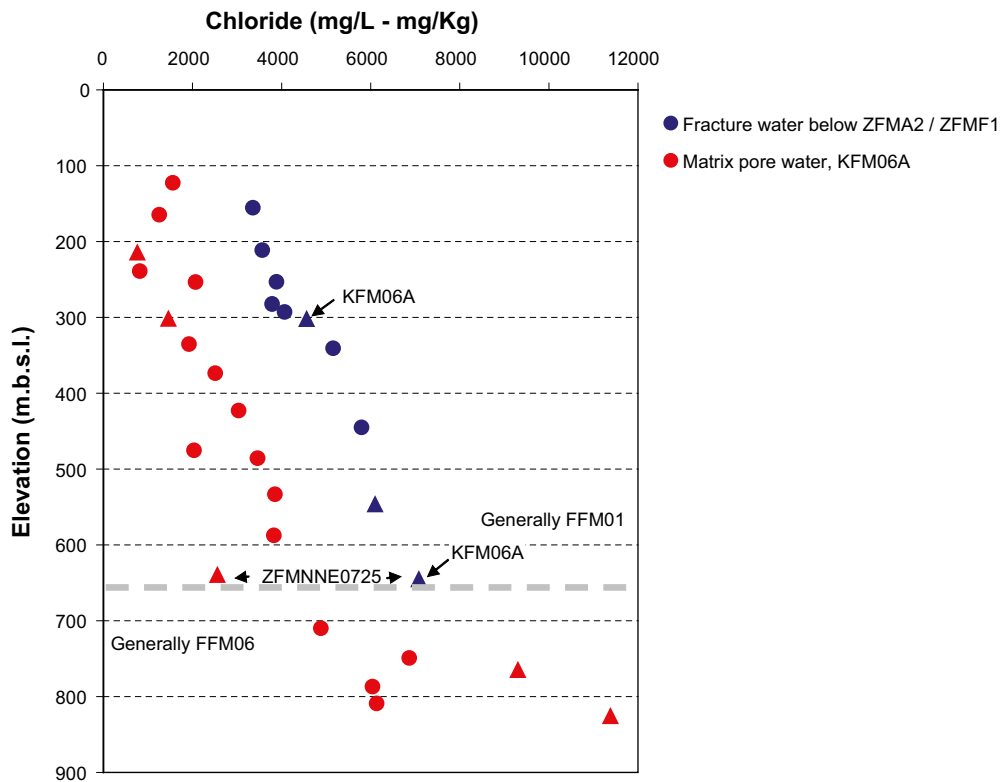


Figure 7-7. Comparison of chloride concentrations between matrix pore water (mg/Kg water) from KFM06A and “fracture water” (mg/L) from borehole sections below deformation zones ZFMA2-ZFMF1 (boreholes HFM22, KFM01D, KFM06A and KFM08A). Samples assigned to fracture domains and deformation zones are shown as filled-in circles and triangles respectively.

7.2.7 Drill site 7

The groundwater composition in the bedrock volume penetrated by the boreholes at drill site 7 (DS7) has been studied in boreholes KFM07A and HFM21. Table 7-10 lists the borehole investigations and borehole sections providing the data included in the data compilation table for fracture domains.

Table 7-10. Boreholes, investigations and borehole sections providing the selected hydrochemical data at DS7 and assigned geological entities.

IDcode	Investigation	Borehole section (m borehole length)	Secmid elevation (m.b.s.l.)	Fracture domain or deformation zone
HFM21	Sampling in connection with pumping tests (HTHB)	97.0–163.0*	100	ZFM1203 (FFM02)
KFM07A	Complete hydrochemical characterization	848.0–1,001.6	790*	ZFMNNW0100, ZFMB8

* Flow anomaly position.
 ** Data record excluded.
 *** DZ not modelled

Available hydrochemical data are scarce also from this drill site. However, groundwater sampled from the only investigated section in borehole KFM07A displayed a surprisingly high chloride concentration (14,400 mg/L) at depth. At this depth, the origin of the water is clearly non-marine.

The chloride concentration is significantly higher than at comparable depth in borehole KFM03A representing fracture domain FFM03. No chloride data are available from fracture domain FFM01 at this depth. The high concentration may be caused by up-coning of deep saline water due to pumping in the steep NNW zone (ZFMNNW0100) subparallel to the strongly foliated bedrock of the marginal fracture domain FFM05. Up-coning effects due to heavy pumping during drilling were observed from hydrochemical logging of the borehole /Berg et al. 2005/. Another hypothesis is that the water composition also represents the conditions in fracture domain FFM01 at depth.

7.2.8 Drill site 8

The groundwater composition in the bedrock volume penetrated by the boreholes at drill site 8 (DS8) has been studied in boreholes KFM08A and HFM22. Table 7-11 lists the borehole investigations and borehole sections providing the data included in the data compilation table stored in the SKB model database.

Groundwater from the borehole section at 546 m depth in borehole KFM08A designated as “DZ not modelled” shows similar non-marine character as the groundwater in KFM01D and KFM06A.

Matrix pore water data are available from borehole KFM08C /Waber and Smellie 2007/. Unfortunately, no fracture water data are available from this borehole. The fracture domain or deformation zone associated with each sample is listed in Table 7-12. Figure 7-8 displays chloride concentrations in matrix pore water from borehole KFM8C together with chloride in “fracture water” from borehole sections below the deformation zones ZFMA2 and ZFMF1 (the foot wall), i.e. mainly fracture domain FFM01, as well as from two observations in deformation zones adjacent to strongly foliated bedrock. The chloride concentrations in matrix water from KFM08C are the ones that most closely resemble fracture water representing the foot wall beneath ZFMA2. The WellCad diagram in Appendix 5 permits comparison of matrix pore water data with geological and hydrogeological properties along the borehole on a detailed scale, which is necessary in the pore water case.

Table 7-11. Boreholes, investigations and borehole sections providing the selected hydrochemical data at DS8 and assigned geological entities.

IDcode	Investigation	Borehole section (m borehole length)	Secmid elevation (m.b.s.l.)	Fracture domain or deformation zone
HFM22	Sampling in connection with pumping tests (HTHB)	60.5–64.0*	50.0	FFM02/FFM01 uncertain
KFM08A	Complete hydrochemical characterization	683.5–690.6	546.4	DZ***

* Flow anomaly position.

** Data record excluded.

*** DZ not modelled.

Table 7-12. Available matrix pore water data along KFM08C and assigned fracture domains or deformation zones.

Matrix pore water	Secup (m borehole length)	Seclow (m borehole length)	Secmid elevation (m.b.s.l.)	Fracture domain or deformation zone
KFM08C	154.55	154.83	131.16	FFM01
KFM08C	254.71	255.12	215.88	FFM01
KFM08C	353.70	354.14	298.58	FFM06
KFM08C	455.51	455.93	383.03	ZFMNNE2312
KFM08C	553.01	553.38	463.27	FFM01
KFM08C	648.41	648.75	540.69	FFM01
KFM08C	751.31	751.59	623.27	FFM01
KFM08C	839.57	839.91	693.38	FFM01
KFM08C	917.04	917.38	754.37	FFM01
KFM08C	938.10	938.50	770.85	FFM01

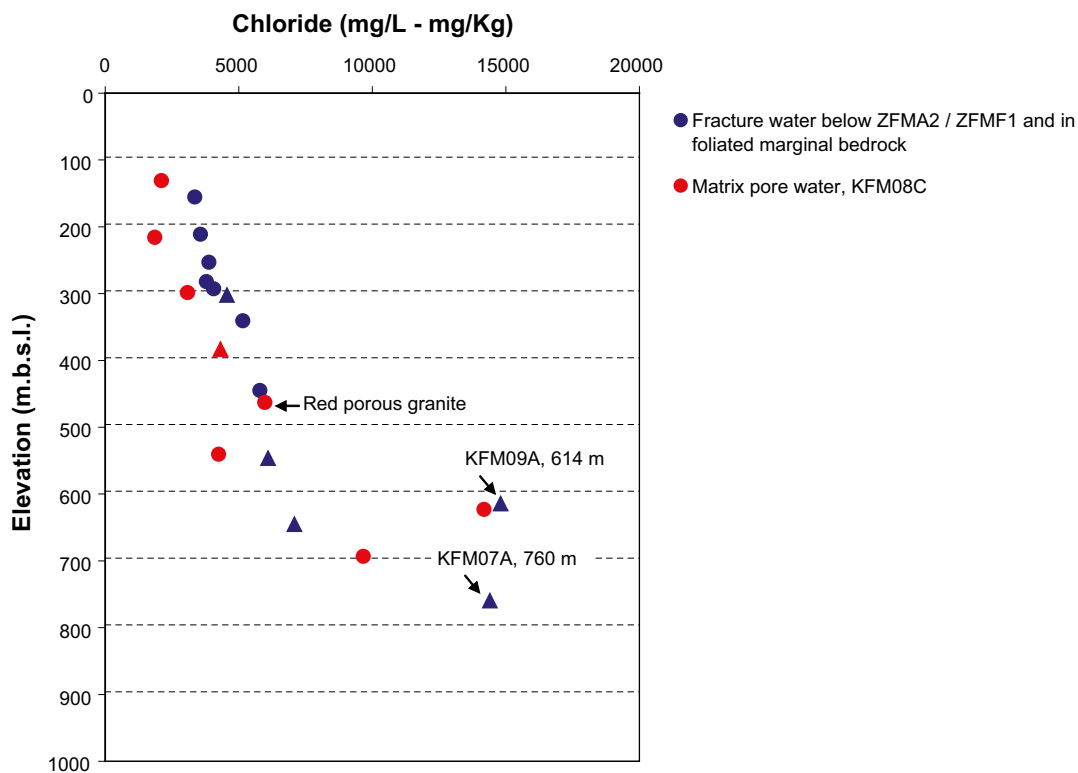


Figure 7-8. Comparison of chloride concentrations between matrix pore water from KFM08A and “fracture water” from borehole sections below deformation zones ZFMA2-ZFMF1 and in deformation zones adjacent to the foliated marginal bedrock (boreholes KFM01D, KFM06A, KFM08A as well as KFM07A and KFM09A). Samples assigned to fracture domains and deformation zones are shown as filled-in circles and triangles, respectively.

7.2.9 Drill site 9

The groundwater composition in the bedrock volume penetrated by the boreholes at drill site 9 (DS9) has been studied in the boreholes, KFM09A, HFM20, HFM23 and HFM25. Table 7-13 lists the borehole investigations and borehole sections providing the data included in the data compilation table available in the SKB model database.

Like borehole KFM07A, this borehole also reaches the strongly foliated bedrock delimiting the lens and the groundwater shows equally high chloride concentration (14,800 mg/L) at depth. Both boreholes penetrate deformation zones at the bottom and these zones seem to be interconnected. Borehole KFM09A is directed from the lens towards the southwest and enters fracture domain FFM04 at the base. Another borehole at drill site DS9, KFM09B, is directed into fracture domain FFM01. The chloride concentrations from hydrochemical logging along boreholes KFM09A and KFM09B are compared in /Lindquist and Nilsson 2006/. Despite the uncertainty due to high flushing water contents and open borehole conditions, the estimated chloride concentration corrected for the flushing water content does not reach similar high values at depth in KFM09B.

Some matrix pore water data are available from a short interval of borehole KFM09B (573.3–586.4 m borehole length), see Table 7-14. These samples were collected soon after observations of vuggy granite during drilling. The intention was to investigate whether these special conditions have an impact on pore water properties. The chloride concentration was found to vary in an irregular manner between 4,670 and 10,500 mg/Kg with the highest concentrations at the beginning and end of the borehole interval.

Table 7-13. Boreholes, investigations and borehole sections providing the selected hydrochemical data at DS9 and assigned geological entities.

IDcode	Investigation	Borehole section (m borehole length)	Secmid elevation (m.b.s.l.)	Fracture domain or deformation zone
HFM20	Sampling in connection with pumping tests (HTHB)	12.0–301.0**	–	FFM02/FFM01
HFM23	Sampling in connection with pumping tests (HTHB)	0.0–211.5**	–	–
HFM25	Sampling in connection with pumping tests (HTHB)	0.0–187.5**	–	–
KFM09A	Complete hydrochemical characterization	785.1–792.2	614.2	ZFMNW1200

* Flow anomaly position.

** Data record excluded.

*** DZ not modelled.

Table 7-14. Available matrix pore water data along KFM09B and assigned fracture domains or deformation zones.

Matrix pore water	Secup (m borehole length)	Seclow (m borehole length)	Secmid elevation (m.b.s.l.)	Fracture domain or deformation zone
KFM09B	573.33	573.61	442.43	ZFMENE2325B
KFM09B	574.36	574.73	443.18	FFM01
KFM09B	576.25	576.57	444.47	FFM01
KFM09B	576.57	576.89	444.70	FFM01
KFM09B	576.89	577.06	444.87	FFM01
KFM09B	577.74	578.04	445.50	FFM01
KFM09B	582.49	582.89	448.84	FFM01
KFM09B	586.37	586.77	451.52	FFM01

7.3 Summary and discussion

As evident from the previous chapter, most hydrochemical data originate from geological entities interpreted as deformation zones in the geological model. This is what could be expected since a certain water yield is necessary (generally $T > 1E-8$ m²/s) for water sampling, and flow anomalies of the requested size are most often found in the zones. Of 51 sampled borehole sections, 35 represented modelled or unmodelled deformation zones, whereas only 16 were associated with interpreted fracture domains. The latter group was mainly found in boreholes KFM01A and KFM01D, representing fracture domains FFM02 and FFM01, respectively. However, two of the key samples originate from great depth and are associated with deformation zones with adjacent bedrock belonging to fracture domains FFM04 (KFM09A) and FFM05 (KFM07A). Figure 7-9 and Figure 7-10 show chloride and magnesium concentrations in relation to fracture domains and deformation zones.

Another difficulty when exploring hydrochemical data in order to seek support for the geological fracture domain model is the relatively low total number of observations and investigated borehole sections (fractures or fracture zones) in each borehole. However, the sections of the two well-investigated boreholes KFM01D and KFM03A represent what seem to be two extremes: the impermeable bedrock of the modelled fracture domain FFM01 in the target area and gently dipping deformation zones penetrating fracture domain FFM03.

The composition of the bedrock groundwater in the depth range 0 to 150 m varies between different boreholes and in an irregular manner which is difficult to relate to geological entities. These fractures and fracture zones are generally characterized by interconnection and high hydraulic transmissivity and they form the so called hydrogeological cage. The pumping time and rate needed to collect samples may therefore have a high impact on the water composition and explain some of the irregularities.

The following observations were made from the hydrochemical data in the depth range 100 to 1,000 m:

- The diagrams in Figure 7-11 and Figure 7-12 may be used to divide data into the following three categories: 1) Data representing conditions within the deformation zones ZFMA2, ZFMF1 and the gently dipping deformation zones in the south-east part of the candidate area as well as within fracture domain FFM02. The only deep flow anomaly assigned to fracture domain FFM03 (KFM03A at 969 m) is also included in this group. 2) Data representing conditions in the bedrock between deformation zones below ZFMA2, i.e. the modelled fracture domain FFM01 down to 450 m depth. 3) Deep groundwater data associated with the deformation zones adjacent to the strongly foliated rocks constituting fracture domains FFM04 and FFM05 along the margins of the target area.
- Groundwater of clear Littorina sea water origin is observed between approximately 100 and 600 m vertical depth and only in deformation zones and fracture domain FFM02. However, all deformation zones in this depth range do not show marine Littorina character. Two exceptions are KFM06A at 302 m assigned to the minor deformation zone ZFMENE0060A and KFM08A at 546 m assigned to a possible, but not deterministically modelled deformation zone. These two data records indicate a mainly non-marine origin. In contrast to the open gently dipping zones, the east-north-east oriented zone ZFMENE0060A is perpendicular to the maximum horizontal stress and the fracture structure is more closed. The extent and orientation of the possible, but not modelled, zone in KFM08A is not fully known.
- High chloride concentrations (exceeding 14,000 mg/L) were measured in borehole sections at 760 m and 614 m depths in boreholes KFM07A and KFM09A, respectively, see Figure 7-11. Both borehole sections represent deformation zones adjacent to fracture domains FFM05 and FFM04 along the north-western and south-western margins of and outside the target volume. The water composition may be representative of the zones themselves, and possibly of the rock volumes outside the tectonic lens. Similar conditions may also prevail at depth in fracture domain FFM01. Representative water composition

data from the rock below ZFMA2 in the target area at depths >450 m are missing, but there are indications of less saline conditions from hydrochemical logging in borehole KFM09B, which is directed into the lens. If the salinity is unique for the deformation zones, it may imply that the zones serve as a discharge route for up-coning deeper saline water. This may or may not have been triggered by pumping of the boreholes.

- The twelve Eh values measured so far in Forsmark groundwaters range from –145 mV to –260 mV and values close to –200 mV are most frequent. The highest value (smallest negative number) was obtained from measurements in the ZFMA2 zone at around 500 m depth in KFM02A whereas the lowest values (largest negative numbers) were measured in two sections of borehole KFM01D (341 and 445 m) assigned to fracture domain FFM01. This may suggest a possible weak connection between connective properties and redox conditions.
- Most rock matrix porewater data from boreholes KFM01D, KFM06A and KFM08C are associated with the fracture domain FFM01 (42 out of 55 samples) and it is more relevant to compare them with fracture waters from the foot wall of zone ZFMA2 in domain FFM01 than with waters with a strong Littorina character. The chloride concentrations in matrix pore water from KFM01D, KFM06A and KFM08C show similar increasing trends with depth. The fracture domain concept is not detailed enough to explain differences in, for example, chloride concentrations between individual samples, and a detailed comparison of geological and hydrogeological properties in a smaller scale will probably be more informative.

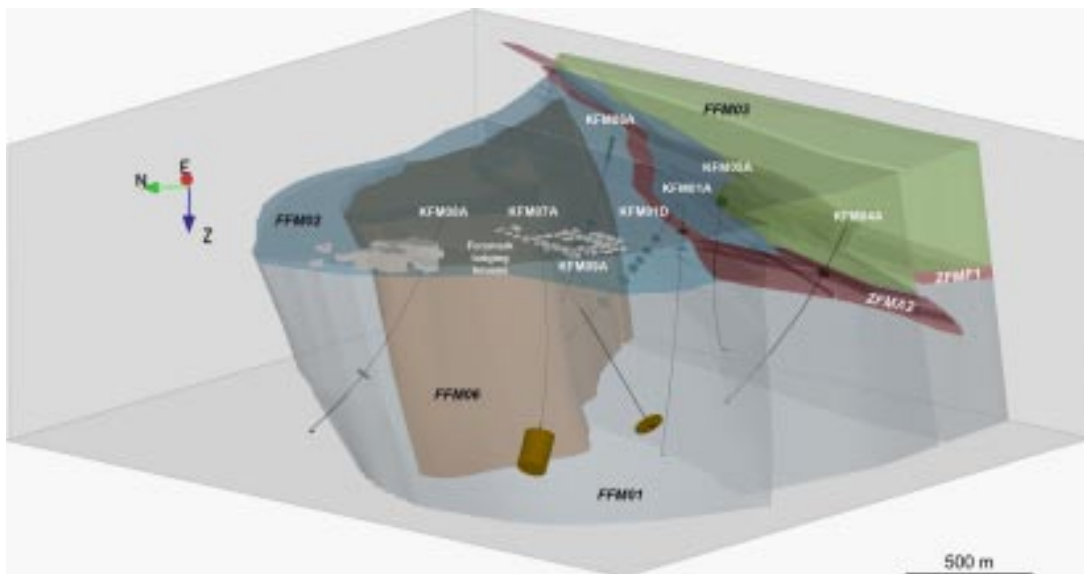


Figure 7-9. View to the east-north-east showing chloride concentrations in the investigated boreholes and borehole sections. The concentrations are proportional to the diameter of the coloured plates/tubes representing the borehole sections. The fracture domains and zones are displayed more clearly in Figure 5-4.

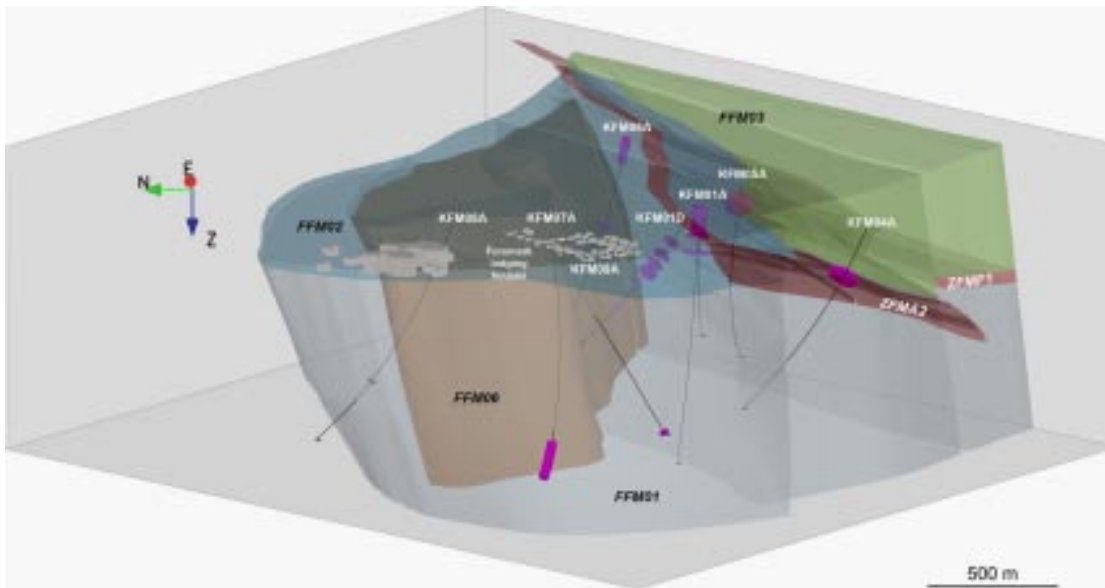


Figure 7-10. View to the east-north-east showing magnesium concentrations in the investigated boreholes and borehole sections. The concentration is proportional to the diameter of the coloured plates/tubes representing the borehole sections. The magnesium concentrations in the groundwater from the two deepest borehole sections of KFM01D are low and the sections may be difficult to observe in the figure. The fracture domains and zones are displayed more clearly in Figure 5-4.

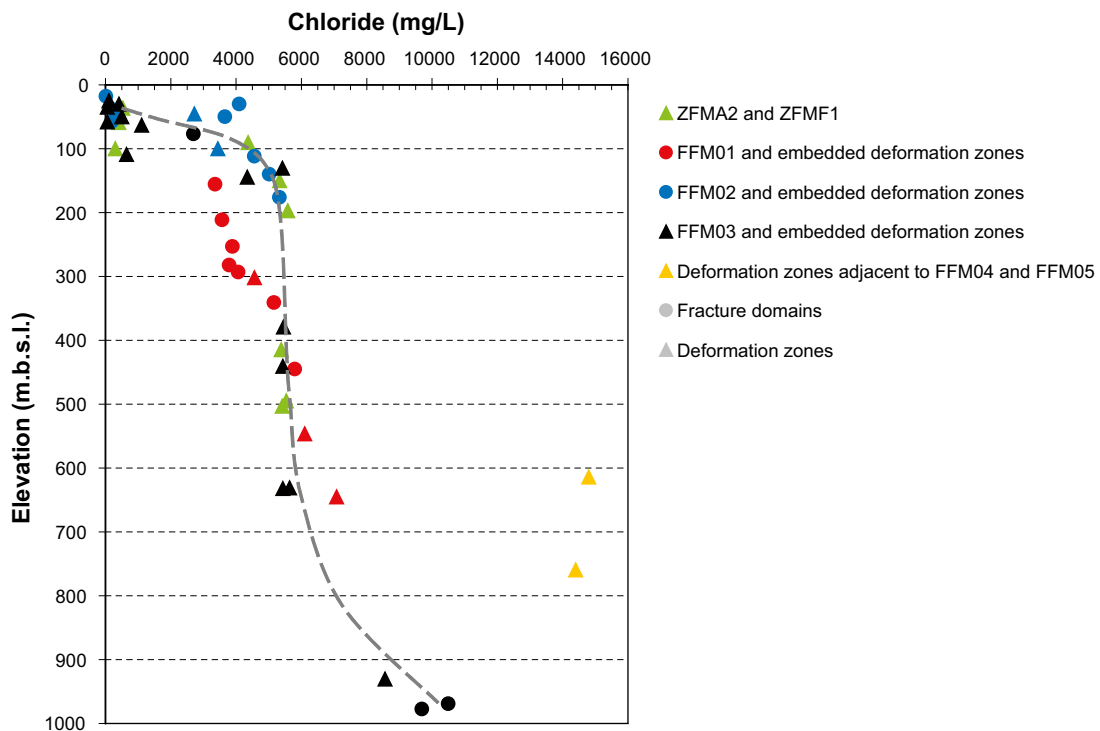


Figure 7-11. Chloride concentration versus vertical depth. Geological entities are indicated by a colour code. Data representing conditions above and adjacent to the deformation zone ZFMA2 as well as from the southeast part of the candidate area are joined by a dashed grey line.

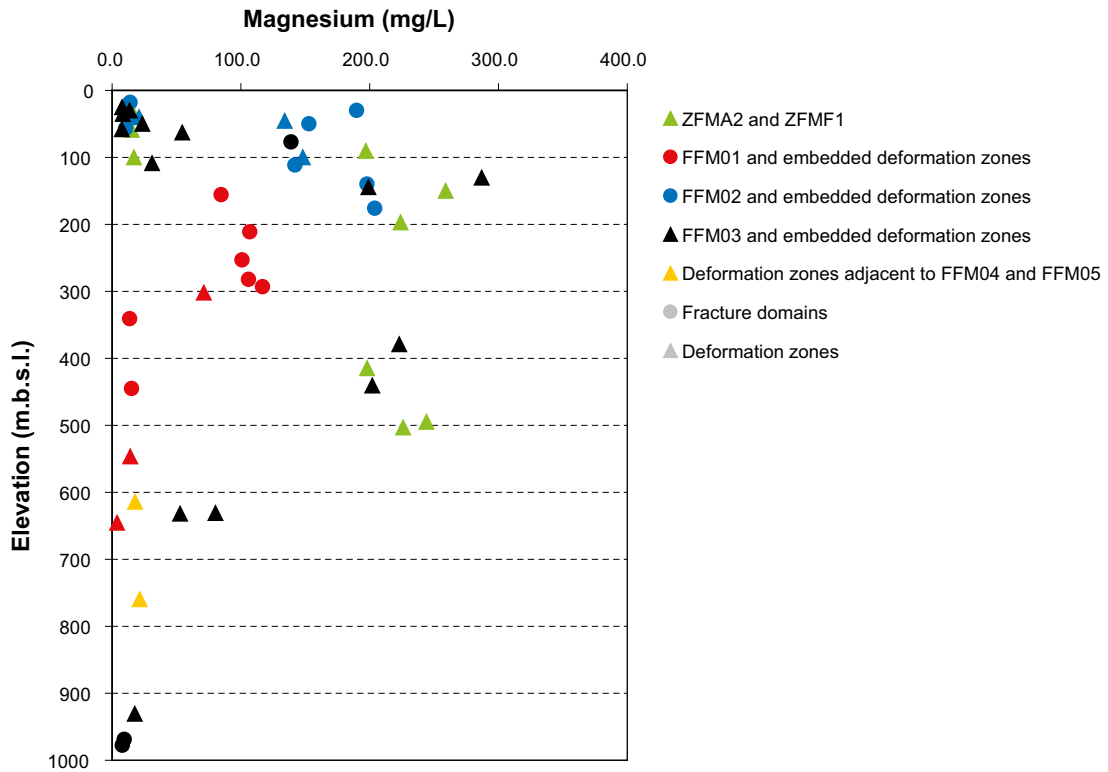


Figure 7-12. Magnesium concentration versus vertical depth. Geological entities are indicated by a colour code.

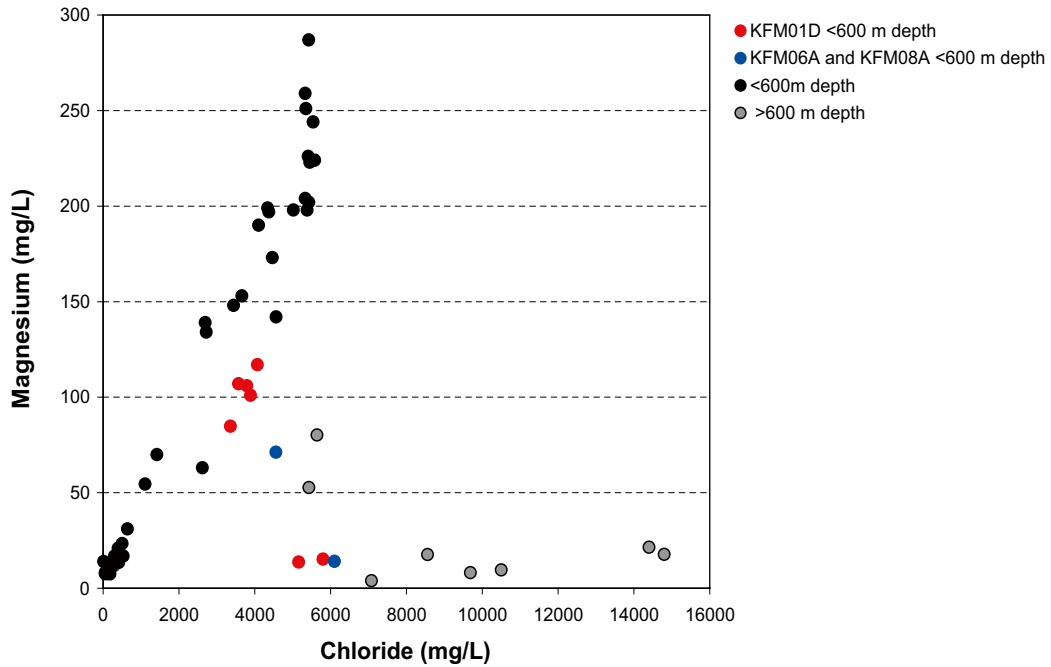


Figure 7-13. Magnesium concentration versus chloride concentration. The three boreholes showing non-marine signatures at relatively shallow depths (KFM01D, KFM06A and KFM08A) are indicated by red and blue colours.

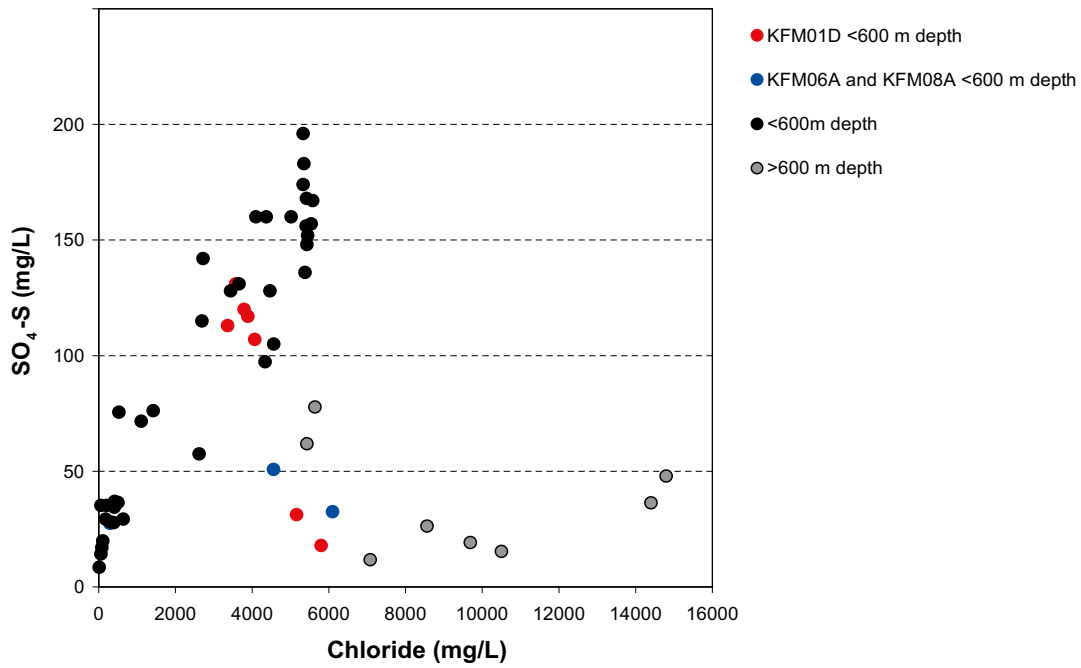


Figure 7-14. Sulphate concentration versus chloride concentration. The three boreholes with non-marine signatures at relatively shallow depths (KFM01D, KFM06A and KFM08A) are indicated by red and blue colours.

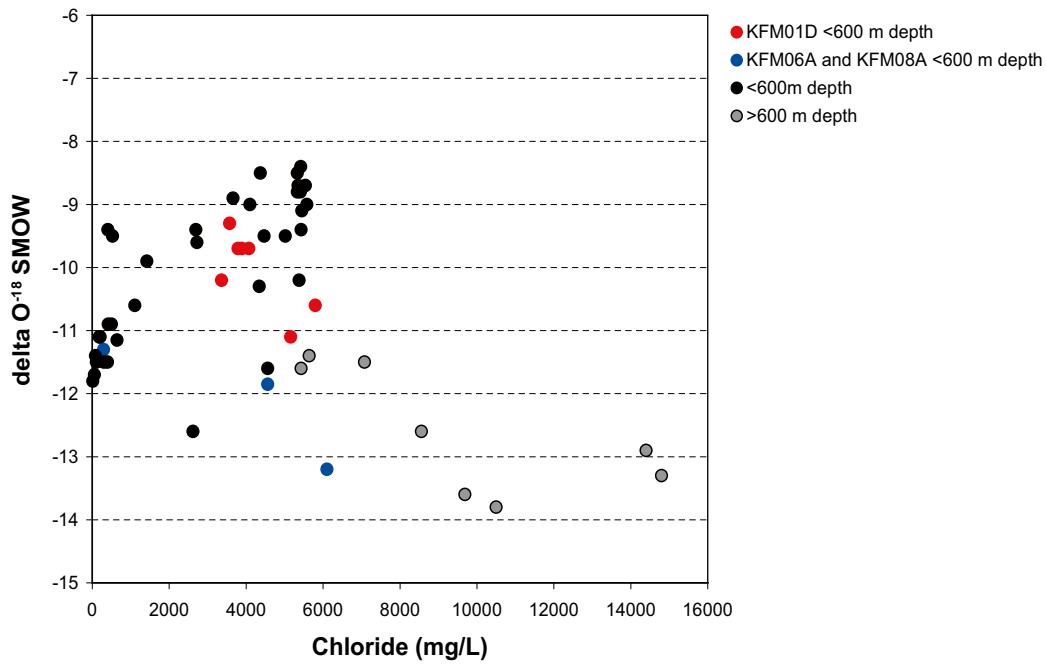


Figure 7-15. $\delta^{18}\text{O}$ ‰ SMOW versus chloride concentration. The three boreholes with non-marine signatures at relatively shallow depths (KFM01D, KFM06A and KFM08A) are indicated by red and blue colours.

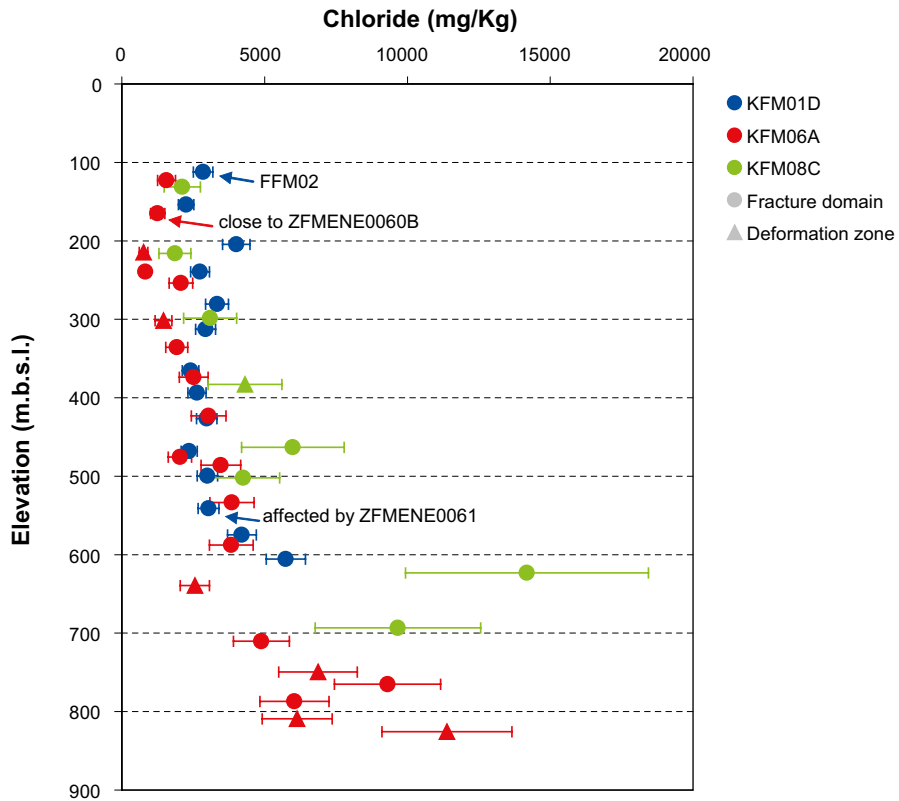


Figure 7-16. Chloride concentrations in matrix pore water from boreholes KFM01D, KFM06A and KFM08C plotted versus elevation. The fracture domain is generally FFM01. Individual positive as well as negative uncertainties have been interpreted for each data point and the size of these uncertainties varies a lot. The error bars in the diagram represent the maximum uncertainty in percent for each borehole when single extreme values are rejected.

8 Rock mechanics data in the context of fracture domains and deformation zones

8.1 Available rock mechanics data and data selection

In this chapter the rock mechanics data available at Forsmark by datafreeze 2.2 are presented for the core-drilled boreholes at each drill site where rock mechanics investigations were carried out. The test programme includes both laboratory and field tests. The laboratory tests results available by data freeze 2.2 are summarized in Table 8-1. The field measurements include rock stress, rock mass characterization and P-wave velocity measurements in boreholes. All sampling for laboratory testing of mechanical properties has been done in batches at different depths. Figure 8-1 show the sampling locations for all uniaxial tests listed in Table 8-1.

The methodology, standard and performance used for the laboratory testing are described in SKB's Method Descriptions for each test:

- Uniaxial compression: SKB MD 190.001e, ver 3.0 (2005-11-01).
- Triaxial compression: SKB MD 190.003e, ver 2.0 (2004-06-07).
- Indirect tensile tests: SKB MD 190.004e, ver 2.0 (2004-06-07).
- Shear tests on fractures: SKB MD 190.005e, ver 3.0 (2005-11-01).
- Tilt tests on fractures: SKB MD 190.006, ver 2.0 (2002-04-16).
- P-wave velocity on core samples: SKB MD 190.002, ver 2.0 (2006-04-26).

Table 8-1. Rock mechanics data from laboratory testing.

	Uniaxial compressive tests	Triaxial tests	Indirect tensile tests	Shear tests on open fractures	Tilt tests on fractures	P-wave velocity on core samples
KFM01A	14 (15)	14	30	18	41	34
KFM01A ¹	6	5	10	15		
KFM01C	8 ⁴	5				
KFM01D		4		36 ³		
KFM02A	14 (15)	12	30	21	40	74
KFM03A	16 (17)	16	40	24	35	68
KFM03B					3	3
KFM04A	14 (15)	11 (12)	33	18	26	34
KFM05A	10	8	20	24	9	32
KFM06A	15 (16)		5	18		30
KFM07A	8	4	6	15		33
KFM08A		6	1 ²	15		33
KFM09A	7 (8)	5	20	18	9	30

Data within parenthesis includes samples containing sealed fractures.

¹ Independent lab.

² Included in the report of KFM07A.

³ These results come from tests on three sealed fractures, each with normal loading and three different magnitudes of normal stress.

⁴ Late data.

Table 8-2. Rock mechanics data from field measurements and empirical characterization.

	RQD	Q	RMR	Rock stress measurements	Sonic velocity
KFM01A	X	5 and 20 m intervals	5 and 20 m intervals		X
KFM01B	X	1 and 5 m intervals	1 and 5 m intervals	Overcoring	X
KFM01C	X				X
KFM01D	X				X
KFM02A	X	5 and 30 m intervals	5 and 30 m intervals		X
KFM03A	X	5 and 30 m intervals	5 and 30 m intervals		X
KFM03B	X				X
KFM04A	X	5 and 30 m intervals	5 and 30 m intervals		X
KFM05A	X				X
KFM06A	X				X
KFM06B	X				X
KFM07A	X			HF/HTPF*	X
KFM07B	X				X
KFM07C	X	1 and 5 m intervals*	1 and 5 m intervals*	Overcoring and HF/HTPF*	
KFM08A	X			HF/HTPF*	X
KFM08B	X				X
KFM08C	X				X
KFM09A	X	1 and 5 m intervals	1 and 5 m intervals	HF/HTPF*	X
KFM09B	X	1 and 5 m intervals	1 and 5 m intervals	HF/HTPF*	X

* Late data.

The laboratory tests were mainly performed at SP, Statens Provningsanstalt (Swedish National Testing and Research Institute). SP performed all laboratory tests except the tilt tests and P-wave velocity measurements on core samples, which were performed by NGI (Norwegian Geotechnical Institute). HUT (Helsinki University of Technology), Finland and NGI, Norway, also performed some laboratory testing as an independent check. The number and type of parallel independent testing is shown in Table 8-1.

Rock mechanics characterization of the rock mass by means of the Rock Quality Index (Q) and Rock Mass Rating (RMR) according to /Andersson et al. 2002, Röshoff et al. 2002/ was carried out for selected boreholes based on the single-hole interpretation (SHI). These boreholes are listed in Table 8-2 and their locations are illustrated in Figure 8-1.

The rock stress measurements were conducted by Vattenfall Power Consultant AB (earlier SwedPower), Sweden, using the overcoring and hydraulic fracturing methods and by MeSy, Germany, using hydraulic fracturing methods. Only data from the overcoring in KFM01B is presented in this report. However, more data will become available once the quality of the data has been controlled (see section 3.2).

Section 8.2 presents the results of the tests available from each drill site. Section 8.3 presents an overview of the laboratory and field test results, taking into account the geological context of the Forsmark site. All results from the tests presented in section 8.3 are included in the rock mechanics data compilation table available in the SKB model database.

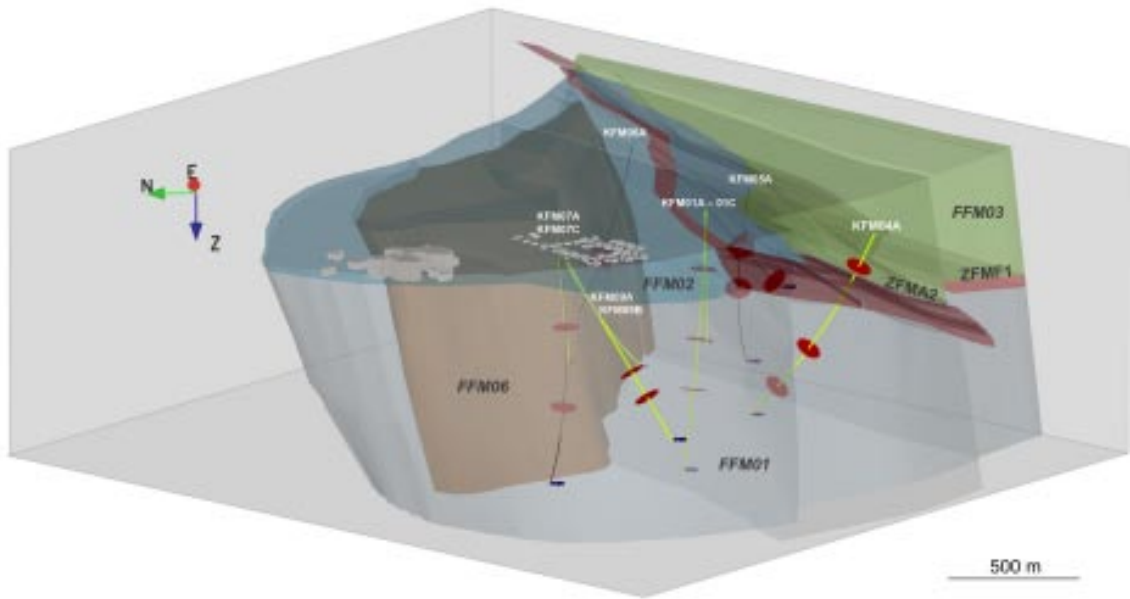


Figure 8-1. View to the east-north-east presenting locations of sampling for UCS tests (red) as listed in Table 8-1 and location of boreholes subject to rock mechanical characterization (Q and RMR) (green) as listed in Table 8-2 with the exception of KFM02A and KFM03A as they are not located in the volume of the local model.

The results are also shown in WellCad diagrams presented in Appendix 6. These diagrams do not include test results from the independent laboratories, nor from the tests performed on sealed fractures.

8.2 Drill site overview

8.2.1 Intact rock properties

The data presented in Table 8-3 to Table 8-14 are per drill site and include the following information from intact rock tests:

- Testing method for each test.
- The borehole section and elevation at which the samples were taken.
- Number of tested samples, with
 - confining pressure for triaxial test,
 - direction of test in relation to foliation for tensile tests,
 - date of testing.
- The rock domain from which the samples are taken.
- The fracture domain or deformation zone to which the samples belong.

Drill site 1

Table 8-3. Rock mechanics investigations in borehole KFM01A.

Testing method	Sample location secup–seclow [m]	Elevation seclow [m.b.s.l]	No. of tested samples	Rock domain RFM	Fracture domain FFM or deformation zone DZ
Uniaxial compressive strength	225.92–229.75	222–225	15 (17 June 2003)	RFM029	FFM01
	496.01–497.9	489–491		RFM029	FFM01
	690.32–690.88			RFM029	FFM01
Triaxial compressive strength	233.29–237.99	229–234	6 conf. 2 MPa 6 conf. 7 MPa 2 conf. 10 MPa (12 July 2004)	RFM029	FFM01
	498.42–499.86	492–493		RFM029	FFM01
	696.62–697.71	686–687		RFM029	FFM01
Indirect tensile strength	231.43–237.49	227–233	15 along foliation 15 perpendicular to foliation (17 June 2003)	RFM029	FFM01
	491.50–498.31	485–491		RFM029	FFM01
	689.84–690.58	679–680		RFM029	FFM01
P-wave velocity transverse borehole core	105.46–162.00	102–158	34 (24–26 July 2003)	RFM029	FFM02
	206.85	203		RFM029	FFM01
	253.35–264.61	249–260		RFM029	FFM01
	304.39–384.65	299–379		RFM029	FFM01
	413.90–632.15	408–623		RFM029	FFM01
	648.56–669.35	639–659		RFM029	ZFMENE2254
688.17–1001.17	678–982	RFM029	FFM01		
Uniaxial compressive strength*	495.46–498.04	489–491	6 (12 July 2004)	RFM029	FFM01
Triaxial compressive strength*	495.14–501.32	488–494	2 conf. 2 MPa	RFM029	FFM01
			2 conf. 7 MPa		
			1 conf. 10 MPa (11 July 2004)		
Indirect tensile strength*	491.54–498.35	485–491	5 along foliation 5 perpendicular to foliation (09 July 2004)	RFM029	FFM01

* Tests conducted at independent laboratory.

Table 8-4. Rock mechanics investigations in borehole KFM01C.

Testing method	Sample location secup–seclow [m]	Elevation seclow [m.b.s.l]	No. of tested samples	Rock domain RFM	Fracture domain FFM or deformation zone DZ
Triaxial compressive strength	398.27–400.44	295–297	1 conf. 5 MPa	RFM029	FFM01 ⁽¹⁾
	411.51–413.40	305–306	2 conf. 10 MPa	RFM029	FFM01 ⁽¹⁾
			2 conf. 20 MPa (05 May 2006)		

⁽¹⁾ Sections which might be affected by DZ.

Table 8-5. Rock mechanics investigations in borehole KFM01D.

Testing method	Sample location secup–seclow [m]	Elevation seclow [m.b.s.l]	No. of tested samples	Rock domain RFM	Fracture domain FFM or deformation zone DZ
Triaxial compressive strength	550.75–551.08	430	1 conf. 5 MPa	RFM029	FFM01
	556.01–556.28	434	1 conf. 10 MPa	RFM029	FFM01
			2 conf. 20 MPa (15 June 2006)		

Drill site 2

Table 8-6. Rock mechanics investigations in borehole KFM02A.

Testing method	Sample location secup–seclow [m]	Elevation seclow [m.b.s.l.]	No. of tested samples	Rock domain RFM	Fracture domain FFM or deforma- tion zone DZ
Uniaxial compressive strength	333.51–334.93	325–327	14 (17 June 2003)	RFM029	FFM03
	527.72–529.48	519–520		RFM029	Possible DZ
	705.55–708.55	695–698		RFM029	FFM01
Triaxial compressive strength	330.33–334.41	322–326	3 conf. 2 MPa 6 conf. 7 MPa 3 conf. 12 MPa (12 July 2004)	RFM029	FFM03
	531.01–531.61	522		RFM029	Possible DZ
	704.09–709.27	694–699		RFM029	FFM01
Indirect tensile strength	330.60–335.90	322–327	15 along foliation 15 perpendicular to foliation (17 June 2003)	RFM029	FFM03
	527.87–537.35	519–528		RFM029	Possible DZ
	704.39–718.22	694–708		RFM029	FFM01
P-wave velocity transverse borehole core	191.50–230.30	184–222	74 (17 June 2003)	RFM029	FFM03
	302.5	294		RFM029	ZFM1189
	310.10–409.35	302–401		RFM029	FFM03
	434.80	426		RFM029	ZFMA2
	447.10–472.80	438–464		RFM029	FFM01 ⁽¹⁾
	481.70–508.25	473–499		RFM029	ZFMF1
	522.80–586.40	514–577		RFM029	Possible DZ
	603.00–891.40	593–879		RFM029	FFM01
	900.25	888		RFM029	ZFMB4
	906.70–917.20	894–905		RFM029	FFM01
	928.20–974.60	915–961		RFM029	FFM01
990.30–997	977–983	RFM029	FFM01		
1002.3	989	–	–		

⁽¹⁾ Sections which might be affected by DZ.

Drill site 3

Table 8-7. Rock mechanics investigations in borehole KFM03A.

Testing method	Sample location secup–seclow [m]	Elevation seclow [m.b.s.l.]	No. of tested samples	Rock domain RFM	Fracture domain FFM or deforma- tion zone DZ
Uniaxial compressive strength	278.29–280.99	269–272	17 (09 July 2004)	RFM017	FFM03
	305.98–308.68	297–300		RFM029	FFM03
	523.82–525.01	514–515		RFM029	FFM03
	670.54–671.22	660		RFM029	FFM03
Triaxial compressive strength	281.35–282.02	272–273	4 conf. 2 MPa 8 conf. 7 MPa 4 conf. 12 MPa (12 July 2004)	RFM017	FFM03
	306.40–306.96	297–298		RFM029	FFM03
	524.29–524.87	514–515		RFM029	FFM03
	671.64–680.82	661–670		RFM029	FFM03
Indirect tensile strength	278.88–281.84	270–273	20 along foliation 20 perpendicular to foliation (09 July 2004)	RFM017	FFM03
	310.07–310.40	301		RFM029	FFM03
	523.13–527.70	513–518		RFM029	FFM03
	670.46–682.15	660–671		RFM029	FFM03
P-wave velocity transverse borehole core	181.90–216.55	173–208	68 (6–13 October 2003)	RFM029	FFM03
	229.05–281.75	220–273		RFM017	FFM03
	202.60–348.05	293–339		RFM029	FFM03
	370.23–392.80	361–383		RFM029	ZFMA4
	410.48–444.35	401–435		RFM029	FFM03
	461.77–630.75	452–620		RFM029	FFM03
	639.25	629		RFM029	ZFMB1
	649.75–794.60	639–783		RFM029	FFM03
	805.20–814.80	794–803		RFM029	ZFMA3
	816.70–940.95	805–928		RFM029	FFM03
953.27–981.70	941–969	RFM029	FFM03		

Table 8-8. Rock mechanics investigations in borehole KFM03B.

Testing method	Sample location secup–seclow [m]	Elevation seclow [m.b.s.l.]	No. of tested samples	Rock domain RFM	Fracture domain FFM or deformation zone DZ
P-wave velocity transverse borehole core	21.65–87.87	13–79	3 (13–15 October 2003)	RFM029	FFM03

Drill site 4**Table 8-9. Rock mechanics investigations in borehole KFM04A.**

Testing method	Sample location secup–seclow [m]	Elevation seclow [m.b.s.l.]	No. of tested samples	Rock domain RFM	Fracture domain FFM or deformation zone DZ
Uniaxial compressive strength	162.02–163.79	134–136	14 (17 June 2003)	RFM018	ZFMNW1200
	586.46–587.56	488–489		RFM029	FFM01
	812.78–813.78	660–661		RFM029	FFM01
Triaxial compressive strength	161.44–165.48	134–137	1 conf. 2 MPa 2 conf. 5 MPa 2 conf. 7 MPa 4 conf. 10 MPa 2 conf. 20 MPa (12 July 2004)	RFM018	ZFMNW1200
	587.69–588.96	489–490		RFM029	FFM01
	814.48–815.36	661–662		RFM029	FFM01
Indirect tensile strength	161.57–164.15	134–136	20 along foliation 13 perpendicular to foliation (17 June 2003)	RFM018	ZFMNW1200
	586.87–588.06	489–490		RFM029	FFM01
	813.34–815.53	660–662		RFM029	FFM01
P-wave velocity transverse borehole core	158.20–166.65	131–138	34 (8 July 2004)	RFM018	ZFMNW1200
	248.00–263.53	209–222		RFM012	FFM04
	402.10–408.25	340–345		RFM012	FFM04
	485.5	408		RFM012	FFM04
	508.85–636.70	427–527		RFM029	FFM01
	660.25	546		RFM029	ZFMWNW0123
	685.35–943.30	565–754		RFM029	FFM01
967.60–999.8	771–793	RFM029	FFM01		

Drill site 5**Table 8-10. Rock mechanics investigations in borehole KFM05A.**

Testing method	Sample location secup–seclow [m]	Elevation seclow [m.b.s.l.]	No. of tested samples	Rock domain RFM	Fracture domain FFM or deformation zone DZ
Uniaxial compressive strength	326.94–328.18	275–276	10 (20 June 2004)	RFM029	FFM01
	560.03–561.05	468–469		RFM029	FFM01
Triaxial compressive strength	329.43–332.89	277–280	2 conf. 5 MPa 4 conf. 10 MPa 2 conf. 20 MPa (20 June 2004)	RFM029	FFM01
	572.68–575.68	478–481		RFM029	FFM01
Indirect tensile strength	330.14–337.09	278–284	20 Foliation not specified (24 September 2004 –07 February 2005)	RFM029	FFM01
	561.05–575.48	469–480		RFM029	FFM01
P-wave velocity transverse borehole core	165.50–226.89	138–191	32 (16 September 2004)	RFM029	FFM02
	250.00–381.15	210–320		RFM029	FFM01
	403.73–422.70	339–355		RFM029	ZFMENE2282
	444.00–569.00	373–475		RFM029	FFM01
	592.12–608.20	494–507		RFM029	ZFMENE0401B
	622.50–679.70	519–566		RFM029	FFM01 ⁽¹⁾
721.30–742.68	599–617	RFM029	FFM01 ⁽¹⁾		

⁽¹⁾ Sections which might be affected by DZ.

Drill site 6

Table 8-11. Rock mechanics investigations in borehole KFM06A.

Testing method	Sample location secup–seclow [m]	Elevation seclow [m.b.s.l]	No. of tested samples	Rock domain RFM	Fracture domain FFM or deforma- tion zone DZ
Uniaxial compressive strength	449.15–450.87	379–381	15 (15 February 2005)	RFM029	FFM01
	483.11–483.39	408		RFM029	FFM01
	495.98–503.50	418–424		RFM029	FFM01
	818.46–820.42	683–685		RFM045	FFM06
Indirect tensile strength	483.39–496.35	408–418	5 Foliation not specified (30 May 2005)	RFM029	FFM01
P-wave velocity transverse borehole core	153.95–194.35	129–164	30 (12 January 2005)	RFM029	FFM01
	222.70–266.10	188–225		RFM029	ZFMENE0060B
	286.55–308.50	242–261		RFM029	FFM01
	329.40–350.45	279–296		RFM029	ZFMENE0060A, ZFMB7
	372.20–502.60	315–424		RFM029	FFM01
	525.08–544.50	442–458		RFM029	ZFMNNE2273
	565.07–607.60	476–511		RFM029	FFM01
	633.15–633.15	532		RFM029	FFM01
	652.80	548		RFM029	Possible DZ
	673.85–715.95	565–600		RFM029	FFM01

Drill site 7

Table 8-12. Rock mechanics investigations in borehole KFM07A.

Testing method	Sample location secup–seclow [m]	Elevation seclow [m.b.s.l]	No. of tested samples	Rock domain RFM	Fracture domain FFM or deforma- tion zone DZ
Uniaxial compressive strength	356.25–356.67	301	8 (1 March 2005)	RFM029	FFM01
	676.39–679.53	564–566		RFM029	FFM01
Triaxial compressive strength	356.97–357.81	301 302	1 conf. 5 MPa 2 conf. 10 MPa 1 conf. 20 MPa (25 August 2005)	RFM029	FFM01
Indirect tensile strength	678.49–681.45	566–568	6 Foliation not specified (30 March 2006)	RFM029	FFM01
P-wave velocity transverse borehole core	201.30	170	33 (1 March 2005)	RFM029	Possible DZ
	219.90–402.00	186–339		RFM029	FFM01
	424.95–486.20	358–409		RFM029	FFM01 ⁽¹⁾
	512.55–783.40	430–650		RFM029	FFM01

⁽¹⁾ Sections which might be affected by DZ.

Drill site 8

Table 8-13. Rock mechanics investigations in borehole KFM08A.

Testing method	Sample location secup–seclow [m]	Elevation seclow [m.b.s.]	No. of tested samples	Rock domain RFM	Fracture domain FFM or deforma- tion zone DZ
Triaxial compressive strength	326.25–326.41	271	2 conf. 5 MPa	RFM029	FFM01 ⁽¹⁾
	398.48–398.63	329	2 conf. 10 MPa	RFM029	FFM01 ⁽¹⁾
	523.64–524.11	426–427	2 conf. 20 MPa	RFM029	FFM01
	618.11–618.42	497	(15 November 2005)	RFM029	FFM01
Indirect tensile strength*	668.54–668.60	533	1 Foliation not specified (30 March 2006)	RFM029	FFM01
P-wave velocity transverse borehole core	200.60–238.70	168–200	33 (24 May 2005)	RFM029	FFM01 ⁽¹⁾
	263.40–299.95	220–250		RFM029	ZFMENE1061A
	321.70	268		RFM029	FFM01 ⁽¹⁾
	343.75–399.00	285–329		RFM029	FFM01
	420.15–457.10	346–375		RFM029	FFM01
	487.90	399		RFM029	ZFMNNW1204
	503.20–521.40	411–425		RFM029	FFM01
	545.70	443		RFM029	Possible DZ
	559.00–621.9	453–499		RFM029	FFM01
	642.40–660.15	514–527		RFM029	FFM01
	680.00	541		RFM029	Possible DZ
700.65–758.75	556–597	RFM029	FFM01		
781.00	612	RFM029	ZFMENE2248		

* This test is included in the report for KFM07C.

⁽¹⁾ Sections which might be affected by DZ.

Drill site 9

Table 8-14. Rock mechanics investigations in borehole KFM09A.

Testing method	Sample location secup–seclow [m]	Elevation seclow [m.b.s.]	No. of tested samples	Rock domain RFM	Fracture domain FFM or deforma- tion zone DZ
Uniaxial compressive strength	482.01–486.10	393–396	8 (15 January 2006)	RFM044	FFM05
	594.90–596.31	479		RFM034	FFM01
Triaxial compressive strength	481.49–481.77	392	1 conf. 5 MPa 2 conf. 10 MPa 2 conf. 20 MPa (15 January 2006)	RFM044	FFM05
	565.83–597.28	457–480		RFM034	FFM01
Indirect tensile strength	466.89–467.02	381	20 Foliation not specified (15 January 2006)	RFM044	FFM05
	479.96–480.03	391		RFM044	FFM05
	563.93–564.13	455–456		RFM034	FFM01
	592.99–595.07	477–479		RFM034	FFM01
P-wave velocity transverse borehole core	200.45	165	30 (15 December 2005)	RFM029	FFM01
	229.80	190		RFM029	ZFMENE0159A, ZFMNNW0100
	255.74	211		RFM044	ZFMENE0159A, ZFMNNW0100
	286.32–500.05	236–407		RFM044	FFM05
	512.10	416		RFM034	FFM05 ⁽²⁾
	530.25–635.40	430–508		RFM012	FFM01
	650.00–665.20	519–530		RFM012	FFM04
	678.77–710.95	539–562		RFM012	FFM04
	725.00–741.90	571–583		RFM018	ZFMNW1200
	759.22–767.55	594–600		RFM018	FFM04 ⁽¹⁾
	796.30	619		RFM018	FFM04

⁽¹⁾ Sections which might be affected by DZ.

⁽²⁾ Section of vuggy rock outside DZ.

8.2.2 Fracture properties

Tests on fractures were performed on core samples collected from boreholes KFM01A, KFM02A, KFM03A, KFM04A, KFM05A, KFM06A, KFM07A and KFM08A, see Table 8-1. Results from two types of tests are available: direct shear tests with constant normal loading and tilt tests.

Available test results from the tilt and shear tests are presented in Table 8-15 to Table 8-25. Each table gives the following information:

- Testing method.
- The borehole section and elevation at which the samples are taken.
- Number of tested samples and
 - the normal stress during each test varying from 0.5–20 MPa,
 - date of testing.
- The rock domain from which the samples are taken.
- The fracture domain or deformation zone to which the samples belong.

Drill site 1

Table 8-15. Rock mechanics investigations on fractures in borehole KFM01A.

Testing method	Sample location secup–seclow [m]	Elevation seclow [m.b.s.l]	No. of tested samples	Rock domain RFM	Fracture domain FFM or deforma- tion zone DZ
Normal loading and shear tests on joints*	228.49–235.77	224–231	6 (each sample tested at normal stress levels 0.5 MPa, 5 MPa, 20 MPa) (09 July 2004)	RFM029	FFM01
	390.43–390.43	385		RFM029	ZFMENE1192
	699.62–699.62	689		RFM029	FFM01
Normal loading and shear tests on joints (NGI)	229.51–235.76	225–231	5 (each sample tested at normal stress levels 0.5 MPa, 5 MPa, 20 MPa) (08 July 2004)	RFM029	FFM01
	390.33–390.33	385		RFM029	ZFMENE1192
Tilt tests	108.64–196.10	105–192	41 (20 February 2003– 24 February 2003)	RFM029	FFM02
	227.16–257.85	224–253		RFM029	FFM01
	268.70–269.00	264		RFM029	ZFMENE1192
	290.75–290.90	286		RFM029	FFM01
	320.46–349.69	315–344		RFM029	FFM01
	386.35–408.61	381–403		RFM029	ZFMENE1192
	433.60–597.64	427–589		RFM029	FFM01
	639.87–670.12	630–660		RFM029	ZFMENE2254
710.90–898.80	700–883	RFM029	FFM01		

* Tests performed with the Type I methodology.

Table 8-16. Rock mechanics investigations on fractures in borehole KFM01D.

Testing method	Sample location secup–seclow [m]	Elevation seclow [m.b.s.l]	No. of tested samples	Rock domain RFM	Fracture domain FFM or deforma- tion zone DZ
Normal loading and shear tests on joints*	482.33–482.83	379	3 (each sample tested at normal stress levels 2 MPa, 5 MPa, 10 MPa) (15 June 2006)	RFM029	FFM01
	587.93–588.28	457		RFM029	FFM01
	658.34–658.58	509		RFM029	FFM01
				RFM029	FFM01

* These tests were performed on sealed fractures.

Drill site 2

Table 8-17. Rock mechanics investigations on fractures in borehole KFM02A.

Testing method	Sample location secup–seclow [m]	Elevation seclow [m.b.s.l]	No. of tested samples	Rock domain RFM	Fracture domain FFM or deforma- tion zone DZ
Normal loading and shear tests on joints*	331.76–331.88	323	7 (each sample tested at normal stress levels 0.5 MPa, 5 MPa, 20 MPa) (9 July 2004)	RFM029	FFM03
	528.31–535.30	519–526		RFM029	Possible DZ
	715.96–717.99	705–707		RFM029	FFM01
Tilt tests	216.57–238.42	209–230	40 (10 June 2003– 17 June 2003)	RFM029	FFM03
	306.64–306.64	298		RFM029	ZFM1189
	310.54–411.39	302–403		RFM029	FFM03
	425.81–425.81	417		RFM029	ZFMA2
	443.26–474.68	434–466		RFM029	FFM01 ⁽¹⁾
	482.08–510.01	473–501		RFM029	ZFMF1
	525.70–578.49	517–569		RFM029	Possible DZ
	614.94–839.54	605–828		RFM029	FFM01

⁽¹⁾ Sections which might be affected by DZ.

* Tests performed with the Type I methodology.

Drill site 3

Table 8-18. Rock mechanics investigations on fractures in borehole KFM03A.

Testing method	Sample location secup–seclow [m]	Elevation seclow [m.b.s.l]	No. of tested samples	Rock domain RFM	Fracture domain FFM or deforma- tion zone DZ
Normal loading and shear tests on joints*	263.90–267.79	257	8 (each sample tested at normal stress levels 0.5 MPa, 5 MPa, 20 MPa) (9 July 2004)	RFM017	FFM03
	306.19–308.54	298–299		RFM029	FFM03
	516.38–518.82	508		RFM029	FFM03
	666.85–670.16	658		RFM029	FFM03
Tilt tests	207.06–217.88	198–209	35 (06 October 2003– 13 October 2003)	RFM029	FFM03
	228.85–287.88	220–279		RFM017	FFM03
	320.39–610.16	311–600		RFM029	FFM03
	640.03–642.88	629–632		RFM029	ZFMB1
	685.81–749.46	675–738		RFM029	FFM03
	804.95–806.01	793–794		RFM029	ZFMA3
	834.35–953.34	823–941		RFM029	FFM03

* Tests performed with the Type I methodology.

Table 8-19. Rock mechanics investigations on fractures in borehole KFM03B.

Testing method	Sample location secup–seclow [m]	Elevation seclow [m.b.s.l]	No. of tested samples	Rock domain RFM	Fracture domain FFM or deforma- tion zone DZ
Tilt tests	39.45–39.45	31	3 (13 October 2003– 15 October 2003)	RFM029	ZFMA5
	47.12–50.12	38–41		RFM029	FFM03

Drill site 4

Table 8-20. Rock mechanics investigations on fractures in borehole KFM04A.

Testing method	Sample location secup–seclo w [m]	Elevation seclo w [m.b.s.l]	No. of tested samples	Rock domain RFM	Fracture domain FFM or deformation zone DZ
Normal loading and shear tests on joints*	111.49–112.46	89–90	6 (each sample tested at normal stress levels 0.5 MPa, 5 MPa, 20 MPa) (9 July 2004)	RFM018	ZFMNW1200
	164.15–164.66	136		RFM018	ZFMNW1200
	807.78–807.91	658		RFM029	FFM01
	822.15–822.27	668		RFM029	FFM01
Tilt tests	488.80–493.59	411–415	26 (8 July 2004)	RFM012	FFM04
	516.88–641.41	434–532		RFM029	FFM01
	654.76–658.64	542–545		RFM029	ZFMWNW0123
	690.78–965.22	570–771		RFM029	FFM01

* Tests performed with the Type I methodology.

Drill site 5

Table 8-21. Rock mechanics investigations on fractures in borehole KFM05A.

Testing method	Sample location secup–seclo w [m]	Elevation seclo w [m.b.s.l]	No. of tested samples	Rock domain RFM	Fracture domain FFM or deformation zone DZ
Normal loading and shear tests on joints*	326.81–333.54	275–281	4 (each sample tested at normal stress levels 0.5 MPa, 5 MPa, 20 MPa) (20 June 2004)	RFM029	FFM01
	563.09–563.23	471		RFM029	FFM01
Normal loading and shear tests on joints*	329.30–336.09	277–283	4 (each sample tested at normal stress levels 0.5 MPa, 5 MPa, 20 MPa) (10 January 2005)	RFM029	FFM01
	575.83–576.50	481		RFM029	FFM01
Tilt tests	370.36–392.03	311–330	9 (16 September 2004)	RFM029	FFM01
	406.91–424.67	342–357		RFM029	ZFMENE2282
	456.73–468.60	383–393		RFM029	FFM01
	598.96–608.29	500–507		RFM029	ZFMENE0401B

* All normal and shear tests in KFM05A were performed with the Type II methodology. On the four samples dated 2005-01-10, normal loading tests were also performed according to the Type III method.

Drill site 6

Table 8-22. Rock mechanics investigations on fractures in borehole KFM06A.

Testing method	Sample location secup–seclo w [m]	Elevation seclo w [m.b.s.l]	No. of tested samples	Rock domain RFM	Fracture domain FFM or deformation zone DZ
Normal loading and shear tests on joints*	395.28–395.38	335	6 (each sample tested at normal stress levels 0.5 MPa, 5 MPa, 20 MPa) (15 February 2005)	RFM029	FFM01
	429.67–429.84	364		RFM029	FFM01
	452.29–453.03	383		RFM029	FFM01
	470.70–470.88	399		RFM029	FFM01
	493.48–493.53	418		RFM029	FFM01

* Shear tests performed with the Type III methodology.

Drill site 7

Table 8-23. Rock mechanics investigations on fractures in borehole KFM07A.

Testing method	Sample location secup–seclow [m]	Elevation seclow [m.b.s.l]	No. of tested samples	Rock domain RFM	Fracture domain FFM or deformation zone DZ
Normal loading and shear tests on joints*	335.99–338.28	285–287	5 (each sample tested at normal stress levels 0.5 MPa, 5 MPa, 20 MPa) (1 March 2005)	RFM029	FFM01

* Shear tests performed with the Type III methodology.

Drill site 8

Table 8-24. Rock mechanics investigations on fractures in borehole KFM08A.

Testing method	Sample location secup–seclow [m]	Elevation seclow [m.b.s.l]	No. of tested samples	Rock domain RFM	Fracture domain FFM or deformation zone DZ
Normal loading and shear tests on joints*	297.80–302.81	249–253	5 (each sample tested at normal stress levels 0.5 MPa, 5 MPa, 20 MPa) (17 October 2005)	RFM029	ZFMENE1061A
	338.39–338.63	282		RFM029	FFM01 ⁽¹⁾
	398.06–398.23	329		RFM029	FFM01
	472.34–472.50	388		RFM029	FFM01

* Shear tests performed with the Type III methodology.

⁽¹⁾ Sections which might be affected by DZ.

Drill site 9

Table 8-25. Rock mechanics investigations on fractures in borehole KFM09A.

Testing method	Sample location secup–seclow [m]	Elevation seclow [m.b.s.l]	No. of tested samples	Rock domain RFM	Fracture domain FFM or deformation zone DZ
Normal loading and shear tests on joints*	431.35–431.52	353	6 (each sample tested at normal stress levels 0.5 MPa, 5 MPa, 20 MPa) (15 January 2006)	RFM044	FFM05
	450.84–451.06	368		RFM044	FFM05
	575.76–575.89	464		RFM034	FFM01
	669.30–669.64	533		RFM012	FFM04
	683.47–684.75	543		RFM012	FFM04
Tilt tests	200.57–200.57	165	9 (13 December 2005– 15 December 2005)	RFM029	FFM01
	221.35–236.18	183–195		RFM029	ZFMENE0159A, ZFMNNW0100
	259.65–259.65	214	RFM044	ZFMENE0159A, ZFMNNW0100	
	292.75–382.75	242 314	RFM044	FFM05	

* Shear tests performed with the Type III methodology.

8.3 Overview of test results

This section presents an overview of the mechanical properties of intact rock and fractures based on evaluation of the test results. Valuable data from the intact rock tests are sorted by rock type and the variation of the parameters with depth is also presented. Test data from independent laboratories and tests on sealed fractures are omitted in the tables and diagrams.

8.3.1 Tests on intact rock

Uniaxial compressive strength (UCS)

The test results classified by rock types are presented in Table 8-26. Most of the tested samples fall within the range 200–270 MPa and represent granite to granodiorite, as well as granodiorite, metamorphic (it should be noticed that only 4 samples of this rock type have been tested). Figure 8-2a illustrates the frequency distribution of the UCS for each rock type. The rock type tonalite to granodiorite presents in general lower strength, with UCS values between 140 to 200 MPa. Pegmatite and pegmatitic granite generally exhibit higher strength, but the range is large. Based on the number of samples tested, it is difficult to draw any conclusion regarding the strength of the aplitic metagranite (referred to in the tables as granite, metamorphic, aplitic).

The presence of sealed fractures has been reported in 6 of the tested samples, of which three are the granite to granodiorite rock type. The UCS values of those samples range from 127 to 187 MPa, which are quite low values compared to the values of all tested samples of this rock type. One sample from pegmatite also has a very low UCS value. However, the UCS obtained for a tonalite to granodiorite sample with sealed fractures lies in the same range as all tested samples of this rock type. It is possible that the presence of sealed fractures causes lower UCS values but no firm conclusions can be drawn from the analyses carried out.

Five samples of granite to granodiorite from KFM01A were tested by HUT for comparison. /Lanaro and Fredriksson 2005/ reported that the average UCS of these samples tested by HUT was 5% higher compared to the results obtained by SP, which are summarized in Table 8-26.

The drilling process and stress release of the core may cause an increase of the pore volume in the core samples with depth. Such induced microfractures may affect the strength of the rock. The plot in Figure 8-2b shows the variation of strength with depth down to 800 m below sea level for the various rock types. The whole population of granite to granodiorite samples seems to indicate a minor decrease of the UCS with depth. According to /Lanaro and Fredriksson 2005/, the P-wave velocity in core samples from KFM02B decreases slightly below c 700 m below sea level, which supports a possible decrease in UCS in this borehole between the uppermost and lowermost test levels. These observations are illustrated by the WellCad and P-wave velocity plots in Appendix 6 and 7.

Table 8-26. Uniaxial compressive strength, USC (MPa), by rock type.

Rock type	Number of samples	Minimum	Mean	Median	Maximum	Standard deviation
Granite to granodiorite, metamorphic, medium grained	68	157	222	221	289	26
Granite, metamorphic, aplitic	4	229	310	320	371	67
Granodiorite, metamorphic	4	222	236	236	249	12
Pegmatite, pegmatitic granite	14	153	230	231	309	40
Tonalite to granodiorite, metamorphic	8	140	156	155	176	13
All intact samples	98	140	222	222	371	39
Only samples with sealed fractures	6	94	152	158	188	37

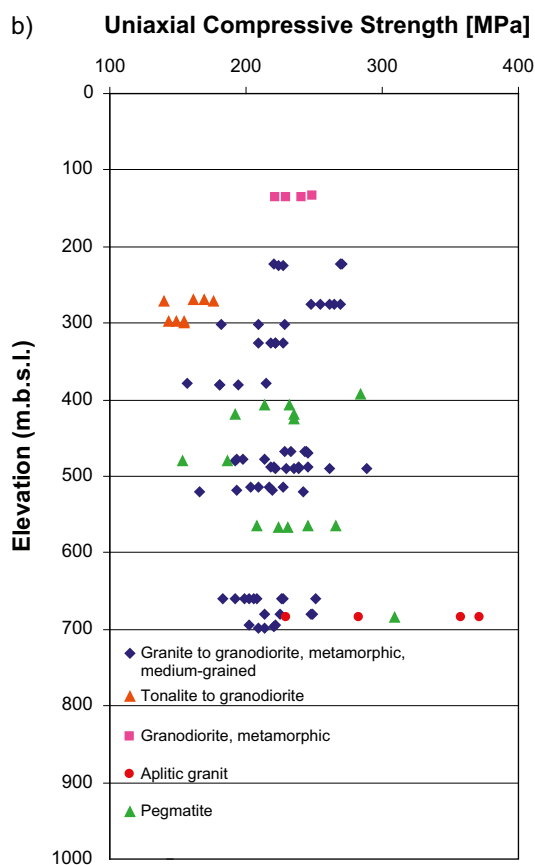
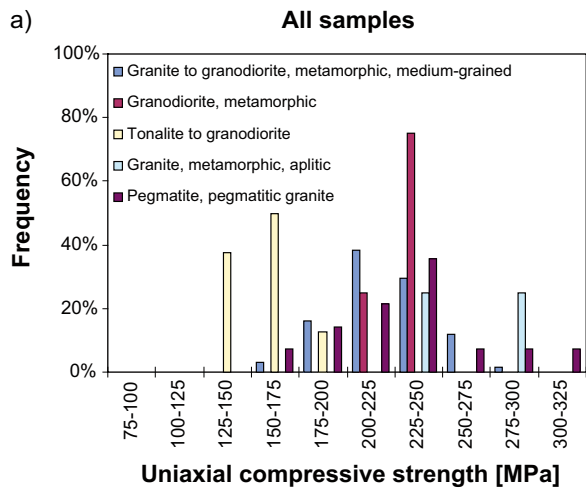


Figure 8-2. Uniaxial compressive strength (UCS) Forsmark 2.2. a) sorted by rock type, b) variation with depth and rock type. Note: the frequencies of different rock types should not be compared with each other from figure a.

Triaxial compressive strength

Triaxial tests were performed in order to evaluate the strength and elastic parameters of the intact rock, as well as the variation of the strength and elastic parameters with increasing stress. The confinement stress was varied in two series namely 2, 7 and 10 MPa and 5, 12 and 20 MPa.

The test results are presented in Table 8-27 and Table 8-28.

Table 8-27. Test results from triaxial testing with confinement stresses 2, 7 and 10 MPa.

Rock type	Confinement stress 2 MPa			Confinement stress 7 MPa			Confinement stress 10 MPa		
	No. of samples	Mean value (MPa)	Std	No. of samples	Mean value (MPa)	Std	No. of samples	Mean value (MPa)	Std
Granite to granodiorite, metamorphic, medium-grained	11	296.7	69.7	16	298.0	68.7	15	319.6	77.0
Granite, granodiorite and tonalite, metamorphic, fine- to medium-grained	0	–	–	0	–	–	1	330.5	–
Granodiorite, metamorphic	1	226.3	–	2	332.8	36.7	0	–	–
Pegmatite, pegmatitic granite	0	–	–	0	–	–	3	319.9	82.2
Tonalite to granodiorite, metamorphic	2	188.8	14.8	4	194.2	12.5	0	–	–

Table 8-28. Test results from triaxial testing with confinement stresses 5, 12 and 20 MPa.

Rock type	Confinement stress 5 MPa			Confinement stress 12 MPa			Confinement stress 20 MPa		
	No. of samples	Mean value (MPa)	Std	No. of samples	Mean value (MPa)	Std	No. of samples	Mean value (MPa)	Std
Granite to granodiorite, metamorphic, medium-grained	7	343.7	78.3	5	277.3	64.9	8	357.0	79.5
Granite, granodiorite and tonalite, metamorphic, fine- to medium-grained	1	260.3	–	0	–	–	2	442.1	21.8
Granodiorite, metamorphic	0	–	–	0	–	–	0	–	–
Pegmatite, pegmatitic granite	2	317.2	80.4	0	–	–	3	321.6	81.8
Tonalite to granodiorite, metamorphic	0	–	–	2	198.3	20.6	0	–	–

Five samples of granite to granodiorite were tested by HUT and compared with the results presented in Table 8-27 and Table 8-28. The results from the two laboratories are in good agreement /Lanaro and Fredriksson 2005/.

Tensile strength (TS)

The indirect tensile strength was evaluated from testing according to the Brazilian test set up, and the results are summarized in Table 8-29. The tests were performed parallel as well as perpendicular to the foliation. Pegmatite and pegmatitic granite generally have lower tensile strength compared to granite, granodiorite and tonalite, fine- to medium-grained. The granodiorite, metamorphic exhibits the highest tensile strength values.

Figure 8-3a presents the frequency distribution of the tensile strength for each main rock type. The test data exhibit wide variation from less than 8 MPa to 22MPa. The new data confirm that the loading direction has a minor influence on the tensile strength /Lanaro and Fredriksson 2005/.

The tests performed by HUT on 10 fully saturated samples of granite to granodiorite give on average tensile strength values that are 18% higher than those presented in Table 8-29 /Lanaro and Fredriksson 2005/.

Table 8-29. Tensile strength, TS (MPa), for the different rock types.

Rock type	Orientation with respect to foliation	No. of samples	Minimum	Mean	Median	Maximum	Standard deviation
Granite to granodiorite, metamorphic, medium-grained	Parallel	55	10	13	13	17	1.6
	Perpendicular	47	10	14	14	18	1.8
	No information	28	11	14		18	1.6
Granite, granodiorite and tonalite, metamorphic, fine to medium-grained	No information	4	14	16	16	19	2.4
Granodiorite, metamorphic	Parallel	5	17	18	17	19	0.7
	Perpendicular	6	17	18	18	20	1.1
Pegmatite, pegmatitic granite	No information	20	7	11	10	17	2.9
Tonalite to granodiorite, metamorphic	Parallel	10	15	16	16	17	0.9
	Perpendicular	10	14	15	15	18	1.2
All intact samples	–	185	7	14	14	20	2.3

Variation of tensile strength with depth is shown in Figure 8-3b. There is a slight trend towards decreasing tensile strength with depth.

Elastic properties of the intact rock

Uniaxial and triaxial testing also provide results on the deformability of the intact sample in terms of the elastic parameters Young's Modulus (E) and Poisson's Ratio (ν). The Young's modulus determined for each rock type from uniaxial and triaxial testing is summarized in Table 8-30 and Table 8-31, respectively. In general, the values from the triaxial loading seem to be lower.

Table 8-30. Young's modulus, E (GPa), by rock type as determined from uniaxial loading.

Rock type	Number of samples	Minimum	Mean	Median	Maximum	Standard deviation
Granite to granodiorite, metamorphic, medium-grained	68	69	76	76	83	2.8
Granite, metamorphic, aplitic	4	80	82	81	86	2.6
Granodiorite, metamorphic	4	73	77	77	81	3.0
Pegmatite, pegmatitic granite	14	71	76	76	86	4.2
Tonalite to granodiorite, metamorphic	8	69	72	71	78	3.3
All intact samples	98	69	76	76	86	3.4
Only samples with sealed fractures	6	72	78	78	83	4.0

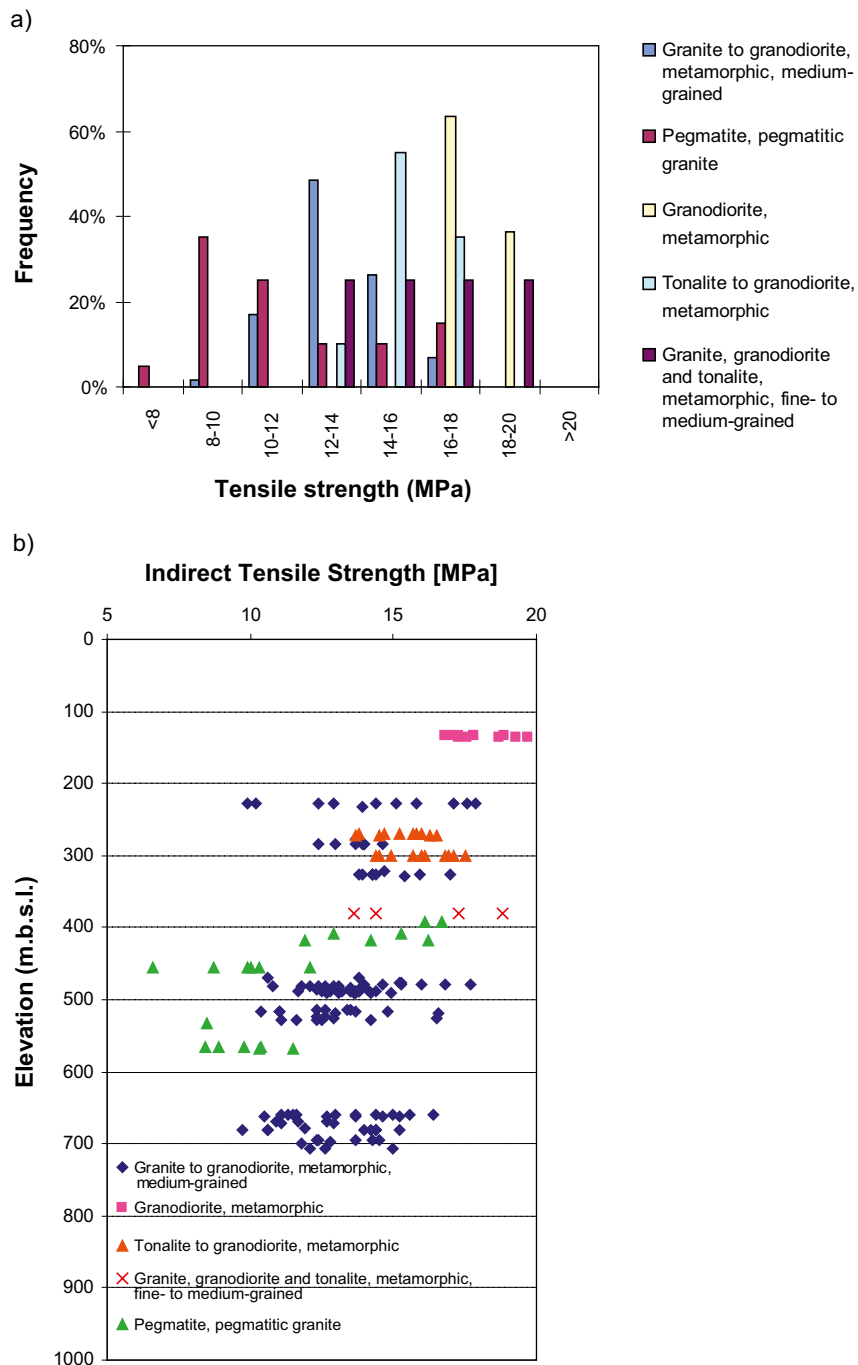


Figure 8-3. Tensile strength a) sorted by rock type, b) variation with depth.

Variation of the Young's Modulus with depth evaluated from the uniaxial and triaxial loading tests is presented in Figure 8-4a and Figure 8-4b, respectively.

A slight decrease in Young's modulus with depth can be observed for the granite to granodiorite in Figure 8-4a. However, these results do not provide any strong evidence of stress dependency of Young's modulus.

The independent testing at HUT of six samples of granite to granodiorite gave an average Young's modulus of 75 GPa /Eloranta 2004/, which is in very good agreement with the values presented in Table 8-30.

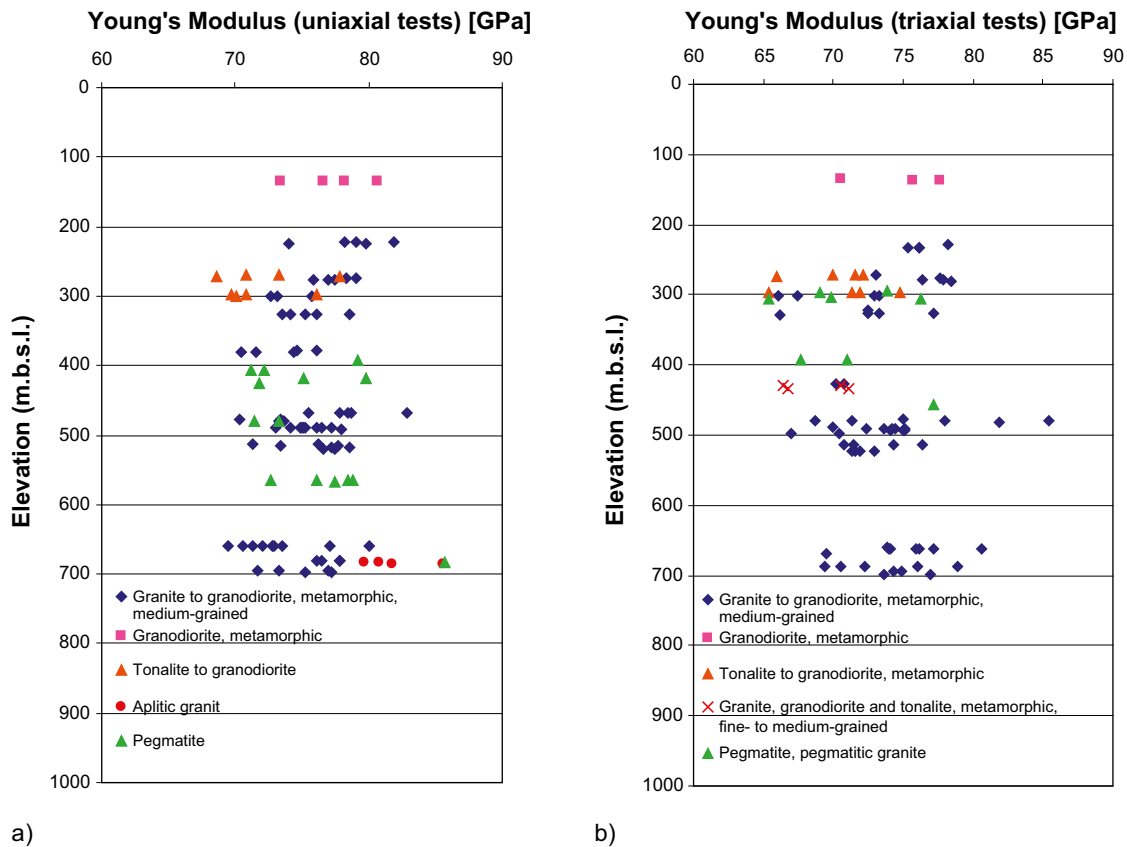


Figure 8-4. Young's Modulus versus depth determined from a) uniaxial testing (UCS) and b) triaxial testing (the confining pressure varies from 2 to 20 MPa).

Table 8-31. Young's modulus, Et (GPa), by rock type as determined from triaxial loading.

Rock type	Number of samples	Minimum	Mean	Median	Maximum	Standard deviation
Granite to granodiorite, metamorphic, medium-grained	62	66	74	74	85	3.7
Granite, granodiorite and tonalite, metamorphic, fine- to medium-grained	4	66	69	69	71	2.4
Granodiorite, metamorphic	3	71	75	76	78	3.7
Pegmatite, pegmatitic granite	8	65	71	70	77	4.2
Tonalite to granodiorite, metamorphic	8	65	70	71	75	3.2
All intact samples	85	65	73	74	85	3.9

The values obtained for Poisson's ratio are evaluated from uniaxial and triaxial tests and summarized in Table 8-32 and Table 8-33, respectively. The values from both tests are in the range 0.15 to 0.30, which are very normal values for hard rock. The values are significantly lower for some rock types when determined from triaxial tests.

Table 8-32. Poisson's ratio, ν (-), by rock type as determined from uniaxial loading.

Rock type	Number of samples	Minimum	Mean	Median	Maximum	Standard deviation
Granite to granodiorite, metamorphic, medium-grained	68	0.14	0.24	0.24	0.30	0.03
Granite, metamorphic, aplitic	4	0.25	0.27	0.26	0.31	0.03
Granodiorite, metamorphic	4	0.19	0.23	0.24	0.25	0.03
Pegmatite, pegmatitic granite	14	0.19	0.29	0.30	0.35	0.04
Tonalite to granodiorite, metamorphic	8	0.23	0.27	0.28	0.34	0.04
All intact samples	98	0.14	0.25	0.25	0.35	0.04
Only samples with sealed fractures	6	0.18	0.24	0.24	0.31	0.05

Table 8-33. Poisson's ratio, ν_t (-), by rock type as determined from triaxial loading.

Rock type	Number of samples	Minimum	Mean	Median	Maximum	Standard deviation
Granite to granodiorite, metamorphic, medium-grained	62	0.15	0.20	0.19	0.26	0.03
Granite, granodiorite and tonalite, metamorphic, fine- to medium-grained	4	0.20	0.24	0.24	0.28	0.04
Granodiorite, metamorphic	3	0.18	0.18	0.18	0.19	0.01
Pegmatite, pegmatitic granite	8	0.17	0.23	0.24	0.28	0.04
Tonalite to granodiorite, metamorphic	8	0.18	0.20	0.20	0.23	0.02
All intact samples	85	0.15	0.20	0.20	0.28	0.03

Variation of Poisson's ratio with depth is illustrated in Figure 8-5a and Figure 8-5b for uniaxial and triaxial test results, respectively. A slight trend with depth can be observed in Figure 8-5a for granite and granodiorite.

The independent testing at HUT of six samples of granite to granodiorite gave an average Poisson's ratio of 0.29 /Eloranta 2004/, with a range of 0.28 to 0.30 /Lanaro and Fredriksson 2005/. These results are not in agreement with the values presented in Table 8-32.

P-wave velocity

The P-wave velocity was measured on cores in two directions, and the difference between the maximum and minimum velocities recorded at the same measurement points provides an indication of the anisotropy of the intact rock. The P-wave velocity for all boreholes is presented in Appendix 7. Figure 8-6 illustrates two different modes of behaviour. In borehole KFM04A, the differences between minimum and maximum values are small, whereas in borehole KFM01A, the differences clearly indicate an anisotropic effect more or less independent of depth. Moreover, a decrease in P-wave velocity with depth might be an indication of the effects of drilling and stress release of the core, causing an increase in the pore volume of the samples with depth. A decrease in velocity with depth is noted in both boreholes. In KFM01A, the decrease is more accentuated below 500 m depth.

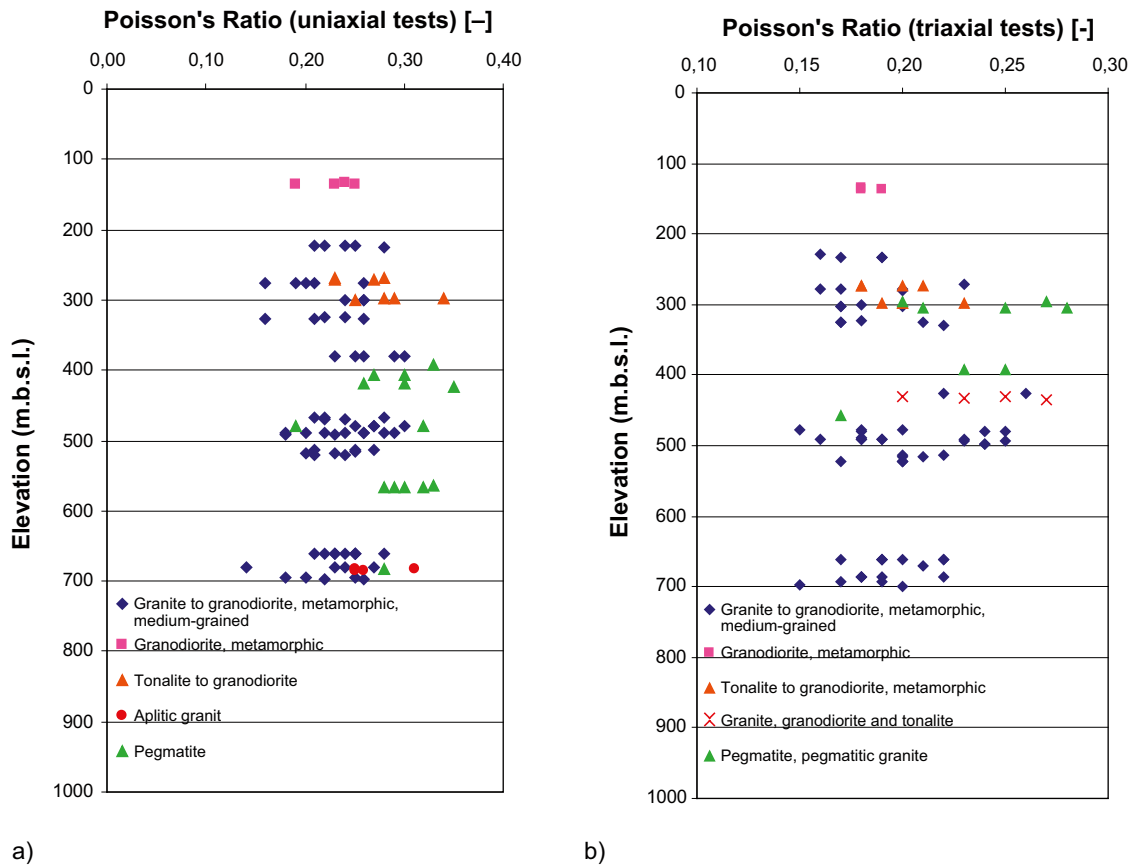


Figure 8-5. Poisson's ratio versus depth: a) uniaxial testing, b) triaxial testing.

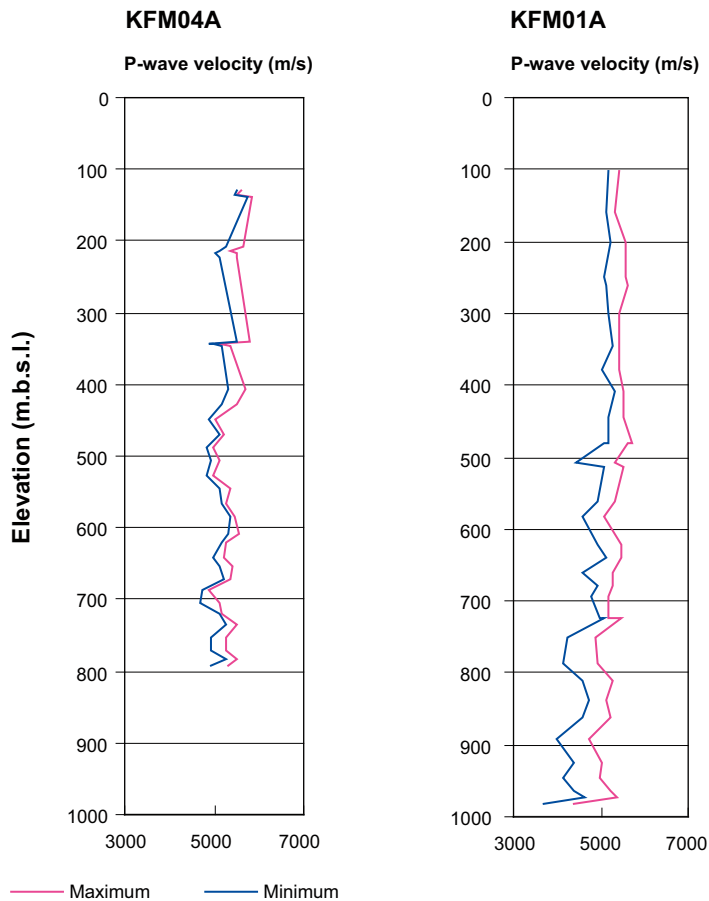


Figure 8-6. P-wave velocity from borehole KFM04A and KFM01A

The minimum and maximum velocities obtained on cores can be compared with the continuous logging of sonic velocity (this dataset is not evaluated in this report). These values are illustrated in the WellCad diagrams in Appendix 6. The sonic velocity shown in these diagrams is filtered to show only the P-wave velocities between 2,000 and 8,000 m/s.

8.3.2 Tests on fractures

Tilt tests

A number of tilt tests were performed on natural fractures in order to evaluate the strength of the fractures. The test results are presented in Table 8-34.

Variation of the evaluated parameters with depth – basic and residual friction angle, JRC_{100} and JCS_{100} – are shown in Figure 8-7 and Figure 8-8. The basic and residual friction angles display a small increase with depth in Figure 8-7. JRC_{100} and JCS_{100} display no variation with depth in Figure 8-8.

Table 8-34. Test results from 163 tilt tests.

Test	Minimum	Mean	Median	Maximum	Standard deviation
Basic friction angle (°)	22.8	30.8	31.2	34.7	2.0
JRC_{100}	2.1	5.8	5.8	9.4	1.5
JCS_{100} (MPa)	33	83	77	156	25
Residual friction angle (°)	17.3	26.4	26.7	33.8	2.9

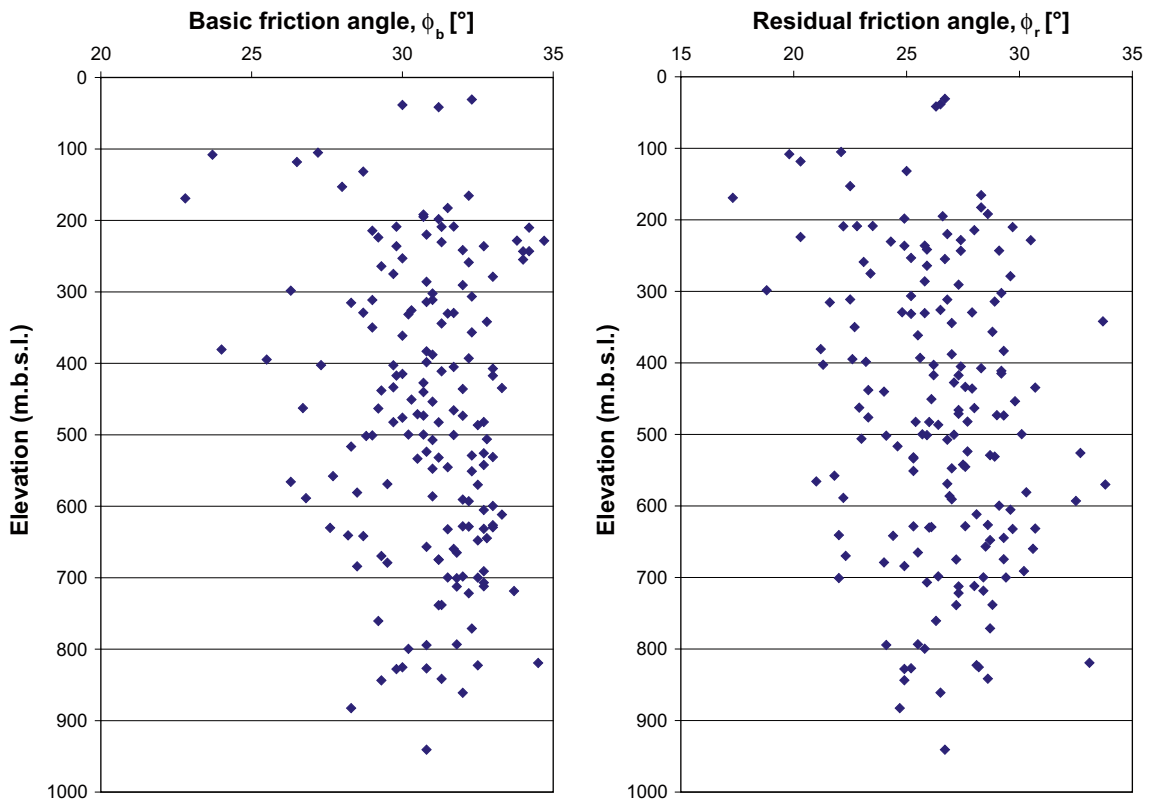


Figure 8-7. Basic friction angle and residual friction angle versus depth.

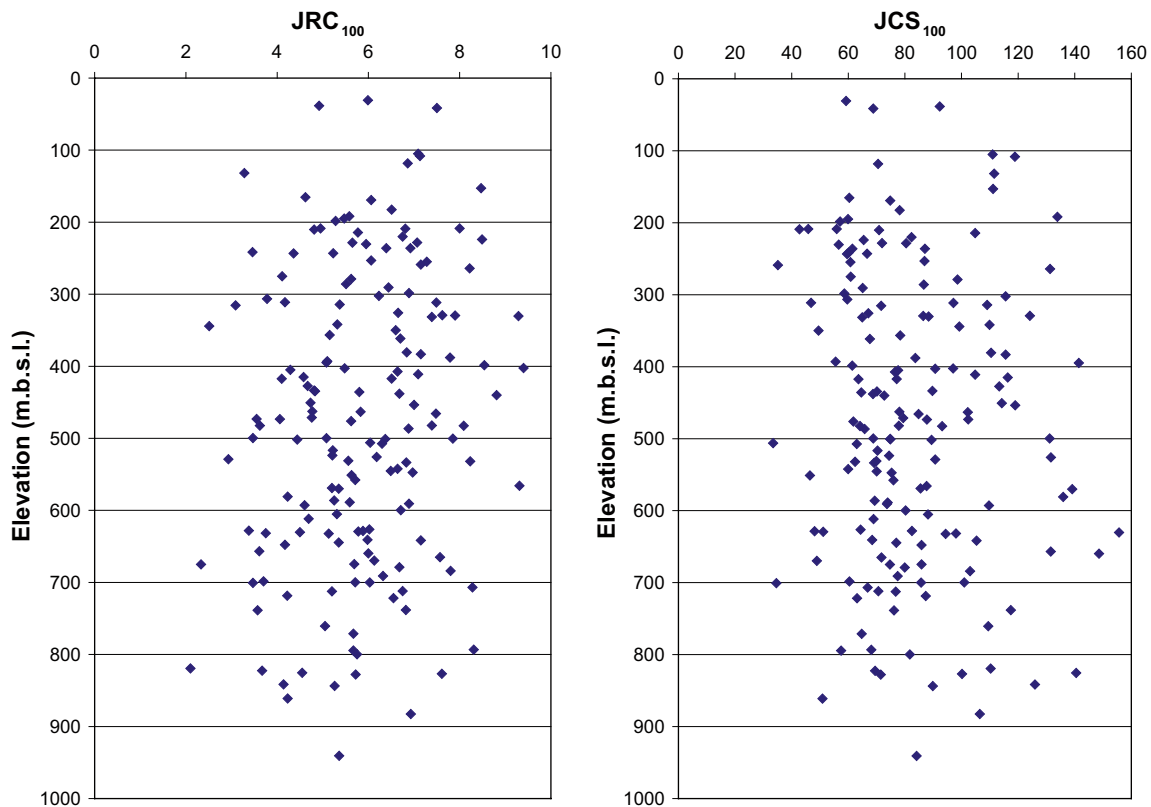


Figure 8-8. JRC_{100} and JCS_{100} (MPa) versus depth.

Normal and shear tests

Specimens containing a natural fracture from boreholes KFM01A to KFM09A were tested with normal stress and shear tests. In the normal loading tests, the joint was loaded and unloaded twice up to a normal stress of 10 MPa (20 MPa on specimens from borehole KFM05A). Direct shear tests with constant normal loading were carried out after the normal loading tests. Each fracture was sheared three times at the normal stress levels 0.5, 5 and 20 MPa.

Successive changes of the test set-up were made resulting in three different test configurations denoted Type I, Type II and Type III, which are briefly described below. The configuration mainly affects the normal stiffness and the friction angle.

Type I: The aim was to use maximum fracture length, resulting in various fracture lengths depending on the formation. The specimens were grouted into specimen holders using a fast-hardening anchoring grout. The normal deformation was measured using an indirect measurement method. A correction of the normal deformation values due to the cement deformation was subsequently carried out based on results from reference tests on steel specimens. The shear test started from an initial state corresponding to a matching fracture at the 0.5 and 20 MPa normal stress level, but not on the 5 MPa level. This test type was used for the tests on specimens from boreholes KFM01A, KFM02A, KFM03A and KFM04A.

Type II: The aim was to use similar fracture areas in the different specimens. The fractures were therefore cut to a length of between 50 and 60 mm. The specimens were also cut parallel to the fractures to obtain equal total heights. The specimens were grouted into smaller specimen holders using an epoxy material. The normal deformation values were corrected for the epoxy deformation based on results from reference tests on steel specimens. The shear test started from the initial state corresponding to a matching fracture at the normal stress level. This test type was used for the tests on specimens from borehole KFM05A.

Type III: The aim was to use similar fracture areas in the different specimens. The fractures were therefore cut to a length of between 50 and 60 mm. The specimens were also cut parallel to the fractures to obtain equal total heights. The specimens were partially grouted into fast-hardening anchoring grout for the normal loading test. The normal deformation was measured directly. The specimens were removed from the holders after the test and grouted into another set of specimen holders using an epoxy material. This configuration was used for the shear tests. The shear test started from an initial state corresponding to a matching fracture at the normal stress level. This test type was used for the tests on specimens from boreholes KFM05A, KFM06A, KFM07A, KFM08A and KFM09A.

Test results from the three types of tests are presented in Table 8-35, Table 8-36 and Table 8-37. Variation of the evaluated parameters with depth are shown in Figure 8-9, Figure 8-10, Figure 8-11, Figure 8-12, Figure 8-13 and Figure 8-14.

Table 8-35. Test results from Type I test (27 tests).

Parameter	Minimum	Mean	Median	Maximum	Standard deviation
Normal stiffness, K_N (MPa/mm)	65	130	114	288	52
Shear stiffness, $K_{S0.5}$ (MPa/mm)	2	10	8	35	7
Shear stiffness, K_{S5} (MPa/mm)	7	29	29	44	8
Shear stiffness, K_{S20} (MPa/mm)	18	32	33	49	9
Dilatancy angle, 0.5 MPa, $\psi_{0.5}$ (°)	0.3	15.9	16.4	27.1	4.9
Dilatancy angle, 5 MPa, ψ_5 (°)	0.5	4.0	4.0	10.9	2.5
Dilatancy angle, 20 MPa, ψ_{20} (°)	0.2	2.7	2.0	9.6	2.1
Peak friction angle, ϕ_p (°)	27.3	34.1	33.7	39.1	2.8
Peak cohesion, c_p (MPa)	0.0	0.6	0.6	1.1	0.3
Residual friction angle, ϕ_r (°)	19.8	30.3	31.2	37.6	5.2
Residual cohesion, c_r (MPa)	0.0	0.5	0.4	1.3	0.3

Table 8-36. Test results from Type II test (8 tests).

Parameter	Minimum	Mean	Median	Maximum	Standard deviation
Normal stiffness, K_N (MPa/mm)	268	340	286	521	110
Shear stiffness, $K_{S0.5}$ (MPa/mm)	5	12	12	23	6
Shear stiffness, K_{S5} (MPa/mm)	18	29	28	46	9
Shear stiffness, K_{S20} (MPa/mm)	18	35	36	52	12
Dilatancy angle, 0.5 MPa, $\psi_{0.5}$ (°)	9.0	14.8	15.6	17.9	3.3
Dilatancy angle, 5 MPa, ψ_5 (°)	2.5	9.0	9.7	13.7	3.4
Dilatancy angle, 20 MPa, ψ_{20} (°)	0.2	3.6	3.9	7.2	2.2
Peak friction angle, ϕ_p (°)	28.1	35.0	35.0	40.8	3.5
Peak cohesion, c_p (MPa)	0.4	1.0	1.1	1.3	0.3
Residual friction angle, ϕ_r (°)	28.7	33.9	33.7	39.1	3.0
Residual cohesion, c_r (MPa)	0.1	0.2	0.2	0.4	0.1

Table 8-37. Test results from Type III test (22 tests).

Parameter	Minimum	Mean	Median	Maximum	Standard deviation
Normal stiffness, K_N (MPa/mm)	328	1,010	827	2,445	530
Shear stiffness, $K_{S0.5}$ (MPa/mm)	1	9	9	20	5
Shear stiffness, K_{S5} (MPa/mm)	7	21	22	32	7
Shear stiffness, K_{S20} (MPa/mm)	18	33	29	51	10
Dilatancy angle, 0.5 MPa, $\psi_{0.5}$ (°)	7.8	13.0	13.2	19.1	3.1
Dilatancy angle, 5 MPa, ψ_5 (°)	3.0	8.0	8.0	13.0	2.4
Dilatancy angle, 20 MPa, ψ_{20} (°)	0.3	2.7	2.6	4.9	1.3
Peak friction angle, ϕ_p (°)	28.5	36.2	36.4	39.9	2.7
Peak cohesion, c_p (MPa)	0.2	0.8	0.7	1.7	0.4
Residual friction angle, ϕ_r (°)	29.6	34.6	34.4	39.2	2.4
Residual cohesion, c_r (MPa)	0.1	0.3	0.3	0.5	0.1

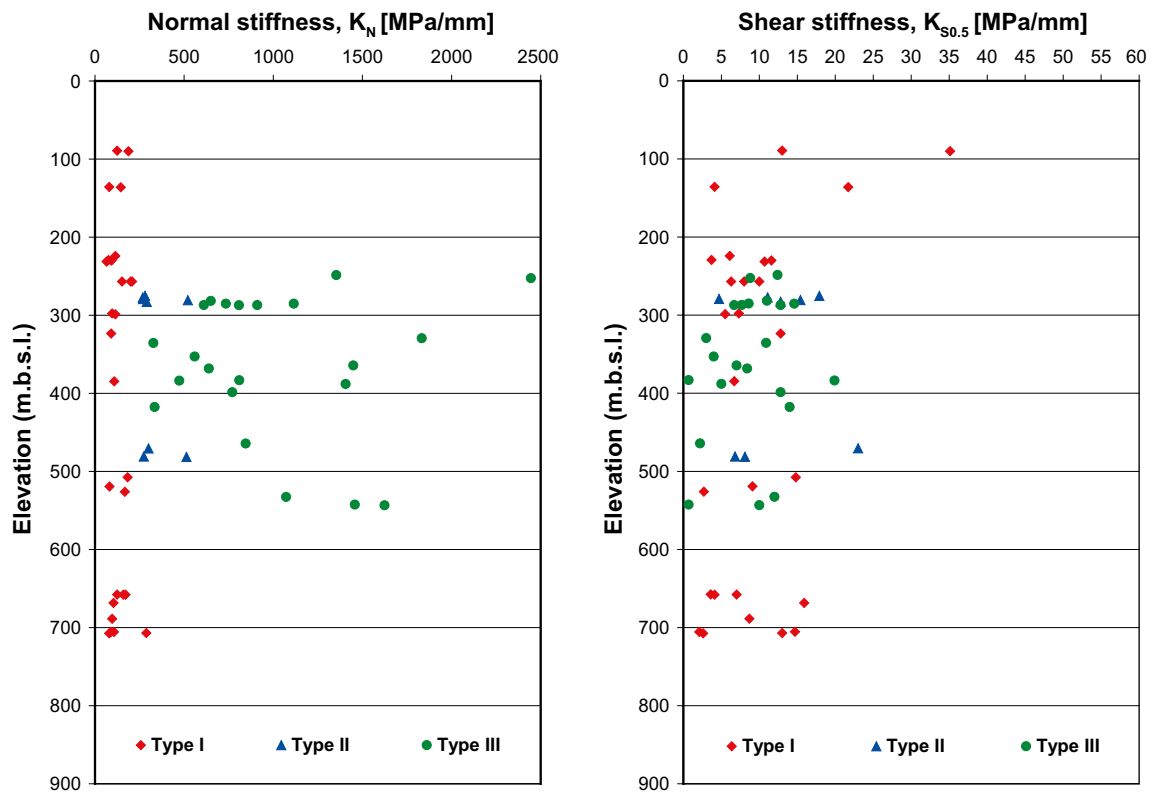


Figure 8-9. Normal stiffness K_N and shear stiffness $K_{S0.5}$ versus depth.

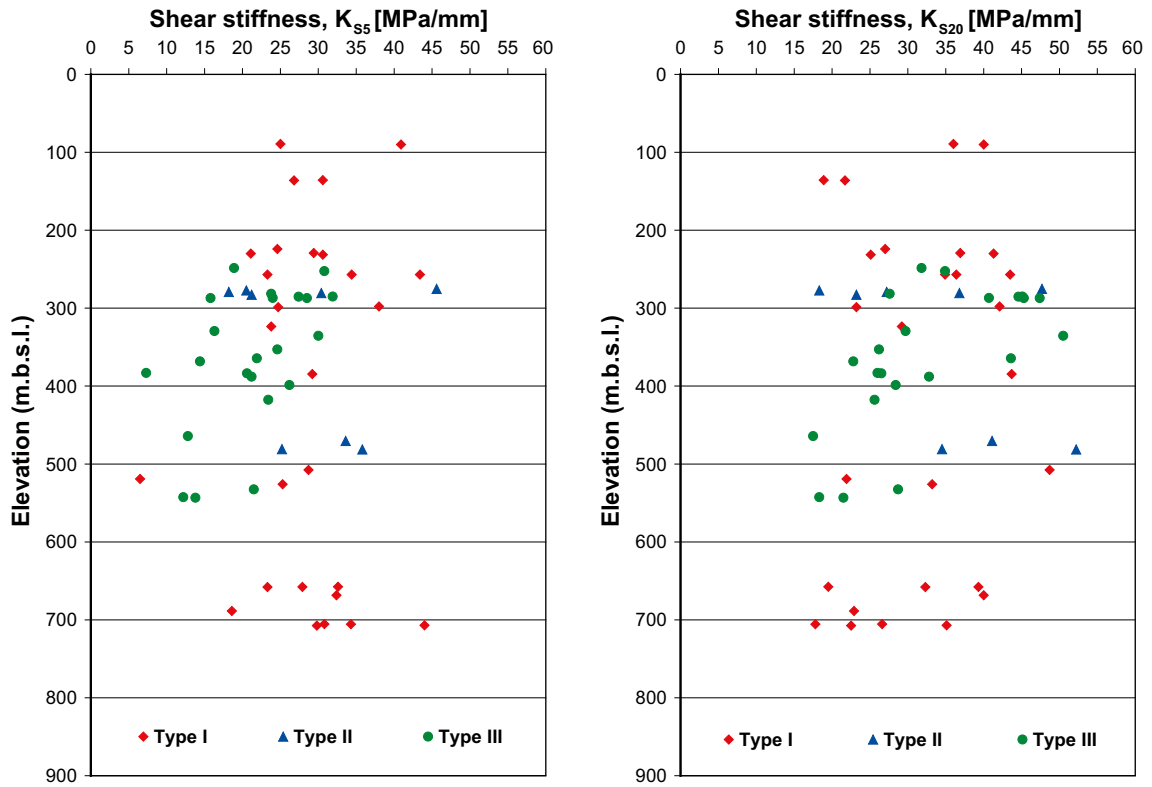


Figure 8-10. Shear stiffness K_{S5} and shear stiffness K_{S20} versus depth.

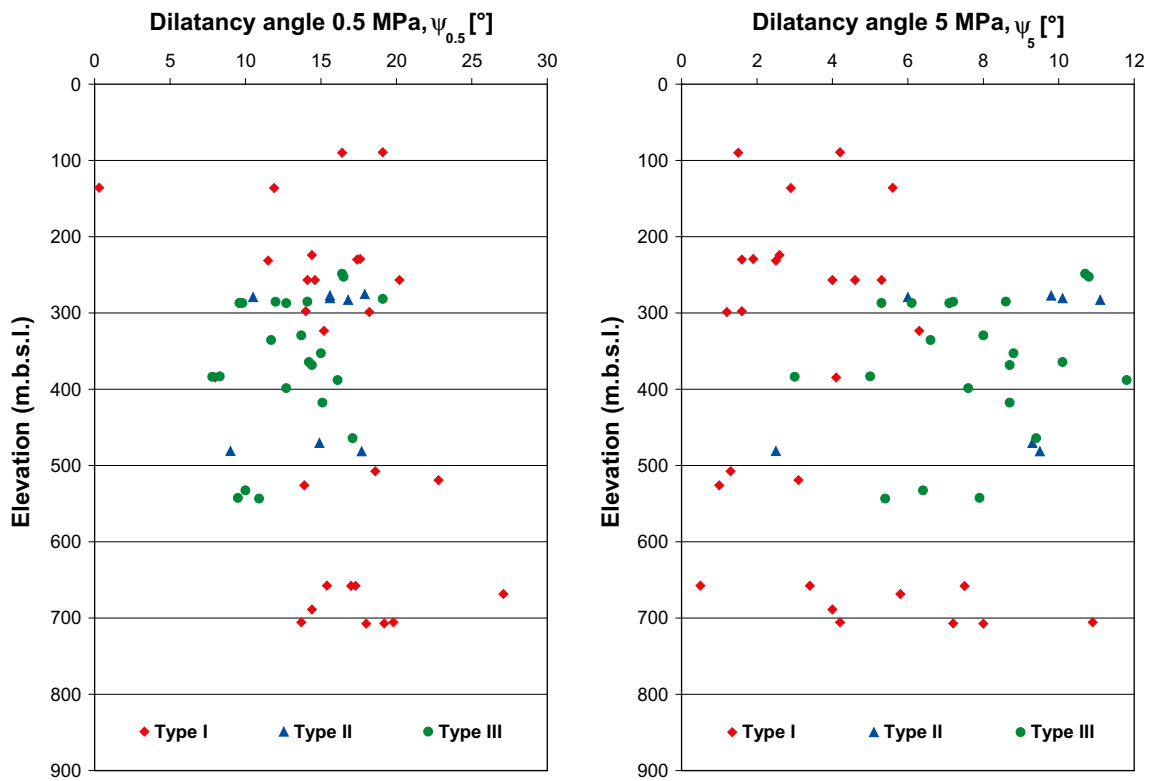


Figure 8-11. Dilatancy angle at 0.5 MPa and dilatancy angle at 5 MPa versus depth.

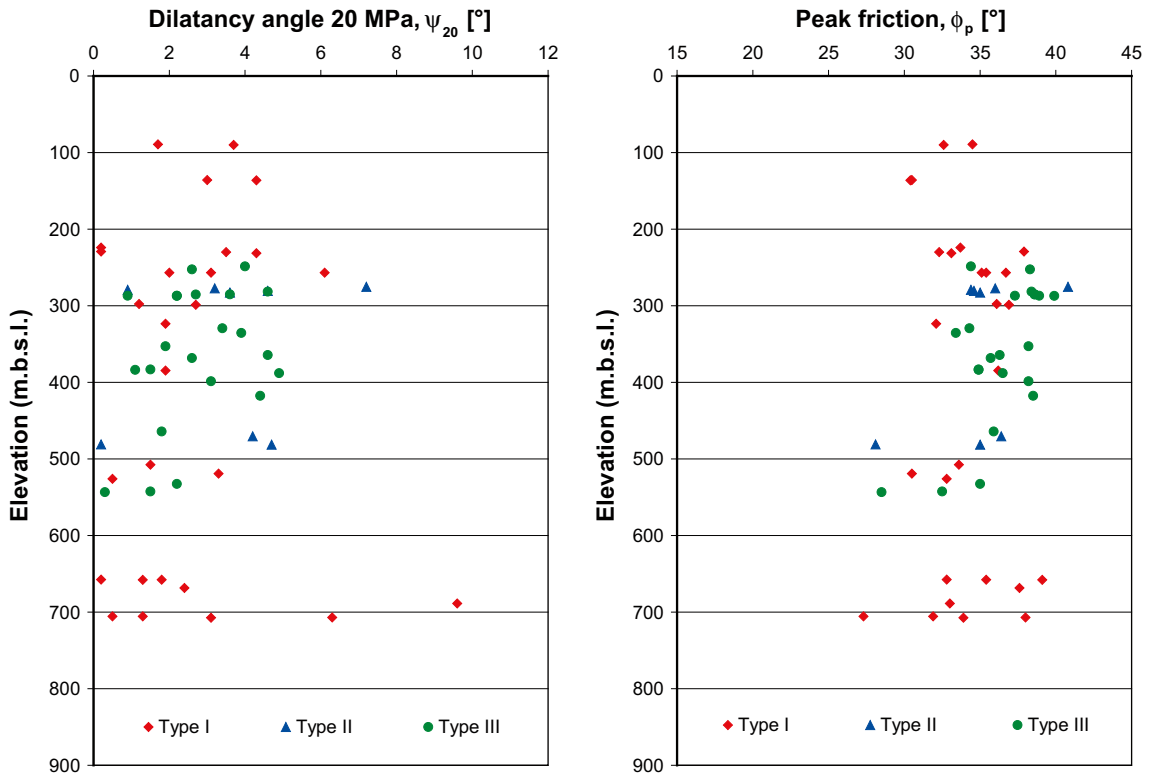


Figure 8-12. Dilatancy angle at 20 MPa and peak friction angle versus depth.

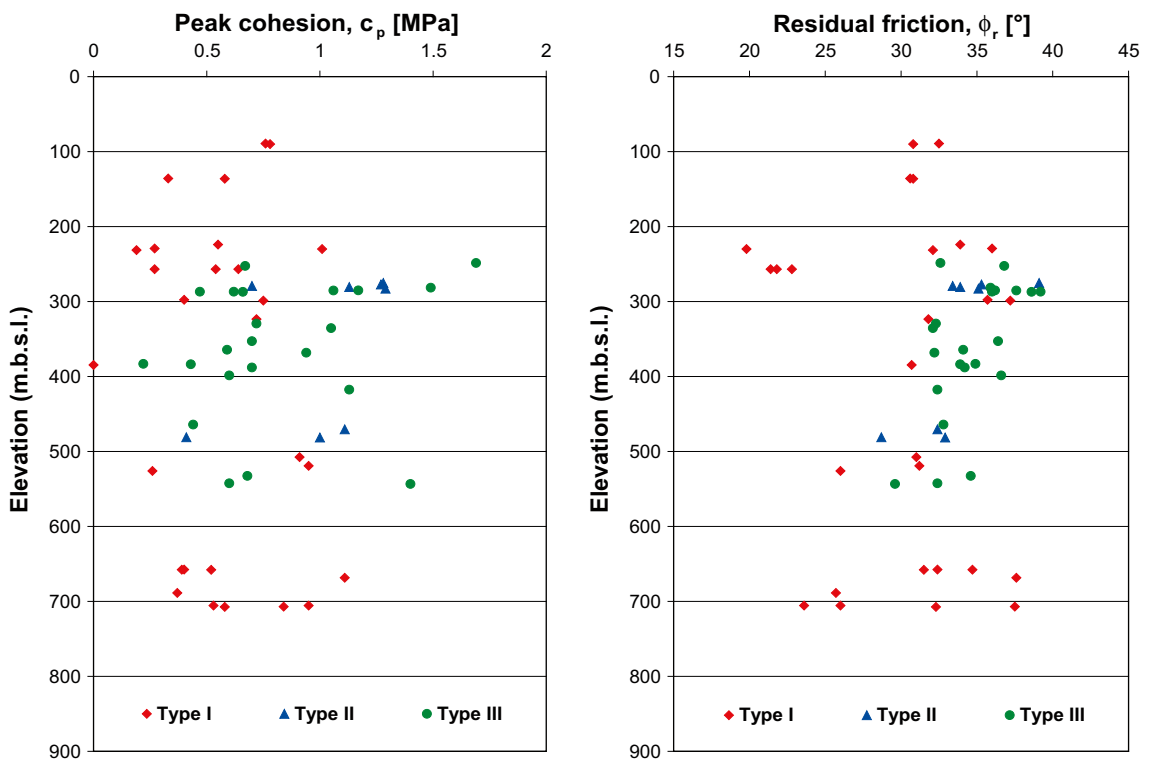


Figure 8-13. Peak cohesion and residual friction angle versus depth.

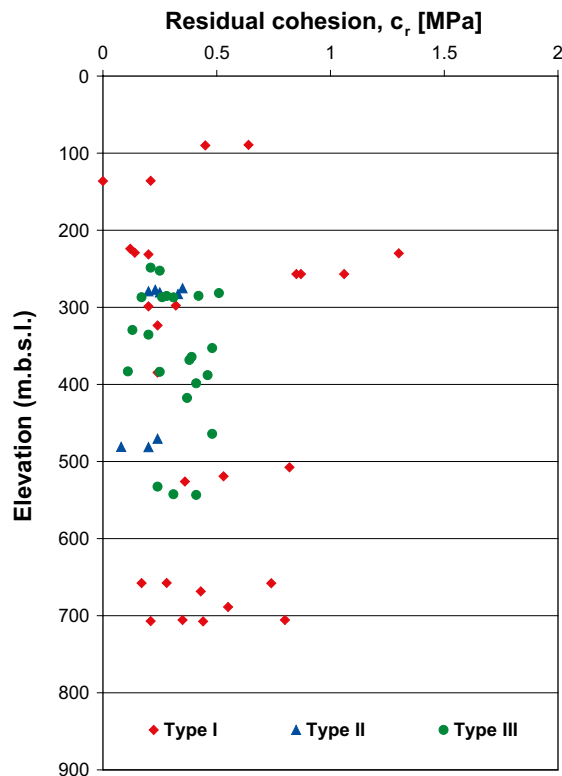


Figure 8-14. Residual cohesion versus depth.

8.3.3 Rock mass characterization

Rock mass characterization of the drill cores was performed using the methods for Rock Mass Quality, Q-system /Barton 2002/ and RMR, Rock Mass Rating /Bieniawski 1989/. These were adjusted according to /Andersson et al. 2002/ and /Röshoff et al. 2002/ in order to take into account the fact that the mapping was done on cores and not on the rock mass (on data from outcrops or tunnel walls).

The rock mass quality characterization determined according to these two systems is presented in Table 8-38 and Table 8-39. The effects of stresses and water pressure are considered separately.

One of the parameters defining the Q system is RQD. RQD (Rock Quality Designation) is a parameter used for measuring the fracture intensity along a standard core length, normally 1 m. The classification in RQD is presented in Table 8-40.

Table 8-38. Q classification.

Q number	Classification
< 1	Very poor rock
1–4	Poor rock
4–10	Fair rock
10–40	Good rock
40–100	Very good rock
100–400	Extremely good rock
> 400	Exceptionally good rock

Table 8-39. RMR classification.

RMR rating	Rock class	Classification
81–100	I	Very good rock
61–80	II	Good rock
41–60	III	Fair rock
21–40	IV	Poor rock
< 20	V	Very poor rock

Table 8-40. RQD classification

RQD	
90–100	Excellent rock
75–90	Good rock
50–75	Fair rock
25–50	Poor rock
<25	Very poor rock

RMR and Q are evaluated on core at intervals of 1, 5, 20 and/or 30 m. Only the 5 m intervals are available for all boreholes characterized with the RMR parameter. Then the RMR and Q values are evaluated in intervals that fit the rock units identified in the single-hole interpretation process.

The mean Q values evaluated for rock units and deformation zones (identified by the original single-hole interpretation) are illustrated for each cored borehole in the rock mechanics WellCad diagrams in Appendix 6, together with RMR (mean value evaluated over intervals corresponding to rock units and deformation zones identified by the original single-hole interpretation). RQD is shown in the integrated diagrams in Appendix 8. The underlying data are included in the data compilation table stored in the SKB model database. Summarized results of the classification for each fracture domain are presented in section 8.4.

8.3.4 Rock stress measurements

The principal stresses in the rock mass are determined by: a) direct measurements using the overcoring and hydraulic fracturing techniques and b) indirect observations from borehole breakout studies and core discing. However, at the time of writing of this report, the results from overcoring in KFM01B are the only available direct measurements reported to Sicada. Data from core discing observations are reported to Sicada from both geological and rock mechanical activities, where the latter include core discing observations only at the overcoring measurement levels (ring-discing). In the geological mapping of core discing, the discing is classified in the form of written comments, which are not easily retrieved for evaluation purposes.

The principal rock stresses were measured at two different levels in borehole KFM01B as shown in Table 8-41 and Table 8-42. The maximum stress (σ_1) ranges from 38.7 to 50.5 MPa. The lowest principal stress (σ_3) is nearly vertical. Stereographic plots in Figure 8-15 and Figure 8-16 illustrate the orientation of the principal stresses in 3D.

Table 8-41. Overcoring stress measurements in KFM01B, upper level.

Borehole length (secup m)	σ_1 (MPa)	Orientation (bearing/dip)	σ_2 (MPa)	Orientation (bearing/dip)	σ_3 (MPa)	Orientation (bearing/dip)
238.94	50.5	102/42	37.4	324/39	29.6	214/23
240.01	38.7	282/12	22.3	187/19	15.6	043/67
242.05	40.2	289/12	32.4	195/17	19.0	053/69

Table 8-42. Overcoring stress measurements in KFM01B, lower level.

Borehole length (secup m)	σ_1 (MPa)	Orientation (bearing/dip)	σ_2 (MPa)	Orientation (bearing/dip)	σ_3 (MPa)	Orientation (bearing/dip)
412.79	42.3	141/28	25.2	030/34	10.3	261/43
471.69	46.8	156/23	14.5	011/62	10.0	252/14

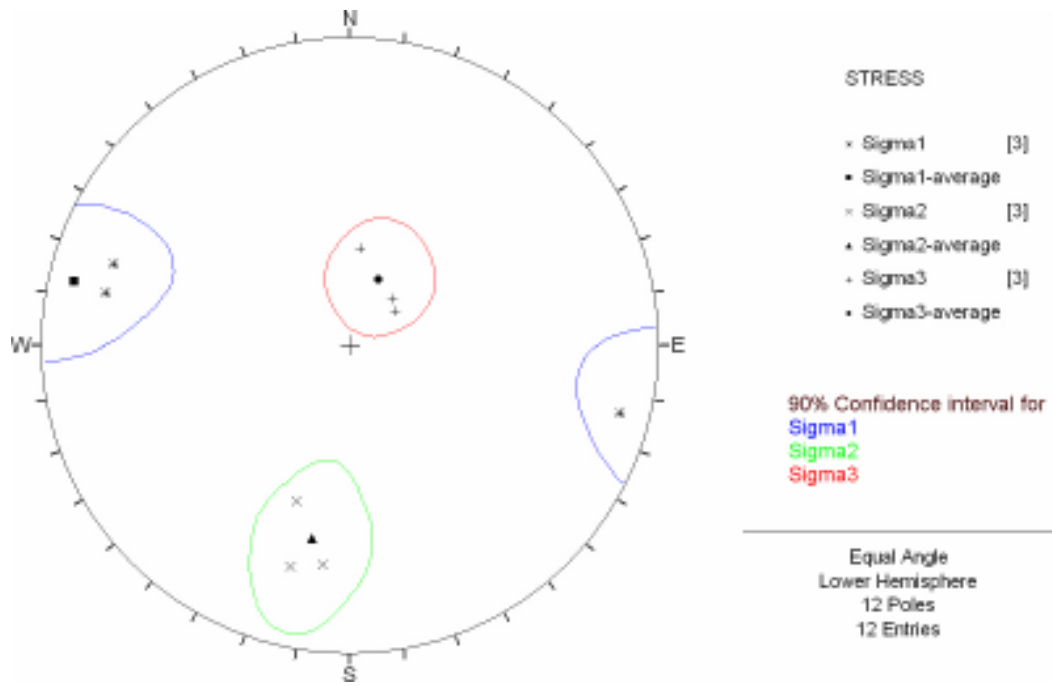


Figure 8-15. Calculated confidence intervals (90%) for the orientation of the major principal stresses σ_1 , σ_2 and σ_3 at level 1 in borehole KFM01B, shown in a lower hemisphere projection /Lindfors et al. 2005/.

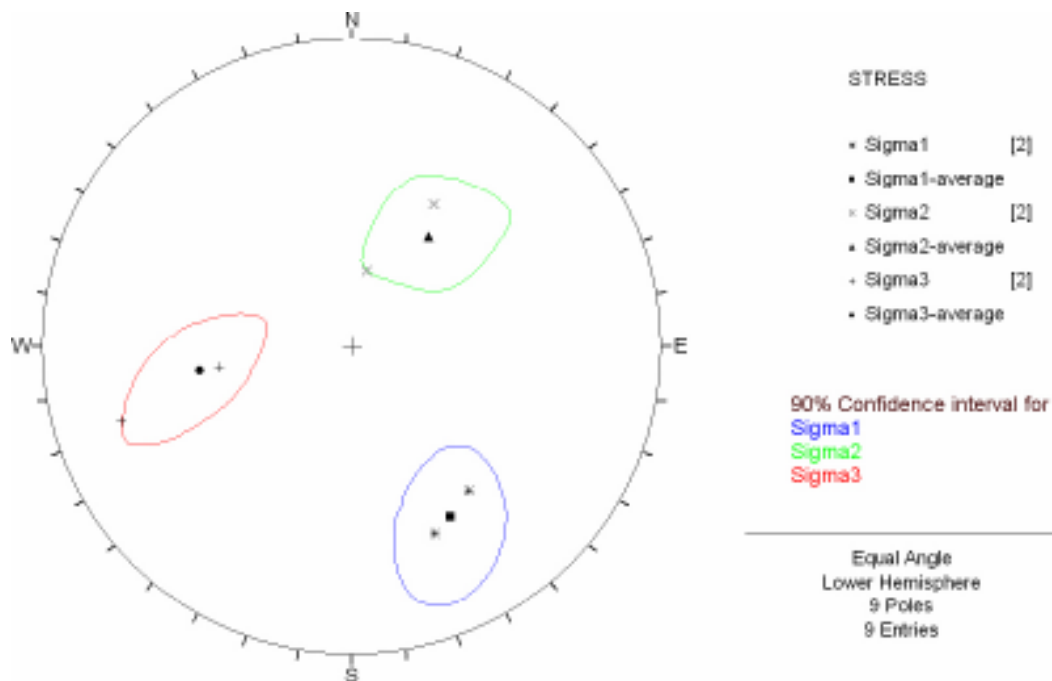


Figure 8-16. Calculated confidence intervals (90%) for the orientation of the major principal stresses σ_1 , σ_2 and σ_3 at level 2 in borehole KFM01B, shown in a lower hemisphere projection /Lindfors et al. 2005/.

8.4 Summary and discussion

In general, the results of the intact rock testing indicate that the strength and elasticity of the intact rock are normal for hard rock in Sweden. The range in uniaxial compressive strength (UCS) is around 150–300 MPa, with a mean value of around 220 MPa. The tonalite to granodiorite displays lower strength. The mean value of the tensile strength is around 14 MPa, with pegmatite exhibiting the lowest value of 7 MPa.

The elastic parameters Young's Modulus (E) and Poisson's Ratio are normal for such rock types, with a mean value for the Young's Modulus of 75 GPa and a range from 68 to 85 GPa for all samples.

The mechanical properties of the intact rock have been analyzed according to the different fracture domains and for all rock types. The results are presented in Table 8-43 to Table 8-49. There are no data from fracture domains FFM02 and FFM04, and very few data from FFM05 (1 sample of pegmatite) and FFM06 (5 samples). The only statistically significant comparisons can be made between samples in FFM01 and FFM03. The UCS properties are lower for FFM03 than for FFM01. When the same rock type (granite to granodiorite) is compared between the two domains (Table 8-44), the mean UCS value is almost identical, but the spread of the properties is much wider in FFM01. Even if there are few samples in FFM06, the results are noticeable. The mean UCS value is much higher in FFM06 than in FFM01 and FFM03 (Table 8-43). Four of the five samples are metagranite and exhibit the highest UCS value and a very wide spread (Table 8-44). The lowest values in FFM03 is obtained from tests on tonalite samples, see Table 8-44 and Figure 8-2a.

The mean value obtained for tensile strength, Table 8-45, does not show any appreciable difference between the three fracture domains FFM01, FFM03 and FFM05. The variations in tensile strength seem to be more closely related to rock types than to fracture domains (Table 8-46).

Table 8-43. Uniaxial compressive strength, UCS (MPa), for all rock types sorted by fracture domain.

FFM	Number of samples	Minimum	Mean	Median	Maximum	Standard deviation
FFM01	63	153	223	224	289	28
FFM03	21	140	196	209	251	34.2
FFM05	1	–	285	–	–	–
FFM06	5	229	310	309	371	58

Table 8-44. Uniaxial compressive strength, UCS (MPa), for comparison between rock type and fracture domains.

FFM	Number of samples	Minimum	Mean	Median	Maximum	Standard deviation
FFM01, granite to granodiorite	51	157	224	222	289	28
FFM03, granite to granodiorite	13	203	220	221	251	13
FFM01, pegmatite	12	153	219	227	251	12.9
FFM06, granite metamorphic	4	229	310	320	371	66.7
FFM03, tonalite to granodiorite, metamorphic	8	140	156	155	176	13

Table 8-45. Tensile strength, TS (MPa), for all rock types sorted by fracture domain.

FFM	Number of samples	Minimum	Mean	Median	Maximum	Standard deviation
FFM01	108	6.6	13	13	18	2.1
FFM03	50	10	14	14	18	2
FFM05	6	14	16	16	19	2

Table 8-46. Tensile strength, TS (MPa), for comparison between rock type and fracture domains.

FFM	Number of samples	Minimum	Mean	Median	Maximum	Standard deviation
FFM01, granite to granodiorite	90	10	13		18	1.7
FFM03, granite to granodiorite	30	10	14	14	17	1.7
FFM01, pegmatite	18	7	11		16	2.5
FFM03, tonalite	20	14	16	16	18	1.1

The value of Young's modulus displays insignificant variations between the fracture domains FFM01 and FFM03, Table 8-47. The values obtained in FFM06 are slightly higher than in both these domains, but the number of samples is also very low. However, this could be explained by the different rock types sampled in this fracture domain, Table 8-48.

Poisson's Ratio is presented in Table 8-49. The values are quite consistent between FFM01, FFM03 and FFM06. The only sample that represents FFM05 has a high value, but within the range of the maximum values obtained for the other fracture domains. There is no significant variation for the same rock type in two different fracture domains, Table 8-50.

Table 8-47. Young's Modulus, E (GPa), for all rock types sorted by fracture domain.

FFM	Number of samples	Minimum	Mean	Median	Maximum	Standard deviation
FFM01	63	69	75	75	83	2.9
FFM03	21	69	74	74	80	3.3
FFM05	1	–	79	–	–	–
FFM06	5	80	83	82	86	3

Table 8-48. Young's Modulus, E (GPa), for comparison between rock type and fracture domains.

FFM	Number of samples	Minimum	Mean	Median	Maximum	Standard deviation
FFM01, granite to granodiorite	51	69	76		83	2.9
FFM03, granite to granodiorite	13	71	75		80	2.8
FFM01, pegmatite	12	71	75		80	3.2
FFM06, granite metamorphic	4	80	82	81	86	2.6

Table 8-49. Poisson's Ratio, ν (-), for all rock types sorted by fracture domain.

FFM	Number of samples	Minimum	Mean	Median	Maximum	Standard deviation
FFM01	63	0.14	0.25	0.25	0.35	0.04
FFM03	21	0.16	0.25	0.25	0.34	0.04
FFM05	1	0.33	0.33	0.33	0.33	–
FFM06	5	0.25	0.27	0.26	0.31	0.03

Table 8-50. Poisson's Ratio, ν (-), for comparison between rock type and fracture domains.

FFM	Number of samples	Minimum	Mean	Median	Maximum	Standard deviation
FFM01, granite to granodiorite	51	0.14	0.24		0.3	0.04
FFM03, granite to granodiorite	13	0.16	0.23		0.27	0.03
FFM01, pegmatite	12	0.19	0.29		0.35	0.04
FFM06, granite metamorphic	4	0.25	0.27	0.26	0.31	0.03

The results from the tilt tests indicate small differences between the fracture domains as presented in Table 8-51 to Table 8-54.

Table 8-51. Basic friction angle ($^{\circ}$) sorted by fracture domain.

FFM	Number of samples	Minimum	Mean	Median	Maximum	Standard deviation
FFM01	64	26.8	30.9	31.1	34.5	1.6
FFM02	7	22.8	26.8	27.2	30.7	2.8
FFM03	41	29.7	31.9	31.7	34.7	1.3
FFM04	2	30.0	30.7	30.7	31.3	0.9
FFM05	5	29.7	31.3	32.0	32.2	1.1

Table 8-52. JRC_{100} (-) sorted by fracture domain.

FFM	Number of samples	Minimum	Mean	Median	Maximum	Standard deviation
FFM01	64	2.1	5.7	5.7	8.5	1.5
FFM02	7	3.3	6.4	6.9	8.5	1.6
FFM03	41	2.3	5.8	5.7	9.3	1.5
FFM04	2	4.6	5.8	5.8	7.1	1.8
FFM05	5	3.5	5.3	5.4	7.2	1.5

Table 8-53. JCS₁₀₀ (MPa) sorted by fracture domain.

FFM	Number of samples	Minimum	Mean	Median	Maximum	Standard deviation
FFM01	64	35	86	84	141	23
FFM02	7	71	105	111	134	23
FFM03	41	33	71	69	117	18
FFM04	2	105	111	111	116	8
FFM05	5	35	66	61	109	27

Table 8-54. Residual friction angle (°) sorted by fracture domain.

FFM	Number of samples	Minimum	Mean	Median	Maximum	Standard deviation
FFM01	64	20.3	26.7	27.0	33.8	2.7
FFM02	7	17.3	22.2	22.1	28.6	3.7
FFM03	41	22.2	26.6	26.8	30.5	2.0
FFM04	2	29.2	29.2	29.2	29.2	0.0
FFM05	5	23.1	25.7	25.9	28.9	2.5

The results of the normal and shear tests have been evaluated in relation to the different fracture domains and the results are presented in Table 8-55 to Table 8-65. The results from the normal and shear tests display wide variation depending on type of test I–III. If only the results from test type III are considered, the evaluated normal stiffness in fracture domain FFM04 is higher than that in the other fracture domains.

Table 8-55. Normal stiffness K_N (MPa/mm) sorted by fracture domain and test type.

FFM	Test type	No. of samples	Minimum	Mean	Median	Maximum	Standard deviation
FFM01	I	11	65	115	96	288	62
FFM01	II	8	268	340	286	521	110
FFM01	III	14	328	888	809	1,833	434
FFM02	I	0	–	–	–	–	–
FFM02	II	0	–	–	–	–	–
FFM02	III	0	–	–	–	–	–
FFM03	I	9	114	148	148	183	34
FFM03	II	0	–	–	–	–	–
FFM03	III	0	–	–	–	–	–
FFM04	I	0	–	–	–	–	–
FFM04	II	0	–	–	–	–	–
FFM04	III	3	1,072	1,385	1,458	1,624	283
FFM05	I	0	–	–	–	–	–
FFM05	II	0	–	–	–	–	–
FFM05	III	4	559	599	599	639	57

Table 8-56. Shear stiffness $K_{S0.5}$ (MPa/mm) sorted by fracture domain and test type.

FFM	Test type	No. of samples	Minimum	Mean	Median	Maximum	Standard deviation
FFM01	I	11	2	8	9	16	5
FFM01	II	8	5	12	12	23	6
FFM01	III	14	1	9	8	20	5
FFM02	I	0	–	–	–	–	–
FFM02	II	0	–	–	–	–	–
FFM02	III	0	–	–	–	–	–
FFM03	I	9	4	8	6	15	5
FFM03	II	0	–	–	–	–	–
FFM03	III	0	–	–	–	–	–
FFM04	I	0	–	–	–	–	–
FFM04	II	0	–	–	–	–	–
FFM04	III	3	1	8	10	12	6
FFM05	I	0	–	–	–	–	–
FFM05	II	0	–	–	–	–	–
FFM05	III	4	4	6	6	8	3

Table 8-57. Shear stiffness K_{S5} (MPa/mm) sorted by fracture domain and test type.

FFM	Test type	No. of samples	Minimum	Mean	Median	Maximum	Standard deviation
FFM01	I	11	19	29	30	44	7
FFM01	II	8	18	29	28	46	9
FFM01	III	14	7	22	23	32	7
FFM02	I	0	–	–	–	–	–
FFM02	II	0	–	–	–	–	–
FFM02	III	0	–	–	–	–	–
FFM03	I	9	25	28	28	33	3
FFM03	II	0	–	–	–	–	–
FFM03	III	0	–	–	–	–	–
FFM04	I	0	–	–	–	–	–
FFM04	II	0	–	–	–	–	–
FFM04	III	3	12	16	14	22	5
FFM05	I	0	–	–	–	–	–
FFM05	II	0	–	–	–	–	–
FFM05	III	4	14	20	20	25	7

Table 8-58. Shear stiffness K_{S20} (MPa/mm) sorted by fracture domain and test type.

FFM	Test type	No. of samples	Minimum	Mean	Median	Maximum	Standard deviation
FFM01	I	11	18	30	27	41	8
FFM01	II	8	18	35	36	52	12
FFM01	III	14	18	36	37	51	10
FFM02	I	0	–	–	–	–	–
FFM02	II	0	–	–	–	–	–
FFM02	III	0	–	–	–	–	–
FFM03	I	9	20	33	31	49	14
FFM03	II	0	–	–	–	–	–
FFM03	III	0	–	–	–	–	–
FFM04	I	0	–	–	–	–	–
FFM04	II	0	–	–	–	–	–
FFM04	III	3	18	23	22	29	5
FFM05	I	0	–	–	–	–	–
FFM05	II	0	–	–	–	–	–
FFM05	III	4	23	25	25	26	2

Table 8-59. Dilatancy angle 0.5 MPa, $\psi_{0.5}$ (°), sorted by fracture domain and test type.

FFM	Test type	No. of samples	Minimum	Mean	Median	Maximum	Standard deviation
FFM01	I	11	11.5	17.3	17.4	27.1	4.1
FFM01	II	8	9.0	14.8	15.6	17.9	3.3
FFM01	III	14	7.8	12.5	12.7	17.1	2.8
FFM02	I	0	–	–	–	–	–
FFM02	II	0	–	–	–	–	–
FFM02	III	0	–	–	–	–	–
FFM03	I	9	15.4	17.4	17.8	18.6	1.4
FFM03	II	0	–	–	–	–	–
FFM03	III	0	–	–	–	–	–
FFM04	I	0	–	–	–	–	–
FFM04	II	0	–	–	–	–	–
FFM04	III	3	9.5	10.1	10.0	10.9	0.7
FFM05	I	0	–	–	–	–	–
FFM05	II	0	–	–	–	–	–
FFM05	III	4	14.4	14.7	14.7	15.0	0.4

Table 8-60. Dilatancy angle 5 MPa, ψ_5 (°), sorted by fracture domain and test type.

FFM	Test type	No. of samples	Minimum	Mean	Median	Maximum	Standard deviation
FFM01	I	11	1.6	5.1	4.2	10.9	3.0
FFM01	II	8	2.5	9.0	9.7	13.7	3.4
FFM01	III	14	3.0	7.5	7.4	11.8	2.3
FFM02	I	0	–	–	–	–	–
FFM02	II	0	–	–	–	–	–
FFM02	III	0	–	–	–	–	–
FFM03	I	9	0.5	1.6	1.3	3.4	1.3
FFM03	II	0	–	–	–	–	–
FFM03	III	0	–	–	–	–	–
FFM04	I	0	–	–	–	–	–
FFM04	II	0	–	–	–	–	–
FFM04	III	3	5.4	6.6	6.4	7.9	1.3
FFM05	I	0	–	–	–	–	–
FFM05	II	0	–	–	–	–	–
FFM05	III	4	8.7	8.8	8.8	8.8	0.1

Table 8-61. Dilatancy angle 20 MPa, ψ_{20} (°), sorted by fracture domain and test type.

FFM	Test type	No. of samples	Minimum	Mean	Median	Maximum	Standard deviation
FFM01	I	11	0.2	3.0	2.4	9.6	2.9
FFM01	II	8	0.2	3.6	3.9	7.2	2.2
FFM01	III	14	0.9	2.9	2.9	4.9	1.3
FFM02	I	0	–	–	–	–	–
FFM02	II	0	–	–	–	–	–
FFM02	III	0	–	–	–	–	–
FFM03	I	9	0.2	1.6	1.7	2.7	1.0
FFM03	II	0	–	–	–	–	–
FFM03	III	0	–	–	–	–	–
FFM04	I	0	–	–	–	–	–
FFM04	II	0	–	–	–	–	–
FFM04	III	3	0.3	1.3	1.5	2.2	1.0
FFM05	I	0	–	–	–	–	–
FFM05	II	0	–	–	–	–	–
FFM05	III	4	1.9	2.3	2.3	2.6	0.5

Table 8-62. Peak friction angle, ϕ_p (°), sorted by fracture domain and test type.

FFM	Test type	No. of samples	Minimum	Mean	Median	Maximum	Standard deviation
FFM01	I	11	27.3	34.3	33.7	39.1	3.5
FFM01	II	8	28.1	35.0	35.0	40.8	3.5
FFM01	III	14	33.4	36.9	36.9	39.9	2.0
FFM02	I	0	–	–	–	–	–
FFM02	II	0	–	–	–	–	–
FFM02	III	0	–	–	–	–	–
FFM03	I	9	32.8	34.7	34.5	36.9	1.8
FFM03	II	0	–	–	–	–	–
FFM03	III	0	–	–	–	–	–
FFM04	I	0	–	–	–	–	–
FFM04	II	0	–	–	–	–	–
FFM04	III	3	28.5	32.0	32.5	35.0	3.3
FFM05	I	0	–	–	–	–	–
FFM05	II	0	–	–	–	–	–
FFM05	III	4	35.7	37.0	37.0	38.2	1.8

Table 8-63. Peak cohesion, c_p (MPa), sorted by fracture domain and test type.

FFM	Test type	No of samples	Minimum	Mean	Median	Maximum	Standard deviation
FFM01	I	11	0.2	0.6	0.6	1.1	0.3
FFM01	II	8	0.4	1.0	1.1	1.3	0.3
FFM01	III	14	0.2	0.7	0.6	1.2	0.3
FFM02	I	0	–	–	–	–	–
FFM02	II	0	–	–	–	–	–
FFM02	III	0	–	–	–	–	–
FFM03	I	9	0.4	0.6	0.6	0.9	0.3
FFM03	II	0	–	–	–	–	–
FFM03	III	0	–	–	–	–	–
FFM04	I	0	–	–	–	–	–
FFM04	II	0	–	–	–	–	–
FFM04	III	3	0.6	0.9	0.7	1.4	0.4
FFM05	I	0	–	–	–	–	–
FFM05	II	0	–	–	–	–	–
FFM05	III	4	0.7	0.8	0.8	0.9	0.2

Table 8-64. Residual friction angle, ϕ_r (°), sorted by fracture domain and test type.

FFM	Test type	No. of samples	Minimum	Mean	Median	Maximum	Standard deviation
FFM01	I	11	19.8	30.5	32.1	37.6	5.9
FFM01	II	8	28.7	33.9	33.7	39.1	3.0
FFM01	III	14	32.1	35.1	34.6	39.2	2.4
FFM02	I	0	–	–	–	–	–
FFM02	II	0	–	–	–	–	–
FFM02	III	0	–	–	–	–	–
FFM03	I	9	31.0	33.8	33.6	37.2	2.7
FFM03	II	0	–	–	–	–	–
FFM03	III	0	–	–	–	–	–
FFM04	I	0	–	–	–	–	–
FFM04	II	0	–	–	–	–	–
FFM04	III	3	29.6	32.2	32.4	34.6	2.5
FFM05	I	0	–	–	–	–	–
FFM05	II	0	–	–	–	–	–
FFM05	III	4	32.2	34.3	34.3	36.4	3.0

Table 8-65. Residual cohesion, c_r (MPa), sorted by fracture domain and test type.

FFM	Test type	No. of samples	Minimum	Mean	Median	Maximum	Standard deviation
FFM01	I	11	0.1	0.5	0.4	1.3	0.4
FFM01	II	8	0.1	0.2	0.2	0.4	0.1
FFM01	III	14	0.1	0.3	0.3	0.5	0.1
FFM02	I	0	–	–	–	–	–
FFM02	II	0	–	–	–	–	–
FFM02	III	0	–	–	–	–	–
FFM03	I	9	0.2	0.4	0.2	0.8	0.3
FFM03	II	0	–	–	–	–	–
FFM03	III	0	–	–	–	–	–
FFM04	I	0	–	–	–	–	–
FFM04	II	0	–	–	–	–	–
FFM04	III	3	0.2	0.3	0.3	0.4	0.1
FFM05	I	0	–	–	–	–	–
FFM05	II	0	–	–	–	–	–
FFM05	III	4	0.4	0.4	0.4	0.5	0.1

The rock mass characterizations by Q-value and RMR have also been evaluated for each fracture domain. Two sets of data are available for classification of the rock mass. One data set is reported in Sicada and entails an interpretation of representative Q and RMR values along intervals that correspond to the rock units and possible deformation zones identified during the single-hole interpretation. However, this set of data is difficult to use for analyzing Q and RMR in relation to the different fracture domains as the limits do not fit. The other set of data is Q and RMR that have been estimated along 1, 5, 20 or 30 m intervals of borehole lengths. Only the 5 m section estimate is available for all boreholes characterized, and this set is used for the analysis of the rock mass characterization inside the represented fracture domains.

The results are presented in Table 8-66 and Table 8-67. The results are given as the mean value of rock quality, the standard deviation and the percentage of the rating class of the mean rock quality for each fracture domain. Only fracture domain FFM06 is not represented in the data. Most of the data comes from FFM01 (56%) and FFM03 (24%). The three other fracture domains FFM02, FFM04 and FFM05 only represent 8, 6 and 6% of the data set, respectively.

In fracture domain FFM01, 87% of the volume has a Q value greater than 40, indicating very high to extremely high quality (with a mean Q value of 543) of the rock mass. About 55% of FFM03 also exhibits Q values characteristic of very high to extremely high quality of the rock mass (with a mean Q value of 270). In comparison, it can be noticed that 54% of the rock mass in FFM02 is classified as good rock with a mean Q value of 24. The proportion of fair rock is very low, and the Q values are never lower than 6.

The same picture of rock mass quality is obtained when RMR is used as a rating method. Both FFM01 and FFM03, as well as FFM04 and FFM05, are characterized for the most part by very good rock (RMR class I), while 55% of FFM02 is characterized by good rock (RMR class II). However, the difference in mean RMR value is too small to be of any rock mechanical significance.

Table 8-66. Q-value evaluated at 5 m intervals for each fracture domain.

	Q<10 (fair rock)			10≤Q<41 (good rock)			Q≥41 (very to extremely good rock)		
	Mean value	Standard deviation	%	Mean value	Standard deviation	%	Mean value	Standard deviation	%
FFM01	6	2.9	1	27	8.5	12	543	653	87
FFM02	7	2.8	9	24	8.8	54	133	211	37
FFM03	7	2.3	4	27	7.5	41	270	465	55
FFM04	10	–	–	23	7.1	32	195	219	68
FFM05	9	–	–	25	9.4	36	86	52.2	64

Table 8-67. RMR-value evaluated at 5 m intervals for each fracture domain.

	III–V (<60)			II (61–80)			I (81–100)		
	Mean value	Standard deviation	%	Mean value	Standard deviation	%	Mean value	Standard deviation	%
FFM01	–	–	–	78	2.0	10	90	4.6	90
FFM02	–	–	–	77	2.1	55	86	4.4	45
FFM03	–	–	–	78	2.1	29	87	3.6	71
FFM04	–	–	–	78	3	28	88	3.9	72
FFM05	–	–	–	77	3.5	31	85	2.9	69

9 Discussion and summary

The fracture domain model was developed based on geological data. In Chapters 6, 7 and 8, primary hydrogeological, hydrogeochemical and rock mechanics data from boreholes have been presented and analyzed in relation to the different fracture domains.

In this section, a brief overview of the visualization of raw borehole data is presented. The implications of the fracture domain model for the geological DFN modelling and the integration of the other disciplines with the fracture domain model are also discussed.

9.1 Visualization of borehole data

A data container has been created in RVS, in order to visualize a selected portion of the primary data from cored boreholes presented in this report by the different disciplines. This visualization allows combinations of different data sets to be studied in 3D together with the fracture domain model and other three dimensional models within the local model volume version 2.2. Thus, when the rock domain and the deformation zone models are finalised, it will be possible to combine the information in the container also with these geological entities.

The data container and the fracture domain model are stored on the appended CD in RVS and MicroStation formats, together with an instruction file that describes the disposition of the data sets.

The data from cored boreholes visualized in the RVS container are listed below.

Geology:

- Rock type
- Rock units from single-hole interpretation
- Rock domains
- Rock alteration
 - Albitization
 - Oxidation
 - Quartz dissolution
- Resistivity 300 cm (Ω m)
- Deformation zones from the extended and modified single-hole interpretation
- Fracture domains.

Hydrogeology:

- Steady-state transmissivity in 100 m section, double packer injection test (PSS-moye 100 m) (m^2/s)
- Steady-state transmissivity in 20 m section, double packer injection test (PSS-moye 20 m) (m^2/s)
- Steady-state transmissivity in 5 m section, double packer injection test (PSS-moye 5 m) (m^2/s)
- Water flow in fracture during non-pumped conditions (open borehole) measured with Posiva Flow Log (m^3/s)
- Steady-state fracture transmissivity measured with Posiva Flow Log (PFL-f) (m^2/s)
- Packer position in borehole.

Hydrogeochemistry:

- Chloride concentration (mg/L)
- Magnesium concentration (mg/L)
- Bromide concentration (mg/L)
- $\delta^{18}\text{O}$ (‰ SMOW).

Rock mechanics:

- Uniaxial compressive strength
 - < 150 (MPa)
 - 150–200 (MPa)
 - 200–250 (MPa)
 - > 250 (MPa)
- Triaxial compressive strength – sampling position
- Strength, Brazilian test – sampling position
- Directed shear tests on, – open fractures – sampling position
- RQD
- RMR.

9.2 Implications of the fracture domain model for geological DFN modelling

The geological DFN model in stage 2.2 will be developed for the target volume of the rock, see definition in Chapter 2. The target volume is divided into three fracture domains FFM01, FFM02 and FFM06. Fracture domain FFM01 occurs inside rock domain RFM029, FFM02 is identified in the upper parts of rock domains RFM029 and RFM045, and fracture domain FFM06 is identified in rock domain RFM045.

The fracture domain model has arisen as a way to refine our conceptual understanding of the Forsmark site. This model was developed using both rock domains and deformation zones in the deterministic modelling work, combined with a reconnaissance survey of fracture frequency in the boreholes. The number of fracture domains is limited in order to permit modifications to be made during a more stringent statistical analysis. For example, examination of the fracture frequency diagrams (Appendix 3) clearly shows that the central part of fracture domain FFM01 may differ from what is observed in boreholes drilled in the NW border of the rock domain RFM029. This may lead to an increase in the number of fracture domains based on other geological controlling parameters.

In geological DFN modelling, data from each fracture domain will be analyzed separately and variability and uncertainty within these domains will be described. These analyses and results will be reported in the forthcoming DFN report and summarised in the integrated geological model report.

9.3 Feedback from other disciplines to geology

This section summarizes the main results and conclusions drawn from the analyses of data from hydrogeology, hydrogeochemistry and rock mechanics in relation to the fracture domains. To illustrate the discussion points, integrated WellCad diagrams have been plotted combining data on geology, hydrogeology, hydrogeochemistry and rock mechanics for all cored boreholes up to data freeze 2.2. These diagrams are presented in Appendix 8. They provide a visual overview of hydraulic data, groundwater composition and rock mechanics properties in relation to rock domains, deformation zones and fracture domains.

The main results and conclusions from the hydrogeological, hydrogeochemical and rock mechanics analyses are summarized below.

- Fracture transmissivity data from boreholes KFM01A, -01D, -05A, -06A, -07A, -07C, -08A and -08C support the subdivision of the foot wall bedrock of deformation zones ZFMA2 and ZFMF1 (bedrock beneath/northwest of the zones) into fracture domains FFM01 and FFM02. Likewise, fracture transmissivity data from boreholes KFM02A, -03A and -10A support the subdivision of the corresponding hanging wall bedrock (bedrock above/southeast of the zones) into fracture domain FFM03. The fracture domain concept in this regard resembles the previously used subdivision of the bedrock within the tectonic lens into hydrogeological subdomains in Forsmark site descriptive model version 1.2, cf /Follin et al. 2005/ and /Hartley et al. 2005/.
- In the case of FFM01, the fracture transmissivities are strongly dominated by horizontal and gently dipping fractures, with a small handful of fractures with strike NE or NNE. This is also true of FFM02. In both fracture domains, the highest transmissivities are associated with horizontal and gently dipping fractures. The orientation of the gently dipping fractures has a NNE component, hence flow is strongly anisotropic in FFM01 and FFM02. In the case of FFM03, flow is more dispersed in terms of orientation (more isotropic). Although horizontal and gently dipping fractures still dominate, they are less concentrated at the centre of the stereonet.
- Stereonets have been computed for FFM01–FFM03 above and below –400 m elevation. The interesting thing here is that even with FFM03 included, fracture transmissivities below –400 m are restricted to horizontal and gently dipping fractures. The distribution of fracture transmissivities is therefore strongly anisotropic in much of the rock, influencing the hydrogeology of the site many kilometres away within the tectonic lens.
- Concerning fracture domains FFM04–FFM06, very little data have been acquired for various reasons. Firstly, FFM04 and FFM05 occur on the edges of the target volume consisting of FFM01, FFM02 and FFM06. Secondly, FFM06 only occurs in a fairly small part of the target volume. Hence, fracture domains FFM04–FFM06 are undersampled in comparison with FFM01–FFM03. However, it should be noted that FFM04 and FFM05 lie outside the volume of rock that will be treated by discrete fracture network modelling. Moreover, the hydraulic characterization of FFM06 performed in KFM06A and KFM08C has not revealed any flowing fractures.
- Hydrogeochemical data from boreholes KFM01A and KFM01D supports subdivision into the two fracture domains FFM02 and FFM01. A clearly marine *Littorina* sea water signature is observed in fracture domain FFM02, which is affected by the gently dipping deformation zone ZFMA2. This marine signature is much less pronounced down to about 300 m depth in fracture domain FFM01 and is absent below this depth. The observed differences may be explained by different connective properties of the two fracture domains.
- Only two selected hydrogeochemical data records can be assigned to fracture domain FFM03. These samples represent a very shallow (82 m) and a deep (969 m) flow anomaly. Up to data freeze 2.2, hydrogeochemical data from the depth range 100 m to 445 m in the rock assigned to fracture domain FFM03 have been lacking. However, recent data from 220 m depth in borehole KFM10A clearly indicate a non-marine signature for the groundwater from fracture domain FFM03 as well (the “hanging wall” above ZFMA2). This may indicate that the non-marine character of the groundwater in the depth range 100–600 m is mainly associated with the bedrock between deformation zones, i.e. fracture domains, whereas the *Littorina* signature is more pronounced in groundwater in deformation zones or in domains strongly affected by fracturing such as fracture domain FFM02.
- No hydrogeochemical data are available from fracture domains FFM04 and FFM05. However, the very saline water sampled at depth in boreholes KFM09A and KFM07A may be representative solely of the deformation zones ZFMNW1200 and ZFMNNW0100 or also

of the adjacent foliated bedrock in FFM04 and FFM05, respectively. It is possible, but less plausible, that similar conditions prevail at depth in fracture domain FFM01. Alternatively, the zones may serve as a discharge path for up-coning deeper saline water, which may have been triggered by pumping in the boreholes. In this case, the water composition is not representative for the sampling depth.

- Most of the available rock matrix pore water data represent fracture domain FFM01 (42 out of 55 samples). It is therefore not possible to distinguish pore water properties related to the different fracture domains. It is likely that the fracture domain concept offers too coarse a classification to explain the variations in pore water composition. A comparison of matrix pore water data with geological and hydrogeological properties on a detailed scale along the boreholes may be more informative.
- The properties of the intact rock do not display clear trends in relation to the fracture domains. This is not to be expected, since sampling for testing of intact rock has been carried out in between significant fractured areas. The only noticeable exception is for uniaxial compressive strength (UCS). UCS is highest in FFM06, but it should be noted that only few samples come from this domain and from domain FFM01. In addition, different levels of sample disturbance due to stress release in the different fracture domains might have affected the laboratory test results.
- The mechanical properties of fractures obtained from tilt test results do not show any significant relation to the fracture domains. The results from the shear tests are difficult to interpret, since different test methods have been employed and they are not represented in all fracture domains. Looking only at test type III, it seems that the properties obtained for rock in fracture domain FFM04 are higher. However, the number of samples is very limited.
- The rock mass quality in Forsmark is in general very to extremely good according to the Q and RMR characterizations. Based on the results of the rock mass qualities (Table 8-66 and Table 8-67), there is a small or even insignificant rock mechanics support for a subdivision into fracture domains based on the values on rock mass qualities. However, fracture domain FFM01 has the highest percentage of very to extremely good rock: 87% (Q) and 90% (RMR) of the characterized borehole length. FFM02 has the lowest percentage, 37% (Q) and 45% (RMR), of the same quality.

10 Conclusions

The following conclusions can be drawn:

- The bedrock inside fracture domains corresponds to the bedrock that remains inside rock domains following exclusion of the bedrock along modelled DZ and possible DZ (not modelled). It forms the basis for the geological DFN modelling work.
- The bedrock judged to be affected by, but situated outside deformation zones, as well as vuggy rock outside deformation zones need to be addressed separately in the geological DFN modelling work.
- On the basis of borehole data, six fracture domains (FFM01–FFM06) have been recognized inside and immediately around the candidate volume. Three of these domains (FFM01, FFM02 and FFM06) lie inside the target volume and need to be addressed in the geological DFN modelling work.
- The results of the geological work are presented in the form of a table and several figures, one for each borehole, that document the occurrence of rock domains, deformation zones and fracture domains in each borehole. A geometric model for fracture domains inside the target volume, based on the data in the boreholes, is also presented.
- Uncertainties in the definition of fracture domains concern:
 1. Intrinsic uncertainties in the rock domain and deformation zone models, stage 2.2.
 2. Intrinsic uncertainties in the data from percussion-drilled boreholes.
 3. Interpretation of the boundaries of deformation zones in boreholes.
 4. Treatment of the bedrock classified as “Affected by DZ” and “Vuggy rock outside DZ”.
 5. Treatment of the bedrock intersected by boreholes from drill sites 6 and 8.
- The allocation of borehole sections to different fracture domains is a current working hypothesis for the geological DFN modelling work undertaken for the Forsmark site. If the stringent statistical analysis indicates that these fracture domains are inadequate for characterizing the variability in fracturing within the target volume, alternatives to the existing domains will need to be introduced. The boundaries of the domains may be changed, or sub-domains may be defined.
- An attempt has been made to integrate the fracture domain concept with data from other disciplines. The hydrogeological data support the subdivision of the bedrock into fracture domains FFM01, FFM02 and FFM03. Few or no data are available for the other three domains.
- The hydrogeochemical data also support the subdivision into fracture domains FFM01 and FFM02. Since few data are available from the bedrock between deformation zones inside FFM03, there is little information on the hydrogeochemical character of the groundwater in this domain. It can be noted that the non-marine character of the groundwater in the depth range 100–600 m is mainly associated with the bedrock between deformation zones, i.e. fracture domains, whereas the Littorina signature is more pronounced in groundwater in deformation zones or in domains strongly affected by fracturing such as fracture domain FFM02.
- No significant differences in intact rock mechanics properties between the fracture domains have been noted, except for those that more likely depend on different mineralogical composition, such as the tonalite in FFM03 and the granite in FFM06, which is altered by albitization.

Acknowledgements

The authors wish to express their warm gratitude for the work carried out by Pär Kinnbom with all the WellCad diagrams in Appendices 2, 5, 6 and 8, to Ingemar Källberg (deceased) and Anders Lindblom for their work with the borehole logs in Appendix 4, and to Kristina Skagius, who completed the complex and painstaking editorial work in preparation for the printing of this report.

References

- Andersson J, Ström A, Almén K-E, Ericsson LO, 2000.** Vilka krav ställer djupförvaret på berget? Geovetenskapliga lämplighetsindikationer och kriterier för lokalisering och platsutvärdering. SKB R-00-15, Svensk Kärnbränslehantering AB.
- Andersson J, Christiansson R, Hudson J, 2002.** Site investigations. Strategy for Rock Mechanics Site Descriptive Model. SKB TR-02-01, Svensk Kärnbränslehantering AB.
- Barton, 2002.** Some new Q-value correlations to assist in site characterisation and tunnel design. *International Journal of Rock Mechanics & Mining Sciences* 39 (2002) 185–216. Pergamon.
- Berg C, Levén J, Nilsson A-C, 2005.** Hydrochemical logging in KFM07A. Forsmark site investigation. SKB P-05-187, Svensk Kärnbränslehantering AB.
- Bienawski ZT, 1989.** Engineering rock mass classifications. John Wiley & Sons.
- Eloranta P, 2004.** Drill hole KFM01A. Uniaxial compression test (HUT). Forsmark site investigation. SKB P-04-176, Svensk Kärnbränslehantering AB.
- Follin S, Stigsson M, Svensson U, 2005.** Regional hydrogeological simulations for Forsmark – numerical modelling using Darcy Tools. Preliminary site description Forsmark area – version 1.2. SKB R-05-60, Svensk Kärnbränslehantering AB.
- Forssman I, Zetterlund M, Rhén I, 2004.** Correlation of Posiva Flow Log anomalies to core mapped features in Forsmark (KFM01A to KFM05A). SKB R-04-77, Svensk Kärnbränslehantering AB.
- Forssman I, Zetterlund M, Forsmark T, Rhén I, 2006.** Correlation of Posiva Flow Log anomalies to core mapped fractures in KFM06A and KFM07A. SKB P-06-56, Svensk Kärnbränslehantering AB.
- Fox A, Hermanson J, 2006.** Identification of additional, possible minor deformation zones at Forsmark through a review of data from cored boreholes. SKB P-06-293, Svensk Kärnbränslehantering AB.
- Hartley L, Cox I, Hunter F, Jackson P, Joyce S, Swift B, Gylling B, Marsic N, 2005.** Regional hydrogeological simulations for Forsmark – Numerical modelling using CONNECTFLOW. Preliminary site description of the Forsmark area. SKB R-05-32, Svensk Kärnbränslehantering AB.
- Lanaro F, Fredriksson A, 2005.** Rock Mechanics Model – Summary of the primary data. Forsmark site investigation. SKB R-05-83, Svensk Kärnbränslehantering AB.
- La Pointe P, Olofsson I, Hermanson J, 2005.** Statistical model of fractures and deformation zones for Forsmark. Preliminary site description Forsmark area – version 1.2. SKB R-05-26, Svensk Kärnbränslehantering AB.
- Lindfors U, Perman F, Sjöberg J, 2005.** Evaluation of the overcoring results from borehole KFM01B. Forsmark site investigation. SKB P-05-66, Svensk Kärnbränslehantering AB.
- Lindquist A, Nilsson K, 2006.** Hydrochemical logging in KFM09B. Forsmark site investigation. SKB P-06-179, Svensk Kärnbränslehantering AB.
- Munier R, Hermanson J, 2001.** Metodik för geometrisk modellering. Presentation och administration av platsbeskrivande modeller. SKB R-01-15, Svensk Kärnbränslehantering AB.

- Munier R, Stenberg L, Stanfors R, Milnes AG, Hermanson J, Triumf C-A, 2003.** Geological Site Descriptive Model. A strategy for the model development during site investigations. SKB R-03-07, Svensk Kärnbränslehantering AB.
- Möller C, Snäll S, Stephens M B, 2004.** Dissolution of quartz, vug formation and new grain growth associated with post-metamorphic hydrothermal alteration in KFM02A. Forsmark site investigation. SKB P-03-77, Svensk Kärnbränslehantering AB.
- Nilsson K, Bergelin A, Lindquist A, Nilsson A-C, 2006.** Hydrochemical characterization in borehole KFM01D. Results from seven investigated borehole sections: 194.0–195.0 m, 263.8–264.8 m, 314.5–319.5 m, 354.9–355.9 m, 369.0–370.0 m, 428.5–435.6 m, 568.0–575.1 m. Forsmark site investigation. SKB P-06-227, Svensk Kärnbränslehantering AB.
- Petersson J, Berglund J, Danielsson P, Skogsmo G, 2005.** Petrographic and geochemical characteristics of bedrock samples from boreholes KFM04A–06A, and a whitened alteration rock. Forsmark site investigation. SKB P-05-156, Svensk Kärnbränslehantering AB.
- Röshoff K, Lanaro F, Jing L, 2002.** Strategy for a Rock Mechanics Site Descriptive Model. Development and testing of the empirical approach. SKB R-02-01, Svensk Kärnbränslehantering AB.
- SKB, 2000.** Samlad redovisning av metod, platsval och program inför platsundersöknings-skedet. Svensk Kärnbränslehantering AB.
- SKB, 2004.** Preliminary site description Forsmark area – version 1.1. SKB R-04-15, Svensk Kärnbränslehantering AB.
- SKB, 2005a.** Preliminary site description Forsmark area – version 1.2. SKB R-05-18, Svensk Kärnbränslehantering AB.
- SKB, 2005b.** Forsmark site investigation. Programme for further investigations of geosphere and biosphere. SKB R-05-14, Svensk Kärnbränslehantering AB.
- SKB, 2005c.** Hydrochemical evaluation. Preliminary site description Forsmark area – version 1.2. SKB R-05-17, Svensk Kärnbränslehantering AB.
- SKB, 2006.** Site descriptive modelling Forsmark stage 2.1 – Feedback for completion of the site investigation including from safety assessment and repository engineering. SKB R-06-38, Svensk Kärnbränslehantering AB.
- Stephens M B, Lundqvist S, Ekström M, Bergman T, Andersson J, 2003.** Bedrock mapping. Rock types, their petrographic and geochemical characteristics, and a structural analysis of the bedrock based on stage 1 (2002) surface data. Forsmark site investigation. SKB P-03-75, Svensk Kärnbränslehantering AB.
- Stephens M B, Lundqvist S, Bergman T, Ekström M, 2005.** Bedrock mapping. Petrographic and geochemical characteristics of rock types based on Stage 1 (2002) and Stage 2 (2003) surface data. Forsmark site investigation. SKB P-04-87, Svensk Kärnbränslehantering AB.
- Teurneau B, Forsmark T, Forssman I, Rhén I, Zinn E, 2007.** Correlation of Posiva Flow Log anomalies to core mapped features in KFM01D, -07C, -08A, -08C, -08D and -10A. SKB P-07-xx, Svensk Kärnbränslehantering AB.
- Waber H N, Smellie J A T, 2005.** Borehole KFM06A: Characterisation of pore water. Part I: Diffusion experiments. Forsmark site investigation. SKB P-05-196, Svensk Kärnbränslehantering AB.
- Waber H N, Smellie J A T, 2007.** Boreholes KFM01D, KFM08C, KFM09B: Characterisation of pore water. Part 1: Diffusion experiments and pore water data. Forsmark site investigation. SKB P-07-119, Svensk Kärnbränslehantering AB.

Specification of available data

Table A1-1. Available bedrock geological and geophysical data and their handling in Forsmark modelling stage 2.2. Report numbers in italics show data available already at data freeze 2.1.

Data specification	Reference to report	Reference in Sicada	Usage in F2.2 analysis/modelling		
Data from core-drilled boreholes					
Technical data in connection with drilling (KFM01A, KFM01B, KFM01C, KFM01D, KFM02A, KFM03A-KFM03B, KFM04A, KFM05A, KFM06A-KFM06B, KFM06C, KFM07A, KFM07B, KFM07C, KFM08A-KFM08B, KFM09A, KFM09B, KFM10A)	<i>P-03-32</i>	AP PF400-02-003	Siting and orientation of boreholes in modelling work.		
	<i>P-04-302</i>	AP PF400-03-041			
	<i>P-03-52</i>	AP PF400-02-042			
	<i>P-03-59</i>	AP PF400-02-016, AP PF400-03-053			
	<i>P-03-82</i>	AP PF400-03-040, AP PF400-03-042			
	<i>P-04-222</i>	AP PF400-03-069			
	<i>P-05-50</i>	AP PF400-03-080, AP PF400-04-052, AP PF400-04-108			
	<i>P-05-142</i>	AP PF400-04-053			
	<i>P-05-172</i>	AP PF400-04-086, AP PF400-04-104			
	<i>P-05-277</i>	AP PF400-05-015			
	<i>P-06-169</i>	AP PF400-05-077 AP PF400-05-102 AP PF400-05-103			
	<i>P-06-170</i>	AP PF400-05-003 AP PF400-05-123			
	<i>P-06-171</i>	AP PF400-05-016			
	<i>P-06-172</i>	AP PF400-05-109			
	<i>P-06-173</i>	AP PF400-05-089 AP PF400-05-108			
	Radar and BIPS-logging, and interpretation of radar logs (KFM01A, KFM01B, KFM01C-KFM01D, KFM02A, KFM03A-KFM03B, KFM04A, KFM05A, KFM06A, KFM06B, KFM06C, KFM07A, KFM07B-KFM09A, KFM08A, KFM08B, KFM08C, KFM09B, KFM10A)	<i>P-03-45</i>		AP PF400-02-044	Data used in borehole mapping (BIPS) and in single hole interpretation (radar logging) with focus on the identification of brittle deformation zones. Input for both rock domain and DZ modelling.
		<i>P-04-79</i>		AP PF400-03-044, AP PF400-03-047	
		<i>P-06-98</i>		AP PF400-05-112, AP PF400-06-014	
		<i>P-04-40</i>		AP PF400-03-002	
		<i>P-04-41</i>		AP PF400-03-002	
<i>P-04-67</i>		AP PF400-03-045			
<i>P-04-152</i>		AP PF400-04-047			
<i>P-05-01</i>		AP PF400-04-047			
<i>P-05-242</i>		AP PF400-05-069			
<i>P-05-53</i>		AP PF400-04-047			
<i>P-06-44</i>		AP PF400-05-067			
<i>P-05-52</i>		AP PF400-05-002			
<i>P-05-158</i>		AP PF400-05-030			
<i>P-05-58</i>		AP PF400-04-047			
<i>P-06-178</i>		AP PF400-06-046			
<i>P-06-64</i>		AP PF400-05-112			
<i>P-06-177</i>	AP PF400-06-046				
Geophysical logging (KFM01A, KFM01B, KFM01C-KFM09B, KFM01D, KFM02A-KFM03A-KFM03B, KFM04A, KFM05A, KFM06A, KFM06C, KFM07A, KFM07B-KFM09A, KFM08A-KFM08B, KFM08C-KFM10A)	<i>P-03-103</i>	AP PF400-03-003	Data used in borehole mapping and in single hole interpretation. Input for both rock domain and DZ modelling.		
	<i>P-04-145</i>	AP PF400-03-089			
	<i>P-06-123</i>	AP PF400-05-119			
	<i>P-06-168</i>	AP PF400-06-013			
	<i>P-04-97</i>	AP PF400-03-046			
	<i>P-04-144</i>	AP PF400-03-089			
	<i>P-04-153</i>	AP PF400-04-048			
	<i>P-05-17</i>	AP PF400-04-085			
	<i>P-05-159</i>	AP PF400-05-008			
	<i>P-05-276</i>	AP PF400-05-068			
	<i>P-06-22</i>	AP PF400-05-098			
<i>P-07-05</i>	AP PF400-06-050				

Data specification	Reference to report	Reference in Sicada	Usage in F2.2 analysis/modelling
Interpretation of geophysical logs (KFM01A-KFM01B, KFM01C-KFM09B, KFM01D, KFM02A-KFM03A-KFM03B, KFM04A, KFM05A, KFM06A, KFM06C, KFM07A, KFM07B-KFM09A, KFM08A-KFM08B, KFM08C-KFM10A)	<i>P-04-80</i> <i>P-04-98</i> P-06-152 P-06-216 <i>P-04-143</i> <i>P-04-154</i> <i>P-05-51</i> P-06-84 <i>P-05-119</i> P-06-126 <i>P-05-202</i> P-06-258	AP PF400-03-048 AP PF400-03-091 AP PF400-06-008 AP PF400-06-014 AP PF400-03-090 AP PF400-03-090 AP PF400-04-118 AP PF400-05-096 AP PF400-05-022 AP PF400-05-118 AP PF400-05-022 AP PF400-06-074	Used in single hole interpretation. Input for both rock domain and DZ modelling.
Vertical seismic profiling (KFM01A and KFM02A)	<i>P-05-168</i>	AP PF400-04-060	Input for DZ modelling.
Electrical measurements at drill sites 4, 7 and 8 (KFM04A, KFM07A and KFM08A)	P-05-265	AP PF400-04-068	Analysis of corrosion observations.
Boremap mapping (KFM01A, KFM01B, KFM01C, KFM01D, KFM02A, KFM03A-KFM03B, KFM04A, KFM05A, KFM06A-KFM06B, KFM06C, KFM07A, KFM07B, KFM07C, KFM08A-KFM08B, KFM08C, KFM09A, KFM09B, KFM10A)	<i>P-03-23</i> <i>P-04-114</i> P-06-133 P-06-132 <i>P-03-98</i> <i>P-03-116</i> <i>P-04-115</i> <i>P-04-295</i> <i>P-05-101</i> P-06-79 <i>P-05-102</i> P-06-80 P-06-205 <i>P-05-203</i> P-06-203 P-06-130 P-06-131 P-06-204	AP PF400-02-014 AP PF400-03-094 AP PF400-05-129 AP PF400-06-045 AP PF400-03-006 AP PF400-03-054 AP PF400-03-100 AP PF400-04-033 AP PF400-04-105 AP PF400-05-079 AP PF400-04-115 AP PF400-05-105 AP PF400-06-060 AP PF400-05-044 AP PF400-06-058 AP PF400-05-095 AP PF400-05-130 AP PF400-06-059	Rock type, ductile deformation in the bedrock, fracture statistics. Data used in identification of rock units and brittle deformation zones in single hole interpretation. Input for rock domain, DZ and DFN modelling.
Comparative geological mapping with the BOREMAP system: 176.5–306.9 m of borehole KFM06C, 9.6–132.2 m of borehole KLX07B	P-06-81 P-06-82	AP PF400-05-086 AP PF400-05-086	Control of the reproducibility of borehole mapping data.
Mineralogical and geochemical analyses of rock types and fracture fillings (KFM01A-KFM01B-KFM02A-KFM03A-KFM03B, KFM04A-KFM05A-KFM06A, KFM06B-KFM06C-KFM07A-KFM08A-KFM08B)	<i>P-04-103</i> <i>P-04-149</i> <i>P-05-156</i> <i>P-05-197</i> P-06-226	AP PF400-03-051 AP PF400-04-032 AP PF400-03-088 AP PF400-04-032 AP PF400-06-077	Mineralogical and geochemical properties of rock types and fracture fillings. Input for rock domain, DZ and DFN modelling.
Petrophysical and in situ gamma-ray spectrometric data from rock types ((KFM01A, KFM02A and KFM03A-KFM03B, KFM04A, KFM05A and KFM06A)	<i>P-04-103</i> <i>P-04-107</i> <i>P-05-204</i>	AP PF400-03-051 AP PF400-03-048 AP PF400-05-031	Physical properties of rock types. Input for rock domain modelling. Data also used for the interpretation of geophysical logs.
Mineralogical and microstructural analyses of vuggy metagranite in KFM02A	<i>P-03-77</i>	AP PF400-03-005	Input for rock domain, fracture domain and DZ modelling.
Mineralogy, geochemistry, porosity and redox capacity of altered rock adjacent to fractures	P-06-209	AP PF400-05-076	Mineralogical and geochemical properties of rock types. Input for rock domain modelling.
Characterisation of brittle deformation zones at Forsmark	P-06-212	AP PF400-06-109	Input for DZ modelling.

Data specification	Reference to report	Reference in Sicada	Usage in F2.2 analysis/modelling
Single hole interpretation (KFM01A-KFM01B, KFM01C-KFM09B, KFM01D, KFM02A, KFM03A-KFM03B, KFM04A, KFM05A, KFM06A-KFM06B, KFM06C, KFM07A, KFM07B-KFM09A, KFM08A-KFM08B, KFM08C-KFM10A)	<i>P-04-116</i> <i>P-04-117</i> P-06-135 P-06-210 <i>P-04-118</i> <i>P-04-119</i> <i>P-04-296</i> <i>P-05-132</i> P-06-83 <i>P-05-157</i> P-06-134 <i>P-05-262</i> P-06-207	AP PF400-04-038 AP PF400-03-007 AP PF400-06-022 AP PF400-06-056 AP PF400-04-022 AP PF400-04-039 AP PF400-04-040 AP PF400-04-114 AP PF400-05-107 AP PF400-05-027 AP PF400-06-011 AP PF400-05-029 AP PF400-06-057	Interpretation used in rock domain and DZ modelling.
Data from percussion-drilled boreholes			
Technical data in connection with drilling (HFM01-HFM03, HFM04-HFM05, HFM06-HFM08, HFM09-HFM10, HFM11-HFM12 and HFM17-HFM19, HFM13-HFM15, HFM16, HFM20-22, HFM23-HFM24-HFM28, HFM25-HFM27-HFM29-HFM30-HFM31-HFM32-HFM38)	<i>P-03-30</i> <i>P-03-51</i> <i>P-03-58</i> <i>P-04-76</i> <i>P-04-85</i> <i>P-04-106</i> <i>P-04-94</i> <i>P-04-245</i> P-05-278 P-06-166	AP PF400-02-008 AP PF400-02-018 AP PF400-02-022 AP PF400-02-036 AP PF400-02-036 AP PF400-03-052 AP PF400-03-067 AP PF400-03-068 AP PF400-03-082 AP PF400-03-059 AP PF400-03-097 AP PF400-03-079 AP PF400-04-054 AP PF400-05-073 AP PF400-05-085 AP PF400-05-081 AP PF400-05-115 AP PF400-05-124 AP PF400-06-054	Siting and orientation of boreholes in modelling work.
Radar and BIPS-logging, and interpretation of radar logs (HFM01-HFM03, HFM04-HFM05, HFM06-HFM08, HFM09-HFM10, HFM11-HFM12, HFM13-HFM15, HFM16-HFM19, HFM20-21, HFM22, HFM24-HFM26-HFM27-HFM29-HFM32, HFM25-HFM28, HFM30-HFM31, HFM38)	<i>P-03-39</i> <i>P-03-53</i> <i>P-03-54</i> <i>P-04-67</i> <i>P-04-39</i> <i>P-04-68</i> <i>P-04-69</i> <i>P-05-64</i> <i>P-05-01</i> <i>P-05-176</i> P-06-64 P-06-44 P-06-178 P-06-177	AP PF400-02-010 AP PF400-02-043 AP PF400-02-043 AP PF400-03-045 AP PF400-03-087 AP PF400-03-087 AP PF400-03-087 AP PF400-04-092 AP PF400-04-047 AP PF400-05-039 AP PF400-05-112 AP PF400-05-067 AP PF400-06-046 AP PF400-06-046	Data used in borehole mapping (BIPS) and in single hole interpretation (radar logging) with focus of identification of brittle deformation zones. Input for both rock domain and DZ modelling.
Geophysical logging (HFM01-HFM03, HFM04-HFM05, HFM06 and HFM08, HFM10-HFM13, HFM14-HFM18, HFM19, HFM20-22, HFM07-HFM24-HFM26-HFM29-HFM32, HFM25-HFM27-HFM28, HFM30-HFM31-HFM38)	<i>P-03-39</i> <i>P-03-103</i> <i>P-03-53</i> <i>P-03-54</i> <i>P-04-144</i> <i>P-04-145</i> <i>P-04-153</i> <i>P-05-17</i> P-06-123 P-06-22 P-07-05	AP PF400-02-010 AP PF400-03-003 AP PF400-02-043 AP PF400-02-043 AP PF400-03-089 AP PF400-03-089 AP PF400-04-048 AP PF400-04-085 AP PF400-05-119 AP PF400-05-061 AP PF400-05-098 AP PF400-06-050	Data used in borehole mapping and in single hole interpretation. Input for both rock domain and DZ modelling.

Data specification	Reference to report	Reference in Sicada	Usage in F2.2 analysis/modelling	
Interpretation of geophysical logs (HFM01-HFM03, HFM04-HFM08, HFM10-HFM13 and HFM16-HFM18, HFM14-HFM15-HFM19, HFM20-22, HFM07-HFM24-HFM26 -HFM29-HFM32, HFM25-HFM27-HFM28, HFM30-HFM31-HFM38)	<i>P-04-80</i>	AP PF400-03-048	Used in single hole interpretation. Input for both rock domain and DZ modelling.	
	<i>P-04-98</i>	AP PF400-03-090		
	<i>P-04-143</i>	AP PF400-03-091		
	<i>P-04-154</i>	AP PF400-03-090		
	<i>P-05-51</i>	AP PF400-03-090		
	<i>P-06-152</i>	AP PF400-04-049		
	<i>P-06-126</i>	AP PF400-04-118		
Boremap mapping (HFM01-HFM03, HFM04-HFM05, HFM06-HFM08, HFM09-HFM12, HFM13-HFM15 and HFM19, HFM16-HFM18, HFM20-22, HFM23-HFM32 and HFM38)	<i>P-03-20</i>	AP PF400-06-008	Data mainly used for identification of rock units and DZ in single hole interpretation. Input for both rock domain and DZ modelling. (Problem with recognition of rock types and mineral coatings along fractures. Also underestimation of the amount of fractures which is derived from BIPS images).	
	<i>P-03-21</i>	AP PF400-06-074		
	<i>P-03-22</i>	AP PF400-02-050		
	<i>P-04-101</i>	AP PF400-02-050		
	<i>P-04-112</i>	AP PF400-03-073		
	<i>P-04-113</i>	AP PF400-03-106		
	<i>P-05-103</i>	AP PF400-03-102		
Single hole interpretation (HFM01-HFM03, HFM04-HFM05, HFM06-HFM08, HFM09-HFM10, HFM11-HFM13 and HFM16-HFM18, HFM14-HFM15 and HFM19, HFM20-22, HFM23-HFM28-HFM30-HFM31-HFM32-HFM38, HFM24-HFM25-HFM27-HFM29)	<i>P-06-206</i>	AP PF400-04-106	Interpretation used in rock domain and DZ modelling.	
	<i>P-04-116</i>	AP PF400-05-128		
	<i>P-04-117</i>	AP PF400-04-038		
	<i>P-04-118</i>	AP PF400-03-007		
	<i>P-04-119</i>	AP PF400-04-022		
	<i>P-04-120</i>	AP PF400-04-039		
	<i>P-04-296</i>	AP PF400-04-043		
Older borehole, tunnel and surface data	<i>P-04-296</i>	AP PF400-04-040	Rock type data from boreholes and tunnels, lineament identification at the nuclear power plant, brittle structures at or close to the surface in the vicinity of the nuclear power plant, and identification of brittle deformation zones. Fracture orientation and mineral coatings from tunnels and boreholes. Input for rock domain, DZ and DFN modelling.	
	<i>P-05-157</i>	AP PF400-04-040		
	<i>P-05-262</i>	AP PF400-05-027		
	<i>P-06-207</i>	AP PF400-05-029		
	<i>P-06-210</i>	AP PF400-06-057		
	<i>P-06-210</i>	AP PF400-06-056		
	<i>P-04-81</i>	AP PF400-02-048		
Surface-based data	<i>P-03-09</i>	AP PF400-02-011	Rock type, rock type distribution, ductile deformation in the bedrock, fracture statistics, and identification of deformation zones at surface. Input for rock domain, DZ and DFN modelling.	
	<i>P-04-91</i>	AP PF400-03-074		
	<i>Bedrock geological map, Forsmark version 1.2 (SKB GIS database)</i>			
	Detailed bedrock mapping with special emphasis on fractures (drill sites 2, 3, 4, 5, 7, and coastal outcrop at Klubbudden)	<i>P-03-12</i>		AP PF400-02-015
		<i>P-03-115</i>		AP PF400-02-015
		<i>P-04-90</i>		AP PF400-03-037
	Detailed bedrock mapping of excavations across lineaments	<i>P-05-199</i>		AP PF400-03-075
<i>P-06-136</i>		AP PF400-03-085		
<i>P-04-88</i>		AP PF400-03-096		
Geochemical analyses of till	<i>P-05-269</i>	AP PF400-03-096	Fracture statistics (orientation, length) and identification of brittle and ductile features at surface. Input for rock domain, DZ and DFN modelling.	
	<i>P-03-118</i>	AP PF400-05-074		
	<i>P-04-88</i>	AP PF400-04-081	Assessment of the geological character of lineaments. Input especially for DZ modelling, but also DFN.	
	<i>P-05-269</i>	AP PF400-05-075		

Data specification	Reference to report	Reference in Sicada	Usage in F2.2 analysis/modelling
Evaluation of the occurrence of late- or post-glacial faulting	<i>P-03-76</i> <i>P-04-123</i>	AP PF400-02-013 AP PF400-03-020	
Mineralogical and geochemical analyses of rock types	<i>P-03-75</i> <i>P-04-87</i>	AP PF400-02-011	Mineralogical and geochemical properties of rock types. Input for rock domain modelling.
Petrophysical and in situ gamma-ray spectrometric data from rock types	<i>P-03-26</i> <i>P-03-102</i> <i>P-04-155</i>	AP PF400-02-011 AP PF400-02-047	Physical properties of rock types. Input for rock domain modelling. Data also used for the interpretation of geophysical logs.
U-Pb, ⁴⁰ Ar/ ³⁹ Ar, (U-Th)/He and Rb-Sr geochronological data from bedrock and fracture minerals	<i>P-04-126</i> P-06-211 P-06-213	AP PF400-02-011 AP PF400-05-048 AP PF400-05-047	Input for conceptual understanding of the geological modelling work.
Production of orthorectified aerial photographs and digital terrain model	<i>P-02-02</i>		
Methodology for construction of digital terrain model for the site	<i>P-04-03</i>		
Marine geological survey of the sea bottom off Forsmark	<i>P-03-101</i>	AP PF400-02-027	
Water depth in shallow lakes	<i>P-04-25</i>	AP PF400-02-005	
Water depth in shallow bays	<i>P-04-125</i>	AP PF400-03-061	
Helicopter-borne, geophysical data (magnetic, EM, VLF and gamma-ray spectrometry data)	<i>P-03-41</i>	AP PF400-02-025	Base data for interpretation of airborne magnetic lineaments.
Electric soundings	<i>P-03-44</i>	AP PF400-02-029	
Inversion of helicopter-borne EM measurements	<i>P-04-157</i>	AP PF400-03-092	
Interpretation of topographic, bathymetric and helicopter-borne geophysical data. Alternative interpretation in and immediately around the candidate area. Assessment of all lineaments in the target area.	<i>P-03-40</i> <i>P-04-29</i> <i>P-04-282</i> <i>P-04-241</i> <i>P-05-261</i>	AP PF400-02-011 AP PF400-02-047 AP PF400-05-036	Identification of magnetic lineaments. Input for DZ modelling.
High-resolution seismic reflection data carried out during stage I and II (including interpretation)	<i>R-02-43</i> <i>P-04-158</i> <i>R-05-42</i>	AP PF400-02-002 AP PF400-03-084 AP PF400-04-078	Identification of seismic reflectors in the bedrock that may correspond to deformation zones or boundaries between different types of bedrock. Input for DZ modelling.
Seismic refraction data	<i>P-05-12</i> P-06-138	AP PF400-04-077 AP PF400-05-034	Identification of low velocity anomalies in the bedrock that may correspond to deformation zones. Input for DZ modelling.
Seismic velocity measurements along excavation across lineaments	<i>P-05-46</i>	AP PF400-04-077	Identification of low velocity anomalies in the bedrock that may correspond to deformation zones. Input for DZ modelling.
Ground geophysical data (magnetic and EM data) close to drill sites 1, 2, 3, 4 and 5, and several lineaments (including interpretation)	<i>P-02-01</i> <i>P-03-55</i> <i>P-03-104</i> P-05-266	AP PF400-02-001 AP PF400-03-031 AP PF400-03-065 AP PF400-05-083	Identification of magnetic lineaments. Input for DZ modelling.
High-resolution ground magnetic measurements	P-06-85 P-06-261	AP PF400-05-082 AP PF400-06-034	Identification of magnetic lineaments. Input for DZ modelling.
Mise-à-la-masse data from drill site 5	<i>P-04-305</i>	AP PF400-04-113	
Regional gravity data	<i>P-03-42</i>	AP PF400-02-026	

Data specification	Reference to report	Reference in Sicada	Usage in F2.2 analysis/modelling
<i>Previous models</i>			
SFR structural models	<i>R-98-05</i> <i>R-01-02</i>		DZ modelling. The subvertical zones 3, 8 and 9 have been extracted from /Axelsson and Hansen 1997/. The sub-horizontal zone H2 has been extracted from the SAFE model /Holmén and Stigsson 2001/.
Forsmark site descriptive model versions 0, 1.1, 1.2 and stage 2.1	<i>R-02-32</i> <i>R-04-15</i> <i>R-05-18</i> <i>R-06-38</i>	The approved models are stored in the SKB model database	Comparison and updating of models.

Table A1-2. Available bedrock hydrogeological data and their handling in Forsmark modelling stage 2.2. Report numbers in italics show data available already at data freeze 2.1.

Data specification	Reference to report	Reference in Sicada	Usage in F2.2
Single-hole data from core-drilled boreholes			
Double-packer injection tests (PSS)			Included in integrated WellCad plots in this report. Further use in modelling will be described in the hydrogeological modelling report based on data freeze 2.2.
KFM01A	P-04-95	AP PF400-03-022	
KFM01C	P-06-165	AP PF400-06-009	
KFM01D	P-06-195	AP PF400-06-017	
KFM02A	<i>P-04-100</i>	AP PF400-04-008	
KFM02A – re-measurement after hydraulic fracturing	<i>P-05-145</i>	AP PF400-04-073	
KFM03A	<i>P-04-194</i>	AP PF400-04-026	
KFM03B	P-04-278	AP PF400-04-064	
KFM04A	<i>P-04-293</i>	AP PF400-04-027	
KFM05A	<i>P-05-56</i>	AP PF400-04-111	
KFM06A and 06B	P-05-165	AP PF400-04-122 AP PF400-05-005	
KFM06C	P-06-23	AP PF400-05-087	
KFM07A	<i>P-05-133</i>	AP PF400-05-006	
KFM07B	P-06-86	AP PF400-05-049	
KFM08A	P-06-194	AP PF400-05-032	
KFM08B	P-05-235	AP PF400-05-004	
KFM09A	P-06-52	AP PF400-05-104	
KFM09B	P-06-122	AP PF400-06-003	
Difference-flow logging (PFL)			
KFM01A	P-03-28 P-04-193	AP PF400-02-040	
KFM01D	P-06-161	AP PF400-06-018	
KFM02A	<i>P-04-188</i>	AP PF400-03-021	
KFM03A	P-04-189	AP PF400-04-041	
KFM04A	<i>P-04-190</i>	AP PF400-04-028	
KFM05A	<i>P-04-191</i>	AP PF400-04-029	
KFM06A	<i>P-05-15</i>	AP PF400-04-076	
KFM07A	<i>P-05-63</i>	AP PF400-04-123	
KFM07C	P-06-247	AP PF400-06-070	
KFM08A	P-05-43	AP PF400-05-007	
KFM08C	P-06-189	AP PF400-06-019	
KFM10A	P-06-190	AP PF400-06-020	
Pumping tests and impeller flow logging			
HFM01, -02, -03	<i>P-03-33</i>	AP PF400-02-019	Will be described in the hydrogeological modelling report based on data freeze 2.2.
HFM04, -05	<i>P-03-34</i>	AP PF400-02-039	
HFM06, -07, -08	<i>P-03-36</i>	AP PF400-02-039	
HFM09, -10	<i>P-04-74</i>	AP PF400-04-017	
HFM11, -12	<i>P-04-64</i>	AP PF400-03-078	
HFM13, -14, -15	<i>P-04-71</i>	AP PF400-03-095	
HFM16	<i>P-04-65</i>	AP PF400-03-101	
HFM17, -18, -19	<i>P-04-72</i>	AP PF400-04-007	
HFM20, -21, -22	P-05-14	AP PF400-04-075 AP PF400-04-091	
HFM24, -32	P-06-96	AP PF 400-05-121	
HFM25, -26	P-06-139	AP PF 400-05-121	
HFM23, -27, -28	P-06-191	AP PF 400-05-121	
HFM29, -30, -31	P-06-192	AP PF 400-06-036	
HFM33, -34, -35	P-06-193	AP PF 400-06-037	

Data specification	Reference to report	Reference in Sicada	Usage in F2.2	
<i>Cross-hole (interference) data</i>				
HFM01, -02, -03	<i>P-03-35</i>	AP PF400-02-023	Will be described in the hydrogeological modelling report based on data freeze 2.2.	
HFM11, -12	<i>P-04-200</i>	AP PF400-03-078		
HFM18, KFM03A	<i>P-04-307</i>	AP PF400-04-065		
HFM16, KFM02A	<i>P-05-78</i>	AP PF400-04-074		
	<i>P-05-37</i>	AP PF400-04-107		
KFM04A, HFM10, -13 -19, HFK252	<i>P-05-186</i>	AP PF400-05-035		
HFM01	<i>P-05-236</i>	AP PF400-05-043		
KFM02A, KFM03A	<i>P-06-09</i>	AP PF400-05-050		
HFM14, KFM05A	<i>P-06-140</i>	AP PF 400-05-125		
HFM14	<i>P-06-188</i>	AP PF 400-06-052		
HFM14	<i>P-06-196</i>	AP PF 400-06-038		
<i>Correlation of structural, hydraulic and hydrogeochemical data</i>				
KFM01A, -02A, -03A, -04A, -05A	R-04-77			Analyses of flow anomalies in relation to fracture domains (see Chapter 6).
KFM06A, -07A	P-06-56			
HFM16, KFM02A	Sicada Field note Forsmark 437		Included in integrated WellCad plots in this report.	
KFM03A	<i>P-04-96</i>	AP PF400-03-070	Further use in modelling will be described in the hydrogeological modelling report based on data freeze 2.2.	
KFM02A, -03A, -04A	<i>P-05-21</i>	AP PF400-04-042		
KFM01B, HFM01, -02, -03, KFM01A	<i>P-04-135</i>	AP PF400-03-049		
KFM01D, 07C, 08A, 08C, 10A	In prep			

Table A1-3. Available hydrogeochemical data and their handling in Forsmark modelling stage 2.2. Report numbers in italics show data available already at data freeze 2.1.

Data specification	Reference to report	Reference in Sicada	Usage in F2.2
<i>Complete chemical characterisation (class 4 and 5) in</i>			Analyses of hydrogeochemical data in relation to fracture domains (see Chapter 7). Included in integrated WellCad plots. The use of the data in the specific modelling approaches will be described in the hydrogeochemical modelling report based on data freezes 2.2 and 2.3.
KFM01A	<i>P-03-94</i>	AP PF400-02-038	
KFM01D	<i>P-06-227</i>	AP PF400-06-053	
KFM02A	<i>P-04-70</i>	AP PF400-03-038	
KFM03A	<i>P-04-108</i>	AP PF400-03-063	
KFM04A	<i>P-04-109</i>	AP PF400-04-001	
KFM05A	<i>P-05-79</i>	AP PF400-04-084	
KFM06A	<i>P-05-178</i>	AP PF400-04-110	
KFM07A	<i>P-05-170</i>	AP PF400-05-012	
KFM08A	<i>P-06-63</i>	AP PF400-05-063	
KFM09A	<i>P-06-217</i>	AP PF400-06-026	
<i>Sampling during drilling and Uranine analyses</i>	<i>Drilling reports</i>		
<i>Hydrochemical logging in</i>			
KFM02A	<i>P-03-95</i>	AP PF400-03-001	
KFM03A	<i>P-03-96</i>	AP PF400-03-056	
KFM04A	<i>P-04-47</i>	AP PF400-03-099	
KFM06A	<i>P-05-33</i>	AP PF400-04-102	
KFM07A	<i>P-05-187</i>	AP PF400-05-033	
KFM08A	<i>P-05-206</i>	AP PF400-05-059	
KFM09A	<i>P-06-95</i>	AP PF400-06-016	
KFM09B	<i>P-06-179</i>	AP PF400-06-048	
<i>Sampling in percussion-drilled boreholes and monitoring wells</i>			
Drill site 1	<i>P-03-47</i>	AP PF400-02-024	
Drill site 2	<i>P-03-48</i>	AP PF400-02-039	
Drill site 3	<i>P-03-49</i>	AP PF400-02-039	
HFM09–HFM19	<i>P-04-92</i>	AP PF400-03-095	
		AP PF400-03-101	
		AP PF400-04-007	
		AP PF400-04-017	
HFM20–HFM22	<i>P-05-48</i>	AP PF400-04-075	
		AP PF400-04-091	
HFM14, HFM23–35	<i>P-06-231</i>	AP PF400-05-121	
		AP PF400-06-036	
		AP PF400-06-037	
<i>Hydrochemical monitoring of percussion and core drilled boreholes</i>			
2005; KFM01A, KFM02A, KFM03A, HFM02, HFM04, HFM13, HFM15, HFM19	<i>P-06-57</i>	AP PF400-05-060	
Sampling/analyses of shallow groundwaters; May 2003–April 2005	<i>P-05-171</i>	AP PF400-04-090	
Samling/analyses of surface waters	<i>P-03-27</i>	AP PF400-03-033	
	<i>P-04-146</i>	AP PF400-02-007	
		AP PF400-03-036	
Sampling/analysis of precipitation	<i>P-05-274</i>	AP PF400-04-071	
	<i>P-05-143</i>	AP PF400-04-089	

Table A1-4. Available rock mechanical data and their handling in Forsmark modelling stage 2.2. Report numbers in italics show data available already at data freeze 2.1.

Data specification	Reference to report	Reference in Sicada	Usage in F2.2	
<i>Uniaxial compressive strength</i>				
KFM01A	<i>P-04-223</i>	AP PF400-03-018	Characterisation of the intact rock; Empirical determination of the rock mass mechanical properties by means of RMR and Q; Theoretical determination of the rock mass mechanical properties by means of numerical modelling.	
KFM01A – Independent determination	<i>P-04-176</i>	AP PF400-04-004		
KFM02A	<i>P-04-224</i>	AP PF400-04-019		
KFM03A	<i>P-04-225</i>	AP PF400-04-020		
KFM04A	<i>P-04-226</i>	AP PF400-04-059		
KFM05A	<i>P-05-97</i>	AP PF400-04-080		
KFM06A	<i>P-05-120</i>	AP PF400-04-121		
KFM07A	<i>P-05-211</i>	AP PF400-05-024		
KFM09A	<i>P-06-27</i>	AP PF400-05-111		
<i>Triaxial compressive strength</i>				
KFM01A	<i>P-04-227</i>	AP PF400-03-018	Characterisation of the intact rock; Empirical determination of the rock mass mechanical properties by means of RMR and Q; Theoretical determination of the rock mass mechanical properties by means of numerical modelling.	
KFM01A – Independent determination	<i>P-04-177</i>	AP PF400-04-004		
KFM01C	<i>P-06-68</i>	AP PF400-06-024		
KFM01D	<i>P-06-214</i>	AP PF400-06-047		
KFM02A	<i>P-04-228</i>	AP PF400-04-019		
KFM03A	<i>P-04-229</i>	AP PF400-04-020		
KFM04A	<i>P-04-230</i>	AP PF400-04-059		
KFM05A	<i>P-05-100</i>	AP PF400-04-080		
KFM07A	<i>P-05-210</i>	AP PF400-05-024		
KFM08A	<i>P-05-217</i>	AP PF400-05-058		
KFM09A	<i>P-06-26</i>	AP PF400-05-111		
<i>Indirect tensile strength</i>				
KFM01A	<i>P-04-170</i>	AP PF400-03-018		Characterisation of the intact rock; Theoretical determination of the rock mass mechanical properties by means of numerical modelling.
KFM01A – Independent determination	<i>P-04-171</i>	AP PF400-04-004		
KFM02A	<i>P-04-172</i>	AP PF400-04-019		
KFM03A	<i>P-04-173</i>	AP PF400-04-019		
		AP PF400-04-020		
KFM04A	<i>P-04-174</i>	AP PF400-04-059		
KFM05A	<i>P-05-98</i>	AP PF400-04-080		
KFM06A	<i>P-05-121</i>	AP PF400-04-121		
KFM07A and KFM08A	<i>P-05-212</i>	AP PF400-05-024		
KFM09A	<i>P-06-28</i>	AP PF400-05-111		
<i>Crack initiation stress</i>				
KFM01A	<i>P-04-223</i>	AP PF400-03-018	Evaluation of the elastic limit of deformation – for addressing spalling and core discing problems.	
KFM02A	<i>P-04-224</i>	AP PF400-04-019		
KFM03A	<i>P-04-225</i>	AP PF400-04-020		
KFM04A	<i>P-04-226</i>	AP PF400-04-059		
KFM05A	<i>P-05-97</i>	AP PF400-04-080		
KFM06A	<i>P-05-120</i>	AP PF400-04-121		
KFM07A	<i>P-05-211</i>	AP PF400-05-024		
KFM09A	<i>P-06-27</i>	AP PF400-05-111		
<i>Direct shear tests</i>				
KFM01A	<i>P-04-175</i> <i>P-05-08</i>	AP PF400-04-005 AP PF400-03-018	Characterisation of the rock fractures – strength and stiffness; Theoretical determination of the rock mass mechanical properties by means of numerical modelling.	
KFM01D	<i>P-06-215</i>	AP PF 400-06-047		
KFM02A	<i>P-05-09</i>	AP PF400-04-019		
KFM03A	<i>P-05-10</i>	AP PF400-04-020		
KFM04A	<i>P-05-11</i>	AP PF400-04-059		
KFM05A	<i>P-05-99</i> <i>P-05-141</i>	AP PF400-04-080 AP PF400-05-013		
KFM06A	<i>P-05-122</i>	AP PF400-04-121		
KFM07A	<i>P-05-213</i>	AP PF400-05-024		
KFM08A	<i>P-05-218</i>	AP PF400-05-058		
KFM09A	<i>P-06-29</i>	AP PF400-05-111		

Data specification	Reference to report	Reference in Sicada	Usage in F2.2
<i>Tilt tests</i>			
KFM01A	<i>P-03-108</i>	AP PF400-03-010 AP PF400-04-011	Characterisation of the rock fracture properties and of the rock mass by RMR and Q.
KFM02A	<i>P-04-08</i>	AP PF400-03-044	
KFM03A and KFM03B	<i>P-04-178</i>	AP PF400-03-077	
KFM04A	<i>P-04-179</i>	AP PF400-04-002	
KFM05A	<i>P-04-205</i>	AP PF400-04-067	
KFM09A	<i>P-06-25</i>	AP PF400-05-110	
<i>P-wave velocity measurements on core samples</i>			
KFM01A	<i>P-03-38</i>	AP PF400-03-010	Correlation between rock mass stresses and foliation.
KFM02A	<i>P-04-09</i>	AP PF400-03-044	
KFM03A	<i>P-04-180</i>	AP PF400-03-077	
KFM04A	<i>P-04-181</i>	AP PF400-04-002	
KFM05A	<i>P-04-203</i>	AP PF400-04-067	
KFM06A	<i>P-05-04</i>	AP PF400-04-112	
KFM07A	<i>P-05-125</i>	AP PF400-05-023	
KFM08A	<i>P-05-216</i>	AP PF400-05-057	
KFM09A	<i>P-06-24</i>	AP PF400-05-110	
<i>Sonic velocity measurements along the boreholes</i>			
KFM01A		AP PF 400-03-003	Correlation with P-velocity along the cores and considerations about damage of the core.
KFM01B		AP PF 400-03-089	
KFM01C		AP PF 400-05-119	
KFM02A		AP PF 400-03-046	
KFM03A		AP PF 400-03-046	
KFM03B		AP PF 400-03-046	
KFM04A		AP PF 400-03-089	
KFM05A		AP PF 400-04-048	
KFM06A		AP PF 400-03-089	
KFM06C		AP PF 400-05-068	
KFM07A		AP PF 400-05-008	
KFM07B		AP PF 400-05-098	
KFM08A		AP PF 400-05-042	
KFM08B		AP PF 400-05-008	
KFM08C		AP PF 400-06-050	
KFM09A		AP PF 400-05-098	
KFM09B		AP PF 400-05-119	
KFM010A		AP PF 400-06-050	
<i>Empirical characterisation</i>			
KFM01A	<i>P-05-112</i>		Characterisation of the rock mass (RMR, Q) – rock mass mechanical properties.
KFM02A	<i>P-05-113</i>		
KFM03A	<i>P-05-114</i>		
KFM04A	<i>P-05-115</i>	AP PF 400-04-039	
KFM01B	<i>P-07-115</i>		
KFM07C	<i>P-07-115</i>		
KFM09A	<i>P-07-115</i>		
KFM09B	<i>P-07-115</i>		
<i>Stress measurements</i>			
KFM01B	<i>P-04-83</i>	AP PF400-03-041	Estimation of the in situ stress field.
KFM02B			
KFM07C			
Evaluation of overcoring result in KFM01B HF and HTPF measurements KFM01A, KFM01B, KFM02A, KFM04A	<i>P-05-66</i> <i>P-04-311</i>	AP PF400-04-016 AP PF400-04-023	Estimation of the in situ stress field.
HF and HTPF measurements – KFM01A, KFM01B, KFM02A, KFM04A – laboratory testing on cores	<i>P-04-312</i>	AP PF400-04-023	
HF and HTPF measurements KFM09A		AP PF400-06-061	
HF and HTPF measurements KFM09B		AP PF400-06-044	
Borehole break-out studies in boreholes KFM01A, KFM01B, KFM02A, KFM03A, KFM03B, KFM04A, KFM05A, KFM06A	<i>P-07-07</i>	AP PF 400-06-062	Indirect observation of rock stresses.

Table A1-5. References to the reports in the SKB series P-, R- and TR- that are referred to in Tables A1-1 to A1-4. Reports with numbers in italics were already available for stage 2.1

<i>P-02-01</i>	Thunehed H, Pitkänen T. Markgeofysiska mätningar inför placering av de tre första kärnborrhålen i Forsmarksområdet.
<i>P-02-02</i>	Wiklund S. Digitala ortofoton och höjdmodeller. Redovisning av metodik för platsundersökningsområdena Oskarshamn och Forsmark samt förstudieområdet Tierp Norra.
<i>P-03-09</i>	Stephens M B, Bergman T, Andersson J, Hermansson T, Wahlgren C-H, Albrecht L, Mikko H. Bedrock mapping. Stage 1 (2002) – Outcrop data including fracture data. Forsmark.
<i>P-03-12</i>	Hermanson J, Hansen L, Olofsson J, Sävås J, Vestgård J. Detailed fracture mapping at the KFM02 and KFM03 drill sites. Forsmark.
<i>P-03-20</i>	Nordman, C. Forsmark site investigation. Boremap mapping of percussion boreholes HFM01–03.
<i>P-03-21</i>	Nordman, C. Forsmark site investigation. Boremap mapping of percussion boreholes HFM04 and HFM05.
<i>P-03-22</i>	Nordman, C. Forsmark site investigation. Boremap mapping of percussion boreholes HFM06–08.
<i>P-03-23</i>	Petersson J, Wägnerud A. Forsmark site investigation. Boremap mapping of telescopic drilled borehole KFM01A.
<i>P-03-26</i>	Mattsson H, Isaksson H, Thunehed H. Forsmark site investigation. Petrophysical rock sampling, measurements of petrophysical rock parameters and in situ gamma-ray spectrometry measurements on outcrops carried out 2002.
<i>P-03-27</i>	Nilsson A-C, Karlsson S, Borgiel M. Forsmark site investigation. Sampling and analysis of surface waters. Results from sampling in the Forsmark area, March 2002 to March 2003.
<i>P-03-28</i>	Rouhiainen P, Pöllänen J. Forsmark site investigation. Difference flow logging of borehole KFM01A.
<i>P-03-29</i>	Barton N. KFM01A. Q-logging.
<i>P-03-30</i>	Claesson L-Å, Nilsson G. Forsmark site investigation. Drilling of a flushing water well, HFM01, and two groundwater monitoring wells, HFM02 and HFM03 at drillsite DS1.
<i>P-03-32</i>	Claesson L-Å, Nilsson G. Forsmark site investigation. Drilling of the telescopic borehole KFM01A at drilling site DS1.
<i>P-03-33</i>	Ludvigson J-E, Jönsson S, Levén, J. Forsmark site investigation. Pumping tests and flow logging. Boreholes KFM01A (0–100 m), HFM01, HFM02 and HFM03.
<i>P-03-34</i>	Ludvigson J-E, Jönsson S, Svensson T. Forsmark site investigation. Pumping tests and flow logging. Boreholes KFM02A (0–100 m), HFM04 and HFM05.
<i>P-03-35</i>	Ludvigson J-E, Jönsson S. Forsmark site investigation. Hydraulic interference tests. Boreholes HFM01, HFM02 and HFM03.
<i>P-03-36</i>	Källgården J, Ludvigson J-E, Jönsson S. Forsmark site investigation. Pumping tests and flow logging. Boreholes KFM03A (0–100 m), HFM06, HFM07 and HFM08.
<i>P-03-38</i>	Tunbridge L, Chryssanthakis P. Forsmark site investigation. Borehole KFM01A. Determination of P-wave velocity, transverse borehole core.
<i>P-03-39</i>	Gustafsson C, Nilsson P. Forsmark site investigation. Geophysical, radar and BIPS logging in boreholes HFM01, HFM02, HFM03 and the percussion drilled part of KFM01A.
<i>P-03-40</i>	Isaksson H. Forsmark site investigation. Interpretation of topographic lineaments 2002.
<i>P-03-41</i>	Rønning H J S, Kihle O, Mogaard J O, Walker P, Shomali H, Hagthorpe P, Byström S, Lindberg H, Thunehed H. Forsmark site investigation. Helicopter borne geophysics at Forsmark, Östhammar, Sweden.
<i>P-03-42</i>	Aaro S. Forsmark site investigation. Regional gravity survey in the Forsmark area, 2002 and 2003.
<i>P-03-44</i>	Thunehed H, Pitkänen, T. Forsmark site investigation. Electric soundings supporting inversion of helicopterborne EM-data.
<i>P-03-45</i>	Aaltonen J, Gustafsson C. Forsmark site investigation. RAMAC and BIPS logging in borehole KFM01A.
<i>P-03-47</i>	Nilsson A-C. Forsmark site investigation. Sampling and analyses of groundwater in percussion drilled boreholes and shallow monitoring wells at drillsite DS1. Results from the percussion boreholes HFM01, HFM02, HFM03, KFM01A (borehole section 0–100 m) and the monitoring wells SFM0001, SFM0002 and SFM0003.
<i>P-03-48</i>	Nilsson A-C. Forsmark site investigation. Sampling and analyses of groundwater in percussion drilled boreholes and shallow monitoring wells at drillsite DS2. Results from the percussion boreholes HFM04, HFM05, KFM02A (borehole section 0–100 m) and the monitoring wells SFM0004 and SFM0005.
<i>P-03-49</i>	Nilsson A-C. Forsmark site investigation. Sampling and analyses of groundwater in percussion drilled boreholes at drillsite DS3. Results from the percussion boreholes HFM06 and HFM08.
<i>P-03-51</i>	Claesson L-Å, Nilsson, G. Forsmark site investigation. Drilling of a flushing water well, HFM05, and a groundwater monitoring well, HFM04, at drillsite DS2.

- P-03-52* **Claesson L-Å, Nilsson, G.** Forsmark site investigation. Drilling of the telescopic borehole KFM02A at drilling site DS2.
- P-03-53* **Nilsson P, Gustafsson C.** Forsmark site investigation. Geophysical, radar and BIPS logging in boreholes HFM04, HFM05, and the percussion drilled part of KFM02A.
- P-03-54* **Nilsson P, Aaltonen J.** Forsmark site investigation. Geophysical, radar and BIPS logging in boreholes HFM06, HFM07 and HFM08.
- P-03-55* **Pitkänen T, Isaksson H.** Forsmark site investigation. A ground geophysical survey prior to the siting of borehole KFM04A.
- P-03-58* **Claesson L-Å, Nilsson, G.** Forsmark site investigation. Drilling of a flushing water well, HFM06 and two groundwater monitoring wells, HFM07 and HFM08, at drillsite DS3.
- P-03-59* **Claesson L-Å, Nilsson, G.** Forsmark site investigation. Drilling of the telescopic borehole KFM03A and the core drilled borehole KFM03B at drilling site DS3.
- P-03-75* **Stephens M B, Lundqvist S, Bergman T, Anderson J, Ekström M.** Forsmark site investigation. Bedrock mapping. Rock types, their petrographic and geochemical characteristics, and a structural analysis of the bedrock based on Stage 1 (2002) surface data.
- P-03-76* **Lagerbäck R, Sundh M.** Forsmark site investigation. Searching for evidence of late- or post-glacial faulting in the Forsmark region. Results from 2002.
- P-03-77* **Möller C, Snäll S, Stephens M B.** Forsmark site investigation. Dissolution of quartz, vug formation and new grain growth associated with post-metamorphic hydrothermal alteration in KFM02A.
- P-03-82* **Claesson L-Å, Nilsson, G.** Forsmark site investigation. Drilling of the telescopic borehole KFM04A and the percussion drilled borehole KFM04B at drilling site DS4.
- P-03-94* **Wacker P, Bergelin A, Nilsson, A-C.** Forsmark site investigation. Complete hydrochemical characterisation in KFM01A. Results from two investigated sections, 110.1–120.8 and 176.8–183.9 m.
- P-03-95* **Wacker P, Nilsson A-C.** Forsmark site investigation. Hydrochemical logging and “clean up” pumping in KFM02A.
- P-03-96* **Berg C, Nilsson A-C.** Forsmark site investigation. Hydrochemical logging in KFM03A.
- P-03-98* **Petersson J, Wängnerud A, Strähle A.** Forsmark site investigation. Boremap mapping of telescopic drilled borehole KFM02A.
- P-03-101* **Elhammer A, Sandkvist Å.** Forsmark site investigation. Detailed marine geological survey of the sea bottom outside Forsmark.
- P-03-102* **Isaksson H, Mattsson H, Thunehed H, Keisu M.** Forsmark site investigation. Interpretation of petrophysical surface data. Stage 1 (2002).
- P-03-103* **Nielsen U T, Ringgaard J.** Forsmark site investigation. Geophysical borehole logging in borehole KFM01A, HFM01 and HFM02.
- P-03-104* **Pitkänen T, Thunehed H, Isaksson H.** Forsmark site investigation. A ground geophysical survey prior to the siting of borehole KFM05A and KFM06A and control of the character of two SW-NE oriented lineaments.
- P-03-108* **Chryssanthakis P.** Forsmark site investigation. Borehole KFM01A. Results of tilt testing.
- P-03-115* **Hermanson J, Hansen L, Vestgård J, Leiner P.** Forsmark site investigation. Detailed fracture mapping of the outcrops Klubbudden, AFM001098 and drill site 4, AFM001097.
- P-03-116* **Petersson J, Wängnerud A, Danielsson P, Strähle A.** Forsmark site investigation. Boremap mapping of telescopic drilled borehole KFM03A and core drilled borehole KFM03B.
- P-03-118* **Nilsson B.** Forsmark site investigation. Element distribution in till at Forsmark – a geochemical study.
- P-04-03* **Brydsten L.** A method for construction of digital elevation models for site investigation program at Forsmark and Simpevarp.
- P-04-08* **Chryssanthakis P.** Forsmark site investigation. Borehole KFM02A. Results of tilt testing.
- P-04-09* **Chryssanthakis P, Tunbridge L.** Forsmark site investigation. Borehole KFM02A. Determination of P-wave velocity, transverse borehole core.
- P-04-25* **Brunberg A-K, Carlsson T, Blomqvist P, Brydsten L, Strömgren M.** Forsmark site investigation. Identification of catchments, lake-related drainage parameters and lake habitats.
- P-04-29* **Isaksson H, Thunehed H, Keisu M.** Forsmark site investigation. Interpretation of airborne geophysics and integration with topography.
- P-04-39* **Gustafsson J, Gustafsson C.** Forsmark site investigation. RAMAC and BIPS logging in borehole HFM11 and HFM12.
- P-04-40* **Gustafsson J, Gustafsson C.** Forsmark site investigation. RAMAC and BIPS logging in borehole KFM02A.
- P-04-41* **Gustafsson J, Gustafsson C.** Forsmark site investigation. RAMAC and BIPS logging in borehole KFM03A and KFM03B.
- P-04-47* **Berg C, Nilsson A-C.** Forsmark site investigation. Hydrochemical logging of KFM04A.

- P-04-64* **Ludvigson J-E, Jönsson S, Jönsson J.** Forsmark site investigation. Pumping tests and flow logging. Boreholes HFM11 and HFM12.
- P-04-65* **Ludvigson J-E, Jönsson S, Hjerne C.** Forsmark site investigation. Pumping tests and flow logging. Boreholes KFM06A (0–100 m) and HFM16.
- P-04-67* **Gustafsson J, Gustafsson C.** Forsmark site investigation. RAMAC and BIPS logging in borehole KFM04A, KFM04B, HFM09 and HFM10.
- P-04-68* **Gustafsson J, Gustafsson C.** Forsmark site investigation. RAMAC and BIPS logging in borehole HFM13, HFM14 and HFM 15.
- P-04-69* **Gustafsson J, Gustafsson C.** Forsmark site investigation. RAMAC and BIPS logging in borehole KFM06A, HFM16, HFM17, HFM18 and HFM19.
- P-04-70* **Wacker P, Bergelin A, Nilsson A-C.** Forsmark site investigation. Hydrochemical characterisation in KFM02A. Results from three investigated borehole sections; 106.5–126.5, 413.5–433.5 and 509.0–516.1 m.
- P-04-71* **Ludvigson J-E, Jönsson S, Jönsson J.** Forsmark site investigation. Pumping tests and flow logging. Boreholes HFM13, HFM14 and HFM15.
- P-04-72* **Ludvigson J-E, Källgården J, Hjerne C.** Forsmark site investigation. Pumping tests and flow logging. Boreholes HFM17, HFM18 and HFM19.
- P-04-74* **Ludvigson J-E, Källgården J, Jönsson J.** Forsmark site investigation. Pumping tests and flow logging. Boreholes HFM09 and HFM10.
- P-04-76* **Claesson L-Å, Nilsson, G.** Forsmark site investigation. Drilling of a flushing water well, HFM10, a groundwater monitoring well in solid bedrock, HFM09, and a groundwater monitoring well in soil, SFM0057, at drilling site DS4.
- P-04-79* **Gustafsson J, Gustafsson C.** Forsmark site investigation. RAMAC and BIPS logging in borehole KFM01B and RAMAC directional re-logging in borehole KFM01A.
- P-04-80* **Mattsson H, Thunehed H, Keisu M.** Forsmark site investigation. Interpretation of borehole geophysical measurements in KFM01A, KFM01B, HFM01, HFM02 and HFM03.
- P-04-81* **Keisu M, Isaksson H.** Forsmark site investigation. Acquisition of geological information from Forsmarksverket. Information from the Vattenfall archive, Räcksta.
- P-04-83* **Sjöberg J.** Forsmark site investigation. Overcoring rock stress measurements in borehole KFM01B.
- P-04-85* **Claesson L-Å, Nilsson, G.** Forsmark site investigation. Drilling of a flushing water well, HFM13, two groundwater monitoring wells in solid bedrock, HFM14–15, and one groundwater monitoring well in soil, SFM0058, at and close to drilling site DS5.
- P-04-87* **Stephens M B, Lundqvist S, Bergman T, Ekström M.** Forsmark site investigation. Bedrock mapping. Petrographic and geochemical characteristics of rock types based on Stage 1 (2002) and Stage 2 (2003) surface data.
- P-04-88* **Cronqvist T, Forssberg O, Mærsk Hansen L, Jonson A, Koyi S, Leiner P, Vestgård J, Petersson J, Skogsmo G.** Forsmark site investigation. Detailed fracture mapping of two trenches at Forsmark.
- P-04-90* **Hermanson J, Hansen L, Vestgård J, Leiner, P.** Forsmark site investigation. Detailed fracture mapping of excavated rock outcrop at drilling site 5, AFM100201.
- P-04-91* **Bergman T, Andersson J, Hermansson T, Zetterström Evins L, Albrecht L, Stephens M, Petersson J, Nordman C.** Forsmark site investigation. Bedrock mapping. Stage 2 (2003) – bedrock data from outcrops and the basal parts of trenches and shallow boreholes through the Quaternary cover.
- P-04-92* **Nilsson D.** Forsmark site investigation. Sampling and analyses of groundwater from percussion drilled boreholes. Results from the percussion boreholes HFM09 to HFM19 and the percussion drilled part of KFM06A.
- P-04-94* **Claesson L-Å, Nilsson G.** Forsmark site investigation. Drilling of a monitoring well, HFM16, at drilling site DS6.
- P-04-95* **Ludvigson J-E, Levén J, Jönsson S.** Forsmark site investigation. Single-hole injection tests in borehole KFM01A.
- P-04-96* **Ludvigson J-E, Jönsson S, Levén J.** Forsmark site investigation. Hydraulic evaluation of pumping activities prior to hydro-geochemical sampling in borehole KFM03A – Comparison with results from difference flow logging.
- P-04-97* **Nielsen U T, Ringgaard J.** Forsmark site investigation. Geophysical borehole logging in borehole KFM02A, KFM03A and KFM03B.
- P-04-98* **Thunehed H.** Forsmark site investigation. Interpretation of borehole geophysical measurements in KFM02A, KFM03A, KFM03B and HFM04 to HFM08.
- P-04-99* **Bergman B, Palm H, Juhlin C.** Forsmark site investigation. Estimate of bedrock topography using seismic tomography along reflection seismic profiles.
- P-04-100* **Källgården J, Ludvigson J-E, Jönsson J.** Forsmark site investigation. Single-hole injection tests in borehole KFM02A.

- P-04-101* **Nordman C.** Forsmark site investigation. Boremap mapping of percussion holes HFM09–12.
- P-04-103* **Petersson J, Berglund J, Danielsson P, Wängnerud A, Tullborg E-L, Mattsson H, Thunehed H, Isaksson H, Lindroos, H.** Forsmark site investigation. Petrography, geochemistry, petrophysics and fracture mineralogy of boreholes KFM01A, KFM02A and KFM03A+B.
- P-04-106* **Claesson L-Å, Nilsson G.** Forsmark site investigation. Drilling of five percussion boreholes, HFM11–12 and HFM17–19, on different lineaments.
- P-04-107* **Mattsson H, Thunehed H, Isaksson H, Kübler L.** Forsmark site investigation. Interpretation of petro-physical data from the cored boreholes KFM01A, KFM02A, KFM03A and KFM03B.
- P-04-108* **Wacker P, Bergelin A, Berg C, Nilsson A-C.** Forsmark site investigation. Hydrochemical characterisation in KFM03A. Results from six investigated borehole sections: 386.0–391.0 m, 448.0–453.0 m, 448.5–455.6 m, 639.0–646.1 m, 939.5–946.6 m, 980.0–1,001.2 m.
- P-04-109* **Wacker P, Bergelin A, Berg C, Nilsson A-C.** Forsmark site investigation. Hydrochemical characterisation in KFM04A. Results from two investigated borehole sections, 230.5–237.6 and 354.0–361.1 m.
- P-04-112* **Nordman C.** Forsmark site investigation. Boremap mapping of percussion boreholes HFM13–15 and HFM19.
- P-04-113* **Nordman C, Samuelsson E.** Forsmark site investigation. Boremap mapping of percussion boreholes HFM16–18.
- P-04-114* **Berglund J, Petersson J, Wängnerud A, Danielsson P.** Forsmark site investigation. Boremap mapping of core drilled borehole KFM01B.
- P-04-115* **Petersson J, Wängnerud A, Berglund J, Danielsson P, Stråhle A.** Forsmark site investigation. Boremap mapping of telescopic drilled borehole KFM04A.
- P-04-116* **Carlsten S, Petersson J, Stephens M, Mattsson H, Gustafsson J.** Forsmark site investigation. Geological single-hole interpretation of KFM01A, KFM01B and HFM01–03 (DS1).
- P-04-117* **Carlsten S, Petersson J, Stephens M, Mattsson H, Gustafsson J.** Forsmark site investigation. Geological single-hole interpretation of KFM02A and HFM04–05 (DS2).
- P-04-118* **Carlsten S, Petersson J, Stephens M, Thunehed H, Gustafsson J.** Forsmark site investigation. Geological single-hole interpretation of KFM03B, KFM03A and HFM06–08 (DS3).
- P-04-119* **Carlsten S, Petersson J, Stephens M, Mattsson H, Gustafsson J.** Forsmark site investigation. Geological single-hole interpretation of KFM04A and HFM09–10 (DS4).
- P-04-120* **Carlsten S, Petersson J, Stephens M, Thunehed H, Gustafsson J.** Forsmark site investigation. Geological single-hole interpretation of HFM11–13 and HFM16–18.
- P-04-123* **Lagerbäck R, Sundh M, Johansson H.** Forsmark site investigation. Searching for evidence of late- or post-glacial faulting in the Forsmark region. Results from 2003.
- P-04-125* **Brydsten L, Strömngren M.** Forsmark site investigation. Water depth soundings in shallow bays in Forsmark.
- P-04-126* **Page L, Hermansson T, Söderlund P, Andersson J, Stephens M B.** Forsmark site investigation. Bedrock mapping U-Pb, $40\text{Ar}/39\text{Ar}$ and (U-Th)/He geochronology.
- P-04-135* **Levén J, Ludvigson J-E.** Forsmark site investigation. Hydraulic interferences during the drilling of borehole KFM01B. Boreholes HFM01, HFM02, HFM03 and KFM01A.
- P-04-143* **Mattsson H, Keisu M.** Forsmark site investigation. Interpretation of borehole geophysical measurements in KFM04A, KFM06A (0–100 m), HFM10, HFM11, HFM12, HFM13, HFM16, HFM17 and HFM18.
- P-04-144* **Nielsen U T, Ringgaard J.** Forsmark site investigation. Geophysical borehole logging in borehole KFM04A, KFM06A, HFM10, HFM11, HFM12 and HFM13.
- P-04-145* **Nielsen U T, Ringgaard J.** Forsmark site investigation. Geophysical borehole logging in borehole KFM01B, HFM14, HFM15, HFM16, HFM17 and HFM18.
- P-04-146* **Nilsson A-C, Borgiel M.** Forsmark site investigation. Sampling and analyses of surface waters. Results from sampling in the Forsmark area, March 2003 to March 2004.
- P-04-149* **Sandström B, Savolainen M, Tullborg E-L.** Forsmark site investigation. Fracture mineralogy. Results from fracture minerals and wall rock alteration in boreholes KFM01A, KFM02A, KFM03A and KFM03B.
- P-04-152* **Gustafsson J, Gustafsson C.** Forsmark site investigation. RAMAC and BIPS logging in borehole KFM05A.
- P-04-153* **Nielsen U T, Ringgaard J.** Forsmark site investigation. Geophysical borehole logging in borehole KFM05A and HFM19.
- P-04-154* **Thunehed H, Keisu M.** Forsmark site investigation. Interpretation of borehole geophysical measurements in KFM05A, HFM14, HFM15 and HFM19.
- P-04-155* **Isaksson H, Mattsson H, Thunehed H, Keisu M.** Forsmark site investigation. Petrophysical surface data Stage 2 – 2003 (including 2002).
- P-04-156* **Marek R.** Forsmark site investigation. A co-ordinated interpretation of ground penetrating radar data from the Forsmark site.
- P-04-157* **Thunehed H.** Forsmark site investigation. Inversion of helicopterborne electromagnetic measurements.

- P-04-158* **Juhlin C, Bergman B.** Reflection seismics in the Forsmark area. Updated interpretation of Stage 1 (previous report R-02-43). Updated estimate of bedrock topography (previous report P-04-99).
- P-04-170* **Jacobsson L.** Forsmark site investigation. Drill hole KFM01A. Indirect tensile strength test.
- P-04-171* **Eloranta P.** Forsmark site investigation. Drill hole KFM01A. Indirect tensile strength test (HUT).
- P-04-172* **Jacobsson L.** Forsmark site investigation. Drill hole KFM02A. Indirect tensile strength test.
- P-04-173* **Jacobsson L.** Forsmark site investigation. Drill hole KFM03A. Indirect tensile strength test.
- P-04-174* **Jacobsson L.** Forsmark site investigation. Drill hole KFM04A. Indirect tensile strength test.
- P-04-175* **Chryssanthakis P.** Forsmark site investigation. Drill hole KFM01A. The normal stress and shear tests on joints.
- P-04-176* **Eloranta P.** Forsmark site investigation. Drill hole KFM01A. Uniaxial compression test (HUT).
- P-04-177* **Eloranta P.** Forsmark site investigation. Drill hole KFM01A. Triaxial compression test (HUT).
- P-04-178* **Chryssanthakis P.** Forsmark site investigation. Boreholes KFM03A and KFM03B Tilt testing.
- P-04-179* **Chryssanthakis P, Tunbridge L.** Forsmark site investigation. Borehole KFM04A Tilt testing.
- P-04-180* **Chryssanthakis P, Tunbridge L.** Forsmark site investigation. Borehole KFM03A. Determination of P-wave velocity, transverse borehole core.
- P-04-181* **Chryssanthakis P, Tunbridge L.** Forsmark site investigation. Borehole KFM04A. Determination of P-wave velocity, transverse borehole core.
- P-04-188* **Rouhiainen P, Pöllänen J.** Forsmark site investigation. Difference flow logging in borehole KFM02A.
- P-04-189* **Pöllänen J, Sokolnicki M.** Forsmark site investigation. Difference flow logging in borehole KFM03A.
- P-04-190* **Rouhiainen P, Pöllänen J.** Forsmark site investigation. Difference flow logging in borehole KFM04A.
- P-04-191* **Pöllänen J, Sokolnicki M, Rouhiainen P.** Forsmark site investigation. Difference flow logging in borehole KFM05A.
- P-04-193* **Rouhiainen P, Pöllänen J, Ludvigson J-E.** Forsmark site investigation. Addendum to Difference flow logging in borehole KFM01A.
- P-04-194* **Källgården J, Ludvigson J-E, Hjerne C.** Forsmark site investigation. Single-hole injection tests in borehole KFM03A.
- P-04-200* **Jönsson S, Ludvigson J-E, Svensson T.** Forsmark site investigation. Hydraulic interference tests. Boreholes HFM11 and HFM12.
- P-04-203* **Chryssanthakis P, Tunbridge L.** Forsmark site investigation. Borehole: KFM05A. Determination of P-wave velocity, transverse borehole core.
- P-04-205* **Chryssanthakis P, Tunbridge L.** Forsmark site investigation. Borehole: KFM05A. Tilt testing.
- P-04-222* **Claesson L-Å, Nilsson G.** Forsmark site investigation. Drilling of the telescopic borehole KFM05A at drilling site DS5.
- P-04-223* **Jacobsson L.** Forsmark site investigation. Borehole KFM01A. Uniaxial compression test of intact rock.
- P-04-224* **Jacobsson L.** Forsmark site investigation. Borehole KFM02A. Uniaxial compression test of intact rock.
- P-04-225* **Jacobsson L.** Forsmark site investigation. Borehole KFM03A. Uniaxial compression test of intact rock.
- P-04-226* **Jacobsson L.** Forsmark site investigation. Borehole KFM04A. Uniaxial compression test of intact rock.
- P-04-227* **Jacobsson L.** Forsmark site investigation. Borehole KFM01A. Triaxial compression test of intact rock.
- P-04-228* **Jacobsson L.** Forsmark site investigation. Borehole KFM02A. Triaxial compression test of intact rock.
- P-04-229* **Jacobsson L.** Forsmark site investigation. Borehole KFM03A. Triaxial compression test of intact rock.
- P-04-230* **Jacobsson L.** Forsmark site investigation. Borehole KFM04A. Triaxial compression test of intact rock.
- P-04-241* **Korhonen K, Paananen M, Paulamäki S.** Interpretation of lineaments from airborne geophysical and topographic data. An alternative model within version 1.2 of the Forsmark modelling project.
- P-04-245* **Claesson L-Å, Nilsson G.** Forsmark site investigation. Drilling of two flushing water wells, HFM21 and HFM22, one groundwater monitoring well in solid bedrock, HFM20, and one groundwater monitoring well in soil, SFM0076.
- P-04-278* **Hjerne C, Jönsson J, Ludvigson J-E.** Forsmark site investigation. Single-hole injection tests in borehole KFM03B.
- P-04-282* **Isaksson H, Keisu M.** Forsmark site investigation. Interpretation of airborne geophysics and integration with topography. Stage 2 (2002–2004).
- P-04-293* **Hjerne C, Ludvigson J-E.** Forsmark site investigation. Single-hole injection tests in borehole KFM04A.
- P-04-295* **Petersson J, Berglund J, Wängnerud A, Danielsson P, Strähle A.** Forsmark site investigation. Boremap mapping of telescopic drilled borehole KFM05A.
- P-04-296* **Carlsten S, Petersson J, Stephens M, Thunehed H, Gustafsson J.** Forsmark site investigation. Geological single-hole interpretation of KFM05A, HFM14–15 and HFM19 (DS5).
- P-04-302* **Claesson L-Å, Nilsson G.** Forsmark site investigation. Drilling of borehole KFM01B at drilling site DS1.

- P-04-305* **Gustafsson J, Nissen J.** Forsmark site investigation. Mise-à-la-masse measurements. An experiment to test the possibility for detecting the outcropping of the fracture zone DZ2 in HFM14.
- P-04-307* **Gokall-Norman K, Svensson T, Ludvigson L-E, Jönsson S.** Forsmark site investigation. Hydraulic interference test. Boreholes HFM18 and KFM03A.
- P-04-311* **Klee G, Rummel F.** Forsmark site investigation. Rock stress measurements with hydraulic fracturing and hydraulic testing of pre-existing fractures in borehole KFM01A, KFM01B, KFM02A and KFM04A. Results from in-situ tests.
- P-04-312* **Rummel F, Weber U.** Forsmark site investigation. Rock stress measurements with hydraulic fracturing and hydraulic testing of pre-existing fractures in borehole KFM01A, KFM01B, KFM02A and KFM04A. Laboratory Core Investigations.
- P-05-01* **Gustafsson J, Gustafsson C.** Forsmark site investigation. RAMAC and BIPS logging in boreholes KFM06A and HFM22.
- P-05-04* **Chryssanthakis P, Tunbridge L.** Forsmark site investigation. Borehole KFM06A. Determination of P-wave velocity, transverse borehole core.
- P-05-08* **Ljunggren B.** Forsmark site investigation. Drill hole KFM01A. Normal loading and shear tests on joints.
- P-05-09* **Ljunggren B.** Forsmark site investigation. Drill hole KFM02A. Normal loading and shear tests on joints.
- P-05-10* **Ljunggren B.** Forsmark site investigation. Drill hole KFM03A. Normal loading and shear tests on joints.
- P-05-11* **Ljunggren B.** Forsmark site investigation. Drill hole KFM04A. Normal loading and shear tests on joints.
- P-05-12* **Toresson B.** Forsmark site investigation. Seismic refraction survey 2004.
- P-05-14* **Jönsson J, Hjerne C, Ludvigson J-E.** Forsmark site investigation. Pumping tests and flow logging. Boreholes HFM20, HFM21 and HFM22.
- P-05-15* **Rouhiainen P, Sokolnicki M.** Forsmark site investigation. Difference flow logging in borehole KFM06A.
- P-05-17* **Nielsen U T, Ringgaard J, Horn F.** Forsmark site investigation. Geophysical borehole logging in borehole KFM06A, HFM20, HFM21, HFM22 and SP-logging in KFM01A and KFM04A.
- P-05-21* **Ludvigson J-E, Levén J.** Forsmark site investigation. Comparison of measured EC in selected fractures in boreholes KFM02A, KFM03A and KFM04A from difference flow logging and hydro-geochemical characterization – Analysis of observed discrepancies in KFM03A.
- P-05-33* **Berg C.** Forsmark site investigation. Hydrochemical logging in KFM06A.
- P-05-37* **Rouhiainen P, Sokolnicki M.** Forsmark site investigation. Difference flow logging in borehole KFM02A during pumping in HFM16.
- P-05-43* **Sokolnicki M, Rouhiainen P.** Forsmark site investigation. Difference flow logging in borehole KFM08A.
- P-05-46* **Toresson B.** Forsmark site investigation. Seismic velocity analysis in excavated trenches.
- P-05-48* **Nilsson D.** Forsmark site investigation. Sampling and analyses of groundwater from percussion drilled boreholes Results from the percussion drilled boreholes HFM20, HFM21 and HFM22.
- P-05-50* **Claesson L-Å, Nilsson G.** Forsmark site investigation. Drilling of the telescopic borehole KFM06A and the core drilled borehole KFM06B at drill site DS6.
- P-05-51* **Mattsson H, Keisu M.** Forsmark site investigation. Interpretation of geophysical borehole measurements from KFM06A and HFM20, HFM21 and HFM22.
- P-05-52* **Gustafsson J, Gustafsson C.** Forsmark site investigation. RAMAC and BIPS logging in borehole KFM07A.
- P-05-53* **Gustafsson J, Gustafsson C.** Forsmark site investigation. RAMAC and BIPS logging in borehole KFM06B.
- P-05-56* **Gokall-Norman K, Ludvigson J-E, Hjerne C.** Forsmark site investigation. Single-hole injection tests in borehole KFM05A.
- P-05-58* **Gustafsson J, Gustafsson C.** Forsmark site investigation. RAMAC and BIPS logging in borehole KFM08B.
- P-05-63* **Sokolnicki M, Rouhiainen P.** Forsmark site investigation. Difference flow logging in borehole KFM07A.
- P-05-64* **Gustafsson J, Gustafsson C.** Forsmark site investigation. RAMAC and BIPS logging in borehole KFM07A (0–100 m), HFM20 and HFM21.
- P-05-66* **Lindfors U, Perman F, Sjöberg J.** Forsmark site investigation. Evaluation of the overcoring results from borehole KFM01B.
- P-05-78* **Gokall-Norman, Ludvigson J-E.** Forsmark site investigation. Hydraulic interference test. Boreholes HFM16, HFM19 and KFM02A.
- P-05-79* **Wacker P, Berg C, Bergelin A, Nilsson A-C.** Forsmark site investigation. Hydrochemical characterisation in KFM05A. Results from an investigated section at 712.6–722.0 m
- P-05-97* **Jacobsson L.** Forsmark site investigation. Borehole KFM05A. Uniaxial compression test of intact rock.
- P-05-98* **Jacobsson L.** Forsmark site investigation. Borehole KFM05A. Indirect tensile strength test.
- P-05-99* **Jacobsson L.** Forsmark site investigation. Borehole KFM05A. Normal stress and shear test on joints.

- P-05-100* **Jacobsson L.** Forsmark site investigation. Borehole KFM05A. Triaxial compression test of intact rock.
- P-05-101* **Petersson J, Skogsmo G, Berglund J, Wängnerud A, Stråhle A.** Forsmark site investigation. Boremap mapping of telescopic drilled borehole KFM06A and core drilled borehole KFM06B.
- P-05-102* **Petersson J, Skogsmo G, Wängnerud A, Berglund J, Stråhle A.** Forsmark site investigation. Boremap mapping of telescopic drilled borehole KFM07A.
- P-05-103* **Berglund J, Döse C.** Forsmark site investigation. Boremap mapping of percussion boreholes HFM20, HFM21 and HFM22.
- P-05-112* **Lanaro F.** Forsmark site investigation. Rock mechanics characterisation of borehole KFM01A.
- P-05-113* **Lanaro F.** Forsmark site investigation. Rock mechanics characterisation of borehole KFM02A.
- P-05-114* **Lanaro F.** Forsmark site investigation. Rock mechanics characterisation of borehole KFM03A.
- P-05-115* **Lanaro F.** Forsmark site investigation. Rock mechanics characterisation of borehole KFM04A.
- P-05-119* **Mattson H.** Forsmark site investigation. Interpretation of geophysical borehole measurements from KFM07A.
- P-05-120* **Jacobsson L.** Forsmark site investigation. Borehole KFM06A. Uniaxial compression test of intact rock.
- P-05-121* **Jacobsson L.** Forsmark site investigation. Drill hole KFM06A. Indirect tensile strength test.
- P-05-122* **Jacobsson L, Flansbjer M.** Forsmark site investigation. Borehole KFM06A. Normal loading and shear test on joints.
- P-05-125* **Chryssanthakis P, Tunbridge L.** Borehole KFM07A. Determination of P-wave velocity transverse borehole core. Forsmark site investigation.
- P-05-132* **Carlsten S, Gustafsson J, Mattsson H, Petersson J, Stephens M.** Forsmark site investigation. Geological single-hole interpretation of KFM06A and KFM06B (DS6).
- P-05-133* **Gokall-Norman K, Svensson T, Ludvigson.** Forsmark site investigation. Single-hole injection tests in borehole KFM07A.
- P-05-141* **Jacobsson L, Flansbjer M.** Forsmark site investigation. Borehole KFM05A Normal stress test with direct and indirect deformation measurement together with shear tests on joints.
- P-05-142* **Claesson L-Å, Nilsson G.** Forsmark site investigation. Drilling of the telescopic borehole KFM07A at drill site DS7.
- P-05-143* **Nilsson D.** Forsmark site investigation. Sampling and analysis of precipitation, years 2002 to 2005.
- P-05-145* **Svensson T, Ludvigson J-E, Hjerne C.** Forsmark site investigation. Single-hole injection tests in borehole KFM02A, re-measurements after hydraulic fracturing.
- P-05-156* **Petersson J, Berglund J, Danielsson P, Skogsmo G.** Forsmark site investigation. Petrographic and geochemical characteristics of bedrock samples from boreholes KFM04A–06A, and a whitened alteration rock.
- P-05-157* **Carlsten S, Gustafsson J, Mattsson H, Petersson J, Stephens M.** Forsmark site investigation. Geological single-hole interpretation of KFM07A and HFM20–21 (DS7).
- P-05-158* **Gustafsson J, Gustafsson C.** Forsmark site investigation. RAMAC and BIPS logging in borehole KFM08A.
- P-05-159* **Nielsen U T, Ringgaard J, Fris Dahl J.** Forsmark site investigation. Geophysical borehole logging in the boreholes KFM07A, KFM08A and KFM08B.
- P-05-165* **Hjerne C, Ludvigson J-E, Lindquist A.** Forsmark site investigation. Single-hole injection tests in boreholes KFM06A and KFM06B.
- P-05-168* **Cosma C, Enescu N, Balu L.** Forsmark site investigation. Vertical seismic profiling from the boreholes KFM01A and KFM02A.
- P-05-170* **Berg C, Wacker P, Nilsson A-C.** Forsmark site investigation. Chemical interpretation in borehole KFM07A Results from the investigated section at 848.0–1,001.6 m.
- P-05-171* **Nilsson A-C, Borgiel M.** Forsmark site investigation. Sampling and analyses of near surface groundwaters Results from sampling of shallow soil monitoring wells, BAT pipes, a natural spring and private wells, May 2003–April 2005.
- P-05-172* **Claesson L-Å, Nilsson G.** Forsmark site investigation. Drilling of the telescopic borehole KFM08A and the core drilled borehole KFM08B at drill site DS8.
- P-05-176* **Gustafsson J, Gustafsson C.** Forsmark site investigation. BIPS logging in the boreholes HFK248, HFK249 and HFK250.
- P-05-178* **Berg C, Wacker P, Nilsson A-C.** Forsmark site investigation. Chemical interpretation in borehole KFM06A. Results from the investigated sections at 266.0–271.0 m, 353.5–360.6 m and 768.0–775.1 m.
- P-05-186* **Gokall-Norman K, Ludvigson J-E, Jönsson S.** Forsmark site investigation. Hydraulic interference test. Boreholes KFM04A, HFM10, HFM13, HFM19 and HFK252.
- P-05-187* **Berg C, Levén J, Nilsson A-C.** Forsmark site investigation. Hydrochemical logging in KFM07A.
- P-05-197* **Sandström B, Tullborg E-L.** Forsmark site investigation. Fracture mineralogy Results from fracture minerals and wall rock alteration in boreholes KFM01B, KFM04A, KFM05A and KFM06A.

- P-05-199 **Leijon, B.** Forsmark site investigation. Investigations of superficial fracturing and block displacements at drill site 5.
- P-05-202 **Mattsson H, Keisu M.** Forsmark site investigation. Interpretation of geophysical borehole measurements from KFM08A and KFM08B.
- P-05-203 **Petersson J, Berglund J, Skogsmo G, Wängnerud A.** Forsmark site investigation. Boremap mapping of telescopic drilled borehole KFM08A and cored drilled borehole KFM08B
- P-05-204 **Mattsson H, Thunehed H, Isaksson H.** Forsmark site investigation. Interpretation of petrophysical data from the cored boreholes KFM04A, KFM05A and KFM06A.
- P-05-206 **Berg C.** Forsmark site investigation. Hydrochemical logging in KFM08A.
- P-05-210 **Jacobsson L.** Forsmark site investigation. Borehole KFM07A. Triaxial compression test of intact rock.
- P-05-211 **Jacobsson L.** Forsmark site investigation. Borehole KFM07A. Uniaxial compression test of intact rock.
- P-05-212 **Jacobsson L.** Forsmark site investigation. Drill hole KFM07A. Indirect tensile strength test including strain measurement.
- P-05-213 **Jacobsson L, Flansbjer M.** Forsmark site investigation. Borehole KFM07A Normal loading and shear tests on joints.
- P-05-216 **Chryssanthakis P, Tunbridge L.** Borehole: KFM08A Determination of P-wave velocity, transverse borehole core. Forsmark site investigation.
- P-05-217 **Jacobsson L.** Forsmark site investigation. Borehole KFM08A Triaxial compression test of intact rock.
- P-05-218 **Jacobsson L, Flansbjer M.** Forsmark site investigation. Borehole KFM08A Normal loading and shear tests on joints.
- P-05-235 **Lindquist A, Ludvigson J-E, Svensson T.** Forsmark site investigation. Single-hole injection tests and pressure pulse tests in borehole KFM08B.
- P-05-236 **Gokall-Norman K, Ludvigson J-E, Jönsson S.** Forsmark site investigation. Hydraulic interference test in borehole HFM01.
- P-05-242 **Gustasson J, Gustafsson C.** Forsmark site investigation. RAMAC and BIPS logging in borehole KFM06C.
- P-05-261 **Johansson R, Isaksson H.** Forsmark site investigation. Assessment of inferred lineaments in the northwestern part of the Forsmark site investigation area. Present knowledge and recommendations for further investigations.
- P-05-262 **Carlsten S, Gustafsson J, Mattsson H, Petersson J, Stephens M.** Forsmark site investigation. Geological single-hole interpretation of KFM08A, KFM08B and HFM22 (DS8).
- P-05-265 **Nissen J, Gustafsson J, Sandström R, Wallin L, Taxén C.** Forsmark site investigation. Some corrosion observations and electrical measurements at drill sites DS4, DS7 and DS8.
- P-05-266 **Isaksson H, Pitkänen T.** Forsmark site investigation. Ground geophysical measurements near the lineament trench AFM001265.
- P-05-269 Forsmark site investigation. Bedrock mapping and magnetic susceptibility measurements in trench AFM001265 for verification of lineament XFM0159A0 (report in print)
- P-05-274 **Nilsson A-C, Borgiel M.** Forsmark site investigation. Sampling and analyses of surface waters. Results from sampling in the Forsmark area, March 2004–June 2005.
- P-05-276 **Nielsen U T, Skjellerup P, Ringgaard J.** Forsmark site investigation. Geophysical borehole logging in the borehole KFM06C.
- P-05-277 **Claesson L-A, Nilsson G.** Forsmark site investigation. Drilling of the telescopic borehole KFM06C at drill site DS6.
- P-05-278 **Claesson L-A, Nilsson G.** Forsmark site investigation. Drilling of monitoring wells HFM23 and HFM28 at drill site DS9 as well as HFM24 and SFM0080 at drill site DS10.
- P-06-09 **Gokall-Norman K, Ludvigson J-E, Jönsson S.** Forsmark site investigation. Hydraulic interference test. Boreholes KFM02A and KFM03A.
- P-06-22 **Nielsen UT, Ringgaard J, Vangkild-Pedersen T.** Forsmark site investigation. Geophysical borehole logging in boreholes KFM09A, KFM07B, HFM25, HFM27 and HFM28.
- P-06-23 **Lindquist A, Ludvigson J-E, Gokall-Norman K.** Forsmark site investigation. Single-hole injection tests in borehole KFM06C.
- P-06-24 **Chryssanthakis P, Tunbridge L.** Forsmark site investigation. Borehole KFM09A Determination of P-wave velocity, transverse borehole core.
- P-06-25 **Chryssanthakis P.** Forsmark site investigation. Borehole: KFM09A Tilt testing.
- P-06-26 **Jacobsson L.** Forsmark site investigation. Borehole KFM09A. Triaxial compression tests of intact rock.
- P-06-27 **Jacobsson L.** Forsmark site investigation. Borehole KFM09A. Uniaxial compression test of intact rock.
- P-06-28 **Jacobsson L.** Forsmark site investigation. Borehole KFM09A. Indirect tensile strength test.
- P-06-29 **Jacobsson L.** Forsmark site investigation. Borehole KFM09A. Normal loading and shear tests on joints.

- P-06-44 **Gustasson J, Gustafsson C.** Forsmark site investigation. RAMAC and BIPS logging in boreholes KFM07B, KFM09A, HFM25 and HFM28.
- P-06-52 **Lindquist A, Ludvigson J-E, Harrström J, Svensson T.** Forsmark site investigation. Single-hole injection tests in borehole KFM09A.
- P-06-56 **Forsman I, Zetterlund M, Forsmark T, Rhén I.** Correlation of Posiva Flow Log anomalies to core mapped features in Forsmark in KFM06A and KFM07A.
- P-06-57 **Berg C, Nilsson A-C.** Forsmark site investigation. Hydrochemical monitoring of percussion- and core drilled boreholes. Results from water sampling and analyses during 2005.
- P-06-63 **Berg C, Bergelin A, Wacker P, Nilsson A-C.** Forsmark site investigation. Hydrochemical characterisation in borehole KFM08A. Results from the investigated section at 683.5–690.6 (690.8) m.
- P-06-64 **Gustasson J, Gustafsson C.** Forsmark site investigation. RAMAC and BIPS logging in boreholes KFM09B, HFM24, HFM26, HFM27, HFM29 and HFM32.
- P-06-68 **Jacobsson L.** Forsmark site investigation. Borehole KFM01C Triaxial compression test of intact rock.
- P-06-79 **Petersson J, Skogsmo, Berglund J, Von Dalwigk I, Wängnerud A, Danielsson P, Strähle A.** Forsmark site investigation. Boremap mapping of telescopic drilled borehole KFM06C.
- P-06-80 **Döse C, Samuelsson E.** Forsmark site investigation. Boremap mapping of telescopic drilled borehole KFM7B.
- P-06-81 **Petersson J, Skogsmo, Berglund J, Strähle A.** Forsmark site investigation. Comparative geological logging with the Boremap system: 176.5–360.9 m of borehole KFM06C.
- P-06-82 **Petersson J, Skogsmo, Berglund J, Strähle A.** Forsmark site investigation. Comparative geological logging with the Boremap system: 9.6–132.2 m of borehole KLX07B.
- P-06-83 **Carlsten S, Gustafsson J, Mattsson H, Petersson J, Stephens M.** Forsmark site investigation. Geological single-hole interpretation of KFM06C.
- P-06-84 **Mattsson H, Keisu M.** Forsmark site investigation. Interpretation of geophysical borehole measurements from KFM06C.
- P-06-85 **Isaksson H, Pitkänen T, Thunehed H.** Forsmark site investigation. Ground magnetic survey and lineament interpretation in an area northwest of Bolundsfjärden.
- P-06-86 **Gokall-Norman K, Lindquist A, Ludvigson J-E, Gustavsson E.** Forsmark site investigation. Single-hole injection tests and pressure pulse tests in borehole KFM07B.
- P-06-87 **Bergman T, Hedenström A.** Forsmark site investigation. Petrographic analysis of gravel and boulders in the Forsmark candidate area.
- P-06-95 **Nilsson K.** Forsmark site investigation. Hydrochemical logging in KFM09A.
- P-06-96 **Jönsson S, Ludvigson J-E.** Forsmark site investigation. Pumping tests and flow logging. Boreholes HFM24, HFM32.
- P-06-98 **Gustasson J, Gustafsson C.** Forsmark site investigation. RAMAC and BIPS logging in boreholes KFM01C and KFM01D.
- P-06-122 **Gustavsson E, Ludvigson J-E, Gokall-Norman K.** Forsmark site investigation. Single-hole injection tests in borehole KFM09B.
- P-06-123 **Nielsen UT, Ringgaard J, Fris Dahl J.** Forsmark site investigation. Geophysical borehole logging in boreholes KFM01C, KFM09B, HFM07, HFM24, HFM26, HFM29 and HFM32.
- P-06-126 **Mattsson H, Keisu M.** Forsmark site investigation. Interpretation of geophysical borehole measurements and petrophysical data from KFM07B, KFM09A, HFM25, HFM27 and HFM28.
- P-06-130 **Petersson J, Skogsmo, Von Dalwigk I, Wängnerud A, Berglund J.** Forsmark site investigation. Boremap mapping of telescopic drilled borehole KFM09A.
- P-06-131 **Petersson J, Skogsmo, Von Dalwigk I, Wängnerud A, Berglund J.** Forsmark site investigation. Boremap mapping of telescopic drilled borehole KFM09B.
- P-06-132 **Petersson J, Skogsmo, Von Dalwigk I, Wängnerud A, Berglund J.** Forsmark site investigation. Boremap mapping of telescopic drilled borehole KFM01D.
- P-06-133 **Döse C, Samuelsson E.** Forsmark site investigation. Boremap mapping of telescopic drilled borehole KFM1C.
- P-06-134 **Carlsten S, Döse C, Gustafsson J, Keisu M, Petersson J, Stephens M.** Forsmark site investigation. Geological single-hole interpretation of KFM09A and KFM07B.
- P-06-135 **Carlsten S, Döse C, Gustafsson J, Petersson J, Stephens M, Thunehed H.** Forsmark site investigation. Geological single-hole interpretation of KFM09B and KFM01C.
- P-06-136 **Mattsson H, Keisu M.** Forsmark site investigation. Detailed fracture mapping of excavated outcrop AFM001264 (DS7) in Forsmark (report in print).
- P-06-138 **Toresson B.** Forsmark site investigation. Seismic refraction survey 2005–2006.
- P-06-139 **Jönsson S, Ludvigson J-E.** Forsmark site investigation. Pumping tests and flow logging. Boreholes HFM25, HFM26.

- P-06-140 **Lindquist A, Ludvigson J-E.** Pumping tests and flow logging in borehole HFM14 and pumping test in KFM05A (0–114 m).
- P-06-152 **Mattsson H, Keisu M.** Forsmark site investigation. Interpretation of geophysical borehole measurements from KFM01C, KFM09B, HFM07, HFM24, HFM26, HFM29 and HFM32 (report in print).
- P-06-161 **Väisäsvaara J, Leppänen H, Pekkanen J.** Forsmark site investigation. Difference flow logging in borehole KFM01D.
- P-06-165 **Gustavsson E, Ludvigson J-E, Hjerne C, Florberger J.** Forsmark site investigation. Single-hole injection tests in borehole KFM01C.
- P-06-166 **Claesson L-A, Nilsson G.** Forsmark site investigation. Drilling of percussion boreholes HFM25–HFM27, HFM29–HFM32, and HFM38 for investigation of different lineaments and to be used as monitoring wells.
- P-06-168 **Nielsen UT, Ringgaard J, Fris Dahl J.** Forsmark site investigation. Geophysical borehole logging in borehole KFM01D.
- P-06-169 **Claesson L-A, Nilsson G.** Forsmark site investigation. Drilling of the cored boreholes KFM09A and KFM09B.
- P-06-170 **Claesson L-A, Nilsson G.** Forsmark site investigation. Drilling of the telescopic boreholes KFM07B and KFM07C at drilling site DS7.
- P-06-171 **Claesson L-A, Nilsson G.** Forsmark site investigation. Drilling of the telescopic borehole KFM08C at drill site DS8.
- P-06-172 **Claesson L-A, Nilsson G.** Forsmark site investigation. Drilling of the telescopic borehole KFM10A at drill site DS10.
- P-06-173 **Claesson L-A, Nilsson G.** Forsmark site investigation. Drilling of borehole KFM01C and the telescopic borehole KFM01D at drill site DS1.
- P-06-177 **Gustafsson J, Gustafsson C.** Forsmark site investigation. RAMAC and BIPS logging in boreholes KFM10A, HFM35 and HFM38.
- P-06-178 **Gustafsson J, Gustafsson C.** Forsmark site investigation. RAMAC and BIPS logging in boreholes KFM08C, HFM30, HFM31, HFM33 and HFM34.
- P-06-179 **Lindquist A, Nilsson K.** Forsmark site investigation. Hydrochemical logging in KFM09B.
- P-06-188 **Lindquist A, Wass E.** Forsmark site investigation. Groundwater flow measurements in conjunction with the interference test with pumping in HFM14.
- P-06-189 **Väisäsvaara J, Leppänen H, Pekkanen J, Pöllänen J.** Forsmark site investigation. Difference flow logging in borehole KFM08C.
- P-06-190 **Sokolnicki M, Pöllänen J, Pekkanen J.** Forsmark site investigation. Difference flow logging in borehole KFM10A.
- P-06-191 **Jönsson S, Ludvigson J-E.** Forsmark site investigation. Pumping tests and flow logging. Boreholes HFM23, HFM27 and HFM28.
- P-06-192 **Lindquist A, Ludvigson J-E.** Forsmark site investigation. Pumping tests and flow logging. Boreholes HFM29, HFM30 and HFM31.
- P-06-193 **Gustavsson E, Jönsson S, Ludvigson J-E.** Forsmark site investigation. Pumping tests and flow logging. Boreholes HFM33, HFM34 and HFM35.
- P-06-194 **Walger E, Hjerne C, Ludvigson J-E, Harrström J.** Forsmark site investigation. Single-hole injection tests and pressure pulse tests in borehole KFM08A.
- P-06-195 **Florberger J, Hjerne C, Ludvigson J-E, Walger E.** Forsmark site investigation. Single-hole injection tests in borehole KFM01D.
- P-06-196 **Gokall-Norman K, Ludvigson J-E.** Forsmark site investigation. Hydraulic interference test in boreholes HFM14.
- P-06-203 **Petersson J, Wängnerud A, von Dalwigk I, Berglund J.** Forsmark site investigation. Boremap mapping of telescopic drilled borehole KFM08C.
- P-06-204 **Döse C, Samuelsson E.** Forsmark site investigation. Boremap mapping of telescopic drilled borehole KFM10A.
- P-06-205 **Petersson J, Andersson U B, Berglund J.** Forsmark site investigation. Boremap mapping of telescopic drilled borehole KFM07C.
- P-06-206 **Döse C, Samuelsson E.** Forsmark site investigation. Boremap mapping of percussion boreholes HFM23–32 and HFM38.
- P-06-207 **Carlsten S, Döse C, Samuelsson E, Petersson J, Stephens M, Thunehed H.** Forsmark site investigation. Geological single-hole interpretation of KFM08C, KFM10A, HFM23, HFM28, HFM30, HFM31, HFM32 and HFM38.
- P-06-209 **Sandström B, Tullborg E-L.** Forsmark site investigation. Mineralogy, geochemistry, porosity and redox capacity of altered rock adjacent to fractures.

- P-06-210 **Carlsten S, Döse C, Gustafsson J, Mattsson H, Petersson J, Stephens M.** Forsmark site investigation. Geological single-hole interpretation of KFM01D, HFM24, HFM25, HFM27 and HFM29.
- P-06-211 **Page L, Hermansson T, Söderlund P, Stephens M.** Forsmark site investigation. ⁴⁰Ar/³⁹Ar and U-Th/He geochronology. Phase II (report in print).
- P-06-212 **Nordgulen Ø, Saintot A.** Forsmark site investigation. The character and kinematics of deformation zones (ductile shear zones, fault zones and fracture zones) at Forsmark (report in print).
- P-06-213 **Sandström B, Page L, Tullborg E-L.** Forsmark site investigation. ⁴⁰Ar/³⁹Ar (adularia) and Rb-Sr (adularia, prehnite, calcite) ages of fracture minerals.
- P-06-214 **Jacobsson L.** Forsmark site investigation. Borehole KFM09A. Triaxial compression tests of intact rock.
- P-06-215 **Jacobsson L.** Forsmark site investigation. Borehole KFM01D. Shear tests on sealed joints.
- P-06-216 **Mattsson H, Keisu M.** Forsmark site investigation. Interpretation of geophysical borehole measurements and petrophysical data from KFM01D.
- P-06-217 **Nilsson K, Bergelin A.** Forsmark site investigation. Hydrochemical characterisation in borehole KFM09A. Results from the investigated section at 785.1–792.2 m.
- P-06-226 **Sandström B, Tullborg E-L.** Forsmark site investigation. Fracture mineralogy. Results from KFM06B, KFM06C, KFM07A, KFM08A, KFM08B (report in print).
- P-06-227 **Nilsson K, Bergelin A, Lindquist A, Nilsson A-C.** Forsmark site investigation. Hydrochemical characterisation in borehole KFM01D. Results from seven investigated borehole sections: 194.0–195.0 m, 263.8–264.8 m, 314.5–319.5 m, 354.9–355.9 m, 369.0–370.0 m, 428.5–435.6 m, 568.0–575.1 m.
- P-06-231 **Berg C.** Forsmark site investigation. Sampling and analyses of groundwater from percussion drilled boreholes. Results from the boreholes HFM14, HFM23, HFM24, HFM25, HFM26, HFM27, HFM28, HFM29, HFM30, HFM32, HFM33, HFM34 and HFM35.
- P-06-247 **Väisesvaara J, Pekkanen J, Pöllänen J.** Forsmark site investigation. Difference flow logging in KFM07C (report in print).
- P-06-258 **Mattsson H, Keisu M.** Forsmark site investigation. Interpretation of geophysical borehole measurements from KFM10A, KFM08C, HFM30, HFM31, HFM33, HFM34, HFM35 and HFM38.
- P-06-261 **Isaksson H, Thunehed H, Pitkänen T, Keisu M.** Forsmark site investigation. Detailed ground and marine magnetic survey and lineament interpretation in the Forsmark area – 2006.
- P-07-05 **Nielsen U T, Ringgaard J.** Forsmark site investigation. Geophysical borehole logging in boreholes KFM08C, KFM10A, HFM30, HFM31, HFM33, HFM34, HFM35 and HFM38.
- P-07-07 **Ringgaard J.** Forsmark site investigation. Mapping of borehole breakout. Processing of acoustical televiewer data from KFM01A, KFM01B, KFM02A, KFM03A, KFM03B, KFM04A, KFM05A, KFM06A and KFM07C (report in print).
- P-07-115 **Bäckström A, Lanaro F.** Forsmark site investigation. Rock mechanics characterisation of boreholes KFM01B, KFM07C, KFM09A and KFM09B (in prep.)
- R-98-05 **Axelsson C-L; Hansen L M.** Update of structural models at SFR nuclear waste repository, Forsmark, Sweden.
- R-01-02 **Holmén J G, Stigsson M.** Modelling of future hydrogeological conditions at SFR.
- R-02-14 **Axelsson C-L, Ekstav A, Lindblad Påsse A.** SFR – Utvärdering av hydrogeologi
- R-02-32 **SKB.** Forsmark – site descriptive model version 0.
- R-02-43 **Juhlin C, Bergman B, Palm H.** Reflection seismic studies in the Forsmark area – stage 1.
- R-04-15 **SKB.** Preliminary site description Forsmark area – version 1.1
- R-04-77 **Forssman I, Zetterlund M, Rhén I.** Correlation of Posiva Flow Log anomalies to core mapped features in Forsmark (KFM01A to KFM05A).
- R-05-18 **SKB.** Preliminary site description Forsmark area – version 1.2.
- R-05-42 **Juhlin C, Palm H.** Forsmark site investigation. Reflection seismic studies in the Forsmark area, 2004: Stage 2.
- R-06-38 **SKB.** Site descriptive modelling Forsmark stage 2.1. Feedback for completion of the site investigation including input from safety assessment and repository engineering.
-

WellCad diagrams for geological data

The identification and description of rock units and especially possible deformation zones in the single hole interpretations (SHI) is a key component in the establishment of the fracture domain concept. In order to illustrate the interplay between base geological and geophysical data and the identification of these geological entities, WellCad diagrams for all the cored boreholes, which show a selected suite of key geological and geophysical data used in the SHI work as well as the results of this work, are shown in Appendix 2. For further discussion of these critical geological and geophysical data, the reader is referred to section 4.2 in the main text.

Title GEOLOGY KFM01A



Site	FORSMARK	Coordinate System	RT90-RHB70
Borehole	KFM01A	Northing [m]	6699529.81
Diameter [mm]	76	Easting [m]	1631397.16
Length [m]	1001.490	Elevation [m.a.s.l.ToC]	3.13
Bearing [°]	318.35	Drilling Start Date	2002-05-07 09:30:00
Inclination [°]	-84.72	Drilling Stop Date	2002-10-28 14:39:00
Date of mapping	2003-01-23 00:00:00	Plot Date	2007-02-26 22:09:57

ROCK TYPE FORSMARK

- Granite, fine- to medium-grained
- Pegmatite, pegmatitic granite
- Granite, granodiorite and tonalite, metamorphic, fine- to medium-grained
- Granite to granodiorite, metamorphic, medium-grained
- Amphibolite
- Calc-silicate rock (skarn)

ROCK ALTERATION

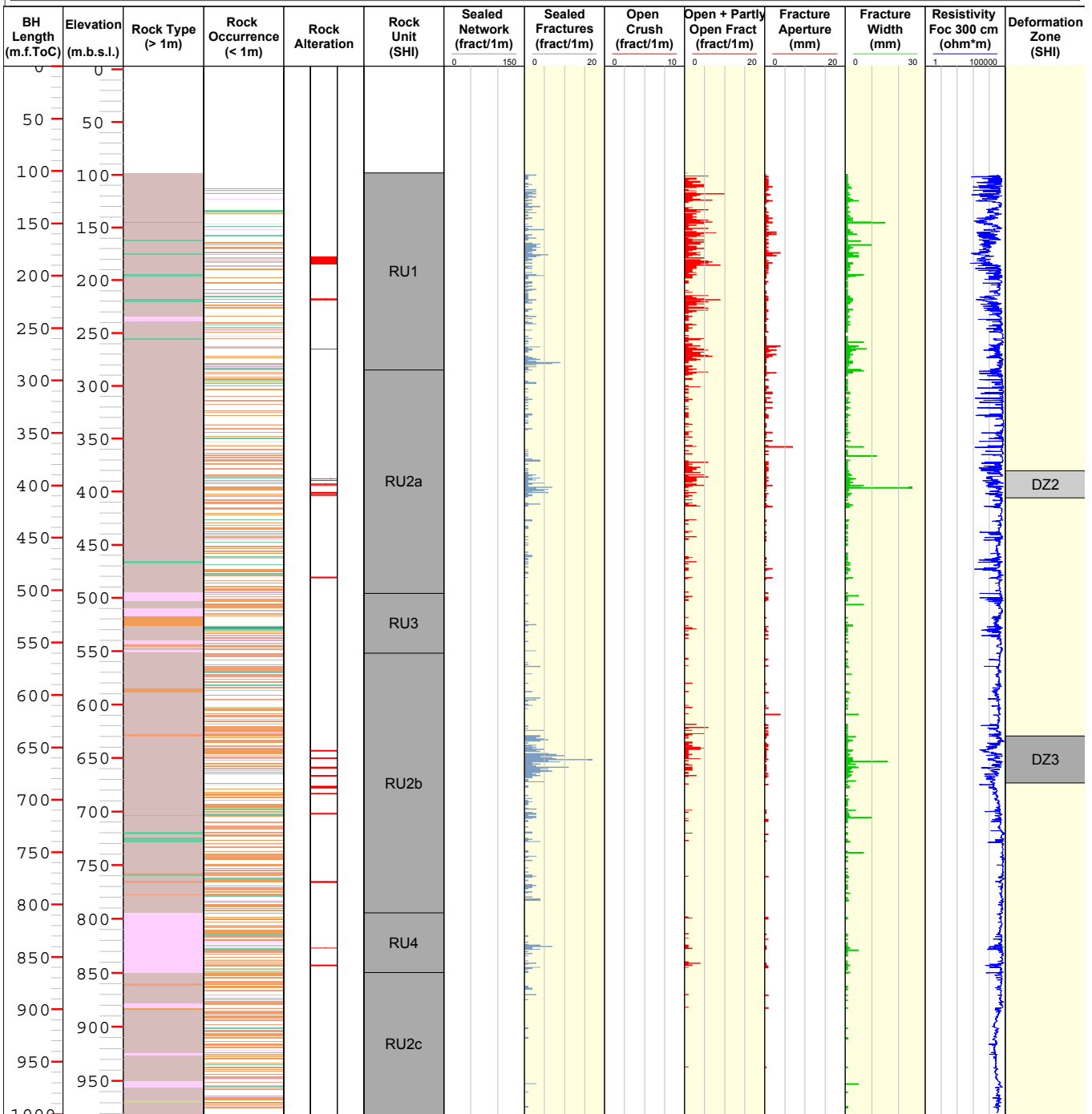
- Oxidized

ROCK UNIT

- High confidence

DEFORMATION ZONE

- Medium confidence
- High confidence

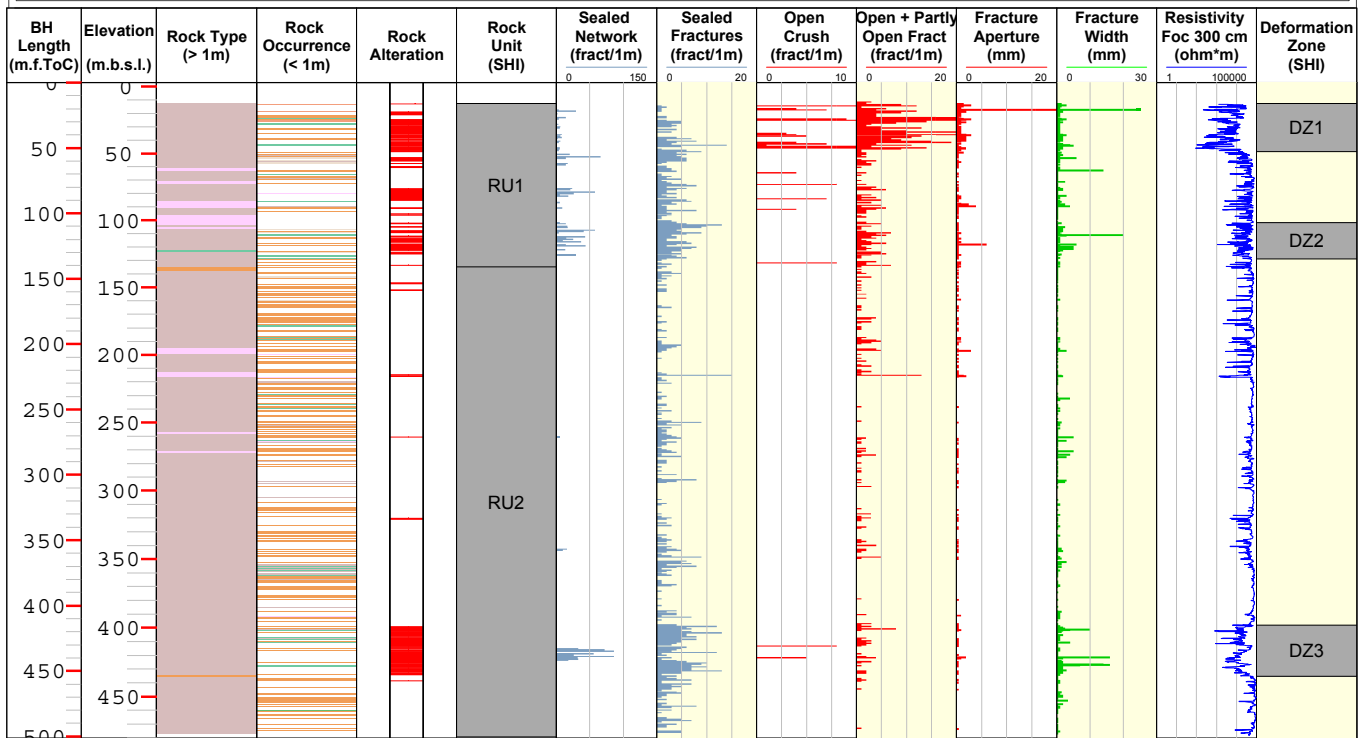


Title GEOLOGY KFM01B



Site	FORSMARK	Coordinate System	RT90-RHB70
Borehole	KFM01B	Northing [m]	6699539.40
Diameter [mm]	76	Easting [m]	1631387.67
Length [m]	500.520	Elevation [m.a.s.l.ToC]	3.09
Bearing [°]	267.59	Drilling Start Date	2003-06-25 07:00:00
Inclination [°]	-79.03	Drilling Stop Date	2004-01-15 15:00:00
Date of mapping	2004-03-05 00:00:00	Plot Date	2007-02-26 22:09:57

ROCK TYPE FORSMARK	ROCK ALTERATION	ROCK UNIT	DEFORMATION ZONE
Pegmatite, pegmatitic granite	Oxidized	High confidence	High confidence
Granite, granodiorite and tonalite, metamorphic, fine- to medium-grained			
Granite to granodiorite, metamorphic, medium-grained			
Amphibolite			



Title GEOLOGY KFM01C



Site	FORSMARK	Coordinate System	RT90-RHB70
Borehole	KFM01C	Northing [m]	6699526.14
Diameter [mm]	76	Easting [m]	1631403.75
Length [m]	450.020	Elevation [m.a.s.l.ToC]	2.91
Bearing [°]	165.35	Drilling Start Date	2005-11-05 13:56:00
Inclination [°]	-49.60	Drilling Stop Date	2005-11-29 13:52:00
Date of mapping	2006-01-17 10:57:00	Plot Date	2007-02-26 22:09:57

ROCK TYPE FORSMARK

- Granite, fine- to medium-grained
- Pegmatite, pegmatitic granite
- Granite, granodiorite and tonalite, metamorphic, fine- to medium-grained
- Granite, metamorphic, aplitic
- Granite to granodiorite, metamorphic, medium-grained
- Amphibolite
- Felsic to intermediate volcanic rock, metamorphic

ROCK ALTERATION

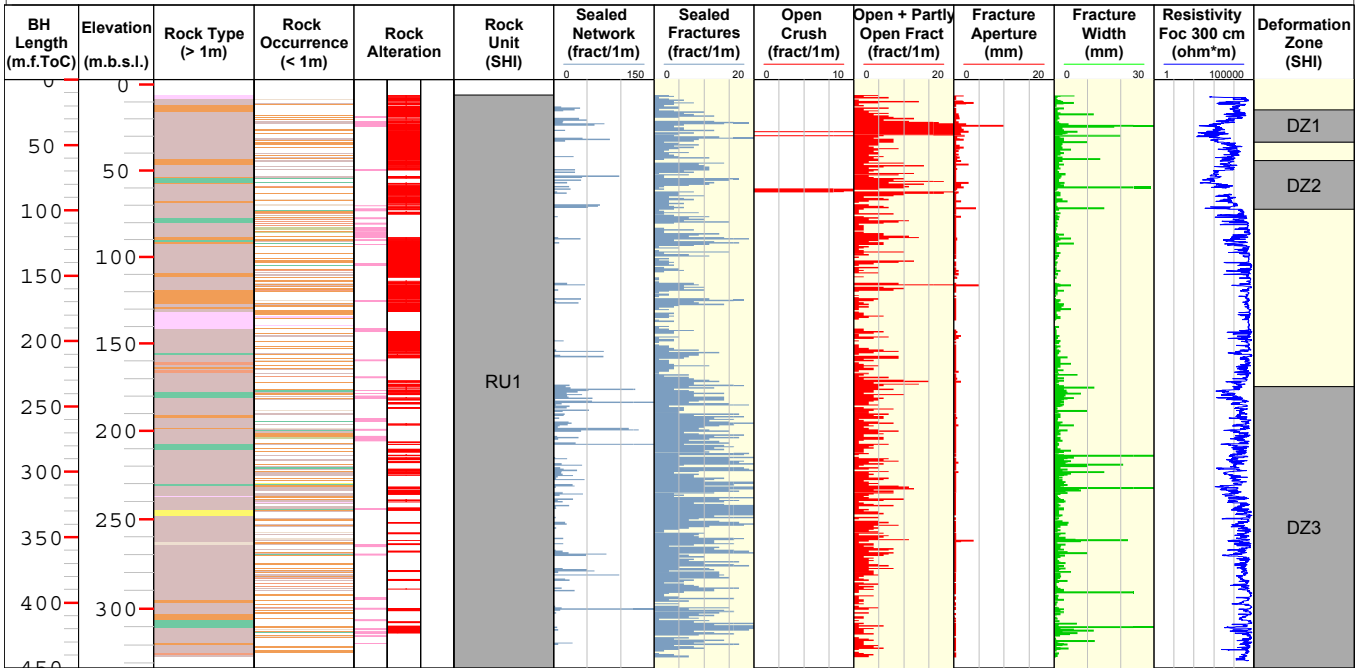
- Albitization
- Oxidized

ROCK UNIT

- High confidence

DEFORMATION ZONE

- High confidence

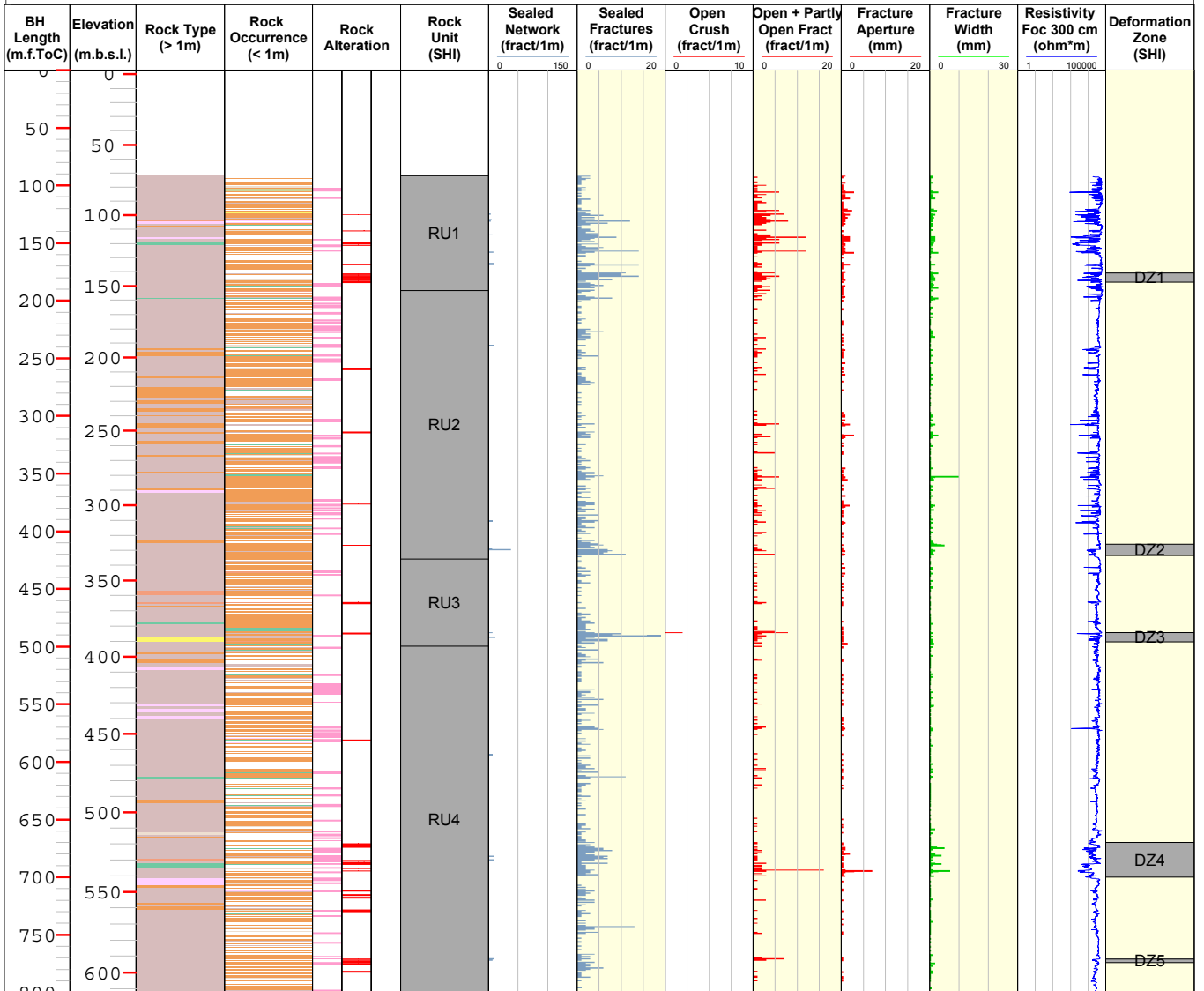


Title GEOLOGY KFM01D



Site	FORSMARK	Coordinate System	RT90-RHB70
Borehole	KFM01D	Northing [m]	6699542.07
Diameter [mm]	76	Easting [m]	1631404.52
Length [m]	800.240	Elevation [m.a.s.l.ToC]	2.95
Bearing [°]	35.03	Drilling Start Date	2005-11-21 07:00:00
Inclination [°]	-54.89	Drilling Stop Date	2006-02-18 10:49:00
Date of mapping	2006-03-28 13:20:00	Plot Date	2007-02-26 22:09:57

ROCK TYPE FORSMARK	ROCK ALTERATION	ROCK UNIT	DEFORMATION ZONE
Granite, fine- to medium-grained	Albitization	High confidence	High confidence
Pegmatite, pegmatitic granite	Oxidized		
Granite, granodiorite and tonalite, metamorphic, fine- to medium-grained			
Granite, metamorphic, aplitic			
Granite to granodiorite, metamorphic, medium-grained			
Amphibolite			
Felsic to intermediate volcanic rock, metamorphic			



Title GEOLOGY KFM02A



Site FORSMARK
 Borehole KFM02A
 Diameter [mm] 77
 Length [m] 1002.440
 Bearing [°] 275.76
 Inclination [°] -85.37
 Date of mapping 2003-04-22 00:00:00

Coordinate System RT90-RHB70
 Northing [m] 6698712.50
 Easting [m] 1633182.86
 Elevation [m.a.s.l.ToC] 7.35
 Drilling Start Date 2002-11-20 14:03:00
 Drilling Stop Date 2003-03-12 21:30:00
 Plot Date 2007-02-26 22:09:57

ROCK TYPE FORSMARK

- Granite, fine- to medium-grained
- Pegmatite, pegmatitic granite
- Granite, granodiorite and tonalite, metamorphic, fine- to medium-grained
- Granite to granodiorite, metamorphic, medium-grained
- Amphibolite

ROCK ALTERATION

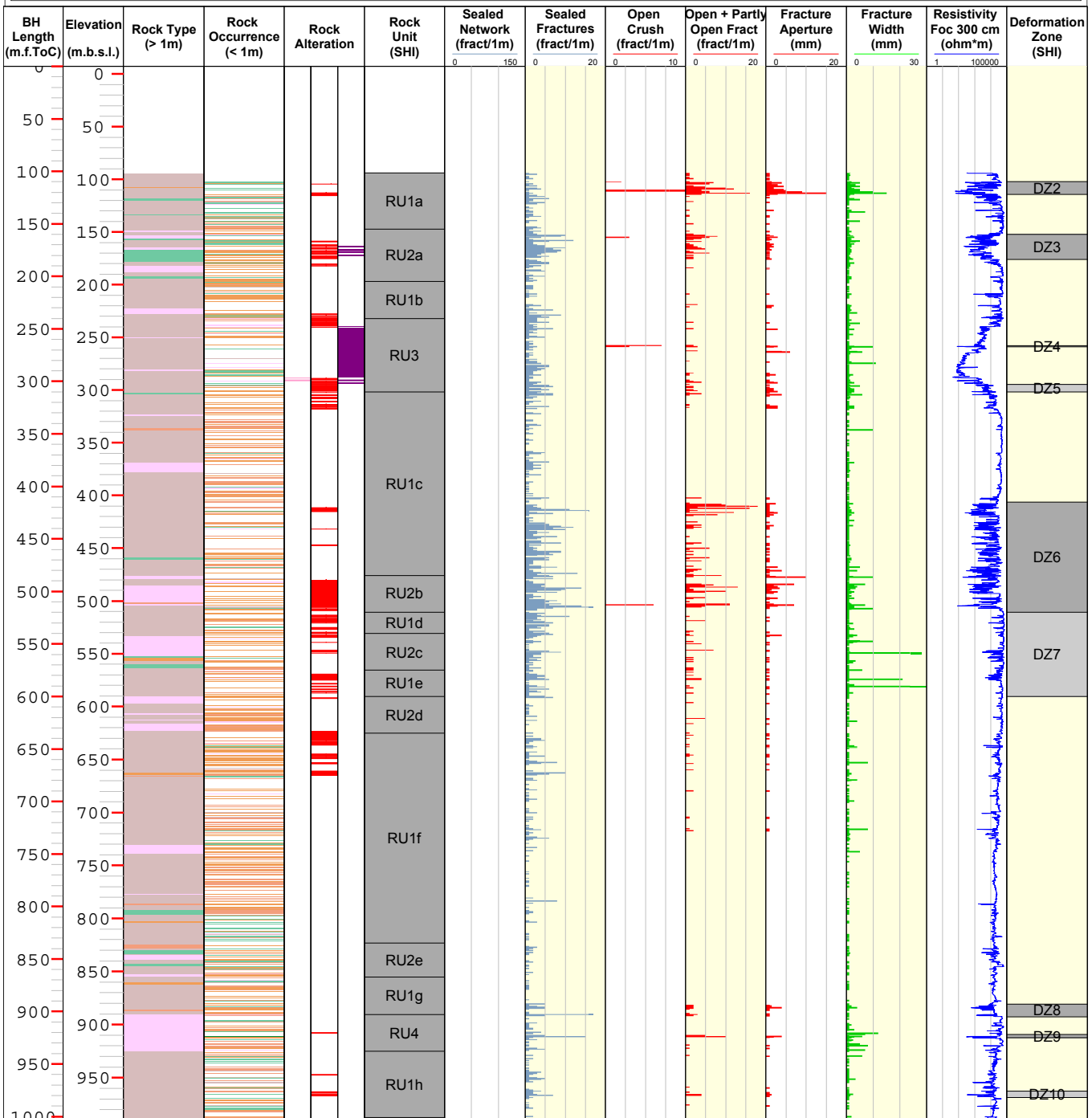
- Quartz dissolution
- Albitization
- Oxidized

ROCK UNIT

- High confidence

DEFORMATION ZONE

- Medium confidence
- High confidence



Title GEOLOGY KFM03A



Site	FORSMARK	Coordinate System	RT90-RHB70
Borehole	KFM03A	Northing [m]	6697852.10
Diameter [mm]	77	Easting [m]	1634630.74
Length [m]	1001.190	Elevation [m.a.s.l.ToC]	8.29
Bearing [°]	271.52	Drilling Start Date	2003-03-18 09:10:00
Inclination [°]	-85.74	Drilling Stop Date	2003-06-23 16:15:00
Date of mapping	2003-08-28 00:00:00	Plot Date	2007-02-26 22:09:57

ROCK TYPE FORSMARK

- Granite, fine- to medium-grained
- Pegmatite, pegmatitic granite
- Granite, granodiorite and tonalite, metamorphic, fine- to medium-grained
- Granite to granodiorite, metamorphic, medium-grained
- Tonalite to granodiorite, metamorphic
- Amphibolite

ROCK ALTERATION

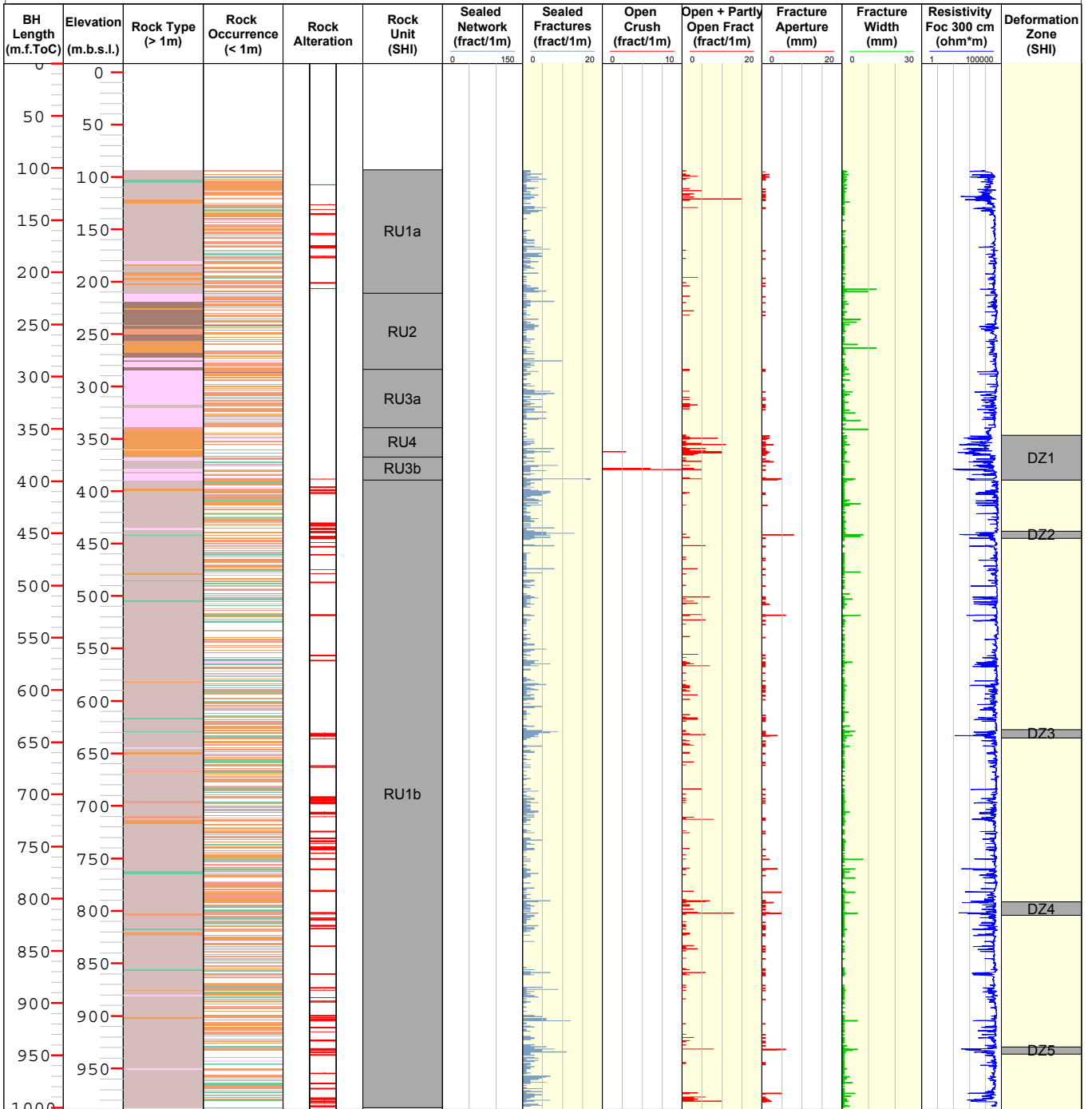
- Oxidized

ROCK UNIT

- High confidence

DEFORMATION ZONE

- High confidence



Title GEOLOGY KFM03B



Site	FORSMARK	Coordinate System	RT90-RHB70
Borehole	KFM03B	Northing [m]	6697844.20
Diameter [mm]	77	Easting [m]	1634618.68
Length [m]	101.540	Elevation [m.a.s.l.ToC]	8.47
Bearing [°]	264.49	Drilling Start Date	2003-06-29 09:30:00
Inclination [°]	-85.29	Drilling Stop Date	2003-07-02 14:05:00
Date of mapping	2003-08-12 00:00:00	Plot Date	2007-02-26 22:09:57

ROCK TYPE FORSMARK

- Granite, fine- to medium-grained
- Pegmatite, pegmatitic granite
- Granite, granodiorite and tonalite, metamorphic, fine- to medium-grained
- Granite to granodiorite, metamorphic, medium-grained
- Amphibolite

ROCK ALTERATION

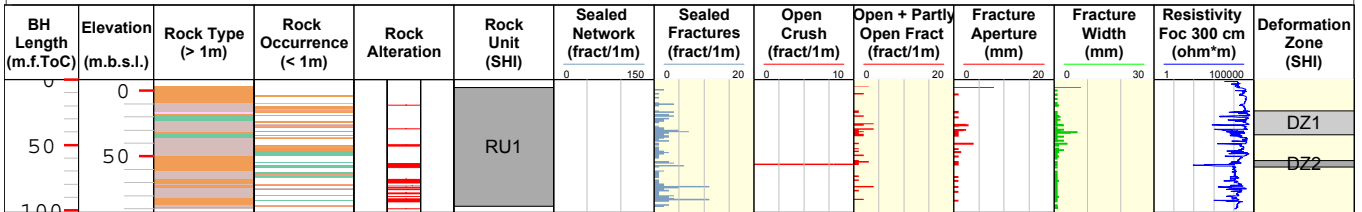
- Oxidized

ROCK UNIT

- High confidence

DEFORMATION ZONE

- Medium confidence
- High confidence



Title GEOLOGY KFM04A



Site	FORSMARK	Coordinate System	RT90-RHB70
Borehole	KFM04A	Northing [m]	6698921.74
Diameter [mm]	77	Easting [m]	1630978.96
Length [m]	1001.420	Elevation [m.a.s.l.ToC]	8.77
Bearing [°]	45.24	Drilling Start Date	2003-05-20 07:00:00
Inclination [°]	-60.07	Drilling Stop Date	2003-11-19 15:15:00
Date of mapping	2003-12-08 00:00:00	Plot Date	2007-02-26 22:09:57

ROCK TYPE FORSMARK

- Granite, fine- to medium-grained
- Pegmatite, pegmatitic granite
- Granite, granodiorite and tonalite, metamorphic, fine- to medium-grained
- Granite to granodiorite, metamorphic, medium-grained
- Granodiorite, metamorphic
- Amphibolite
- Felsic to intermediate volcanic rock, metamorphic

ROCK ALTERATION

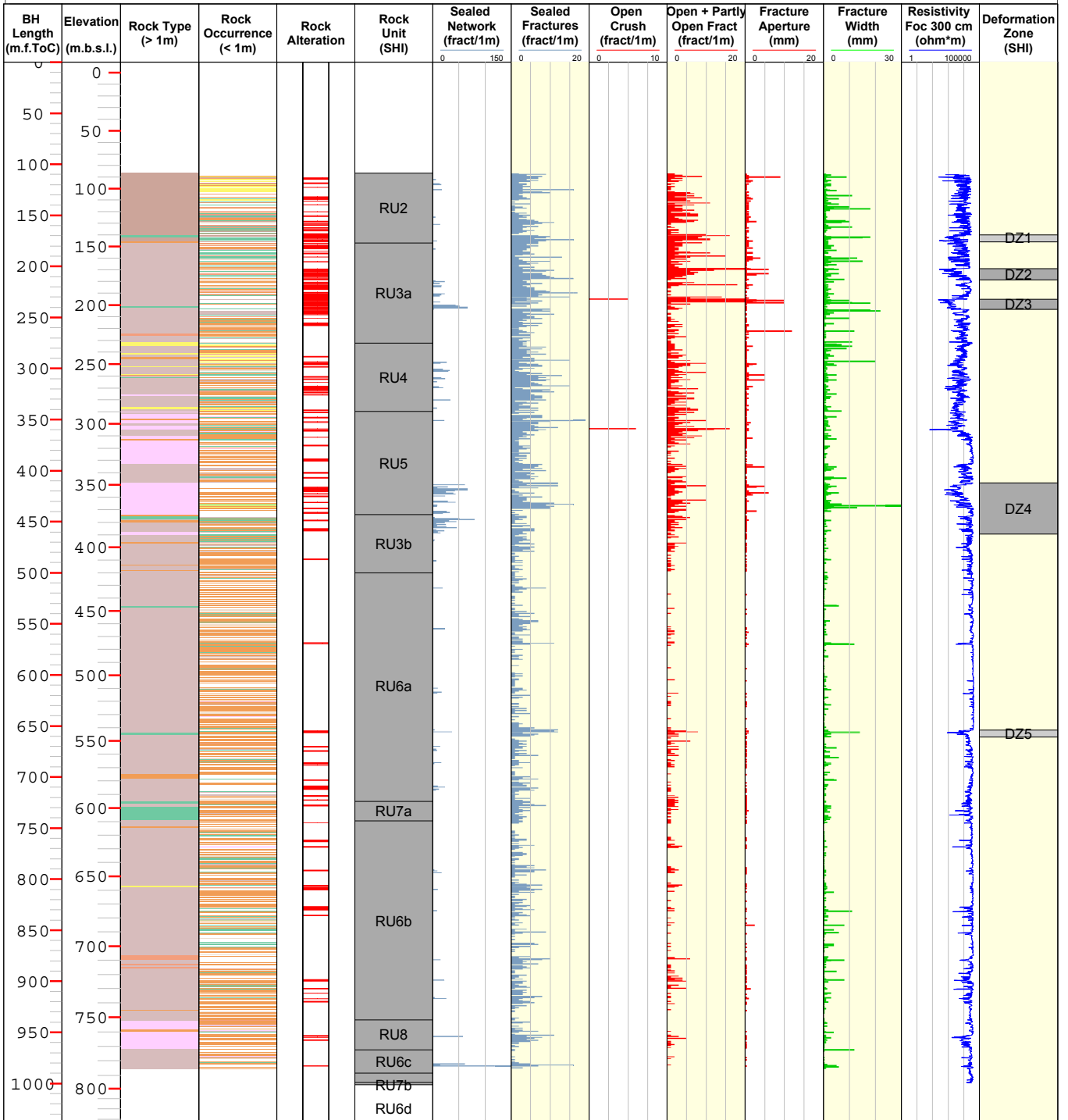
- Oxidized

ROCK UNIT

- High confidence

DEFORMATION ZONE

- Medium confidence
- High confidence



Title GEOLOGY KFM05A



Site	FORSMARK	Coordinate System	RT90-RHB70
Borehole	KFM05A	Northing [m]	6699344.85
Diameter [mm]	77	Easting [m]	1631710.80
Length [m]	1002.710	Elevation [m.a.s.l.ToC]	5.53
Bearing [°]	80.93	Drilling Start Date	2003-11-23 14:30:00
Inclination [°]	-59.80	Drilling Stop Date	2004-05-05 10:00:00
Date of mapping	2004-05-24 00:00:00	Plot Date	2007-02-26 22:09:57

ROCK TYPE FORSMARK

- Granite, fine- to medium-grained
- Pegmatite, pegmatitic granite
- Granite, granodiorite and tonalite, metamorphic, fine- to medium-grained
- Granite to granodiorite, metamorphic, medium-grained
- Amphibolite
- Felsic to intermediate volcanic rock, metamorphic

ROCK ALTERATION

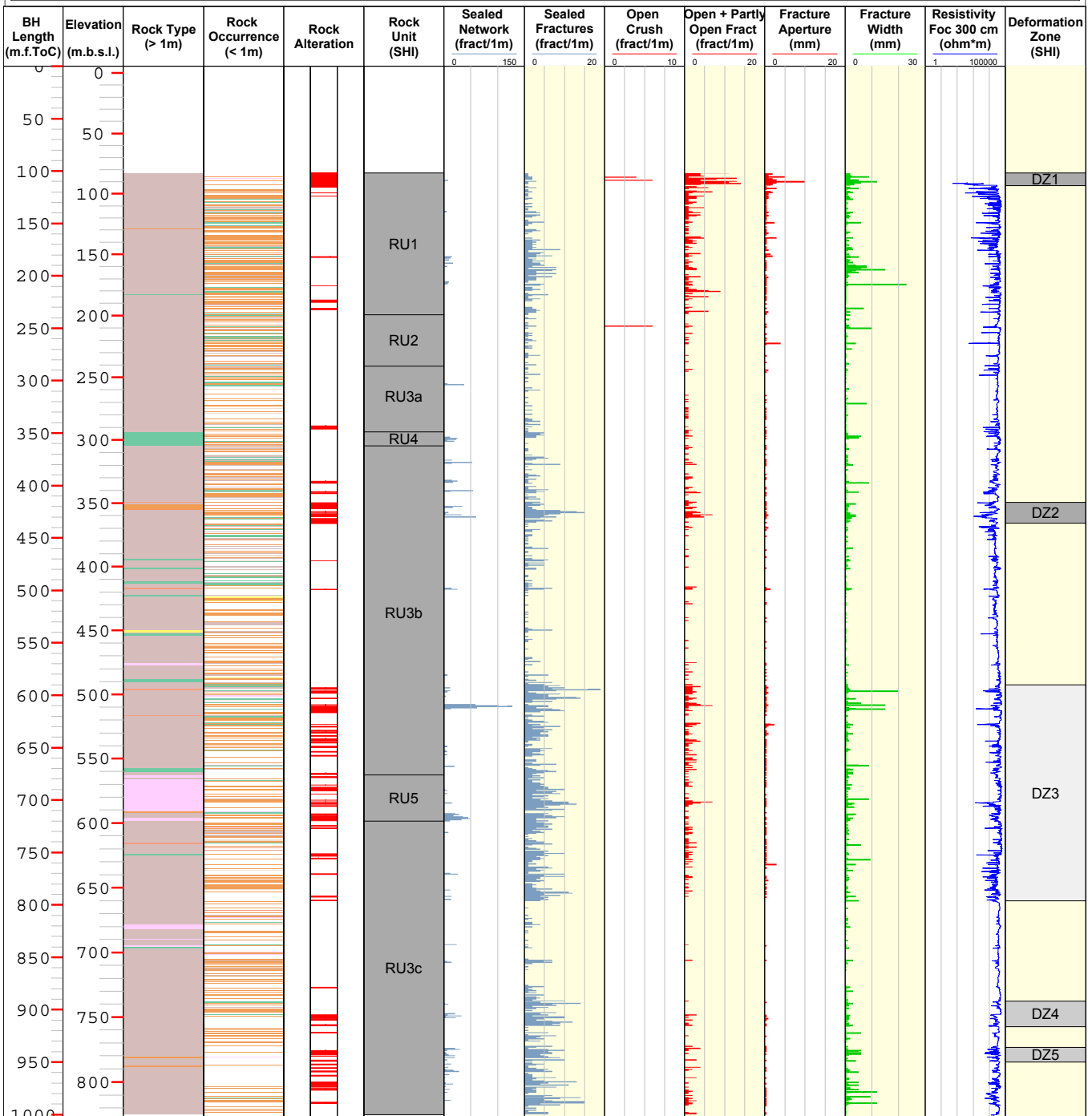
- Oxidized

ROCK UNIT

- High confidence

DEFORMATION ZONE

- Low confidence
- Medium confidence
- High confidence

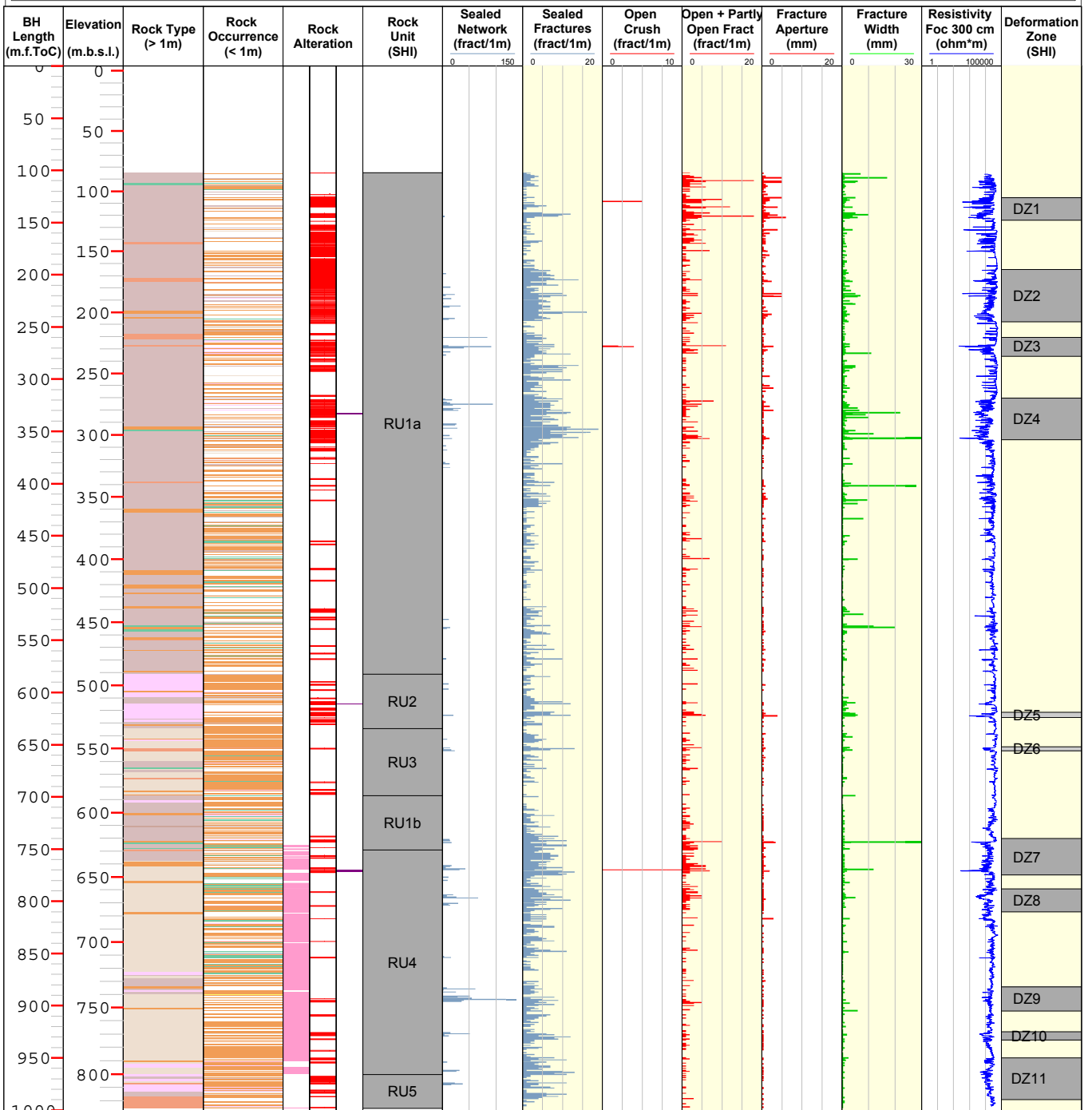


Title GEOLOGY KFM06A



Site	FORSMARK	Coordinate System	RT90-RHB70
Borehole	KFM06A	Northing [m]	6699732.88
Diameter [mm]	77	Easting [m]	1632442.51
Length [m]	1000.640	Elevation [m.a.s.l.ToC]	4.10
Bearing [°]	300.92	Drilling Start Date	2003-11-11 16:25:00
Inclination [°]	-60.24	Drilling Stop Date	2004-09-21 03:37:00
Date of mapping	2004-11-02 00:00:00	Plot Date	2007-02-26 22:09:57

ROCK TYPE FORSMARK		ROCK ALTERATION		ROCK UNIT		DEFORMATION ZONE	
	Granite, fine- to medium-grained		Quartz dissolution		High confidence		Medium confidence
	Pegmatite, pegmatitic granite		Albitization		High confidence		High confidence
	Granite, granodiorite and tonalite, metamorphic, fine- to medium-grained		Oxidized				
	Granite, metamorphic, aplitic						
	Granite to granodiorite, metamorphic, medium-grained						
	Granodiorite, metamorphic						
	Amphibolite						



Title GEOLOGY KFM06B



Site	FORMARK	Coordinate System	RT90-RHB70
Borehole	KFM06B	Northing [m]	6699732.24
Diameter [mm]	77	Easting [m]	1632446.41
Length [m]	100.330	Elevation [m.a.s.l.ToC]	4.13
Bearing [°]	296.96	Drilling Start Date	2004-05-26 07:00:00
Inclination [°]	-83.51	Drilling Stop Date	2005-02-08 14:00:00
Date of mapping	2005-03-12 18:51:00	Plot Date	2007-02-26 22:09:57

ROCK TYPE FORMARK

- Pegmatite, pegmatitic granite
- Granite, granodiorite and tonalite, metamorphic, fine- to medium-grained
- Granite to granodiorite, metamorphic, medium-grained

ROCK ALTERATION

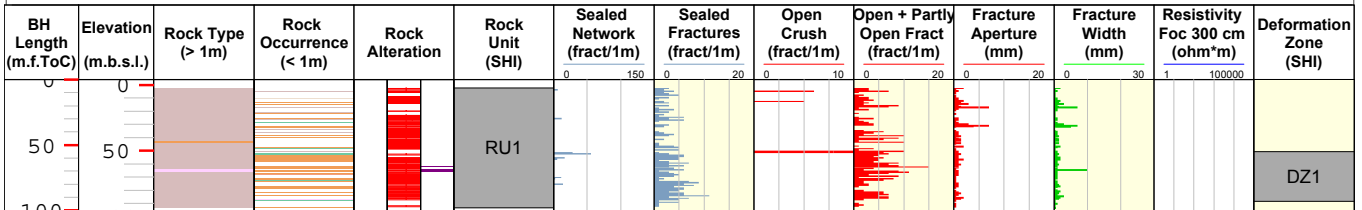
- Quartz dissolution
- Oxidized

ROCK UNIT

- High confidence

DEFORMATION ZONE

- High confidence

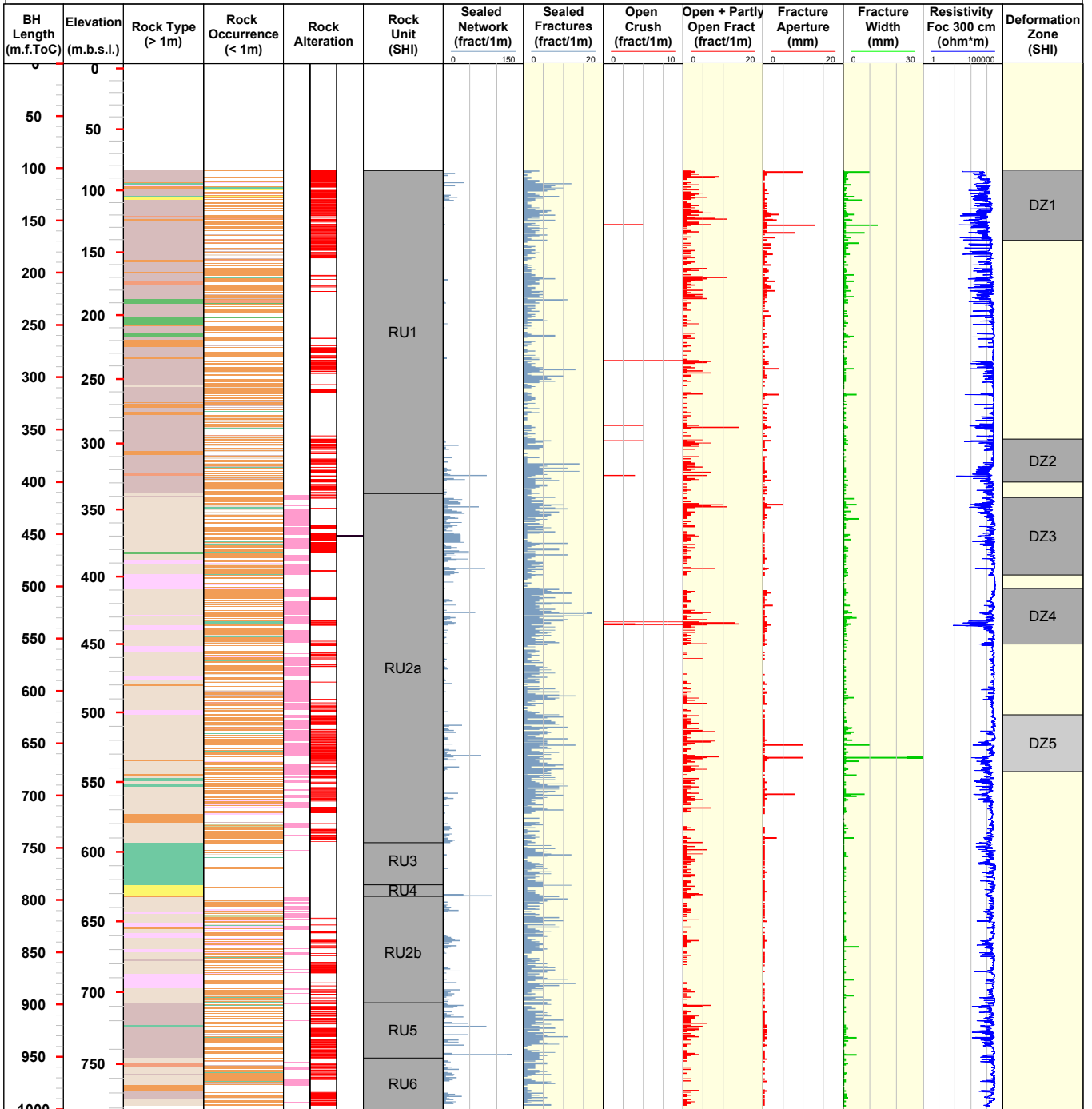


Title **GEOLOGY KFM06C**



Site	FORSMARK	Coordinate System	RT90-RHB70
Borehole	KFM06C	Northing [m]	6699740.96
Diameter [mm]	76	Easting [m]	1632437.03
Length [m]	1000.910	Elevation [m.a.s.l.ToC]	4.09
Bearing [°]	26.07	Drilling Start Date	2005-03-09 08:30:00
Inclination [°]	-60.11	Drilling Stop Date	2006-06-05 00:00:00
Date of mapping	2005-08-29 08:00:00	Plot Date	2007-04-22 23:43:02

ROCK TYPE FORSMARK	ROCK ALTERATION	ROCK UNIT	DEFORMATION ZONE
Granite, fine- to medium-grained	Albitization	High confidence	Medium confidence
Pegmatite, pegmatitic granite	Quartz dissolution		High confidence
Granite, granodiorite and tonalite, metamorphic, fine- to medium-grained	Oxidized		
Granite, metamorphic, aplitic			
Granite to granodiorite, metamorphic, medium-grained			
Diorite, quartz diorite and gabbro, metamorphic			
Amphibolite			
Felsic to intermediate volcanic rock, metamorphic			



Title GEOLOGY KFM07A



Site	FORSMARK	Coordinate System	RT90-RHB70
Borehole	KFM07A	Northing [m]	6700127.08
Diameter [mm]	77	Easting [m]	1631031.57
Length [m]	1002.100	Elevation [m.a.s.l.ToC]	3.33
Bearing [°]	261.47	Drilling Start Date	2004-06-07 11:40:00
Inclination [°]	-59.28	Drilling Stop Date	2004-12-09 11:40:00
Date of mapping	2005-01-17 15:59:00	Plot Date	2007-02-26 22:09:57

ROCK TYPE FORSMARK

- Granite, fine- to medium-grained
- Pegmatite, pegmatitic granite
- Granite to granodiorite, metamorphic, medium-grained
- Amphibolite
- Felsic to intermediate volcanic rock, metamorphic

ROCK ALTERATION

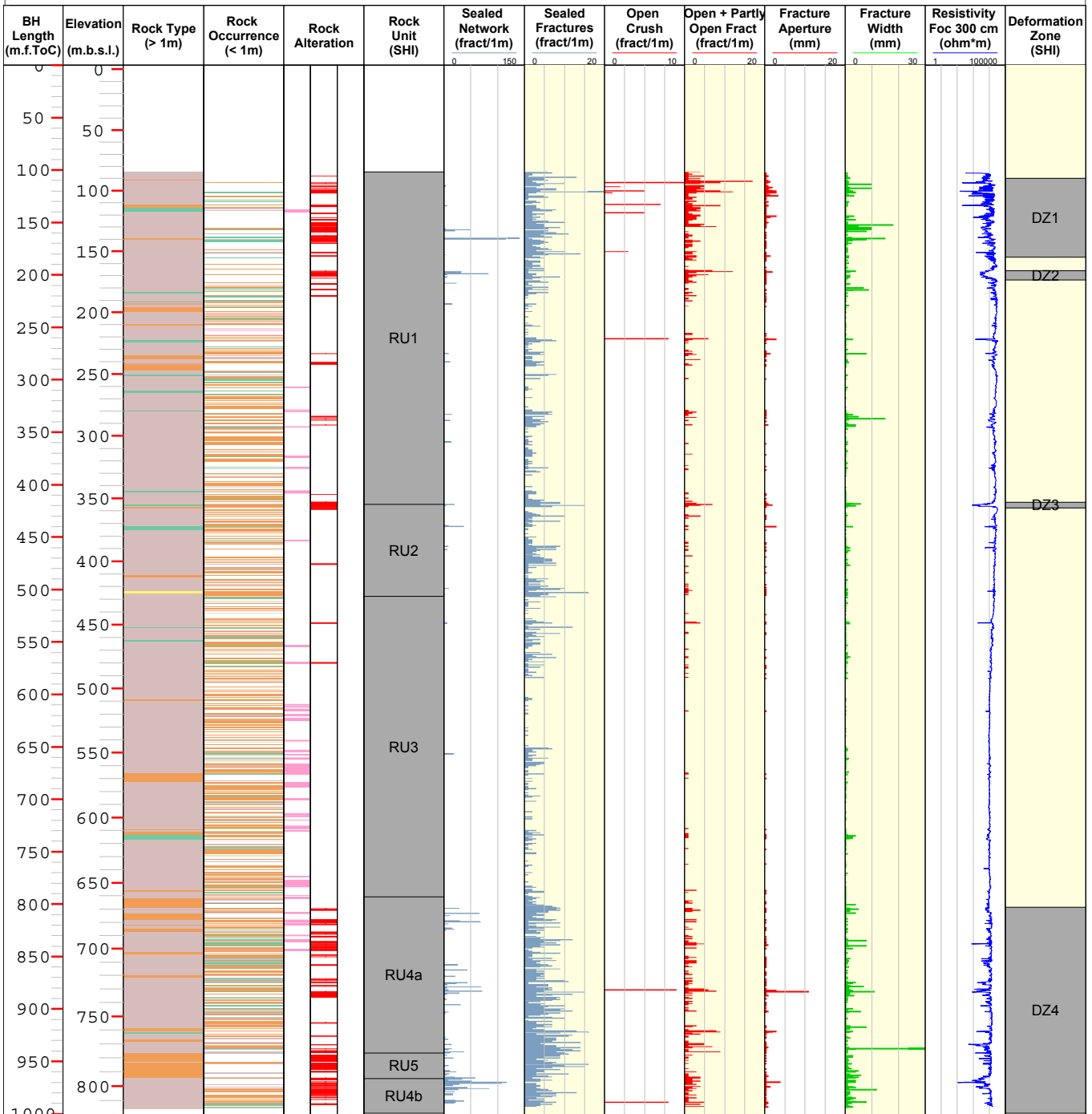
- Albitization
- Oxidized

ROCK UNIT

- High confidence

DEFORMATION ZONE

- High confidence

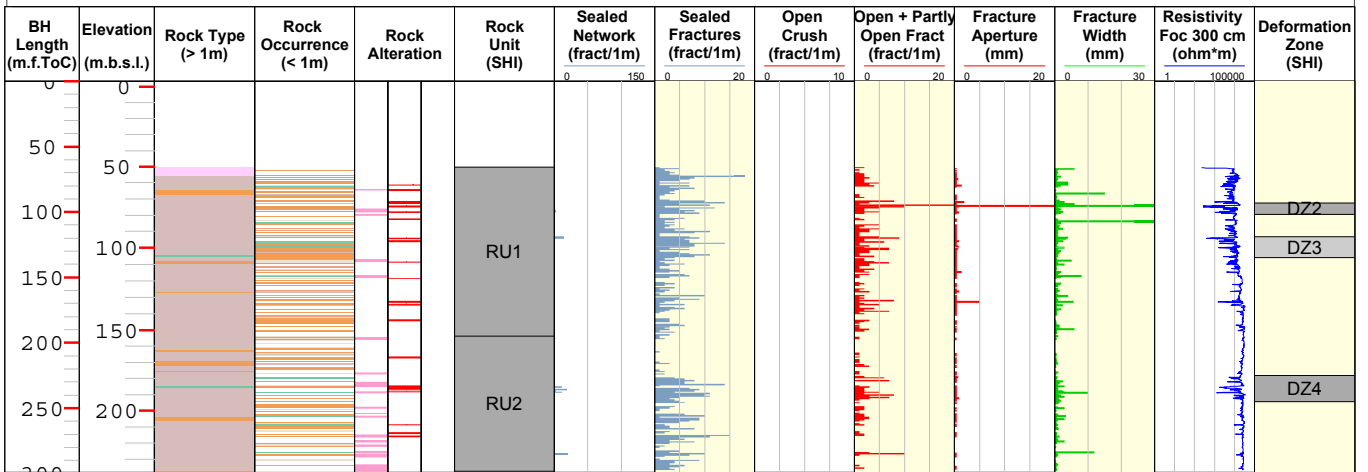


Title GEOLOGY KFM07B



Site	FORSMARK	Coordinate System	RT90-RHB70
Borehole	KFM07B	Northing [m]	6700123.62
Diameter [mm]	76	Easting [m]	1631036.83
Length [m]	298.930	Elevation [m.a.s.l.ToC]	3.36
Bearing [°]	134.35	Drilling Start Date	2005-05-31 16:20:00
Inclination [°]	-54.73	Drilling Stop Date	2005-10-18 10:24:00
Date of mapping	2005-11-10 10:03:00	Plot Date	2007-02-26 22:09:57

ROCK TYPE FORSMARK	ROCK ALTERATION	ROCK UNIT	DEFORMATION ZONE
Pegmatite, pegmatitic granite	Albitization	High confidence	Medium confidence
Granite, granodiorite and tonalite, metamorphic, fine- to medium-grained	Oxidized		High confidence
Granite to granodiorite, metamorphic, medium-grained			
Amphibolite			

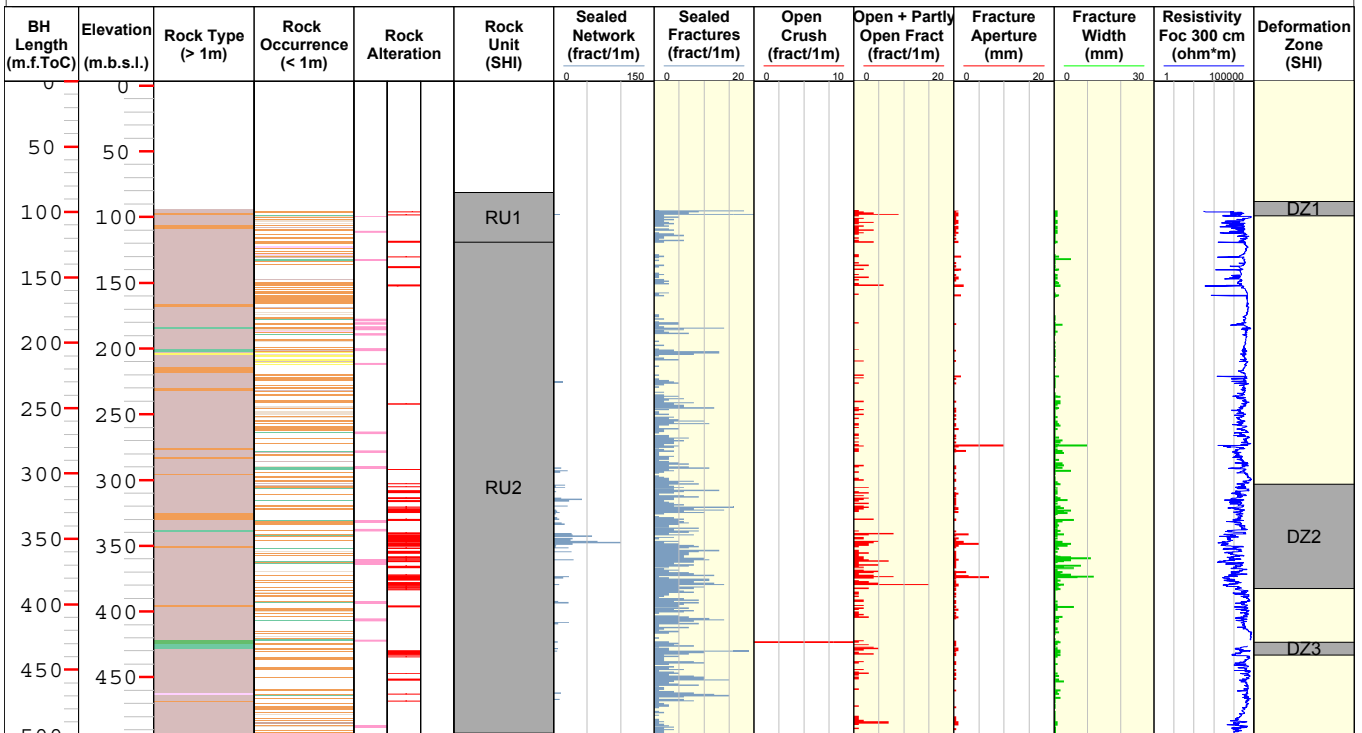


Title GEOLOGY KFM07C



Site	FORSMARK	Coordinate System	RT90-RHB70
Borehole	KFM07C	Northing [m]	6700125.61
Diameter [mm]	76	Easting [m]	1631034.45
Length [m]	500.340	Elevation [m.a.s.l.ToC]	3.35
Bearing [°]	142.71	Drilling Start Date	2006-03-30 00:00:00
Inclination [°]	-85.32	Drilling Stop Date	2006-08-08 00:00:00
Date of mapping	2006-09-04 09:21:00	Plot Date	2007-02-26 22:09:57

ROCK TYPE FORSMARK	ROCK ALTERATION	ROCK UNIT	DEFORMATION ZONE
Pegmatite, pegmatitic granite	Albitization	High confidence	High confidence
Granite, granodiorite and tonalite, metamorphic, fine- to medium-grained	Oxidized		
Granite to granodiorite, metamorphic, medium-grained			
Diorite, quartz diorite and gabbro, metamorphic			
Amphibolite			
Felsic to intermediate volcanic rock, metamorphic			

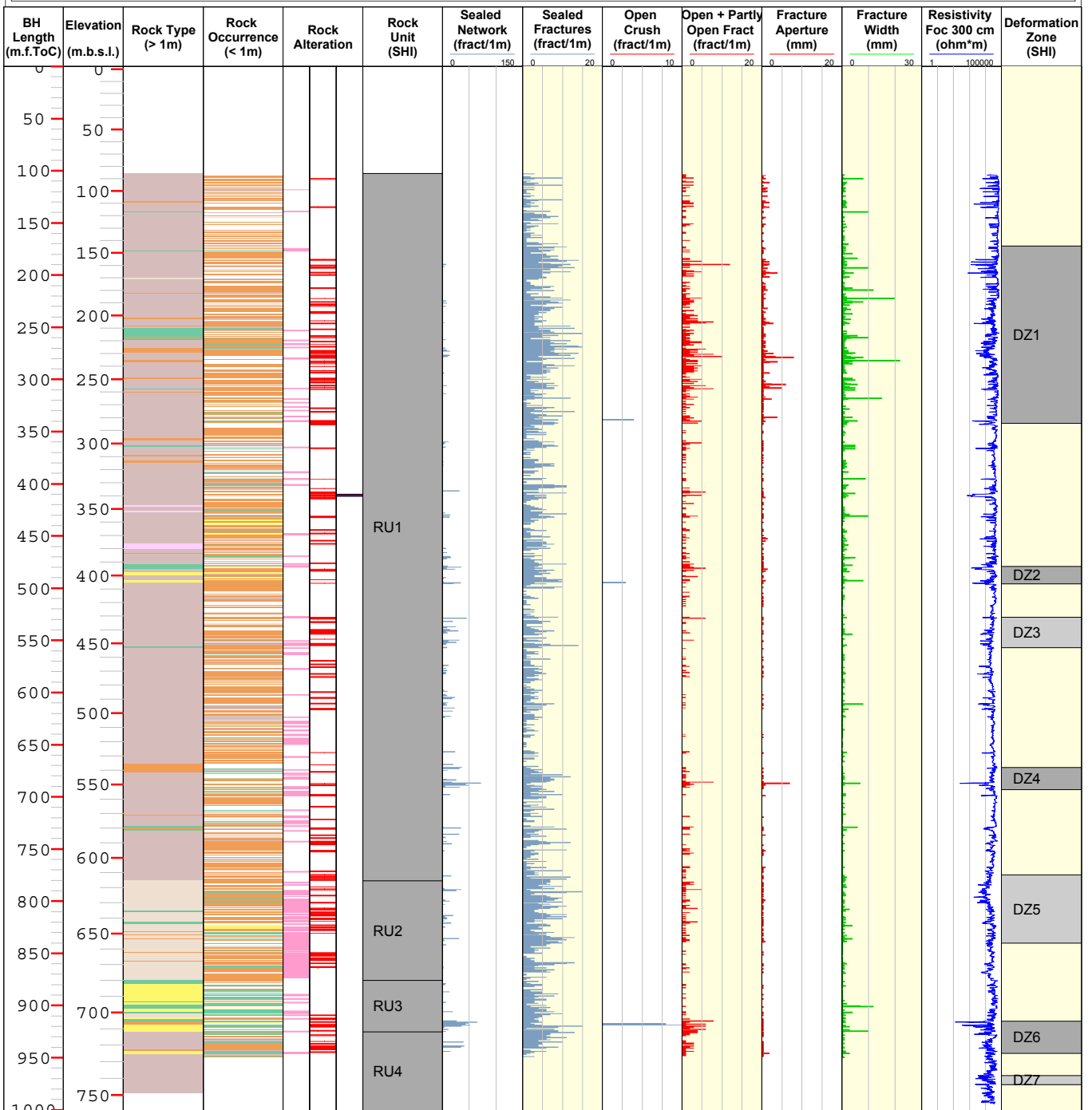


Title GEOLOGY KFM08A



Site	FORSMARK	Coordinate System	RT90-RHB70
Borehole	KFM08A	Northing [m]	6700494.49
Diameter [mm]	77	Easting [m]	1631197.06
Length [m]	1001.190	Elevation [m.a.s.l.ToC]	2.49
Bearing [°]	321.00	Drilling Start Date	2004-09-13 11:03:00
Inclination [°]	-60.84	Drilling Stop Date	2005-03-31 10:40:00
Date of mapping	2005-05-11 10:43:00	Plot Date	2007-03-04 22:14:36

ROCK TYPE FORSMARK		ROCK ALTERATION		ROCK UNIT	DEFORMATION ZONE
	Pegmatite, pegmatitic granite		Albitization		High confidence
	Granite, granodiorite and tonalite, metamorphic, fine- to medium-grained		Quartz dissolution		Medium confidence
	Granite, metamorphic, aplitic		Oxidized		High confidence
	Granite to granodiorite, metamorphic, medium-grained				
	Amphibolite				
	Felsic to intermediate volcanic rock, metamorphic				

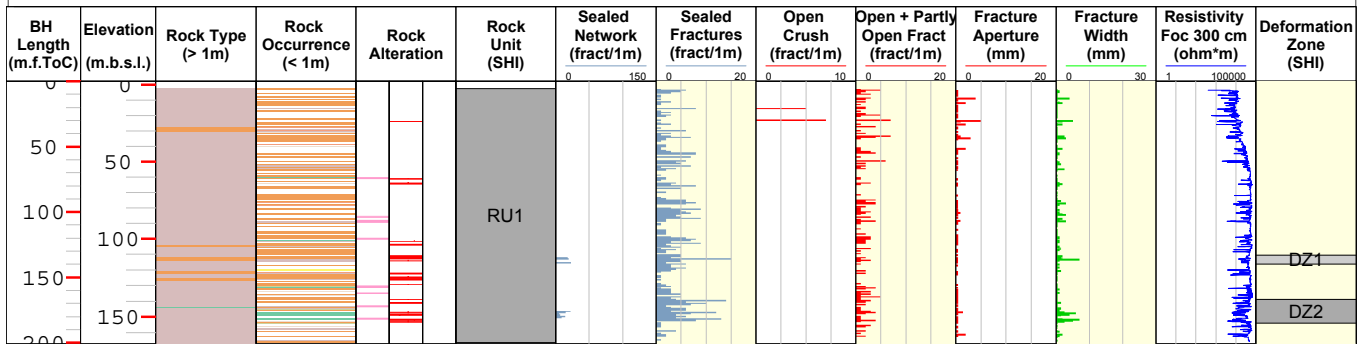


Title GEOLOGY KFM08B



Site	FORSMARK	Coordinate System	RT90-RHB70
Borehole	KFM08B	Northing [m]	6700492.75
Diameter [mm]	76	Easting [m]	1631173.27
Length [m]	200.540	Elevation [m.a.s.l.ToC]	2.25
Bearing [°]	270.45	Drilling Start Date	2005-01-11 16:04:00
Inclination [°]	-58.84	Drilling Stop Date	2005-01-26 14:51:00
Date of mapping	2005-05-02 14:49:00	Plot Date	2007-02-26 22:09:57

ROCK TYPE FORSMARK	ROCK ALTERATION	ROCK UNIT	DEFORMATION ZONE
Pegmatite, pegmatitic granite	Albitization	High confidence	Medium confidence
Granite to granodiorite, metamorphic, medium-grained	Oxidized		High confidence
Amphibolite			

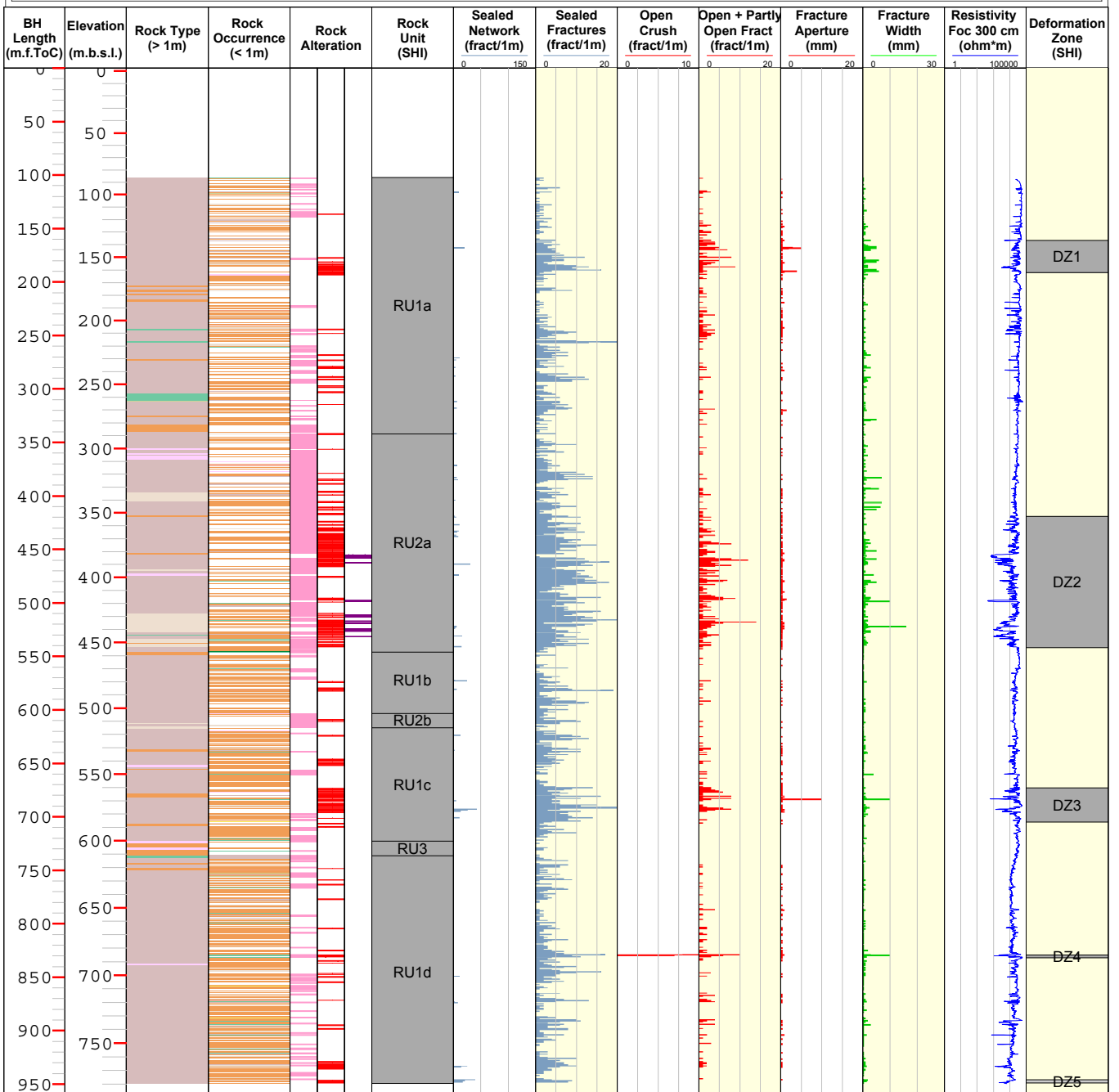


Title GEOLOGY KFM08C



Site	FORSMARK	Coordinate System	RT90-RHB70
Borehole	KFM08C	Northing [m]	6700495.88
Diameter [mm]	77	Easting [m]	1631187.57
Length [m]	951.080	Elevation [m.a.s.l.ToC]	2.47
Bearing [°]	35.88	Drilling Start Date	2006-01-30 16:00:00
Inclination [°]	-60.47	Drilling Stop Date	2006-05-09 06:00:00
Date of mapping	2006-06-20 15:25:00	Plot Date	2007-02-26 22:09:57

ROCK TYPE FORSMARK		ROCK ALTERATION		ROCK UNIT	DEFORMATION ZONE
	Pegmatite, pegmatitic granite		Quartz dissolution		High confidence
	Granite, granodiorite and tonalite, metamorphic, fine- to medium-grained		Albitization		Medium confidence
	Granite, metamorphic, aplitic		Oxidized		High confidence
	Granite to granodiorite, metamorphic, medium-grained				
	Amphibolite				
	Calc-silicate rock (skarn)				

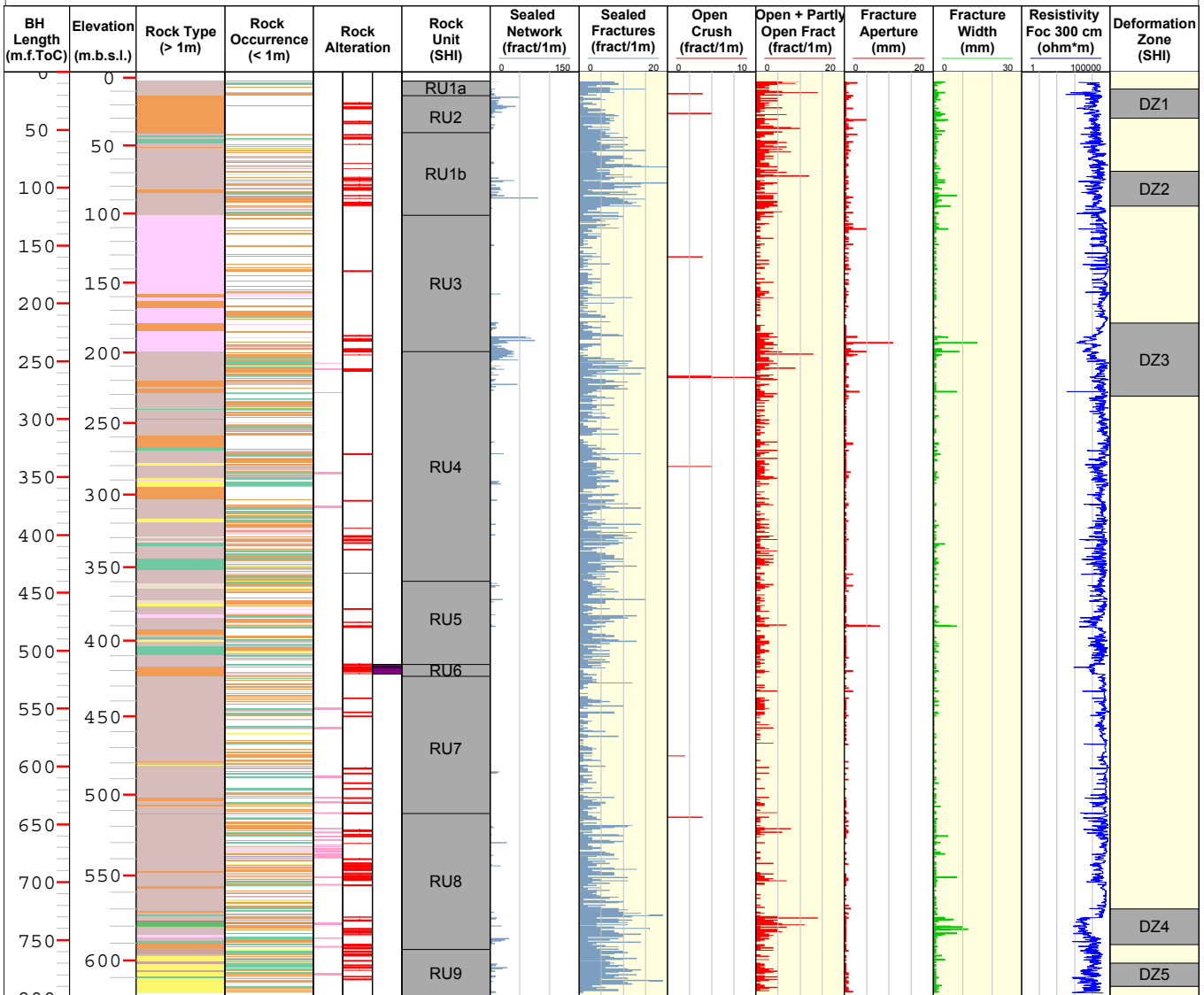


Title GEOLOGY KFM09A



Site	FORSMARK	Coordinate System	RT90-RHB70
Borehole	KFM09A	Northing [m]	6700115.04
Diameter [mm]	77	Easting [m]	1630647.50
Length [m]	799.670	Elevation [m.a.s.l.ToC]	4.29
Bearing [°]	200.08	Drilling Start Date	2005-08-31 00:00:00
Inclination [°]	-59.45	Drilling Stop Date	2005-10-27 13:00:00
Date of mapping	2005-11-29 20:07:00	Plot Date	2007-03-04 22:14:36

ROCK TYPE FORSMARK		ROCK ALTERATION	ROCK UNIT	DEFORMATION ZONE
	Pegmatite, pegmatitic granite			
	Granite, granodiorite and tonalite, metamorphic, fine- to medium-grained			
	Granite, metamorphic, aplitic			
	Granite to granodiorite, metamorphic, medium-grained			
	Granodiorite, metamorphic			
	Tonalite to granodiorite, metamorphic			
	Diorite, quartz diorite and gabbro, metamorphic			
	Amphibolite			

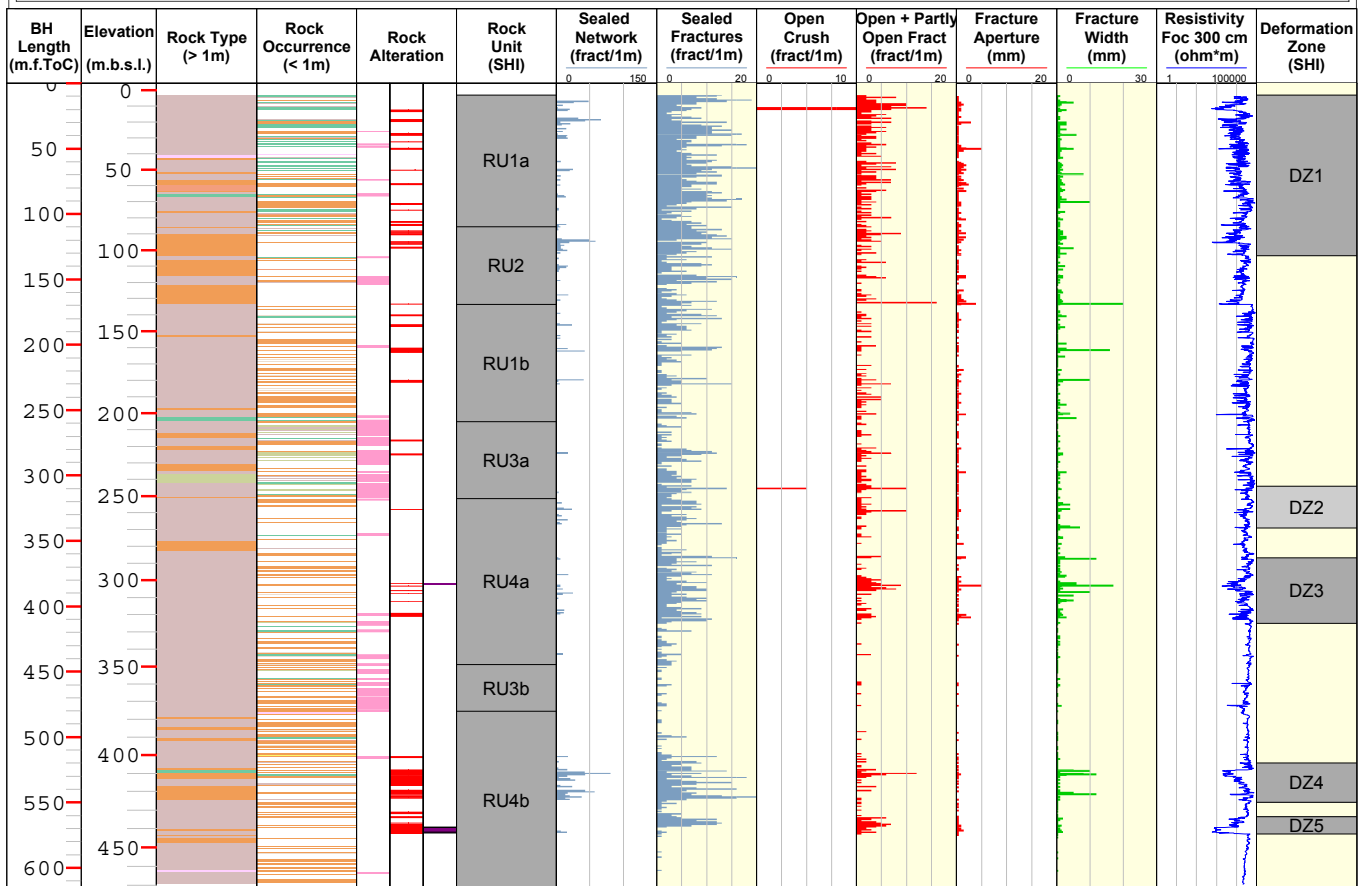


Title GEOLOGY KFM09B



Site	FORSMARK	Coordinate System	RT90-RHB70
Borehole	KFM09B	Northing [m]	6700119.89
Diameter [mm]	77	Easting [m]	1630638.78
Length [m]	616.450	Elevation [m.a.s.l.ToC]	4.30
Bearing [°]	140.83	Drilling Start Date	2005-11-16 00:00:00
Inclination [°]	-55.07	Drilling Stop Date	2005-12-19 00:00:00
Date of mapping	2006-02-05 10:35:00	Plot Date	2007-03-04 22:14:36

- | | | | |
|--|------------------------|------------------|-------------------------|
| ROCK TYPE FORSMARK | ROCK ALTERATION | ROCK UNIT | DEFORMATION ZONE |
| Granite, fine- to medium-grained | Albitization | High confidence | Medium confidence |
| Pegmatite, pegmatitic granite | Quartz dissolution | | High confidence |
| Granite, granodiorite and tonalite, metamorphic, fine- to medium-grained | Oxidized | | |
| Granite to granodiorite, metamorphic, medium-grained | | | |
| Amphibolite | | | |
| Calc-silicate rock (skarn) | | | |



Title GEOLOGY KFM10A



Site FORSMARK
 Borehole KFM10A
 Diameter [mm] 16
 Length [m] 500.160
 Bearing [°] 10.42
 Inclination [°] -50.12
 Date of mapping 2006-06-20 10:59:00

Coordinate System RT90-RHB70
 Northing [m] 6698629.17
 Easting [m] 1631715.90
 Elevation [m.a.s.l.ToC] 4.51
 Drilling Start Date 2005-12-06 09:00:00
 Drilling Stop Date 2006-06-01 12:25:00
 Plot Date 2007-03-04 22:14:36

ROCK TYPE FORSMARK

- Granite, fine- to medium-grained
- Pegmatite, pegmatitic granite
- Granite, granodiorite and tonalite, metamorphic, fine- to medium-grained
- Granite to granodiorite, metamorphic, medium-grained
- Amphibolite

ROCK ALTERATION

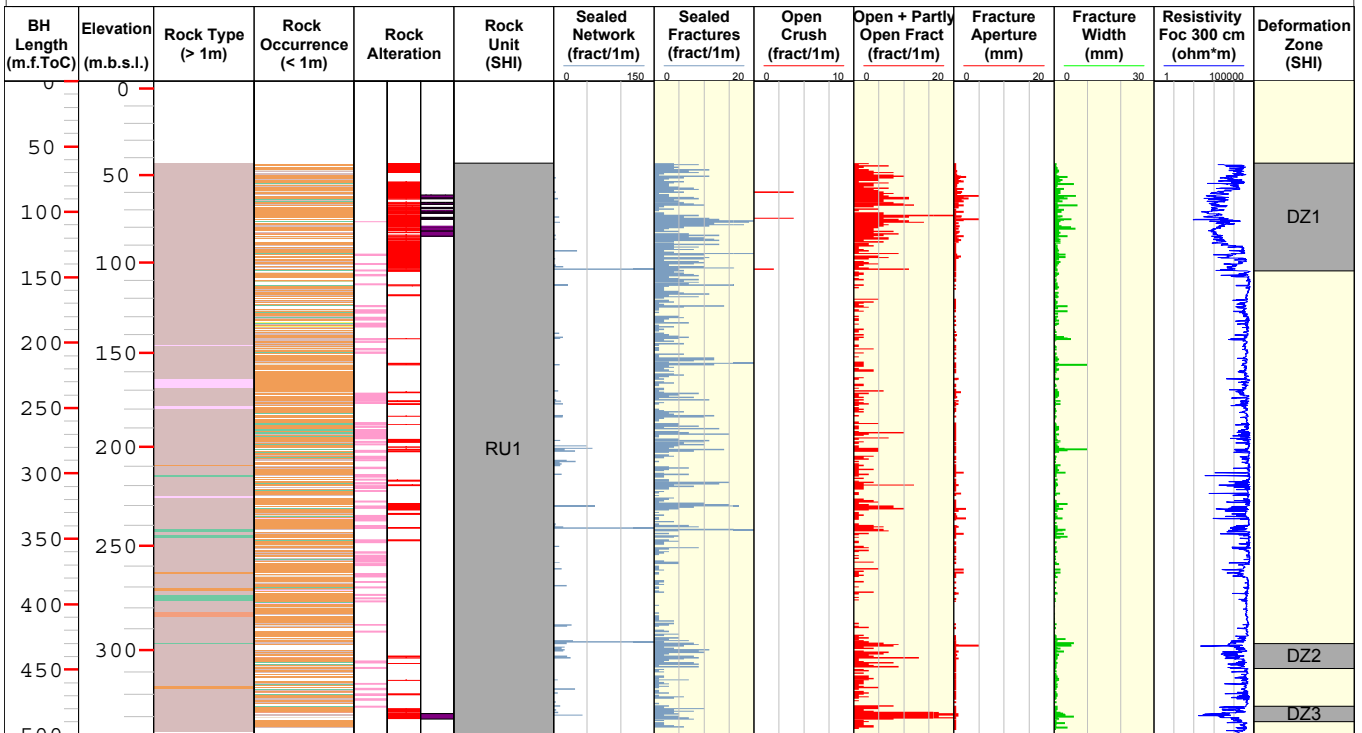
- Quartz dissolution
- Albitization
- Oxidized

ROCK UNIT

- High confidence

DEFORMATION ZONE

- High confidence



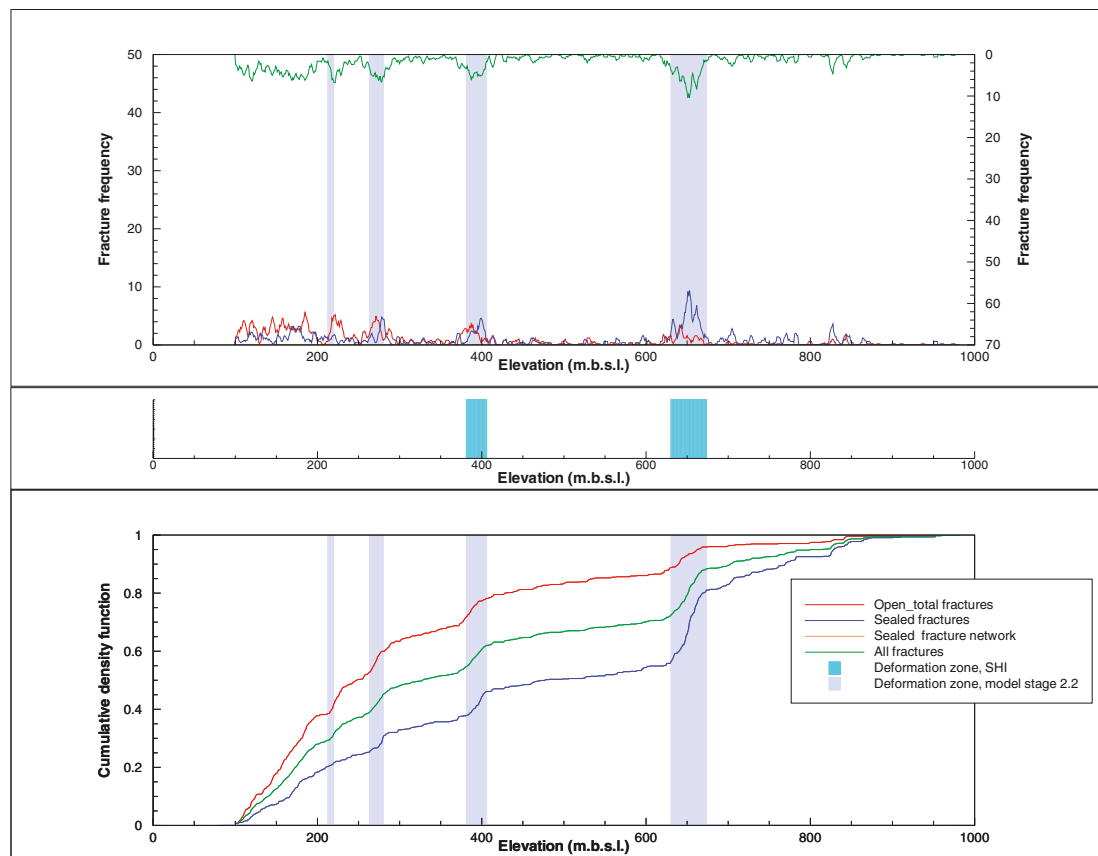
Fracture frequency distribution diagrams for all boreholes

Fracture frequency distribution diagrams have been used in order to gain a first assessment of significant variations in fracture frequency in the bedrock that is not affected by geological anomalies such as deformation zones. This analysis addresses the variation in the frequency of different types of fractures in each cored borehole. In this way, the variation with depth of different types of fractures at different locations inside the candidate volume can be assessed.

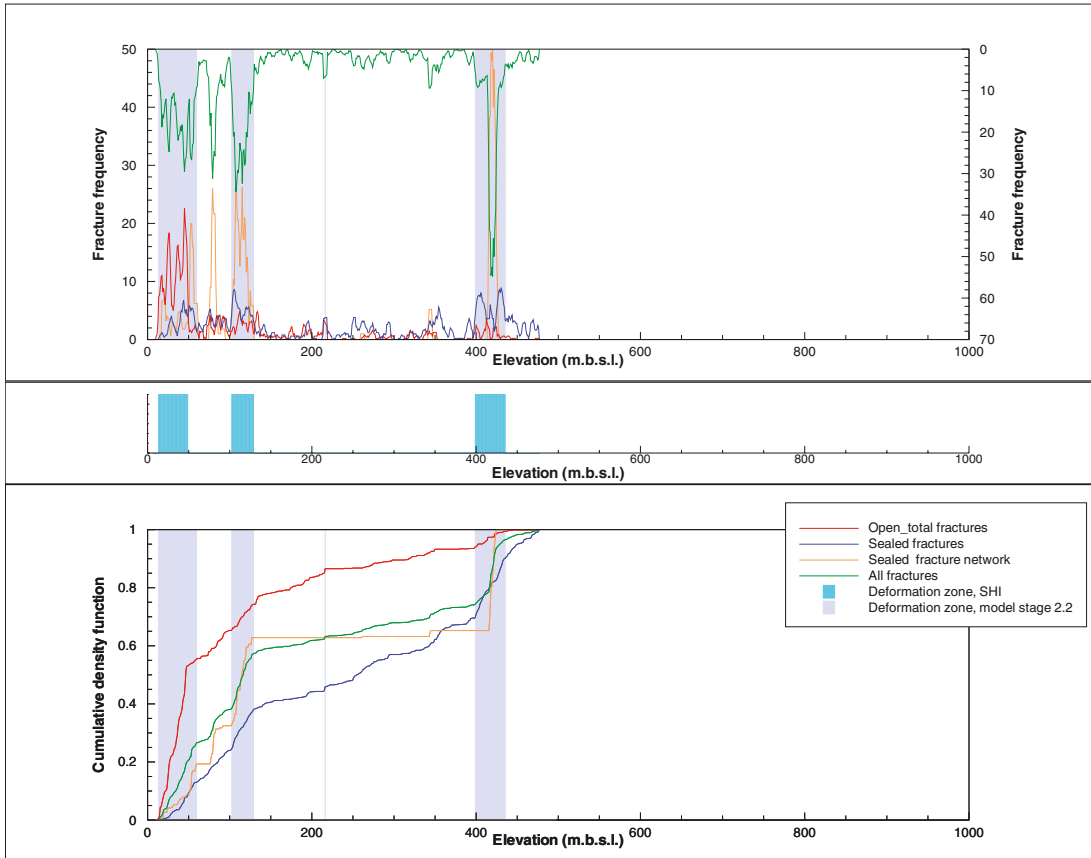
The fracture frequency distribution diagrams for all the cored boreholes are presented in Appendix 3. The upper diagram is a moving average plot with a 5 m window and 1 m steps, and the lower diagram is a cumulative frequency plot. The deformation zones modelled during stage 2.2, as well as additional possible zones recognised during the extended single hole interpretation work, are marked on both diagrams. Possible deformation zones, as defined in the single hole interpretation, are presented, for comparison purposes, in the middle part of the figure.

Contrasting modes of variation for fracture frequency in the cored boreholes KFM01A and KFM03A were already recognised in model version 1.2 /SKB 2005a/. The KFM01A mode, with a marked concentration of open and partly open fractures in the upper part of the bedrock outside the influence of deformation zones, is also conspicuous in boreholes KFM01D, KFM05A, KFM07B and KFM07C. The KFM03A mode, with a more even distribution of open fractures along the borehole outside the influence of deformation zones, is also conspicuous in borehole KFM08C and, after taking account of the occurrence of deformation zones, even in boreholes KFM02A and KFM08A. For further discussion of these fracture frequency distributions, the reader is referred to section 4.5 in the main text.

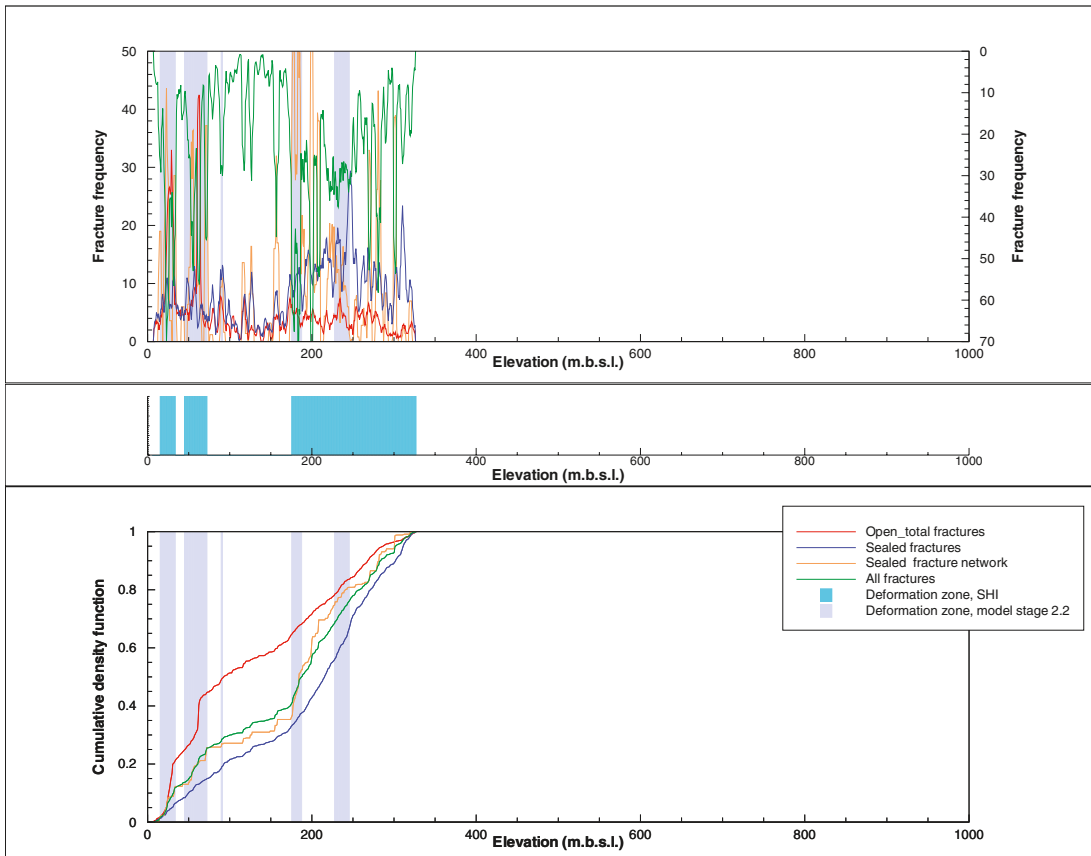
Borehole KFM01A



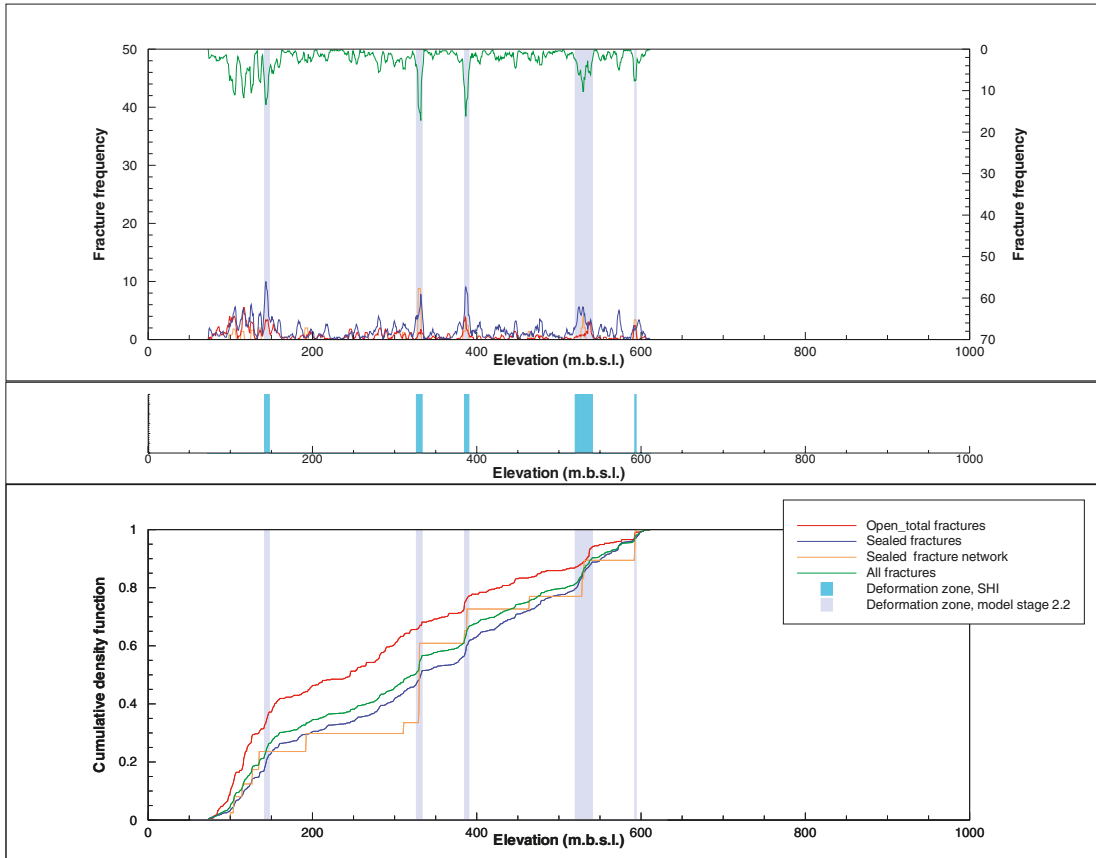
Borehole KFM01B



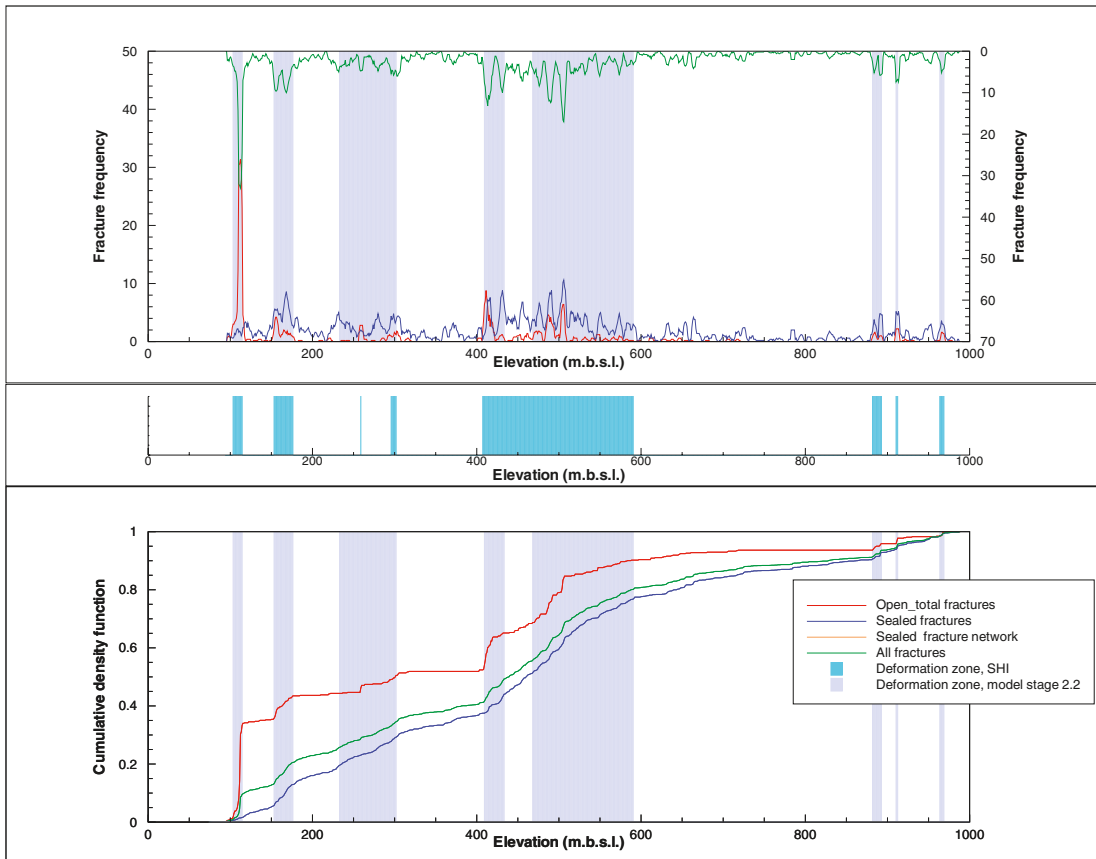
Borehole KFM01C



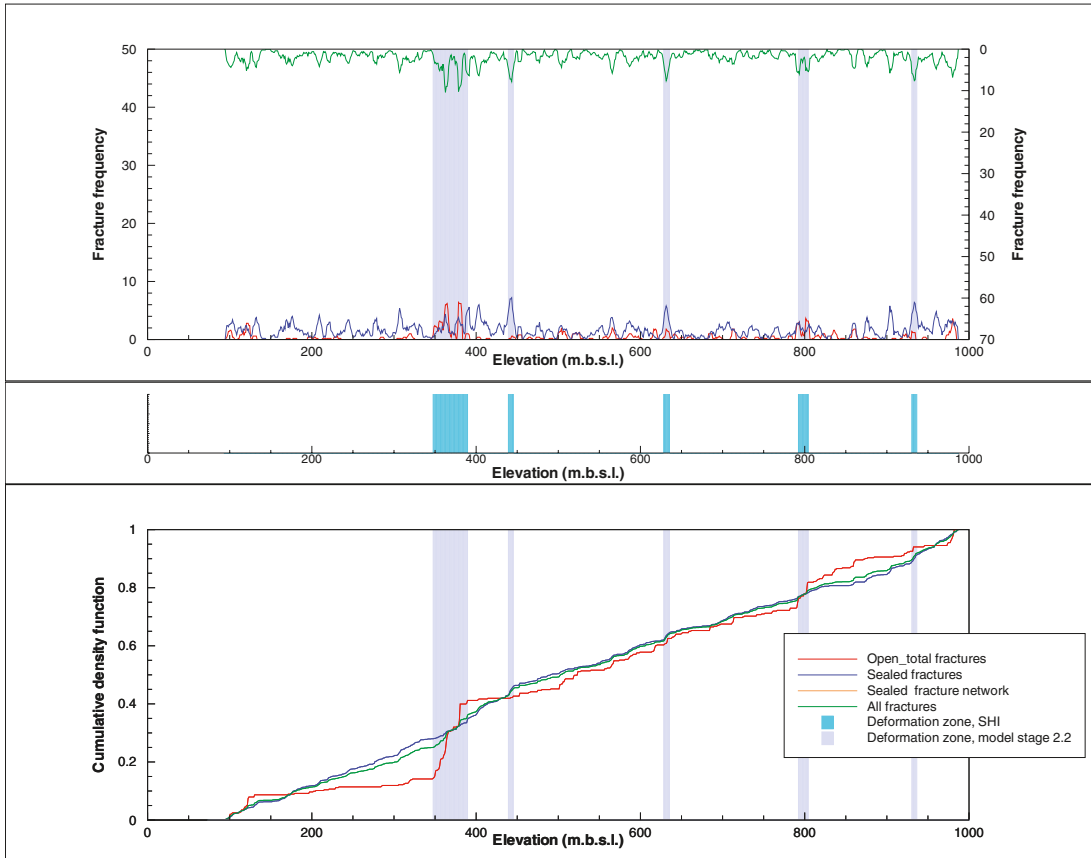
Borehole KFM01D



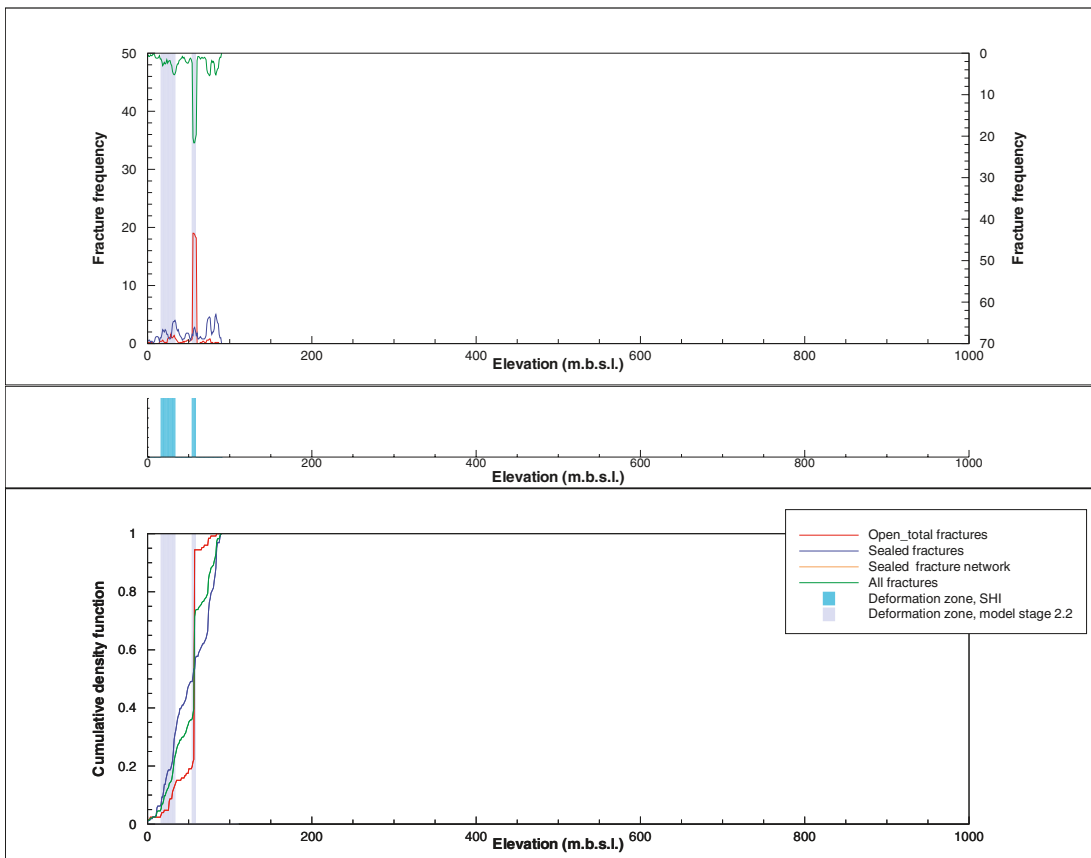
Borehole KFM02A



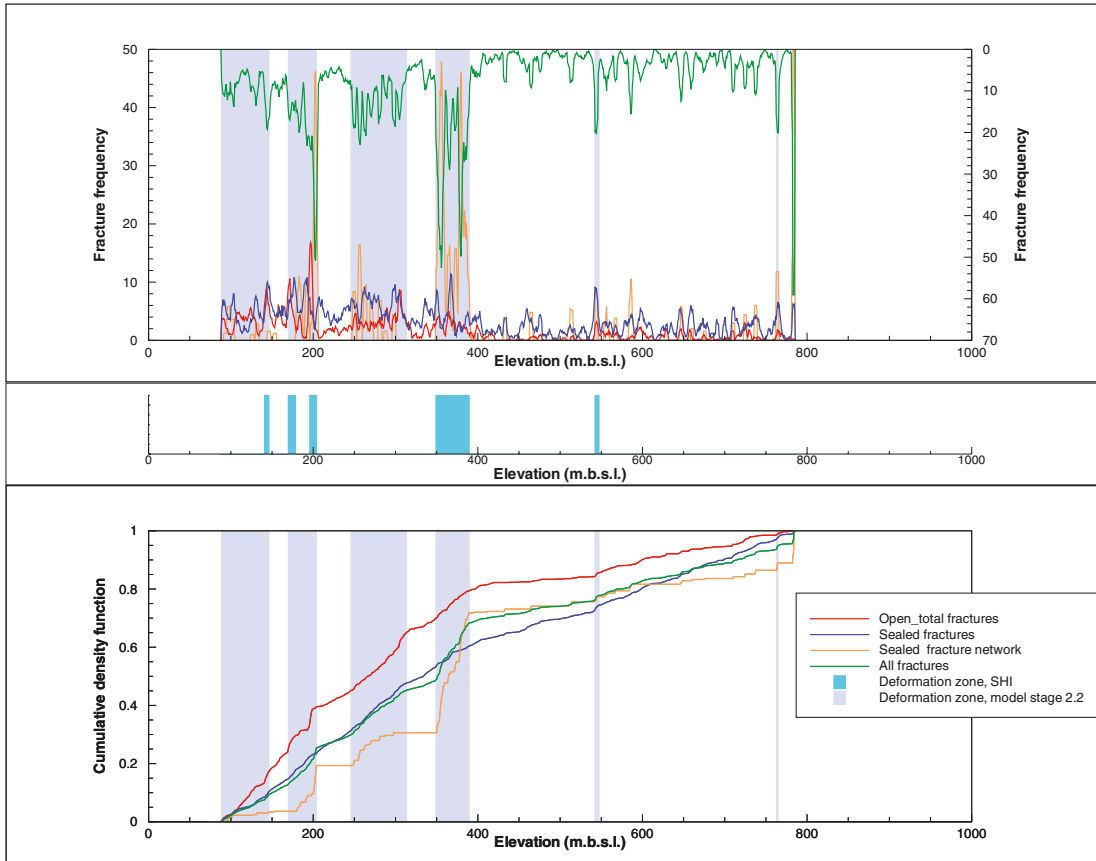
Borehole KFM03A



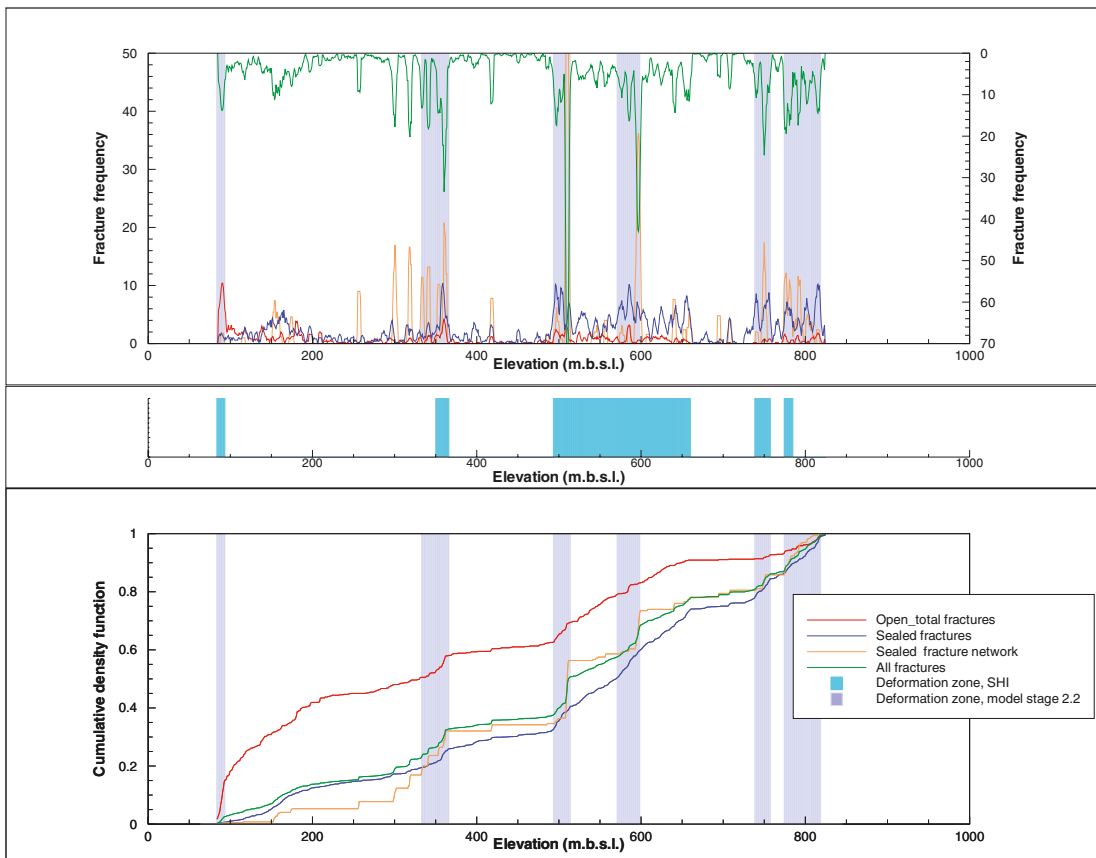
Borehole KFM03B



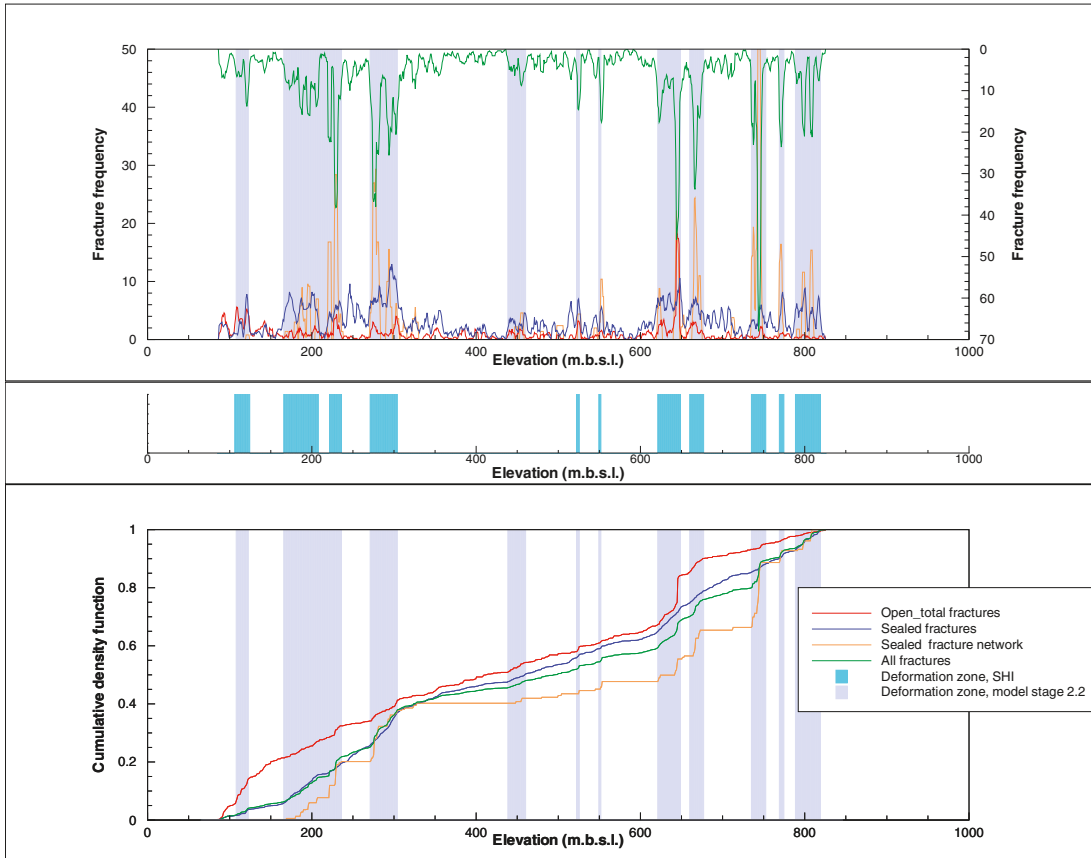
Borehole KFM04A



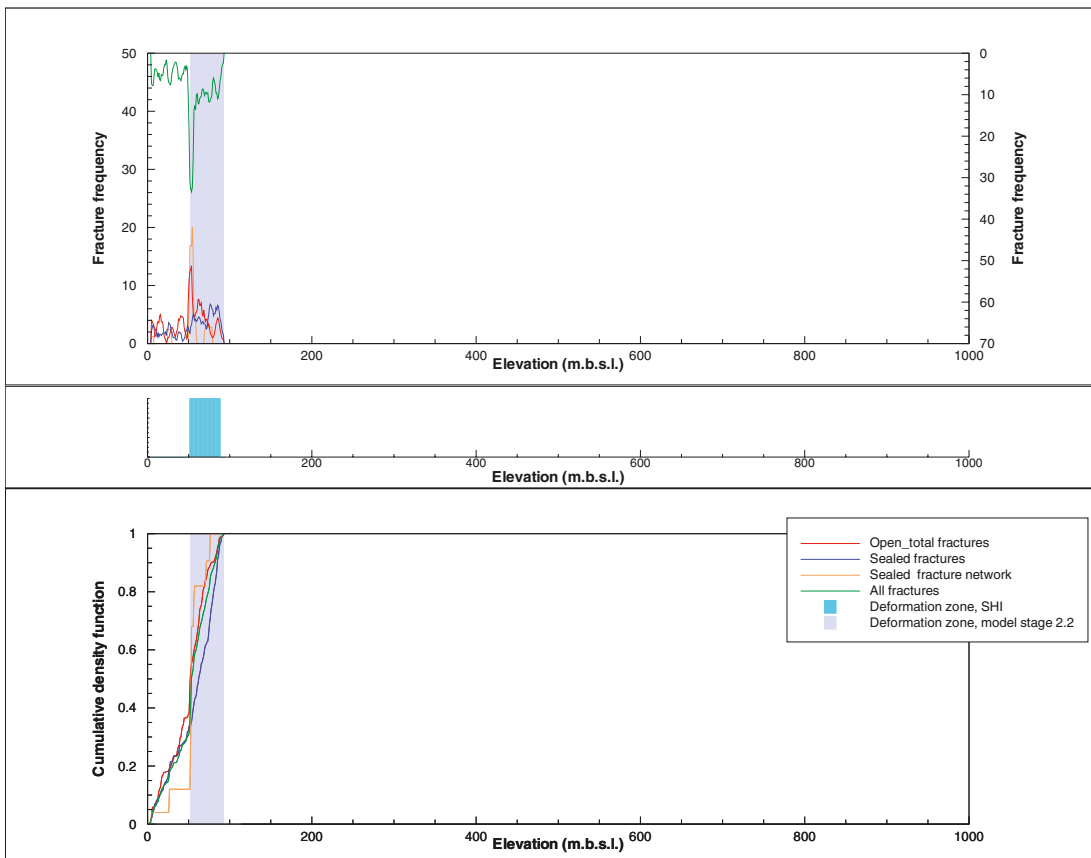
Borehole KFM05A



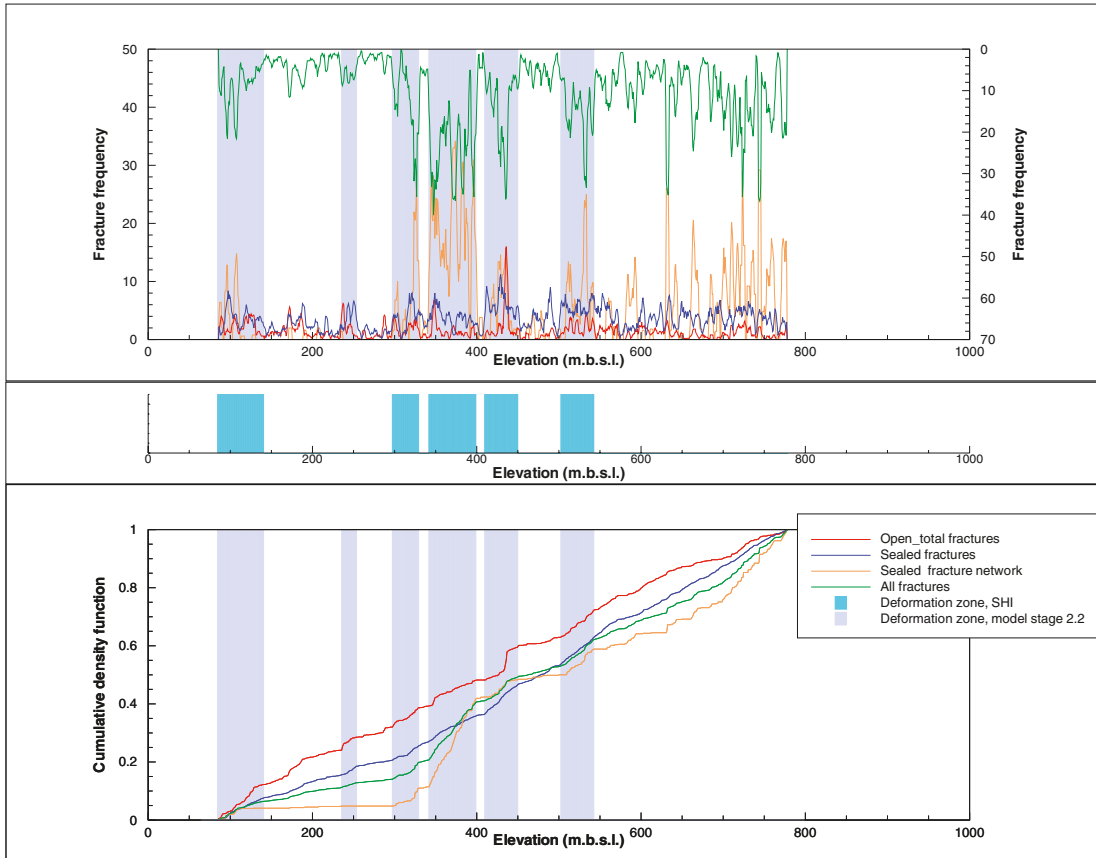
Borehole KFM06A



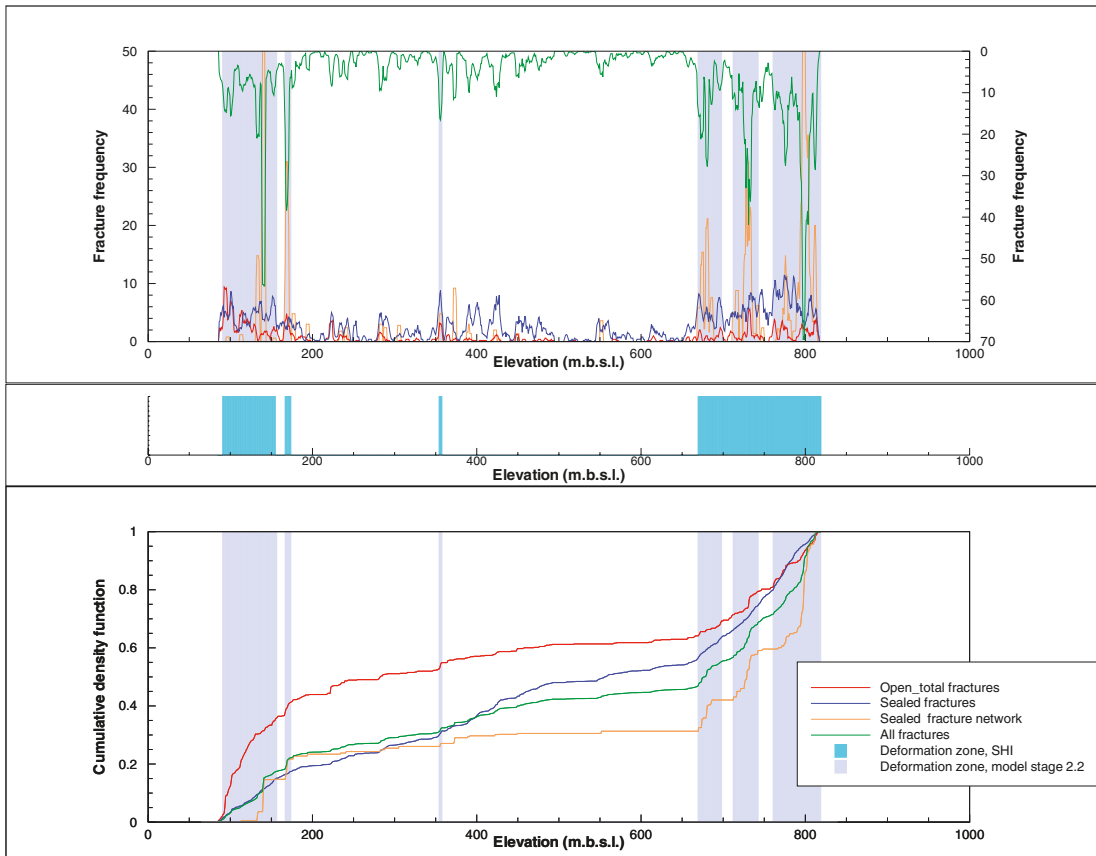
Borehole KFM06B



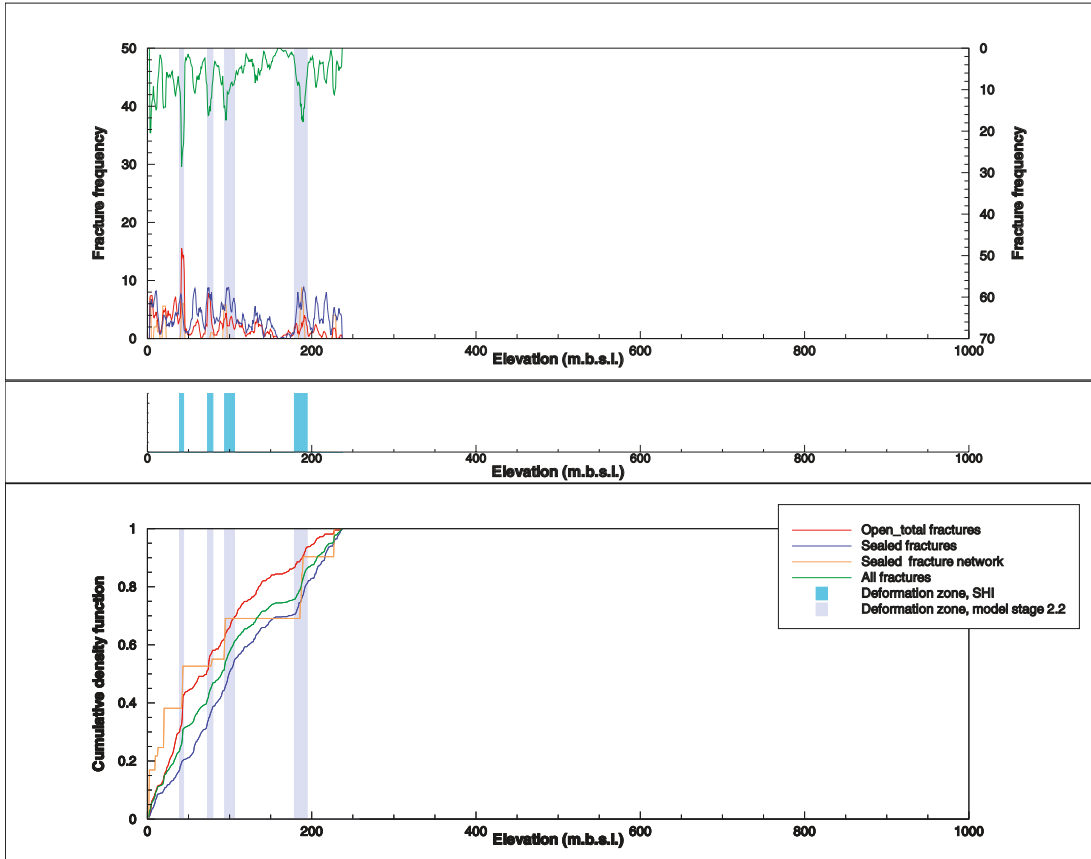
Borehole KFM06C



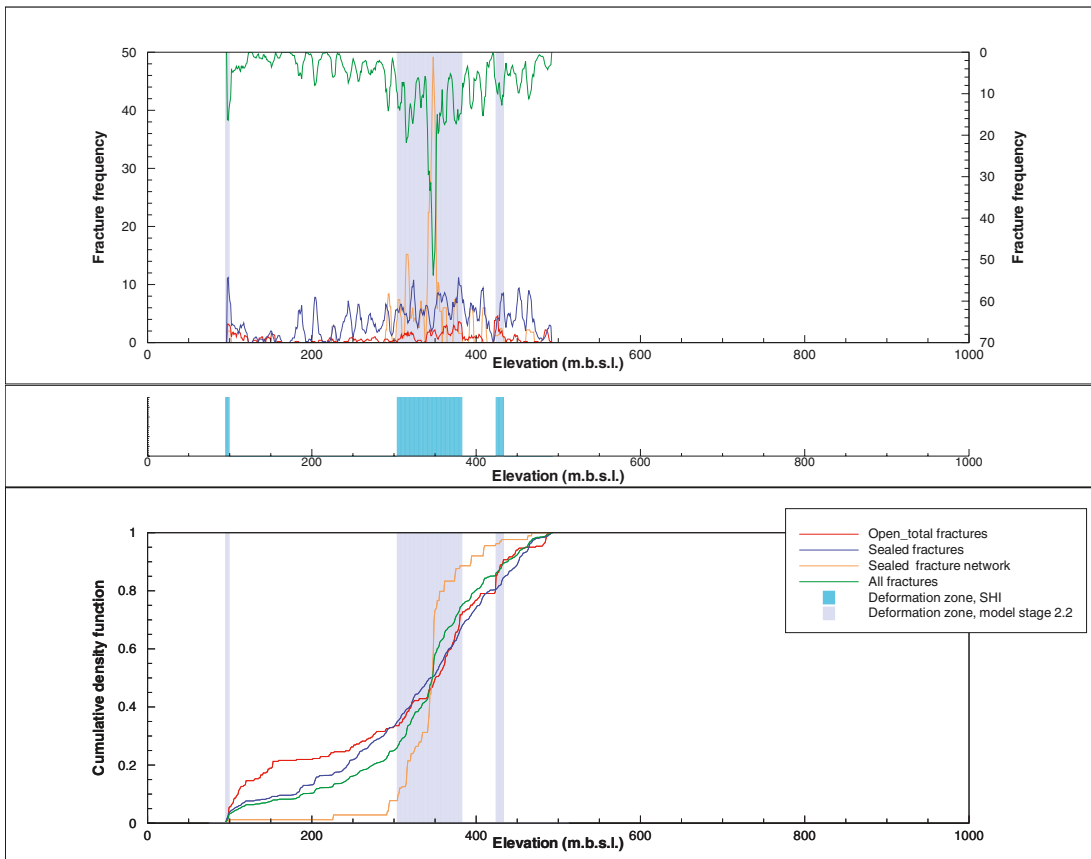
Borehole KFM07A



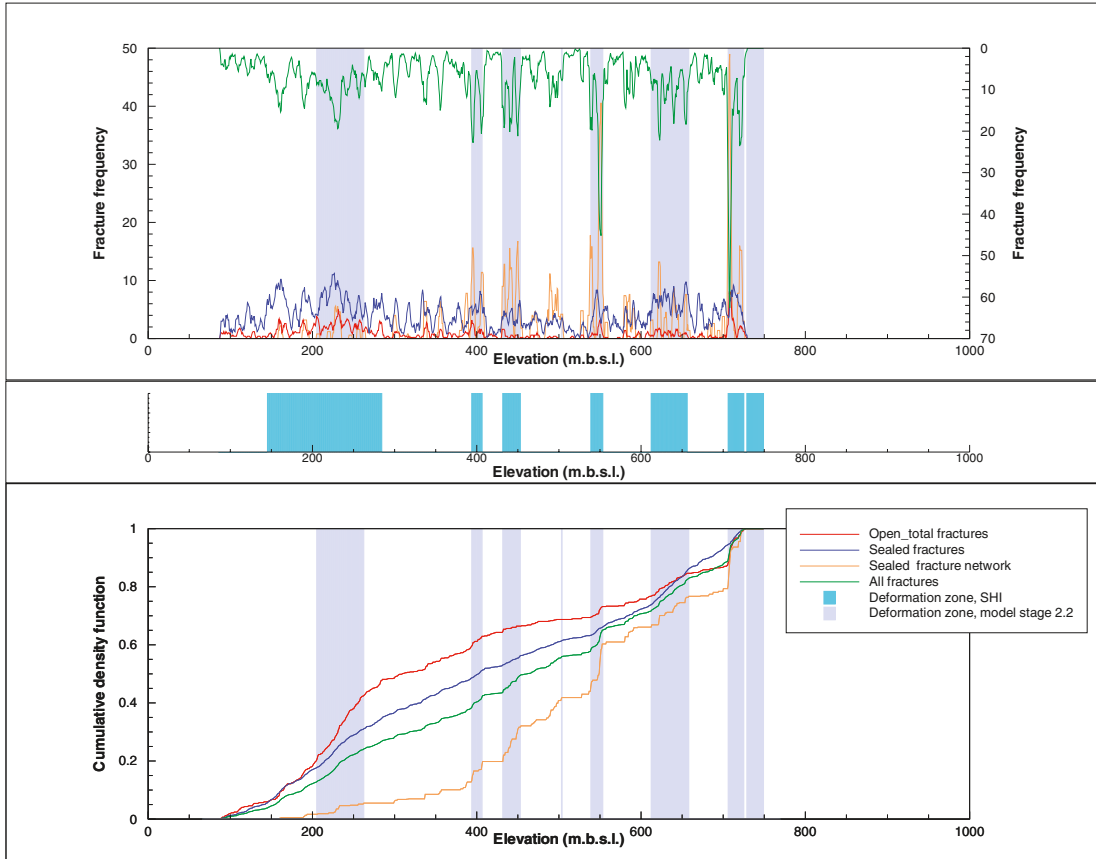
Borehole KFM07B



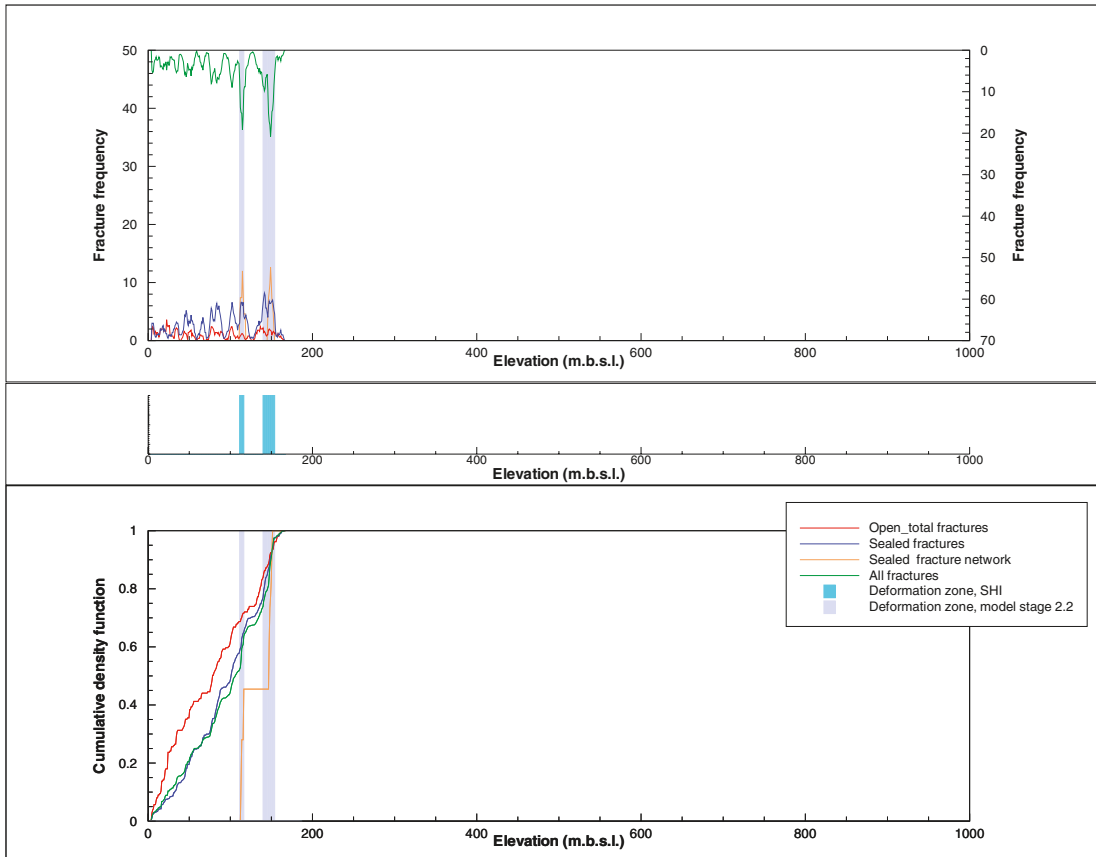
Borehole KFM07C



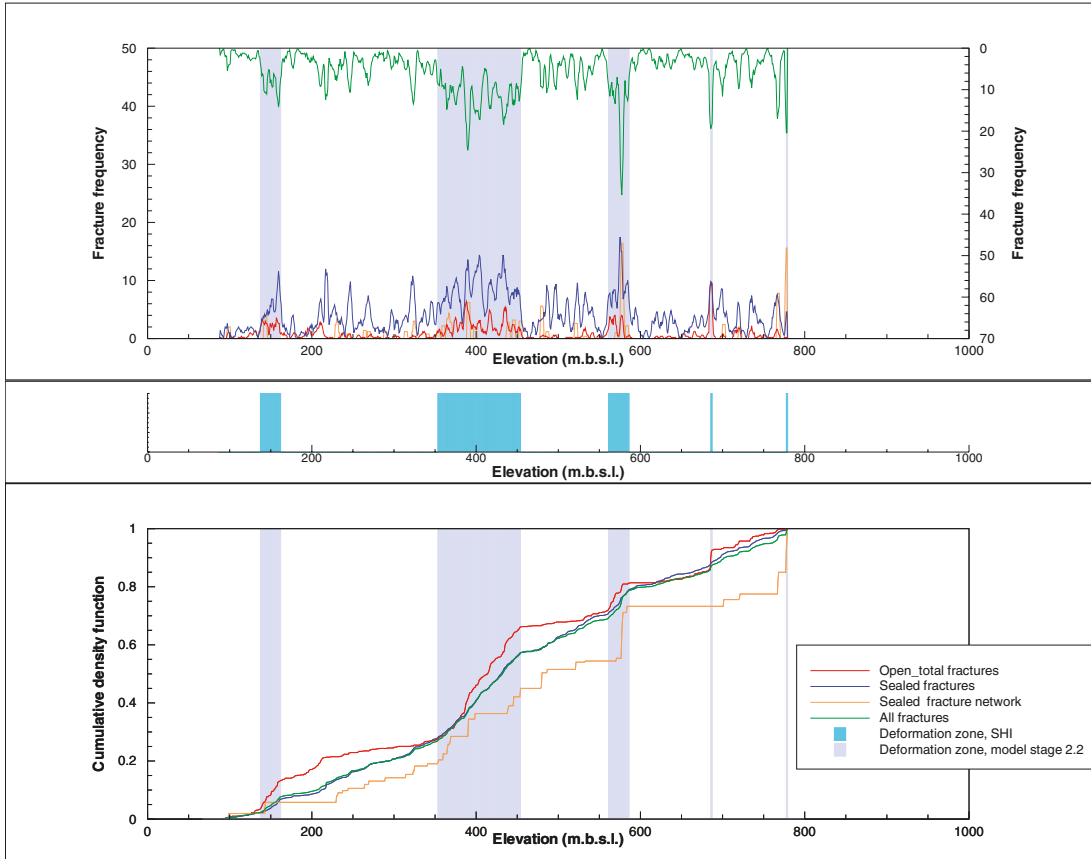
Borehole KFM08A



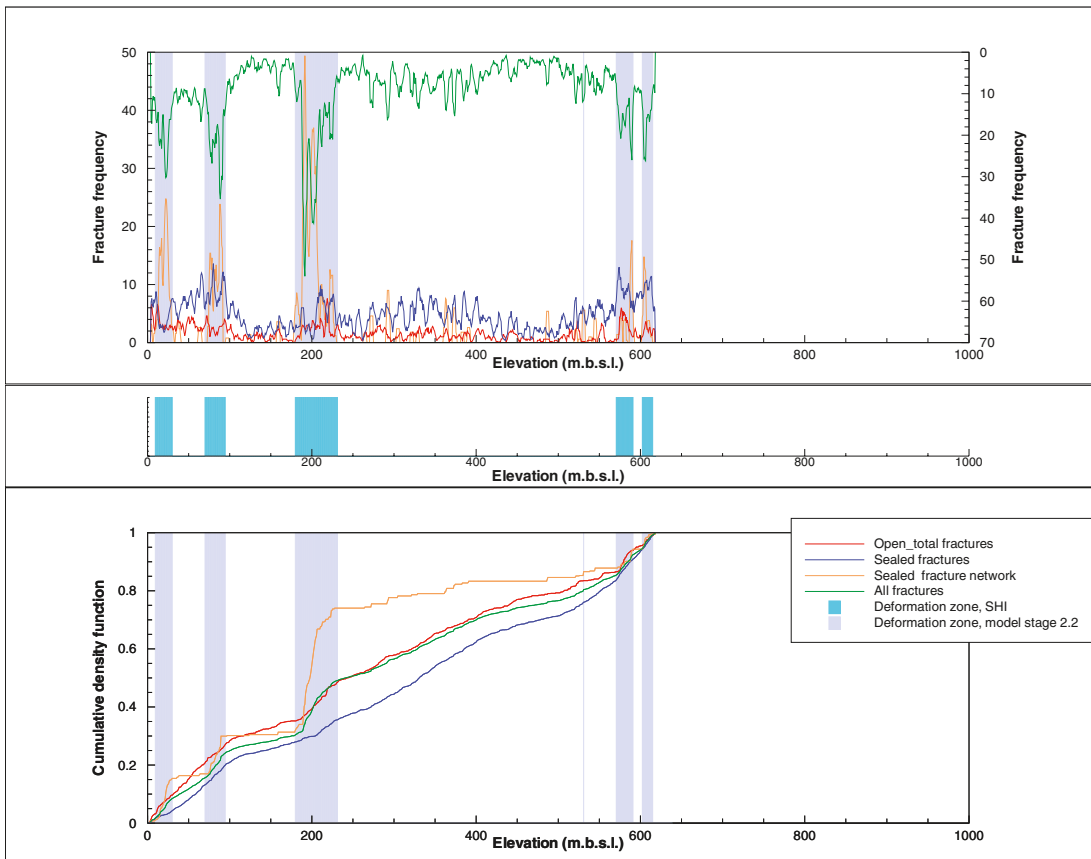
Borehole KFM08B



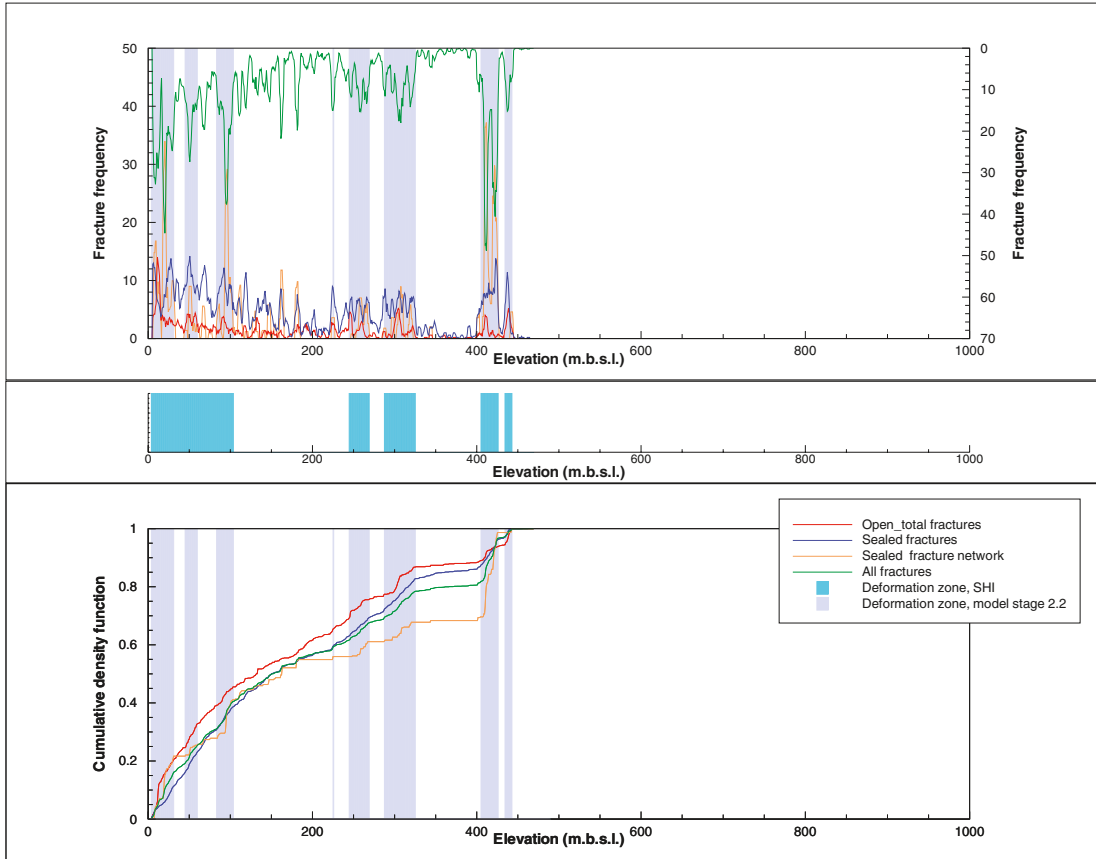
Borehole KFM08C



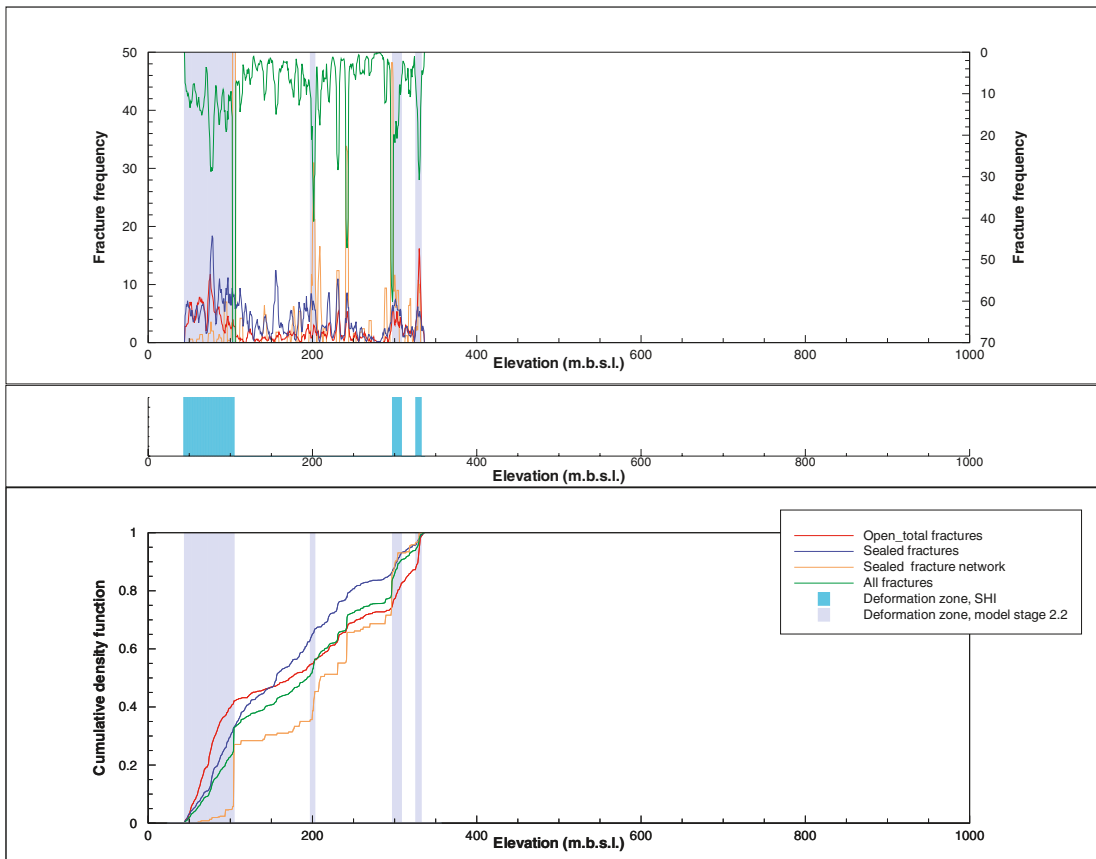
Borehole KFM09A



Borehole KFM09B



Borehole KFM10A



Presentation of fracture domains in each cored borehole

Fracture domains at the Forsmark site (FFM), which have been distinguished in each cored borehole during modelling stage 2.2, are presented in Appendix 4. These domains are shown in relation to modelled rock domains (RFM) and deformation zones (ZFM), and an overview of rock units (RU) and possible deformation zones (DZ) in the single hole interpretation (SHI) and extended single hole interpretation (ESHI). For further discussion of fracture domains in each borehole, the reader is referred to section 5.2 in the main text.

Explanation to legend in the figures. Rock groups

Different groups of rocks at the Forsmark site are distinguished on the basis of their relative age. The four groups, A to D, are defined in the table below.

Groups of rock types

All rocks are affected by brittle deformation. The fractures generally cut the boundaries between the different rock types. The boundaries are predominantly not fractured.

Rocks in Group D are affected only partly by ductile deformation and metamorphism.

Group D
(c 1,851 million years)

- Fine- to medium-grained granite and aplite (111058). Pegmatitic granite and pegmatite (101061).

Variable age relationships with respect to Group C. Occur as dykes and minor bodies that are commonly discordant and, locally, strongly discordant to ductile deformation in older rocks.

Rocks in Group C are affected by penetrative ductile deformation under lower amphibolite-facies metamorphic conditions.

Group C
(c 1,864 million years)

- Fine- to medium-grained granodiorite, tonalite and subordinate granite (101051).

Occur as lenses and dykes in Groups A and B. Intruded after some ductile deformation in the rocks belonging to Groups A and B with weakly discordant contacts to ductile deformation in these older rocks.

Rocks in Groups A and B are affected by penetrative ductile deformation under amphibolite-facies metamorphic conditions.

Group B
(c 1,886–1,865 million years)

- Biotite-bearing granite (to granodiorite) (101057) and aplitic granite (101058), both with amphibolite (102017) as dykes and irregular inclusions. Local albitisation (104) of granitic rocks.

- Tonalite to granodiorite (101054) with amphibolite (102017) enclaves. Granodiorite (101056).

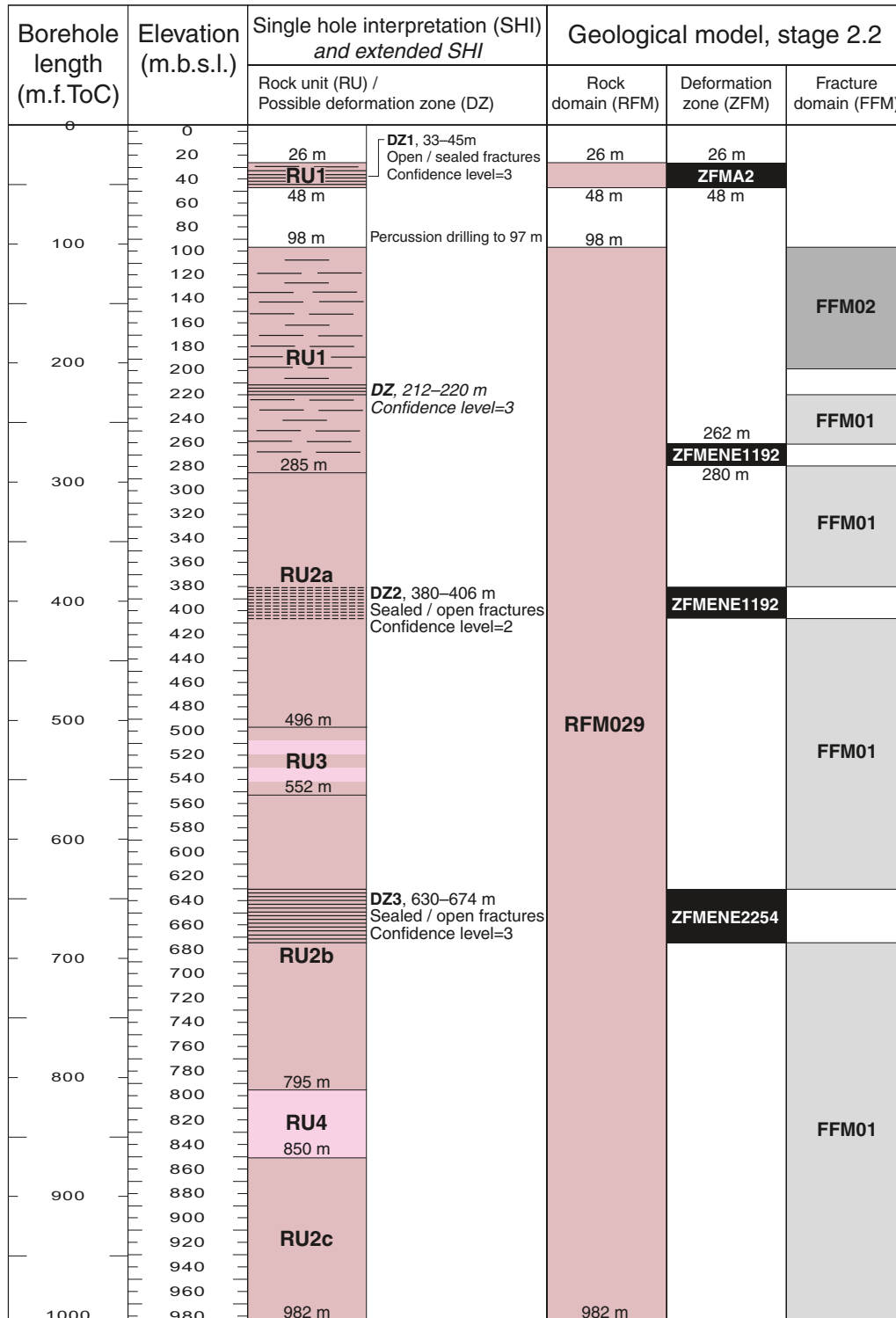
- Ultramafic rock (101004). Gabbro, diorite and quartz diorite (101033).

Group A
(supracrustal rocks older than 1,885 million years)

- Sulphide mineralisation, possibly epigenetic (109010).

- Volcanic rock (103076), calc-silicate rock (108019) and iron oxide mineralisation (109014). Subordinate sedimentary rocks (106001).

KFM01A

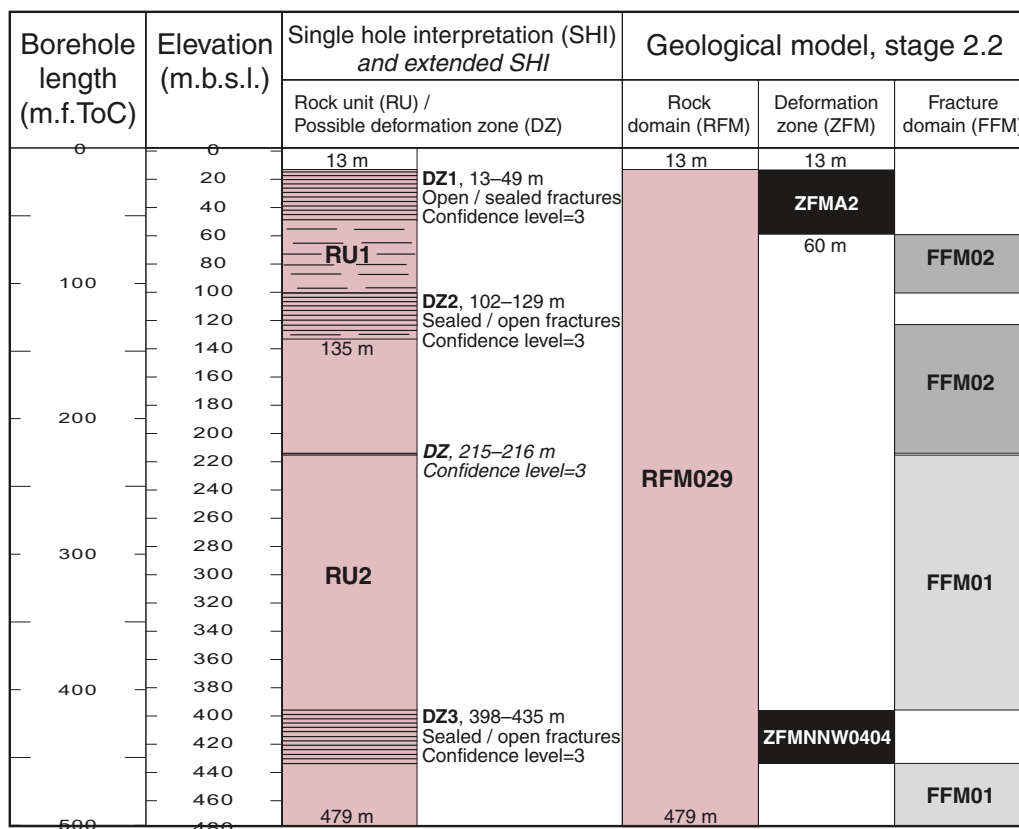


Legend for single hole interpretation

- | | |
|--|---|
| <ul style="list-style-type: none"> Increased frequency of fractures relative to other borehole sections outside deformation zones Brittle deformation zone, probable Brittle deformation zone, certain | <p>Rock type</p> <p>Group C</p> <ul style="list-style-type: none"> Granodiorite to tonalite, metamorphic, fine- to medium-grained <p>Group B</p> <ul style="list-style-type: none"> Granite (to granodiorite), metamorphic, medium-grained |
|--|---|

The elevation of a modelled deformation zone is only provided in the cases where the zone boundaries differ from the single hole interpretation. The base of FFM02 is placed at 199 m beneath sea level

KFM01B

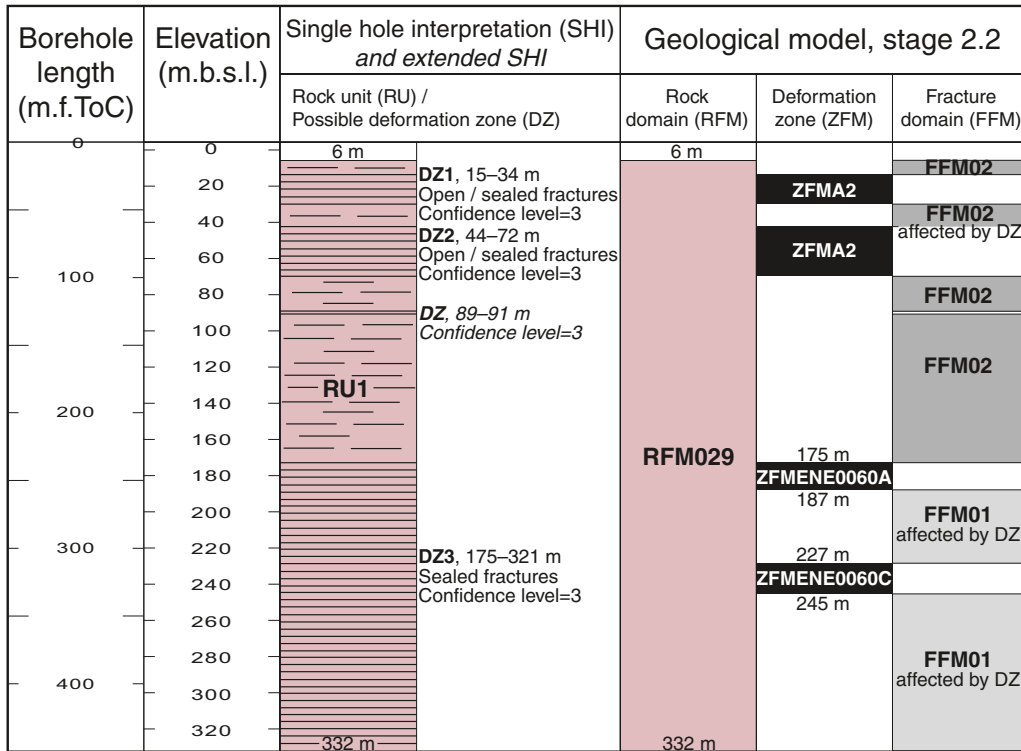


Legend for single hole interpretation

- | | |
|---|---|
| <p> Increased frequency of fractures relative to borehole sections outside the deformation zone in the lower part of the borehole</p> <p> Brittle deformation zone, certain</p> | <p>Rock type
Group B</p> <p> Granite (to granodiorite), metamorphic, medium-grained</p> |
|---|---|

The elevation of a modelled deformation zone is only provided in the cases where the zone boundaries differ from the single hole interpretation. The base of FFM02 is placed at 215 m beneath sea level

KFM01C

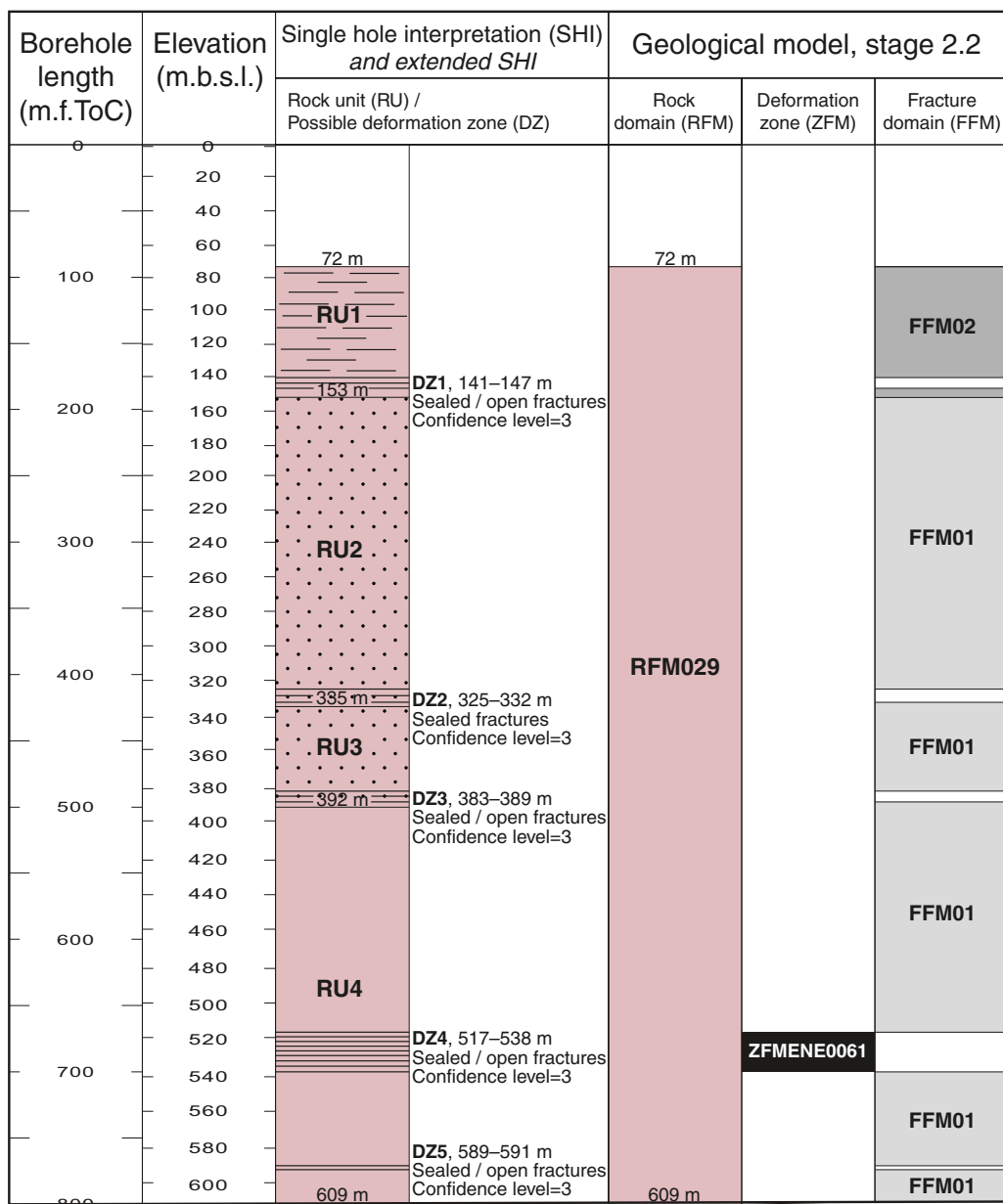


Legend for single hole interpretation

- | | |
|--|---|
| <ul style="list-style-type: none"> Increased frequency of fractures relative to lowermost part of borehole Brittle deformation zone, certain | <p>Rock type</p> <p>Group B</p> <ul style="list-style-type: none"> Granite (to granodiorite), metamorphic, medium-grained |
|--|---|

The elevation of a modelled deformation zone is only provided in the cases where the zone boundaries differ from the single hole interpretation

KFM01D



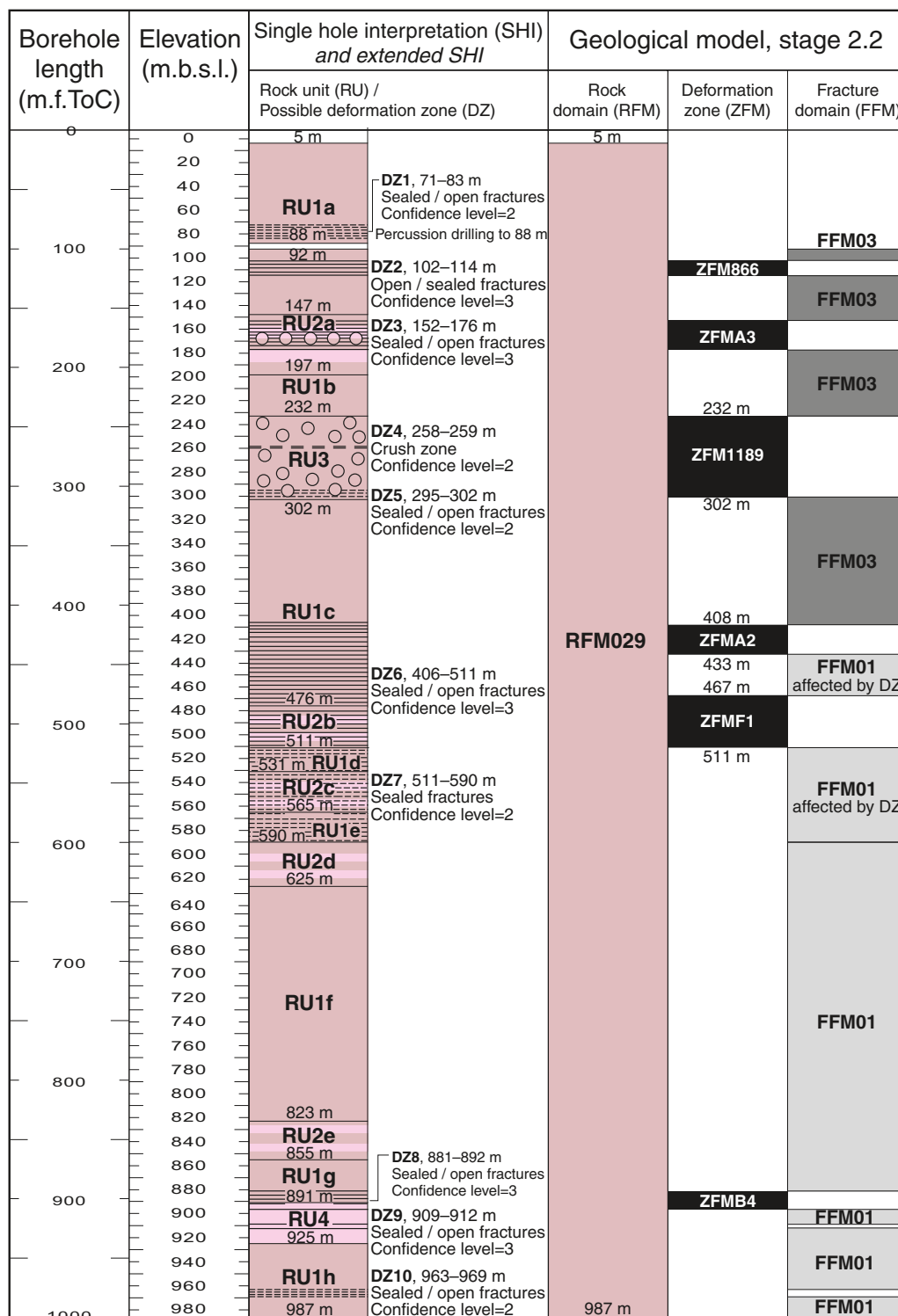
Legend for single hole interpretation

- Increased frequency of fractures relative to other borehole sections outside deformation zones
- Brittle deformation zone, certain

Rock type Group B

- Granite (to granodiorite), metamorphic, fine- to medium-grained. Static recrystallisation in RU3
- Granite (to granodiorite), metamorphic, medium-grained

KFM02A



Legend for single hole interpretation

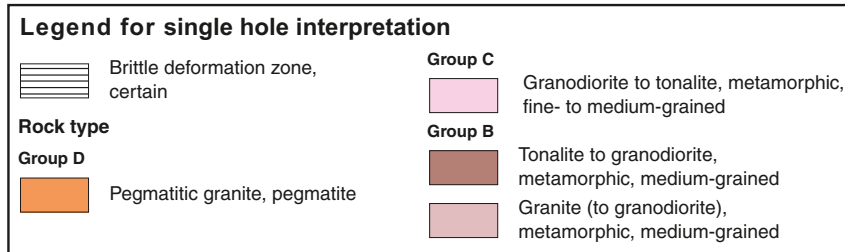
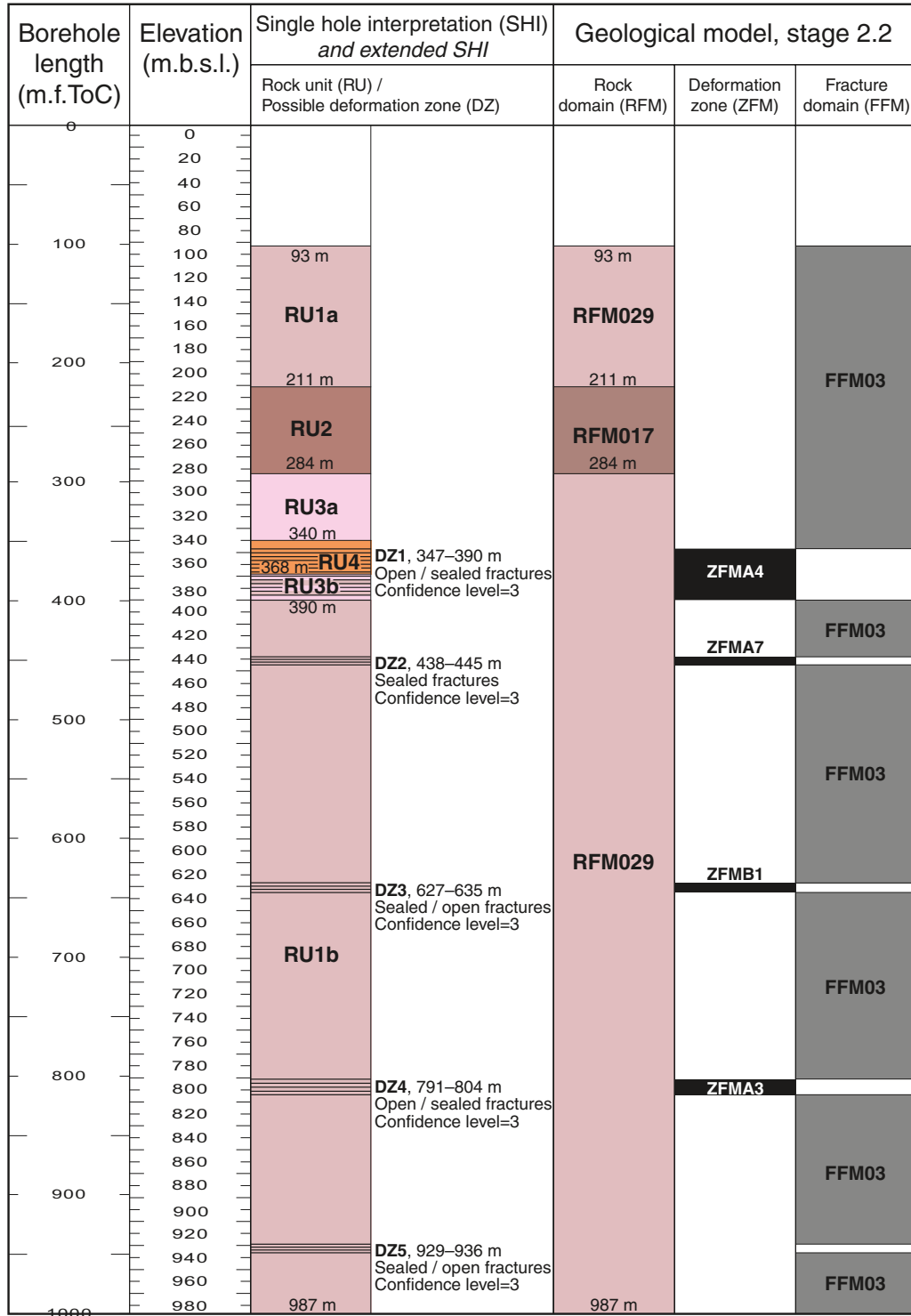
- Brittle deformation zone, probable
- Brittle deformation zone, certain
- Strongly altered, vuggy rock

Rock type

- Group C**
- Granodiorite to tonalite, metamorphic, fine- to medium-grained
- Group B**
- Granite (to granodiorite), metamorphic, medium-grained

The elevation of a modelled deformation zone is only provided in the cases where the zone boundaries differ from the single hole interpretation


KFM03A




KFM03B

Borehole length (m.f.ToC)	Elevation (m.b.s.l.)	Single hole interpretation (SHI) <i>and extended SHI</i>		Geological model, stage 2.2		
		Rock unit (RU) / Possible deformation zone (DZ)		Rock domain (RFM)	Deformation zone (ZFM)	Fracture domain (FFM)
0	0	2 m.a.s.l.		2 m.a.s.l.		
50	20	DZ1, 15–33 m Sealed / open fractures Confidence level=2	RFM029		ZFMA5	FFM03
	40	RU1 DZ2, 53–58 m Sealed / open fractures				FFM03
	60	Sealed / open fractures				
	80	88 m Confidence level=3		88 m		FFM03

Legend for single hole interpretation

 Brittle deformation zone, probable


 Brittle deformation zone, certain

Rock type

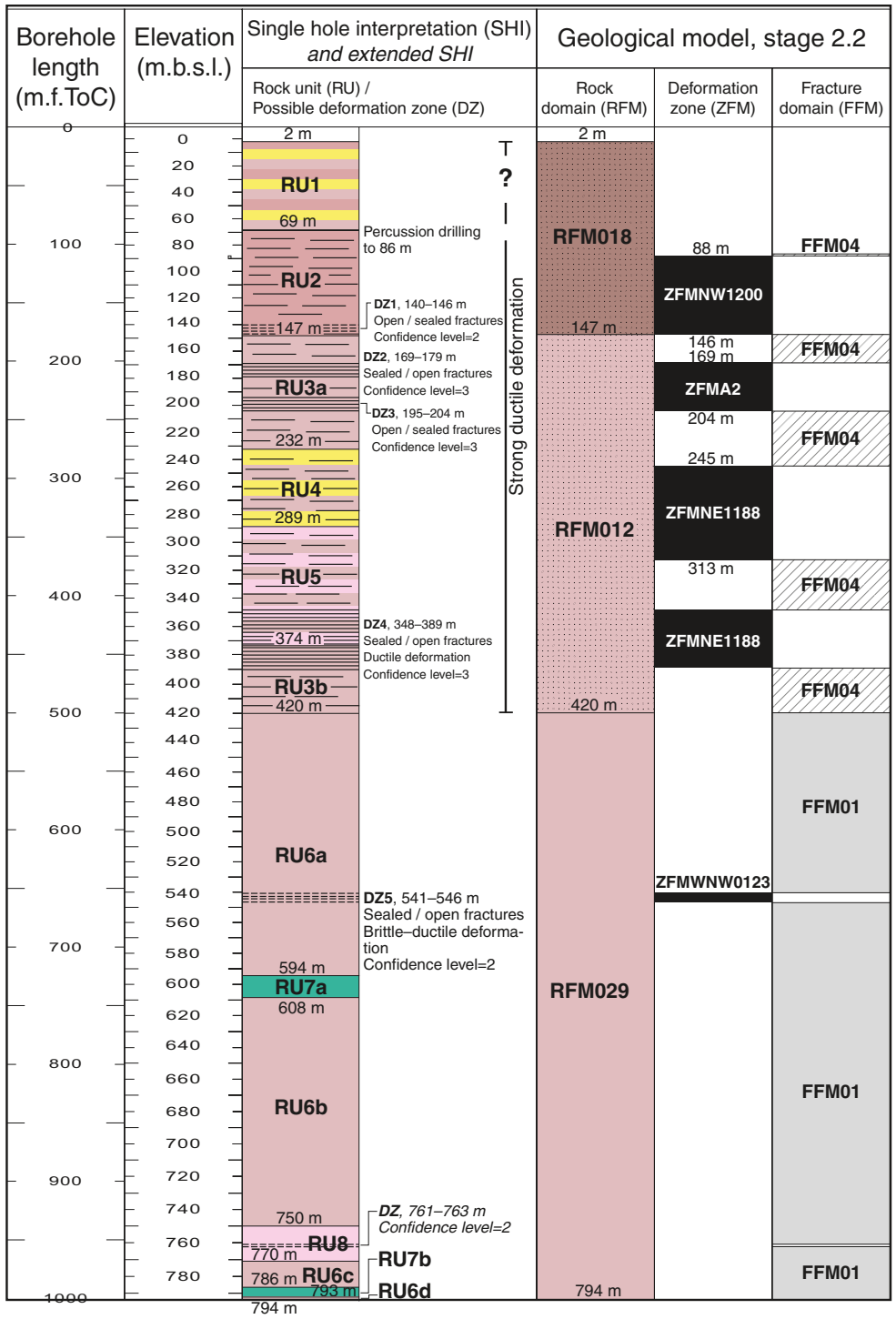
Group D

 Pegmatitic granite, pegmatite

Group B

 Granite (to granodiorite), metamorphic, medium-grained

KFM04A

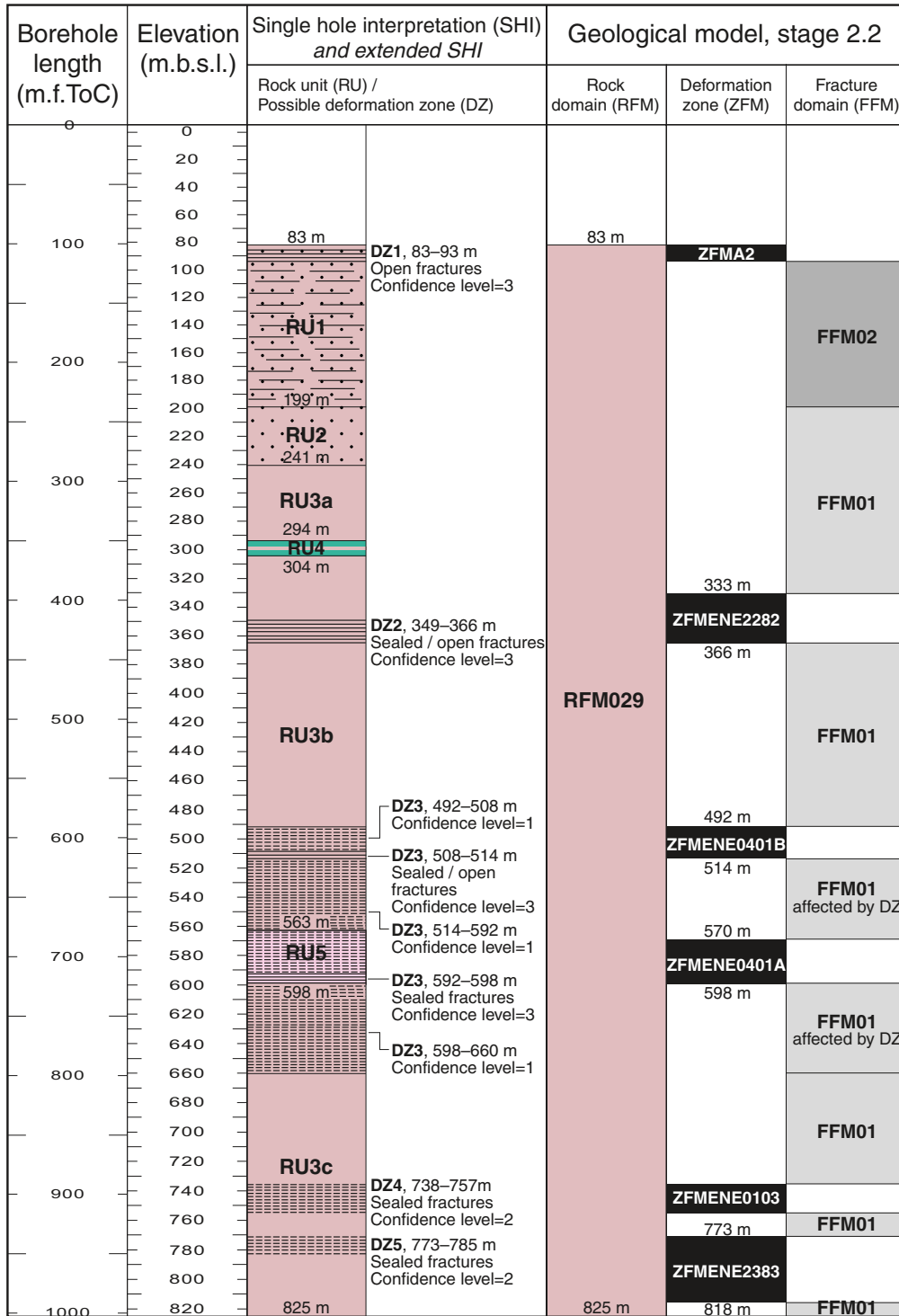


Legend for single hole interpretation

- | | | |
|--|---|---|
| <ul style="list-style-type: none"> Increased frequency of fractures relative to other borehole sections outside deformation zones Brittle deformation zone, probable Brittle deformation zone, certain | <p>Rock type</p> <p>Group C</p> <ul style="list-style-type: none"> Granodiorite to tonalite, metamorphic, fine- to medium-grained <p>Group B</p> <ul style="list-style-type: none"> Granite (to granodiorite), metamorphic | <ul style="list-style-type: none"> Felsic to intermediate metavolcanic rock Granodiorite, metamorphic Amphibolite |
|--|---|---|

The elevation of a modelled deformation zone is only provided in the cases where the zone boundaries differ from the single hole interpretation

KFM05A



Legend for single hole interpretation

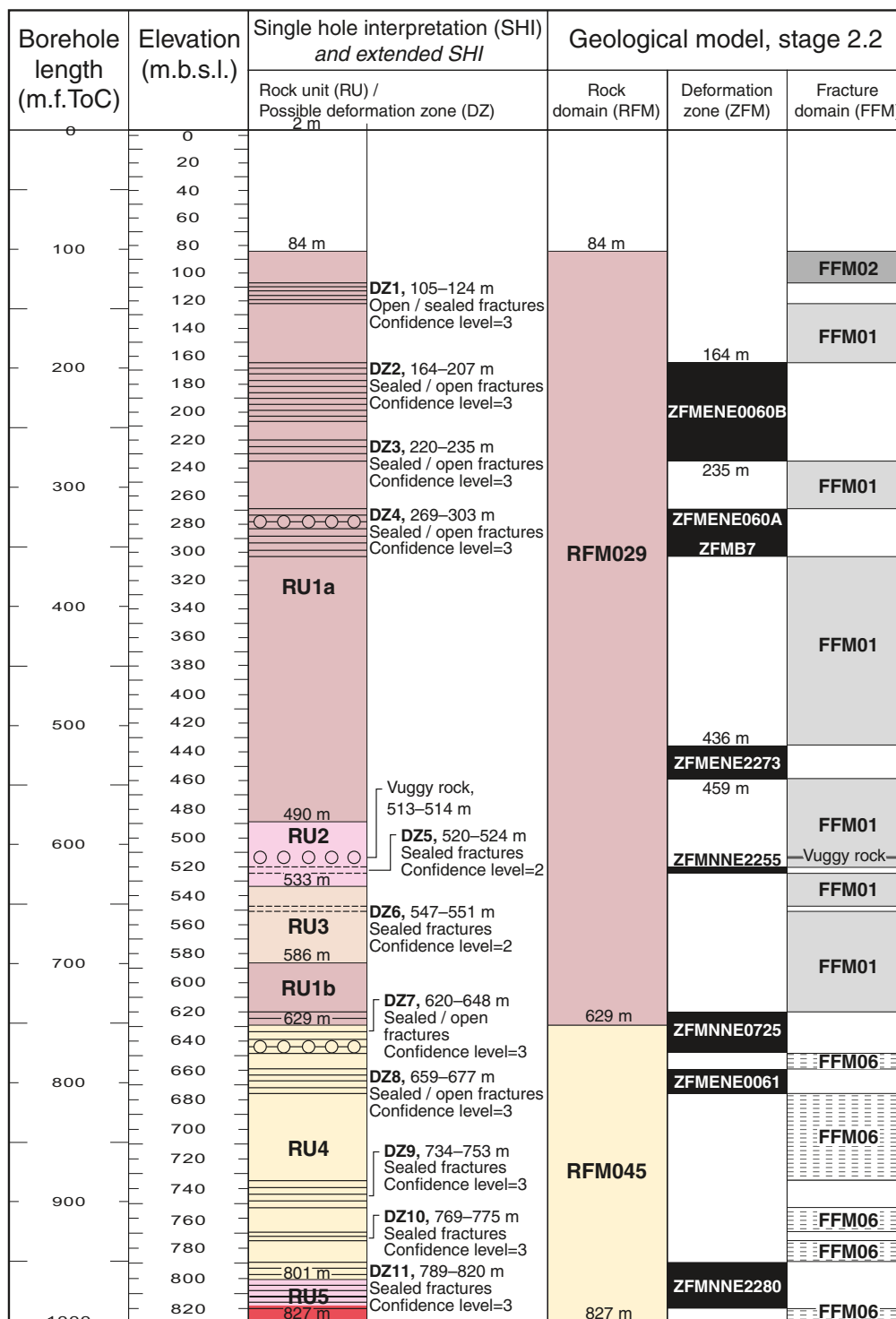
- Increased frequency of fractures relative to other borehole sections outside deformation zones
- Brittle deformation zone, probable or possible
- Brittle deformation zone, certain

Rock type

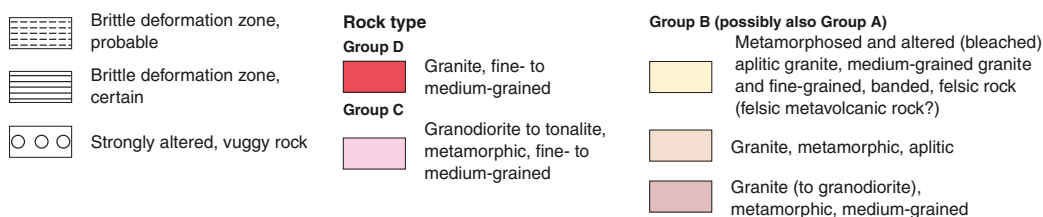
- Group C** Granodiorite to tonalite, metamorphic, fine- to medium-grained
- Group B** Granite (to granodiorite), metamorphic, fine- to medium-grained
- Granite (to granodiorite), metamorphic, medium-grained
- Amphibolite

The elevation of a modelled deformation zone is only provided in the cases where the zone boundaries differ from the single hole interpretation

KFM06A



Legend for single hole interpretation



The elevation of a modelled deformation zone is only provided in the cases where the zone boundaries differ from the single hole interpretation. The base of FFM02 is placed at 107 m beneath sea level. The top of FFM01 is placed at 122 m beneath sea level

KFM06B

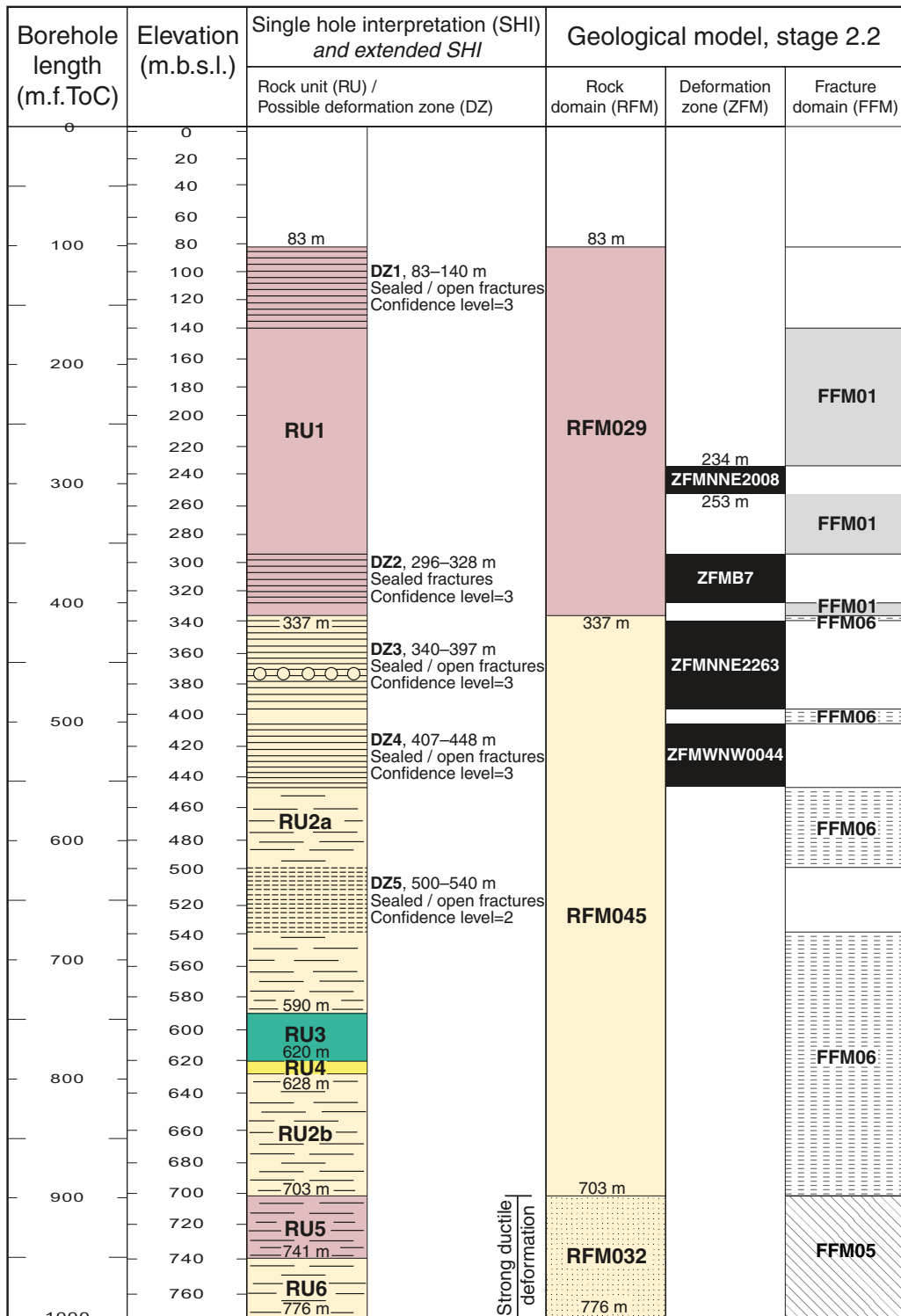
Borehole length (m.f.ToC)	Elevation (m.b.s.l.)	Single hole interpretation (SHI) <i>and extended SHI</i>		Geological model, stage 2.2		
		Rock unit (RU) / Possible deformation zone (DZ)	Rock domain (RFM)	Deformation zone (ZFM)	Fracture domain (FFM)	
0	0	2 m	2 m			
50	20 40 60 80	<div style="background-color: #d9ead3; padding: 2px; text-align: center;">RU1</div>	<div style="background-color: #d9ead3; padding: 2px; text-align: center;">RFM029</div>		<div style="background-color: #d9ead3; padding: 2px; text-align: center;">FFM02</div>	
		<div style="background-color: #d9ead3; padding: 2px; text-align: center;"> </div>	<div style="background-color: #d9ead3; padding: 2px; text-align: center;">93 m</div>	<div style="background-color: #d9ead3; padding: 2px; text-align: center;"> </div>	<div style="background-color: #d9ead3; padding: 2px; text-align: center;"> </div>	<div style="background-color: #d9ead3; padding: 2px; text-align: center;"> </div>
		DZ1, 51–88 m Open / sealed fractures Confidence level=3		<div style="background-color: #d9ead3; padding: 2px; text-align: center;">93 m</div>	<div style="background-color: #d9ead3; padding: 2px; text-align: center;"> </div>	<div style="background-color: #d9ead3; padding: 2px; text-align: center;"> </div>
				<div style="background-color: #d9ead3; padding: 2px; text-align: center;"> </div>	<div style="background-color: #d9ead3; padding: 2px; text-align: center;"> </div>	<div style="background-color: #d9ead3; padding: 2px; text-align: center;"> </div>

Legend for single hole interpretation

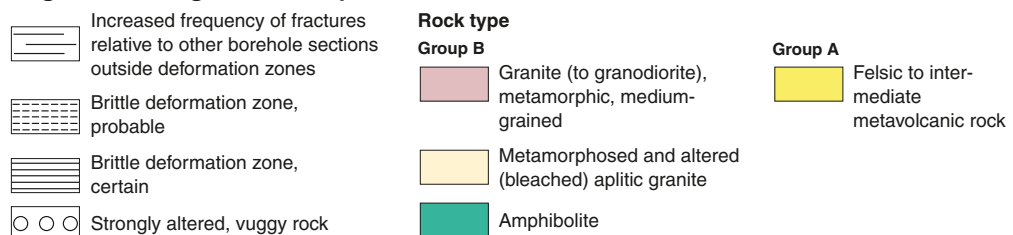
- Brittle deformation zone, certain
- Strongly altered, vuggy rock

- Rock type**
Group B
- Granite (to granodiorite), metamorphic, medium-grained

KFM06C

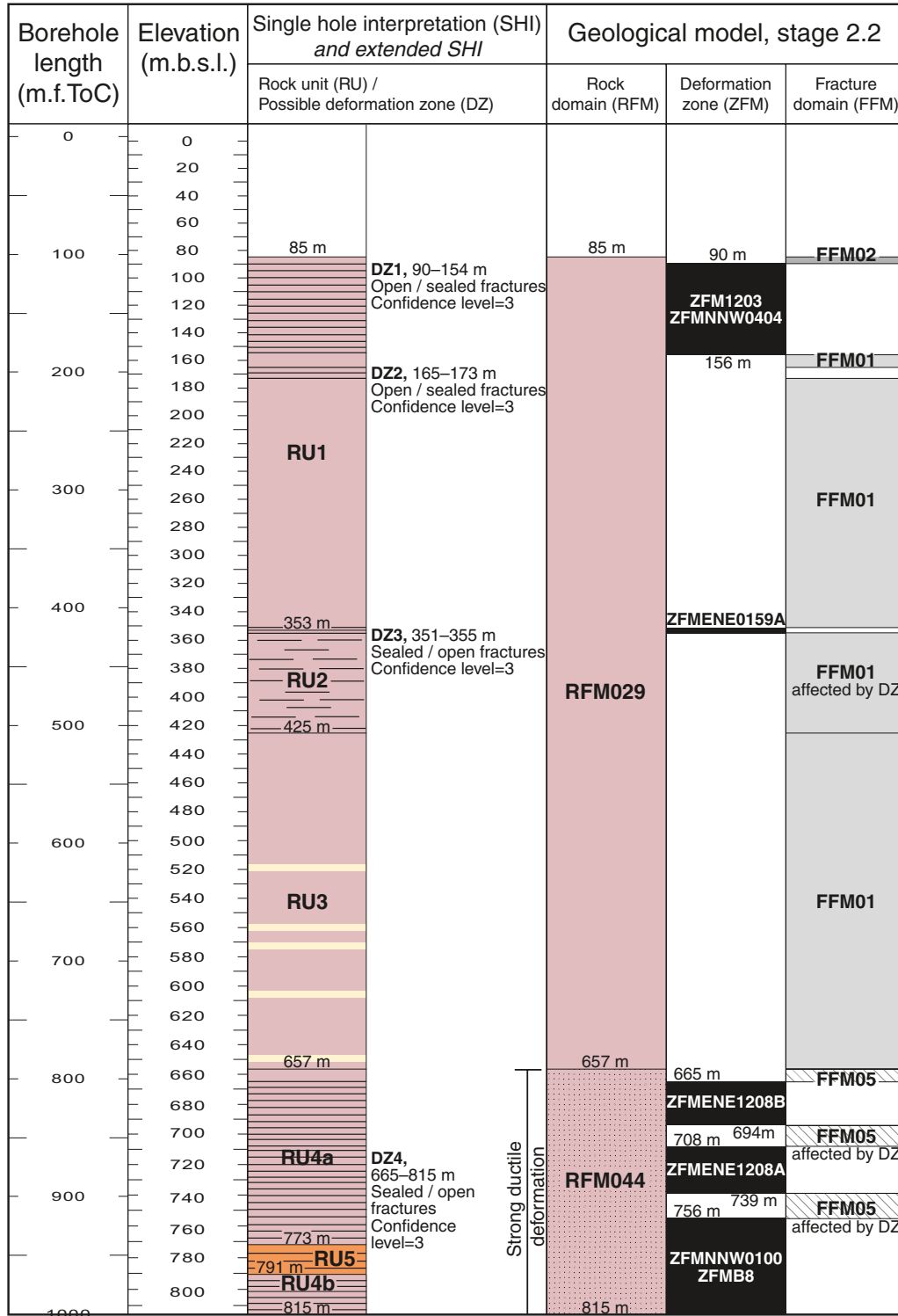


Legend for single hole interpretation

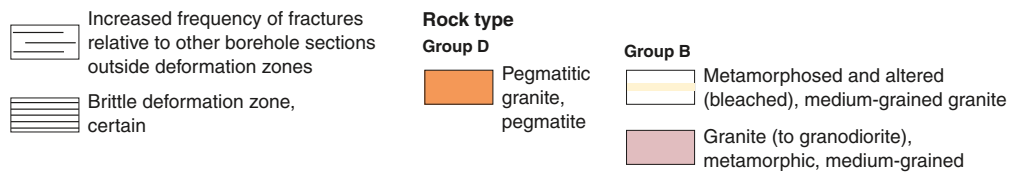


The elevation of a modelled deformation zone is only provided in the cases where the zone boundaries differ from the single hole interpretation

KFM07A

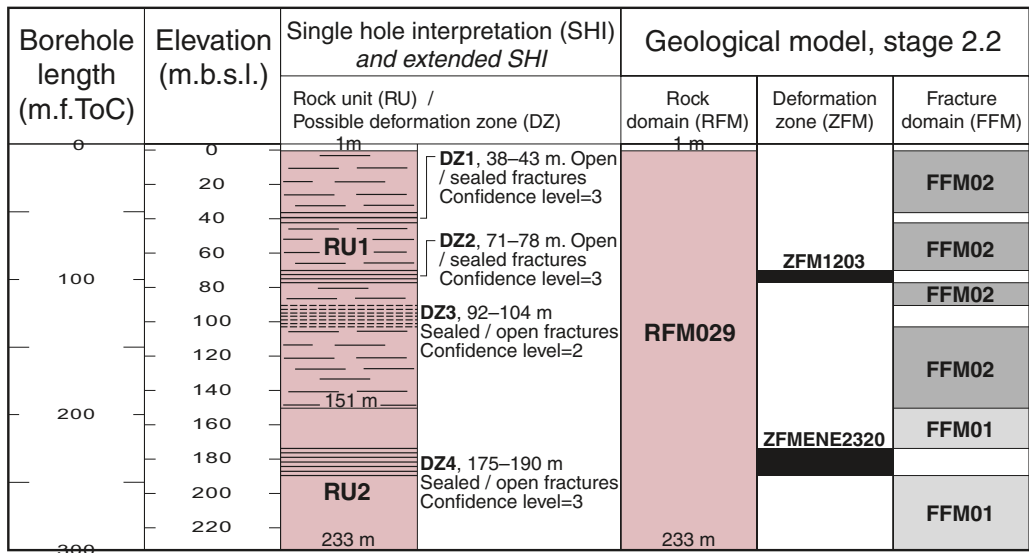


Legend for single hole interpretation

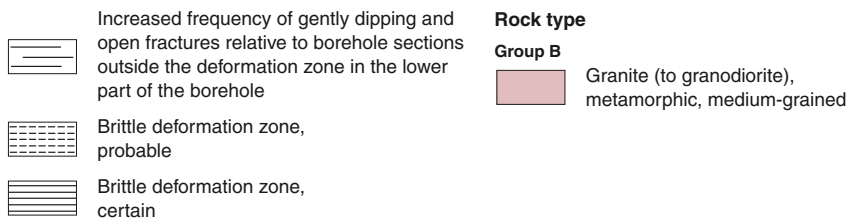


The elevation of a modelled deformation zone is only provided in the cases where the zone boundaries differ from the single hole interpretation

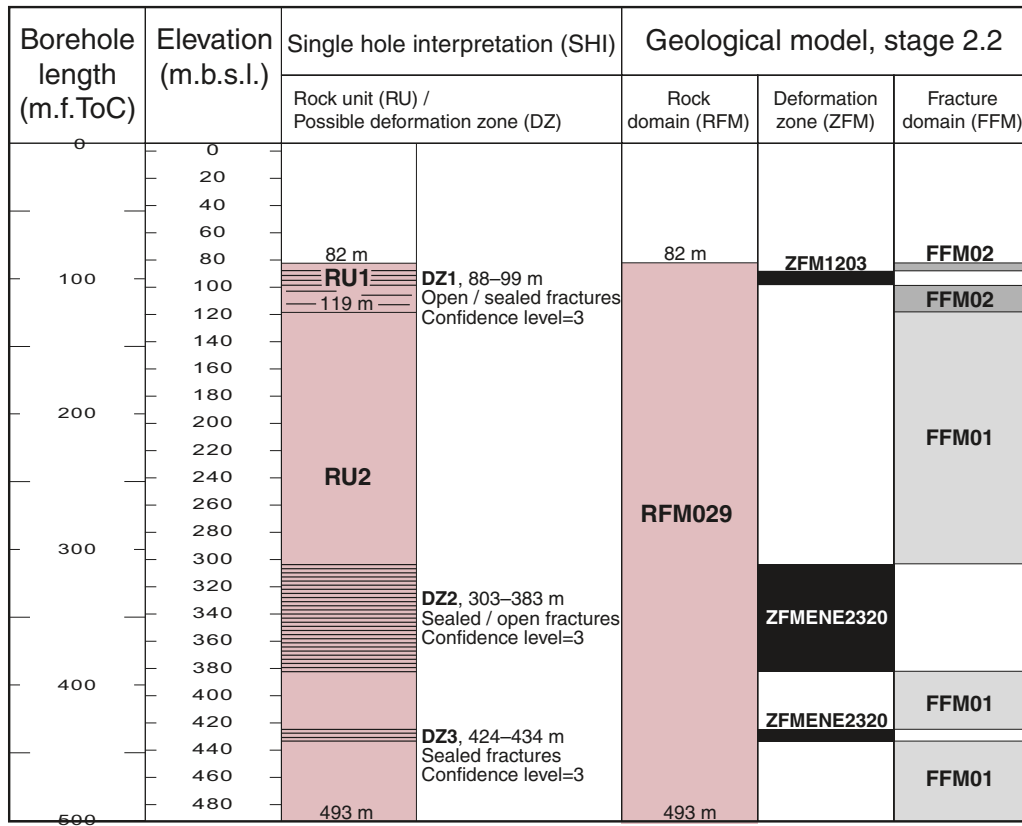
KFM07B



Legend for single hole interpretation



KFM07C



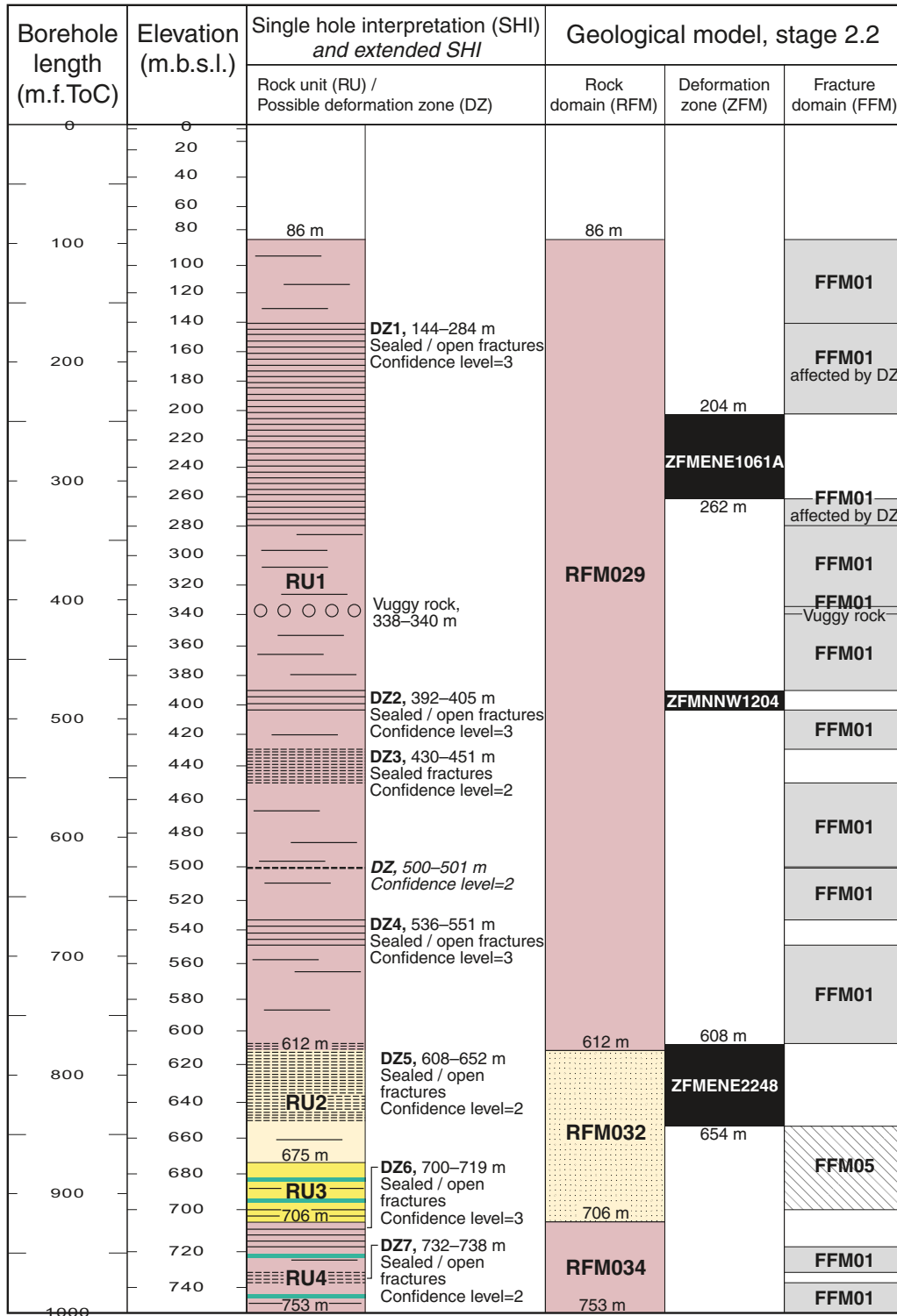
Legend for single hole interpretation

- Increased frequency of fractures relative to other borehole sections outside deformation zones
- Brittle deformation zone, certain

Rock type Group B

- Granite (to granodiorite), metamorphic, medium-grained

KFM08A



Legend for single hole interpretation

- Increased frequency of sealed fractures relative to majority of borehole sections outside deformation zones at Forsmark
- Brittle deformation zone, probable
- Brittle deformation zone, certain
- Strongly altered, vuggy rock

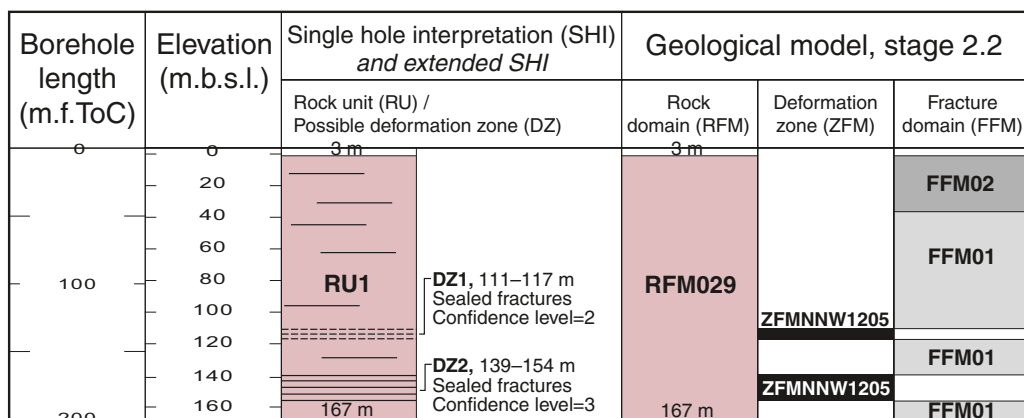
Rock type

- Group B**
- Amphibolite
- Metamorphosed and altered (bleached), aplitic granite
- Granite (to granodiorite), metamorphic, medium-grained

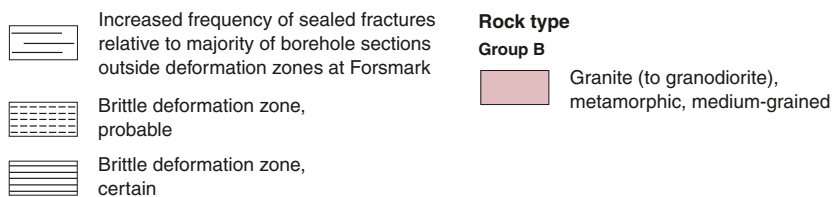
- Group A**
- Felsic metavolcanic rock

The elevation of a modelled deformation zone is only provided in the cases where the zone boundaries differ from the single hole interpretation

KFM08B

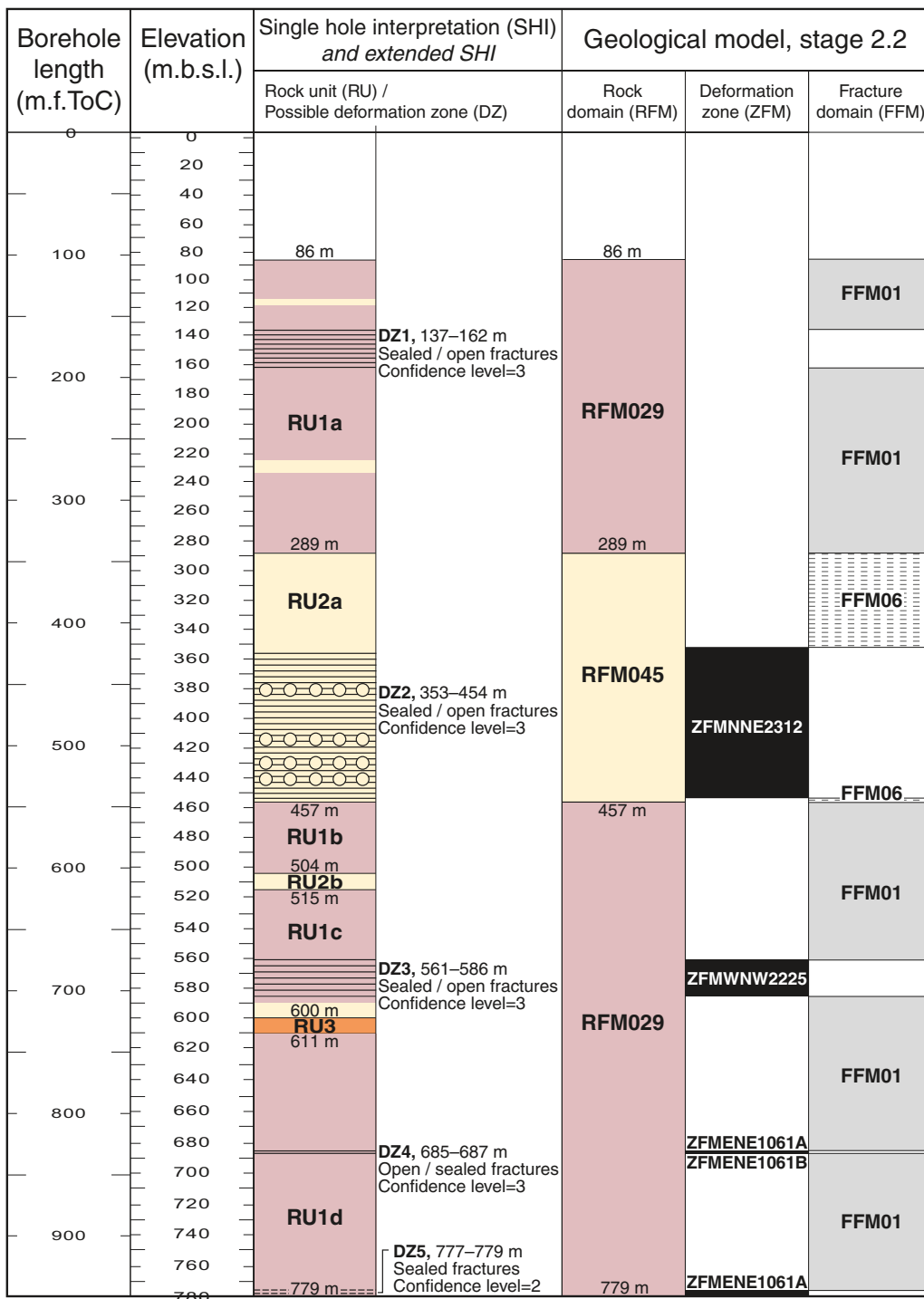


Legend for single hole interpretation



The base of FFM02 is placed at 37 m beneath sea level

KFM08C



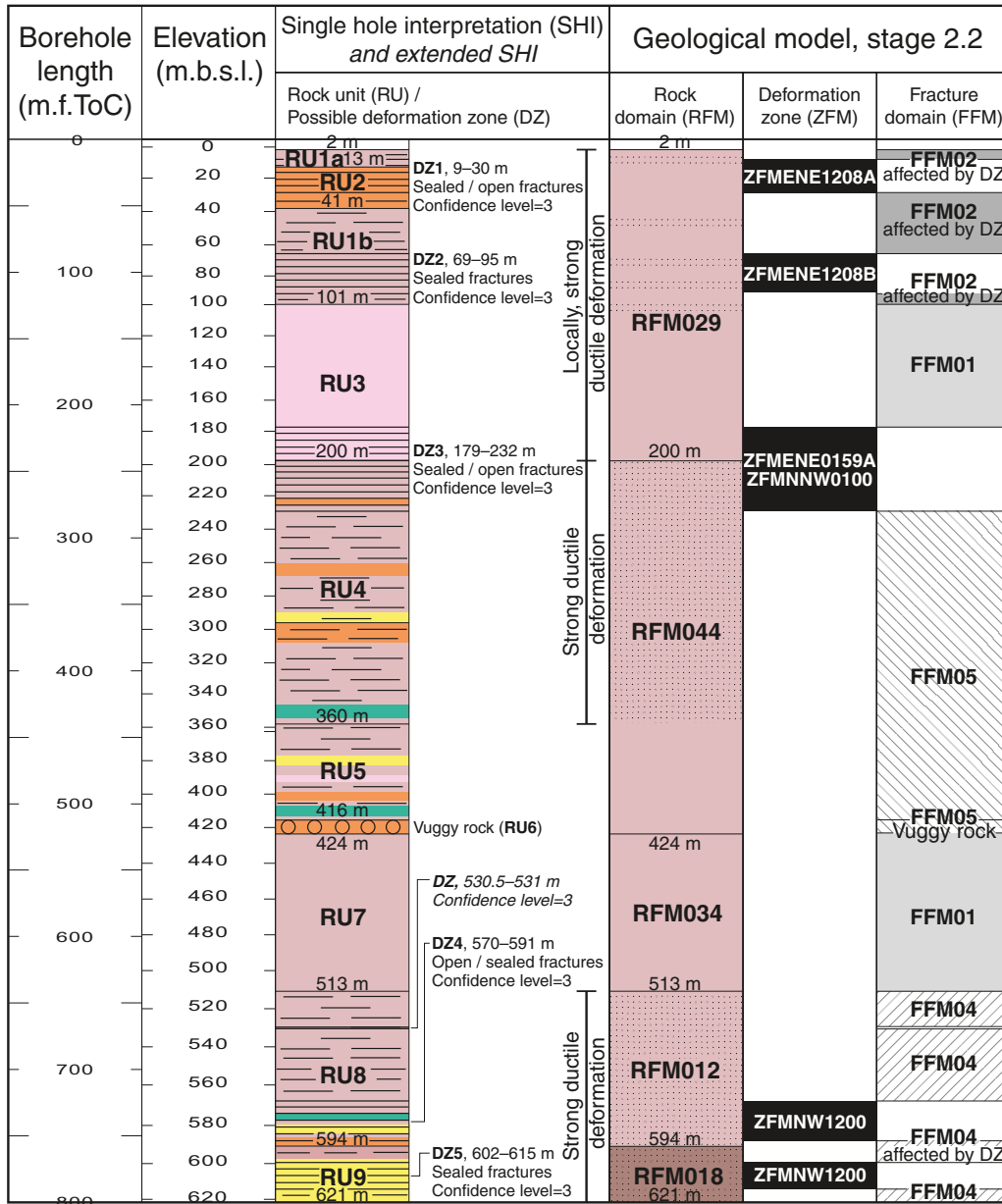
Legend for single hole interpretation

- Brittle deformation zone, probable
- Brittle deformation zone, certain
- Strongly altered, vuggy rock

Rock type

- Group D**
- Pegmatitic granite, pegmatite
- Group B**
- Metamorphosed and altered (bleached) medium-grained granite and aplitic granite
- Granite (to granodiorite), metamorphic, medium-grained

KFM09A



Legend for single hole interpretation

- Increased frequency of fractures relative to other borehole sections outside deformation zones
- Brittle deformation zone, certain
- Strongly altered, vuggy rock

Rock type

- Group D**
- Pegmatitic granite, pegmatite

Group C

- Granodiorite to tonalite, metamorphic, fine- to medium-grained

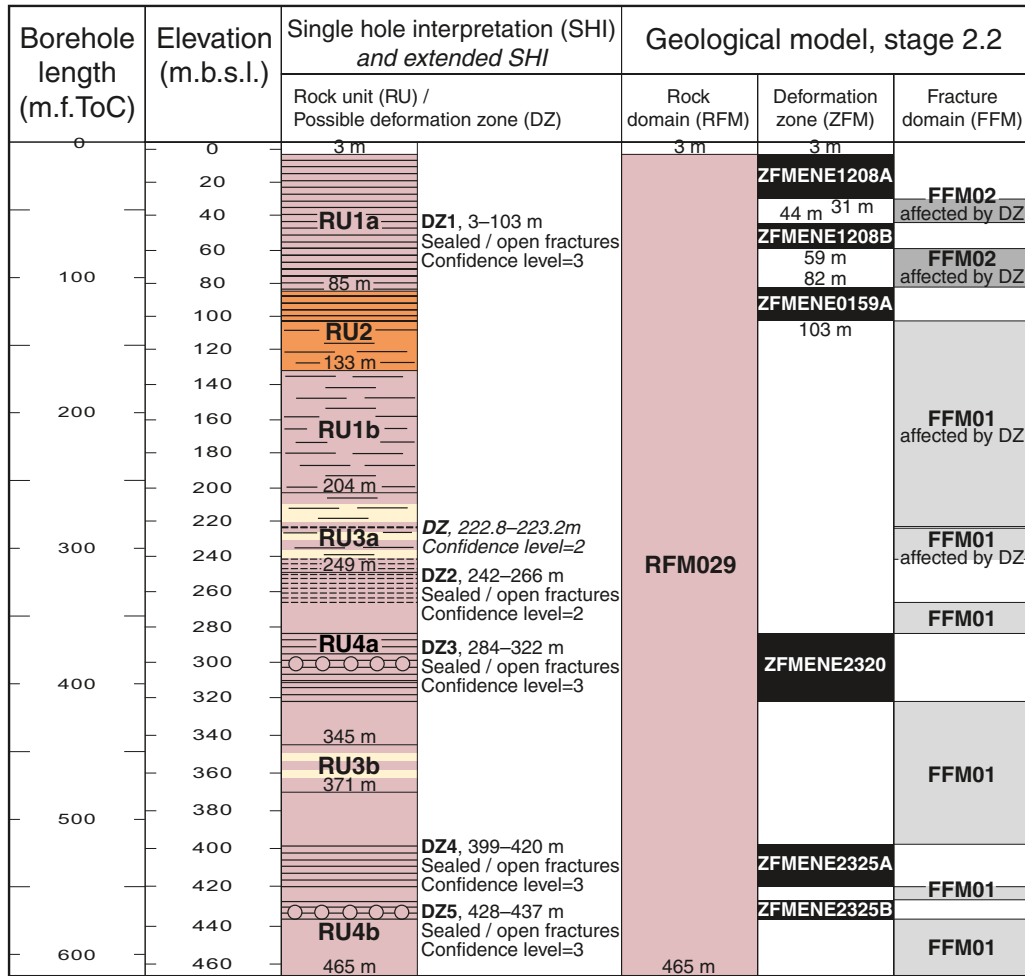
Group B

- Granite (to granodiorite), metamorphic, medium-grained
- Granodiorite, metamorphic
- Amphibolite, quartz-bearing metadiorite

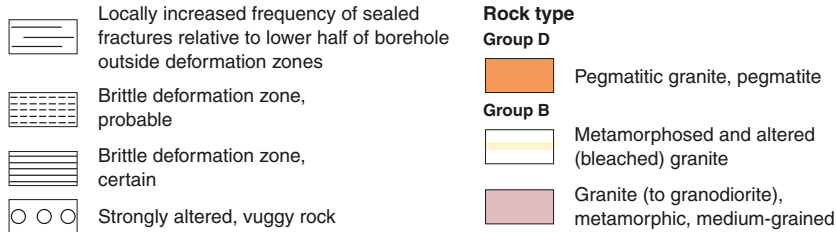
Group A

- Felsic to intermediate metavolcanic rock

KFM09B



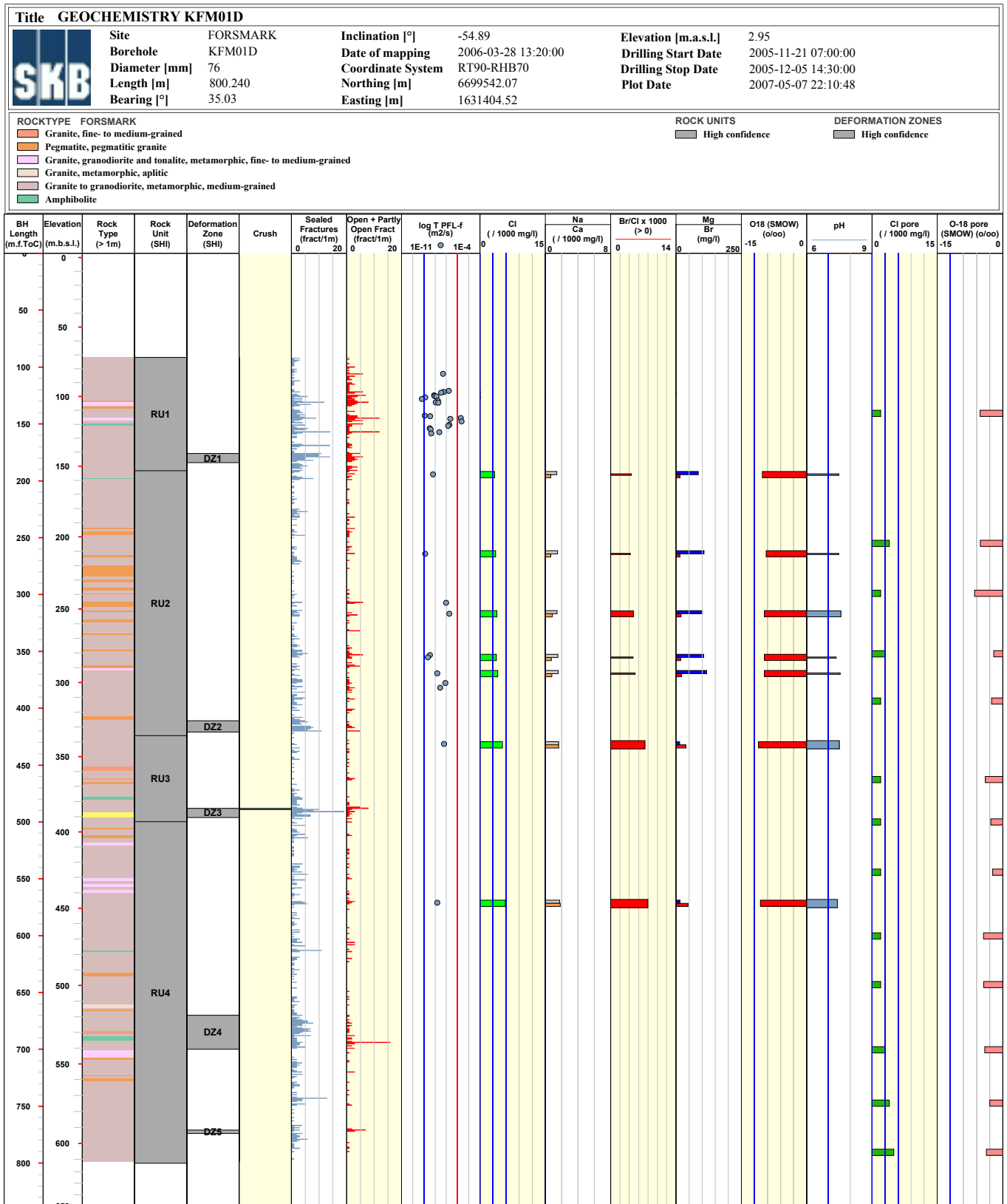
Legend for single hole interpretation



The elevation of a modelled deformation zone is only provided in the cases where the zone boundaries differ from the single hole interpretation

WellCad diagrams for hydrogeochemical data

WellCad diagrams for a number of the cored boreholes, showing a selected suite of hydrogeochemical data in the context of some base geological and hydrogeological data.



Title GEOCHEMISTRY KFM03A



Site	FORSMARK	Inclination [°]	-85.74	Elevation [m.a.s.l.]	8.29
Borehole	KFM03A	Date of mapping	2003-08-28 00:00:00	Drilling Start Date	2003-03-18 09:10:00
Diameter [mm]	77	Coordinate System	RT90-RHB70	Drilling Stop Date	2003-03-28 14:30:00
Length [m]	1001.190	Northing [m]	6697852.10	Plot Date	2007-05-08 22:21:06
Bearing [°]	271.52	Easting [m]	1634630.74		

ROCKTYPE FORSMARK

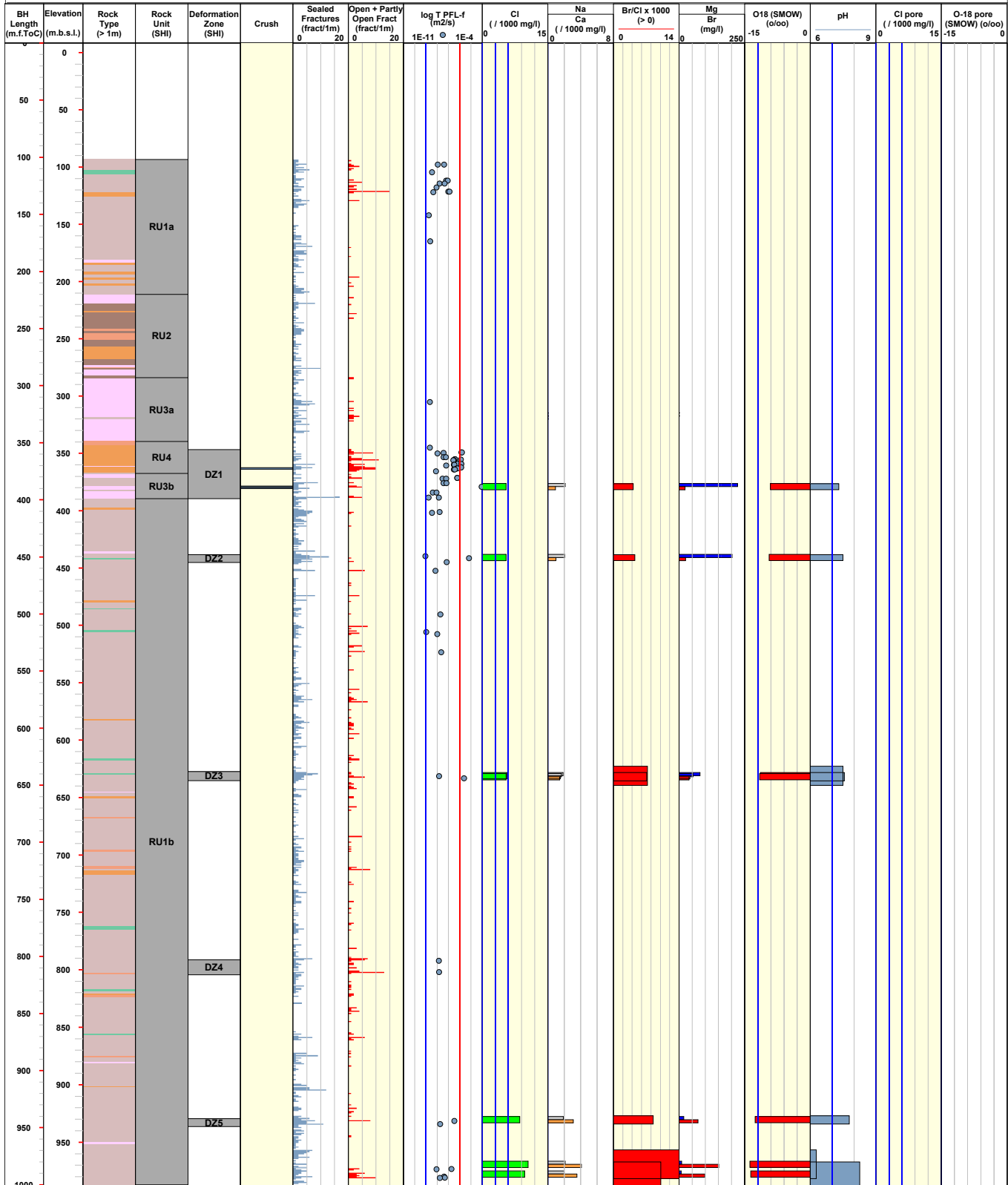
- Granite, fine- to medium-grained
- Pegmatite, pegmatitic granite
- Granite, granodiorite and tonalite, metamorphic, fine- to medium-grained
- Granite to granodiorite, metamorphic, medium-grained
- Tonalite to granodiorite, metamorphic
- Amphibolite

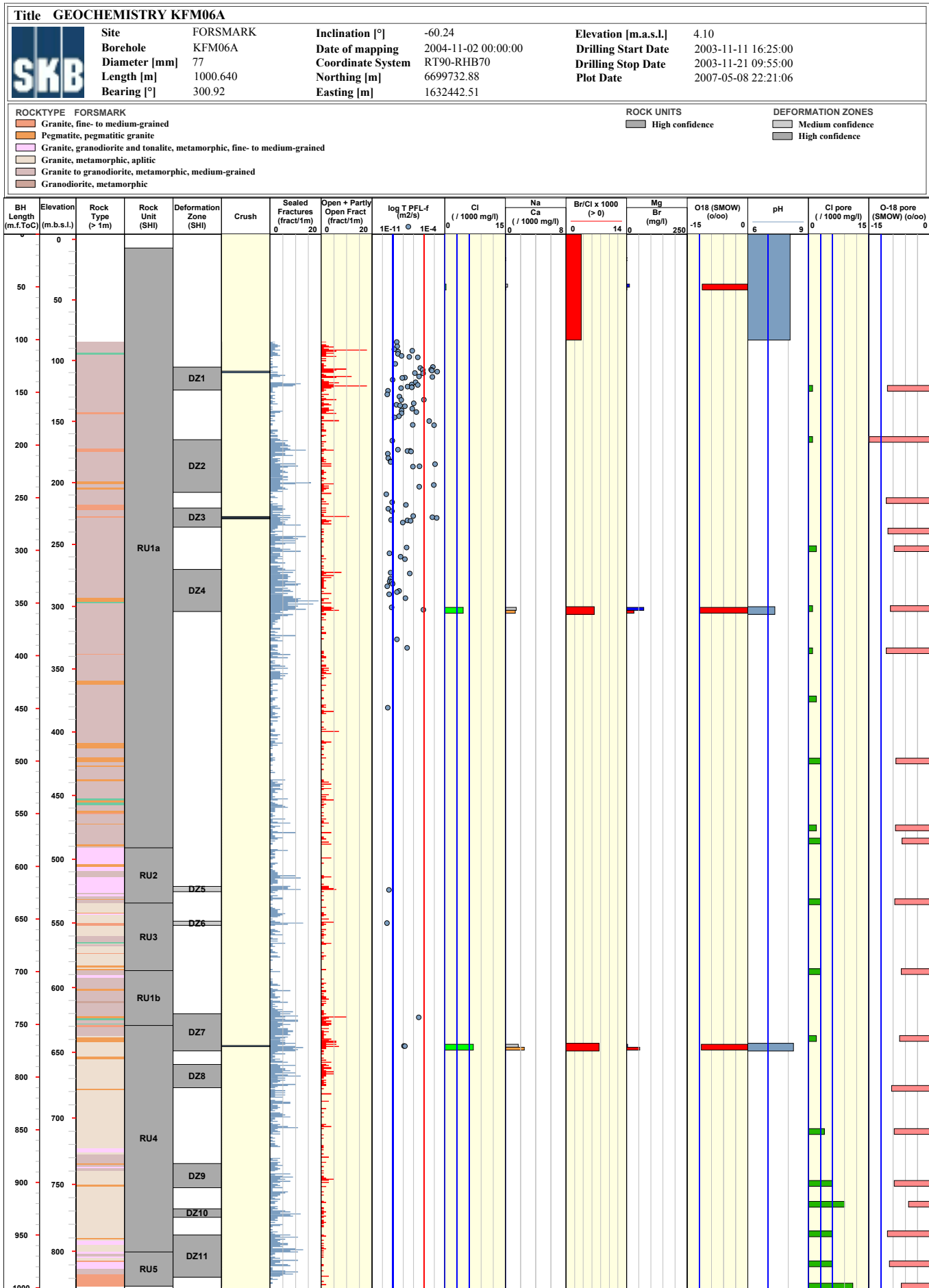
ROCK UNITS


High confidence

DEFORMATION ZONES

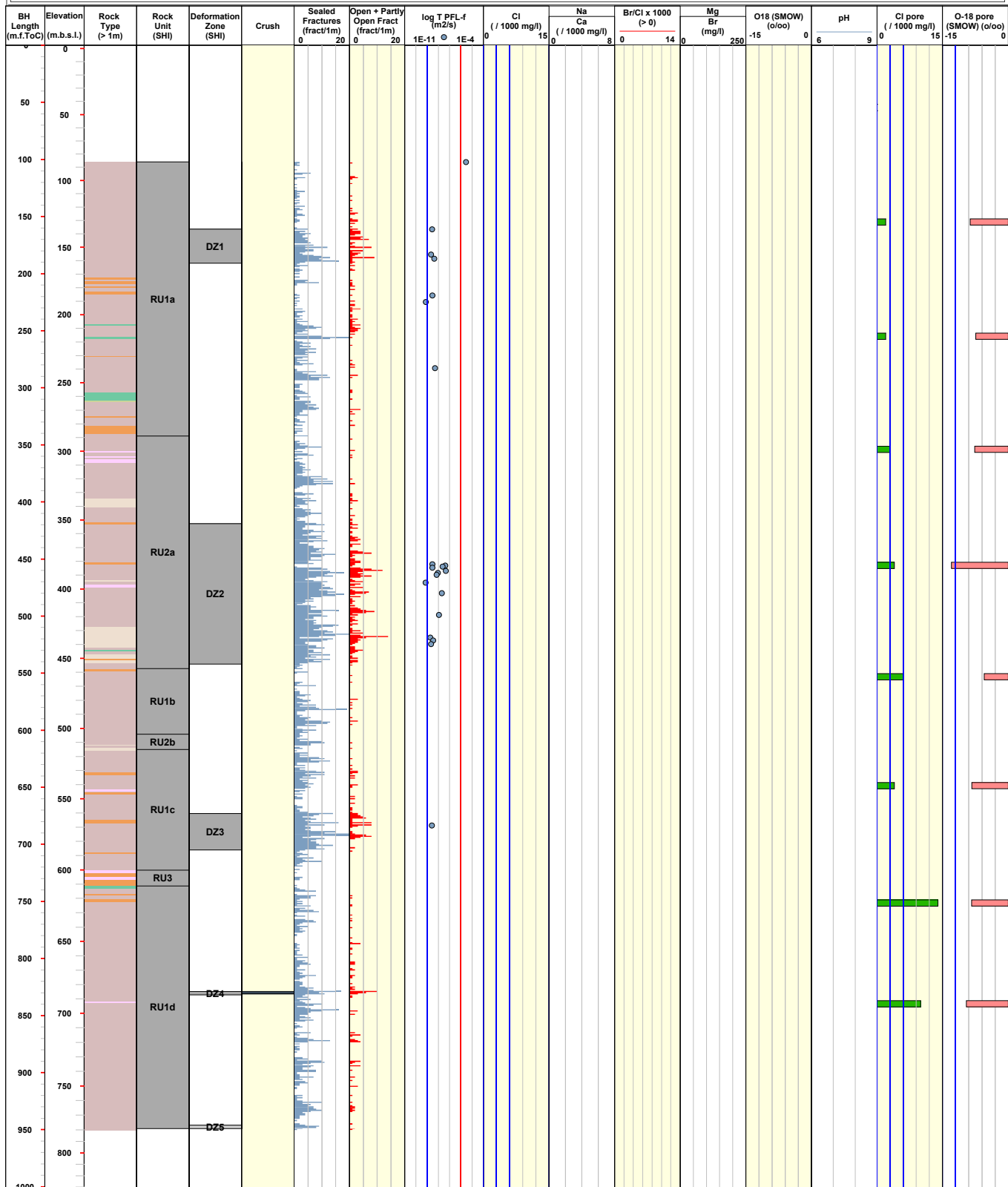
High confidence





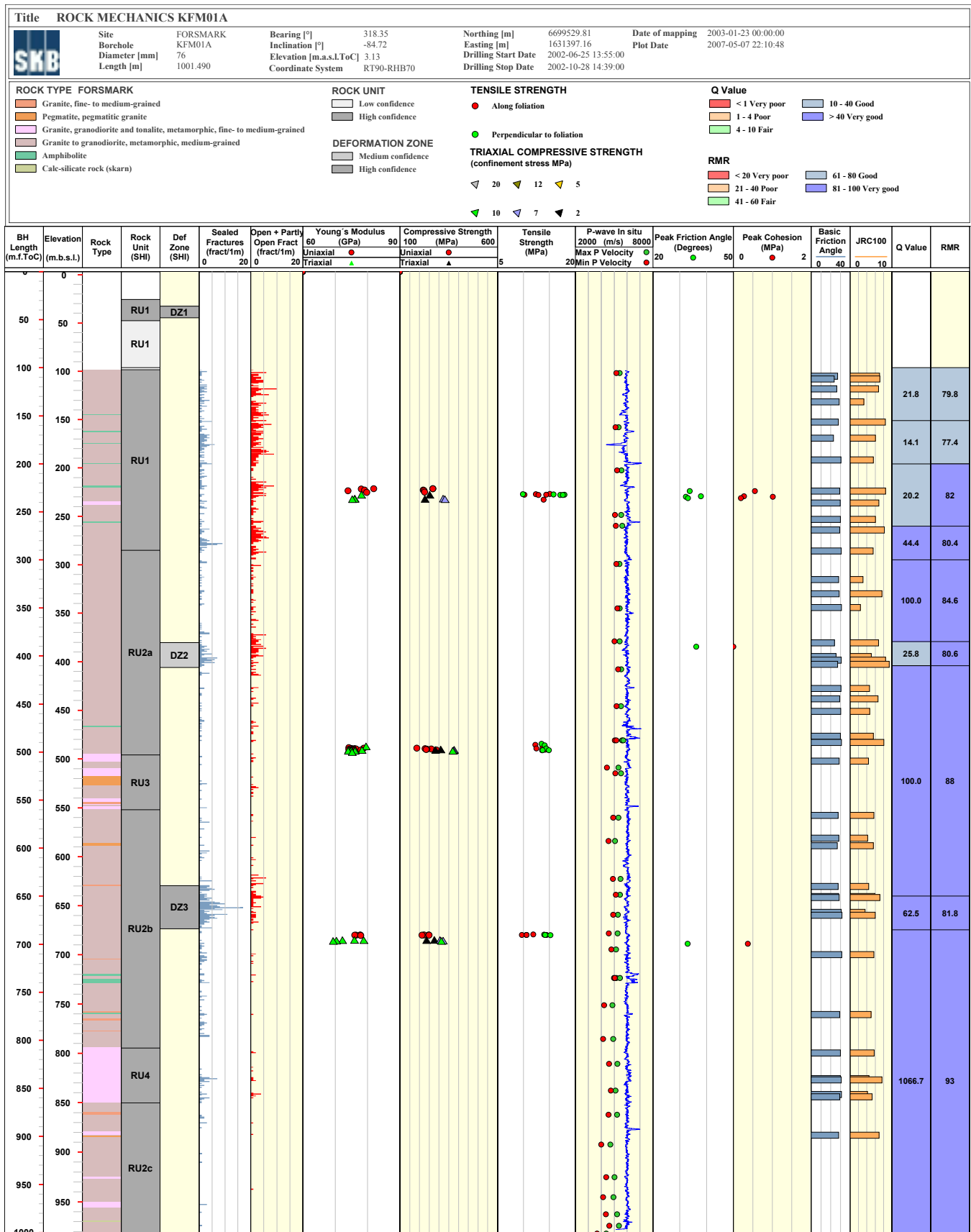
Title GEOCHEMISTRY KFM08C		Site FORSMARK	Inclination [°] -60.47	Elevation [m.a.s.l.] 2.47
	Borehole KFM08C	Date of mapping 2006-06-20 15:25:00	Drilling Start Date 2005-04-14 00:00:00	
	Diameter [mm] 77	Coordinate System RT90-RHB70	Drilling Stop Date 2005-04-26 00:00:00	
	Length [m] 951.080	Northing [m] 6700495.88	Plot Date 2007-05-08 22:21:06	
	Bearing [°] 35.88	Easting [m] 1631187.57		

ROCKTYPE FORSMARK	ROCK UNITS	DEFORMATION ZONES
<ul style="list-style-type: none"> Pegmatite, pegmatitic granite Granite, granodiorite and tonalite, metamorphic, fine- to medium-grained Granite, metamorphic, aplitic Granite to granodiorite, metamorphic, medium-grained Amphibolite Calc-silicate rock (skarn) 	<ul style="list-style-type: none"> High confidence 	<ul style="list-style-type: none"> Medium confidence High confidence

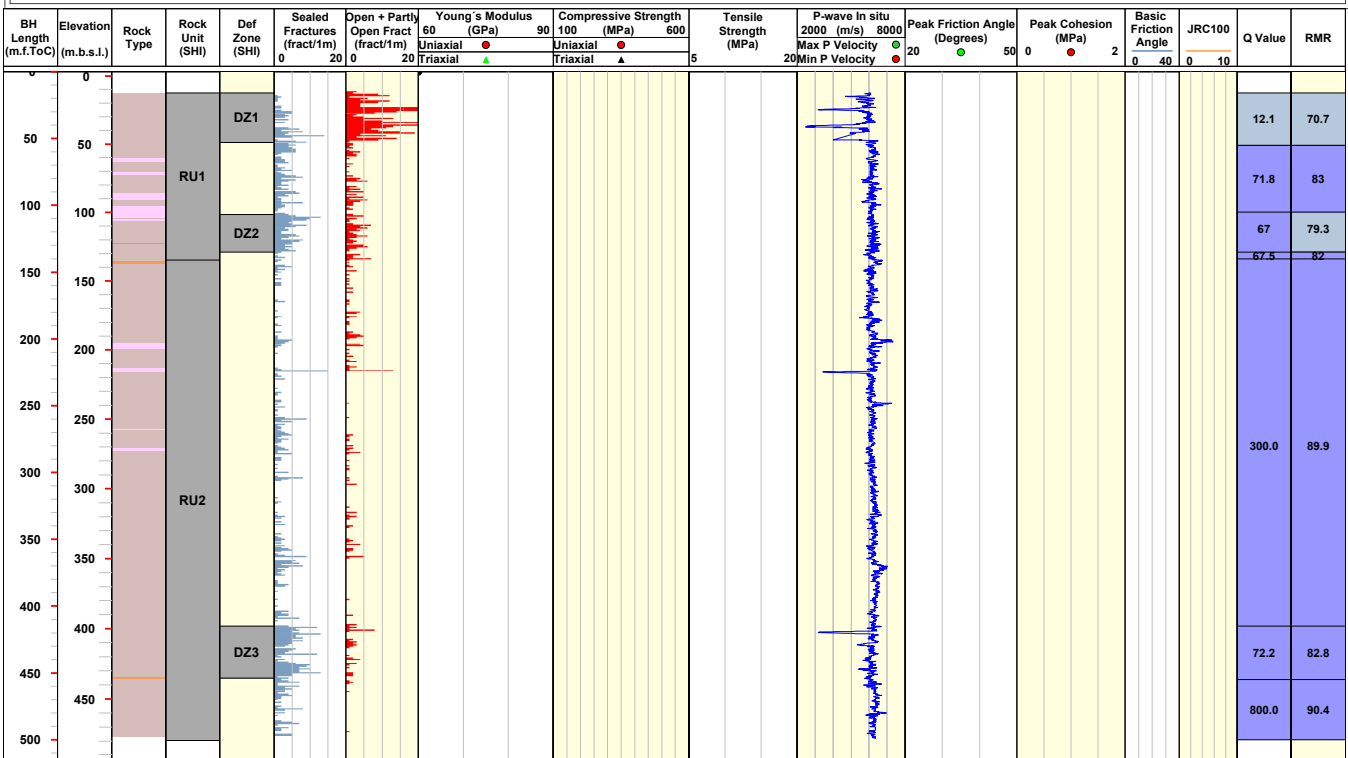


WellCad diagrams for rock mechanics data

WellCad diagrams for all the cored boreholes, showing a selected suite of rock mechanical data in the context of some base geological and geophysical data.

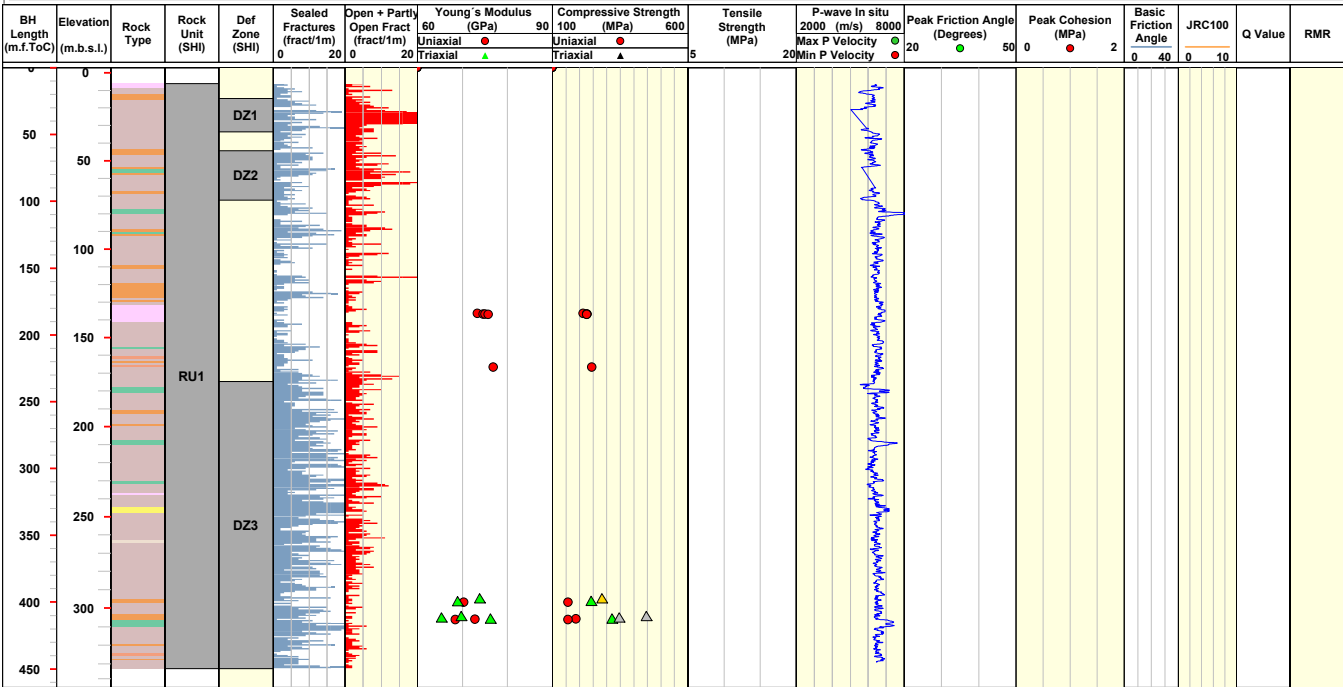


Title ROCK MECHANICS KFM01B									
	Site	FORSMARK	Bearing [°]	267.59	Northing [m]	6699539.40	Date of mapping	2004-03-05 00:00:00	
	Borehole	KFM01B	Inclination [°]	-79.03	Easting [m]	1631387.67	Plot Date	2007-05-06 22:11:24	
	Diameter [mm]	76	Elevation [m.a.s.l.ToC]	3.09	Drilling Start Date	2003-07-29 11:00:00			
	Length [m]	500.520	Coordinate System	RT90-RHB70	Drilling Stop Date	2004-01-15 15:00:00			
ROCK TYPE FORSMARK			ROCK UNIT		TENSILE STRENGTH		Q Value		
<ul style="list-style-type: none"> Pegmatite, pegmatitic granite Granite, granodiorite and tonalite, metamorphic, fine- to medium-grained Granite to granodiorite, metamorphic, medium-grained Amphibolitic 			<ul style="list-style-type: none"> High confidence 		<ul style="list-style-type: none"> < 1 Very poor 1 - 4 Poor 4 - 10 Fair 10 - 40 Good > 40 Very good 				
			DEFORMATION ZONE		TRIAXIAL COMPRESSIVE STRENGTH		RMR		
			<ul style="list-style-type: none"> High confidence 		<ul style="list-style-type: none"> < 20 Very poor 21 - 40 Poor 41 - 60 Fair 61 - 80 Good 81 - 100 Very good 				

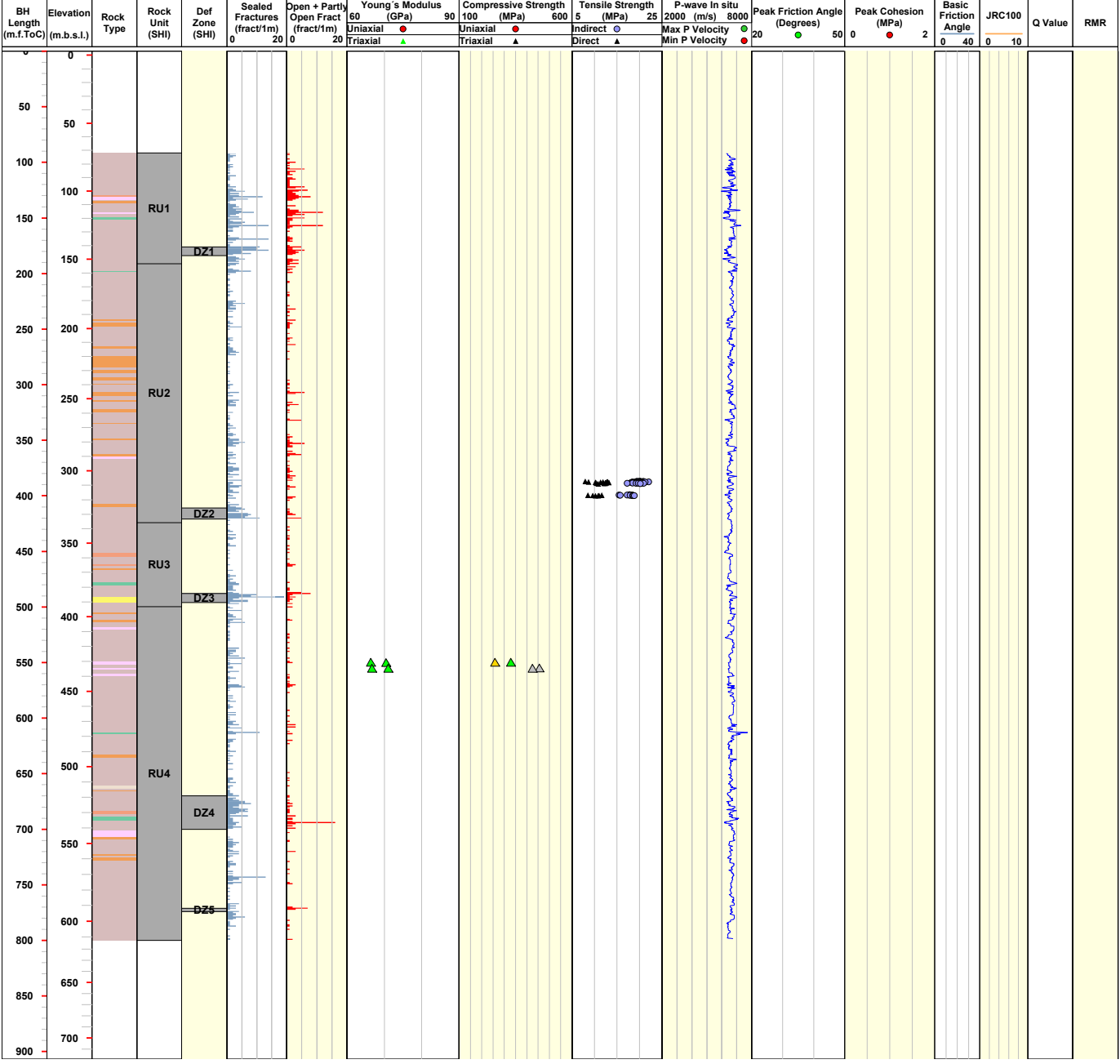


Title ROCK MECHANICS KFM01C									
	Site	FORMSARK	Bearing [°]	165.35	Northing [m]	6699526.14	Date of mapping	2006-01-17 10:57:00	
	Borehole	KFM01C	Inclination [°]	-49.60	Easting [m]	1631403.75	Plot Date	2007-05-06 22:11:24	
	Diameter [mm]	76	Elevation [m.a.s.l.ToC]	2.91	Drilling Start Date	2005-11-05 13:56:00			
	Length [m]	450.020	Coordinate System	RT90-RHB70	Drilling Stop Date	2005-11-29 13:52:00			

ROCK TYPE FORMSARK		ROCK UNIT		TENSILE STRENGTH		Q Value	
	Granite, fine- to medium-grained		High confidence		< 1 Very poor		10 - 40 Good
	Pegmatite, pegmatitic granite				1 - 4 Poor		> 40 Very good
	Granite, granodiorite and tonalite, metamorphic, fine- to medium-grained	DEFORMATION ZONE		TRIAXIAL COMPRESSIVE STRENGTH (confinement stress MPa)			
	Granite, metamorphic, aplitic		High confidence		2		7
	Granite, granodiorite, metamorphic, medium-grained				10		
	Amphibolite				5		12
	Felsic to intermediate volcanic rock, metamorphic				20		20



Title ROCK MECHANICS KFM01D											
	Site	FORSMARK	Bearing [°]	35.03	Northing [m]	6699542.07	Date of mapping	2006-03-28 13:20:00			
	Borehole	KFM01D	Inclination [°]	-54.89	Easting [m]	1631404.52	Plot Date	2007-05-10 22:13:25			
	Diameter [mm]	76	Elevation [m.a.s.l.ToC]	2.95	Drilling Start Date	2005-12-18 13:44:00					
	Length [m]	800.240	Coordinate System	RT90-RHB70	Drilling Stop Date	2006-02-18 10:49:00					
ROCK TYPE FORSMARK			ROCK UNIT			TENSILE STRENGTH			Q Value		
<ul style="list-style-type: none"> Granite, fine- to medium-grained Pegmatite, pegmatitic granite Granite, granodiorite and tonalite, metamorphic, fine- to medium-grained Granite, metamorphic, aplitic Granite to granodiorite, metamorphic, medium-grained Amphibolite Felsic to intermediate volcanic rock, metamorphic 			<ul style="list-style-type: none"> High confidence 			<ul style="list-style-type: none"> Foliation not specified Foliation not specified 			<ul style="list-style-type: none"> < 1 Very poor 1 - 4 Poor 4 - 10 Fair 10 - 40 Good > 40 Very good 		
DEFORMATION ZONE			TRIAXIAL COMPRESSIVE STRENGTH (confinement stress MPa)			RMR					
<ul style="list-style-type: none"> High confidence 			<ul style="list-style-type: none"> 2 7 10 5 12 20 			<ul style="list-style-type: none"> < 20 Very poor 21 - 40 Poor 41 - 60 Fair 61 - 80 Good 81 - 100 Very good 					



Title ROCK MECHANICS KFM02A

SKB Site FORSMARK Borehole KFM02A Diameter [mm] 77 Length [m] 1002.440 Bearing [°] 275.76 Inclination [°] -85.37 Elevation [m.a.s.l.ToC] 7.35 Coordinate System RT90-RHB70 Northing [m] 6698712.50 Easting [m] 1633182.86 Date of mapping 2003-04-22 00:00:00 Plot Date 2007-05-06 22:11:24 Drilling Start Date 2003-01-08 14:23:00 Drilling Stop Date 2003-03-12 21:30:00

ROCK TYPE FORSMARK
 Granite, fine- to medium-grained
 Pegmatite, pegmatitic granite
 Granite, granodiorite and tonalite, metamorphic, fine- to medium-grained
 Granite to granodiorite, metamorphic, medium-grained
 Amphibolite

ROCK UNIT
 High confidence

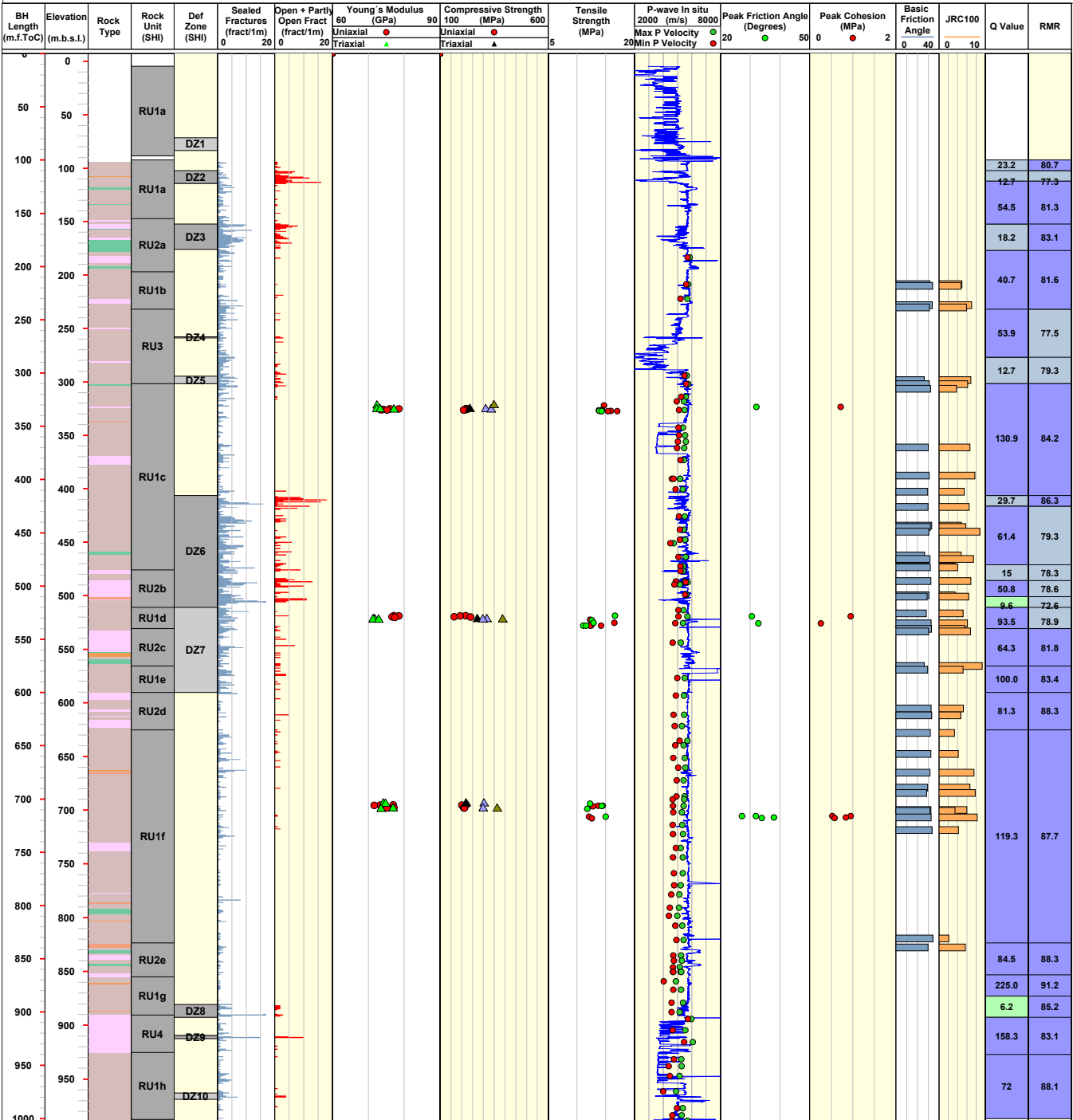
TENSILE STRENGTH
 Perpendicular to foliation
 Along foliation

Q Value
 < 1 Very poor
 1 - 4 Poor
 4 - 10 Fair
 10 - 40 Good
 > 40 Very good

DEFORMATION ZONE
 Medium confidence
 High confidence

TRIAXIAL COMPRESSIVE STRENGTH
 (confinement stress MPa)
 2 5 7 12 10 20

RMR
 < 20 Very poor
 21 - 40 Poor
 41 - 60 Fair
 61 - 80 Good
 81 - 100 Very good



Title ROCK MECHANICS KFM03A

SKB Site FORSMARK Borehole KFM03A Diameter [mm] 77 Length [m] 1001.190 Bearing [°] 271.52 Inclination [°] -85.74 Elevation [m.a.s.l.ToC] 8.29 Coordinate System RT90-RHB70 Northing [m] 6697852.10 Easting [m] 1634630.74 Drilling Start Date 2003-04-16 11:33:00 Drilling Stop Date 2003-06-23 16:15:00 Date of mapping 2003-08-28 00:00:00 Plot Date 2007-05-06 22:11:24

ROCK TYPE FORSMARK
 Granite, fine- to medium-grained
 Pegmatite, pegmatitic granite
 Granite, granodiorite and tonalite, metamorphic, fine- to medium-grained
 Granite to granodiorite, metamorphic, medium-grained
 Tonalite to granodiorite, metamorphic
 Amphibolite

ROCK UNIT
 High confidence

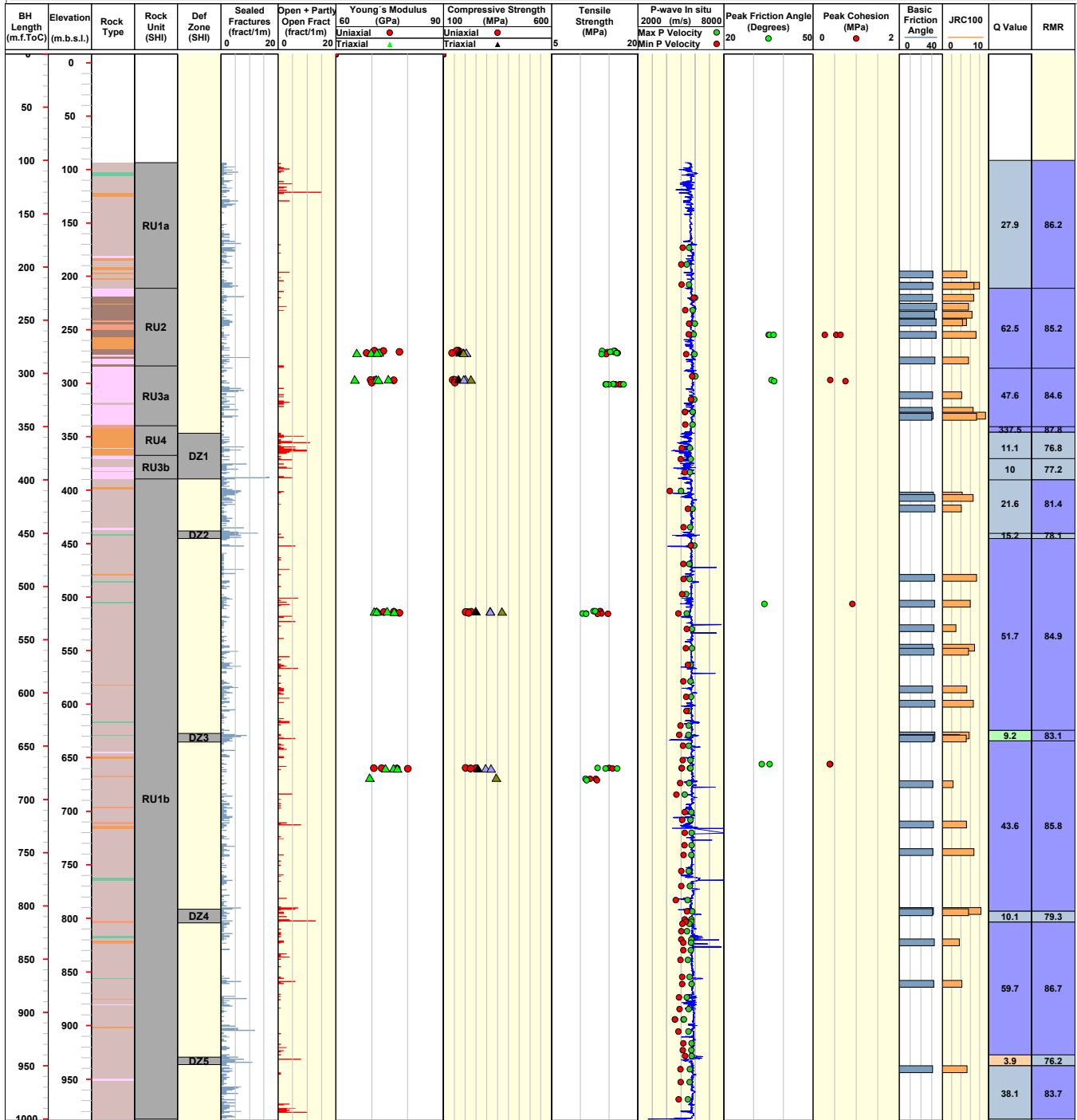
TENSILE STRENGTH
 Perpendicular to foliation
 Along foliation

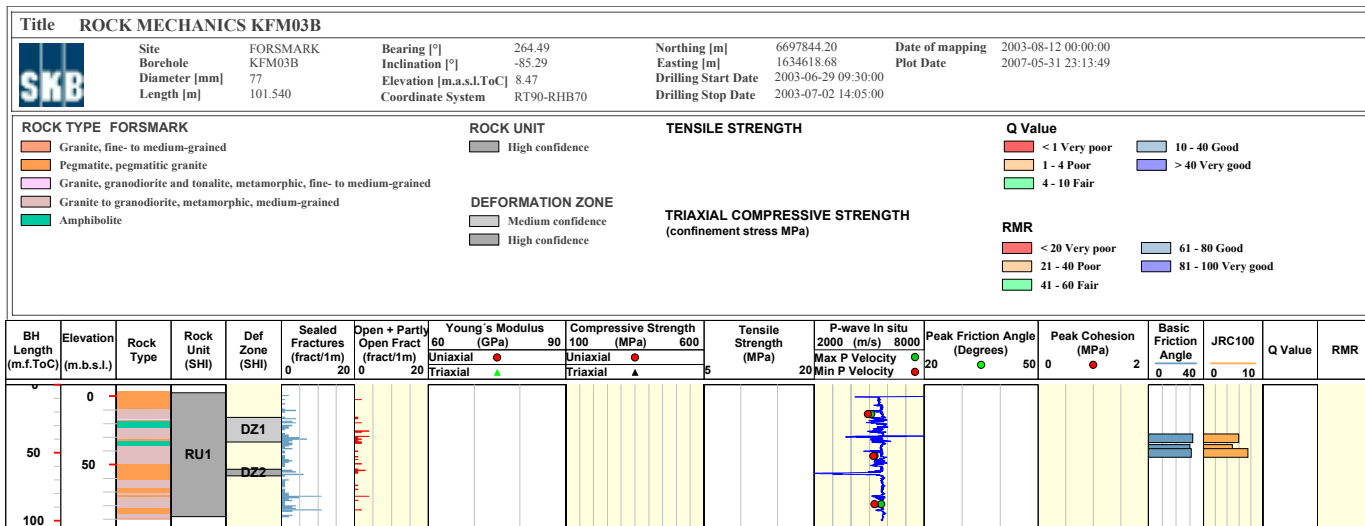
DEFORMATION ZONE
 High confidence

TRIAXIAL COMPRESSIVE STRENGTH
 (confinement stress MPa)
 2 5 7 12 10 20

Q Value
 < 1 Very poor
 1 - 4 Poor
 4 - 10 Fair
 10 - 40 Good
 > 40 Very good

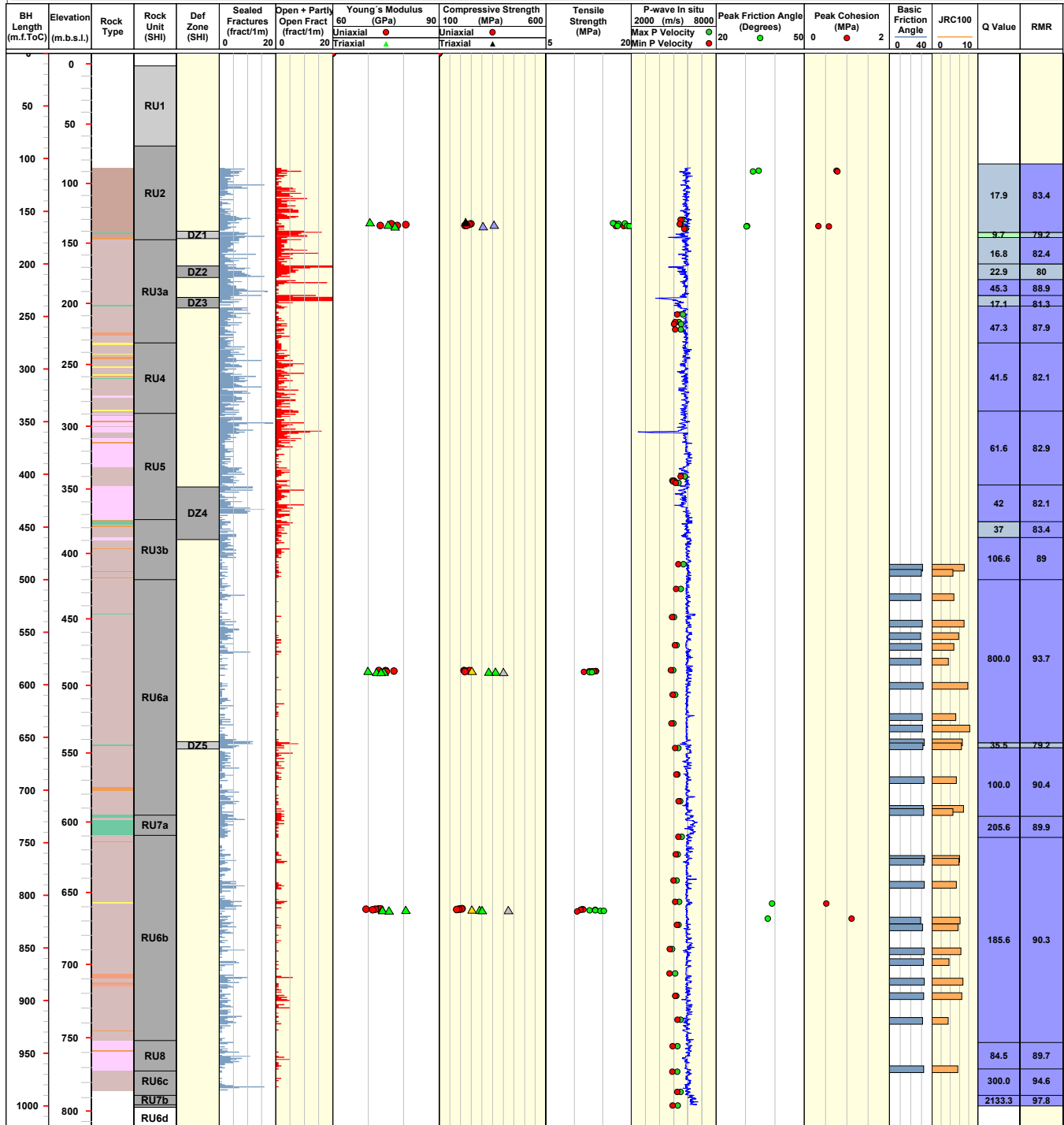
RMR
 < 20 Very poor
 21 - 40 Poor
 41 - 60 Fair
 61 - 80 Good
 81 - 100 Very good

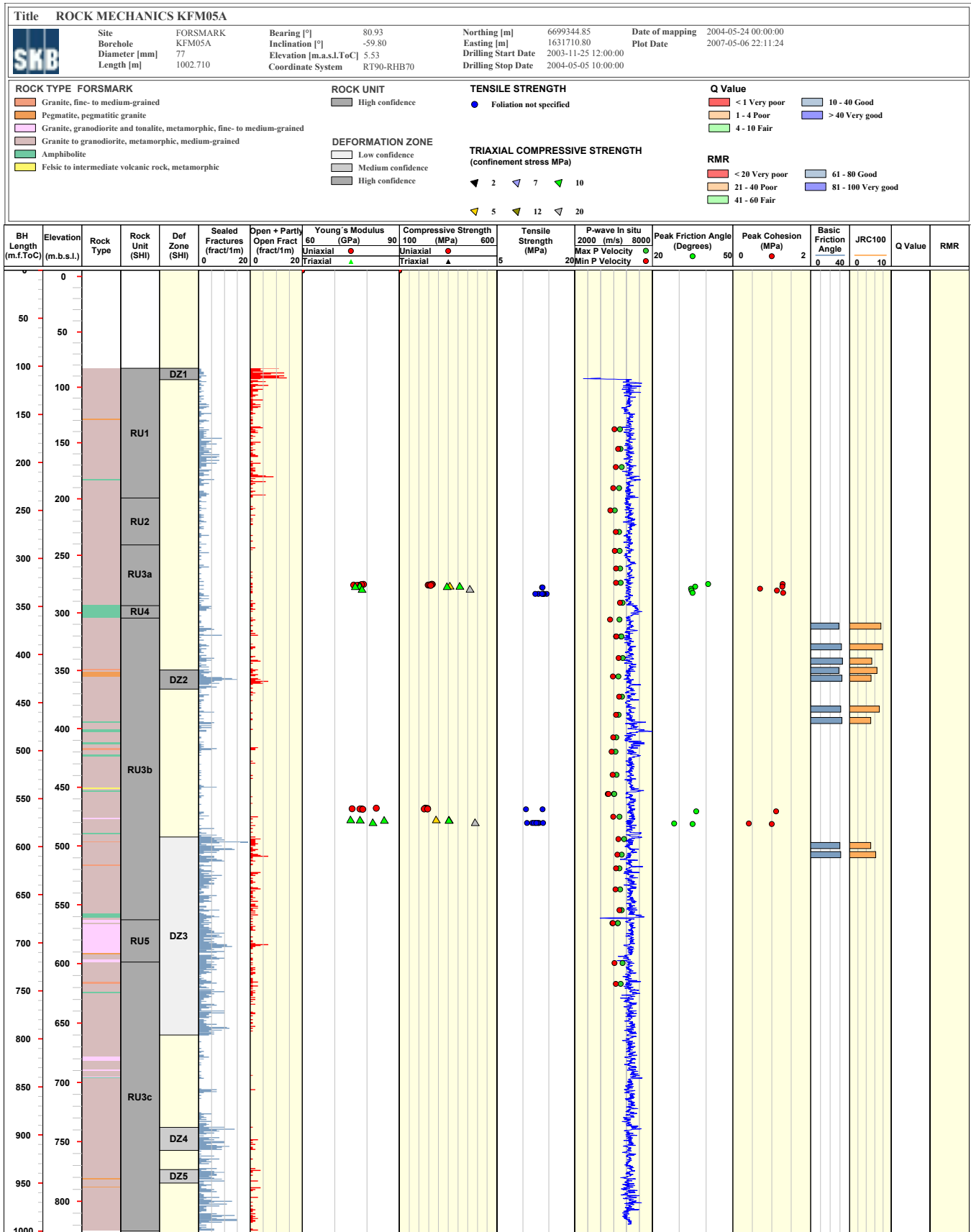





Title ROCK MECHANICS KFM04A		Site FORSMARK		Bearing [°] 45.24	Northing [m] 6698921.74	Date of mapping	2003-12-08 00:00:00	
	Borehole KFM04A	Inclination [°] -60.07		Easting [m] 1630978.96	Plot Date			2007-05-06 22:11:24
	Diameter [mm] 77	Elevation [m.a.s.l.ToC] 8.77		Drilling Start Date	2003-08-25 11:17:00			
	Length [m] 1001.420	Coordinate System RT90-RHB70		Drilling Stop Date	2003-11-19 15:15:00			

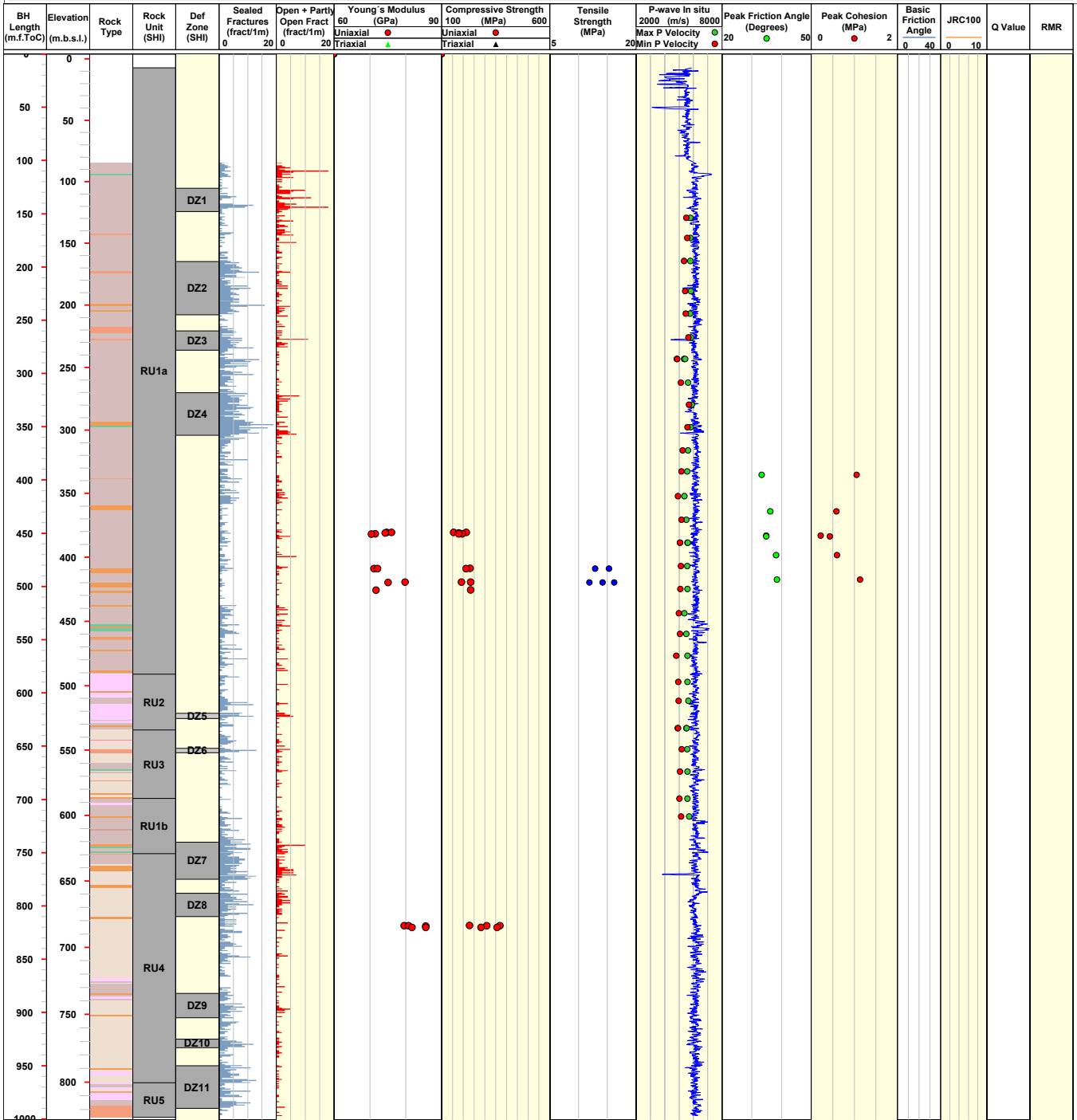
ROCK TYPE FORSMARK		ROCK UNIT		TENSILE STRENGTH		Q Value	
	Granite, fine- to medium-grained		Medium confidence		Perpendicular to foliation		< 1 Very poor
	Pegmatite, pegmatitic granite		High confidence		Along foliation		1 - 4 Poor
	Granite, granodioritic and tonalite, metamorphic, fine- to medium-grained	DEFORMATION ZONE		TRIAXIAL COMPRESSIVE STRENGTH			4 - 10 Fair
	Granite to granodiorite, metamorphic, medium-grained		Medium confidence	(confinement stress MPa)			10 - 40 Good
	Granodiorite, metamorphic		High confidence		2		> 40 Very good
	Amphibolite				7		61 - 80 Good
	Felsic to intermediate volcanic rock, metamorphic				10		81 - 100 Very good
					5		41 - 60 Fair
					12		61 - 80 Good
					20		81 - 100 Very good

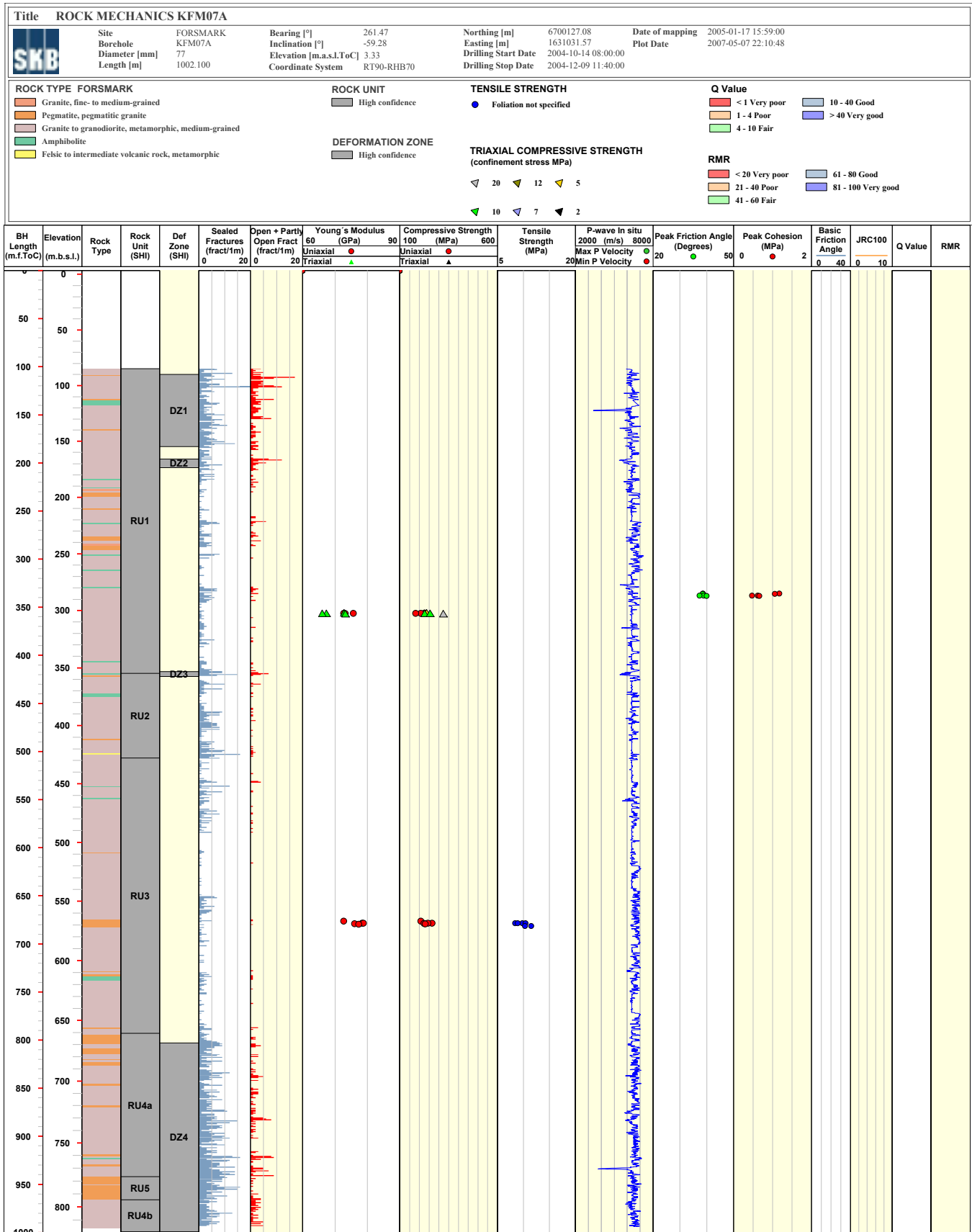


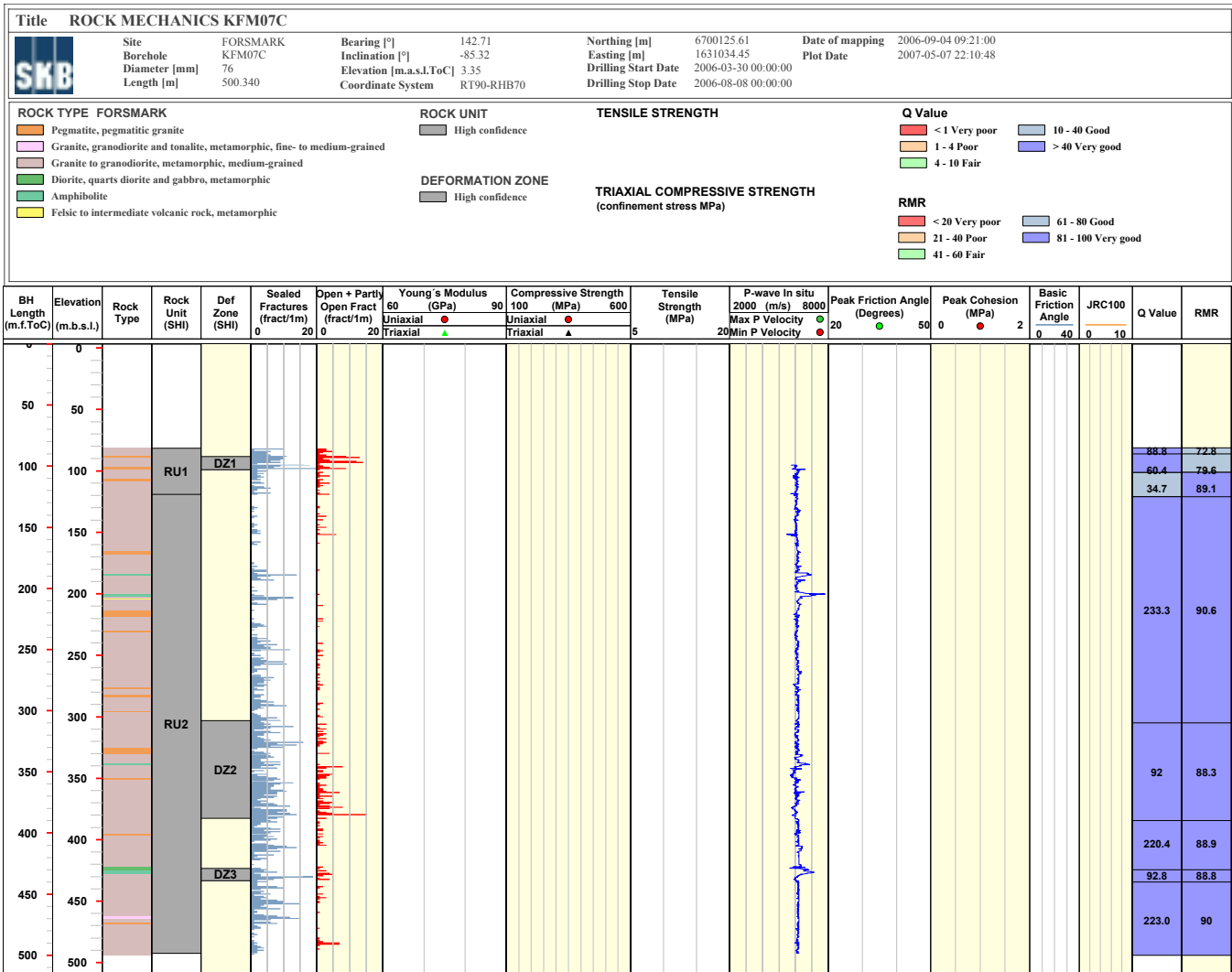


Title ROCK MECHANICS KFM06A		Site FORSMARK		Bearing [°] 300.92	Northing [m] 6699732.88	Date of mapping 2004-11-02 00:00:00
	Borehole KFM06A	Inclination [°] -60.24	Easting [m] 1632442.51	Plot Date 2007-05-07 22:10:48		
	Diameter [mm] 77	Elevation [m.a.s.l.ToC] 4.10	Drilling Start Date 2004-06-14 14:00:00			
	Length [m] 1000.640	Coordinate System RT90-RHB70	Drilling Stop Date 2004-09-21 03:37:00			

ROCK TYPE FORSMARK	ROCK UNIT	TENSILE STRENGTH	Q Value
<ul style="list-style-type: none"> Granite, fine- to medium-grained Pegmatite, pegmatitic granite Granite, granodiorite and tonalite, metamorphic, fine- to medium-grained Granite, metamorphic, aplitic Granite to granodiorite, metamorphic, medium-grained Granodiorite, metamorphic Amphibolite 	<ul style="list-style-type: none"> High confidence 	<ul style="list-style-type: none"> Foliation not specified 	<ul style="list-style-type: none"> < 1 Very poor 1 - 4 Poor 4 - 10 Fair 10 - 40 Good > 40 Very good
	DEFORMATION ZONE	TRIAXIAL COMPRESSIVE STRENGTH (confinement stress MPa)	RMR
	<ul style="list-style-type: none"> Medium confidence High confidence 	<ul style="list-style-type: none"> < 20 Very poor 21 - 40 Poor 41 - 60 Fair 61 - 80 Good 81 - 100 Very good 	

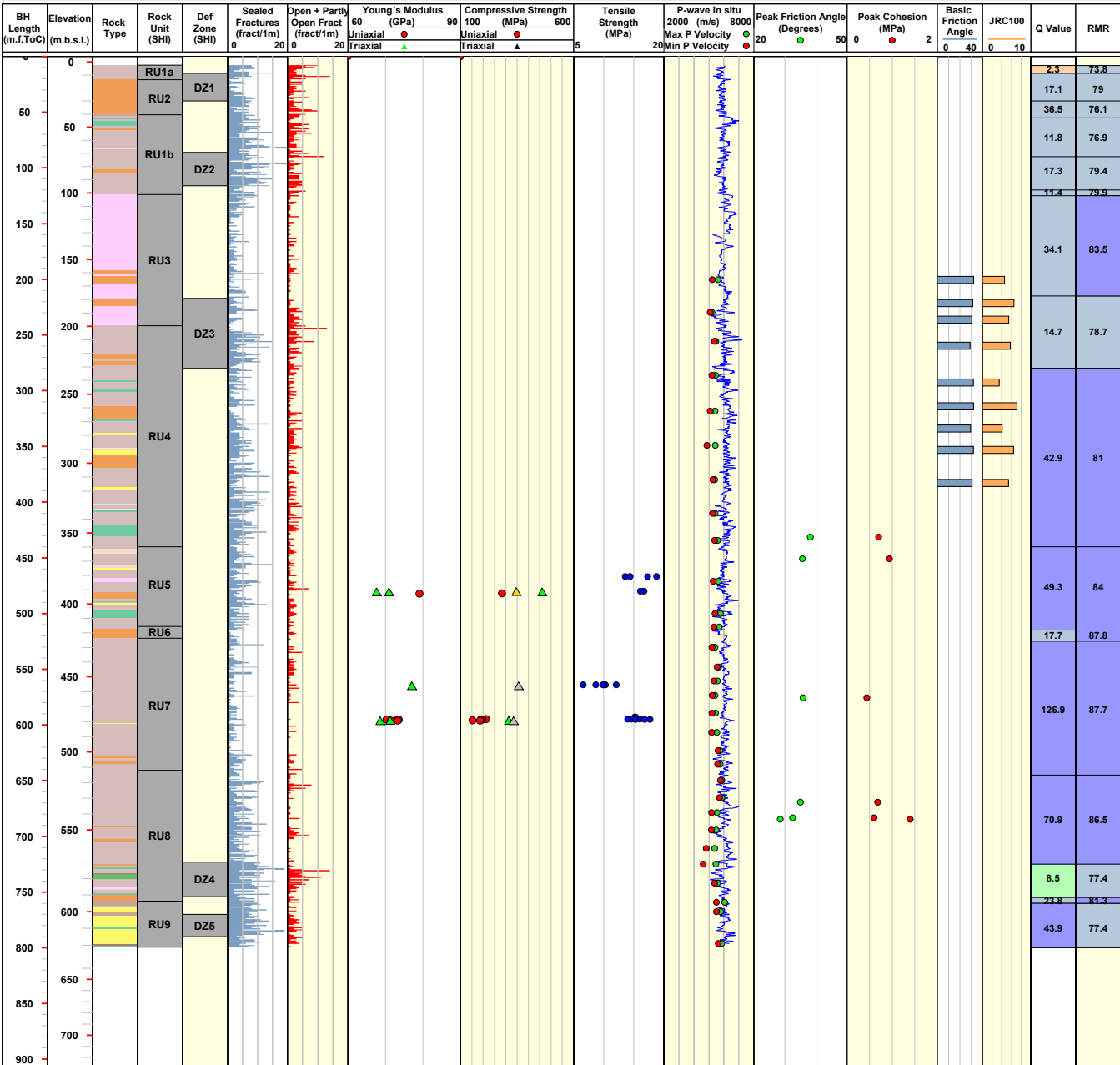






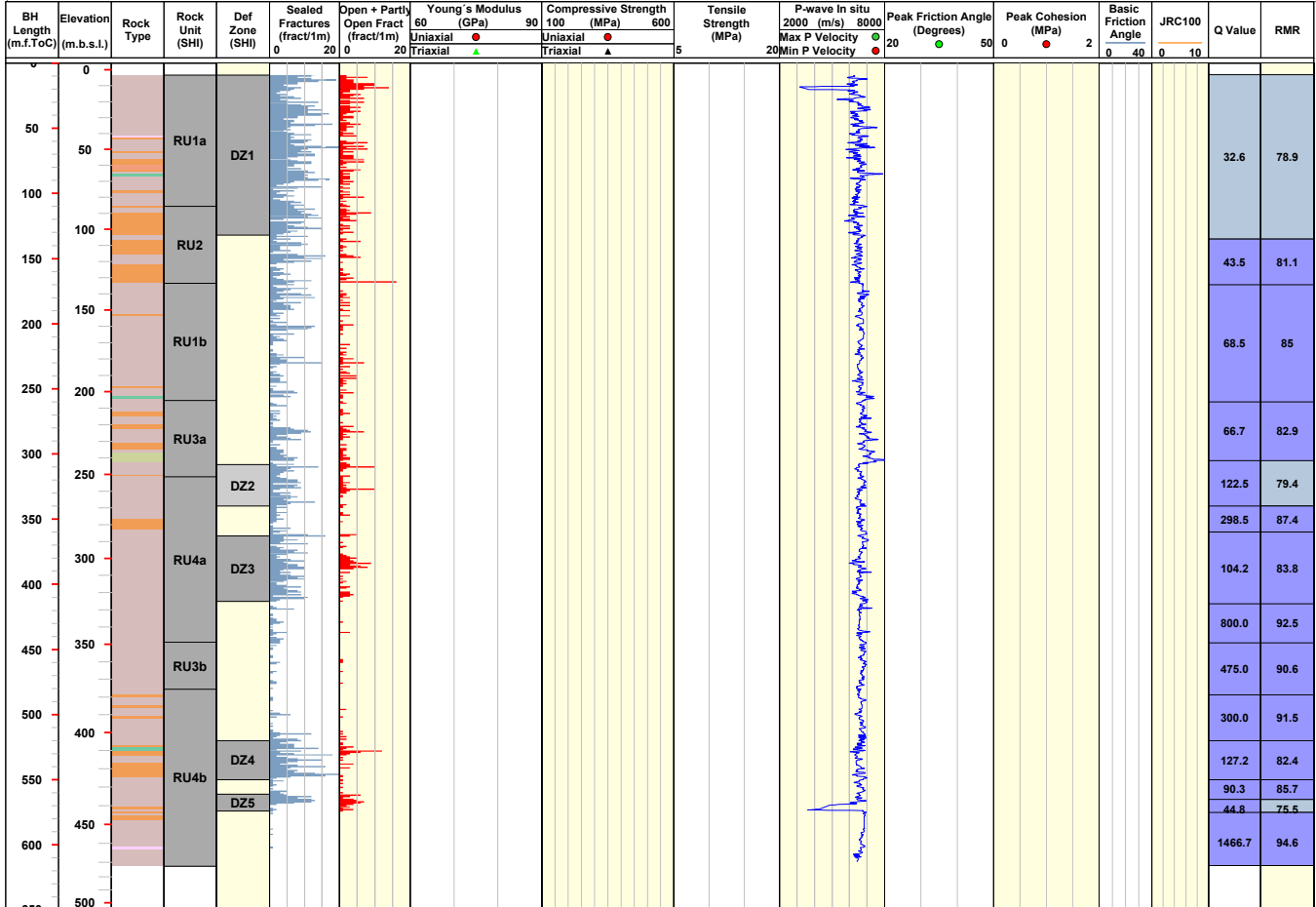
Title ROCK MECHANICS KFM09A		Site FORSMARK		Bearing [°] 200.08	Northing [m] 6700115.04	Date of mapping 2005-11-29 20:07:00
	Borehole KFM09A	Inclination [°] -59.45	Easting [m] 1630647.50	Plot Date 2007-05-07 22:10:48		
	Diameter [mm] 77	Elevation [m.a.s.l.ToC] 4.29	Drilling Start Date 2005-08-31 00:00:00			
	Length [m] 799.670	Coordinate System RT90-RHB70	Drilling Stop Date 2005-10-27 13:00:00			

ROCK TYPE FORSMARK <ul style="list-style-type: none"> Pegmatite, pegmatitic granite Granite, granodiorite and tonalite, metamorphic, fine- to medium-grained Granite, metamorphic, aplitic Granite to granodiorite, metamorphic, medium-grained Granodiorite, metamorphic Tonalite to granodiorite, metamorphic Diorite, quartz diorite and gabbro, metamorphic Amphibolite 	ROCK UNIT <ul style="list-style-type: none"> High confidence 	TENSILE STRENGTH <ul style="list-style-type: none"> Foliation not specified 	Q Value <ul style="list-style-type: none"> < 1 Very poor 1 - 4 Poor 4 - 10 Fair 10 - 40 Good > 40 Very good
	DEFORMATION ZONE <ul style="list-style-type: none"> High confidence 	TRIAxIAL COMPRESSIVE STRENGTH (confinement stress MPa) <ul style="list-style-type: none"> 20 12 5 10 7 2 	RMR <ul style="list-style-type: none"> < 20 Very poor 21 - 40 Poor 41 - 60 Fair 61 - 80 Good 81 - 100 Very good



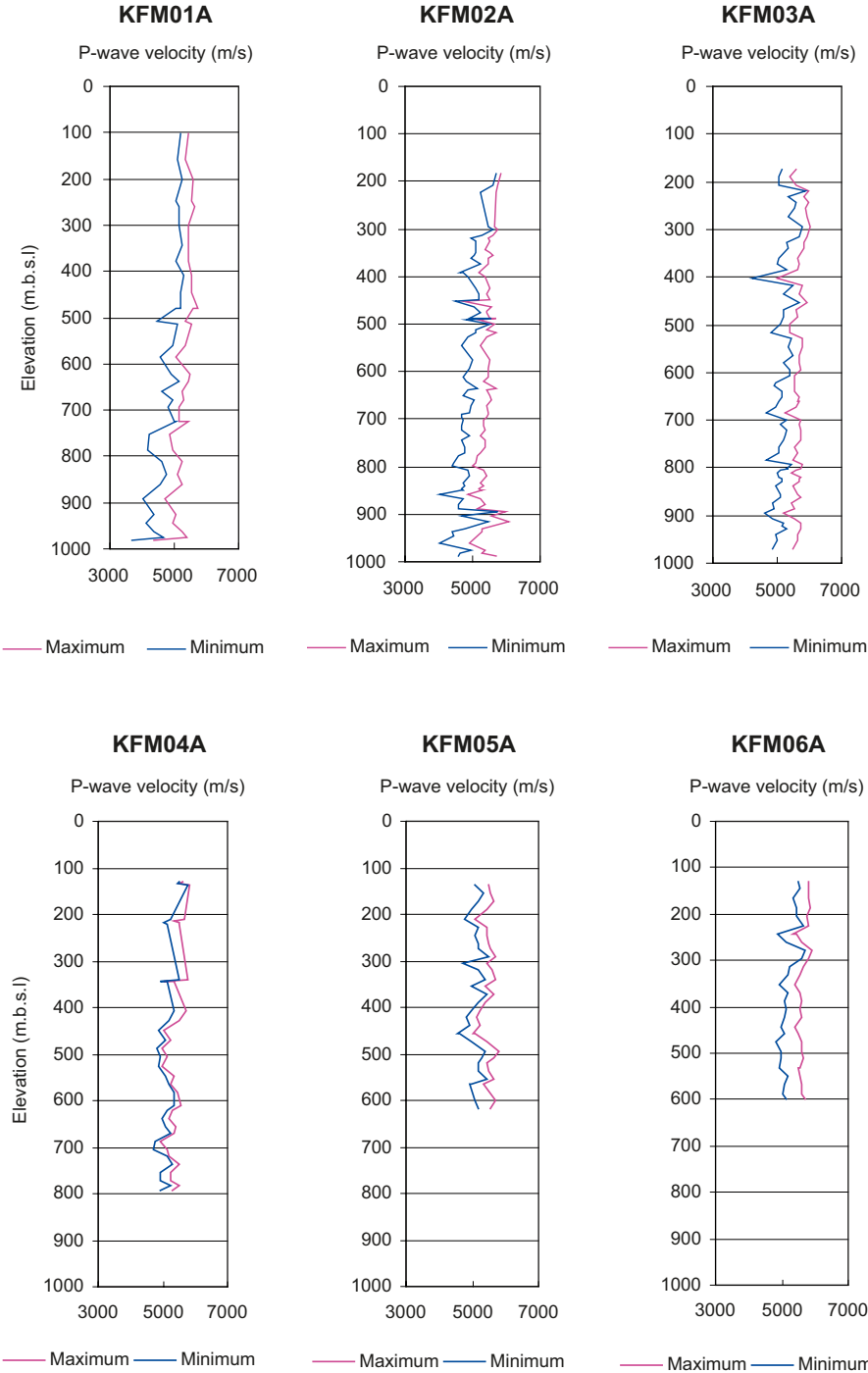
Title ROCK MECHANICS KFM09B									
	Site	FORMARK	Bearing [°]	140.83	Northing [m]	6700119.89	Date of mapping	2006-02-05 10:35:00	
	Borehole	KFM09B	Inclination [°]	-55.07	Easting [m]	1630638.78	Plot Date	2007-05-07 22:10:48	
	Diameter [mm]	77	Elevation [m.a.s.l.ToC]	4.30	Drilling Start Date	2005-11-16 00:00:00			
	Length [m]	616.450	Coordinate System	RT90-RHB70		Drilling Stop Date	2005-12-19 00:00:00		

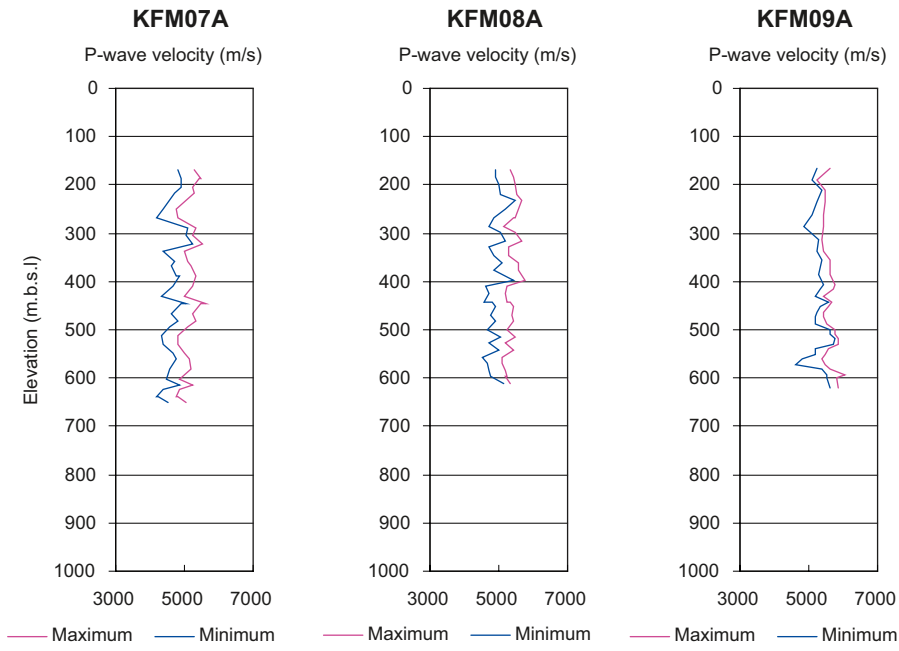
ROCK TYPE FORMARK		ROCK UNIT		TENSILE STRENGTH		Q Value	
	Granite, fine- to medium-grained		High confidence		< 1 Very poor		10 - 40 Good
	Pegmatite, pegmatitic granite		Medium confidence		1 - 4 Poor		> 40 Very good
	Granite, granodiorite and tonalite, metamorphic, fine- to medium-grained		High confidence		4 - 10 Fair		
	Granite to granodiorite, metamorphic, medium-grained			TRIAXIAL COMPRESSIVE STRENGTH		RMR	
	Amphibolite			(confinement stress MPa)			< 20 Very poor
	Calc-silicate rock (skarna)						21 - 40 Poor
							41 - 60 Fair
							61 - 80 Good
							81 - 100 Very good



P-wave velocity plots

P-wave velocity measured on the borehole cores.





Integrated WellCad diagrams

WellCad plots for all the cored boreholes, showing a selected suite of hydrogeological, hydrogeochemical and rock mechanical data in the context of the geological model at stage 2.2.

SKB **INTEGRATED DATA KFM01A**

Site FORSMARK 318.35
 Borehole KFM01A -84.72
 Diameter [mm] 76
 Length [m] 1001.490

Bearing [°] 318.35
 Inclination [°] -84.72
 Date of mapping 2003-01-23 00:00:00

Coordinate System RT90-RHB70
 Northing [m] 669529.81
 Easting [m] 1631397.16
 Elevation [m.a.s.l. ToC] 3.13

Drilling Start Date 2002-06-25 13:55:00
 Drilling Stop Date 2002-10-28 14:39:00
 Plot Date 2007-05-02 22:12:12

ROCK DOMAIN V2.2
 RFM029 Granite to granulite, metamorphic, medium-grained

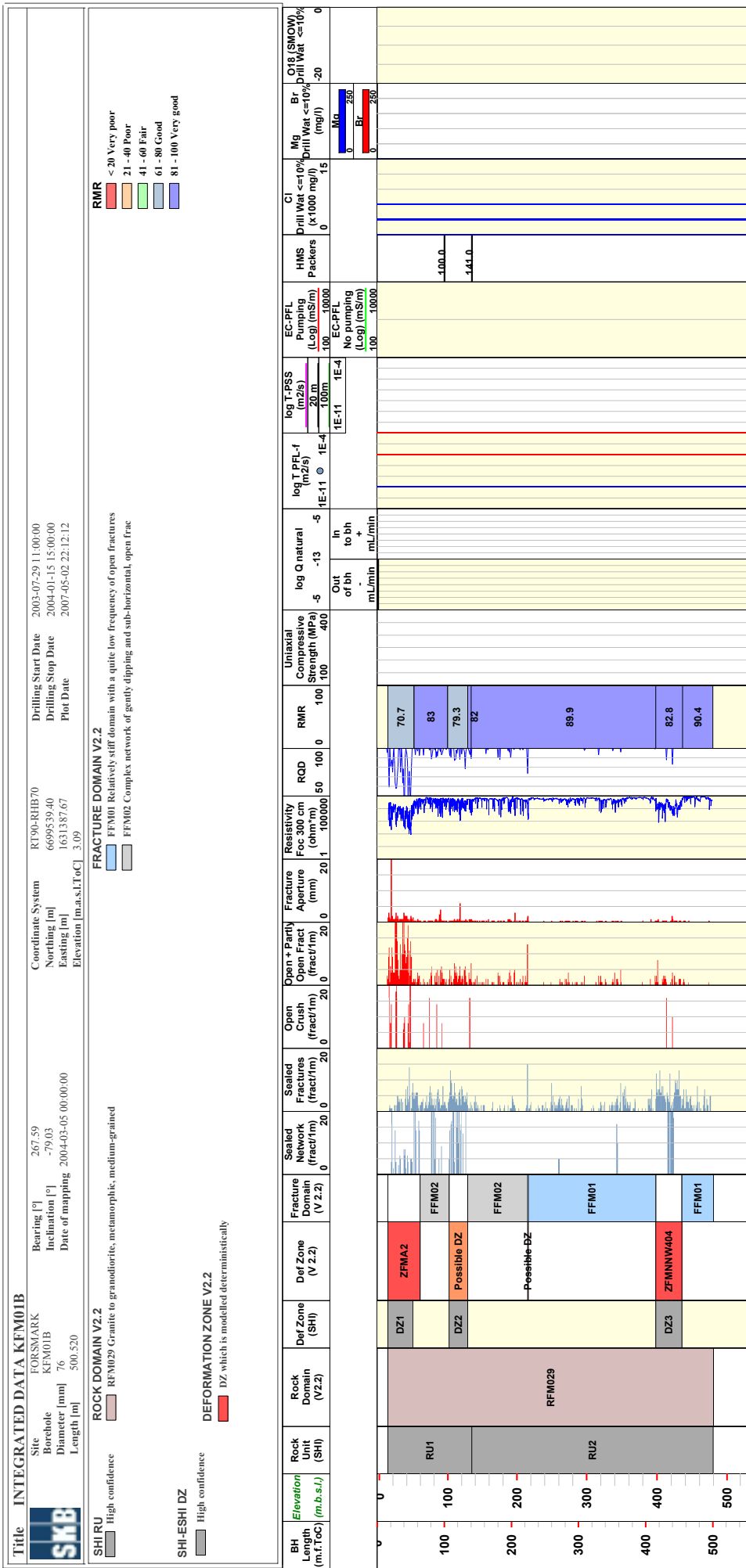
FRACTURE DOMAIN V2.2
 FFM01 Relatively stiff domain with a quite low frequency of open fractures
 FFM02 Complex network of gently dipping and sub-horizontal, open frac

DEFORMATION ZONE V2.2
 DZ2 which is modelled deterministically

SHI-ESHI DZ
 High confidence
 Medium confidence
 High confidence



BH Length (m.f.ToC)	Elevation (m.b.s.l.)	Rock Unit (SHI)	Rock Domain (V2.2)	Def Zone (SHI)	Def Zone (V2.2)	Fracture Domain (V2.2)	Sealed Network Fractures (frac/fm)	Sealed Fractures (frac/fm)	Open Crush (frac/fm)	Open Fractures (frac/fm)	Open + Partly Open Fractures (frac/fm)	Fracture Aperture (mm)	Resistivity Foc 300 cm (ohm*m)	RQD	RMR	Uniaxial Compressive Strength (MPa)	log Q natural	log T PFL-f (m2/s)	log T-PSS (m2/s)	EC-PFL Pumping (Log) (mS/m)	CI Drill Wat <=10% (x1000 mg/l)	Mg Drill Wat <=10% (mg/l)	Br Drill Wat <=10% (mg/l)	O16 (SNOW) Drill Wat <=10%	
100	100	RU1	RFM029			FFM02									79.8										
200	200	RU1	RFM029		Possetts DZ	FFM01									77.4										
300	300	RU1	RFM029		ZFMNE1192	FFM01									82										
400	400	RU2a	RFM029	DZ2	ZFMNE1192	FFM01									80.4										
500	500	RU3	RFM029			FFM01									84.6										
600	600	RU3	RFM029			FFM01									80.6										
700	700	RU2b	RFM029	DZ3	ZFMNE2254	FFM01									88										
800	800	RU4	RFM029			FFM01									81.8										
900	900	RU2c	RFM029			FFM01									93										



Title INTEGRATED DATA KFM01C



Site FORSMARK
 KFM01C
 Borehole Diameter [mm] 76
 Length [m] 450.020

Bearing [°] 165.35
 Inclination [°] -49.60
 Date of mapping 2006-01-17 10:57:00

Coordinate System R190-RHB70
 Northing [m] 669526.14
 Easting [m] 1631403.75
 Elevation [m.a.s.l. to C] 2.91

Drilling Start Date 2005-11-05 13:56:00
 Drilling Stop Date 2005-11-29 13:52:00
 Plot Date 2007-05-02 22:12:12

ROCK DOMAIN V2.2

High confidence RFM029 Granite to granodiorite, metamorphic, medium-grained

FRACTURE DOMAIN V2.2

FFM01 Relatively stiff domain with a quite low frequency of open fractures
 FFM02 Complex network of gently dipping and sub-horizontal, open frac

RMR

< 20 Very poor
 21 - 40 Poor
 41 - 60 Fair
 61 - 80 Good
 81 - 100 Very good

SHI-RU

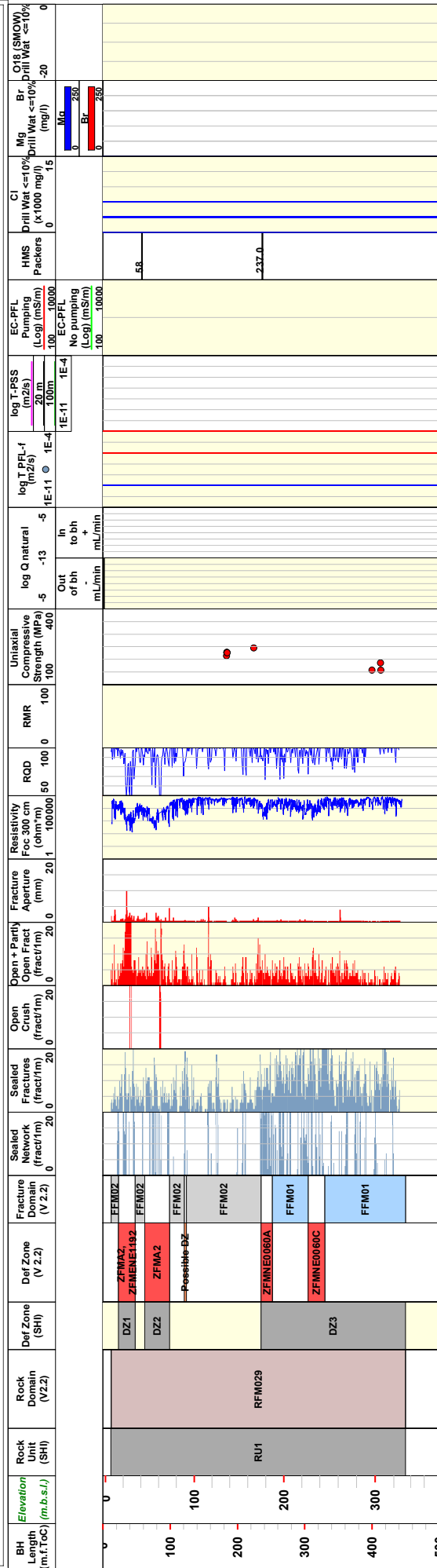
High confidence

SHI-ESI DZ

High confidence

DEFORMATION ZONE V2.2

DZ which is modelled deterministically



Title **INTEGRATED DATA KFM02A**

Site FORSMARK
 Borehole KFM02A
 Diameter [mm] 77
 Length [m] 1002.440

Bearing [°] 275.76
 Inclination [°] -85.37
 Date of mapping 2003-04-22 00:00:00

Coordinate System R 190-RHB70
 Northing [m] 6698712.50
 Easting [m] 1633182.86
 Elevation [m a.s.l.] 7.35

Drilling Start Date 2003-01-08 14:23:00
 Drilling Stop Date 2003-03-12 21:30:00
 Plot Date 2007-05-02 22:12:12

SHI RU
 High confidence
 Medium confidence
 High confidence

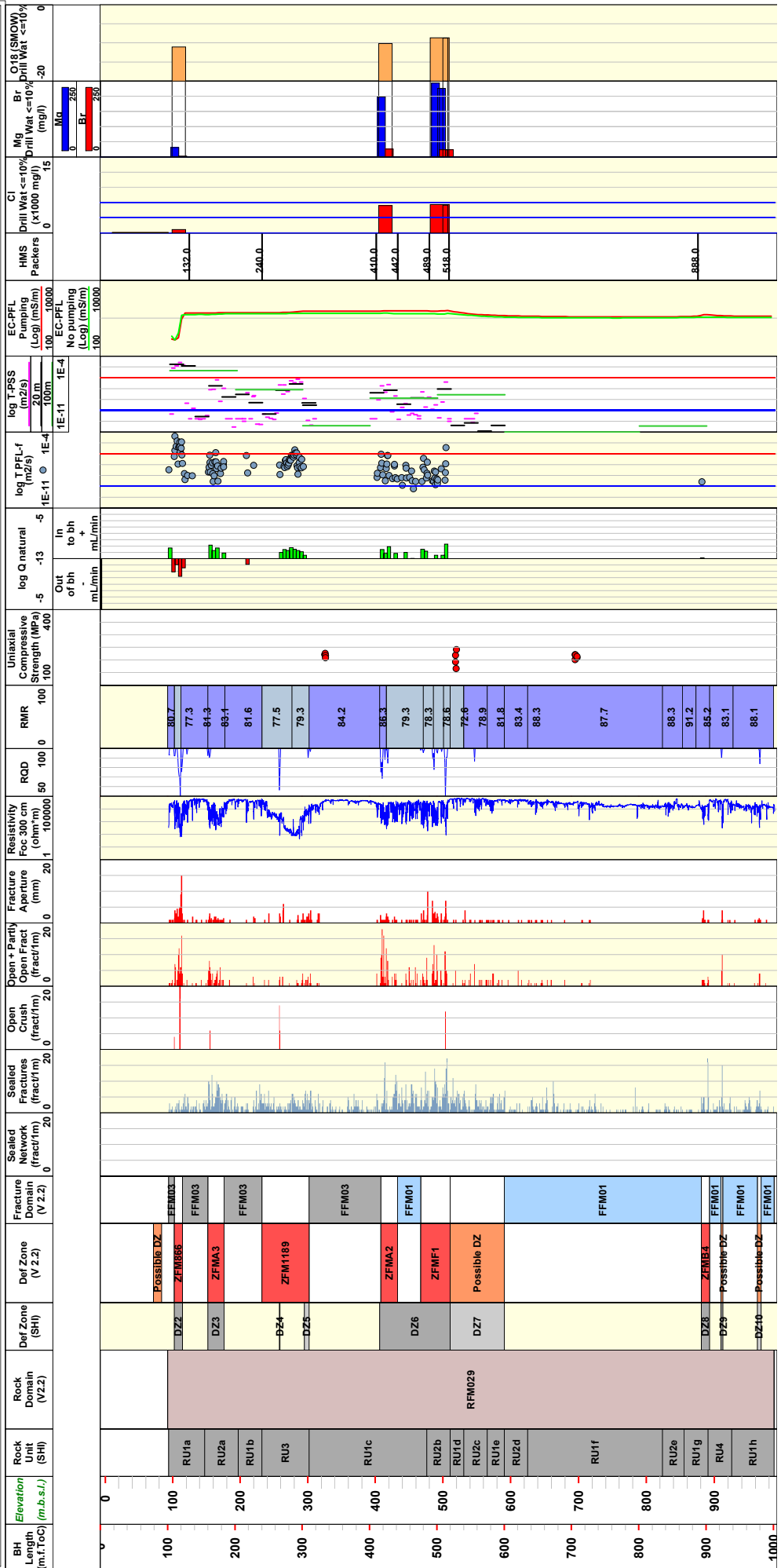
ROCK DOMAIN V2.2
 RFM029 Granite to granodiorite, metamorphic, medium-grained

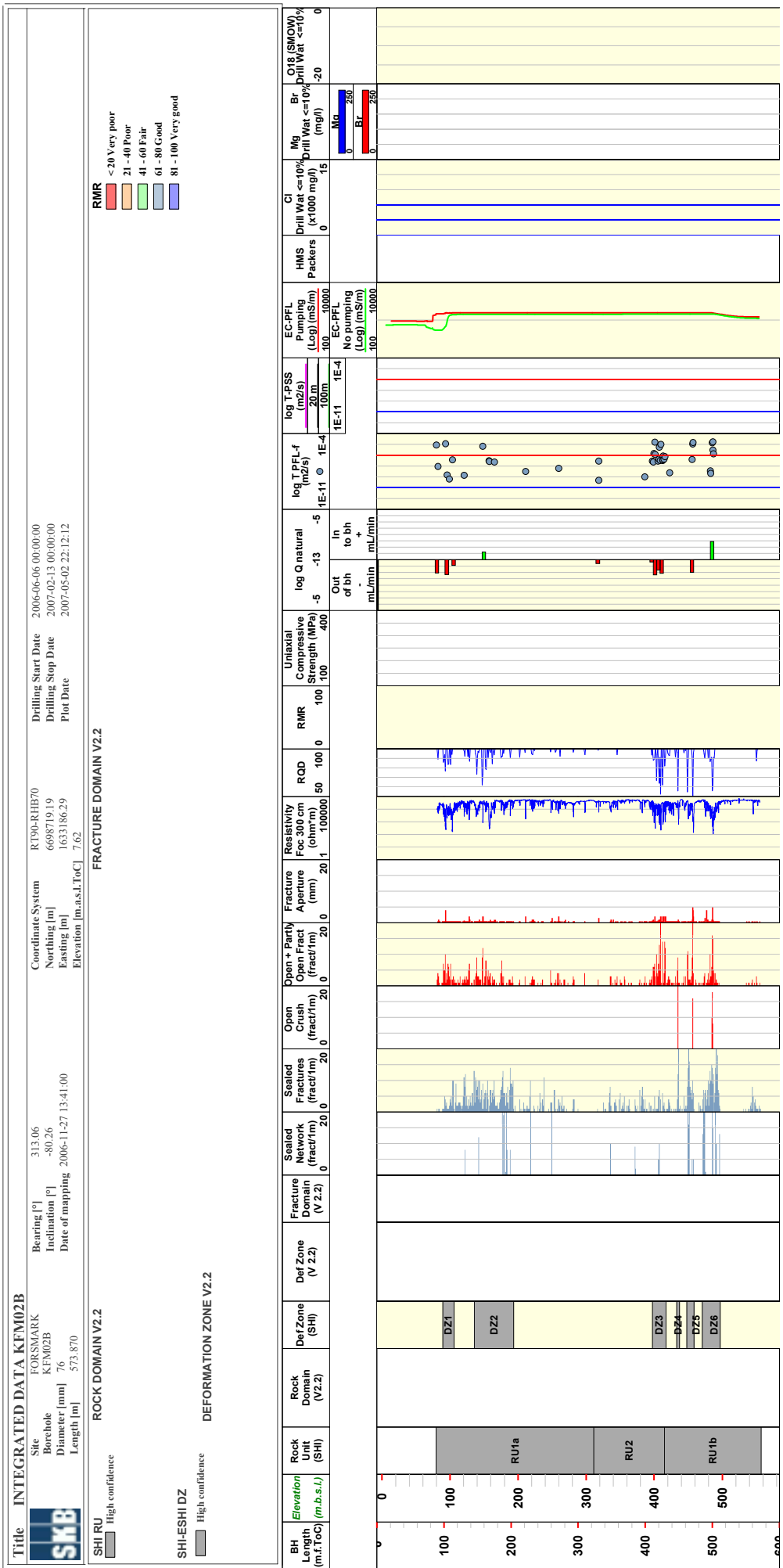
FRACTURE DOMAIN V2.2
 FFM01 Relatively stiff domain with a quite low frequency of open fractures
 FFM03 High freq. of gently dipping DZ, both containing sealed and open frac

RMR
 <20 Very poor
 21-40 Poor
 41-60 Fair
 61-80 Good
 81-100 Very good

SHI-ESHI DZ
 High confidence
 Medium confidence
 High confidence

DEFORMATION ZONE V2.2
 DZ which is modelled deterministically





Title INTEGRATED DATA KFM03A

Site FORSMARK 271.52
 Borehole KFM03A -85.74
 Diameter [mm] 77
 Length [m] 1001.190

Coordinate System R190-RHB70
 Northing [m] 6697852.10
 Easting [m] 1634630.74
 Elevation [m.a.s.l./ToC] 8.29

Drilling Start Date 2003-04-16 11:33:00
 Drilling Stop Date 2003-06-23 16:15:00
 Plot Date 2007-05-02 22:12:12

SHI RU
 High confidence

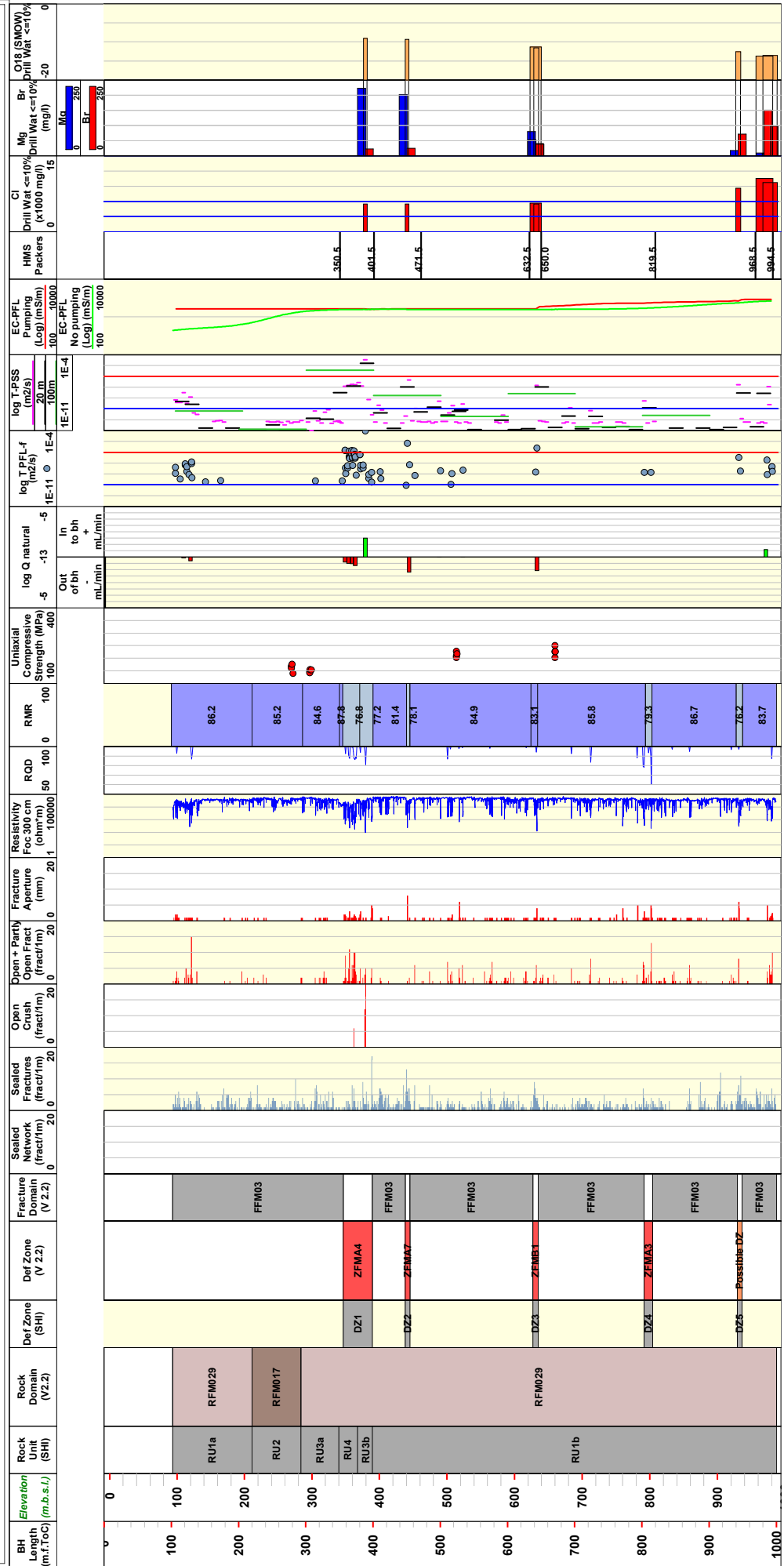
ROCK DOMAIN V2.2
 RFM017 Tonalite to granodiorite, metamorphic
 RFM029 Granite to granodiorite, metamorphic, medium-grained

SHI-ESHI DZ
 High confidence

DEFORMATION ZONE V2.2
 DZ, which is modelled deterministically

FRACTURE DOMAIN V2.2
 FFM03 High freq of gently dipping, DZ, both containing sealed and open frac

RMR
 <20 Very poor
 21-40 Poor
 41-60 Fair
 61-80 Good
 81-100 Very good



Title INTEGRATED DATA KFM04

Site FORSMARK
 Borehole KFM04A
 Diameter [mm] 77
 Length [m] 1001.420

Bearing [°] 45.24
 Inclination [°] -60.07
 Date of mapping 2003-12-08 00:00:00

Coordinate System R190-RHD70
 Northing [m] 6698921.74
 Easting [m] 1630978.96
 Elevation [m.a.s.l.] 8.77

Drilling Start Date 2003-08-25 11:17:00
 Drilling Stop Date 2003-11-19 15:15:00
 Plot Date 2007-05-02 22:12:12

SHI RU

High confidence
 RFM012 Granite to granodiorite, metamorphic, medium-grained
 RFM018 Tonalite to granodiorite, metamorphic
 RFM029 Granite to granodiorite, metamorphic, medium-grained

ROCK DOMAIN V2.2

FFM01 Relatively stiff domain with a quite low frequency of open fractures
 FFM04 Strong bedrock anisotropy with ductile strain / struc

SHI-ESHI DZ
 Medium confidence
 High confidence

DEFORMATION ZONE V2.2

DZ4 which is modelled deterministically

RMR
 <20 Very poor
 21 -40 Poor
 41 -60 Fair
 61 -80 Good
 81 -100 Very good

EC-PFL Pumping (Log) (mS/m)
 EC-PFL No pumping (Log) (mS/m)

log T-PFL-f (m2/s)
 log T-PSS (m2/s)

log Q natural
 Out of bh
 In to bh

Uniaxial Compressive Strength (MPa)

RMR

RQD

Resistivity Foc 300 cm (ohm*m)

Fracture Aperture (mm)

Open + Partly Open Fract (fract/m)

Open Crush (fract/m)

Sealed Fractures (fract/m)

Sealed Network (fract/m)

Fracture Domain (V.2.2)

Def Zone (SHI)

Def Zone (V.2.2)

Rock Domain (V.2.2)

Rock Unit (SHI)

BH Length (m.t. TOC)

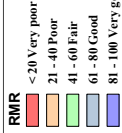
Elevation (m.b.s.l.)

HMS Packers

CI Drill Wat <=10% (x1000 mg/l)

Mg Br Drill Wat <=10% (mg/l)

O18 (SMOW) Drill Wat <=10%



Title INTEGRATED DATA KFM05A

Site FORSMARK KFM05A
 Borehole Diameter [mm] 77
 Length [m] 1002.710

Coordinate System RT90-RHB70
 Northing [m] 669344.85
 Easting [m] 1631710.80
 Elevation [m.a.s.l./ToC] 5.53

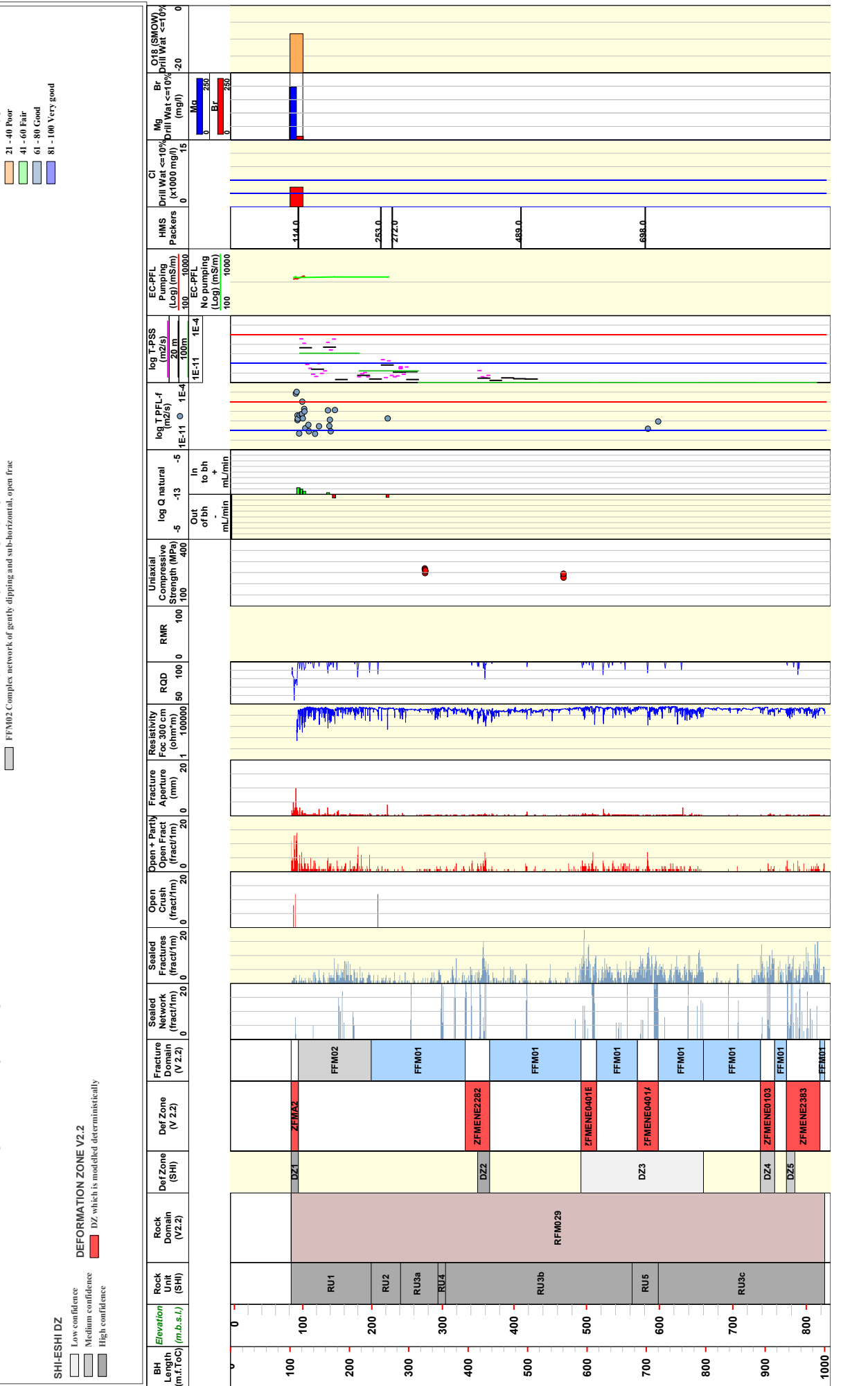
Drilling Start Date 2003-11-25 12:00:00
 Drilling Stop Date 2004-05-05 10:00:00
 Plot Date 2007-05-02 22:12:12

SHI-RU High confidence
 SHI-ESHI DZ Low confidence
 Medium confidence
 High confidence

ROCK DOMAIN V2.2
 RFM029 Granite to gneiss, medium-grained
 RFM01 Relatively stiff domain with a quite low frequency of open fractures
 RFM02 Complex network of gently dipping and sub-horizontal, open frac

DEFORMATION ZONE V2.2
 DZ1 which is modeled deterministically
 DZ2
 DZ3
 DZ4
 DZ5

RMR
 < 20 Very poor
 21 - 40 Poor
 41 - 60 Fair
 61 - 80 Good
 81 - 100 Very good



Title INTEGRATED DATA KFM06A

Site: FORSMARK KFM06A
 Borehole: KFM06A
 Diameter [mm]: 77
 Length [m]: 1000.640
 Bearing [°]: 300.92
 Inclination [°]: -60.24
 Date of mapping: 2004-11-02 00:00:00
 Coordinate System: RT90-RHB70
 Northing [m]: 669732.88
 Easting [m]: 163242.51
 Elevation [m.a.s.l./ToC]: 4.10
 Drilling Start Date: 2004-06-14 14:00:00
 Drilling Stop Date: 2004-09-21 03:37:00
 Plot Date: 2007-05-02 22:12:12

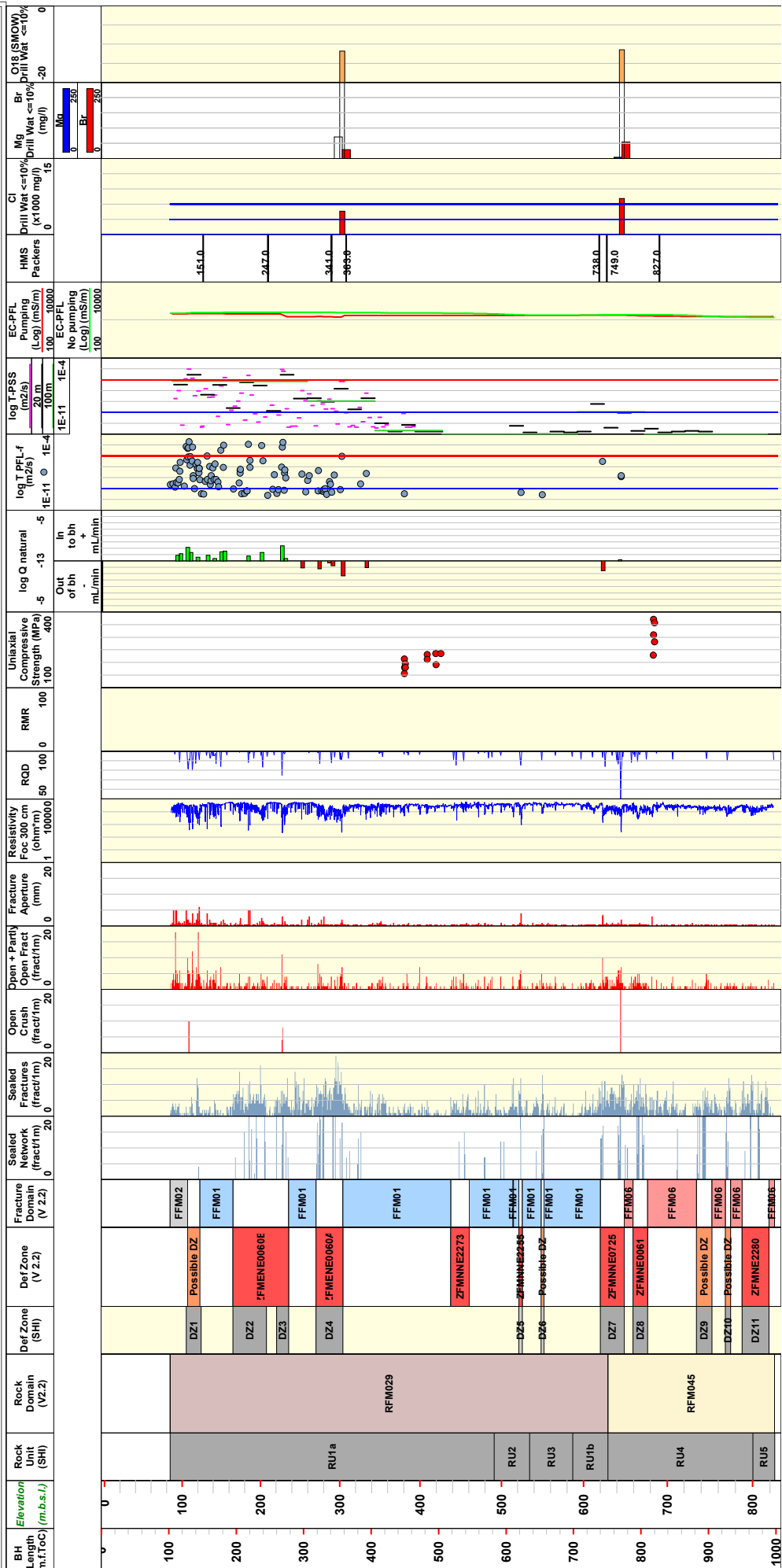
ROCK DOMAIN V2.2
 SHI RU High confidence
 SHI RU Medium confidence
 SHI RU High confidence
 RFM029 Granite to granodiorite, metamorphic, medium-grained
 RFM045 Aplitic granite, medium-grained granite and felsic volcanic rock, metamorphic and, in part, albitised
 RFM06 Common occurrence of fine-grained, albitised granitic rock

SHI-ESHI DZ
 DZ1 Possible DZ
 DZ2 ZFMENE060E
 DZ3
 DZ4 ZFMENE060A
 DZ5 ZFMINE2273
 DZ6 ZFMINE2255
 DZ7 ZFMINE0725
 DZ8 ZFMINE0601
 DZ9 Possible DZ
 DZ10 Possible DZ
 DZ11 ZFMINE2280

DEFORMATION ZONE V2.2
 DZ which is modelled deterministically

FRACTURE DOMAIN V2.2
 FFM01 Relatively stiff domain with a quite low frequency of open fractures
 FFM02 Complex network of gently dipping and sub-horizontal, open frac
 FFM06 Common occurrence of fine-grained, albitised granitic rock

RMR
 < 20 Very poor
 21 - 40 Poor
 41 - 60 Fair
 61 - 80 Good
 81 - 100 Very good



Title **INTEGRATED DATA KFM06B**

Site FORSMARK
 Borehole KFM06B
 Diameter [mm] 77
 Length [m] 100.330

Bearing [°] 296.96
 Inclination [°] -83.51
 Date of mapping 2005-03-12 18:51:00

Coordinate System RT90-RHB70
 Northing [m] 6699732.24
 Easting [m] 1632446.41
 Elevation [m.a.s.l./ToC] 4.13

Drilling Start Date 2004-05-26 07:00:00
 Drilling Stop Date 2005-02-08 14:00:00
 Plot Date 2007-05-02 22:12:12

SHIRU **ROCK DOMAIN V2.2**

High confidence RFM029 Granite to gneiss, medium-grained

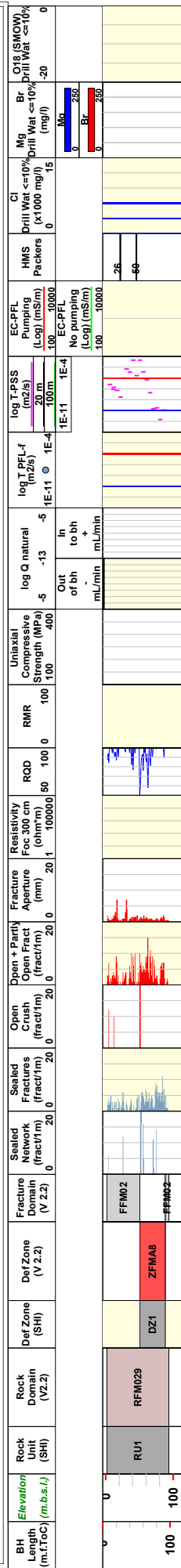
FRACTURE DOMAIN V2.2

FFM02 Complex network of gently dipping and sub-horizontal, open frac

SHI-ESHI DZ

High confidence **DEFORMATION ZONE V2.2**
 DZ which is modelled deterministically

RMR
 < 20 Very poor
 21 - 40 Poor
 41 - 60 Fair
 61 - 80 Good
 81 - 100 Very good



Title INTEGRATED DATA KEM06C

Site FORSMARK KEM06C
 Borehole Diameter [mm] 76
 Length [m] 1000.910
 Bearing [°] 26.07
 Inclination [°] -60.11
 Date of mapping 2005-08-29 08:00:00
 Coordinate System RT90-RHB70
 Northing [m] 6699740.96
 Easting [m] 1632437.03
 Elevation [m.a.s.l./ToC] 4.09
 Drilling Start Date 2005-04-26 14:30:00
 Drilling Stop Date 2006-06-05 00:00:00
 Plot Date 2007-05-02 22:12:12

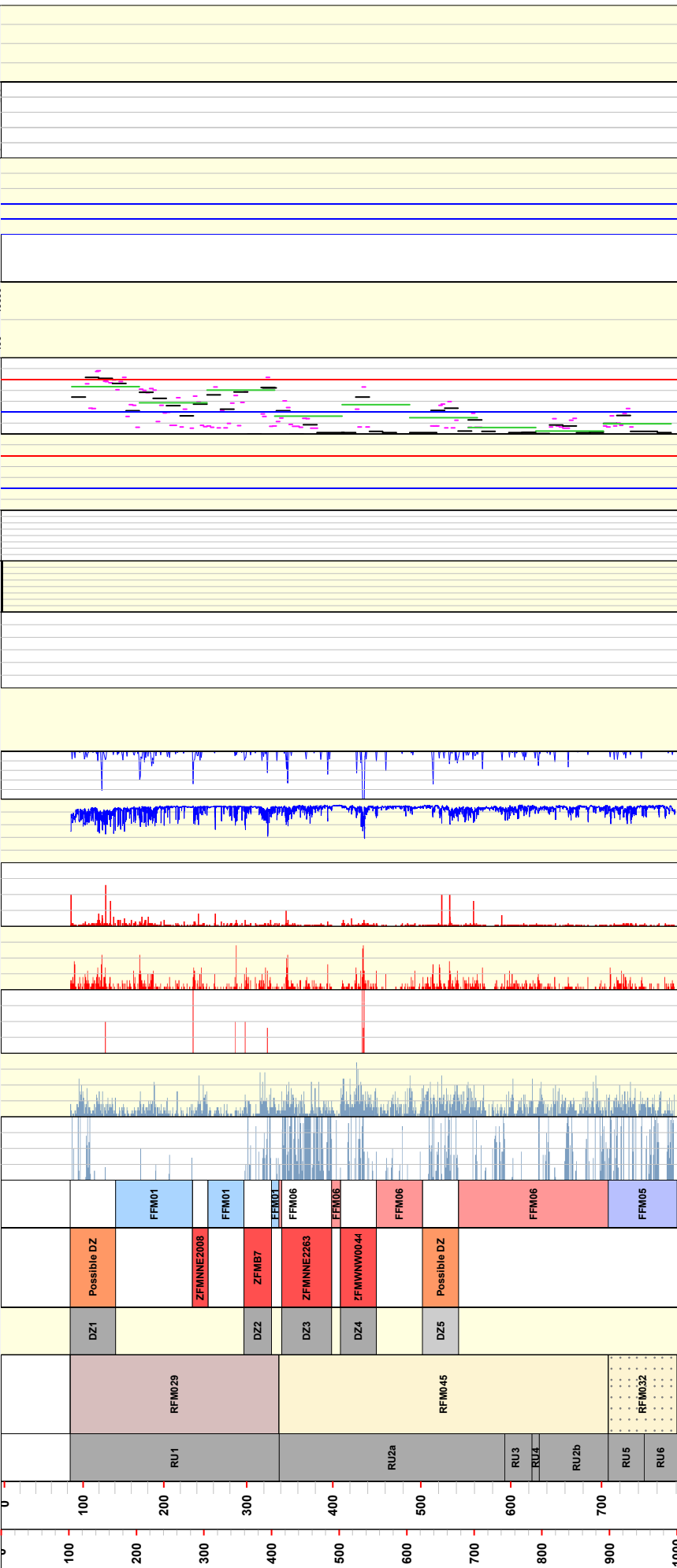
SHI RU
 High confidence
 Medium confidence
 High confidence

SHI-ESHI DZ
 High confidence
 Medium confidence
 High confidence

ROCK DOMAIN V2.2
 RFM029 Granite to granodiorite, metamorphic, medium-grained
 RFM037 Aplitic granite, medium-grained granite and felsic volcanic rock, metamorphic and, in part, albitised
 RFM045 Aplitic granite, medium-grained granite and felsic volcanic rock, metamorphic and, in part, albitised
 RFM066 Common occurrence of fine-grained, albitised granitic rock

DEFORMATION ZONE V2.2
 DZ1 Possible DZ
 DZ2
 DZ3
 DZ4
 DZ5 Possible DZ

FRACTURE DOMAIN V2.2
 FFM01 Relatively stiff domain with a quite low frequency of open fractures
 FFM05 Strong bedrock anisotropy with high ductile strain, folded ductile strata, and occurrence of felsic meta-igneous rocks
 FFM06 Common occurrence of fine-grained, albitised granitic rock



Title: INTEGRATED DATA KFM07A

Site FORSMARK KFM07A
 Borehole Diameter [mm] 77
 Length [m] 1002.100

Bearing [°] 261.47
 Inclination [°] -59.28
 Date of mapping, 2005-01-17 15:59:00

Coordinate System RT90-R14B70
 Northing [m] 6700127.08
 Easting [m] 1631031.57
 Elevation [m.a.s.l./ToC] 3.33

Drilling Start Date 2004-10-14 08:00:00
 Drilling Stop Date 2004-12-09 11:40:00
 Plot Date 2007-05-02 22:12:12

SHI RU High confidence

ROCK DOMAIN V2.2
 RFM029 Granite to granodiorite, metamorphic, medium-grained
 RDM044 Granite to granodiorite, metamorphic, medium-grained

FRACTURE DOMAIN V2.2

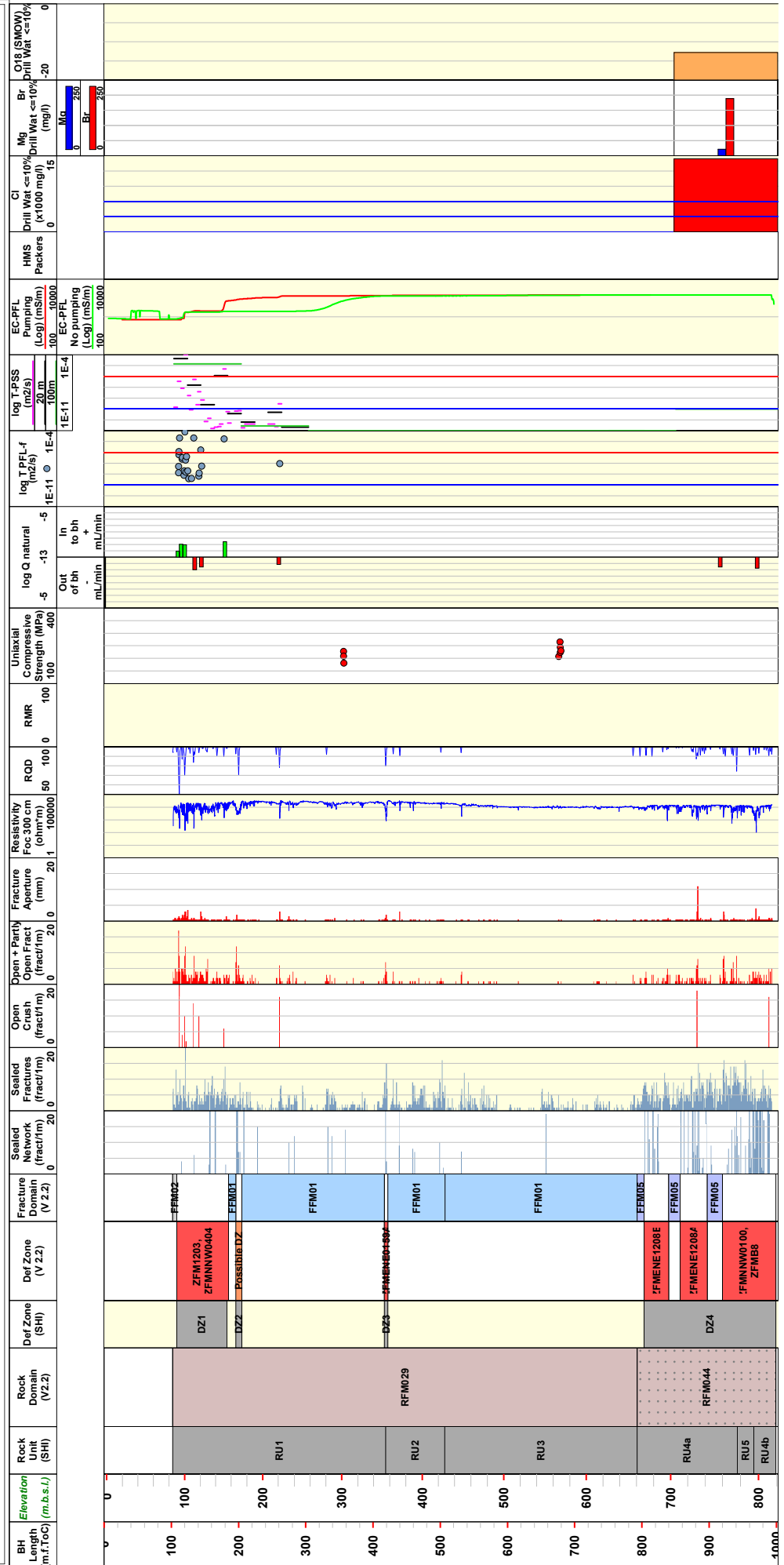
FFM01 Relatively stiff domain with a quite low frequency of open fractures
 FFM02 Complex network of gently dipping and sub-horizontal, open frac
 FFM05 Strong bedrock anisotropy with high ductile strain, folded ductile struc, and occurrence of fibric meta-igneous rocks

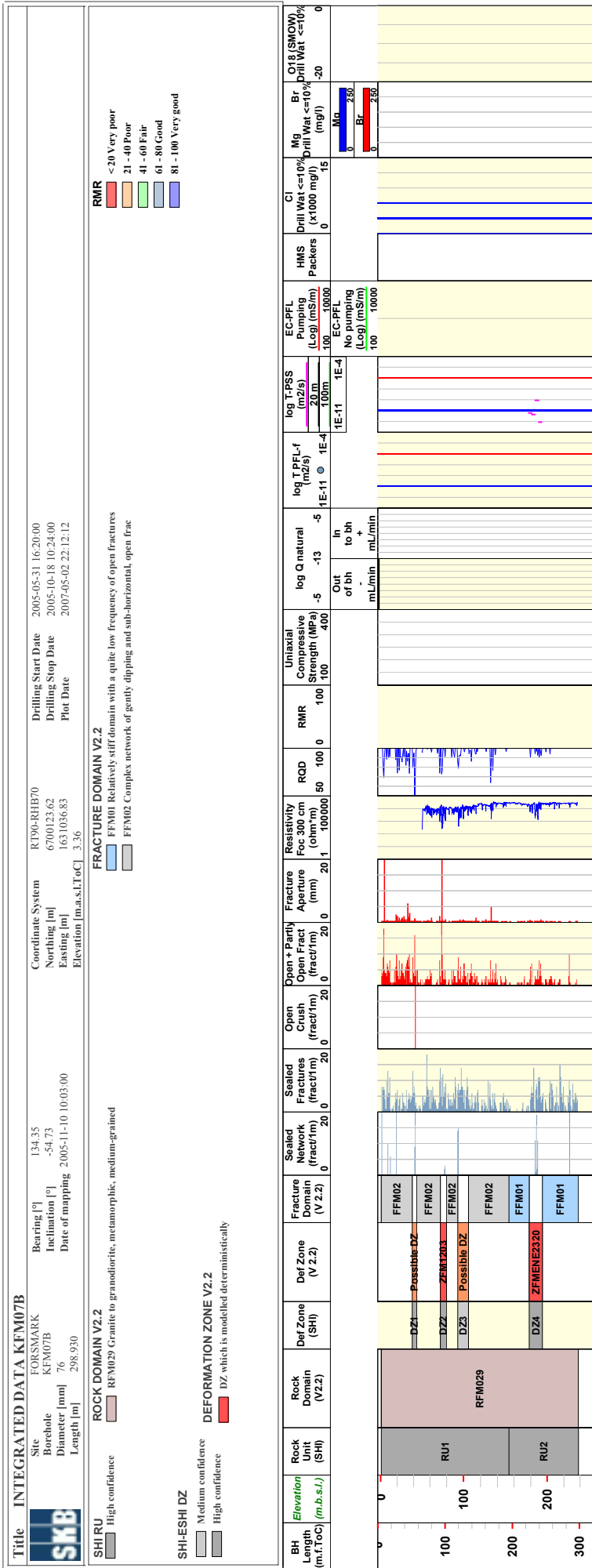
RMR
 <20 Very poor
 21 - 40 Poor
 41 - 60 Fair
 61 - 80 Good
 81 - 100 Very good

SHI-ESHI DZ High confidence

DEFORMATION ZONE V2.2

DZ which is modelled deterministically





Title INTEGRATED DATA KFM07C



FORMS MARK
KFM07C
Site 142.71
Borehole -85.32
Diameter [mm] 76
Length [m] 500.340
Date of mapping 2006-09-04 09:21:00

Coordinate System R190-RHB70
Northing [m] 6700125.61
Easting [m] 1631034.45
Elevation [m.a.s.l./ToC] 3.35
Drilling Start Date 2006-03-30 00:00:00
Drilling Stop Date 2006-08-08 00:00:00
Plot Date 2007-05-02 22:12:12

ROCK DOMAIN V2.2

High confidence RTM029 Granite to gneiss, metamorphic, medium-grained

FRACTURE DOMAIN V2.2

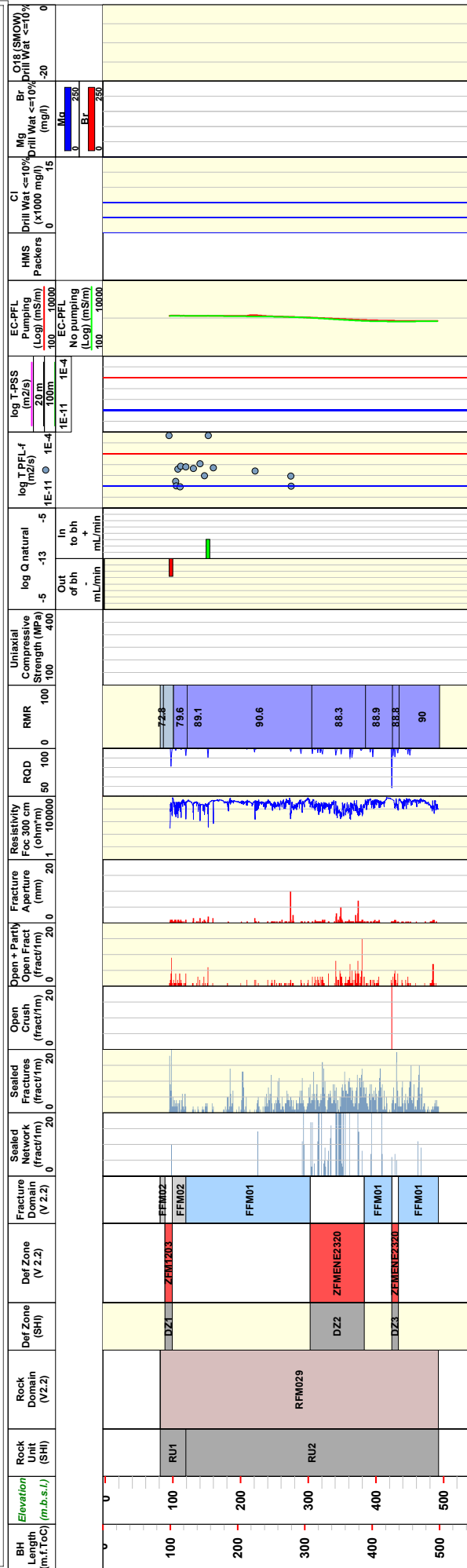
FFM01 Relatively stiff domain with a quite low frequency of open fractures
FFM02 Complex network of gently dipping and sub-horizontal, open frac

RMR
 < 20 Very poor
 21 - 40 Poor
 41 - 60 Fair
 61 - 80 Good
 81 - 100 Very good

SHI-ESH1 DZ
 High confidence

DEFORMATION ZONE V2.2

DZ which is modelled deterministically



Title **INTEGRATED DATA KFM08B**

Site FORSMARK
 KFM08B
 Borehole Diameter [mm] 76
 Length [m] 200.540

Bearing [°] 270.45
 Inclination [°] -58.84
 Date of mapping 2005-05-02 14:49:00

Coordinate System RT90-RHB70
 Northing [m] 6700492.75
 Easting [m] 1631173.27
 Elevation [m.a.s.l.±0.1] 2.25

Drilling Start Date 2005-01-11 16:04:00
 Drilling Stop Date 2005-01-26 14:51:00
 Plot Date 2007-05-02 22:12:12

SHI RU

High confidence
 Medium confidence
 High confidence

ROCK DOMAIN V2.2

RFM029 Granite to granodiorite, metamorphic, medium-grained

SHI-ESHI DZ

High confidence
 Medium confidence
 High confidence

FRACTURE DOMAIN V2.2

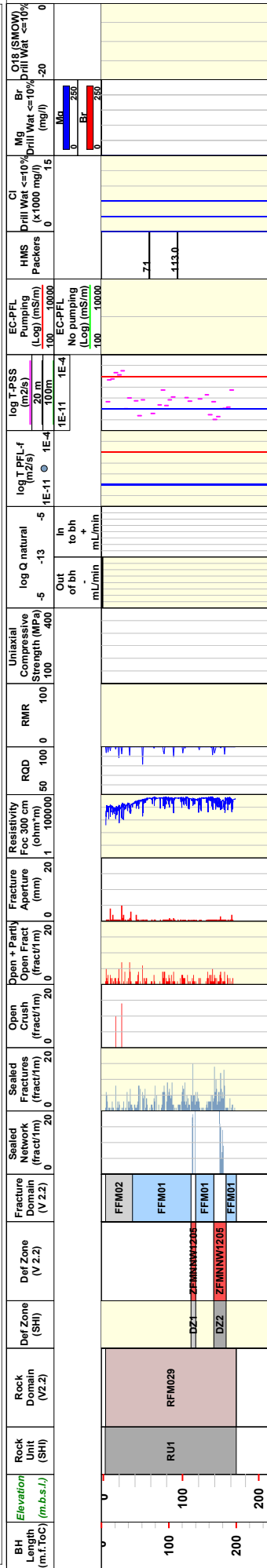
FFM01 Relatively stiff domain with a quite low frequency of open fractures
 FFM02 Complex network of gently dipping and sub-horizontal, open frac

RMR

< 20 Very poor
 21 - 40 Poor
 41 - 60 Fair
 61 - 80 Good
 81 - 100 Very good

DEFORMATION ZONE V2.2

High confidence
 DZ which is modelled deterministically



Title INTEGRATED DATA KFM08C

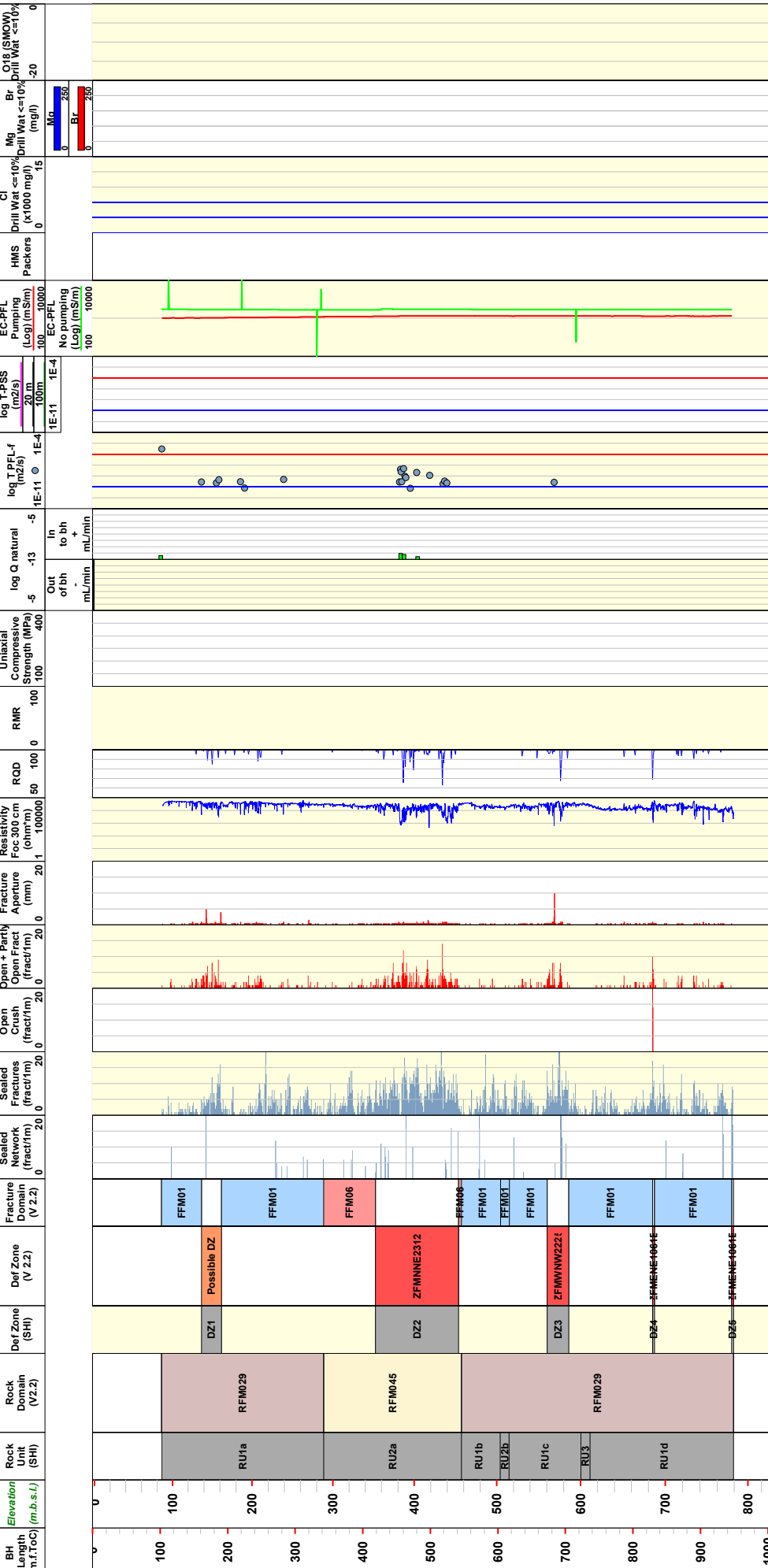
Site FORSMARK KFM08C **Bearing [°]** 35.88 **Coordinate System** R190-R1H270 **Drilling Start Date** 2006-01-30 16:00:00
Borehole Diameter [mm] 77 **Inclination [°]** -60.47 **Northing [m]** 6700495.88 **Drilling Stop Date** 2006-05-09 06:00:00
Date of mapping 2006-06-20 15:25:00 **Easting [m]** 1631187.57 **Plot Date** 2007-05-02 22:12:12
Length [m] 951.080 **Elevation [m.a.s.l.ToC]** 2.47

ROCK DOMAIN V2.2
 SHI RU High confidence RFM029 Granite to granodiorite, metamorphic, medium-grained
 Medium confidence RFM045 Aplitic granite, medium-grained granite and felsic volcanic rock, metamorphic and, in part, albitised
 High confidence RFM06 Common occurrence of fine-grained, albitised granitic rock

SHI-ESHI DZ
 High confidence DZ1
 Medium confidence Possible DZ
 High confidence DZ2
 DZ3
 DZ4
 DZ5

DEFORMATION ZONE V2.2
 High confidence DZ1
 Medium confidence Possible DZ
 High confidence DZ2
 DZ3
 DZ4
 DZ5

FRACTURE DOMAIN V2.2
 FFM01 Relatively stiff domain with a quite low frequency of open fractures
 FFM06 Common occurrence of fine-grained, albitised granitic rock



Title INTEGRATED DATA KFM09A

Site FORSMARK
 Borehole KFM09A
 Diameter [mm] 77
 Length [m] 799.670

Coordinate System RT90-RHB70
 Northing [m] 6700115.04
 Easting [m] 1630647.50
 Elevation [m.a.s.l. ToC] 4.29

Drilling Start Date 2005-08-31 00:00:00
 Drilling Stop Date 2005-10-27 13:00:00
 Plot Date 2007-05-02 22:12:12

SHI RU
 High confidence

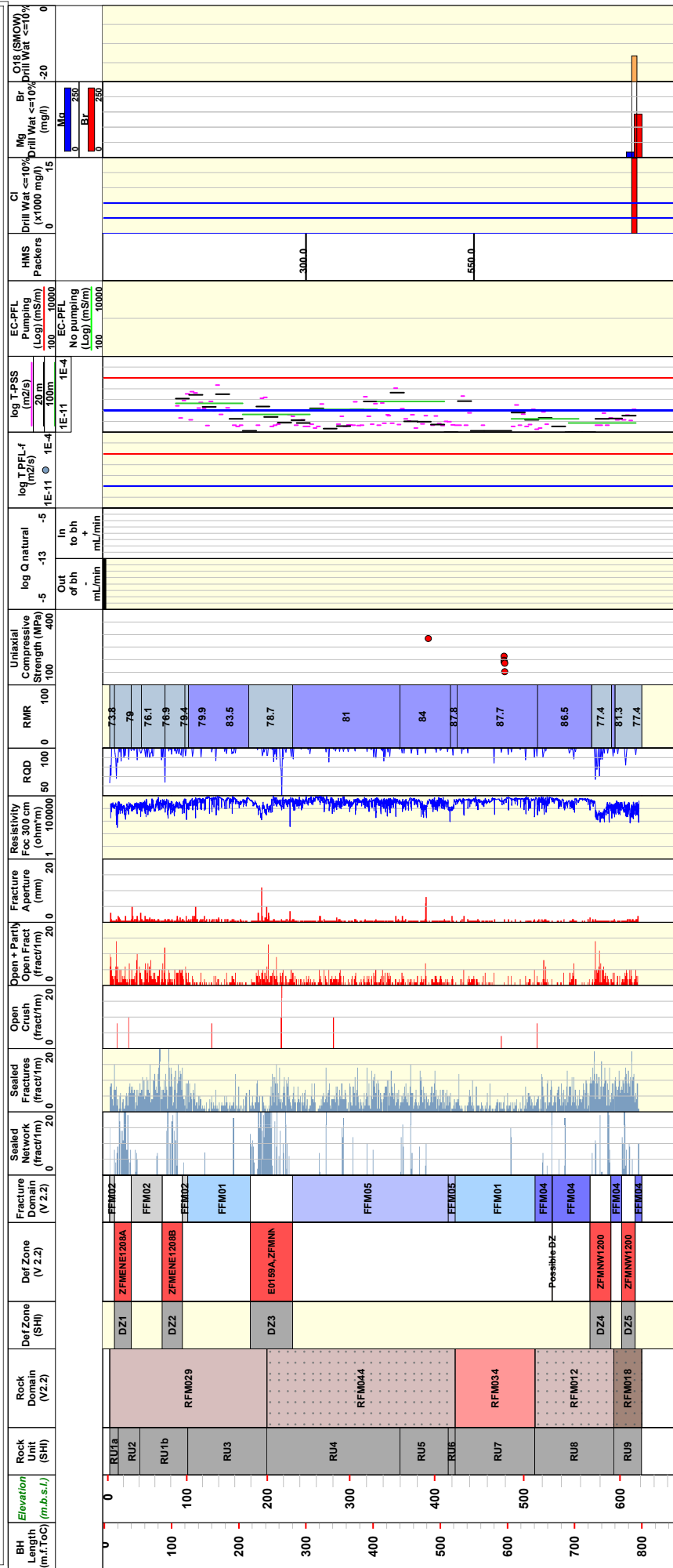
ROCK DOMAIN V2.2
 RFM012 Granite to granodiorite, metamorphic, medium-grained
 RFM018 Tonalite to granodiorite, metamorphic
 RFM029 Granite to granodiorite, metamorphic, medium-grained
 RFM034 Granite to granodiorite, metamorphic, medium-grained
 RFM044 Granite to granodiorite, metamorphic, medium-grained

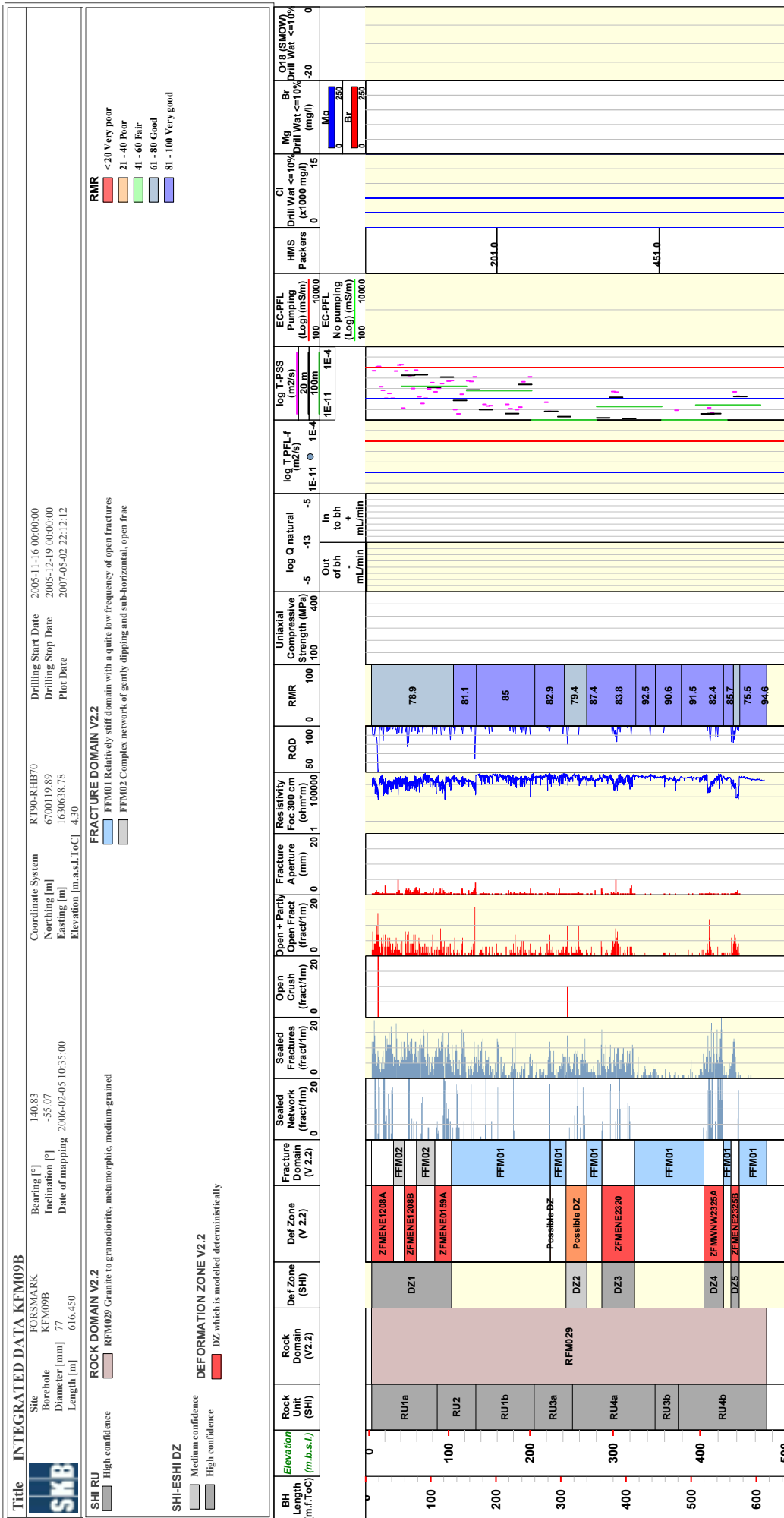
FRACTURE DOMAIN V2.2
 FFM01 Relatively stiff domain with a quite low frequency of open fractures
 FFM02 Complex network of gently dipping and sub-horizontal, open frac
 FFM04 Strong bedrock anisotropy with ductile strain / struc
 FFM05 Strong bedrock anisotropy with high ductile strain , folded ductile struc, and occurrence of felsic meta-igneous rocks

RMR
 < 20 Very poor
 21 - 40 Poor
 41 - 60 Fair
 61 - 80 Good
 81 - 100 Very good

SHI-ESH1-DZ
 High confidence

DEFORMATION ZONE V2.2
 DZ which is modelled deterministically





Title INTEGRATED DATA KFM10A

FORMS MARK
 KFM10A
 Site Bearing [°] 10.42
 KFM10A Inclination [°] -50.12
 Borehole Diameter [mm] 16
 Date of mapping 2006-06-20 10:59:00
 Length [m] 500.160

Coordinate System R190-RHB70
 Northing [m] 6698629.17
 Easting [m] 1631715.90
 Elevation [m.a.s.l./ToC] 4.51
 Drilling Start Date 2006-03-14 15:15:00
 Drilling Stop Date 2006-06-01 12:25:00
 Plot Date 2007-05-02 22:12:12

ROCK DOMAIN V2.2

High confidence RFM029 Granite to granodiorite, metamorphic, medium-grained

FRACTURE DOMAIN V2.2

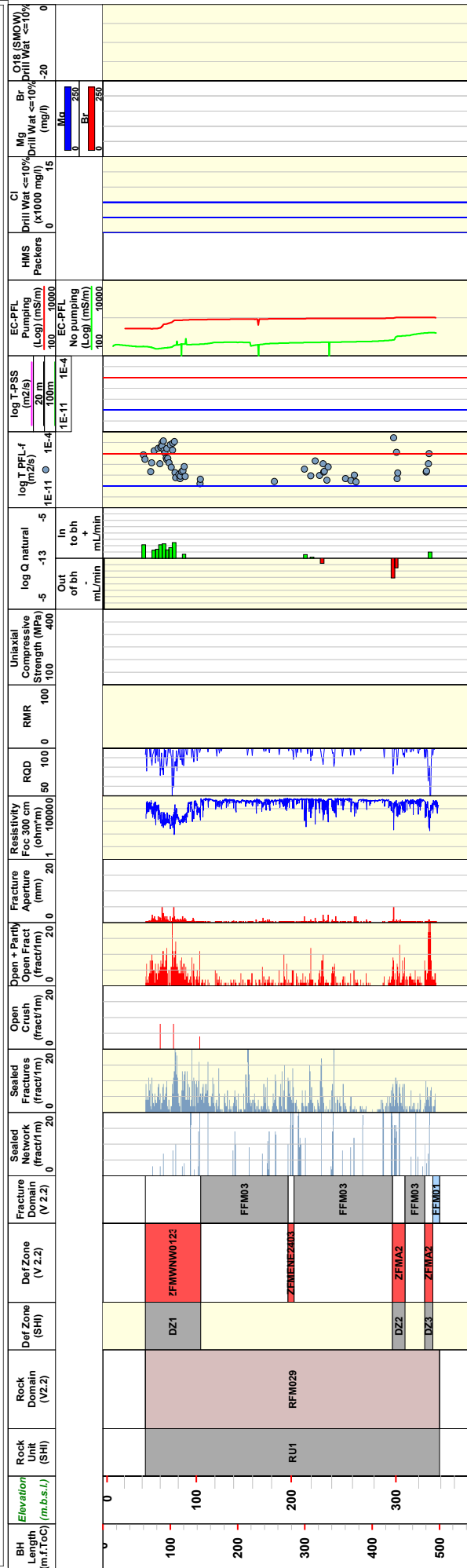
FFM01 Relatively stiff domain with a quite low frequency of open fractures
 FFM03 High freq of gently dipping DZ, both containing sealed and open frac

RMR
 < 20 Very poor
 21 - 40 Poor
 41 - 60 Fair
 61 - 80 Good
 81 - 100 Very good

SHI RU High confidence
 SHI-ESHI DZ High confidence

DEFORMATION ZONE V2.2

DZ which is modelled deterministically



Documentation of data files on the CD-Rom

The following information is found on the appended CD:

- Wellcad diagrams for geological data (Appendix 2).
- Fracture frequency diagrams (Appendix 3).
- Documentation of fracture domains in each cored boreholes (Appendix 4).
- Wellcad diagrams for hydrogeochemical data (Appendix 5).
- Wellcad diagrams for rock mechanical data (Appendix 6).
- Integrated Wellcad diagrams (Appendix 8).
- 3D container with the fracture domain model and a selected portion of primary borehole data in Microstation format together with an instruction file that describes the disposition of the data sets.